Electrical Engineering

Registered U. S. Patent Office

for January 1937—

A Million-Cycle Telephone System		4
Abrasion—A Factor in Electrical Brush Wear	V. P. Hessler	8
Lightning Protection for Transmission Lines	A. W. Gothberg and A. S. Brookes	13
Inductive Co-ordination	J. O'R. Coleman and R. F. Davis	17
Two-Reaction Theory of Synchronous Machines	S. B. Crary	27
Proposed Transformer Standards	J. E. Clem	32
Sealed-Off Ignitrons for Welding Control	David Packard and J. H. Hutchings	37
Contributions to Synchronous-Machine Theory	A. S. Langsdorf	41
Synchronous Machine With Solid Cylindrical Rotor	C. Concordia and H. Poritsky	49
Electrical Characteristics of Suspension Insulators	C. L. Dawes and Reuben Reiter	59
Short-Time Spark-Over of Gaps	J. H. Hagenguth	67
A Single-Element Polyphase Directional Relay	A. J. McConnell	77
Ultrahigh-Speed Reclosing of Transmission Lines	Philip Sporn and D. C. Prince	81
Pole Flexibility as a Factor in Line Design	H. P. Seelye and Myron Zucker	91
Lightning Investigation on Transmission Lines—VI	W. W. Lewis and C. M. Foust	101
Arc Characteristics—Flashing on Commutators	R. E. Hellmund	107
A Review of Overhead Secondary Distribution	W. P. Holben	114
Contact Drop and Wear of Sliding Contacts	R. M. Baker and G. W. Hewitt	123
Watt-Hour Meter Bearings	I. F. Kinnard and J. H. Goss	129
Trends in Distribution Overcurrent Protection	G. F. Lincks and P. E. Benner	138
Expansion Theorems for Ladder Networks	M. G. Malti and S. E. Warschawski	153
A New Electrostatic Precipitator	G. W. Penney	159
Dielectric Strength of Transformer Insulation	P. L. Bellaschi and W. L. Teague	164
Development of a Modern Watt-Hour Meter	I. F. Kinnard and H. E. Trekell	172
A New Service Restorer	E. F. Sixtus and W. R. Nodder	180
Impulse-Generator Voltage Charts	J. L. Thomason	183

News 190

The Cover

"The Welder"
Photo by Basil McLean

VOLUME 56 NUMBER 1

Published monthly by the

American Institute of Electrical Engineers

(Founded 1884)

A. M. MacCutcheon, President

H. H. Henline, National Secretary
G. Ross Henninger, Editor
Floyd A. Lewis, Associate Editor
C. A. Graef, Advertising Manager

Publication Committee—I. Melville Stein, *chairman* C. O. Bickelhaupt J. W. Barker O. W. Eshbach
H. H. Henline L. W. W. Morrow H. S. Osborne D. M. Simmons W. H. Timbie

Entered as second class matter at the Post Office, Easton, Pa., April 20, 1932, under the Act of Congress March 3, 1879. Accepted for mailing at special postage rates provided for in Section 1103, Act of October 3, 1917, authorized on August 3, 1918. ¶ Publication Office: 20th & Northampton Streets, Easton, Pa. Editorial and Advertising Offices at the headquarters of the Institute, 33 West 39th Street, New York

High Lights

Synchronous Machines. Synchronous machines are analyzed in 3 papers in this issue. In the first, synchronous-machine theory has been extended to include the effect of armature-circuit capacitance in the general equations for the performance of a salient-pole machine (*pages 41–8*). The second paper presents an extension of the 2-reaction theory of synchronous machines (*pages 27–31*). The third paper presents a mathematical analysis of the synchronous machine from the point of view of field-distribution theory, a departure from the usual method of considering machine performance by means of circuit theory (*pages 49–58*).

Lightning Investigations. Lightning investigations on power systems are reported in 2 papers in this issue. One shows that lightning protection for low-voltage lines, particularly wood-pole lines, may be obtained at low cost by using lightning-protector tubes on one phase of a 3-phase circuit, the conductor so equipped becoming a shielding conductor for the others (*pages 13–16*). The second paper reports the results obtained during 1935 and 1936 in an investigation that has been carried on over a period of several years on certain lines (*pages 101–06*).

Watt-Hour Meters. Watt-hour meters form the subject of 2 papers in this issue. One discusses meter bearings; sapphire jewels and cobalt-tungsten pivots have been found superior in tests on a number of materials. Lubrication is recommended for bearings of the pivot type, but not for the ball type (*pages 129–37*). In the second paper, factors affecting the performance of watt-hour meters, and their influence in the design of a new type of meter, are described (*pages 172–9*).

Suspension-Insulator Characteristics. Suspension-insulator units have electrical characteristics that vary with time, humidity, and stress. Moisture and corona have been found to produce deposits that affect the surface resistance and cause a hysteresis effect in the characteristics. Temperature affects the characteristics indirectly, in that absolute humidity of air is a function of temperature (*pages 59–66*).

Winter Convention. Final arrangements for the Institute's 1937 winter convention to be held in New York, N. Y., January 25–29, are being completed. The convention will mark the resumption of a 5-day winter convention schedule, and will include the usual social and entertainment features and inspection trips, in addition to the 13 technical sessions scheduled (*pages 190–2*).

Inductive Co-ordination. A study of inductive co-ordination of common-neutral power-distribution systems and telephone circuits, conducted jointly by power and communication engineers, has led to some important conclusions concerning this problem. It is believed that where power and telephone people view the matter as a mutual responsibility and fully co-operate, adequate over-all co-ordination readily can be secured (*pages 17–26*).

Pole Flexibility. Flexibility of poles may be of importance under certain conditions in the design of an overhead line, although poles ordinarily are considered rigid. A paper in this issue describes the general method of attacking the problem of pole flexure, and solutions are given in detail. Simpler rules for use in the field also are mentioned (*pages 91–100*).

Reclosure of Lines. Reclosure of circuit breakers on high-voltage transmission lines with the maximum speed that physical phenomena will permit makes possible a high degree of service continuity from a single transmission line. A complete operation in approximately 20 cycles on a 60-cycle system is said to effect a material reduction in outages caused by lightning (*pages 81–90*).

Overhead Distribution. Secondary distribution by overhead conductors and transformers has been studied by 5 companies from an economic standpoint, and a comparison of the results of these studies indicates that the progressive method of distribution design, which provides additions rather than replacements, is the most economical (*pages 114–22*).

Brush Wear. Results of investigations of the wear of electrical brushes are presented in 2 papers in this issue. In one, abrasion is shown to be an important factor in brush wear (*pages 8–12*). The other shows that wear of both rings and brushes can be reduced by operating them in an oxygen-free gas (*pages 132–8*).

Expansion Theorems. Solutions for the current-electromotive force relations of networks such as filters and artificial lines, which lead to difference equations, may be given in the form of expansion theorems similar to Heaviside's expansion theorem and its extensions by the application of Laplace transformations (*pages 153–8*).

Service Restorer. Automatic service restorers for high-capacity transmission and distribution systems have been improved greatly during the last few years, but the need for such equipment on systems of lower capacity has necessitated the development of a new type of unit (*pages 180–3*).

Transformers. Transformers are discussed in 2 papers in this issue. The first outlines certain proposed changes in the AIEE transformer standards (*pages 32–6*). The second paper presents the results of a series of dielectric tests on transformer oil and solid insulation (*pages 164–71*).

Impulse Generator Charts. Comparison of the voltage waves of impulse generators for commercial testing on the basis of the constants of the generator circuit as well as wave shape is suggested in a paper in this issue; charts for selecting circuit constants are included (*pages 183–8*).

Directional Relay. A relay of the polyphase directional type having only a single element has been developed by the use of multiple poles. Reducing the number of elements has reduced the size and weight of the relay, and has resulted in low inertia and high speed (*pages 77–80*).

Sealed-Off Ignitrons. Ignitrons offer a means of control for resistance welding by their ability to supply very large currents for fractions of a cycle. Principles of design and manufacturing technique for both glass and metal tubes of the sealed-off type are discussed in this issue (*pages 37–40*).

Spark-Over of Gaps. Spark-over of sphere and rod gaps, insulators, bushings, and solid insulation for very short time lags has been investigated and some data obtained for the range from 0.2 to 4 microseconds, on which little has been published (*pages 67–76*).

Distribution Protection. Adequate overcurrent protection on distribution systems is necessary in order that a utility company may maintain proper continuity of service; some modern trends are discussed in this issue (*pages 138–53*).

Electrostatic Precipitator. In order to keep abreast of the rapidly growing need for better methods of cleaning air, a new electrostatic precipitator has been devised (*pages 159–63*).

Cruise to Bermuda. A post-convention cruise to Bermuda at special rates is offered those attending the AIEE 1937 winter convention (*pages 191, 192*).

Prizes for Papers. All technical papers presented at Institute meetings during the calendar year 1936 are eligible for prizes (*page 193*).

Commutator Flashing. A knowledge of arc characteristics is of value in investigations of commutator flashing (*pages 107–13*).

Statements and opinions given in articles and papers appearing in ELECTRICAL ENGINEERING are the expressions of contributors, for which the Institute assumes no responsibility. Correspondence is invited on all controversial matters. ¶ Subscriptions—$12 per year to United States, Mexico, Cuba, Porto Rico, Hawaii, Philippine Islands, Central and South America, Haiti, Spain, Spanish Colonies; $13 to Canada; $14 elsewhere. Single copy $1.50. ¶ Address changes must be received by the fifteenth of the month to be effective with the succeeding issue. Copies undelivered because of incorrect address cannot be replaced without charge. ¶ ELECTRICAL ENGINEERING is indexed annually by the Institute, weekly and monthly by *Engineering Index*, and monthly by *Industrial Arts Index*; abstracted monthly by *Science Abstracts* (London). ¶ Copyright 1937 by the American Institute of Electrical Engineers. Number of copies this issue—20,700.

Electrical Engineering

Published Monthly by
American Institute of Electrical Engineers
FOUNDED 1884

VOLUME 56, NO. 1 ▼ ▼ ▼ JANUARY 1937

We Present

The Easy-Reading Page

IN AN EFFORT to relieve readers of eye-strain, with its attendant fatigue and discomfort, or worse, ELECTRICAL ENGINEERING introduces with this issue some of the indirect results of extensive research by noted illumination and research authorities in the field of "effective seeing"—a hopeful step toward a much-needed "easy-reading page." This issue is printed on new paper of an improved quality, blended and toned scientifically to provide the foundation for an effective non-glare easy-reading page. Typography, too, has been modified in the interests of reader-comfort. Even the ink, which after all makes a periodical out of otherwise blank paper, has been specially compounded to contribute toward the desired results, and in all probability will be improved still further in the future.

Concerning this change, Maurice Holland (A'23, M'30) director, division of engineering and industrial research, National Research Council, has written the following statement:

"I have been advised on good authority that 70 per cent of our current knowledge comes to us through the medium of the printed page. Therefore, especially in view of the recent notable advances in the science and art of electrical illumination, it would seem that we have not carried through to the ultimate conclusion, so far as the reader is concerned.

"Particularly as exemplified in the 'better light, better sight' campaign, much scientific and technical effort has been focused with pronounced success on such modern illuminants as the 'IES lamps.' But all this has had to do with the *source* of the light. Therefore, it seems not only timely, but highly important that thoughtful attention should be given to the question of effective *utilization* of light, particularly with reference to the printed page.

"The advance samples of the January 1937 issue of ELECTRICAL ENGINEERING that I have seen represent the nearest to a scientifically developed easy-reading page that so far has been produced through the media of the graphic arts. It is a definite contribution. It is a definite challenge. An easy-reading page involves not only the paper on which it is printed, but, to be most effective, should represent the co-operative effort of printers, ink manufacturers, type designers, and other elements of the graphic arts."

Frankly an experiment, this step represents ELECTRICAL ENGINEERING's effort to serve its readers in the most effective manner possible. Comments are invited.

A Million-Cycle Telephone System

Fig. 1. View showing structure of coaxial cable

ABOUT 2 years ago a new wide-band system for multichannel telephone transmission over coaxial cables was described in an AIEE paper.[1] An experimental system has now been installed between New York and Philadelphia. The various tests and trials which are planned for this system have not been carried far enough to justify a formal AIEE technical paper for presentation and discussion. Meanwhile, the considerable interest that has been aroused in the system has led to this brief statement of its principal features and its general technical performance as so far measured, which has been prepared by M. E. Strieby (M'22) carrier transmission research engineer of the Bell Telephone Laboratories, Inc., New York, N. Y.

The coaxial cable itself has been installed between the long-distance telephone buildings in New York and Philadelphia, a distance of 94.5 miles. It has been equipped with repeaters, at intervals of about 10 miles, capable of handling a frequency band of about 1,000,000 cycles.

This million-cycle system is designed to handle 240 simultaneous 2-way telephone conversations. Only a part of the terminal apparatus has been installed, sufficient in this case to enable adequate tests to be made of the performance of the entire system. A general view of the New York terminal is shown in figure 2. Some preliminary test conversations have been held over the system both in its normal arrangement for providing New York-Philadelphia circuits, and with certain special arrangements whereby the circuit was looped back and forth many times to provide an approximate equivalent of a very long cable circuit. The performance has been up to expectations, and no important technical difficulties have arisen to cast doubt upon the future usefulness of such systems. Much work remains to be done, however, before coaxial systems suitable for general commercial service can be produced.

The Coaxial Cable

Figure 1 shows a photograph of the particular cable used in this installation. It contains 2 coaxial units, each having a 0.265-inch inside diameter, together with 4 pairs of 19-gauge paper-insulated wires, the whole enclosed in a lead sheath having a $^{7}/_{8}$-inch outside diameter. The central conductor of the coaxial units is a 13-gauge copper wire insulated with hard-rubber disks at intervals of $^{3}/_{4}$ inch. The outer conductor is made up of 9 overlapping copper tapes which form a tube 0.02 inch thick; this is held together with a double wrapping of iron tape.

The transmission losses of this coaxial conductor at various frequencies are shown in figure 5. This attenuation is about 4 per cent higher than is calculated for a solid copper tube of the same dimensions and material. Another matter of importance is the shielding obtained from

1. Systems for Wide Band Transmission Over Coaxial Lines, by L. Espenschied and M. E. Strieby, Electrical Engineering (AIEE Transactions), volume 53, 1934, pages 1371–80.

Fig. 2. The New York terminal of the coaxial system

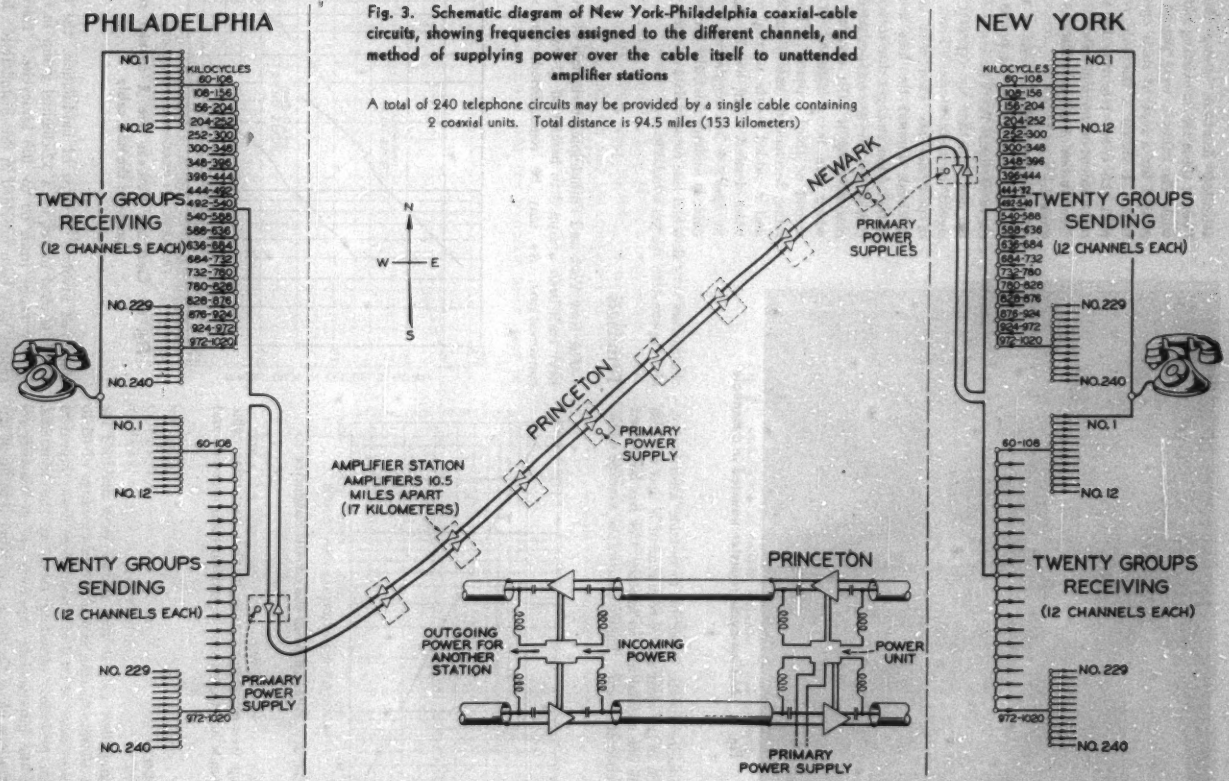

Fig. 3. Schematic diagram of New York-Philadelphia coaxial-cable circuits, showing frequencies assigned to the different channels, and method of supplying power over the cable itself to unattended amplifier stations

A total of 240 telephone circuits may be provided by a single cable containing 2 coaxial units. Total distance is 94.5 miles (153 kilometers)

Fig. 4. Million-cycle repeater mounted in a manhole

attended locations along the line. Four of these are in existing manholes, while the other 2 were placed above ground for a test of such operation. Figure 4 shows a manhole repeater with the cover removed for routine replacement of vacuum tubes. Figure 8 shows one of the installations above ground.

The measured gain of a typical repeater is shown by the points on the curve of figure 7. The curve itself is the line loss that the repeater is designed to compensate. Three stages of pentodes are used with negative feedback around the last 2 stages. Attenuation changes due to temperature of the line are compensated automatically by a pilot channel device which has been installed at every second or third repeater. The regulating mechanism uses 4 small tubes and is added to the normal repeater when desired. The amplifiers shown in figure 8 are regulating. As the cable is underground, the temperature changes are very slow and but meager data on the accuracy of compensation are yet available.

one conductor to the other or to outside interference. Inasmuch as the most severe requirement is that of cross talk from one coaxial unit to another, this has been used as a criterion of design. Figure 6 shows the average meas-

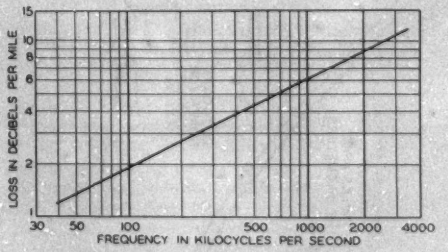

Fig. 5. Attenuation of the coaxial conductor

ured high-frequency cross talk in this particular cable on a 10-mile length without repeaters, both near-end and far-end.

Repeaters

The amplifiers used in this system were designed for about a 10-mile spacing and a frequency range of 60 to 1,024 kilocycles. A total of 10 complete 2-way repeaters has been provided, including those at the terminals. Two of the intermediate repeaters are at existing repeater stations along the route, the other 6 being at un-

Terminals

The New York and Philadelphia terminals of the cable have each been equipped to handle 36 2-way telephone conversations. As may be remembered, the scheme

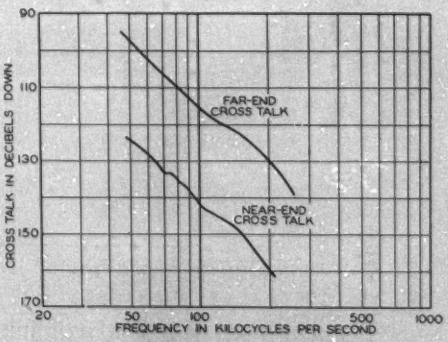

Fig. 6. Cross talk between the 2 coaxial conductors in the new cable

employed involves 2 steps of modulation, the first of which is used to set up a 12-channel group in the frequency range from 60 to 108 kilocycles. Three such groups have been provided in this installation. In order

to transmit at the higher frequencies, a second step of modulation is used in which an entire 12-channel group is moved to the desired frequency location by a "group" modulator. Six such group modulators have been provided at various frequencies throughout the range, including both the top and bottom. Patching facilities have been provided so that any 12-channel group may be transmitted over any one of the high frequency paths. A typical frequency characteristic of one of the channels is shown in figure 9. It may be observed that relatively high quality has been obtained, due largely to the use of crystal filters, even though the channels are spaced throughout the frequency range at 4,000-cycle intervals.

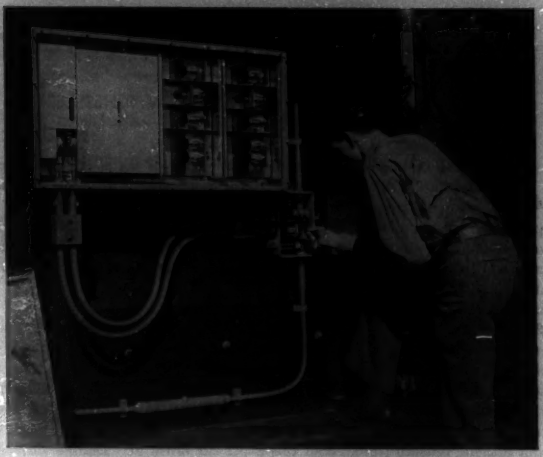

Fig. 8. Installation of coaxial repeater above ground

Preliminary Tests

As already noted, various long circuits have been built up by looping back and forth through the coaxial system. One setup over which conversations were successfully carried out consisted of 5 voice-frequency links in tandem, each link being 760 miles long, giving a total circuit length of 3,800 miles. This setup included, in each direction, 70 stages of modulation and the equivalent of 400 line amplifiers, the transmission passing 20 times through each one of the 20 one-way line amplifiers constituting the 10 2-way repeaters.

This demonstrated that the complete assemblage of parts, including filters which divide the frequency range into the required bands, modulators which produce the necessary frequency transformations, and amplifiers which counteract the line attenuation, introduced very little distortion. Many problems require further consideration, however, before these systems will be ready for design and production for general use. The final systems must have such refinement that they are suitable for transcontinental distances; the tremendous amplifications needed for such distances must have very precisely designed regulation systems, particularly where aerial construction is involved; noise and cross talk must not accumulate over the long distances; the repeaters must have such stability and reliability that continuity of service will be assured with hundreds of repeaters operating in series and each repeater handling several hundred different communications.

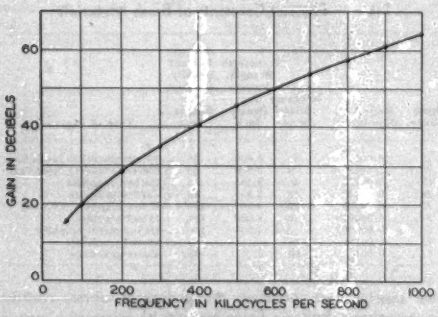

Fig. 7. Gain-frequency characteristic of coaxial repeater

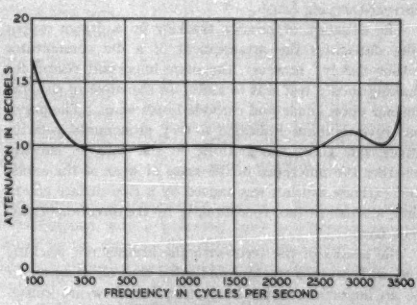

Fig. 9. Frequency characteristic of a typical speech channel

Abrasion—A Factor in Electrical Brush Wear

By V. P. HESSLER
ASSOCIATE AIEE

An investigation of the effect of abrasion upon electrical brush wear is reported in this paper. Tests of the rate of wear of anode and cathode brushes, and of brushes carrying current and those that did not, show that abrasion is an important factor in electrical brush wear.

A BRIEF résumé of the literature on electrical brush wear was reported by the author in a previous paper.[1] A more complete review of this literature has also been reported by the author in another publication.[2] In the interest of brevity, these publications will be assumed to be available to the reader. The investigations reported in this paper represent an extension of the previous work, all of which has been carried on under the auspices of the Iowa Engineering Experiment Station. In the previous investigations the brushes were operated with the anode and cathode brushes (throughout this paper the brush at which the conventional current flow is from the brush to the ring is called the anode brush) on separate paths, for the purpose of obtaining fundamental information concerning the wear of brushes at different polarities. These experiments have been extended to include the condition of brushes tracking and brushes trailing. That is, with brushes tracking, the anode and cathode brushes are both operated on the same path; with brushes trailing, a brush not carrying current is operated on the same path with a current-carrying brush.

The situation of brushes tracking on a drawn copper ring duplicates the arrangement of a d-c commutator rather closely; however, the more important reason for making such a test was to ascertain the effect of the ring surface upon anode and cathode brush wear. The previous investigations indicated a very pronounced polarity effect, but there was nothing in the data to indicate whether the difference in the rates of wear of the anode and cathode brushes was caused by a ring-surface condition, a brush-surface condition, or by the direction of current flow.

The results of the tests with the brushes not tracking and with brushes tracking indicated that abrasion might be an important factor in electrical brush wear; consequently a series of tests was run with brushes trailing, with the hope of evaluating the magnitude of this factor in brush wear. It was assumed that if a brush carrying current were operated on the same ring simultaneously with a brush not carrying current, both might lose material at the same rate as a result of abrasion, while the current-carrying brush would lose additional material as a result of the current flow. This assumption proved to be substantially correct.

Apparatus Used in the Tests

All of the tests were made upon drawn electrolytic-copper rings. The rings were rolled from strip copper, brazed on the inside of the hoop and pressed upon cast aluminum disks. The rings were turned true and finished with the shaft rotating in its own bearings, so it was possible to maintain the ring eccentricity below 0.0005 inch.

The brush holders were of the radial type. The dimensions of the brushes were $\frac{1}{2}$ by $\frac{1}{2}$ by 2 inches. It was realized that a brush of these dimensions in a radial brush holder might be subject to chatter, but it caused no apparent difficulty. The brushes were fitted very closely, and the rings were always rotated in the same direction. Double surfaces were observed on the brush faces only during the running-in period. The brush holders were mounted 90 degrees apart on vertical and horizontal diameters. The rings were always rotated in the direction from the lower brush to the upper brush, because the author thought that less of the material abraded from the preceding brush would be carried under the following brush with such an arrangement.

Some of the physical characteristics of the brush materials are given in table I. The tests ordinarily were conducted on 4 rings simultaneously. The 4 pairs of brushes were connected in series and the group connected to an 80-volt d-c generator through a variable resistor. By dropping a large part of the circuit voltage in the variable resistor and operating the generator under conditions corresponding to a point high on its saturation curve it was possible to maintain a constant circulating current through the brushes.

Table I—Physical Constants of Brush Materials

Brush Grade	Resistivity, Ohm-Inches	Hardness (Sclero-scope)	Transverse Strength, Pounds Per Square Inch	Normal Current Density, Amperes Per Square Inch	Type of Material
A	0.0020	65	3,600	55	Electrographitic lampblack
B	0.00225	54	2,960	60	Electrographitic lampblack
C	0.00106	40	3,500	45	Carbon graphite
D	0.00142	40	3,500	45	Carbon graphite
E	0.0000084	20	4,900	115	Metal graphite
F	0.000010	16	4,000	100	Metal graphite
G	0.00000242	5	9,700	150	Heavy metal graphite
H	0.0014	76		65	Electrographitic
I	0.0013	60		65	Electrographitic

A paper recommended for publication by the AIEE committee on electrical machinery. Manuscript submitted September 23, 1936; released for publication November 27, 1936.

V. P. Hessler is assistant professor of electrical engineering at Iowa State College, Ames. The author wishes to express his appreciation to the National Carbon Company and the Morganite Brush Company for furnishing the brushes which were used in the tests.

1. For all numbered references see list at end of paper.

The temperature and humidity were maintained constant throughout the tests by means of automatically controlled air-conditioning equipment. The atmosphere was kept as nearly dust free as possible by means of a specially designed dust collector, but no attempt was made to make quantitative measurements of the dust condition.

The rate of wear was determined by measuring the length of the brushes at the beginning and again at the end of a run by means of a micrometer with an electrical contact arrangement. The rate of wear is represented by the ratio of the change in length during the run to the duration of the run. The unit "inches per 100,000 hours" was chosen simply for ease of calculation and presentation of the data. A rate of wear of 11.4 inches per 100,000 hours is equivalent to a life of one year per inch.

The data on contact drop were obtained by means of an auxiliary copper-leaf brush, which was lowered to the ring whenever readings were desired. Each test brush was equipped with a potential lead to eliminate errors caused by the shunt voltage drop, and the contact voltage drop was corrected for the voltage drop through the brush material.

A more complete description of the apparatus is included in a previous paper on brush wear.[1] The same apparatus, except for a few minor changes in brush-holder mountings, was used in these tests.

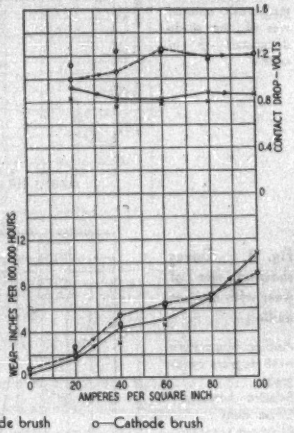

Fig. 1. Curves showing rate of wear and contact voltage drop with brushes tracking

Ambient temperature—45 degrees centigrade
Relative humidity—50 per cent
Ring material—Copper
Brush material—Electrographitic lampblack, designated as material *A* in table I
Ring speed—3,500 feet per minute
Brush pressure—3 pounds per square inch

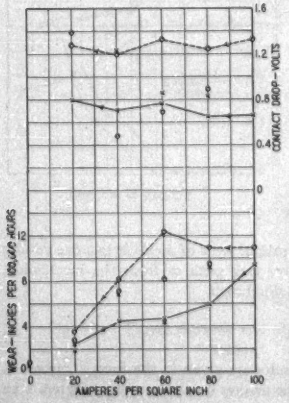

Fig. 2. Curves showing rate of wear and contact voltage drop with brushes tracking

Test conditions identical with those of figure 1, except that the brush material was of the grade designated *B* in table I

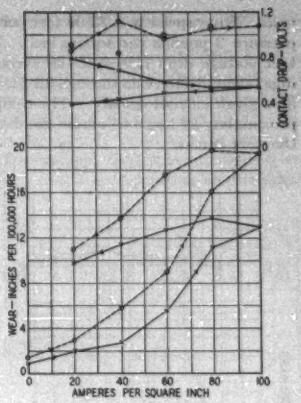

Fig. 3. Curves showing rate of wear and contact voltage drop with brushes tracking

Test conditions identical with those of figure 1, except that the brush material was of the grade designated *C* in table I

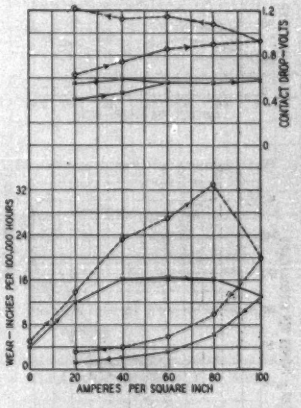

Fig. 4. Curves showing rate of wear and contact voltage drop with brushes tracking

Test conditions identical with those of figure 1, except that the brush material was of the grade designated *D* in table I

Test Procedure

The brushes always were sanded carefully and run for several hours with a nominal current before any readings were taken. The rings were sanded at the beginning of each series of tests and then not cleaned again until the beginning of the next series of tests. The temperature and the relative humidity were held constant at 45 degrees centigrade and 50 per cent, respectively, throughout the

tests. Ring speed was 3,500 feet per minute and brush pressure 3 pounds per square inch. The curves of contact voltage drop represent the average of several readings taken at intervals throughout the period of operation at a given current density. The equipment was run approximately 24 hours to obtain the data for each point on the wear curves.

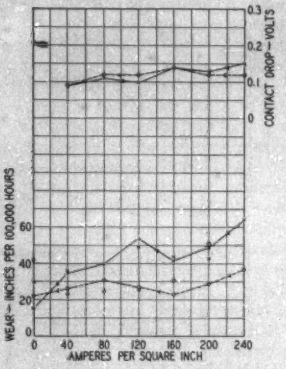

Fig. 5. Curves showing rate of wear and contact voltage drop with brushes tracking

Test conditions identical with those of figure 1, except that the brush material was of the grade designated *E* in table I

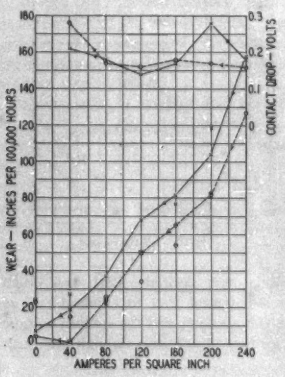

Fig. 6. Curves showing rate of wear and contact voltage drop with brushes tracking

Test conditions identical with those of figure 1, except that the brush material was of the grade designated *F* in table I

The experiments with brushes tracking simply consisted of arranging 2 brushes on the same path of a given ring and obtaining wear and contact voltage drop data. The arrangement was somewhat more involved in the case of brushes trailing, for which 4 brushes were mounted on each ring in such a manner that a pair of brushes operated on each of 2 ring paths. The electrical circuit was arranged to carry current through one brush of each pair, to reverse the current through the first 2 brushes, or to connect to the other 2 brushes on a given ring. This arrangement made it possible to observe whether the results obtained were peculiar to a given brush and holder or could be duplicated on other brushes. Also it gave some idea of the time required for changes in film formation to take place. The sequence of readings represents approximately 24-hour periods of operation. In all trailing tests, except for figures 12 and 13, identical brushes were used in all 4 positions on the ring. The tests for figures 13 and 14 were conducted with one metallic brush and one nonmetallic brush on each path, for the purpose of studying whether the higher rate of wear of metallic brushes results from a more abrasive ring path or from the mechanical structure of the metallic brush.

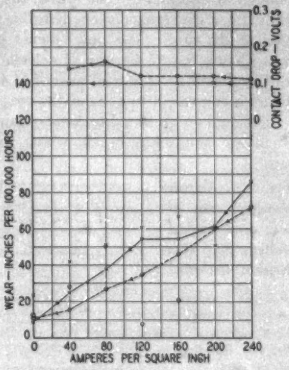

Fig. 7. Curves showing rate of wear and contact voltage drop with brushes tracking

Test conditions identical with those of figure 1, except that the brush material was of the grade designated *G* in table I

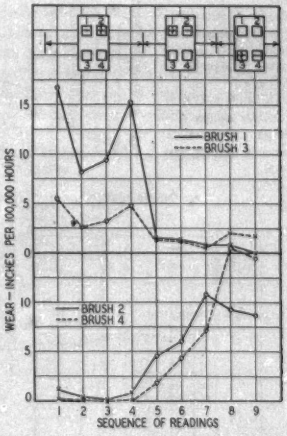

Fig. 8. Curves showing rate of wear with brushes trailing

Ambient temperature—45 degrees centigrade
Relative humidity—50 per cent
Ring material—Copper
Brush material—Electrographitic lampblack, designated as material *H* in table I
Ring speed—3,500 feet per minute
Brush pressure—3 pounds per square inch
x—Anode brush
o—Cathode brush

Results of Tests

All of the test results are given in the form of curves in figures 1 to 13. The arrows on the curves of figures 1 to

7 indicate the sequence in which the tests were made. For example, in figure 3, tests were started at zero current; the current was increased to 100 amperes per square inch and reduced to 20 amperes per square inch by 20-ampere increments. For most cases only the descending or ascending curves are shown. The experimental points not connected by curves represent the other values.

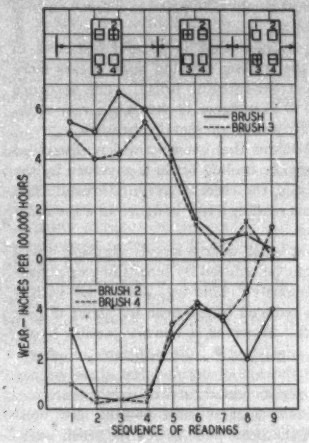

Fig. 9. Curves showing rate of wear with brushes trailing

Test conditions identical with those of figure 8, except that the brush material was of the grade designated *I* in table I

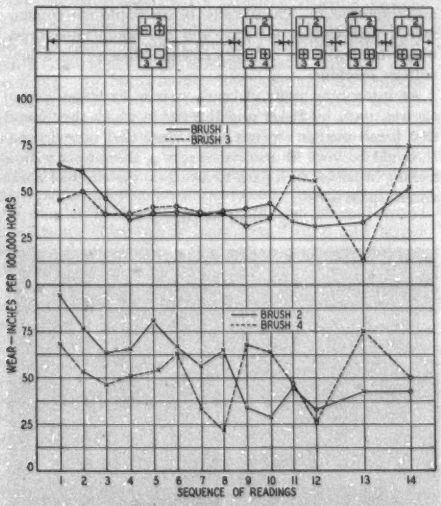

Fig. 10. Curves showing rate of wear with brushes trailing

Test conditions identical with those of figure 8, except that the brush material was of the grade designated *E* in table I

Figures 1 to 7 represent the results of the tests with brushes tracking

The results for various brush materials with brushes trailing are given in figures 8 to 13. The boxes at the top of each figure represent the electrical connection and mechanical arrangement of the 4 brushes on a ring. The minus sign indicates the cathode brush and the plus sign the anode brush. For example, the left box in figure 8 indicates that brushes 1 and 3 are operating on the same

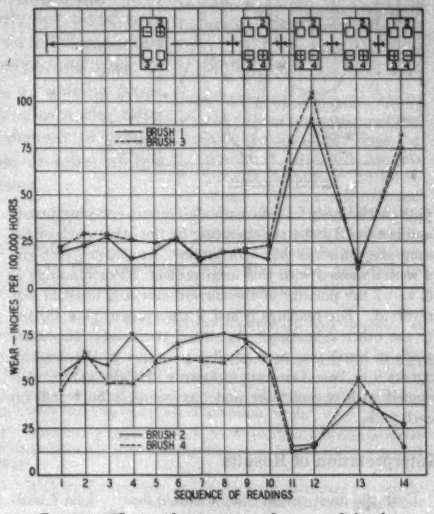

Fig. 11. Curves showing rate of wear with brushes trailing

Test conditions identical with those of figure 8, except that the brush material was of the grade designated *F* in table I

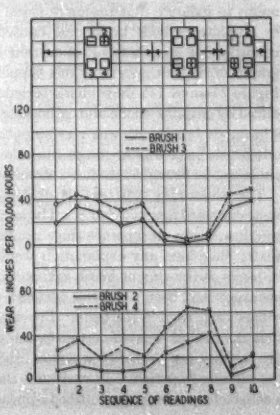

Fig. 12. Curves showing rate of wear with brushes trailing

Test conditions identical with those of figure 8, except that brushes 1 and 2 were of grade *I* and brushes 3 and 4 were of grade *F*

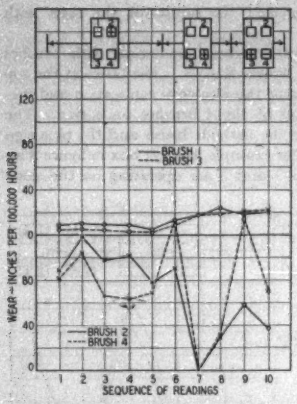

Fig. 13. Curves showing rate of wear with brushes trailing

Test conditions identical with those of figure 8, except that brushes 1 and 2 were of grade *F* and brushes 3 and 4 were of grade *I*

path, with brush 1 as the cathode-current-carrying brush, and brushes 2 and 4 are operating on the other path of the same ring with 2 as the anode brush. Readings 1, 2, 3, and 4 were obtained with this arrangement. For readings 5, 6, and 7 the polarity of the current-carrying brushes was reversed. For readings 8 and 9 the current was shifted to the other 2 brushes. As stated previously, the same grade of brush was used in all 4 positions in the tests of figures 8 to 11. The tests of figures 12 and 13 were conducted with one metallic and one nonmetallic brush on each path.

Interpretation of Results

Even the most casual comparison of figures 1 to 7 with the curves of the previous paper[1] indicates that there is a fundamental difference between operating brushes tracking and not tracking. With brushes of both polarities operating on the same path practically all of the difference in wear which was previously observed disappears. This seems to indicate that the more rapid wear of the carbon or graphite cathode brush was caused by a ring-surface condition set up as a result of current flow. Photomicrographs of ring surfaces show this supposition to be correct. Figure 14*a* and 14*b* show characteristic ring paths as produced by graphite anode and cathode brushes, respectively. The anode-brush path was very smooth, whereas the cathode-brush path was so rough that the peaks and valleys could not be brought into focus simultaneously.

The reader may note that the arrows are reversed on the wear curves of figures 3 and 4. These curves were obtained simultaneously on separate rings mounted upon the same shaft; therefore, any explanation would have to be made in terms of the ring or brush materials. No difference in operation has been observed between the various drawn copper rings used in the tests. Previous tests have shown that the rate of wear of certain brush grades decreases as the brushes are "run in" whereas others increase during the running-in period. In each case the ring may present a satisfactory uniformly polished appearance. No doubt, the same phenomenon has occurred in figures 3 and 4.

The results presented in figures 8 to 13 show definitely that brush wear is largely abrasion resulting from a ring-surface condition set up by current flow. In general, the trailing brush wears at almost the same rate as the current carrying brush. The sequence of readings from 4 to 7 in figure 9 indicates that a surface condition affecting the rate of wear is being established. If the wear were purely electrical, the reversal would take place in a much shorter period.

It is interesting to note that in several instances in figures 10 and 11 the trailing metallic brush wears more rapidly than the current-carrying brush. The sequence of readings from 10 to 14 in figure 11 shows in a very striking manner the polarity effect on metallic brushes.

Figures 12 and 13 show that even for widely dissimilar materials the wear of the trailing brush is governed by the nature and polarity of the current-carrying brush. The decrease in wear from reading 6 to 7 in figure 13 was caused by cleaning the ring.

After showing that brush wear is largely abrasion it was thought that it might be reduced by burnishing or polishing the ring continuously. This was attempted with a cotton tape, which reduced brush wear by about 60 per cent in the first tests. However, it was not possible to obtain these results consistently. An attempt to obtain better results with the aid of certain fine abrasives resulted in tremendously increased rates of brush wear.

The foregoing results suggest using metallic and nonmetallic brushes on the same path to reduce brush wear, but no commercial machine seems to be adaptable to such an arrangement. The metallic brush would not commutate a high-voltage machine and the nonmetallic brush would not have the current-carrying capacity for a low-voltage machine.

An interesting study of brush wear in hydrogen and in air was made by Baker and Hewitt[2] in which they found that brush wear in air was many times that in hydrogen. It would be very instructive to repeat these tests with a trailing brush on each path to ascertain the effect of abrasion in these tests.

(*Concluded on page 16*)

Fig. 14. Photomicrographs of ring surfaces

Left—Path of anode brush. Right—Path of cathode brush

Lightning Protection for Transmission Lines

By A. W. GOTHBERG
ASSOCIATE AIEE

A. S. BROOKES
ASSOCIATE AIEE

To meet the need for lightning protection on low-voltage transmission lines at moderate cost, and particularly for wood-pole lines, a design is presented in this paper that has high insulation strength and uses, in place of a ground wire, a shielding phase conductor with a lightning protector tube. Lightning currents are drained to ground with a minimum number of tubes of low current rating.

THE RESULTS of many years of lightning-research work have been applied to steel-tower transmission lines with great improvements in operating results. In general, there has been less accomplished in improving wood-pole line design. The records of the company with which the writers are associated show lightning outages on unprotected wood-pole lines to be 48 per 100 miles of line per year as compared to a rate of 5 for steel-tower lines with 2 ground wires. Such relatively poor performance shows the need for improved protection.

Early investigators attempted to prevent line outages by increasing insulation. Measurements of stroke currents indicate that some outages can be prevented by over-insulation but that obtaining reliable operation by the use of high insulation is costly and impractical.

The most widely used form of protection consists of ground wires to intercept all direct strokes. These are very effective when properly installed with adequate clearances and low-impedance ground connections. In many cases, however, the cost of the extra wire and of enlarging the structures for increased clearances and heavier loading cannot be economically justified. Particularly in the case of wood construction, low-resistance grounds may be difficult and expensive to obtain. In addition, unless special precautions are taken, the ground lead will render useless a portion of the normal wood insulation. The use of additional wires and larger structures naturally increases construction and maintenance costs.

A recent and increasingly popular protection scheme consists in the installation of lightning protector tubes[1,2] to drain surge currents from the phase wires and extinguish the resulting power arc. It is customary to install a tube for each phase on protected structures. Where ground resistances are low, strokes to one wire will cause phase-to-ground faults. Where more than one wire is struck or where ground resistances are high, the tubes will have to interrupt phase-to-phase short-circuit currents. On power systems using neutral resistors or reactors, co-ordination may be difficult since present tubes are effective only within a limited range of short-circuit currents. A given tube will not interrupt currents below its rating and will fail because of excessive internal pressures on currents in excess of its rating. In general, tubes are effective, although a large number are required to secure protection on lines with short span lengths and high ground resistances.

Summary

Without departing radically from present practices with wood-pole lines, a design is proposed for improved lightning performance. Use is made of wood insulation and a shielding conductor with lightning-protector tubes. Computation methods are shown so that the recommendations may be adapted to local conditions. It may be concluded that:

1. It is possible on low-voltage transmission lines to secure at moderate cost a large reduction in lightning outages.
2. It is possible to secure the advantages of a ground wire without the cost of the additional wires and heavier structures.
3. Protection may be secured by the use of low-rating lightning-protector tubes on one phase of a 3-phase circuit.
4. A method of protection is presented which may be used on higher voltage lines with economies resulting from the elimination of ground wires.
5. With the assumptions used and by using a standard pole top the proposed design shows an estimated reduction in lightning outages of approximately 75 per cent.

Proposed System of Protection

The proposed design is an attempt to secure at moderate cost a line combining the advantages of the 3 present protection methods as follows:

1. One phase of each circuit is made a shielding conductor by locating it so that the remaining phases will be shielded from direct strokes.
2. Lightning currents are drained from the shielding conductor by means of a lightning-protector tube.
3. The remaining phases are isolated from the shielding conductor and tube ground circuit by insulation sufficient to prevent phase-to-phase faults. This allows the use on each structure of a single tube designed to withstand only phase-to-ground currents which, in general, are much less than phase-to-phase currents.

Construction Features

Figure 1 shows the described features incorporated in a single-circuit wood-pole top. The location of

A paper recommended for publication by the AIEE committee on power transmission and distribution. Manuscript submitted October 20, 1936; released for publication November 10, 1936.

A. W. Gothberg is an engineering assistant in the Public Service Electric and Gas Company, Newark, N. J. A. S. Brookes is assistant engineer in the electric distribution department of the same company.

1. For all numbered references see list at end of paper.

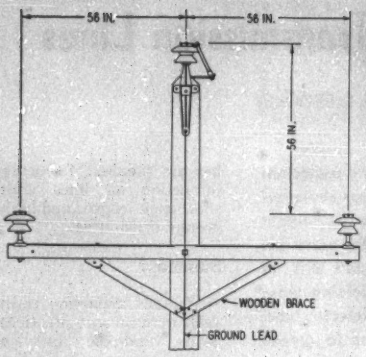

Fig. 1 (left). Single - circuit pole showing shielding conductor and lightning protector tubes

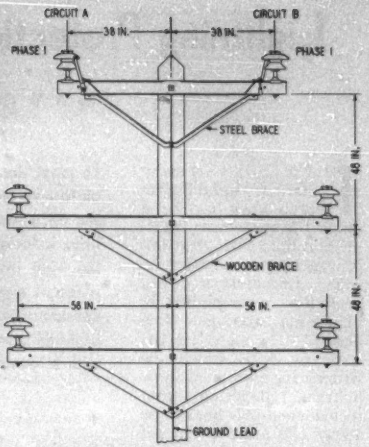

Fig. 2 (right). Double - circuit pole showing shielding conductor and lightning protector tubes

the shielding conductor with reference to the other phase wires may be determined by use of the conventional shielding angle[3] or by assuming a cloud height and considering the distances to the line conductors.[4] For a structure of the size shown the shielding-angle method was used as giving the more conservative results.

To prevent flashovers between the tube ground lead and the lower phase wires without excessively close tube spacings requires the use of insulation having high impulse strength. In the design shown this is obtained by the use of wooden crossarm braces. The breakdown strength for the combination shown is 645 kv at 4 microseconds. Insulation values for other desired forms of construction may be obtained from an earlier paper.[5] For most practical designs only the breakdown strength of the insulators and wood need be considered since it is lower than that of the direct path through air.

The tube is placed as shown so as to drain lightning currents from the shielding conductor to ground. The mounting arrangement must be such that the breakdown of the tube and associated gap is at all times less than that of the insulator and the wood between the insulator pin and tube mounting.

The single-circuit pole top may be expanded to provide for an additional circuit as shown in figure 2. The same clearances are maintained and tubes are installed on the 2 top shielding conductors. It is important that the same phase of each circuit be on the top arm so that, in the event of a stroke involving the top 2 conductors, the tubes will not be required to interrupt phase-to-phase currents.

Distance Between Protected Poles

The expected number of outages and the magnitude of lightning strokes to a line[6] in a territory with an isokeraunic level of 30 are shown in figure 3. While this curve is for a steel-tower line with 2 ground wires, it may be used without serious error for a wood-pole line. This curve is used to find the line performance for an equivalent lightning level. For example, a design for strokes up to 4,000 kv gives an expected

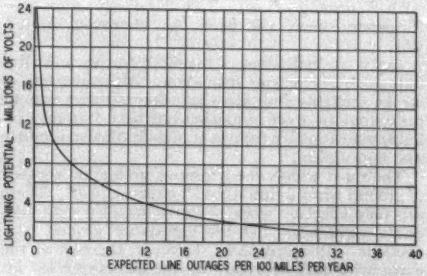

Fig. 3. Expectancy curve of lightning outages

outage rate of 12 per 100 miles per year as compared with a rate of 48 for an unprotected line, a reduction in outages of 75 per cent.

Assuming a surge impedance of 200 ohms for the lighting channel and 4,000 kv as the stroke potential, the stroke current is 20,000 amperes. Since the ground current theoretically may reach double this value, it is necessary to use a tube heavy enough to withstand 40,000 amperes surge current.

A computation of the voltages appearing on the shielding conductor for a stroke to a protected pole involves the use of a rate of voltage rise in the stroke. A rate of 1,000 kv per microsecond is believed to be a value which should give conservative results. Neglecting the length of the ground lead, the initial voltage on the shielding conductor E_L at the struck pole is

$$E_L = E_{stroke} \times \frac{2Y_0}{Y_0 + 2Y_1 + Y_2} = E_s b_0$$

where

Y_0 = surge admittance of stroke
Y_1 = surge admittance of shielding conductor

Y_3 = surge admittance of ground
a is used for reflection factors
b is used for refraction factors

Sufficiently accurate results are secured by considering only the reflections from the first 2 protected poles on each side of the struck pole. The reflection factor at the struck pole is

$$a_1 = \left(1 - \frac{2Y_1}{Y_3 + 2Y_1 + Y_2}\right)$$

The reflection factors at the first and second protected poles away are

$$a_2 = a_3 = \left(1 - \frac{2Y_1}{2Y_1 + Y_2}\right)$$

Similarly the refraction factors are

$$b_1 = \frac{2Y_1}{Y_3 + 2Y_1 + Y_2} \qquad b_2 = b_3 = \frac{2Y_1}{2Y_1 + Y_2}$$

The reduction factors at the struck pole for successive reflections found by using the lattice method[4] are:

Reflection	Reduction Factors
First	$A = -a_2b_1$
Second	$B = a_2b_1(a_2b_1 - b_2^2 - a_1a_2)$
Third	$C = a_2^2b_1(b_1b_2^2 + b_2^2 - 3a_1b_2^2 - a_2b_2^2 - a_2b_1^2 - a_1^2a_2)$
Fourth	$D = a_2^2b_1(b_1b_2^4 + 4a_1a_2b_1b_2^2 + a_2^2b_1b_2 + a_2^2b_1b_2^2 + a_2b_2^2 + a_1^2a_2^2b_1 + a_1a_2b_2^2 - 2a_2b_1^2b_2^2 - a_1b_2^4 - 3a_1^2a_2b_2^2 - 2a_1a_2^2b_2^2 - a_2^2b_2^2 - a_2b_1b_2^2 - a_1a_2^2b_1^2 - a_1^2a_2^2)$

Where the rate of voltage rise de/dt in the stroke equals 1,000 kv per microsecond, $d/1{,}000$ may be used for elapsed time in microseconds after the initial contact of the stroke with the shielding conductor where d is the distance between protected poles (con-

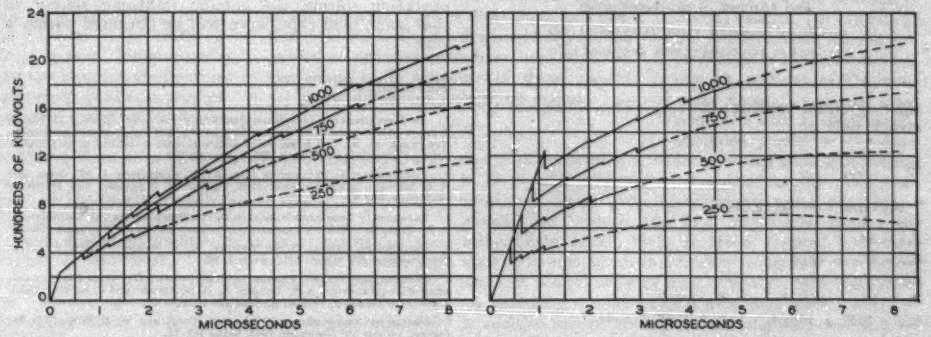

Figs. 4 and 5. Curves for voltage on shielding conductor for stroke to protected pole (left) and to unprotected pole (right)

Ground resistance, 50 ohms; rate of voltage rise in stroke, 1,000 kv per microsecond; numbers on curves are distances between poles in feet

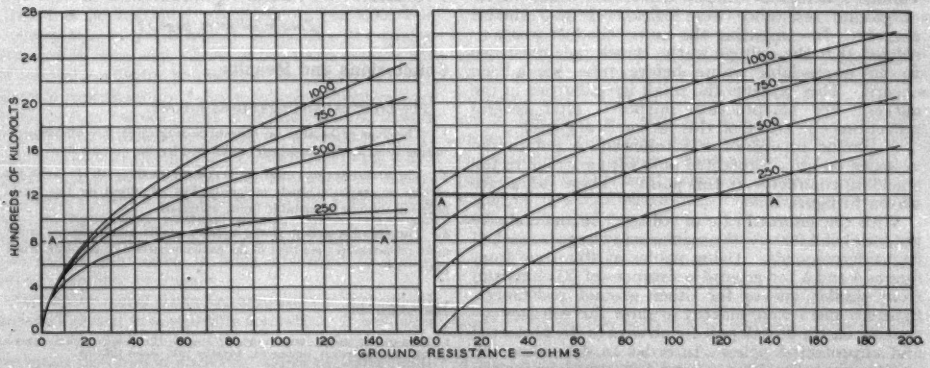

Figs. 6 and 7. Curves for voltage on shielding conductor with stroke of 20,000 amperes to protected pole (left) and to unprotected pole (right) for various ground resistances

Voltage required for flashover of unprotected pole shown by *AA*; numbers on curves are distances between poles in feet

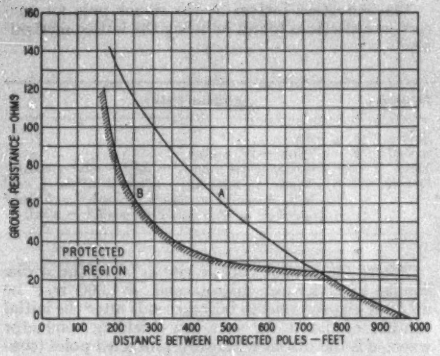

Fig. 8. Curves showing relation between ground resistance and spacing of protector tubes

A—Limit of protected region, unprotected pole
B—Limit of protected region, protected pole

sidering equal spacing) in feet. The voltage at the struck pole is:

$$E_L = \frac{d}{1{,}000} \times \frac{de}{di} \times b_1$$

At time $t = 2d/1{,}000$

$$E_{nd} = 2E_L$$
$$E_{nd} = 4E_L - 4E_LA$$
$$E_{nd} = 6E_L - 8E_LA - 4E_LB$$
$$E_{nd} = 8E_L - 12E_LA - 8E_LB - 4E_LC$$
$$E_{nd} = 10E_L - 16E_LA - 12E_LB - 8E_LC - 4E_LD$$

With values obtained as shown, figure 4 was plotted for ground resistances of 50 ohms, giving the voltages at the struck pole as a function of time for various spacings of tubes. Curves for other values of ground resistance were calculated in a similar manner. In computing the curves the fact was considered that the voltage at the struck pole must rise to an appreciable value before tube breakdown occurs. This explains the small irregularities in the curves. For all practical purposes, after several reflections the effect of this factor is negligible.

A similar procedure was followed to obtain the voltages on an unprotected pole with a stroke to the shielding conductor at this point. These values are shown in figure 5.

With the assumed rate of voltage rise and a stroke potential of 4,000 kv, the maximum voltage is reached in 4 microseconds. Using values at this time from figures 4 and 5 for ground resistances of 50 ohms and from similar curves for other ground resistances, figures 6 and 7 were plotted to show the voltages appearing on the struck pole for strokes to the protected and unprotected poles. In order to determine the correct ground resistances and tube spacings for the proposed design, the impulse breakdown values of the insulation between the lower phase wires and the ground lead or ground are shown as straight lines on the curves. These values were increased by 30 per cent to allow for coupling between the shielding conductor and other phase wires. The intersections of the straight lines and the curves are plotted in figure 8 to show the maximum ground resistance for safe protection with given tube spacings. Local conditions will dictate whether it is more economical to use closely spaced tubes or to take steps to lower ground resistances.

It is realized that there may be some disagreement in regard to the assumptions made for these calculations but the values chosen are considered sufficiently conservative and accurate to give a co-ordinated installation. Future investigations will probably yield more accurate data but these should affect the figures for expected line performance rather than the fundamental design.

At the present time several 26-kv lines are being rebuilt incorporating the features of this proposed design. It is expected that these lines will be in operation during the coming lightning season so that some field experience will be obtained within a year.

References

1. An Experimental Lightning Protector for Insulators, J. J. Torok. A paper (AIEE number 31–9) presented at the 1931 AIEE winter convention, New York, N. Y., and from which abstracts were published in Electrical Engineering, volume 50, July 1931, pages 498–502.

2. The Expulsion Protective Gap, K. B. McEachron, I. W. Cross, and H. L. Melvin. AIEE Transactions, volume 52, September and December 1933, pages 884–91.

3. Progress in Lightning Research in the Field and in the Laboratory, F. W. Peek, Jr. AIEE Transactions, volume 48, April 1929, pages 436–48.

4. Critique of Ground Wire Theory, L. V. Bewley. AIEE Transactions, volume 50, March 1931, pages 1–18.

5. Impulse and Dynamic Flashover Studies of 26-Kv Wood Pole Transmission Construction, A. S. Brookes, R. N. Southgate, and E. R. Whitehead. AIEE Transactions, volume 51, June 1933, pages 494–501.

6. Design of Transmission Lines, J. J. Torok and W. R. Ellis. *Electric Journal*, volume 30, November 1933, pages 467–71.

Abrasion—A Factor in Electrical Brush Wear

(*Continued from page 12*)

Conclusions and Results

The principal findings are as follows:

1. The wear of brushes on concentric rings is largely abrasion resulting from a ring condition established by the current flow.

2. The abrasive ring condition is caused by the cathode brush for carbon or graphite brush materials, but is caused by the anode brush in the case of metallic brush materials.

3. The abrasive action of the anode metallic brush path is much more pronounced than that of the cathode carbon or graphite brush path.

References

1. Electrical Brush Wear V. P. Hessler. Electrical Engineering (AIEE Transactions) volume 54, October 1935 pages 1050–54.

2. The Effect of Various Operating Conditions upon Electrical Brush Wear and Contact Drop V. P. Hessler. Bulletin 122 Iowa Engineering Experiment Station, 1935.

3. Brush Wear in Hydrogen and in Air, R. M. Baker and G. W. Hewitt. *Electric Journal*, volume 33, June 1936, pages 287–9.

Inductive Co-ordination of Common-Neutral Power-Distribution Systems and Telephone Circuits

By J. O'R. COLEMAN
MEMBER AIEE

R. F. DAVIS
ASSOCIATE AIEE

Early installations of 3-phase 4-wire power distribution systems of the multigrounded or common-neutral type in some cases created noise problems involving neighboring telephone circuits. Operating experience, studies of specific situations and comprehensive co-operative research over a period of years have developed means of largely avoiding difficulties of this character. The relative importance of various features of the power and telephone systems which have been found to affect the noise-induction problems involved is discussed here, and the general co-operative procedures most helpful in conversions to, or extensions of, these types of power distribution systems, are outlined.

PRIOR to about 1915, delta-connected 2,300-volt 3-phase primary circuits were used extensively for the distribution of electric current. While some distribution networks throughout the country still operate in this manner, the marked increase in load densities, starting about 1915, often made the retention of the 2,300-volt delta system impracticable. In a few instances the development of the particular network was at a point where it was feasible to change from the 2,300-volt delta to a 4,600-volt delta arrangement, but in other cases the existing equipment represented too great an investment for a complete change of this character.

From studies of various methods of caring for the augmented load densities, it was found that the existing equipment could largely be saved and the capacity of the distributing networks substantially increased by converting them to a 2,300/4,000-volt star-connected 4-wire primary system. By about 1925 this system had extended to most of the larger cities and most power companies had found it economical to use in at least some parts of their territories.

In using the 2,300-volt equipment on the 4,000-volt 4-wire system it was necessary to stabilize the neutral conductor in some way. Most of the 4-wire systems had the neutral conductor grounded at the substation only, although sometimes low-voltage lightning arresters were placed on it at various points in the distribution network to aid in its stabilization in case of a break in it. In some instances, at the time of the installation of the 4-wire system, the primary neutral was connected at various points in the network to driven ground rods thus resulting in a multigrounded neutral system. In at least one instance the neutral conductor was not solidly grounded even at the substation, it being connected to ground through lightning arresters.

The experiences of the power companies with the multigrounded neutral were generally favorable. It was found to be more reliable and to embrace some simplifications over other distribution methods. While the early multigrounded neutral arrangements were obtained by making connections to ground along the primary neutral conductor and interconnecting it, at service transformers, to well-grounded secondary neutrals, a further simplification in the arrangement was readily apparent.

It will be noted in figure 1 that this interconnection of the primary and secondary neutrals resulted in 2 grounded neutrals on the pole line in all sections where the secondary neutral existed. In extending the multigrounded neutral arrangement or in reconstructing existing portions of the network, these 2 neutrals were combined into a single well-grounded conductor continuous in all portions of a feeder area and often continuous in all parts of a substation area or of several contiguous substation areas. This arrangement, called the "common-neutral," which was first extensively applied in Minneapolis, Minn., by S. B. Hood, resulted in certain savings in equipment and relief of congested pole heads and in a neutral network most effectively grounded since all secondary neutral grounds were thus made available, in addition to any driven grounds along the pole line.

The operation of this system in Minneapolis showed many advantages in the protection of secondary networks from the effects of voltage rises under abnormal conditions. In addition, a paper presented in 1925 by Mr. Hood[1] pointed out that over a period of 3 years the rate of transformer failure was reduced to $^{6}/_{10}$ of 1 per cent per annum. This excellent performance in transformers arose undoubtedly from the fact that with the "common-neutral" or interconnected neutral arrangements the lightning arresters are connected directly around the transformers. Later studies showed that the connection of the lightning arresters directly between the primary conductors and secondary neutral provides a degree of protection which cannot readily be obtained in any other way.[2–7]

In urban areas, the multigrounded or common-neutral method of distribution introduced, in some instances, noise induction in nearby telephone circuits. In view

A paper recommended for publication by the AIEE committees on (1) communication and (2) power transmission and distribution. Manuscript submitted October 1, 1936; released for publication November 27, 1936.

J. O'R. COLEMAN is engineer of the Edison Electric Institute, New York, N. Y.; R. F. DAVIS is in the engineering department of the American Telephone and Telegraph Company, New York, N. Y.

The authors wish to acknowledge their indebtedness to their many co-workers who aided in carrying on the various investigations on which this paper is based.

1. For all numbered references see list at end of paper.

of this fact an extensive co-operative investigation was undertaken by project committee No. 6 of the Joint Subcommittee on Development and Research of the National Electric Light Association and Bell Telephone System to determine the factors involved in the co-ordination of

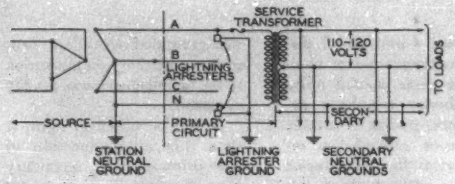

Fig. 1A. Simplified feeder operating with primary neutral grounded at source only

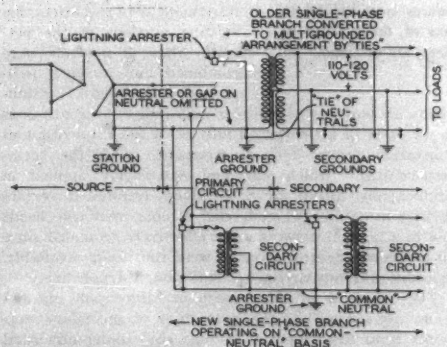

Fig. 1B. Simplified feeder operating with multiple grounds on primary neutral—older part of feeder having ties between primary and secondary and new extensions being of common-neutral arrangement

local power distribution systems and telephone systems. A study was carried out in Minneapolis during the years 1924–26 having as its primary objective the determination of the factors involved where the telephone distribution was largely in aerial cable. The investigation was continued in Elmira, N. Y., in 1926–29 to embrace the factors introduced when the exchange telephone plant was of open-wire construction.[8] Supplementing these detailed technical studies, an investigation of certain economic features of various arrangements of power and telephone distributing methods and of their practical application under varying conditions was carried out in California in 1928–29. As a result of these investigations the various factors involved in the co-ordination of multigrounded or common-neutral power systems and telephone distribution systems were determined and certain practices developed for the co-ordination of these systems under various conditions in urban areas.[9]

The purpose of this paper is that of briefly outlining a few of the more important features of power and telephone circuits affecting noise co-ordination. Following such a review there is presented a list of measures which

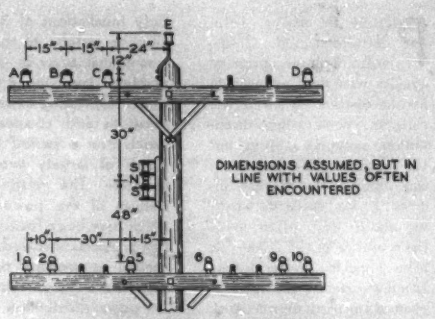

Fig. 2. Effect of relative positions on joint-use pole of power and telephone conductors on coefficients of induction for voltages and currents

Direct Metallic Circuit Induction In Untransposed Telephone Circuits

Magnetic Induction at 1,000 Cycles
Volts Metallic per Ampere of Power-Circuit Current per 1,000 Feet of Exposure

Type of Power Circuit	Induction Component	Power Conductors*	Pair 1–2	Pair 5–6	Pair 9–10	Avg
Single phase	Residual	A & N	0.021	0.043	0.0044	0.022
		C & N	0.0044	0.018	0.0053	0.0092
		E & N	0.0002	0.023	0.0013	0.0082
2 phase wires and neutral	Residual	A, C, & N	0.013	0.031	0.005	0.016
		A, D, & N	0.008	0.018	0.009	0.012
3 phase	Residual	A, B, C, & N	0.019	0.033	0.005	0.017
		A, C, D, & N	0.007	0.01	0.004	0.007
2 phase wires and neutral	Balanced	A, C, & N	0.017	0.026	0.0009	0.015
		A, D, & N	0.026	0.13	0.026	0.061
3 phase	Balanced	A, B, C, & N	0.015	0.023	0.012	0.017
		A, C, D, & N	0.023	0.123	0.026	0.057

* In each case, conductor "N" is a multigrounded neutral, the other wires being phase conductors. Assumed 50 per cent of the residual current in the neutral and 50 per cent in the ground.

Electric Induction
Volts per Kilovolt Va/Kv

Type of Power Circuit	Induction Component	Power Conductors*	Pair 1–2	Pair 5–6	Pair 9–10	Avg
Single phase	Residual	A & N	7	19	3	9.7
		C & N	2	7.3	2.3	3.9
		E & N	0.4	9	0.2	3.2
2 phase wires and neutral	Residual	A, C, & N	5	13	2.6	6.9
		A, D, & N	2	7	2	3.7
3 phase	Residual	A, B, C, & N	2.8	10	2	5.0
		A, C, D, & N	1.4	2.2	0.7	1.4
2 phase wires and neutral	Balanced	A, C, & N	3	7	0.4	3.5
		A, D, & N	6	30	5	13.7
3 phase	Balanced	A, B, C, & N	2.7	5.8	0.4	3.0
		A, C, D, & N	5.6	27	5.4	12.7

* Wires S and S assumed continuous through exposure and grounded.

extended experience has shown will, where given proper consideration by both parties, enable multigrounded or common-neutral power circuits and telephone circuits to live harmoniously. No attempt is made, however, to reiterate the extensive technical information obtained

Table I*—Average Current and Voltage Wave Shapes of 2,300/4,000-Volt 3-Phase 4-Wire Distribution Circuits

Frequency in Cycles per Second	Order of Harmonic	Phase-to-Neutral Voltage at Bus	Current in Industrial Feeder (in Amperes)				Current in Residential Feeder (in Amperes)			
			Light Load		Heavy Load		Light Load		Heavy Load	
			Phase	Residual	Phase	Residual	Phase	Residual	Phase	Residual
60		2380	85		130		53		99	
180	3	*16*	*1.1*	*2.6*	*1.1*	*2.9*	*1.3*	*5.2*	*1.9*	*6.0*
300	5	21	1.0	0.15	1.3	0.16	0.43	0.21	0.75	0.29
420	7	6.4	0.3	0.03	0.3	0.05	0.13	0.06	0.17	0.08
540	9	*1.7*	*0.04*	*0.04*	*0.04*	*0.13*	*0.04*	*0.09*	*0.04*	*0.09*
660	11	1.9	0.07	0.01	0.09	0.01	0.04	0.01	0.06	0.02
780	13	1.8	0.08	0.01	0.05	0.01	0.02	0.01	0.04	0.01
900	15	*0.42*	*0.01*	*0.01*	*0.01*	*0.03*	*0.01*	*0.01*	*0.01*	*0.01*
1,020	17	0.90	0.03	0.01	0.07	0.01	0.02	0.01	0.03	0.01
1,140	19	0.87	0.02		0.04		0.01	0.01	0.02	0.01
1,260	21	*0.16*				*0.01*			*0.01*	*0.01*
1,380	23	1.4	0.05		0.06		0.01		0.03	0.01
1,500	25	2.1	0.06	0.01	0.09	0.01	0.01	0.01	0.03	0.01
1,620	27	*0.79*		*0.01*	*0.01*	*0.02*			*0.01*	*0.01*
1,740	29	1.5	0.03		0.03	0.01	0.01		0.02	0.01
1,860	31	1.4	0.01		0.02				0.01	
TIF**		9.7	11.2		8.9		6.6		5.8	
Kv. T or I. T.		23.2	733	193	1,160	330	346	238	571	283

Note: Values for triple harmonics are in *italic* type.
* Tables 31 and 32, pages 235–6 of volume II of Engineering Reports of Joint Subcommittee on Development and Research.
** New weighting—see Engineering Report No. 33 of Joint Subcommittee on Development and Research.

from the investigations outlined above as these are adequately covered in the references cited.

Recent Trends

During the past few years there has been extensive conversion from other types of urban power distribution to the multigrounded or common-neutral system of primary distribution. Where there exists a 3-phase 3-wire delta circuit the system is converted by making the secondary neutral network continuous, reinforcing it where necessary, and making the required changes in transformer connections. Where there is a 3-phase 4-wire unigrounded primary system the conversion is, as previously mentioned, made by interconnecting the primary and the secondary neutral at each load transformer, generally removing the primary neutral only at the time of major rebuilding. In either case extensions are usually made using a single neutral in the secondary position.

In the urban areas most of the multigrounded or common-neutral systems are of the 2,300/4,000-volt class, although there are a few instances where 4,600-volt systems have been converted. At the present time there is being constructed a 6,900/12,000-volt common-neutral distribution system at Wichita, Kan.

The distinct trend in power distribution practice has been, in no small measure, influenced by the improved over-all protection features readily obtained by the multigrounded neutral arrangement as well as by certain equipment savings. The recent emphasis placed on the electrification of rural areas and the distinct need for maximum service continuity on rural power circuits have increased the interest in the use of the multigrounded or common-neutral method of distribution in rural areas. The rural systems are generally of the 7,600/13,200-volt class, although 4,600/8,000-volt circuits have been used to some extent.

The factors affecting inductive co-ordination involved in the use of the common-neutral method of distribution in rural areas, are somewhat different from those encountered in urban areas. This is largely due to the lower load densities, the greater lengths of circuits, higher operating voltages and to the somewhat different types of equipment employed in rural telephone distribution. These factors were investigated by the Joint Subcommittee on Development and Research during the summers of 1935 and 1936 and the more important considerations determined.[10]

Factors Influencing Inductive Co-ordination

In any problem of inductive co-ordination it is convenient to subdivide the factors influencing co-ordination into those relating to the inductive influence of the power circuit, the inductive susceptiveness of the telephone circuit and the inductive coupling between the 2 types of circuits. As far as urban distribution circuits are concerned the load current unbalance of the power circuit is usually the controlling influence factor. For rural distribution circuits the unbalanced charging currents are generally more important than the unbalanced load currents. Likewise, in an exchange telephone circuit the admittance and impedance unbalances of the 2 sides of the circuit are usually the controlling factors in its inductive susceptiveness. As far as coupling between the power and telephone circuits is concerned this is largely controlled by their relative positions and the lengths of the exposure. For urban areas their relative positions are largely fixed by the normal arrangement of conductors and cables on jointly used poles. In rural areas power and telephone circuits are generally at roadway separation although some joint use exists. In urban areas considerable control can often be exercised over the coupling by planning the routes of the main feeds of the 2 services so as to avoid long sections of close exposure. In rural areas

where there are no paralleling routes close together it is generally necessary for both services to use the same roads and therefore the opportunity to control the coupling by the co-operative planning of routes is much reduced. Certain quantitative indications of the extent to which this measure of co-ordination is applicable in the 2 types of areas are shown in the illustrative examples in the appendix.

Power Circuits

Power systems operate, for the most part, at frequencies of 60 cycles and below. Telephone circuits, on the other hand, depend mainly upon frequencies above about 200 cycles for the transmission of speech. Ordinarily, therefore, the effects of induction from the fundamental-frequency currents and voltages in neighboring power lines are negligible as far as telephone-circuit noise is concerned. It is quite generally recognized, however, that it is impracticable commercially to build rotating machinery and transformers which are entirely free from harmonics. There are, therefore, harmonics present on all operating power systems, and it is the harmonic-frequency components induced into telephone circuits from these power-system harmonics that are of major importance from the noise standpoint.[11]

In any distribution circuit the harmonic currents present will fall within the following classes: load currents, transformer-exciting currents, and line-charging currents. With a uni-grounded neutral the load currents and the transformer-exciting currents are practically entirely confined to the wires of the circuit. Where the neutral is multigrounded, the vector sum of the currents in the phase conductors (residual current) will divide between the neutral conductor and the paralleling earth path as determined by the relative impedances of these 2 paths. While there is some variation in the division of the return current between the neutral and ground paths, for most practical purposes this division may be assumed to be about half in each path at all the frequencies of interest.

As pointed out above, in the case of a line operating with uni-grounded neutral, the earth-return components of the load and transformer-exciting currents are ordinarily negligibly small. However, this is not true of the line-charging current which is chiefly a function of the magnitude and frequency of the impressed voltage, the circuit length, and, at nontriple harmonic frequencies, of the balance of the admittances to ground of the various phase conductors. While multigrounding the neutral ordinarily increases the earth-return components of the load and transformer-exciting currents, it has been found, due to the parallel path provided by the neutral wire, on an average to decrease slightly the amount of charging current in the earth.

In an urban distribution system where the load density is relatively high, the load currents and transformer-exciting currents are relatively large and the line-charging currents are usually negligible. In such a system multigrounding the neutral results in an increase in the current returning through the earth and a consequent increase in the inductive influence of the power distribution system.

In rural areas, however, where the load density is low and the load currents and transformer-exciting currents are relatively small, the line-charging currents become significant. In general, under such conditions the multigrounding of the neutral does not increase the magnitude of the ground-return current at frequencies of interest from the noise-induction viewpoint. Under certain conditions the magnitude of this ground-return current may actually be substantially decreased by the multigrounding of the neutral. This effect is more marked for the higher-voltage circuits.

The harmonics present in a distribution circuit may be divided into: (1) triple harmonics, that is, the third harmonic and odd multiples of it; and (2) nontriple harmonics that is, the odd harmonics, starting with and including the fifth, which are not multiples of 3. The triple harmonics in a 3-phase system are in phase in the 3 line conductors so that their residual value (vector sum) is the arithmetic sum of their magnitudes in the 3 phase wires. The nontriple harmonics are spaced, in time phase, the same as the 60-cycle fundamental, and the magnitude of the residual current (vector sum) for these harmonics is usually much less than their arithmetic sum. If these harmonics were perfectly balanced the residual current for these frequencies would be zero. In exposures involving 3-phase sections of line the balance of the nontriple harmonics between phases is influenced by the degree of balance of the loads and single-phase branches, and therefore has an important effect in reducing the over-all influence of the power system. In exposures involving single-phase extensions, or extensions consisting only of 2 phase wires and a neutral wire, this advantage of the balancing of the nontriple harmonics is, of course, not obtainable.

The extent to which induction from the nontriple harmonic voltages and currents in power-distribution circuits can be controlled by power-circuit transpositions is ordinarily very limited. Usually, due to the large number of exposure discontinuities arising from changes in the power or telephone circuits, the power-circuit transpositions are quite ineffective. This is particularly true in cases where the induction from the ground-return current is controlling. In specific cases where considerable wave-shape distortion exists and the induction from the balanced voltages and currents may therefore be relatively im-

Table II*—Relative Importance of Circuit Unbalances

	500 Cycles			1,000 Cycles		
	Contribution From:			Contribution From:		
Type of Service	Station	Cable	Office	Station	Cable	Office
Individual (bridged ringers)	Negligible	3	3	Negligible	20	20
Party-line (grounded 8-*A* ringers)	100	3	3	100	20	20

*See page 72 of volume I of Engineering Reports of Joint Sub-Committee on Development and Research.

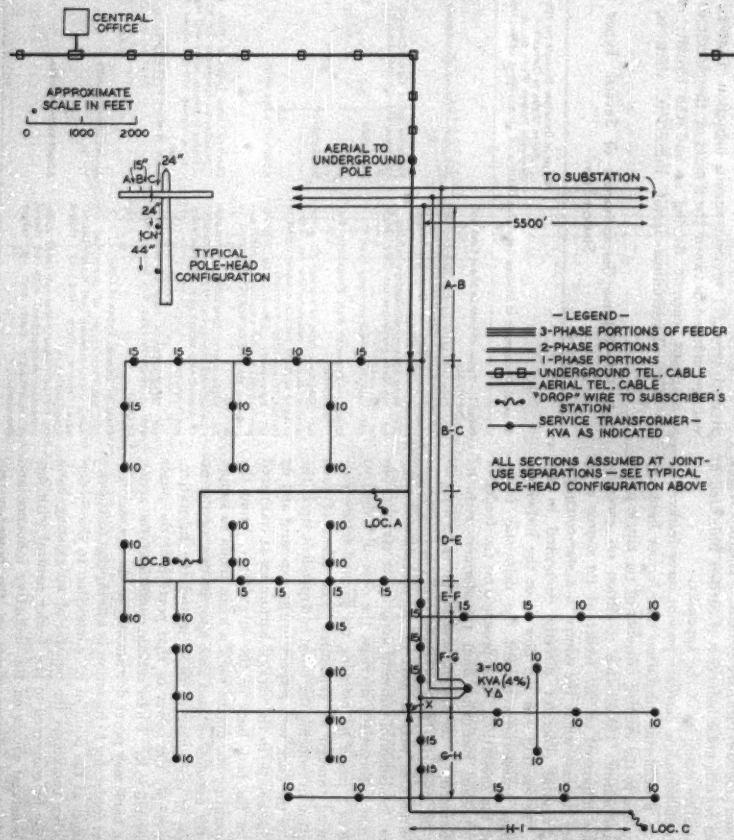

Fig. 3. Example of possible arrangement of feeder layout in an urban area where long aerial telephone cable is exposed to a heavily loaded single-phase feeder

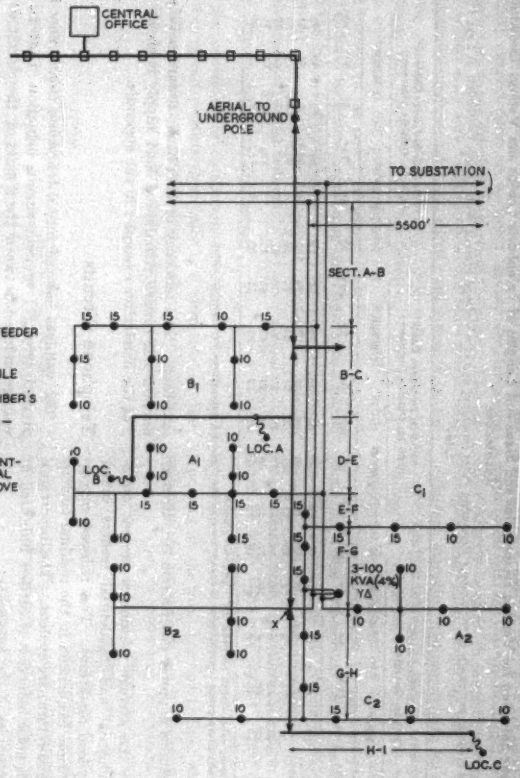

Fig. 4. Example of possible rearrangement of feeder layout shown in figure 3 to reduce magnitudes of "ground-return" currents

Table III—Magnetic Shielding for Various Frequencies and Sizes and Lengths of Telephone Cables and Various Grounding Resistances

Calculated Values of e_r/e_i (in per cent); e_r = Voltage Remaining After Shielding and e_i = Voltage Present With Sheath Grounded at One Point Only

Frequency in Cycles per Second	Full-Sized Cable (2.61 In. Outside Diameter)						101-Pair 24-Gauge Cable (0.85 In. Outside Diameter)						54-Pair 24-Gauge Cable (0.64 In. Outside Diameter)					
	1 Mile*			3 Miles*			1/3 Mile*			1 Mile*			1/3 Mile*			1 Mile*		
	0**	5**	10**	0**	5**	10**	0**	5**	10**	0**	5**	10**	0**	5**	10**	0**	5**	10**
180	14	82	94	14	50	71	60	95	99	60	89	95	71	96	99	71	92	96
300	8.5	65	85	8.5	33	52	42	89	96	42	77	89	57	91	96.5	57	82	91
420	6	52	76	6	24	40	31.5	81	93	31.5	65	81	44.5	84	93.5	44.5	71	84
540	5	43.5	71	5	19	32	25	73	88	25	55.5	73	37	77	90	37	63	77
660	4	37	64	4	16	27	21	66	84	21	47.5	66	31	71	86	31	55	71
1000	3	25.5	44.5	3	11	18	15	51	72	15	35	51	22	56	74.5	22	41	56

* Refers to distances along cable sheath between the 2 grounding points.
** Refers to total grounding impedance (approximate d-c resistance) of the 2 ground connections, expressed in ohms.

portant, transpositions in power-distribution circuits may be found helpful.

Table I shows the average harmonics present on 3-phase 4-wire industrial and residential feeders under light- and heavy-load conditions. The reduced magnitudes of the nontriple frequencies in the residual current (neutral and ground-return) are evident. The importance of this as regards noise induction is further indicated in the illustrative examples of the appendix.

The triple-harmonic currents present on a feeder supplied from a delta-star substation transformer bank are generally due to the exciting currents of the single-phase load transformers. Under this condition no excessive triples are impressed on the feeder at its source as is sometimes the case where the source is a star-connected grounded-neutral generator directly connected to the feeder. The exciting currents flow from the individual single-phase transformers toward the delta-star transformer in the substation. The presence on the feeder of a large 3-phase star-delta load transformer with its neutral connected to the system neutral, provides a parallel path for supplying part of these triple-harmonic exciting currents as well as part of the unbalanced nontriple and fundamental currents and, under certain conditions, may substantially decrease the over-all inductive influence of a feeder by reducing the ground-return current flowing through an exposure. The effect of such a connection in reducing the noise is dependent upon the location of the bank with respect to the exposure and its relative impedance to the various harmonics as compared to that of the path back to the substation. From the power operating standpoint such a bank tends to supply part of the unbalanced load and also, in case of the interruption of one phase between it and the substation, tends to supply the power to that portion of the phase still connected to it. Under certain conditions, the action of such a bank may prove detrimental to the operation of the power feeder due to its action in attempting to balance the voltages at the point of its connection to the feeder. Under other conditions the neutral of an existing bank can readily be connected to the feeder neutral with distinctly beneficial effects on the inductive influence and with little or no adverse effects on the power-system operation. The tendency of such banks toward noise reduction and toward unbalanced load supply is shown in 2 of the illustrative examples in the appendix.

Telephone Circuits

The voltages induced into a telephone circuit may be divided into: (1) metallic-circuit induction, that is, a voltage induced between the 2 sides of the circuit with a resultant current flowing around the circuit; and (2) the longitudinal-circuit induction, that is, a

Table IV—Relative Susceptiveness of Several Types of Station Sets

General Description of Station Set	Noise in Receiver Branch for 100 Noise Units to Ground—Average Power Wave Shape (One Station on Line—Effect of Set Only)
Class 1—Types of Sets in Most Common Use Today	
(a) Side-tone type of party-line set using 8A ringers or equivalents (one end of ringer grounded). (Common-battery talking and signaling)	350 noise units, approximately
(b) Same type—local-battery talking	120 noise units, approximately
(c) Magneto party-line set (52A ringer or equivalent)	120 noise units, approximately
(d) Individual-line set—any type	Negligible
Class 2—Types of Sets Frequently Encountered	
(a) Side-tone type of 4-party full-selective or 8-party semiselective set (using relay or cathode tube to connect ringer to circuit during ringing period)	Negligible
(b) Four-party selective or 8-party semiselective sets employing high impedance ringers or relays connected to ground	About 30 noise units
(c) Eight-party selective (harmonic ringing) sets employing ringers connected to ground and tuned to 4 different ringing frequencies	Limited data indicate that, depending on frequency for which ringer is tuned, noise will range from about 100 to about 400 units
(d) Ground-return rural circuits (usually of magneto type and having code ringing)	3,500 or more noise units
Class 3—Special Types of Sets	
(a) Side-tone type of party-line set using split-condenser and higher-impedance ringer (one end of ringer grounded)	About 20 noise units
(b) Type of party-line set using split-condenser arrangement with 8A ringer or equivalents (one end of ringer grounded)	About 90 noise units

voltage induced along the conductors such that the resultant current flows in a circuit having the telephone conductors as one side and the earth as the other. This latter voltage may also result in noise, due to its action upon telephone-circuit unbalances, setting up currents in the voice channel (metallic circuit). For either type of voltage, the induction may be "electric," that is, from the voltage on the power circuit, or "magnetic" from the current in the power circuit.

The local telephone circuit may be divided into 3 parts: (*a*) the central-office equipment, (*b*) the line conductors, and (*c*) the subscriber equipment. Interoffice circuits include only the first 2 items.

(*a*) Central-Office Equipment

The central-office equipment associated with a subscriber circuit consists essentially of 2 elements: (1) line signaling equipment connected to the circuit for indicating to the operator, or to the dial equipment, the desire of a subscriber to start a call; and (2) a linking or switching circuit or circuits for interconnecting 2 subscriber circuits either directly or through intervening trunk circuits and providing supervision during the call.

The line signaling equipment with its associated relay is either bridged across the line or arranged so that when 2 subscriber circuits are interconnected, any ground connections on the line relays are automatically opened. The line signaling equipment is not, therefore, ordinarily a factor in noise considerations. Occasionally, however, the effect on noise of the ground connection on the line signaling equipment requires specific treatment when the longitudinal-circuit induction is sufficiently high. The noise in such instances occurs either during the preanswering period before the line relay is "cut-off" or, in certain types of switchboards, on conversations between 2 persons on the same line (party-line) where the use of a switching circuit in the office is unnecessary.

The linking or switching equipment in the central office may consist of a pair of wires with bridged supervisory relays, as in the case of a magneto office, or may be a complicated arrangement of relays, repeating coils, condensers, etc., as in the case of common-battery offices of the manual or dial type. The necessary ground connections of the latter type of apparatus introduce the possibility of the unbalances in the equipment contributing to the over-all noise when the longitudinal-circuit induction on the outside conductors is impressed on the switching circuits. Ordinarily in urban areas, due either to the frequency make-up of the longitudinal-circuit induction or to the relationships of the various impedances-to-ground, the amount of noise contributed by the central-office equipment is relatively low. This is readily evident from table II which shows, at 500 and 1,000 cycles, the relative proportions of over-all noise due to the action of induced voltages on station, cable, and central-office unbalances. Cases arise, however, quite frequently where the relative circuit impedances or the frequency

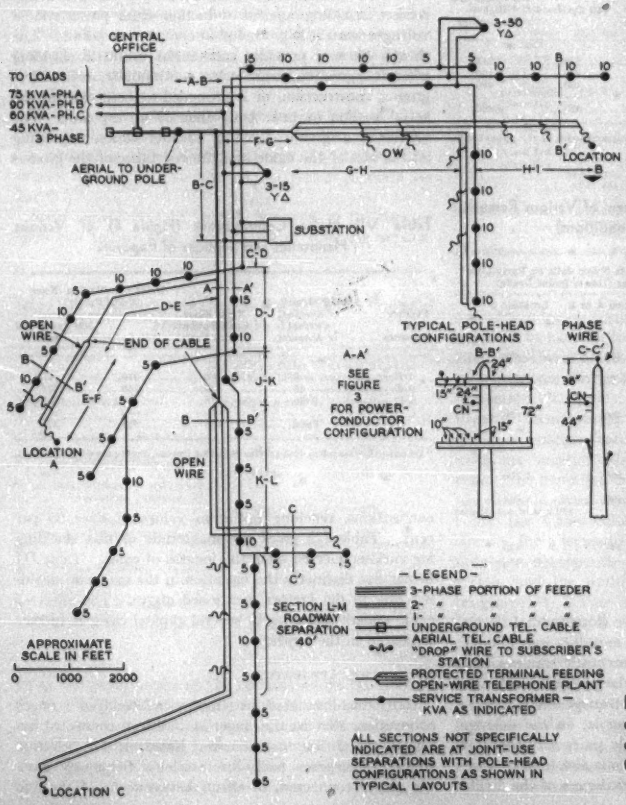

Fig. 5. Example of exposure conditions between 2,300–4,000-volt distribution feeder and exchange telephone plant in suburban and rural area

make-up of the induction or both are such that the noise contribution from the unbalances in the central-office equipment becomes important. Such cases usually involve long subscriber or interoffice trunk circuits and particularly where sections of open-wire construction are present. Values of the unbalances in certain types of central-office equipment are given on page 91 of volume I of the Engineering Reports of the Joint Subcommittee on Development and Research.

(*b*) Line Conductors

Where the telephone line conductors are in open wire, the induced voltage between conductors (metallic-circuit)

Table V—Noise Contributions (Figure 3) of Various Harmonics and Sections of Exposure

Section of Exposure	RMS Magnitude of Residual Current in Amperes	Approximate Total Noise Contribution* (Noise Units)	Approximate Noise Contribution (Noise Units) From: 180 Cycles	300 Cycles and Higher Frequencies
A-B	210	1,240	270	1,215
B-E	157	1,130	250	1,100
E-I	30–107	500	100	490
	Total	2,870	620	2,800

* Location *C*—For party-line service using 8A ringers, during heavy power loads.

Table VI—Comparison of Effectiveness of Various Remedial Measures (Figure 3 Conditions)

Type of Remedial Measure	Approximate Noise Units on Party-Line Stations (Heavy Power Loads) Location A or B	Location C
1. Before applying remedial measures	1,800	2,870
2. Using special telephone station sets	75	125
3. Avoiding exposure in section *A-B* by co-operative planning of routes	560	1,630
4. Cable-sheath shielding by tying aerial and underground telephone cables at junction pole and connecting aerial sheath to 1-ohm ground at point *X*	1,160	1,700
5. Interconnecting 300-kva star-delta bank with system neutral	1,430	1,800
		170 kva of unbalanced load
6. Combination of measures 3, 4, and 5	365	420

as well as along these conductors (longitudinal-circuit) must be considered. The direct metallic-circuit induction can be greatly reduced by systematic transpositions in the telephone circuit. Due to the physical limitations in a practical layout of telephone transpositions, the reduction in metallic-circuit induction is, on the average, from 60 to 80 per cent on nonpole pairs and about 90 per cent on pole pairs. Transpositions also tend to lessen the capacitance and inductance unbalances of the 2 sides to ground and to other circuits, thereby reducing the effect of the longitudinal-circuit induction on such unbalances. The improved balance of the mutual impedances between the various telephone conductors is, of course, distinctly beneficial in reducing cross talk, and transpositions are generally used for limiting the cross talk where open-wire telephone circuits extend for substantial distances.

The construction of telephone cables is such that there is inherently very close spacing between the conductors, and they are frequently transposed due to the continuous twisting of the pairs in manufacture. Due to this close spacing and frequent transposing there is practically no voltage induced between the wires of a cable pair or quad (group of 4 conductors). The unbalance to ground of the conductors of the present type of cable is so small that it is not ordinarily a contributing factor to noise induction. It may be noted, however, from table II that in cases where the central-office unbalances are of importance, the effect of shunt or series unbalances in the cables also needs consideration.

The lead sheath of a telephone cable provides practically perfect shielding against induction from power-system voltages when it is grounded at one or more points. The sheath likewise provides substantial magnetic shielding when it is grounded more or less continuously, as in underground construction, or is grounded at both ends of the aerial section or near both ends of an exposure. The degree of magnetic shielding effected varies, depending on the size of the cable and the resistance of the ground

Table VII—Noise Contributions (Figure 4) of Various Harmonics and Sections of Exposure

Section of Exposure	RMS Magnitude of Residual Current in Amperes	Total Noise Contribution* (Noise Units)	Noise Contribution (Noise Units) From: 180 Cycles	300 Cycles and Higher
A-B	6	280	270	75
B-E	45	370	250	275
E-I	5–45	150	100	115
	Total	735	620	375

* Location *C*—for party-line service using 8A ringers, during heavy power loads.

connections, reaching optimum values of over 90 per cent. Table III gives the magnitude of this shielding for various selected sizes and lengths of cable. Table III brings out distinctly the variation in the magnetic shielding due to the factors mentioned above. The effect of cable sheath shielding in several typical cases is further indicated in the appendix.

(*c*) Station Apparatus

Individual-line stations employ a "bridged" ringer connection, that is, the ringer is, in effect, connected between the 2 line conductors. However, for selective signaling purposes party-line stations, frequently have the ringer connected, in effect, between one of the line

conductors and ground. The unbalance of the party-line station equipment is therefore affected by the impedance of the ringer and its point of connection in the station equipment. The relative susceptiveness of several types of station sets to noise-frequency induction is shown in table IV.

Table IV shows that, with advance planning in areas where noise induction is or may likely become a matter of importance, much can be accomplished by the use of station sets of decreased inductive susceptiveness. Where such types of apparatus are substituted in existing plant, except in gradual replacements or in connection with general rearrangement programs, the expense is, naturally, increased.

Inductive Coupling

As stated above, the inductive coupling between exchange telephone plant and power-distribution circuits in urban areas is largely controlled by such factors as the street layouts and the joint use of poles. However, by co-operative planning of routes it is frequently practicable to secure lower coupling by avoiding long exposures between the main feeds of the 2 plants. As shown by the illustrative examples this procedure is, where applicable, very beneficial.

In rural areas where both distribution services must ordinarily be carried along the highways the opportunity for controlling the coupling between the 2 classes of circuits by co-operative planning of routes is much reduced.

Some benefit may be gained, however, in the case of open-wire construction, particularly at joint-use separations, by arangements of the conductors on the pole so as to avoid excessive spacings. As shown on figure 2, certain arrangements tend to minimize the amount of noise induction arising from the power-circuit voltages and currents. This beneficial effect is, however, much less noticeable at roadway separations.

Table VIII—Comparison of Effectiveness of Various Remedial Measures (Figure 4)

Type of Remedial Measure	Approximate Noise Units on Party-Line Stations (Heavy Power Loads)	
	Location A or B	Location C
1. Before applying remedial measures	480	735
2. Using special telephone station sets	25–30	40–50
3. Avoiding exposure in section a-b by co-operative planning of routes	190	460
4. Interconnecting 300-kva star-delta bank with system neutral	330	535
		26 kva of unbalanced load
5. Cable-sheath shielding—grounding at junction pole and to 1-ohm ground at *X*	325	420
6. Combinations of measure 3, 4, and 5	85	245

Summary and Conclusions

Since about 1915 there has been a continued increase in the use of the multigrounded or common-neutral arrangement of power distribution in this country. At the present time, approximately half of the distribution is by 4,000-volt multigrounded or common-neutral circuits. A large part of the higher-voltage rural distribution is also operating with this arrangement.

In general it may be said that for the lower-voltage 2,300/4,000-volt distribution circuits, the use of the multigrounded or common-neutral arrangement may be expected to increase the inductive influence of the power circuits. Unless attention is given to co-operative planning to secure features beneficial from the inductive-co-ordination standpoint, noise problems may result either in restricted or extensive areas. With proper attention to the co-ordination features[9] such noise situations as develop are largely in the nature of isolated cases and can usually be cared for by relatively minor changes or adjustments in either or both plants.

For the higher-voltage (11–13 kv) rural distribution circuits, there seems to be little difference, from the noise-induction standpoint, between the uni-grounded 4-wire system and the multigrounded or common-neutral arrangement.[10] Under many conditions the placing of multiple grounds on the neutral will result in noise reductions due to the effect, previously mentioned, of the multigrounded neutral on the line-charging currents. It is interesting to note that experience to date with the multigrounded or common-neutral circuit in rural areas has shown that many of the measures of co-ordination applicable in urban areas will prove similarly helpful in rural communities.

The measures of co-ordination which investigations

Table IX—Noise at Various Locations (Figure 5) and for Various Types of Telephone Service

Location	Type of Telephone Service	Total Noise Units	Contribution (Noise Units) From: Cable Exposures	Contribution (Noise Units) From: Open-Wire Exposures	Remarks
A	1. Common-battery party-line stations (class 1-c table IV)	225–345	220–270	45–215	Open-wire noise dependant on effectiveness of telephone transpositions
	2. Magento party-lines (class 1-c table IV)	85–225	75 app.	40–215	
	3. Individual line (class 1-d table IV)	40–210	25–35	About 10–210	Lower values of noise on circuits controlled by effects of station sets — higher values by effectiveness of telephone transpositions
B	1	170–1,300	10–100	170–1,190	
	2	75–1,175	20– 35	70–1,175	
	3	60–1,175	About 20	55–1,175	
C	1	400–975	285–325	275–925	Noise in cable section due to office and cable unbalances
	2	150–870	110–125	110–860	
	3	100–860	60	75–860	

and operating experiences have shown to be practicable and effective include:

1. Co-operative planning by both parties to avoid not only severe exposure conditions but also types of equipment likely to aggravate the possible noise-induction situation.

2. A reasonable degree of balance of the loads between the 3 phases of the power circuit. In the higher-voltage rural circuits this also includes the lengths of branches consisting of 1 or 2 phase wires and neutral.

3. The avoidance of unnecessarily heavily loaded branches consisting of 1 or 2 phase wires and neutral.

4. The prevention of excessive overexcitation of transformers.

5. The grounding, where necessary, of aerial telephone cables at or near both ends of an exposure to obtain the benefits of magnetic shielding.

6. The use of adequately co-ordinated telephone transpositions on open-wire extensions and the avoidance of severe unbalances in the open-wire conductors.

7. The correction of badly distorted voltage or current wave shape on the power system.

8. The connection of the neutral point of 3-phase star-delta load banks to the system neutral conductor.

9. The use of telephone station apparatus, on party-line service, of lower susceptiveness.

10. Occasionally the use of arrangements or apparatus to minimize the effects from unbalances in central office equipment.

It is, of course, essential in successfully co-ordinating the power distribution and telephone circuits that, as in other co-ordination situations, the power and telephone people view the matter as a mutual responsibilty and fully co-operate in the application of the tools available. Experience over a period of years has now shown that where this is done adequate over-all co-ordination can be readily secured.[13]

Appendix

For the sake of brevity, the detailed calculations and some of the minor assumptions for the following examples have been omitted.

Illustrative Example 1

The purpose of this example is to show, for average power-system wave shapes:

1. The noise-induction problem that might be created by the exposure of a reasonably long aerial telephone cable in an urban area with a heavily loaded single-phase feeder. It features:
(*a*) The relative importance of triple and nontriple harmonic induction, and
(*b*) The extent to which planning of routes, grounding of cable sheaths, etc., might improve the situation.

2. The change in the noise magnitudes for the same situation with the various single-phase loads well distributed among all 3 phases. Under this condition, attention is directed to:
(*a*) The change in the relative importance of the triple and nontriple harmonic induction.
(*b*) The amount of reduction obtained by the same remedial measures tried in 1-*b* above.

Figure 3 shows a possible method of supplying the single-phase loads in a rather extensive part of an urban area. The general layout shown in figure 3 is such that all of the current for the feeder area traverses a considerable part of the exposure. Under this quite extreme condition—essentially single-phase supply for a relatively large area—the noise at location *C* under heavy-load conditions would be about as shown in table V.

Table X—Comparison of Effectiveness of Various Remedial Measures

Type of Remedial Measure	Approximate Noise Units at: Location A 1*	2	3	Location B 1	2	3	Location C 1	2	3
1. Before applying measures	225–345	85–225	40–210	170–1,200	75–1,175	60–1,175	400–975	150–870	100–860
2. Using special telephone sets	40–210	40–210	Neg. change	60–1,175	60–1,175	Neg. change	100–880	100–860	Neg. change
3. Avoiding exposure section *B-C* by co-operating planning	130–250	65–220	Neg. change	Neg. change			350–950	115–860	Neg. change
4. Interconnecting neutral of 150-kva star-delta bank	180–310	Neg. change		150–1,175	Neg. change		370–950	Neg. change	
5. Average degree of co-ordinated telephone transpositions	250	80	50	200	175	175	340	175	130
6. Telephone transpositions + cable - sheath shielding**	210	70	50	180	175	175	320	165	130
7. Combination of 4, 5, and 6	185	65	50	160	155	155	310	160	125

* Type of station apparatus shown on table IX.
** Cable was assumed to be grounded at junction pole at end of section *F-G* to 2.5-ohm ground; at other junction poles to grounds exceeding 10 ohms.

It is evident from table V that most of the party-line stations fed by the aerial telephone cable would need treatment. It will be noted from table VI that completely replacing the existing party-line stations with special station apparatus will, to a large extent, care for the situation since, in this case, the amount of noise contributed by the cable and central-office unbalances would aggregate less than 150 units. Other measures either singly or in combination, probably more economical in their application, would provide substantial reductions in noise, but would not be adequate for the more severely exposed stations.

Assume, however, that instead of supplying the single-phase loads in the area shown on figure 3 from one phase only, the single-phase loads were distributed reasonably uniformly among the phases. This would be advantageous not only by the noise-reduction possibilities, which will be more fully discussed, but also by the improved regulation attainable on the feeder. Figure 4 shows a possible rearrangement of figure 3 along these lines and table VII shows the noise conditions with the feeder arrangements of figure 4.

A comparison of tables V and VII shows that the noise from the nontriple harmonics has been very materially reduced by the balancing of loads made possible by the more favorable feeder arrangement of figure 4, although that from the triple harmonics has been inappreciably changed. The net effect has been a reduction of nearly 75 per cent in the noise on the party-line stations served by the telephone cable. The reductions afforded by various remedial measures are shown in table VIII.

It is evident from table VIII that, by the application of various of the measures of co-ordination, the need for an extensive rearrangement of either plant is avoided.

Illustrative Example 2

The purpose of this example is to show the extent to which remedial measures of the type generally applicable in urban areas (see example 1) may be applied in a less thickly settled area where exposures to 2.3/4-kv multigrounded-neutral arrangements are encountered under average conditions of power-system wave shape. In detail the example covers:
(*a*) The extent to which such measures as co-operative planning of routes and use of star-delta load banks may be ineffective.
(*b*) The importance, particularly under joint-use conditions, of noise directly induced into the metallic circuit of open-wire tele-

(*Concluded on page 189*)

Two-Reaction Theory of Synchronous Machines

By S. B. CRARY
ASSOCIATE AIEE

An extension of the 2-reaction theory of synchronous machines as developed by R. H. Park is given in this paper for machines having capacitance in the armature circuit. General equations for predetermination of the performance under certain abnormal conditions of machines having balanced 3-phase capacitance in the armature circuit are presented.

THIS PAPER is an extension of the method of analysis by R. H. Park[1,2,3] in that the effect of armature circuit capacitance is included in the general equations for the performance of a salient-pole synchronous machine. These equations are of sufficient generality so that the operation of a synchronous or induction machine having balanced 3-phase capacitance in the armature circuit can be predetermined for the condition of 3-phase short circuit, sudden application of capacitance load, self-excitation, running out of synchronism, hunting, pulling into step, etc. The method of approach is such that the general impedance operators which have been utilized by recent writers[5-10] can also be used in studying the effect of capacitance in the armature circuit. Such impedance operators include the effect of additional rotor circuits. It is believed that a theoretical basis for the study of the performance of synchronous or induction machines as influenced by capacitance is particularly important at this time, with the increased use of series and shunt capacitors for voltage regulation purposes.

An interesting application of the general equations is to the problem of self-excitation of a machine connected to a circuit containing capacitance. Criteria are developed which indicate the regions in which self-excitation may occur for the case of a synchronous machine connected to a capacitance load or through series capacitance to a system.

List of Symbols

All constants are in per-unit values in terms of normal kilovolt-amperes and voltage, and correspond wherever possible with established nomenclature.

$x_c = 1/c$ = capacitance reactance
x_d = synchronous reactance of direct-axis armature circuit
x_d' = direct-axis transient reactance
x_d'' = direct-axis subtransient reactance
$x_d(p)$ = impedance operator relating the direct-axis armature flux linkages with the direct-axis armature current
x_q = synchronous reactance of quadrature-axis armature circuit
x_q' = quadrature-axis transient reactance
x_q'' = quadrature-axis subtransient reactance
$x_q(p)$ = impedance operator relating the quadrature-axis armature flux linkages with the quadrature-axis armature current
$G_d(p)$ = operator relating the direct-axis armature linkages with the direct-axis field excitation voltage
$G_q(p)$ = operator relating the quadrature-axis armature flux linkages with the quadrature-axis field excitation voltage
r = armature circuit resistance
e = system voltage
E_{fd} = direct-axis field-excitation voltage
E_{fq} = quadrature-axis field-excitation voltage
e_d = direct-axis armature voltage
e_q = quadrature-axis armature voltage
e_0 = zero-sequence armature voltage
ψ_d = direct-axis armature flux linkages
ψ_q = quadrature-axis armature flux linkages
ψ_0 = zero-sequence armature flux linkages
i_d = direct-axis armature current
i_q = quadrature-axis armature current
i_0 = zero-sequence current
e_a, e_b, e_c = phase voltages
i_a, i_b, i_c = phase currents
ψ_a, ψ_b, ψ_c = phase flux linkages
T_o' = open-circuit field time constant in electrical radians
p = d/dt
s = slip
t = time in electrical radians; unit time is the time required for the rotor to pass one electrical radian at normal frequency
δ = angular displacement in electrical radians
1 = Heaviside's unit function

General Analysis

This analysis is based on the definition of an ideal synchronous machine as given in reference 1. A knowledge of the material in references 1 and 2 by R. H. Park is assumed in the following development.

Park gives the following relations:

$$\left.\begin{aligned} i_d &= \tfrac{2}{3}[i_a\cos\theta + i_b\cos(\theta-120) + i_c(\cos\theta+120)] \\ i_q &= -\tfrac{2}{3}[i_a\sin\theta + i_b\sin(\theta-120) + i_c(\sin\theta+120)] \end{aligned}\right\} \quad (1)$$

$$\left.\begin{aligned} e_d &= \tfrac{2}{3}[e_a\cos\theta + e_b\cos(\theta-120) + e_c\cos(\theta+120)] \\ e_q &= -\tfrac{2}{3}[e_a\sin\theta + e_b\sin(\theta-120) + e_c\sin(\theta+120)] \end{aligned}\right\} \quad (2)$$

$$\left.\begin{aligned} \psi_d &= \tfrac{2}{3}[\psi_a\cos\theta + \psi_b\cos(\theta-120) + \psi_c\cos(\theta+120)] \\ \psi_q &= -\tfrac{2}{3}[\psi_a\sin\theta + \psi_b\sin(\theta-120) + \psi_c\sin(\theta+120)] \end{aligned}\right\} \quad (3)$$

$$\left.\begin{aligned} e_a &= p\psi_a - ri_a \\ e_b &= p\psi_b - ri_b \\ e_c &= p\psi_c - ri_c \end{aligned}\right\} \quad (4)$$

A paper recommended for publication by the AIEE committee on electrical machinery. Manuscript submitted October 16, 1936; released for publication November 6, 1936.

S. B. CRARY is in the engineering division of the central-station department, Electric Company, Schenectady, N. Y.

1. For all numbered references see list at end of paper.

and

$$\left.\begin{aligned}\psi_d &= G_d(p)\,E_{fd} - x_d(p)\,i_d\\ \psi_q &= G_q(p)\,E_{fq} - x_q(p)\,i_q\end{aligned}\right\} \quad (5)$$

If the effect of armature circuit capacitance is to be included, equations 4 become

$$\left.\begin{aligned}e_a &= p\,\psi_a - \left(r + \frac{x_c}{p}\right) i_a\\ e_b &= p\,\psi_b - \left(r + \frac{x_c}{p}\right) i_b\\ e_c &= p\,\psi_c - \left(r + \frac{x_c}{p}\right) i_c\end{aligned}\right\} \quad (6)$$

or

$$\left.\begin{aligned}pe_a &= p^2\,\psi_a - (p\,r + x_c)\,i_a\\ pe_b &= p^2\,\psi_b - (p\,r + x_c)\,i_b\\ pe_c &= p^2\,\psi_c - (p\,r + x_c)\,i_c\end{aligned}\right\} \quad (7)$$

Differentiating equations 2,

$$\left.\begin{aligned}pe_d &= \frac{2}{3}\left[\cos\theta\, pe_a + \cos(\theta-120)\, pe_b + \cos(\theta+120)\, pe_c\right] -\\ &\quad \frac{2}{3}\left[e_a \sin\theta + e_b \sin(\theta-120) + e_c \sin(\theta+120)\right] p\theta\\ pe_q &= -\frac{2}{3}\left[\sin\theta\, pe_a + \sin(\theta-120)\, pe_b + \sin(\theta+120)\, pe_c\right] -\\ &\quad \frac{2}{3}\left[e_a \cos\theta + e_b \cos(\theta-120) + e_c \cos(\theta+120)\right] p\theta\end{aligned}\right\} \quad (8)$$

Using equations 2 and 7, equations 8 become

$$\left.\begin{aligned}pe_d - e_q p\theta &= \frac{2}{3}\left[\cos\theta\, p^2\psi_a + \cos(\theta-120)\, p^2\psi_b + \cos(\theta+120)\, p^2\psi_c\right] -\\ &\quad \frac{2}{3} r\left[\cos\theta\, pi_a + \cos(\theta-120)\, pi_b + \cos(\theta+120)\, pi_c\right] -\\ &\quad \frac{2}{3} x_c\left[\cos\theta\, i_a + \cos(\theta-120) i_b + \cos(\theta+120) i_c\right]\\ pe_q + e_d p\theta &= -\frac{2}{3}\left[\sin\theta\, p^2\psi_a + \sin(\theta-120)\, p^2\psi_b + \sin(\theta+120)\, p^2\psi_c\right] +\\ &\quad \frac{2}{3} r\left[\sin\theta\, pi_a + \sin(\theta-120)\, pi_b + \sin(\theta+120)\, pi_c\right] +\\ &\quad \frac{2}{3} x_c\left[\sin\theta i_a + \sin(\theta-120) i_b + \sin(\theta+120) i_c\right]\end{aligned}\right\} \quad (9)$$

In order to express equations 9 in terms of direct- and quadrature-axis quantities rather than phase quantities, the following relations will be used. Differentiating equations 3,

$$\left.\begin{aligned}p\psi_d &= \frac{2}{3}\left[\cos\theta\, p\psi_a + \cos(\theta-120)\, p\psi_b + \cos(\theta+120)\, p\psi_c\right] + \psi_q p\theta\\ p\psi_q &= -\frac{2}{3}\left[\sin\theta\, p\psi_a + \sin(\theta-120)\, p\psi_b + \sin(\theta+120)\, p\psi_c\right] - \psi_d p\theta\end{aligned}\right\} \quad (10)$$

Differentiating equations 10,

$$\begin{aligned}p^2\psi_d &= \frac{2}{3}\left[\cos\theta\, p^2\psi_a + \cos(\theta-120)\, p^2\psi_b + \cos(\theta+120)\, p^2\psi_c\right] -\\ &\quad \frac{2}{3}\left[\sin\theta\, p\psi_a + \sin(\theta-120)\, p\psi_b + \sin(\theta+120)\, p\psi_c\right] p\theta +\\ &\quad p\theta\, p\psi_q + \psi_q p^2\theta \qquad (11a)\end{aligned}$$

$$\begin{aligned}p^2\psi_q &= -\frac{2}{3}\left[\sin\theta\, p^2\psi_a + \sin(\theta-120)\, p^2\psi_b + \sin(\theta+120)\, p^2\psi_c\right] -\\ &\quad \frac{2}{3}\left[\cos\theta\, p\psi_a + \cos(\theta-120)\, p\psi_b + \cos(\theta+120)\, p\psi_c\right] p\theta -\\ &\quad p\theta\, p\psi_d - \psi_d p^2\theta \qquad (11b)\end{aligned}$$

Substituting equations 10 in equations 11,

$$\left.\begin{aligned}&\frac{2}{3}\left[\cos\theta\, p^2\psi_a + \cos(\theta-120)\, p^2\psi_b + \cos(\theta+120)\, p^2\psi_c\right] =\\ &p^2\psi_d - 2p\theta\, p\psi_q - \psi_d(p\theta)^2 - \psi_q p^2\theta -\\ &\frac{2}{3}\left[\sin\theta\, p^2\psi_a + \sin(\theta-120)\, p^2\psi_b + \sin(\theta+120)\, p^2\psi_c\right] =\\ &p^2\psi_q + 2p\theta\, p\psi_d - \psi_q(p\theta)^2 + \psi_d p^2\theta\end{aligned}\right\} \quad (12)$$

Differentiating equations 1,

$$\left.\begin{aligned}&\frac{2}{3}\left[\cos\theta\, pi_a + \cos(\theta-120)\, pi_b + \cos(\theta+120)\, pi_c\right] = pi_d - i_q p\theta -\\ &\frac{2}{3}\left[\sin\theta\, pi_a + \sin(\theta-120)\, pi_b + \sin(\theta+120)\, pi_c\right] = pi_q + i_d p\theta\end{aligned}\right\} \quad (13)$$

Substituting equations 1, 12, and 13 in equations 9 and simplifying,

$$p(e_d - p\psi_d + ri_d + \psi_q p\theta) + x_c i_d = p\theta(e_q - p\psi_q + ri_q - \psi_d p\theta) \qquad (14)$$

$$p(e_q - p\psi_q + ri_q - \psi_d p\theta) + x_c i_q = -p\theta(e_d - p\psi_d + ri_d + \psi_q p\theta) \qquad (15)$$

The expression for the zero-sequence voltage may be obtained by substituting equations 6 in the equation for the zero-sequence voltage given in reference 2, equation 6. This yields

$$e_0 = p\psi_0 - \left(r + \frac{x_c}{p}\right) i_0 \qquad (15a)$$

where

$$\psi_0 = \frac{1}{3}\left(\psi_a + \psi_b + \psi_c\right)$$

$$i_0 = \frac{1}{3}\left(i_a + i_b + i_c\right)$$

Equations 14, 15, and 15a can be used directly in place of equations 8, 9, and 10 of reference 2 in order that the effect of balanced armature circuit capacitance can be included in determining the performance of a synchronous machine. It may be noted that if $x_c = 0$, the case when $c = \infty$, the solution of equations 14, 15, and 15a is that given by equations 8, 9, and 10 of reference 2.

In the following are applications of equations 14 and 15 to problems involving the performance of a synchronous machine and balanced capacitance.

Application to Self-Excitation of a Synchronous Machine

The phenomenon of self-excitation of a synchronous machine connected to a capacitive load or to a system through series capacitance is evidenced by the building up of machine armature voltage to values which are limited by machine or circuit saturation, it being impossible to control completely the terminal voltage by variation in the field-excitation voltage. A common cause for the occurrence of the

phenomenon is the connection of a synchronous machine to a transmission circuit whose line-charging kilovolt-amperes exceed the line-charging capacity of the generator. The following analysis indicates the regions in which this phenomenon will and will not occur. Saturation can be neglected in such an analysis as its effect is chiefly to limit the voltage of self-excitation and not to alter the values of circuit constants which cause it to occur, except for the case when the initial excitation is high enough to produce appreciable saturation.

Consider the case of a machine running at constant speed with constant excitation voltage and connected to a balanced shunt capacitive load or through a balanced series capacitance to an infinite bus, $\dot{p}\theta = (1-s)$, $\Delta E_{fd} = \Delta E_{fq} = 0$. Substituting equations 5 in equations 14 and 15 for these conditions and simplifying,

$$p e_d - (1-s)e_q = \{[(1-s)^2 - p^2]x_q(p) - pr - x_c\}i_d + (1-s)[2px_q(p)+r]i_q \quad (16)$$

$$p e_q + (1-s)e_d = -(1-s)[2px_d(p)+r]i_d + \{[(1-s)^2 - p^2]x_q(p) - pr - x_c\}i_q \quad (17)$$

Solving equations 16 and 17 simultaneously for the currents i_d and i_q,

$$i_d = -\frac{\{[p^2+(1-s)^2]Z_q(p)+px_c\}e_d + \{[p^2+(1-s)^2](1-s)x_q(p)-(1-s)x_c\}e_q}{A(p)} \quad (18)$$

$$i_q = \frac{\{[p^2+(1-s)^2](1-s)x_d(p)-(1-s)x_c\}e_d - \{[p^2+(1-s)^2]Z_d(p)+px_c\}e_q}{A(p)} \quad (19)$$

where

$$A(p) = [p^2+(1-s)^2][Z_d(p)Z_q(p)+(1-s)^2x_d(p)x_q(p)] + x_c[pZ_d(p)+pZ_q(p)-(1-s)^2x_d(p)-(1-s)^2x_q(p)+x_c] \quad (20)$$

and

$$Z_d(p) = px_d(p) + r \qquad Z_q(p) = px_q(p) + r$$

The currents i_d and i_q will increase indefinitely if any of the roots of the denominator of the operational expression for i_d and i_q, which is obtained by rationalizing $A(p)$, have positive real values. Therefore, the criterion of Hurwitz[11] or of Routh,[12] for determining if a positive real root exists, can be used for testing whether or not self-excitation will occur for a given set of machine and circuit constants.

Equation 20 is a general expression which may be used for determining if self-excitation will occur in a salient pole or a symmetrical rotor machine having any number of rotor circuits.

Using the roots of the denominator to determine if self-excitation will occur is similar to the method employed by M. Takahashi.[4] He analyzed quite completely the case of a symmetrical rotor machine with a single rotor winding and to a limited extent a salient-pole machine with a single field winding. When the same special cases were studied the results obtained from equation 20 were found to be in general agreement with his work.

An analysis by Rudenberg[13] based on graphical methods describes the chief aspects of the phenomenon and can be used for determining the effect of saturation in limiting the voltage of self-excitation. The graphical method of analysis is limited, however, in that it cannot be used for a quantitative determination of the effect of additional rotor circuits on the regions of self-excitation.

Consider the special case of a salient-pole machine running at synchronous speed, with no rotor circuits other than the direct-axis field circuit. For this case, $s = 0$,

$$x_d(p) = \frac{x_d'T_o p + x_d}{T_o p + 1}$$

and

$$x_q(p) = x_q$$

Substituting these values in equation 20 and rationalizing, the operational expression for the denominator of the currents is

$$\begin{aligned} D(p) = {} & x_q x_d' T_o p^5 + \\ & [x_d x_q + r T_o(x_d' + x_q)]p^4 + \\ & [2x_q x_d' T_o + r(x_d + x_q) + T_o x_c(x_d' + x_q) + T_o r^2]p^3 + \\ & [2x_d x_q + r T_o(x_d' + x_q) + x_c(x_d + x_q) + r^2 + T_o 2rx_c]p^2 + \\ & [x_q x_d' T_o + r(x_d + x_q) - T_o x_c(x_d' + x_q) + 2rx_c + T_o(x_c^2 + r^2)]p + \\ & [x_d x_q - x_c(x_d + x_q) + x_c^2 + r^2] \end{aligned} \quad (21)$$

Self-excitation will occur if any of the roots of $D(p)$, equation 21, have a positive real value.

For the numerical case of

$$x_d = 1.0,\ x_d' = 0.30,\ x_q = 0.6,\ T_o = 1{,}000,\text{ and } T_o = 0$$

the regions of self-excitation are shown on figure 1. The shaded area is a region of self-excitation for the case of $T_o = 1{,}000$ as well as for the case when $T_o = 0$, indicating that the phenomenon of self-excitation is possible in a salient-pole machine for the condition when the field circuit is open. For normal values of armature resistance, r, when the field circuit is closed, self-excitation occurs for values of x_c between x_d and x_d'.

Armature Resistance Neglected. For the case of $r = 0$, equation 21 reduces to

$$\begin{aligned} D(p) = {} & x_d' x_q T_o p^5 + x_d x_q p^4 + T_o[2x_d' x_q + x_c(x_q + x_d')]p^3 + \\ & [2x_d x_q + x_c(x_q + x_d)]p^2 + T_o[x_d' x_q - x_c(x_q + x_d') + x_c^2]p + \\ & [x_d x_q - x_c(x_q + x_d) + x_c^2]p \end{aligned} \quad (22)$$

By applying Routh's criterion the following array is obtained (common coefficients which are positive in value are omitted following the first 2 rows):

$x_d' x_q T_o$	$T_o[2x_d' x_q + x_c(x_q + x_d')]$	$T_o[x_d' x_q - x_c(x_q + x_d') + x_c^2]$
$x_d x_q$	$[2x_d x_q + x_c(x_q + x_d)]$	$[x_d x_q - x_c(x_q + x_d) + x_c^2]$
x_q	$[x_c - x_q]$	
$x_q[3x_d + x_c]$	$[x_d - x_c][x_q - x_c]$	
$[x_c - x_q]$		
$[x_c - x_q][x_d - x_c][x_q - x_c]$		

Therefore, self-excitation occurs when

$$x_c < x_q \quad \text{and} \quad x_q < x_c < x_d \quad \text{or} \quad x_c < x_d \quad (23)$$

Accordingly, with zero resistance the phenomenon of self-excitation can occur for any value of capacitance less than that corresponding to the direct-axis synchronous reactance. Practically, however, as shown in figure 1, only a small amount of resistance decreases the range of self-excitation from (x_d to 0) to (x_d to x_d').

Field Switch Open. For the case of $T_o = 0$, equa-

tion 21 yields the following array when Routh's criterion is applied:

$$x_d x_q \qquad 2x_d x_q + x_c(x_d + x_q) + r^2 \qquad x_d x_q - x_c(x_d + x_q) + x_c^2 + r^2$$

$$r(x_d + x_q) \qquad r(x_d + x_q) + x_c^2 \qquad 0$$

$$\left\{\begin{matrix}(x_d+x_q)x_d x_q + \\ x_c(x_d^2 + x_q^2) + r^2(x_d + x_q)\end{matrix}\right\} \qquad \left\{\begin{matrix}(x_d+x_q)x_d x_q - x_c(x_d+x_q)^2 \\ +(x_c^2 + r^2)(x_d + x_q)\end{matrix}\right\}$$

$$\left\{\begin{matrix}2(x_d+x_q)^2 + 2r^2(x_d+x_q) \\ +x_c(x_d - x_q)^2\end{matrix}\right\}$$

$$[x_d x_q - x_c(x_d + x_q) + (x_c^2 + r^2)]$$

Therefore, the values of x_c which will result in self-excitation when the field circuit is open are

$$\frac{x_d + x_q - \sqrt{(x_d - x_q)^2 - 4r^2}}{2} < x_c < \frac{x_d + x_q + \sqrt{(x_d - x_q)^2 - 4r^2}}{2} \quad (24)$$

If $x_d = x_q$, which is the case of a machine with laminated cylindrical rotor, self-excitation cannot occur when the field circuit is open. Equation 24 describes the region of self-excitation for values of x_c between x_d and x_q as shown in figure 1.

Infinite Field Time Constant. For the case of $T_o = \infty$ equation 21 yields a similar expression to that obtained for the case when $T_o = 0$ except x_d' replaces x_d. Accordingly, the values of x_c which will result in self-excitation when $T_o = \infty$ are

$$\frac{x_d' + x_q - \sqrt{(x_d' - x_q)^2 - 4r^2}}{2} < x_c < \frac{x_d' + x_q + \sqrt{(x_d' - x_q)^2 - 4r^2}}{2} \quad (25)$$

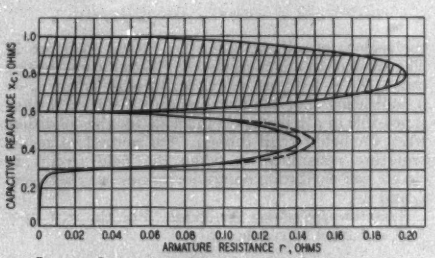

Fig. 1. Regions of self-excitation for a salient-pole synchronous machine

$x_d = 1.0$ $\qquad x_d'' = x_d' = 0.30$
$x_q'' = x_q' = x_q = 0.60$ $\qquad T_o = 1{,}000$
Shaded area applies for field circuit opened or closed
Dotted line applies for $T_o = \infty$ (approximate solution)

Equation 25 is a good approximation to the actual case when T_o is large for the region between x_q and x_d' as shown by figure 1.

This section may be summarized as follows:

1. For a machine having rotor circuits additional to the field circuit, the regions of self-excitation can be determined by numerical substitution in equation 20.

2. For most practical purposes the regions of self-excitation can be determined by equations 24 and 25 for the case of a synchronous machine without an amortisseur winding.

3. For normal values of armature circuit resistance, values of capacitive reactance between x_d and x_d' for a machine without an amortisseur will result in self-excitation.

4. A value of series armature resistance greater than both $(x_d - x_q)/2$ and $(x_q - x_d')/2$ will prevent the phenomenon from occurring, for a machine without an amortisseur.

5. The above results are a theoretical explanation of the difficulties sometimes encountered (*a*) when a capacitance shunt load greater than the line charging capacity is connected to a synchronous machine and (*b*) when a synchronous machine is connected to a source of voltage through a series capacitance.

Applications to a 3-Phase Fault

Equations 14 and 15 will be applied to the case of a 3-phase fault on a synchronous machine running at synchronous speed initially open-circuited having capacitance in its armature circuit. This is also equivalent to suddenly throwing on a capacitive load. The currents i_d and i_q for this case can be determined by substituting $e_d = 0$, $e_q = -e_{qo}1$, and $s = 0$ in equations 18 and 19. This yields

$$i_d = \frac{(p^2 + 1)x_q(p) - x_c}{A(p)} e_{qo}1 \quad (26)$$

$$i_q = \frac{(p^2 + 1)Z_d(p) + px_c}{A(p)} e_{qo}1 \quad (27)$$

where $A(p)$ is given by equation 20 with $s = 0$.

Equations 26 and 27 are operational expressions for the currents i_d and i_q which can be solved by means of Heaviside's expansion theorem, the roots of the denominator being determined by means of Graeffes[14] root-squaring method. Having determined the current i_d and i_q, the phase currents i_a, i_b, and i_c are obtained by substituting in equation 14 of reference 2.

The general solution of the operational expressions for the current, particularly when the effect of more than one rotor circuit is considered, involves a great deal of algebraic work. However, considerable information as regards the phenomena being studied can be obtained by making use of certain simplifying assumptions. The following is an example to illustrate this.

Suppose that it is required to determine the maximum possible voltage which may occur across the terminals of a synchronous machine when it is suddenly thrown on to a very large capacitive load. This also corresponds to the case of a short circuit occurring on the system side of the capacitance of a machine having series capacitors in its armature circuit. Let the machine and capacitor constants be as follows:

$$x_d = 1.0,\ x_q = 0.60,\ x_d' = 0.35,\ r = 0.05,\ T_o = 1{,}000,\ x_c = 0.20$$

From the values chosen it is apparent that the value of capacitance of 0.20 does not lie between x_d' and x_d and therefore it will be assumed that self-excitation does not occur for these constants. Practically, for this assumption to be valid, x_c should be definitely less than x_d' by a small amount, as the effect of saturation, which has been neglected, is to reduce the effective value of transient reactance.

The maximum short-circuit current can be calculated on the basis that $T_o = \infty$ and $r = 0$, which neglects the decrements in current and voltage. This results in a fair approximation for the current and voltage during the first few cycles after the fault is

applied and in a considerable simplification in the algebraic work. For these conditions equations 26 and 27 yield

$$i_d = \frac{0.60\,p^3 + 0.40}{0.21\,p^4 + 0.61\,p^3 + 0.06}\,1$$

$$i_q = \frac{0.35\,p^3 + 0.55\,p}{0.21\,p^4 + 0.61\,p^3 + 0.06}\,1$$

which gives

$$i_d = 6.67 - 0.81\cos 1.67\,t - 5.83\cos 0.32\,t$$
$$i_q = 0.452\sin 1.67\,t + 2.82\sin 0.32\,t$$

Substituting the values of i_d and i_q in

$$i_a = i_d\cos(t+\alpha) - i_q\sin(t+\alpha)$$

and simplifying,

$$i_a = 6.67\cos(t+\alpha) - 0.63\cos(0.67\,t-\alpha) - 4.33\cos(0.68\,t-\alpha) - 0.18\cos(2.67\,t+\alpha) - 1.51\cos(1.32\,t+\alpha)$$

The voltage across the capacitor is

$$V_a = \frac{1}{c}\int i_a\,dt$$

$$= 1.33\sin(t+\alpha) - 0.01\sin(2.67\,t+\alpha) - 0.23\sin(1.32\,t+\alpha) - 1.29\sin(0.68\,t-\alpha) - 0.19\sin(0.67\,t-\alpha)$$

indicating a possible maximum transient voltage across the capacitor of 3 times normal. The actual maximum voltage across the capacitor would be somewhat less because the effect of armature circuit resistance, which was neglected, would be to damp out the components having frequencies other than normal frequency. The voltage across the capacitor immediately after the armature circuit transients have died away corresponds to that given in the first term of the above expression for voltage.

From these results, the conclusion is reached that during the first few cycles immediately following the short circuit, the voltage across the capacitor will be from 1.3 to 3.0 times normal line-to-ground voltage, depending upon the value of armature circuit resistance.

The sustained voltage is

$$V_a = \frac{0.20\times 1}{1.0 - 0.20}\times\sin(t+\alpha) = 0.25\sin(t+\alpha)$$

By these comparatively simple calculations, it is evident that the transient voltage across the capacitance will be considerably greater than that corresponding to the sustained voltage, and that the maximum possible voltage is approximately 3.0 times normal.

Approximate Field Time Constant. An approximate value for the time constant of the field circuit under the condition of capacitive load can be determined by dividing the coefficient of p^1 by the coefficient of p^0 in equation 21. This yields, when terms in the coefficient for p^1 which do not include T_o are neglected,

$$T_{d'} = \frac{(x_d - x_c)(x_q - x_c) + r^2}{(x_{d'} - x_c)(x_q - x_c) + r^2}\,T_o \qquad (28)$$

This time constant is valid only when $T_{d'}$ and T_o are comparatively large. Although approximate, it does indicate with good accuracy the values of x_c which will cause $T_{d'}$ to become negative and accordingly produce self-excitation.

Application to Small Angular Oscillation

Park gives for the change in electrical torque for small changes in angular displacement of a synchronous machine connected to an infinite bus (equation 60, reference 1)

$$\Delta T = [\psi_{do} + i_{qo}x_q(p)]\,\Delta i_q - [\psi_{qo} + i_{do}x_d(p)]\,\Delta i_d \qquad (29)$$

By substituting the following relations in equations 14 and 15, Δi_d and Δi_q can be determined:

$$\psi_d = \psi_{do} + \Delta\psi_d \qquad e_d = e_{do} + \Delta e_d \qquad i_d = i_{do} + \Delta i_d$$
$$\psi_q = \psi_{qo} + \Delta\psi_q \qquad e_q = e_{qo} + \Delta e_q \qquad i_q = i_{qo} + \Delta i_q$$
$$p\delta = 1 + p\,\Delta\delta$$

This yields,

$$\left.\begin{aligned} e_{qo} &= \psi_{do} + x_c\,i_{do} - r\,i_{qo} \\ e_{do} &= -\psi_{qo} - x_c\,i_{qo} - r\,i_{do} \end{aligned}\right\} \qquad (30)$$

and

$$\left.\begin{aligned} &p\,\Delta e_d - \Delta e_q - e_{qo}p\,\Delta\delta = p^3\Delta\psi_d - 2p\,\Delta\psi_q - 2\psi_{do}p\,\Delta\delta - \Delta\psi_d - \psi_{qo}p^2\Delta\delta - rp\,\Delta i_d + r\,\Delta i_q + ri_{qo}p\,\Delta\delta - x_c\Delta i_d \\ &p\,\Delta e_q + \Delta e_d + e_{do}p\,\Delta\delta = p^3\Delta\psi_q + 2p\,\Delta\psi_d - 2\psi_{qo}p\,\Delta\delta - \Delta\psi_q + \psi_{do}p^2\Delta\delta - rp\,\Delta i_q - r\,\Delta i_d - ri_{do}p\,\Delta\delta - x_c\Delta i_q \end{aligned}\right\} \qquad (31)$$

$$\left.\begin{aligned} \psi_{do} &= E_{fd} - x_d i_{do} \\ \psi_{qo} &= -x_q i_{qo} \end{aligned}\right\} \qquad (32)$$

Substituting equations 32 in equations 30 and solving for the initial currents,

$$i_{do} = \frac{E_{fd}(x_q - x_c) - (x_q - x_c)e\cos\delta_o - r\,e\sin\delta_o}{(x_d - x_c)(x_q - x_c) + r^2} \qquad (33)$$

$$i_{qo} = \frac{E_{fd}\,r - e\,r\cos\delta_o + (x_d - x_c)\,e\sin\delta_o}{(x_d - x_c)(x_q - x_c) + r^2} \qquad (34)$$

From equation 28 of reference 1,

$$e_d = e\sin(\delta_o + \Delta\delta) \qquad e_q = e\cos(\delta_o + \Delta\delta)$$

Since $\Delta\delta$ is small,

$$\Delta e_d = e\cos\delta_o\,\Delta\delta \qquad \Delta e_q = -e\sin\delta_o\,\Delta\delta$$

Also from equations 5,

$$\Delta\psi_d = -x_d(p)\,\Delta i_d \qquad \Delta\psi_q = -x_q(p)\,\Delta i_q$$

Substituting these relations in equations 31,

$$\left.\begin{aligned} &[-e\cos\delta_o - 2\psi_{qo}p + \psi_{do}p^2 - ri_{do}p]\,\Delta\delta = [2px_d(p) + r]\,\Delta i_d + [p^2x_q(p) - x_q(p) + rp + x_c]\,\Delta i_q \\ &[-e\sin\delta_o - 2\psi_{do}p - \psi_{qo}p^2 + ri_{qo}p]\,\Delta\delta = [p^2x_d(p) - x_d(p) + rp + x_c]\,\Delta i_d - [2px_q(p) + r]\,\Delta i_q \end{aligned}\right\} \qquad (35)$$

Equations 35 can be solved for Δi_d and Δi_q and substituted in equation 29 for the incremental torque. Therefore,

$$\Delta T = f(p)\,\Delta\delta$$

The response to a sudden change in the electrical angular displacement, $\Delta\delta 1$, may be determined by

(*Concluded on page 36*)

Proposed Transformer Standards

By J. E. CLEM
MEMBER AIEE

During the past 2 years the AIEE transformer subcommittee* has proposed changes in the AIEE transformer standards; this paper is presented to bring these changes before the Institute.

1—Transformer Insulation Levels

DURING previous years the transformer subcommittee established insulation levels for transformers connected to circuits operating at standard voltages. These requirements have been passed on to the ASA sectional committee on transformers (V. M. Montsinger, chairman), and on to the standards sub-committee (W. M. Dann, chairman). The ASA transformer standards subcommittee has taken these insulation levels and incorporated them in the standards with slight modifications not affecting the fundamental requirements. A memorandum of the proposed ASA standards was submitted to the transformer subcommittee and approved with minor changes and recommended for immediate use. These proposed standards follow and are essentially as given in the proposed ASA transformer standards as material in Sections II, III, and IV.

A—Standards Common to Transformers, Regulators, and Reactors

Insulation Level. Table I gives the relations between established rated circuit voltages, limits of rated apparatus voltages, and required basic insulation levels, for transformers and other induction apparatus covered by the standards. Column 1 gives the values of established circuit voltages. Column 2 gives the limits of rated apparatus voltages permissible for the corresponding insulation levels. Columns 3 and 4 give the required standard insulation levels in terms of the spacings of rod gaps used in making impulse tests, and of the low-frequency dielectric test.

A bank of modern large transformers

Table I

Rated Circuit Voltage—Volts	Limit of Rated Apparatus Voltage—Kv	Basic Insulation Level: Impulse Test Gap Spacing—Inches	Basic Insulation Level: Alternating Voltage Dielectric Test—Kv
120			
240			
480			
600	1.2	0.8	10
2,400			
2,500	2.5	1.6	15
4,160			
4,330			
4,800	5.0	2.2	19
6,900	8.66	3.3	26
11,500			
13,800	15.0	4.5	34
25,000	25.0	7.1	51
34,500	34.5	10.2	70
46,000	46.0	13.5	93
69,000	69.0	20.6	139
92,000	92.0	27.5	185
115,000	115.0	34.7	231
138,000	138.0	42.1	277
161,000	161.0	49.0	323
196,000	196.0	60.0	393
230,000	230.0	70.4	461
287,500	287.5	88.0	578
345,000	345.0	105.6	691

Note 1—When apparatus is suitable for wye connection, the name plate shall be so marked and the circuit (line-to-line) voltage rating shall determine the required basic insulation level and bushing requirements. For example, if a transformer is designed for a high voltage of 6,900/11,950Y the name plate shall be marked accordingly and the transformer will be in the 15-kv insulation class.

Note 2—Exceptions to these standards will be found in the specific sections.

B—Standards for Distribution and Power Transformers

In the ASA standards for distribution and power transformers the same introductory paragraphs and the table will be reproduced, with footnotes essentially as follows:

Note 1—When transformers are suitable for wye connection the name plate shall be so marked and the circuit (line-to-line) voltage rating shall determine the insulation level. For example:
Single-phase transformers for 8,660 volts or below shall be suitable for connection in star (wye) and shall be capable of withstanding tests as shown in table II.

C—Standards for Instrument Transformers

In the ASA standards for instrument transformers the introductory paragraph on insulation level is again reproduced, with suitable wording to make it apply to instru-

A paper recommended for publication by the AIEE committee on electrical machinery. Manuscript submitted September 16, 1936; released for publication November 25, 1936.

J. E. Clem is electrical engineer in the central station department of the General Electric Company, Schenectady, N. Y.; he was chairman of the transformer subcommittee* of the AIEE committee on electrical machinery, 1934–36.

* Personnel of Transformer Subcommittee of AIEE Committee on Electrical Machinery, 1935–36: J. E. Clem, *chairman*; G. M. Armbrust, F. F. Brand, E. S. Bundy, F. A. Lane, A. C. Monteith, L. C. Nichols, J. R. North, H. J. Scholz, E. D. Treanor, and F. J. Vogel.

Table II

Transformer Voltage Rating	Impulse Test Gap Spacing—Inches	Alternating Voltage Dielectric Test—Kv
Single-phase transformers		
2,400 delta/4,160 star	2.2	19
4,800 delta/8,320 star	3.3	26
6,900 delta/11,950 star	4.5	34
3-phase transformers		
2,400 delta or star	1.6	15
4,800 delta or star	2.2	19
6,900 delta or star	3.3	26

(The reference to table II appears as a note in the main table opposite 1.2–2.5–5.0–8.66 kv transformer voltages.)

Note 3—*Exception*—Transformers designed to permit star-connected operation on circuits of 92,000 volts and above with the neutral solidly grounded, may be designed, when so specified, to be capable of withstanding only an induced-voltage test corresponding to that required for the next lower rated circuit voltage class.

Note 4—Transformers may be provided with regulation taps for voltages not exceeding 10 per cent above the rated circuit voltage.

Table III

Transformer Voltage Rating	Impulse Test Gap Spacing—Inches	Alternating Voltage Dielectric Test—Kv
Single-phase transformers		
2,400 delta/4,160 star	2.2	19
4,800 delta/8,320 star	3.3	26
6,900 delta/11,950 star	4.5	34
3-phase transformers		
2,400 delta or star	1.6	15
4,800 delta or star	2.2	19
6,900 delta or star	3.3	26

(The reference to table III appears as a note in the main table opposite 1.2–2.5–5.0–8.66 kv transformer voltages.)

Note 3—The next-lower insulation level may be specified when it is adequate. For example:

(*a*) For potential transformers for 15 kv or below when exposure to impulse voltage is low.

(*b*) *Exception*—Transformers designed to permit star-connected operation on circuits of 92,000 volts and above with the neutral solidly grounded, may be designed, when so specified, to be capable of withstanding only an induced voltage test corresponding to that required for the next lower rated circuit voltage class.

Note 4—Voltage ratings of current transformers are the maximum voltages for which they are applicable. For co-ordinated insulation, current transformers having the same test-gap ratings as other apparatus in the circuit should be selected.

ment transformers, together with the table, and the footnotes are essentially as follows:

Note 1—When potential transformers are suitable for wye connection, the name plate shall be so marked and the circuit (line-to-line) voltage rating shall determine the insulation level. For example: Single-phase potential transformers for 8,660 volts or below shall be suitable for connection in star (wye) and shall be capable of withstanding tests as shown in table III.

2—Impulse Tests on Transformers

Initially the impulse test code required 5 tests to be made. In the "Recommended Transformer Standards" by Putman and Clem, published in ELECTRICAL ENGINEERING, December 1934, this was changed to require 3 tests. Since that time the wording designating the tests has been changed to the following:

(*a*) Apply a wave just sufficient to cause flashover of the specified test gap under existing conditions of humidity and air density.

(*b*) Apply a wave sufficient to cause flashover of the bushing. For this test the applied voltage must be at least 5 per cent in excess of the standard minimum flashover voltage for the standard bushing under standard conditions of humidity and air density.

Note—When oversized bushings are used they shall be equipped with suitable gaps to provide the same standard minimum impulse flashover as for the standard bushing.

(*c*) Apply a wave having a crest not less than 90 per cent of the standard minimum flashover voltage of the standard bushing under existing conditions of humidity and air density. No flashover of the bushing shall occur during the test.

Standard atmospheric conditions for these tests are a temperature of 25 degrees centigrade, air density corresponding to 760 millimeters of mercury and a humidity corresponding to a vapor pressure of 15.46 millimeters.

These changes in wording are the result of changes made from time to time to make the test requirements more explicit.

Table IV—Insulation Requirements for Current Limiting Reactors

Limit of Rated Apparatus Voltage—Kv	Low-Frequency Dielectric Test Applied Voltage—Kv	
	Oil Insulated	Air Insulated
1.2	12	20
2.5	17	25
5.	21	30
8.66	29	40
15.0	36	60
25.0	58	85
34.5	80	115
46.0	106	
69.0	157	
92	209	
115	261	
138	312	
161	364	
196	444	
230	520	
287.5	648	
345	780	

3—Insulation Requirements—Current Limiting Reactors

There are, in general, 2 types of construction for current-limiting reactors—oil insulated and air insulated. The insulation has in practice departed somewhat from former Institute standards and the ASA sectional committee has modified these values in accordance with table IV and the AIEE transformer subcommittee recommends that these values be put into immediate use.

4—Transformer for Mercury Arc Rectifiers

The transformer subcommittee does not agree with the present recommendations of the mercury arc rectifier. Subcommittee for the insulation of mercury-arc-rectifier transformers. It recommends higher test voltages based

Table V

D-C Voltage —Volts	Limit of Rated Apparatus Voltage —Kv	Alternating Voltage Dielectric Test —Kv
0– 700	1.2	10
701– 1,500	2.5	15
1,501– 3,000	5.0	19
3,001– 5,000	8.66	26
5,001– 8,750	15.0	34
8,751–15,000	25.0	51
15,001–20,000	34.5	70

on voltage classifications which agree with those for other transformers.

It is reasonable to insulate primaries of rectifier transformers according to conventional transformer practice. The secondaries of these transformers are not, as a rule, exposed to lightning directly, and, accordingly, the next lower insulation level might be considered. However, the secondaries are exposed to overvoltages inherent in the operation of the rectifying equipment, so that a reduction in the low-frequency dielectric test does not seem advisable. Accordingly, the insulation of the secondary windings of these transformers should also follow conventional transformer practice after the proper insulation class of the transformer secondary winding has been agreed upon. However, the impulse tests for other transformers have been set up with overvoltages for lightning in mind. Rectifier transformers are subject only to overvoltages inherent in their operation which may be different in their character and frequency of occurrence, and, therefore, it seems advisable to study the question of the proper impulse test further.

There might be some question as to the secondary voltage rating to be used in selecting the insulation level on account of the variation in connections used to obtain the same d-c voltage. This occurs because the transformer secondary voltage for the same d-c voltage may be different for different schemes of connections. It appears reasonable that the most consistent results would be obtained if the d-c voltage was made the basis for determining the voltage class. It was agreed that the voltage class should be determined by the formula:

$$\text{Voltage class} = 2 \times \frac{\text{Rated d-c voltage}}{1.17}$$

The rated d-c voltage divided by 1.17 gives the corresponding open-circuit voltage to neutral of the rectifier

Table VI—Bushing Characteristics

Transformers Larger than 500 Kva (Power). Transformers 500 Kva and Smaller (Distribution)

Rated Circuit Voltage—Kv (1)	Maximum Rated Apparatus Voltage—Kv (2)	Power Transformers: Equivalent Rod Gap—Inches (3) (4)	Power Transformers: Impulse Flashover Kv (5) (6)	Power Transformers: 60-Cycle Flashover Dry—Kv (6) (8)	Power Transformers: 60-Cycle Flashover Wet—Kv (7) (8)	Distribution Transformers: Equivalent Rod Gap—Inches (3) (4)	Distribution Transformers: Impulse Flashover Kv (5) (6)	Distribution Transformers: 60-Cycle Flashover Dry—Kv (6) (8)	Distribution Transformers: 60-Cycle Flashover Wet—Kv (7) (8)
0.12									
0.24									
0.48									
0.60	1.2	2.25	64	25	12	0.875	35	11	7
2.4									
2.5	2.5								
4.16									
4.33									
4.80	5.0	3.4	82	40	27	2.3	65	27	18
6.9	8.66	4.5	98	50	35	3.5	83	40	27
11.5									
13.8	15.0	5.75	120	65	45	4.7	102	53	37
23.0	25.0	8.1	160	85	60	7.5	150	78	55
34.5	34.5	11.4	215	115	85	10.6	200	110	80
46.0	46.0	15.0	270	150	120	14.1	255	140	105
69	69	22.3	385	215	165	21.6	375	205	155
92	92	29.6	500	280	210				
115	115	36.7	600	340	260				
138	138	44.0	710	405	310				
161	161	51.2	815	460	355				
196	196	62.3	980	555	430				
230	230	73.0	1,135	640	500				
287.5	287.5	92.3	1,400	760	610				
345	345	110.5	1,675						

For circuit voltages 92 kv and above use power transformer bushing values.

1. Column 1 gives the values of rated circuit voltages recommended in the NEMA-NELA report on preferred voltage ratings dated October 1928, for the purpose of establishing values to be used in designing and testing electrical apparatus.

Note: Rated circuit voltages of 92,000, 196,000, and 287,500 volts have been added to the NEMA-NELA list.

2. Column 2 gives the maximum rated apparatus voltages permissible for the corresponding insulation levels.

3. The equivalent rod gap for distribution transformer bushings is based on the transformer subcommittee recommendation standardizing the minimum impulse flashover for bushings at 5 per cent above the flashover of the test gap. The equivalent rod gap for power-transformer bushings for voltage classifications 69 kv and below represents existing practice. These values are minimum and must be met.

4. When bushing and equivalent rod gap are tested in parallel at minimum gap flashover with the 1.5 x 40 microsecond positive wave. 50–50 flashover of the equivalent gap and bushing should occur at minimum flashover voltage.

5. Average minimum flashover voltage with the 1.5x40 microsecond positive wave. Based on curves and tolerance of rod-gap flashover data agreed upon by the NEMA-EEI subcommittee on correlation of laboratory data, September 26, 1935. The tolerance applies to the recorded flashover voltage only (see note 3).

6. Flashover voltages are average values and are given for standard conditions of air density and humidity.

7. Wet flashover voltages are average values based on 0.1-inch precipitation per minute at an angle of 45 degrees with water having a resistivity of 12,000 ohms per centimeter cube and at standard air density.

8. The tolerance on the 60-cycle dry- and wet-flashover voltages shall be 5 per cent under standard conditions of air density and humidity.

9. All flashover values are based on the revised sphere-gap calibration data agreed upon by the sphere gap calibration subcommittee of the instruments and measurements committee. See ELECTRICAL ENGINEERING, page 783, July 1936.

transformer for any half wave 3-phase connection or double-Y connection with interphase. For the same d-c voltage, 6 or more phase half-wave connections have slightly lower corresponding transformer open-circuit voltages; single-phase connections, which are not common in power sizes, have somewhat greater open-circuit voltages. Commutation effects will, in general, result in a slightly higher a-c/d-c voltage ratio than at open circuit. Twice the maximum a-c voltage to neutral of the transformer secondary winding is equal to or greater than the maximum a-c voltage between secondary bushings and so is used to define the voltage class.

Application of this formula gives the following, with some slight rounding off of values:

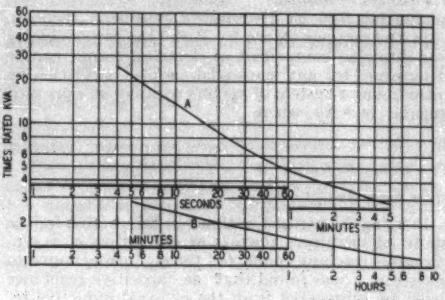

Fig. 1

Duration of Load	Load in Multiples of Continuous Rating	Curve
4 seconds	25	A
10 seconds	13.7	A
30 seconds	6.7	A
60 seconds	4.75	A
5 minutes	2.8	A
30 minutes	1.85	B
60 minutes	1.6	B
2 hours	1.4	B
5 hours	1.2	B

Required Insulation Level of Transformers for Mercury Arc Rectifiers

PRIMARY WINDINGS

The primary windings of rectifier transformers shall be insulated in accordance with standard transformer requirements.

SECONDARY WINDINGS

The secondary windings of rectifier transformers shall be insulated in accordance with table V. It is recommended that this practice be put into immediate use.

5—Bushing Standards

Due to recent changes in the sphere-gap calibration curves it became necessary to modify the 60-cycle flashover data of transformer bushings. In addition the NEMA-EEI laboratory subcommittee on correlation of laboratory data revised the rod-gap flashover data which in turn required a slight change in the tabulation bushing impulse-flashover voltages. The standard bushing characteristics with these changes shown in table VI was approved and is recommended for immediate use.

Tests to verify the flashover of bushings should be made on the basis of the new calibration curve and the new flashover values. If, however, it is required to verify the old flashover values then the old calibration curves shall be used.

6—Use of Sphere-Gap Calibration Curves

Since the subcommittee of the instruments and measurements committee on sphere gap calibration has revised the sphere-gap calibration curves, it is recommended that these new calibrations be put into immediate use in the testing of transformers. The new calibration curves have been published on page 783 of the July 1936 issue of ELECTRICAL ENGINEERING.

The new calibration curves are given only for the case of one sphere grounded. It was recommended that these same curves also be used for the case of nongrounded spheres, providing the ratio of gap spacing to sphere diameter does not exceed 1/4. A review of the data has indicated that with this precaution the error will be quite small.

7—Short-Time Heating and Overloading of Distribution Transformers

The subcommittee's report on the short time overloading of oil-immersed power transformers were given in a paper entitled "Overloading of Power Transformers" by V. M. Montsinger and V. M. Dann, ELECTRICAL ENGINEERING, October 1934, page 1353. Since that time the subcommittee has drawn up a guide for the short-time heating and overloading of certain sizes of distribution transformers. These curves apply to transformers 100 kva and smaller below 15,000 volts, and to network transformers 500 kva and smaller. Other distribution transformers are covered by the paper just mentioned.

Guide—Short-Time Heating and Overload—Distribution Transformers

Distribution transformers operate under varying load-time curves, generally with relatively low load factor. It is possible to apply higher than rated load for short periods without encroaching too seriously on the life of the insulation or the oil. Since the shape of the load curve is variable from day to day and from season to season, and is not subject to easy control, there is no exact method of calculating the correct size of transformer for a given location.

The deterioration of insulation proceeds at different rates, depending upon the temperature, and the end point is not definite unless some characteristic is arbitrarily chosen. Calculations of the life on the basis of assumed

load curves are therefore of somewhat uncertain value. Many such calculations integrating the effect of time and temperature have been made, however, and they tend to check data from experience which in itself is not exact, but this agreement gives some foundation for setting up a curve which should prove a useful guide in overloading distribution transformers without materially affecting the length of life which has been obtained in the past.

Such a curve representing the magnitude and duration of permissible daily overloads starting at no-load temperature has been compiled and is shown as that portion of figure 1 for times longer than 5 minutes, curve *B*. This section of the curve should be of value in the application of distribution transformers, particularly in determining the economic size of transformer required to carry the expected load, with due regard for short-time peak overloads.

The short-time portion of the curve, that is, for times less than 5 minutes, curve *A*, is based on what may be termed, in general, short circuits, whose occurrence is accidental and not premeditated as with a daily recurrent load. They may occur at any time, and hence the worst condition—occurrence after full load—must be assumed. The frequency with which they occur can only be estimated. This portion, curve *A*, of the curve will be useful in the application of primary fuse links or network transformer fuses to meet thermal protective requirements. This portion of the curve is essentially a time-current curve of distribution transformers based on not reducing their normal expected life. A fuse link to provide thermal protection for such a transformer should lie below and to the left of the transformer curve. The inherent thermal ability of fuse links is much smaller than that of the transformer windings and therefore it cannot be expected that such links will provide thermal protection for periods exceeding approximately 5 minutes.

The short-time portion, curve *A*, of the curve may also be used to determine the ability of distribution transformers to operate as grounding transformers only, and to indicate the required time and current settings of protective devices used in the neutral of such transformers to clear them in the case of sustained faults. If distribution transformers connected as grounding transformers are also required to carry load, it should be recognized that the probable more frequent occurrence of line-to-ground faults will result in a shorter life than if the transformers were operated as normal distribution units subjected to occasional secondary faults. In addition, the normal impedance of distribution transformers is usually too low for them to function as grounding transformers unless additional external impedance is added, thus requiring a study of each particular case.

These 2 proposed curves are blended to form a composite continuous curve based on the limiting condition of a 30-degree daily average ambient. For lower ambients the same increase of load may be permitted as has been standardized for use on power transformers, one per cent for each degree below 30 degrees centigrade, but no further increase shall be made below a temperature of zero degrees centigrade.

Continuous duty on distribution transformers in high ambients is so unusual as to constitute a special situation which should be presented when transformers for such service are purchased.

Two-Reaction Theory of Synchronous Machines

(*Continued from page 31*)

evaluating $f(p)$ by Heaviside's expansion theorem.

In the manner shown by Park[3] the synchronizing and damping component of electrical torque can be determined for any sinusoidal angular oscillation by introducing a system of vectors rotating at s per unit angular velocity, where

$\Delta\delta = |\Delta\delta| \sin st$

T_s = real part of $f(jS)$

sT_d = imaginary part of $f(jS)$

In using the method outlined in this section for the study of sustained hunting or oscillation of a synchronous machine connected through capacitance to a system, it was found that the capacitive reactance could be subtracted from the external inductive reactance and the problem analyzed in the usual manner with good approximation, for those cases when the natural oscillation frequency of the machine being studied was small compared with normal frequency of the terminal voltage.

References

1. Definition of an Ideal Synchronous Machine and Formula for the Armature Flux Linkages, R. H. Park. *General Electric Review*, volume 31, June 1928, pages 332–4.

2. Two-Reaction Theory of Synchronous Machines—Generalized Method of Analysis—Part I, R. H. Park. AIEE Transactions, volume 48, July 1929, pages 716–27.

3. Two-Reaction Theory of Synchronous Machines—II, R. H. Park, AIEE Transactions, volume 52, June 1933, pages 352–5.

4. Transient Phenomena of an Alternator Upon Condensive Load, M. Takahashi. Researches of the Electrotechnical Laboratory, Tokyo, Japan, No. 350, August 1933.

5. Starting Performance of Salient Pole Synchronous Motors, T. M. Linville. AIEE Journal, volume 49, Feb. 1930, pages 145–7.

6. The Operational Impedances of a Synchronous Machine, M. L. Waring and S. B. Crary. *General Electric Review*, volume 35, Nov. 1932, pages 578–82.

7. Torque Angle Characteristics of Synchronous Machines Following System Disturbances, S. B. Crary and M. L. Waring. AIEE Transactions, volume 51, Sept. 1932, pages 764–73; discussion pages 773–4.

8. The Application of Tensors to the Analysis of Rotating Electrical Machinery, Gabriel Kron. A serial in the *General Electric Review*, beginning in volume 38, April 1935, page 181.

9. Pull-In Characteristics of Synchronous Motors, D. R. Shoults, S. B. Crary, and A. H. Lauder. Electrical Engineering (AIEE Transactions), volume 54, December 1935, pages 1385–95.

10. Salient-Pole Motors Out of Synchronism, A. H. Lauder. Electrical Engineering, volume 55, June 1936, pages 636–49.

11. Ueber die Bedingungen, unter welchen eine Gleichung nur Wurzeln mit negativen reelen Theilen besitzt, A. Hurwitz. *Mathematische Annalen*, Berlin, volume 46, 1895, pages 273–84.

12. Advanced Rigid Dynamics (a book), E. J. Routh. Macmillan and Co., New York, 1884, page 168.

13. Elektrische Schaltvorgänge und Verwandte Störungserscheinungen in Starkstromanlagen (a book), Reinhold Rüdenberg. Julius Springer Berlin, 1933, section 42, page 359.

14. Mathematics of Modern Engineering (a book), R. B. Doherty and E. G. Keller. John Wiley and Sons, Inc., New York, 1936, page 98.

Sealed-Off Ignitrons for Welding Control

By DAVID PACKARD
ASSOCIATE AIEE

J. H. HUTCHINGS
ASSOCIATE AIEE

Accurate control of high currents for resistance welding may be obtained by igniter-type mercury-cathode tubes capable of conducting 7,000 amperes in impulses of from less than 0.01 second to several seconds duration. This paper describes design principles and manufacturing technique for tubes of the sealed-off type.

IN THE PROCESS of resistance welding, parts to be welded are placed between high-conductivity electrodes, pressure is applied, and an impulse of current passed through the electrodes and work. The region of highest resistance, where most of the heat is developed when the current flows, is the point of contact between the pieces being welded.

When making large welds, very high currents are required to produce sufficient heat to melt the metals. It is desirable to accomplish this heating and subsequent cooling very quickly so that the melted zone does not travel from the joint through the pieces to their outer surfaces. In this way short weld timing leaves a bridge of cooler metal adjacent to each electrode, thus minimizing oxidation and deformation. This short timing, if coupled with high accuracy of current and time control, simplifies the welding of metals otherwise very difficult to weld. Thus there are encountered 2 principal requirements of any device used to control current to a resistance welder:

1. Ability to pass very high currents. Welding depends upon high currents to develop the necessary heat.

2. Quick response. The device must respond quickly if it is to follow the signal impulses and so give the desired short and accurate timing.

The Ignitron

These requirements have been satisfied by the ignitron,[1,2,3] which may be either a sealed-off tube or a continuously pumped tank, the fundamentals of operation being the same in both cases. The ignitron is a mercury-arc rectifier having a special control electrode or igniter used for initiating the arc. Once the arc is established by passing an impulse of current through the igniter, it continues for the remainder of that half-cycle during which the anode is positive with respect to its cathode. During the negative half-cycle the arc is completely extinguished and control is regained. When the anode again becomes more positive than the cathode the arc may be re-established if desired by passing another impulse of current through the igniter. In this way alternating voltage enables one to regain control every cycle. Thus the ignitron and thyratron effect similar control over the flow of current.

In welding service, 2 ignitrons are connected "back to back" in series with the welding transformer primary as shown in figure 1. By energizing the igniter of each unit at the proper instant during each conducting cycle, 2-way or alternating conduction of current is permitted. Each ignitron passes current during half of each conducting cycle, and so control is regained every half-cycle. When the weld has been completed, conduction is stopped by removing excitation from the igniters. Two ignitrons thus act as a quickly responding contactor.

The ignitron satisfies the 2 requirements previously stated for the following reasons:

1. Use of a mercury-pool cathode makes possible the conduction of extraordinarily high instantaneous currents. Cathode life at these high currents should be very long.

2. Quick and accurate response is attained through use of the igniter electrode. When the proper impulse of current is applied to the igniter, the arc starts in less than 100 microseconds. Conduction stops at the instant an anode becomes negative, thus all conducting periods end at approximately the same point on the voltage wave.

It is therefore evident that the ignitron is sufficiently responsive for use in the welding field. If it is coupled

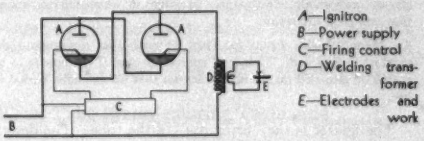

Fig. 1. Schematic diagram of "back to back" connection

with some suitable igniter firing circuit the necessary degree of over-all timing accuracy may be obtained.

A synchronous thyratron control[4] panel is commonly used with ignitrons in welding installations to supply this igniter firing control. This control panel or "brain" of the device makes possible initiation of the arc at any predetermined point on the voltage wave. Very short timing may be attained by firing only one ignitron and doing so just before the end of the positive half cycle. This procedure makes possible a conduction period much

A paper recommended for publication by the AIEE committees on electric welding and electronics. Manuscript submitted October 28, 1936; released for publication November 25, 1936.

DAVID PACKARD is a test engineer for the General Electric Company, Schenectady, N. Y. J. H. HUTCHINGS is an electrical engineer in the vacuum tube engineering department of the same company.

1. For all numbered references see list at end of paper.

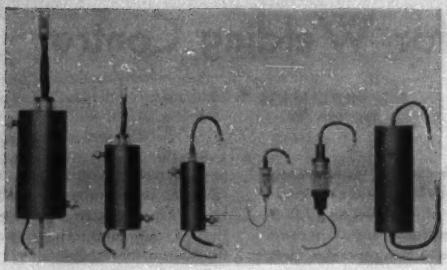

Fig. 2. Sealed-off ignitrons of the water-cooled (3 at left) and air-cooled (3 at right) types

shorter than one-half cycle. By uniformly starting the arc at one point on the voltage wave, the variability of current transients and hence of welds is minimized.

Design Problems of the Sealed-Off Tube

In the development of a line of sealed-off ignitrons the design problems appear in the following natural divisions:

1. The igniter must be properly designed and located in each tube if reliable ignition of the arc is desired.

2. A current path through the tube of good conductivity must be provided to carry the high current. Peak, average, and root-mean-square currents must all be considered.*

3. Heat removal must be sufficiently effective to limit cathode, arc stream, and anode temperatures to values at which reliable operation and good life result.

4. Manufacturing technique must be such that a vacuum-tight product is obtained. This is of course essential if the unit is to be sealed off and still maintain its vacuum over an extended period of life.

The igniter is the "firing pin" of the tube. The design that has been adopted consists of a small rod of treated silicon carbide with the part dipping in the mercury pointed to a logarithmic shape.[5] The igniter is mounted on an insulating bushing in the mercury pool, making it possible to have terminals at the ends of the tube only.

The electron current from the cathode comes from a number of small spots on the pool of mercury.[6] The first spot is started by a spark from the igniter, and it divides into more spots as the current demand is increased until at high currents the emission comes from a great many small spots, each supplying from 5 to 15 amperes. One condition for determining pool size is satisfied by providing sufficient area so that the cathode spots, starting at the igniter, do not travel to the edge of the pool and anchor on the envelope in the time allotted to a single conduction interval. If this occurs, material may be sputtered from the metal walls of the tube. This requirement is easily fulfilled in normal operation since the arc has only one-half cycle during which to travel. Another consideration at the cathode is to provide large contact area between the pool and the cathode lead for the dual purpose of current and heat conduction.

The cross-sectional area of the tube influences the maximum peak current the tube will conduct without failure. As the current density in the arc stream is increased above a certain value the voltage drop in the tube, and consequently the loss per unit current, increases rapidly. This and other considerations set a current density above which it is not practical to operate. In 550-volt welder service successful operation has been obtained with arc stream current densities exceeding 500 amperes per square inch. The envelope sizes have been selected from a preferred number series of standard seamless steel tubing, thus tending to cause peak current capacities to fall in a similar series.

The anode size is determined by both the average and root-mean-square or effective currents. The heat generated at the surface depends upon the average current. The heat generated in the conducting parts is a function of the effective current. Thus both the area and the conduction cross section must be considered. The anode lead must be designed to conduct the effective current.

Heat Removal

When conducting, a gas-filled tube has a voltage drop from anode to cathode of the same order of magnitude as the ionization potential of the gas. This voltage is roughly independent of the current being carried by the arc and in the case of these mercury-pool tubes is approximately 15 volts. This drop causes power loss which appears as heat within the tube.

A mercury-pool tube of any one design and operating under certain current and voltage conditions will perform satisfactorily only when the temperatures of the various parts lie below definite limiting values. It is particularly important to limit the mercury-vapor pressure in the tube. This pressure is determined by the temperature of the cooler parts. If the temperature limits are exceeded, current may be carried in either direction when the igniter is not energized and conduction is not desired. Bad welds may result from such failures. A tube which fails by carrying current in the forward direction is commonly said to "shoot through." One which carries current in the reverse direction is said to "arc back."

The limiting condensed-mercury temperatures of ignitrons now available lie between 50 and 125 degrees centigrade. This means that relatively small temperature differences, between some tube parts and cooling medium, are available for removal of heat.

In the case of low-power ignitrons, air cooling of both ends has been accomplished by providing good paths for conduction of heat from anode and cathode to larger and cooler external parts. An example of this type of

*The highest instantaneous value of current conducted will be referred to hereafter as peak anode current or simply peak current. Large welds require high peak currents.
Average anode current per tube is obtained by averaging the instantaneous values over the rated averaging period. This period is usually sufficiently long to include several welds and the intervening off periods. Both the size of the welds and the frequency at which they are made determine the average current. Root-mean-square current, as referred to in this paper, is measured or calculated in the usual manner considering both the time of current flow and the time off included in the rated averaging period of the tube.

cooling is seen in the 2 smaller tubes shown in figure 2. Radiation and forced ventilation are utilized to remove the heat from tubes of intermediate size. Parts of the tube, the anode in particular, are allowed to operate at high temperatures and so radiate effectively. Parts controlling mercury temperature, such as those parts in the region of the pool cathode, are cooled mainly by forced ventilation. An example of this class of ignitron is the tube on the right side of figure 2.

The amount of heat generated at the cathode of a high-current tube cannot easily be transmitted by conduction through the mercury pool and other cathode parts. It is also difficult to conduct this heat through glass side walls. Temperature drop along either of these paths may be sufficiently great to give inner or effective temperatures higher than are allowable even though the outside of the tube is kept at low temperature. This fact has caused the adoption of metal construction for higher power tubes.

Coupling the metal design with water cooling, as shown in figure 3, results in the cooling water and arc stream being separated only by about $^1/_{16}$ inch of metal, the thickness of the inner envelope. As shown in this illustration, the sides of the ignitron are cooled over their entire length by use of a water jacket. Rather close spacing between the 2 cylinders forming the jacket is used to increase water velocity and so provide better heat transfer.

Fig. 3. Cut-away view of a large water-cooled ignitron

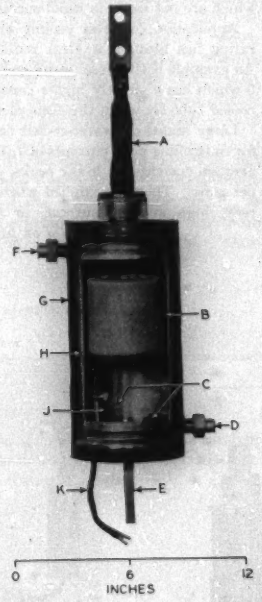

A—Anode connection
B—Anode
C—Space for mercury pool
D—Water inlet
E—Cathode connection
F—Water outlet
G—Water jacket
H—Tube envelope
J—Igniter
K—Igniter connection

In order to avoid air pockets and to keep coolest water in contact with the pool cathode, water enters at the bottom of the jacket and flows out at the top.

The top seal and the central part of the mercury pool are kept cool by use of heavy tube-end pieces, or headers, welded to the cooled envelope. In one tube of large diameter, these ends are over $^1/_8$ inch thick, thus providing a good path for heat conduction. In this way effective cooling, and hence effective control of mercury-vapor pressure, has been attained.

Corrosion and Hydrogen Diffusion With Water Cooling

Water cooling, though it solved many problems, introduced the new ones of corrosion and hydrogen diffusion.

Early developmental tube models employed ordinary steel envelopes and water jackets. Passage of water through the cooling chamber caused considerable rusting. In addition, many of the hydrogen ions* present in the water filtered through the steel envelope into the tube and soon rendered it gassy and inoperable. Ordinary steel is no effective barrier to the hydrogen ion, and while the water may be treated to prevent corrosion and diffusion this does not appear at present to be economical in welding applications. While this seepage of hydrogen through the envelope might be tolerated if the unit were being pumped continuously, it obviously cannot be permitted in sealed-off tubes.

These difficulties of corrosion and hydrogen diffusion were overcome by the use of stainless steel envelopes and jackets. This material is practically impervious to the hydrogen ion at operating temperatures. Since water comes in contact only with stainless steel and the brass pipe fittings, corrosion should be extremely slow, thus permitting very long tube life from this consideration.

Metal Tube Manufacturing Technique

Initially ignitrons were made of glass by adopting the technique then used in making hot-cathode rectifiers and thyratrons. A new glass-to-metal seal, utilizing an alloy called "fernico," and the application of thyratron control to welding introduced an entirely new technique which is now utilized in ignitron manufacture. Fernico, which is an alloy of iron, nickel, and cobalt, has an expansion characteristic which closely matches that of certain glasses.[7] It can be drawn, machined, and welded. This material makes possible strain-free glass-to-metal seals which are relatively easy to manufacture and free from leaks. All of the insulating bushings of these sealed-off ignitrons are made with such seals. The anode bushing of a large water-cooled tube is shown in figure 4.

This figure also shows some of the important welds. The fernico cup on the top is welded onto the anode lead which is designed to carry 1,500 amperes, effective value. The fernico piece on the bottom is welded onto

* Ordinary tap water has a hydrogen concentration of roughly 1×10^{-7} mole per liter.

the steel head which forms the end of the tube. This head is seam welded into a piece of seamless steel tubing forming the envelope. If a water jacket is desired, the tube envelope is flared out at each end beyond the header and a longer cylinder is seam welded on the outside as shown in figure 3. Welding machines equipped with thyratron control, using ignitron or thyratron power tubes, make these vacuum-tight welds and other welds where consistent high quality is essential. Thus ignitrons are an important part of ignitron manufacture.

Even the air-cooled tubes made mainly of glass have been manufactured with metal tube technique. The essential difference in this case is that a larger piece of glass is used between the 2 fernico seals, for the glass is the insulating bushing and tube envelope as well. Although this glass construction has been quite popular, metal tubes are being made in all except the smaller sizes where the glass involved is of about the same size as the anode bushing of a larger tube. Figure 5 shows the smallest ignitron tube before being evacuated beside an anode bushing of a larger ignitron. This tube is made from parts of a similar but larger bushing.

This new technique used in ignitron manufacture has many advantages over older methods:

1. The vacuum-tight seals are mechanically strong and provide good support for heavy anodes and leads required by high current capacity.

2. The metal construction provides good heat transfer and simplifies water cooling.

3. The manufacturing processes may be closely controlled and do not require highly skilled labor, therefore they are less costly.

4. The metal construction gives a product more accordant with industrial psychology.

Some of these construction features have promise of use in other fields. The metal-to-glass seals may be used as insulating bushings in other apparatus. The stainless-steel seam-welded water-jacket construction offers a simple cooler for heat transfer in other devices, and the welding used throughout the line exemplifies what can be done with modern welding technique.

Performance of the Tubes

These general design principles have been applied to ignitrons for a wide range of applications. All of the smaller tubes are air-cooled, and are used where the welds are either small or are made infrequently. The smallest tube is $1^1/_2$ inches in diameter and 3 inches long, yet it will control currents up to several hundred amperes. With this tube small welds such as are used in jewelry manufacture may be controlled. The demand for larger air-cooled tubes has been met with several other sizes, the largest of which will pass peak currents up to several thousand amperes, and can be used to time large welds which are not made in rapid succession.

Application of water cooling to tubes of intermediate rating has brought a great reduction in size and cost. An example is the small water-cooled unit shown in figure 6 which has a slightly higher capacity than the large air-cooled tube shown in the same picture.

Large sealed-off water-cooled tubes are now practical for controlling peak currents of 7,000 amperes or more and average currents, at lower peaks, as high as 250 amperes per tube. They are applied where either high peak current, high average current, or both are encountered.

(*Concluded on page 66*)

Fig. 4. A high-current anode bushing before seals have been made

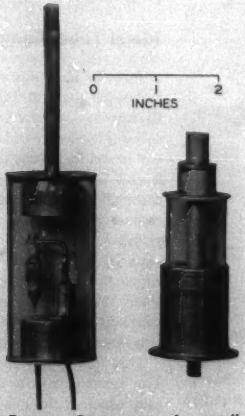

Fig. 5. Comparison of a small ignitron with the anode bushing of a larger tube

Fig. 6. A small water-cooled tube (left) that has greater current capacity than the air-cooled tube (right)

Contributions to Synchronous-Machine Theory

By A. S. LANGSDORF
FELLOW AIEE

In this paper the 2-reaction theory of synchronous machines is extended, for steady-state conditions, to present some new deductions apparently not previously known.

IT HAS long been known that the cylindrical-rotor theory, based essentially upon the concept that the synchronous impedance is a constant for all loads and for all positions of the armature winding relative to the rotor, leads to gross inconsistencies when applied to salient-pole machines. The Blondel 2-reaction theory, and its extension by Doherty and Nickle,[1] have pointed the way to numerous improvements which bring the theory much more nearly into accord with the facts, but the conclusions thus far published have stopped short of a complete presentation of some exceedingly interesting deductions. It is the purpose of this paper to point out some features, apparently not previously known, which follow quite simply and naturally from the 2-reaction theory. This treatment is here limited to steady-state operation, perhaps not as important as the transient case of sudden short circuit, but the results are nevertheless of fundamental interest.

It is desirable, partly by way of introduction, but mainly to facilitate future comparisons, to review briefly the essential features of the cylindrical-rotor theory, as applied to the case of a synchronous motor; the extension to the case of the generator then follows directly. Thus, in figure 1, let

V = terminal voltage
E = counter electromotive force or excitation voltage
I = armature current
Z_s = synchronous impedance
X_s = synchronous reactance
R_a = effective resistance
$\varphi_z = \tan^{-1} X_s/R_a$
φ = angle of phase displacement between V and I

all of these quantities referring to one phase of the winding.

The power (per phase) developed by the machine, including core loss, friction, and windage, is

$$P = VI \cos \varphi - I^2 R_a \tag{1}$$

whence

$$I^2 - \frac{V}{R_a} I \cos \varphi = -\frac{P}{R_a} \tag{2}$$

Adding to both sides of this equation the constant term $(V/2R_a)^2$, it becomes

$$I^2 + \left(\frac{V}{2R_a}\right)^2 - 2\left(\frac{V}{2R_a}\right) I \cos \varphi = \left(\frac{V}{2R_a}\right)^2 - \frac{P}{R_a} \tag{3}$$

The quantity $V/(2R_a)$ is obviously a current in phase with V, and it is a constant. Consequently the equation states that the sum of the squares of I and $V/(2R_a)$, minus twice their product times the cosine of the included angle, is a constant, provided P is constant. This suggests the ordinary cosine law of trigonometry, and indicates the well-known construction, figure 2, for the circular current locus subject to the condition of constant power.

The vector diagram, figure 1, shows further that

$$(IZ_s)^2 = V^2 + E^2 - 2VE \cos \delta \tag{4}$$

where δ is the variable torque angle, whence

$$I^2 = \left(\frac{V}{Z_s}\right)^2 + \left(\frac{E}{Z_s}\right)^2 - 2\left(\frac{V}{Z_s}\right)\left(\frac{E}{Z_s}\right) \cos \delta \tag{5}$$

Here V/Z_s is a constant current lagging behind V by angle φ_z, as in figure 3, and E/Z_s is a constant provided the excitation is held fixed. The same cosine law then shows that the current locus for a fixed excitation is a circle, figure 3, having its center at D, and it is readily shown that D is a point on the zero-power circle. It is to be particularly noted that this construction points to the conclusion that an unexcited motor ($E = 0$) can develop no power, which is not in accord with experimental facts.

Equivalent Impedance, 2-Reaction Theory

Applying the 2-reaction theory, the vector diagram takes the form of figure 4, where, as usual, ψ is the phase displacement between the armature current and the component $(-E)$ of the impressed voltage which balances the counter electromotive force. In this diagram

$$I_q = I \cos \psi \tag{6}$$
$$I_d = I \sin \psi$$

represent, respectively, the components of armature current in the transverse (cross) axis and in the direct axis of the machine; also

$$X_q = X_q' + X_l \tag{7}$$
$$X_d = X_d' + X_l$$

where X_q' and X_d' are the reaction reactances in the 2 axes; and X_l is the true leakage reactance, assumed to be the same in both axes.

From the diagram it is seen that

$$V \sin \delta = I_q X_q + I_d R_a \tag{8}$$
$$E - V \cos \delta = I_d X_d - I_q R_a \tag{9}$$

A paper recommended for publication by the AIEE committee on electrical machinery. Manuscript submitted September 8, 1936; released for publication November 30, 1936.

A. S. LANGSDORF is dean of the schools of engineering and architecture at Washington University, St. Louis, Mo.

1. For all numbered references see list at end of paper.

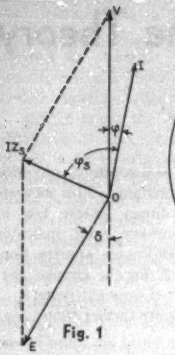

Fig. 1

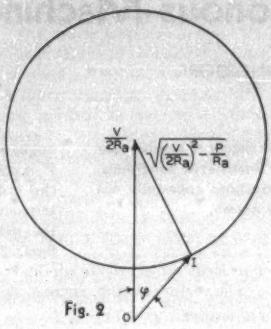

Fig. 2

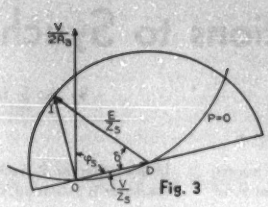

Fig. 3

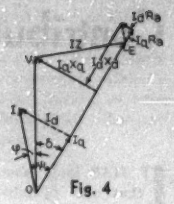

Fig. 4

which may be written in the form

$$V \sin \delta = I(X_q \cos \psi + R_a \sin \psi) = IZ_q \sin (\psi + \varphi_q) \tag{10}$$

$$E - V \cos \delta = I(X_d \sin \psi - R_a \cos \psi) = -IZ_d \cos (\psi + \varphi_d) \tag{11}$$

where

$$\left.\begin{aligned} Z_q &= \sqrt{R_a^2 + X_q^2} \\ Z_d &= \sqrt{R_a^2 + X_d^2} \\ \varphi_q &= \tan^{-1} \frac{X_q}{R_a} \\ \varphi_d &= \tan^{-1} \frac{X_d}{R_a} \end{aligned}\right\} \tag{12}$$

It is also plain from figure 4 that the equivalent impedance drop in the machine is the vector sum of V and E, that is, IZ, and

$$(IZ)^2 = (V \sin \delta)^2 + (E - V \cos \delta)^2 \tag{13}$$

Substituting equations 10 and 11 in equation 13,

$$Z^2 = [Z_q \sin (\psi + \varphi_q)]^2 + [-Z_d \cos (\psi + \varphi_d)]^2 \tag{14}$$

which is at once recognizable as the polar equation of an ellipse with Z and ψ as the dependent and independent variables.

The graph of Z as a function of ψ may be quite simply constructed as in figure 5. The positions of the major and minor axes, which define the maximum and minimum values of Z, are found by differentiating equation 14 with respect to ψ and setting the result equal to zero; thus

$$\frac{d}{d\psi}(Z)^2 = -Z_d^2 \sin 2(\psi + \varphi_d) + Z_q^2 \sin 2(\psi + \varphi_q) = 0 \tag{15}$$

which, when solved for ψ, gives

$$\tan 2\psi = \frac{Z_q^2 \sin 2\varphi_q - Z_d^2 \sin 2\varphi_d}{Z_d^2 \cos 2\varphi_d - Z_q^2 \cos 2\varphi_q} \tag{16}$$

On substituting in equation 16 the relations grouped as equation 12, this reduces to

$$\tan 2\psi = \frac{2 \tan \psi}{1 - \tan^2 \psi} = \frac{R_a}{\frac{1}{2}(X_d + X_q)} = \cot \alpha \tag{17}$$

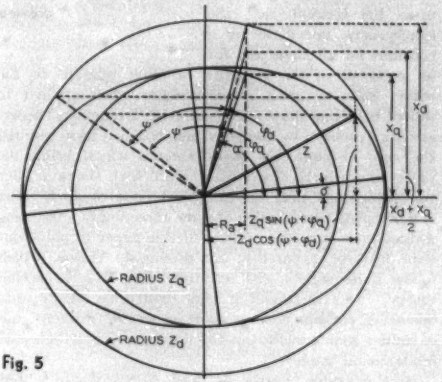

Fig. 5

or

$$\tan \psi = -\frac{\frac{1}{2}(X_d + X_q)}{R_a} \pm \sqrt{1 + \left(\frac{\frac{1}{2}(X_d + X_q)}{R_a}\right)^2} \tag{18}$$

thus defining 2 values of ψ, 90 degrees apart, one of which corresponds to the maximum, the other to the minimum, value of Z. It may be noted in passing that the major axis of the ellipse is tipped up from the horizontal axis of reference at an angle σ such that

$$\tan \sigma = \frac{Z_q \sin\left(\frac{\pi}{4} + \frac{\alpha}{2} - \varphi_q\right)}{Z_d \cos\left(\frac{\pi}{4} + \frac{\alpha}{2} - \varphi_d\right)}$$

The maximum and minimum values themselves are most simply determined by transforming equation 14 to the form

$$Z^2 = \frac{Z_d^2 + Z_q^2}{2} + \frac{Z_d^2}{2} \cos 2(\psi + \varphi_d) - \frac{Z_q^2}{2} \cos 2(\psi + \varphi_q) \tag{19}$$

which, when expanded and rearranged, using equation 12, becomes

$$Z^2 = \frac{Z_d^2 + Z_q^2}{2} - (X_d - X_q)\sqrt{R_a^2 + \left(\frac{X_d + X_q}{2}\right)^2} \times \sin (2\psi + \alpha) \tag{20}$$

where the angle α, defined by equation 17, has the meaning indicated in figure 5.

The variation of the equivalent impedance Z as a function of ψ may be studied in another way by observing from figure 5 that its complex value may be written

$$Z = -Z_d \cos(\psi + \varphi_d) + jZ_q \sin(\psi + \varphi_q)$$
$$= \left(-R_a + j\frac{X_d + X_q}{2}\right)\epsilon^{-j\psi} - j\frac{X_d - X_q}{2}\epsilon^{j\psi} \quad (21)$$

This equation has the simple geometrical interpretation shown in figure 6; that is, when $\psi = 0$, Z is made up of the directed magnitude $OA = \left(-R_a + j\frac{X_d + X_q}{2}\right)$ combined with the directed magnitude $AB = -j\frac{X_d - X_q}{2}$, giving as resultant $Z_{\psi=0} = OB = -R_a + jX_q$. For any arbitrary value of ψ, OA swings clockwise, to OA', while AB swings in a counterclockwise direction to $A'B'$, thus giving $Z = OB'$ for the particular value of ψ indicated in the diagram. It will be noted that the angle between OA' and $A'B'$ is always $2\psi - \alpha'$, where α' is the complement of the constant angle α that appears in figure 5 and which is defined by equation 17. Finally, therefore, the variation of Z may be illustrated by the extremely simple diagram, figure 7, from which

$$Z^2 = (OC)^2 + (CP)^2 - 2(OC)(CP)\cos(2\psi - \alpha')$$
$$= \frac{Z_d^2 + Z_q^2}{2} - (X_d - X_q)\sqrt{R_a^2 + \left(\frac{X_d + X_q}{2}\right)^2} \times \cos(2\psi - \alpha') \quad (22)$$

which is the same as equation 20.

The variation of Z as a function of ψ may now be shown as in figure 8, which is constructed from figure 7 by assigning various values to ψ and plotting the results in rectangular co-ordinates. It is seen that Z passes through 2 complete cycles of values for each cycle in the value of ψ, but the curve is not a simple harmonic function of ψ as might at first glance be supposed to be the case; it fluctuates between limits equally spaced on either side of the ordinate $\sqrt{R_a^2 + (X_d + X_q)^2}/2$, but the upper loops are slightly longer than the lower ones, as may be seen from the fact that in figure 7 the arc through C, having O as center, divides the small circle into 2 unequal parts, so that $a > b$ in figure 8.

Otherwise expressed, when the square root of such an expression as equation 22 is evaluated by means of the binomial theorem, terms appear that involve the ascending powers of the term $\cos(2\psi - \alpha')$, which means that the curve of figure 8 really consists of a fundamental (of double frequency) and a series of higher harmonics.

It has long been known that the reactance of a salient-pole machine varies cyclically when measured at a series of successively different positions of the field poles relatively to the winding, but it has heretofore been assumed[3] that the reactance is expressible as

$$X = X_{aver} + X' \cos(2\theta + \gamma)$$

where X_{aver} is the average value over an arc of one pole pitch, X' is the maximum deviation from the average, and θ is the angle, in electrical degrees, measured from an arbitrarily selected reference point on the armature surface. The analysis here presented shows conclusively that this assumption is not strictly correct, though it becomes very nearly so if X_d and X_q are not greatly different.

Current Locus, Constant Excitation

Equations 8 and 9, when solved for I_q and I_d, yield the following relations:

$$I_q = \frac{VX_d \sin\delta - R_a(E - V\cos\delta)}{X_dX_q + R_a^2} = \frac{VZ_d\cos(\delta - \varphi_d) - ER_a}{X_dX_q + R_a^2} \quad (23)$$

$$I_d = \frac{VR_a \sin\delta + X_q(E - V\cos\delta)}{X_dX_q + R_a^2} = \frac{VZ_q\sin(\delta - \varphi_q) + EX_q}{X_dX_q + R_a^2} \quad (24)$$

The form of these 2 expressions suggests a simple geo-

Fig. 6

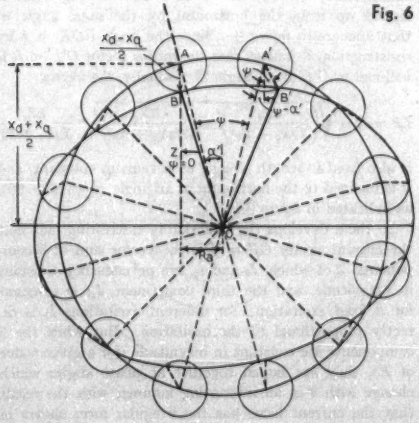

Fig. 7 (right)

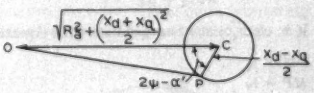

Fig. 8 (below)

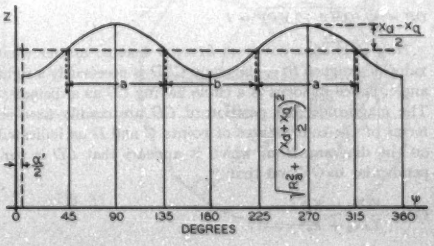

metrical construction for the current locus if E is maintained constant. Thus, in figure 9, OV represents the fixed terminal voltage and $-OE$ is the excitation voltage, fixed as to magnitude, but displaced from OV by the variable torque angle δ. The lines $OD = (VZ_d)/(X_dX_q + R_a^2)$ and $OC = (VZ_q)/(X_dX_q + R_a^2)$, representing the constant coefficients that appear in equations 23 and 24, are drawn at the fixed angles φ_d and φ_q, respectively, with OV. Accordingly, when perpendiculars are dropped from the points D and C upon the line OE, it follows that

$$OK = \frac{VZ_d}{X_dX_q + R_a^2} \times \cos(\delta - \varphi_d)$$

and

$$GC = \frac{VZ_q}{X_dX_q + R_a^2} \times \sin(\delta - \varphi_q)$$

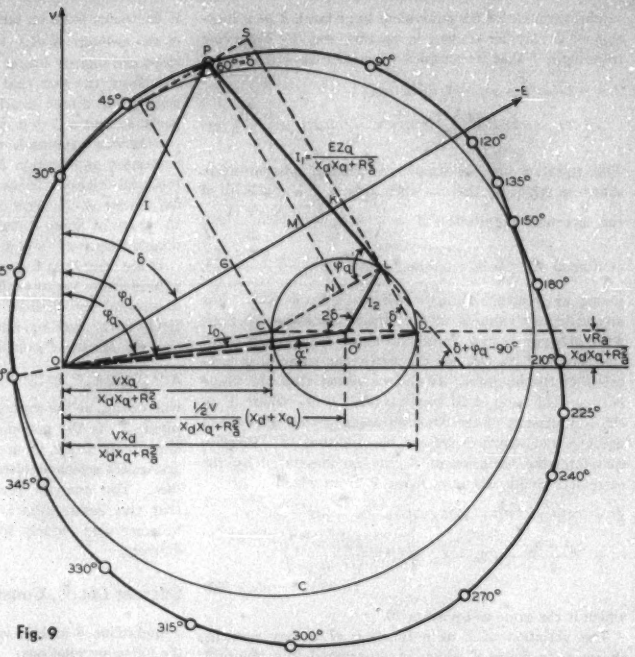

Fig. 9

On subtracting from OK the fixed length

$$KM = LN = \frac{ER_a}{X_dX_q + R_a^2}$$

and adding to GC (which must be considered negative in the diagram since $\delta < \varphi_q$) the fixed length

$$CQ = NP = \frac{EX_q}{X_dX_q + R_a^2}$$

it is clear that in accordance with equations 23 and 24

$$OM = I_q$$
$$MP = I_d$$

and

$$OP = \sqrt{(OM)^2 + (MP)^2} = I$$

Now it is apparent from figure 9 that no matter what value is assigned to δ, the angle CLD is necessarily a right angle, hence its locus is a circle having CD as a diameter. The magnitude and position of CD are readily fixed in terms of the co-ordinates of points C and D as indicated on the diagram, from which it appears that CD is perpendicular to OV and that

$$CD = \frac{V(X_d - X_q)}{X_dX_q + R_a^2}$$

The center of the circle CLD is at O', which has the co-ordinates

$$\left(\frac{V}{X_dX_q + R_a^2}, \frac{X_d + X_q}{2}, \frac{VR_a}{X_dX_q + R_a^2}\right)$$

consequently the line $OO' = I_0$ is fixed in length and is tipped up from the horizontal by the same angle α' that appears in figure 6. Since the angle $CDK = \delta$ by construction, it follows that the radius vector $O'L = I_2$ is inclined to $O'C$ at an angle 2δ. Finally, the vector

$$LP = I_1 = \sqrt{\left(\frac{ER_a}{X_dX_q + R_a^2}\right)^2 + \left(\frac{EX_q}{X_dX_q + R_a^2}\right)^2} = \frac{EZ_q}{X_dX_q + R_a^2}$$

is also fixed in length so long as E remains constant, and it is inclined to the horizontal at an angle $(\delta + \varphi_q - 90)$, as indicated in figure 9.

So there develops the remarkably interesting fact that the current vector $OP = I$ is the vector sum of 3 components, 2 of which, I_0 and I_2, are permanently constant in magnitude, and the third component, I_1, is constant for a fixed excitation; for different excitations I_1 is directly proportional to the excitation. But while the 3 components are constant in magnitude (for a given value of E), they are linked together at phase angles which change with δ in an interesting manner, with the result that the current locus has the irregular form shown in

figure 9, which has been drawn for the condition $E = (^5/_4)V$, and $Z_d/Z_q = {}^5/_3$.

Expressed in complex notation,

$$I = I_0 + I_2 + I_1 \tag{25}$$

where

$$I_0 = \frac{V}{X_d X_q + R_a^2}\sqrt{R_a^2 + \left(\frac{X_d + X_q}{2}\right)^2}\, e^{j\alpha'} = I_0(\cos\alpha' + j\sin\alpha') \tag{26}$$

$$I_2 = -\frac{V}{X_d X_q + R_a^2}\cdot\frac{X_d - X_q}{2}\, e^{-j2\delta} = -I_2(\cos 2\delta - j\sin 2\delta) \tag{27}$$

$$I_1 = -j\frac{EZ_q}{X_d X_q + R_a^2}\, e^{-j(\delta+\varphi_q)} = -I_1[\sin(\delta+\varphi_q) + j\cos(\delta+\varphi_q)] \tag{28}$$

These results may at this point be compared with those of the cylindrical rotor theory. To do so it is only necessary to impose the condition that $Z_d = Z_q = Z_s$, or $X_d = X_q = X_s$. When this is done, the vector I_2 vanishes; the points O' and D, figure 9, coalesce with point C, which then has the co-ordinates

$$\frac{VX_s}{X_s^2 + R_a^2} = \frac{V}{Z_s}\sin\varphi_s$$

and

$$\frac{VR_a}{X_s^2 + R_a^2} = \frac{V}{Z_s}\cos\varphi_s$$

which are the same as those of point D, figure 3; and the irregular current locus of figure 9 degenerates to a simple excitation circle of the type shown in figure 3. This circle is indicated in figure 9 as curve C', having its center at C and a radius equal to LP.

To construct the current loci corresponding to different values of the excitation voltage E, it is only necessary to modify the dimensions of triangle LPN in the desired ratio; otherwise all construction lines remain the same as in figure 9. The effect of varying E from zero to $(^7/_2)V$, by steps of $V/2$, is shown in figure 10.

Figure 10 brings out vividly some extremely interesting characteristics. One of them, known to be an experimental fact, is that an unexcited motor ($E = 0$) is capable of carrying a theoretical maximum load corresponding to the power circle P_1, drawn tangent to the small circle $E = 0$. The remaining power circles, indicated as P_2, P_3, . . . P_8, are all drawn tangent to the curves of constant excitation, and the points of tangency have as their loci the curve marked "stability limit."

Another point of interest is the shape of the excitation curves, which bulge outward to the left, and descend below the zero power circle more than they rise within it. This is a natural consequence of the difference between the action of the machine as a generator (outside the circle $P = 0$) and the action as a motor within the circle $P = 0$. On the right, beyond the stability limit, the curves are flattened when E is large, they develop a concave depression as E becomes smaller, and finally, for sufficiently small values of E, this depression becomes a re-entrant loop.

The nature of this re-entrant loop is shown somewhat more clearly in figure 11, where the points O and O' and the small circle on CD as a diameter have the same meaning as in figure 9. The small triangle shown in successive positions in figure 11 is the same as triangle LPS, figure 9; for values of δ from zero to 150 degrees, inclusive, the triangle is cross-hatched; in the remaining positions it is left blank to avoid confusion.

The interesting linkage of the vectors OO', $O'L$, and LP of figure 9 led to the construction of a working model in which the 2 movable vectors were ruled with India ink on strips of transparent sheet celluloid, suitably pivoted together. Placing these links in the positions corresponding to $\delta = 0$, and then moving them bit by bit as the torque angle was gradually increased from zero to 360 degrees, it was possible to photograph the model in successive positions, thereby yielding a film suitable for use in a moving-picture projector. It is quite interesting to observe this animated vector diagram, which has been

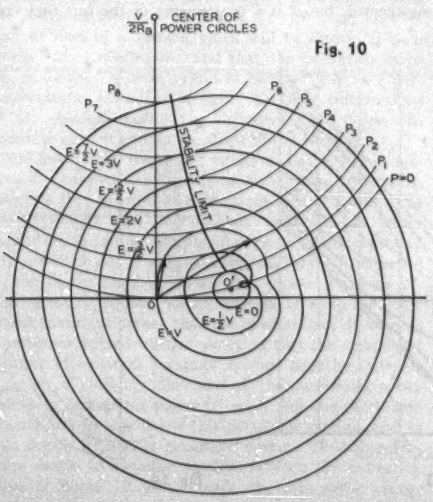

Fig. 10

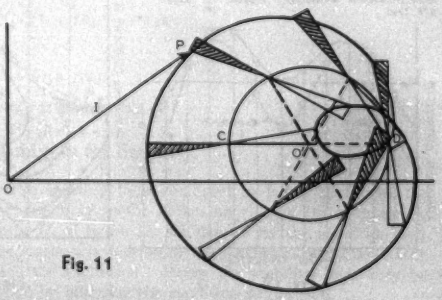

Fig. 11

so made that the excitation locus is drawn as the vectors move.

While no particular importance attaches to the fact, it may be noted that the excitation which marks the point of division between those excitation loops wholly exterior to circle CD, and those which lie partly inside it, is determined by the consideration that

$$I_1 = \frac{EZ_q}{X_dX_q + R_a^2} = CD = \frac{V(X_d - X_q)}{X_dX_q + R_a^2}$$

or

$$E = \frac{V(X_d - X_q)}{Z_q} \qquad (29)$$

and that the point of osculation between this limiting loop and the circle occurs at a value of δ such that $\delta = 180 - \alpha'$.

When the armature current $I(= OP)$, figure 11, is plotted in rectangular co-ordinates as a function of the torque angle δ, curve 1 of figure 12 results. For the sake of comparison, there has been drawn on the same diagram, as curve 2, the variation of armature current when $E = 0$, the ordinates being taken directly from the circle CD of figure 11. Curve 2 will be recognized in terms of the now familiar slip test; it is the envelope of an oscillogram of the armature current taken with the field unexcited and the rotor turned at a speed differing slightly from synchronism.* Curve 1 of figure 12 is then the envelope of the armature current oscillogram taken in the same manner but with the field magnetized to a small fraction of normal excitation. It can be seen from figure 10 that in the case of both curves 1 and 2 the machine is acting as a motor for somewhat less than half of the interval corresponding to slipping a double pole pitch, and is a generator the remainder of the time; but in the case of curve 1, whose polar equivalent has the re-entrant loop projecting outside the zero power circle, the initial motor action is followed by a brief period of generator action, then by another short motoring interval, before the full period of generator action sets in.

One additional feature worthy of consideration is the effect of negative excitation, that is, of reversing the field polarity. It is obvious that if E is reversed in sign, the effect is to reverse the phase of vector LP, figure 9; but figure 11 shows that for any position of vector $O'L$ the excitation triangle LPS necessarily appears in 2 diametrically opposite positions, hence the excitation loci with reversed excitation are identical in form with those shown in figures 10 and 11, but the sequence of values is reversed. In any case the locus passes through a region lying within the zero-power circle and motor action is possible.

The V-Curves

The V-curves constructed from figure 10 are just as distinctively different from those usually derived from the cylindrical rotor theory as are the excitation curves of figure 10 in comparison with the customary circles (figure 3). The V-curves are shown in figure 13, and it will be seen that those portions lying below the stability line H_2 resemble quite closely the curves determined by actual test. Curve H_1, passing through the lowest points of the curves, defines the condition for unity power factor; unlike the corresponding curve derived from the cylindrical-rotor theory, it does not have a point of minimum excitation at a value of armature current greater than zero; on the contrary, the minimum excitation consistent with unity power factor occurs when $E = V$.

While it is quite true that any discussion of the V-curves lying above the stability curve H_2 is academic in the sense that these portions of the curves are beyond the practical limits of operation, they still possess several points of theoretical interest. One of them is that the curve corresponding to zero power lies partly *inside* a curve corresponding to a positive amount of (motor) power. This result, when first encountered, was quite unexpected, but it is a consequence of the fact that the

* The slip test seems to have been first developed and used by K. H. Hagg; see *L'Eclairage Electrique*, 11, IX, 1909; also article by J. A. Schouten, *Elektrotechnische Zeitschrift*, volume 31, page 877, 1910.

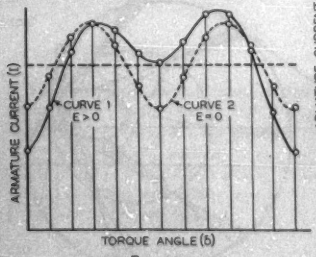

Fig. 12

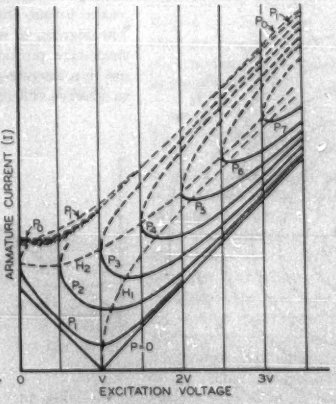

Fig. 13

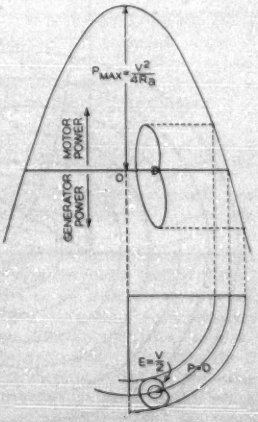

Fig. 14

Fig. 15

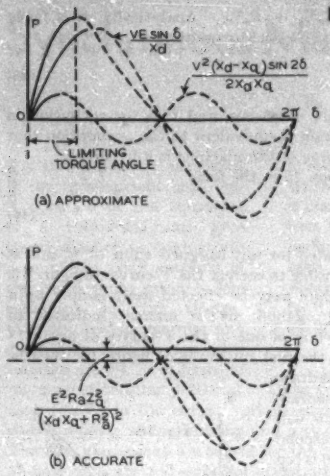

excitation loops of figure 10 are indented for values of the torque angle approaching 180 degrees; some indication that this phenomenon actually occurs is to be found in the experimental curves published[3] by Douglas, Engeset, and Jones; the effect is likewise indicated by J. F. H. Douglas's closing remarks in the discussion of that paper.

Perhaps the simplest way to visualize the relations represented by the V-curves is to regard them as contour lines of a surface which has as co-ordinates the dependent variable I and the 2 independent variables E and P. When this idea is carried back to figure 10, it follows that the power circles $P = O$, P_1, P_2, . . . etc., are likewise contour lines of a surface which will be shown to be a paraboloid of revolution; and that the excitation loops are sections of general cylinders having their axes perpendicular to the plane of figure 10. The intersections of the paraboloid and the cylinders then define the armature current and fix the shape of the V-curve.

The proof that the power circles of figure 10 are sections of a paraboloid follows immediately from equation 1, which is the equation of a parabola having I and P as the dependent and independent variables, all other quantities, including the phase angle φ, being constant. The condition $\cos \varphi = 1$ obviously defines the diametral section of the paraboloid, which is shown as figure 14. The vertex of the paraboloid, corresponding to the theoretical maximum power that the machine can develop as a motor, is defined by the condition that the right-hand member of equation 3 cannot become negative, whence $P_{max.} = V^2/(4R_a)$. The base of the paraboloid corresponds to zero motor power ($P = 0$), but the paraboloid extends indefinitely below this particular section, and in that region represents generator power. It is therefore quite simple to visualize conditions when the excitation loops of figure 10 pass outside the zero-power circle; the geometrical meaning is that the excitation cylinder intersects the power paraboloid below the "base" of the latter. The curve of intersection corresponding to $E = (1/2)V$ is shown in vertical projection in figure 14.

Condition for Unity Power Factor

Inspection of figure 4 shows that when $\varphi = 0$ (i. e., $\cos \varphi = 1$), $\psi = \delta$. Consequently equations 10 and 11 become

$$V \sin \delta = IZ_q \sin (\delta + \varphi_q) \tag{30}$$

$$E - V \cos \delta = -IZ_d \cos (\delta + \varphi_d) \tag{31}$$

from which

$$\sin \delta = \frac{EIX_q}{(V - IR_a)^2 + I^2X_dX_q} \tag{32}$$

$$\cos \delta = \frac{E(V - IR_a)}{(V - IR_a)^2 + I^2X_dX_q} \tag{33}$$

Now it will be seen from figure 9 that when the current vector $I(= OP)$ is in phase with V the algebraic sum of the quadrature components of I_0, I_2, and I_1 is zero. Hence, from equations 26, 27, and 28,

$$I_0 \cos \alpha' - I_2 \cos 2\delta - I_1 \sin (\delta + \varphi_q) = 0 \tag{34}$$

and

$$I \cos \alpha' = \frac{V}{X_dX_q + R_a^2} \cdot \frac{X_d + X_q}{2} \tag{35}$$

$$I_2 = \frac{V}{X_dX_q + R_a^2} \cdot \frac{X_d - X_q}{2} \tag{36}$$

$$I_1 = \frac{EZ_q}{X_dX_q + R_a^2} \tag{37}$$

From equations 30 and 31 it is now possible to express $\cos 2\delta$ and $\sin (\delta + \varphi_q)$ in terms of E, I, and the machine constants, and on substituting all these relations in equation 34 the final result is

$$[(V - IR_a)^2 + I^2X_dX_q]^2 = E^2[(V - IR_a)^2 + I^2X_q^2] \tag{38}$$

which is the complete equation of curve H_1, figure 13. It is obviously an equation of the fourth degree, but if it may be assumed that IX_d and IX_q are not large in comparison with $(V - IR_a)$ it is a reasonable approximation to write

$$E^2 = (V - IR_a)^2 + I^2X_dX_q$$

or

$$E^2 = V^2 + I^2X_dX_q \tag{39}$$

which is a hyperbola.

Condition for Stability

The stability limit indicated in figure 10 (drawn for the region of motor action only), and its counterpart, curve H_3 of figure 13, are defined by the condition that the machine is developing the maximum power consistent with the excitation. Hence the stability limit may be found by imposing the condition $dP/d\delta = 0$.

In order to express without any simplifying approximations the power developed (P) as a function of the torque angle (δ), use may be made of the concept underlying the 2-reaction theory that the armature winding is subjected to the action of 2 fictitious sets of field poles in addition to the actual poles. One of these fictitious sets of poles lines up with the actual poles and either magnetizes or demagnetizes the latter depending upon the phase conditions; the other fictitious set of poles lies midway between the actual poles. The cross-magnetizing component of armature current, I_q, reacts directly with the net flux in the direct axis to produce torque and power, while the direct component of current, I_d, reacts directly with the transverse flux. Referring to the particular phase conditions represented in figure 4, it follows that the power developed is given by

$$P = (E - I_d X_d)I_q + (I_q X_q)I_d$$
$$= EI_q - I_q I_d(X_d - X_q) \tag{40}$$

Substituting for I_q and I_d the values given by equations 23 and 24, the complete expression for the power is found to be

$$P = \frac{VEZ_d Z_q{}^2 \cos(\delta - \varphi_d) + VER_a Z_q(X_d - X_q)\sin(\delta - \varphi_q) - V^2 Z_d Z_q(X_d - X_q)\sin(\delta - \varphi_q)\cos(\delta - \varphi_d) - E^2 R_a Z_q{}^2}{(X_d X_q + R_a{}^2)^2} \tag{41}$$

whence the accurate expression for the stiffness or coupling factor is

$$\frac{dP}{d\delta} = \frac{VER_a Z_q(X_d - X_q)\cos(\delta - \varphi_q) - VEZ_d Z_q{}^2 \sin(\delta - \varphi_d) - V^2 Z_d Z_q(X_d - X_q)\cos(2\delta - \varphi_d - \varphi_q)}{(X_d X_q + R_a{}^2)^2} \tag{42}$$

If, in equations 41 and 42 the approximation is made that terms involving R_a may be neglected, and that correspondingly $\varphi_d = \varphi_q = 90$ degrees, they reduce to

$$P = \frac{VE}{X_d}\sin\delta + \frac{V^2(X_d - X_q)}{2X_d X_q}\sin 2\delta \tag{43}$$

$$\frac{dP}{d\delta} = \frac{VE}{X_d}\cos\delta + \frac{V^2(X_d - X_q)}{X_d X_q}\cos 2\delta \tag{44}$$

which are the same as those derived by Doherty and Nickle by a somewhat different procedure, but which has the disadvantage that it masks some of the finer points of the theory. The differences between the accurate and the approximate expressions are shown graphically in figure 15.

Effect of Saturation

The full effect of saturation of the magnetic circuit is apparently beyond the scope of any reasonably simple analysis. Approximate methods have been proposed by Doherty and Nickle,[1] and also by Blondel.[4,5] Ordinarily it is sufficiently accurate to assume that the saturation in the armature iron and in the path of the cross field is negligible, and that the significant saturation occurs in the pole cores.[1] These assumptions lead to the conclusion that the reactances X_d and X_q may be treated as constant, from which it follows that in figure 9 the only component vector which is affected by saturation is $LP = (EZ_d)/(X_d X_q + R_a{}^2)$. Analytically, it is fairly accurate to write Froehlich's equation

$$E = \frac{aF}{b + F} \tag{45}$$

where a and b are constants, and F is the excitation in ampere-turns, which is equivalent to the assumption that the saturation curve of the machine is a hyperbola.

Writing equation 45 in the form

$$F = \frac{bE}{a - E} \tag{46}$$

F may be computed for any assigned value of E, and it then becomes possible to correct the V-curves of figure 13. The same procedure may be effected quite simply by a purely graphical method in the manner indicated in figure 16. A portion of one of the V-curves of figure 13 is reproduced in the first quadrant of figure 16, and the saturation curve is drawn in the fourth quadrant. For any excitation voltage, E_1, the corresponding field excitation is represented by F_1, and the 2 values of current corresponding thereto are I_1 and I_1', which may then be laid off to the left of F_1 in the third quadrant. The effect is seen to be to stretch the V-curves, the amount of stretch increasing rapidly as the field excitation becomes greater, provided the saturation is sufficient to yield a definite knee to the saturation curve.

Fig. 16

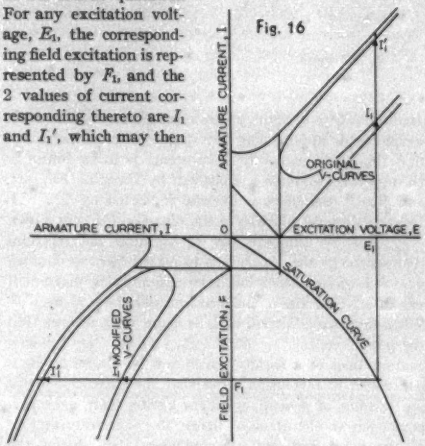

References

1. Synchronous Machines—I, R. E. Doherty and C. A. Nickle. AIEE Transactions, volume 45, 1926, page 912.

2. Variable Armature Leakage Reactance in Salient-Pole Synchronous Machines, V. Karapetoff. AIEE Transactions, volume 45, 1926, page 729.

3. Complete Synchronous Motor Excitation Characteristics, J. F. H. Douglas, E. D. Eugeset, and R. H. Jones. AIEE Transactions, volume 44, 1925, page 164.

4. Synchronous Motors and Converters, A. Blondel (translated by C. O. Mailloux). 1913, part 3.

5. *Revue General d'Electrique*, volume 5, 1919, pages 811 and 843.

Synchronous Machine With Solid Cylindrical Rotor

By C. CONCORDIA
ASSOCIATE AIEE

H. PORITSKY
Member Am. Math. Soc.

In this paper a rigorous mathematical analysis of a synchronous machine with solid cylindrical rotor is presented. The analysis embodies a departure from the usual method of considering machine performance by means of circuit theory, and presents an attack from the point of view of field-distribution theory. Such an analysis is desirable, for it provides a definite means of considering the effect of eddy currents in the solid iron rotor.

IN this paper are presented the development and application of the equations of a cylindrical-rotor synchronous machine, taking into account the eddy currents in the solid iron rotor. The equations for the electromagnetic field in the rotor and air gap due to stator and rotor currents are set up in terms of the magnetic vector potential. These field equations are then related to the circuit voltage equations of a symmetric 3-phase stator winding and a single field winding. The final expressions are solved for the case of symmetric 3-phase currents and constant speed and applied to the calculation of 3-phase short-circuit current, field-current build-up, and flux decay.

In previous treatments of electrical machines, circuit analysis has been the predominant tool. Some of the machine constants have been computed with the aid of coefficients found from flux plots, or by taking into account nonuniform distribution of current in conductors, or the actual circuits replaced by equivalent sinusoidally distributed windings, but always the actual analysis has been of a circuit. In this paper a departure is made by considering the behavior of solid-rotor synchronous machines from the point of view of field-distribution theory. This is particularly desirable since no definite circuit in which the rotor eddy currents must flow presents itself in the actual machine. Previous analyses of solid-rotor machine performance have represented the rotor by an equivalent circuit computed from steady-state eddy-current relations. The present treatment by going back to fundamentals and avoiding the short cuts of the ordinary engineering circuit theory thus presents an opportunity to test the validity of such representation for calculations of transient phenomena. The differential equations governing the field distributions are set up from Maxwell's equations. These are expressed in terms of a magnetic vector potential, introduced in order to correlate them for the rotor and stator, since as ordinarily expressed in terms of electric intensity they are valid only for systems at rest.

Assumptions

The analysis is based on the following assumptions:

1. The rotor permeability is a constant.
2. The stator permeability is infinite.
3. The presence of slots is neglected in both rotor and stator, a uniform equivalent gap being used.
4. The machine is so long that end effects may be neglected; thus the field is 2-dimensional.
5. The circuit conductors are of negligible depth and are distributed on the rotor and stator surfaces (see also assumption 3).
6. The rotor and stator surface curvatures are small compared to the air gap length.
7. To take account of the end effects and slot leakage, provisional corrective terms (so-called leakage inductances) are included in the circuit equations. In correlating the calculations with test results these terms are found to be very important and it is intended to investigate the effect of eddy currents in the leakage fluxpaths as the next step in the development of the theory.

It may be stated broadly that the present purpose is to compute correctly the effect of eddy currents in the main flux path. The results are here compared to similar calculations for a laminated rotor machine, so that the effect of the solid rotor body may be seen directly.

The Field Equations

Maxwell's equations for the electromagnetic field, for the present case, and for axes fixed in the medium, are

$$\nabla \times H = 0.4\pi i \tag{1}$$

$$\nabla \times E = -10^{-8} \frac{\partial}{\partial t} B = -\mu 10^{-8} \frac{\partial}{\partial t} H \tag{2}$$

$$\nabla \cdot B = 0 \quad (\nabla \cdot H = 0), \quad \nabla \cdot E = 0 \tag{3}$$

where all quantities are in practical cgs units

In conducting regions they yield

$$\nabla^2 E = 4\pi\mu 10^{-9} \frac{\partial}{\partial t} i \tag{4a}$$

or, since

$$i = \lambda E, \tag{4b}$$

$$\nabla^2 E = 4\pi\lambda\mu\, 10^{-9} \frac{\partial}{\partial t} E = \beta^2 \frac{\partial}{\partial t} E = \beta^2 \rho E \tag{5a}$$

while in nonconducting regions

$$\nabla^2 E = 0 \tag{5b}$$

At surfaces (such as the rotor and stator surfaces) where current sheets are flowing, the last equations are replaced

A paper recommended for publication by the AIEE committee on electrical machinery. Manuscript submitted October 30, 1936; released for publication December 3, 1936.

C. CONCORDIA is an engineer in the central station department of the General Electric Company, Schenectady, N. Y. H. PORITSKY is in the engineering general department of the same company.

1. For all numbered references, see list at end of paper.

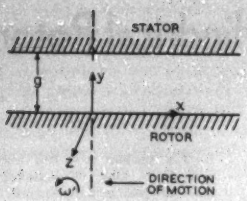

Fig. 1. Orientation of co-ordinate system in the rotor

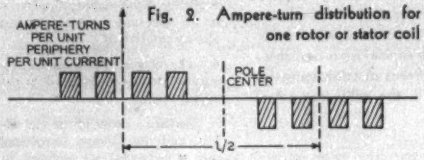

Fig. 2. Ampere-turn distribution for one rotor or stator coil

by a boundary condition specifying the discontinuity in the normal derivative of E. Thus if along a surface (y = constant) there is a current sheet in the z-direction of linear intensity I, then:

$$\Delta H_z = -0.4\pi I \tag{6a}$$

where ΔH_z is the increment or discontinuity in H_z.

From equations 6a and 2

$$\frac{\partial}{\partial t}(\Delta H_z) = \Delta \frac{\partial}{\partial t} H_z = -10^8 \Delta \left(\frac{1}{\mu}\frac{\partial E}{\partial y}\right) = -0.4\pi \frac{\partial}{\partial t} I \tag{6b}$$

For long rotors, neglecting end effects, the currents and induced voltages may be assumed to point in the z-direction (i.e., to be parallel to the rotor axis) and to be functions only of x, y; while the magnetic field is normal to the z axis and also independent of z. Therefore, let

$$E_z = E = E(x, y)$$

and obtain from equation 2

$$\frac{\partial}{\partial t} H_x = -\frac{10^8}{\mu}\frac{\partial}{\partial y} E \qquad \frac{\partial}{\partial t} H_y = +\frac{10^8}{\mu}\frac{\partial E}{\partial x} \tag{7}$$

This shows that the magnetic field can be expressed in terms of a single (now scalar) function E as far as its changes are concerned. However, this induced electric field E is not invariant under motions relative to the axes employed. Therefore, to compute the proper induced voltages in coils in motion with respect to the field, as e.g., in the stator coils due to the motion of the rotor and to take account of static magnetic fields, we introduce a vector magnetic potential ψ defined in the original system of co-ordinates by the relation

$$\psi = \int_{-\infty}^{t} E dt \tag{8}$$

whereupon equations 2, 3, and 5a may be replaced by

$$H = -\frac{10^8}{\mu} \nabla \times \psi \tag{9}$$

$$\nabla \cdot \psi = 0 \tag{10}$$

$$\nabla^2 \psi = 4\pi\mu 10^{-8} i \tag{11}$$

and boundary condition of equation 6b by

$$\Delta\left(\frac{1}{\mu}\frac{\partial \psi}{\partial y}\right) = 4\pi 10^{-8} I \tag{12}$$

The vector potential can be defined by this set of equations and since it points in the z-direction still offers the possibility of expressing the magnetic and electric fields in terms of a single scalar function. This function (or rather, $-10^8\ \psi$) may be interpreted as the total flux enclosed between the point in question and a reference point and is in fact perfectly analogous to the flux linkage of circuit theory.

The Circuit Currents

As explained under the assumptions, it will be assumed throughout the following that a proper mean radius has been chosen both for rotor and stator and that smooth cylindrical surfaces of these mean radii actually replace the slotted rotor and stator surfaces. The armature and field windings are considered to be ribbon-like and to lie on these surfaces. Developing the rotor and stator surfaces along parallel plane surfaces in accordance with assumption 6, and replacing the rotor and stator by semi-

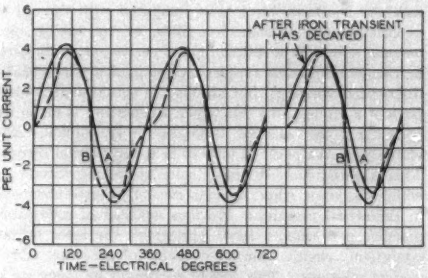

Fig. 3. Short-circuit current of a turbine generator
Phase-a switch closed at instant of minimum linkage
Case 1 — $l_s = 0.18$, $\mu = 100$
A—With solid rotor *B*—With laminated rotor

infinite blocks and the rotation ω' about the z-axis by an equivalent translation, we arrive at figure 1. Suppose the rotor is rotating with angular velocity ω'. Since Maxwell's equations are for axes fixed in conducting materials, we take x, y, z axes fixed in the rotor as shown and let x_1, y, z be similar axes fixed relative to the stator. Thus

$$x_1 = x - r\int \omega' dt \tag{13}$$

Consider one rotor coil with current I_r, and several stator coils with currents I_a, I_b, ... The actual ampere-turn distribution due to these currents may be as shown

in figure 2. The rectangular blocks correspond in position to the slots. (It should, of course, be understood that figure 2 is only representative and the number, height, and spacing of the ampere-turn blocks depend on the machine being analyzed.) If the equation of this curve is $a(x)$, then the ampere turns due to rotor current I_r is $I_r a(x)$. The function $a(x)$ is periodic of period l, and is odd about the pole center and even about a line midway between adjacent poles.

Hence

$$a(x) = \sum_{n=1,3,5,\ldots} A_n \cos n\alpha x, \quad \alpha = \frac{2\pi}{l} \tag{14}$$

Similar ampere turn curves apply to each stator coil. For one of these coils, e.g., we have:

Ampere turns $= I_a\, b\,(x_1)$

where b is again odd and even as above, and

$$b(x_1) = \sum_{n=1,3,\ldots} B_n \cos n\alpha x_1 \tag{15}$$

If there are 3 stator coils with similar winding distributions, obtained from that of coil a by translating through 120 and 240 electrical degrees, the total stator ampere turns are

$$I_s(x_1) = I_a b(x_1) + I_b\left(x_1 + \frac{l}{3}\right) + I_c b\left(x_1 - \frac{2l}{3}\right) \tag{16}$$

To find the field, we express the stator ampere turns also in terms of x, i.e., in terms of co-ordinates fixed with respect to the rotor and then solve the equations

$$\nabla^2\psi = 0 \tag{17}$$

in the gap, and

$$[\nabla^2 - \beta^2 p]\psi = 0 \tag{18}$$

in the rotor for the vector potential ψ, picking the solution which: (a) is zero for $y = -\infty$; (b) is continuous at the rotor (and stator) surface; and (c) is such that at the rotor and stator surfaces $y = 0$, $y = g$, $-\Delta H_x = 0.4\pi$ times the surface current density.

By equation 12 these conditions are:

$$\frac{\partial}{\partial y}\psi\Big|_{y=0+} - \frac{1}{\mu}\frac{\partial}{\partial y}\psi\Big|_{y=0-} = 4\pi\, 10^{-9} I_r(x) \tag{19}$$

$$-\frac{\partial}{\partial y}\psi\Big|_{y=g-} = 4\pi\, 10^{-9} I_s(x) \tag{20}$$

The induced electric field E can now be found from the relation

$$E = \frac{\partial}{\partial t}\psi \tag{21}$$

Coil Voltage Equations

With E known, the voltage equations for the coils may be obtained by adding to the applied voltage the integral of the induced voltage E over the length of the coil. For the rotor coil:

$$RI_r = e_r + Zk\int_0^l a(x)E(x)dx \tag{22}$$

To treat the stator coils which are now moving relative to the x, y, z system, recall that the function $-10^8\psi$ is a measure of the instantaneous flux linking any point.

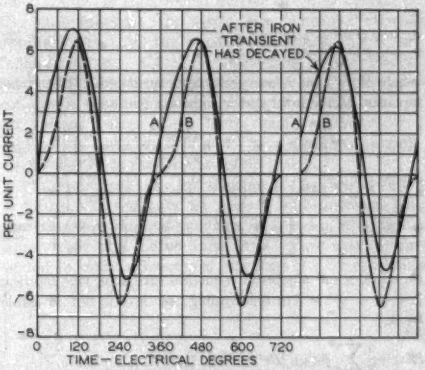

Fig. 5. Short-circuit current of a turbine generator

Phase-a switch closed at instant of minimum linkage
Case 2—$l_s = 0.09$, $\mu = 100$
A and B—Same as for figure 3

Thus to find the induced electromotive force in a coil in motion relative to the x, y, z system, e.g., a stator coil fixed in the x_1, y, z axes of the stator, we need only express ψ in terms of x_1, y, z and then use an equation similar to equation 21:

$$E(x_1) = \frac{\partial}{\partial t}\psi\,(x_1, y, t) \tag{23}$$

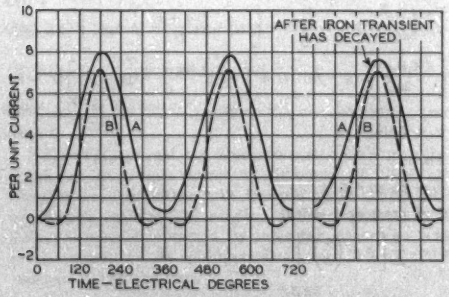

Fig. 4. Short-circuit current of a turbine generator

Phase-a switch closed at instant of maximum linkage; other conditions same as for figure 3

For stator coil a the electromotive force equation is

$$r_s I_a = e_a + Zk \int_0^l b(x_1) E(x_1) dx_1 \tag{24}$$

Similar equations hold for the other 2 stator coils.

Current With Constant Speed

We now assume constant rotor speed. Then from equation 13,

$$\begin{aligned} x_1 &= x - r(\omega' t + \gamma/k) \\ &= x - (\omega t + \gamma) r/k \end{aligned} \tag{25}$$

or

$$\alpha x_1 = \alpha x - \omega t - \gamma$$

To simplify the solution we represent the applied voltages by the relations

$$\left.\begin{aligned} e_a &= C e^{j\omega t} + C' e^{-j\omega t} + e_0 \\ e_b &= C \alpha^2 e^{j\omega t} + C' \alpha e^{-j\omega t} + e_0 \\ e_c &= C \alpha e^{j\omega t} + C' \alpha^2 e^{-j\omega t} + e_0 \end{aligned}\right\} \tag{26}$$

where $\alpha = e^{j2\pi/3} = -1/2 + j\sqrt{3}/2$ is the primitive cube root of unity. In the case of balanced 3-phase sinusoidal voltages, C, C' might be chosen so as to yield real voltages e or else C' might be made to vanish and the real parts of the resulting complex voltages and currents identified with the physical voltages and currents.

The stator currents may be expressed in similar form as

$$\left.\begin{aligned} I_a &= D e^{j\omega t} + D' e^{-j\omega t} + i_0 \\ I_b &= \alpha^2 D e^{j\omega t} + \alpha D' e^{-j\omega t} + i_0 \\ I_c &= \alpha D e^{j\omega t} + \alpha^2 D' e^{-j\omega t} + i_0 \end{aligned}\right\} \tag{27}$$

where D, D', and i_0 are yet to be determined. Then from equation 16 the total stator ampere-turns are:

$$\begin{aligned} I_s(x_1) = D e^{j\omega t} &\left[b(x_1) + \alpha b\left(x_1 + \frac{l}{3}\right) + \alpha^2 b\left(x_1 + \frac{2l}{3}\right)\right] + \\ D' e^{-j\omega t} &\left[b(x_1) + \alpha b\left(x_1 + \frac{l}{3}\right) + \alpha^2 b\left(x_1 + \frac{2l}{3}\right)\right] + \\ i_0 &\left[b(x_1) + b\left(x_1 + \frac{l}{3}\right) + b\left(x_1 + \frac{2l}{3}\right)\right] \end{aligned} \tag{28}$$

or, after some algebraic reduction utilizing the relation $1 + \alpha^n + \alpha^{2n} = 3$ or 0 according as n is or is not divisible by 3,

$$\begin{aligned} I_s(x) = \frac{3}{2} \sum_{n=0,\,\pm 6,\ldots} B_{|n+1|} &\left[D e^{j(n+1)(\alpha x - \gamma) - j n \omega t} + \right. \\ &\left. D' e^{-j(n+1)(\alpha x - \gamma) + j n \omega t}\right] + i_0 \frac{3}{2} \sum_{n=\pm 1,\,\pm 3,\ldots} B_{|3n|} \left[e^{j3n(\alpha x - \omega t - \gamma)} + \right. \\ &\left. e^{-j3n(\alpha x - \omega t - \gamma)}\right] \end{aligned} \tag{29a}$$

In terms of x_1, or referred to the stator,

$$\begin{aligned} I_s(x_1) = \frac{3}{2} \sum_{n=0,\,\pm 6,\ldots} B_{|n+1|} &\left[D e^{j\omega t + j(n+1)\alpha x_1} + D' e^{-j\omega t - j(n+1)\alpha x_1}\right] + \\ &\frac{3}{2} \sum_{n=\pm 1,\,\pm 3,\ldots} B_{|3n|} \left[e^{j3n\alpha x_1} + e^{-j3n\alpha x_1}\right] \end{aligned} \tag{29b}$$

From equation 29 it is seen that if $i_0 = 0$ and D and D' are constants, I_s may be described either as a sinusoidal wave $e^{\pm j(\alpha x - \gamma)}$ stationary relative to the rotor but modulated by a function fixed relative to the stator or as a sinusoidal wave stationary relative to the rotor plus harmonic waves which travel along the rotor with speeds only slightly less than that of the rotor.

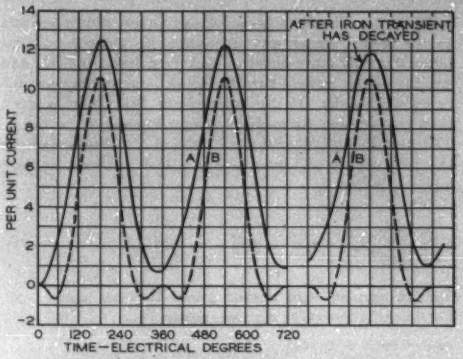

Fig. 6. Short-circuit current of a turbine generator

Phase-a switch closed at instant of maximum linkage; other conditions same as for figure 5

Now suppose the I_r, D, D' vary as e^{pt}, i.e., substitute $I_r e^{pt}$ for I_r, etc., where the new I_r, D, D', and i_0 are constants, and solve the field equations 17, 18, subject to the boundary conditions expressed by equations 19 and 20, and with the current distributions expressed by equations 14 and 29a simultaneously present. From the resulting ψ find E by means of equations 21 and 23, then substitute in equations 22 and 24 to obtain the circuit voltage equations (see appendix II). Considering only the fundamental components, there result the following 4 linear equations in I_r, D, D', and i_0,

$$\left[(R + Lp) + \frac{KA_1^2}{aQ} p \cosh ag \right] I_r + \frac{3KA_1B_1p}{2aQ} (De^{-j\gamma} + D'e^{j\gamma}) = e_r \tag{30a}$$

$$\left[\frac{KA_1B_1e^{j\gamma}}{2aQ} (p + j\omega) \right] I_r + \left[r_s + \frac{(uq + v)}{Q} (p + j\omega) \right] D = C \tag{30b}$$

$$\left[\frac{KA_1B_1e^{-j\gamma}}{2aQ} (p - j\omega) \right] I_r + \left[r_s + \frac{(uq + v)}{Q} (p - j\omega) \right] D' = C' \tag{30c}$$

$$[r_s + k_0 p] i_0 = e_0 \tag{30d}$$

where

$$K = 2\pi 10^{-9} Z l k$$

$$Q = q \cosh ag + \sinh ag$$

$$q = \frac{\beta}{\mu\delta} \left[p + \left(\frac{a}{\beta}\right)^2 \right]^{\frac{1}{2}}$$

$$u = l_s \cosh ag + \frac{3KB_1^2}{2a} \sinh ag$$

$$v = l_s \sinh ag + \frac{3KB_1^2}{2a} \cosh ag$$

In these equations there have been included field and armature leakage inductances which were omitted from the previous steps of the development in order to avoid undue complication. Solving equations 30 for the currents I_r, D, D' in terms of the applied voltages, we find

$$\Delta I_r = a^3[(p^2+\omega^2)(uq+v)^2 + r_s Q[r_s Q + 2p(uq+v)]]e_r - \frac{3}{2}KA_1B_1ap[r_sQ(Ce^{-j\gamma} + C'e^{j\gamma}) + (uq+v)[(p-j\omega)Ce^{-j\gamma} + (p+j\omega)C'e^{j\gamma}]] \quad (31a)$$

$$\Delta D = -\frac{1}{2}KA_1B_1ae^{j\gamma}[(p^2+\omega^2)(uq+v) + r_s(p+j\omega)Q]e_r + \left[(R+Lp)a^2Q[(p-j\omega)(uq+v) + r_sQ] + KA_1^2ap\left\{\frac{1}{2}(p-j\omega)[uQ+\cosh a_2(uq+v)] + r_sQ\cosh a_2\right\}\right]C + KA_1^2ap\frac{3KB_1^2}{4a}(p+j\omega)e^{2j\gamma}C' \quad (31b)$$

$$\Delta D' = -\frac{1}{2}KA_1B_1ae^{-j\gamma}[(p^2+\omega^2)(uq+v) + r_s(p-j\omega)Q]e_r + \left[(R+Lp)a^2Q[(p+j\omega)(uq+v) + r_sQ] + KA_1^2ap\left\{\frac{1}{2}(p+j\omega)[uQ+\cosh a_2(uq+v)] + r_sQ\cosh a_2\right\}\right]C' + KA_1^2ap\frac{3KB_1^2}{4a}(p-j\omega)e^{-2j\gamma}C \quad (31c)$$

where

$$\Delta = (R+Lp)a^2[(p^2+\omega^2)(uq+v)^2 + r_sQ[r_sQ+2p(uq+v)]] + KA_1^2ap[(p^2+\omega^2)u(uq+v) + r_s[Q(r_s\cosh a_2 + up) + \cosh a_2(uq+v)p]] \quad (31d)$$

Electrical Torque

The torque may best be computed by considering the interaction of the stator current with the normal component of flux at the stator surface. We then have in cgs units (ergs),

$$\text{Torque} = -0.1\,rZk\int_0^l I_s(x_1)\,[H_y(x_1)]_{y=g}dx_1 \quad (32)$$

Considering only the fundamental component, we have

$$I_s(x_1) = \frac{3}{2}B_1[De^{j(\omega t+ax_1)} + D'e^{-j(\omega t+ax_1)}] \quad (33)$$

$$[H_y(x_1)]_{y=g} = \frac{0.4\pi A_1}{Q}I_r\sin(ax_1+\omega t+\gamma) + \frac{1.2\pi B_1(\cosh a_2 + q\sinh a_2)}{2jQ}[De^{j(ax_1+\omega t)} - D'e^{-j(ax_1+\omega t)}] \quad (34)$$

If I_s and H_y are real, the expressions above will give the instantaneous torque correctly; however, if they are complex we must either take the real parts before substituting in equation 32 or else add to equation 32 a similar expression obtained by replacing either the field or the current by its conjugate imaginary and take the real part of half the sum.

The Operational Solution and Its Evaluation

In the above solution time entered as e^{pt} (or $e^{p(t+j\omega)}$ where p was a constant. The solution can be adapted, however, to the study of arbitrary applied voltages and in particular to various transient problems by regarding them as operational expressions. Thus if the expressions for I_r, D, D' in equation 31 be considered to operate on the unit function, the result represents the currents obtained when, in the applied voltages, e_r, C, C' are replaced by e_r1, $C1$, $C'1$. According to the modern interpretation of operational calculus the operational solution is obtained merely by superposing the solutions for various values of p. More exactly the operational expressions just described are to be viewed as the coefficients of e^{pt}/p in the Bromwich integral.

The equivalent time functions cannot be directly found in tables. To evaluate the operational expressions, note that they are rational fractions in p and q, q being the square root of a factor linear in p. They may be converted to rational fractional functions of q by expressing p in terms of q, as

$$p = \left(\frac{a}{\beta}\right)^2[(\mu q)^2 - 1] \quad (35)$$

If the resulting functions of q are now expanded in partial fractions the result is of the form

$$\sum_n \frac{a_n}{q-q_n}$$

where q_n are the q roots of the denominator Δ expressed in terms of q. Replacing q by its equivalent in p, there is obtained

$$f(p) = \sum_n \frac{b_n}{\left[p+\left(\frac{a}{\beta}\right)^2\right]^{\frac{1}{2}} - c_n} \quad (36)$$

In this form $f(p)1$ may be evaluated (it will be noted that the operational expressions in p correspond to the

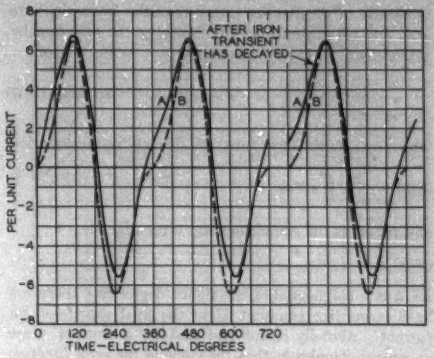

Fig. 7. Short-circuit current of a turbine generator

Phase-a switch closed at instant of minimum linkage
Case 3 — $l_s = 0.09$, $\mu = 1{,}000$
A and *B*—Same as for figure 3

integrand of the Fourier rather than the Bromwich integral, and thus operate on $p1$, that is on the unit impulse, rather than on 1) by the formula[1]

$$\frac{1}{(p+\rho)^{\frac{1}{2}}+c}\,1 = \frac{1}{c^2-\rho}\left[e^{-\rho t}\,erf(\rho t)^{\frac{1}{2}} - ce^{(c^2-\rho)t}erfc(ct^{\frac{1}{2}})\right] \quad (37)$$

where $erf(x)$ is the error function, defined by the equation

$$erf(x) = \frac{2}{\sqrt{\pi}}\int_0^x e^{-x^2}dx$$

and $erfc(x)$ is the complementary error function

$$erfc(x) = 1 - erf(x)$$

As Δ is a polynomial of the eighth degree in q there will be 8 terms like equation 37 in the final expression for current. Actually it is found that the q roots of Δ are in general complex so that the value of the error function of $(ct^{\frac{1}{2}})$ cannot be found in tables but must be computed by expansion in series.

It is of interest to indicate the degree of complexity of the result and its simplification as affected by further assumptions:

1. In general an eighth degree equation in q must be solved.
2. If the field resistance R is zero, the degree reduces to 6.
3. If the armature resistance r is zero, only a cubic need be solved.
4. If both field and armature resistance are zero, the denominator is reduced to linear factors.
5. If the $(p\psi)$ terms of the stator induced voltage are neglected in comparison to the $(\omega\psi)$ or "generated" voltage terms, a fourth degree equation must be solved.
6. If in addition to assumption 5 the field resistance is neglected, only a quadratic equation need be solved.

Applications to 3-Phase Short Circuits

As an example of the application of equations 31 the 3-phase short circuit current of a turbine-generator from no load has been computed. In order to simplify the work the armature and field circuit resistances have been neglected. This should not affect the result very much within the first few cycles.

For this condition the armature current equations may be reduced to:

$$\Delta D = \left[-(p-j\omega)\left\{\left(LaQ+\frac{1}{2}KA_1{}^2\cosh a\right)(uq+v) + \frac{1}{2}KA_1{}^2uQ\right\} + (p+j\omega)\frac{1}{2}KA_1{}^2\frac{3}{2}\frac{KB_1{}^2}{a}\right]jVe^{j\gamma} \quad (38a)$$

$$D' = \text{conjugate of } D \quad (38b)$$

where

$$\Delta = (p^2+\omega^2)[La(uq+v) + KA_1{}^2u](uq+v) \quad (38c)$$

D may be at once evaluated by formula 37 since the 6 q-roots of Δ are evident by inspection.

The current for a solid-rotor machine has been compared directly with that for a similar machine with laminated rotor in order to show clearly the effect of the solid iron.

Case 1

Figures 3 and 4 show the results for a turbine-generator of normal design. Figure 3 is for short circuit at the instant of zero flux linkage in phase a ($\gamma = 90°$), while figure 4 is for short circuit at the instant of maximum flux linkage in phase a ($\gamma = 0$). The principal constants of this machine are:

Number of poles = 4
Speed = 1,800 rpm
$\pi Z/2l$ = 1.91 = ratio of length to diameter
$2g/l$ = 0.0425 = ratio of air gap to pole pitch
Rotor λ = 57,200 (ohms per centimeter cube)$^{-1}$
L = 0.05 per unit (corresponding to field leakage = $\frac{3}{2}\left(\frac{B_1}{A_1}\right)^2 0.05$ = 0.09 per unit)
l_s = 0.18 per unit
Rotor μ = 100

Case 2

Figures 5 and 6 show the effect of reducing the armature leakage l_s to half its previous value, or to 0.09 per unit, all other constants remaining unchanged.

Case 3

Figures 7 and 8 show the effect of a higher permeability. For this case,

l_s = 0.09 per unit
μ = 1,000

The expressions for current in the 3 cases given are, with normal full-load current as the unit,

Case 1. $l_s = 0.18$, $\mu = 100$

$$i_a = (4.24 - 1.75F_c + 1.02F_s)\cos\gamma - (3.58 + 0.20e^{9.91t}\,erfc(30.8t^{\frac{1}{2}}))\times \cos(\omega t+\gamma) + (-0.46 + 1.29F_c + 0.12F_s)\cos(2\omega t+\gamma) + (-0.84 + 1.02F_c + 1.75F_s)\sin\gamma + 1.18e^{114.4t}erfc(10.7t)^{\frac{1}{2}} \sin(\omega t+\gamma) - (0.33 + 0.12F_c - 1.29F_s)\sin(2\omega t+\gamma) \quad (39a)$$

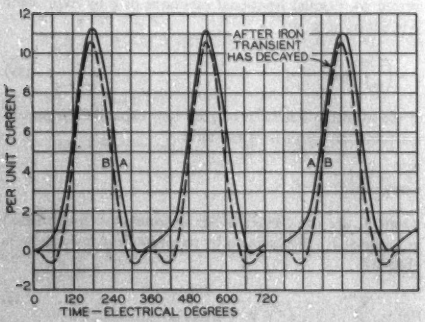

Fig. 8. Short-circuit current of a turbine generator

Phase-a switch closed at instant of maximum linkage; other conditions same as for figure 7

Case 2. $l_a = 0.09, \mu = 100$

$$i_a = (5.60 - 3.51F_c + 4.09F_s)\cos\gamma - (5.30 + 0.25e^{1.43\frac{1}{2}}erfc(38.2i^{\frac{1}{2}}))\times \cos(\omega t + \gamma) + (-0.05 + 2.80F_c - 1.41F_s)\cos(2\omega t + \gamma) + (-2.58 + 4.09F_c + 3.51F_s)\sin\gamma + 4.15e^{2.93i}erfc(18.1i^{\frac{1}{2}}) \sin(\omega t + \gamma) - (1.60 - 1.41F_c - 2.80F_s)\sin(2\omega t + \gamma) \quad (39b)$$

Case 3. $l_a = 0.09, \mu = 1{,}000$

$$i_a = (3.14 - 0.24F_c + 2.43F_s)\cos\gamma - 5.29\cos(\omega t + \gamma) + (2.15 + 0.19F_c - 1.53F_s)\cos(2\omega t + \gamma) + (-0.52 + 2.43F_c + 0.24F_s)\sin\gamma + 0.95e^{2.29i}erfc(57.4i^{\frac{1}{2}}) \sin(\omega t + \gamma) - (0.42 - 1.53F_c - 0.19F_s)\sin(2\omega t + \gamma) \quad (39c)$$

where F_c, F_s are the Fresnel integrals defined by the equations

$$F_c = \int_0^{xt} \frac{\cos x\,dx}{(2\pi x)^{\frac{1}{2}}}, \quad F_s = \int_0^{xt} \frac{\sin x\,dx}{(2\pi x)^{\frac{1}{2}}} \quad (40)$$

The Fresnel integrals, rather than error functions as might be expected from formula 37, are present since with reasonable values of μ the significant q roots have very nearly equal real and imaginary components and

$$erf(xe^{\pm j\pi/4}) = \sqrt{2}e^{\pm j\pi/4}\,[F_c(x^2) \mp j\,F_s(x^2)]$$

This relation may be shown as follows:

Let

$$y^2 = \mp jz$$

then at

$$y = xe^{\pm j\pi/4}$$

and

$$z = x^2$$

$$erf(xe^{\pm j\pi/4}) = \frac{2}{\sqrt{\pi}}\int_0^{xe^{\pm j\pi/4}} e^{-y^2}dy = e\sqrt{2}^{\mp j/4}\int_0^{x^2}\frac{e^{\mp jz}dz}{\sqrt{2\pi z}}$$

$$= \sqrt{2}\,e^{\pm j\pi/4}\int_0^{x^2}\frac{(\cos z \mp j\sin 2)dz}{\sqrt{2\pi z}} = \sqrt{2}e^{\pm j\pi/4}[F_c(x^2) \mp jF_s(x^2)]$$

Tables of both the error function and the Fresnel integral are given in reference 7.

The coefficients of the trigonometric functions in equations 39 have been plotted in Figs. 9, 10, 11 so that they may be compared directly to the corresponding coefficients for the laminated-rotor machine without the necessity of considering the instant of short circuit.

For a laminated rotor ($\lambda = 0$) the short-circuit current equations reduce to

CASE 1

$$i_a = 2.23\cos\gamma - 3.59\cos(\omega t + \gamma) + 1.36\cos(2\omega t + \gamma) \quad (41a)$$

CASE 2

$$i_a = 3.11\cos\gamma - 5.28\cos(\omega t + \gamma) + 2.17\cos(2\omega t + \gamma) \quad (41b)$$

CASE 3

$$i_a = 3.08\cos\gamma - 5.27\cos(\omega t + \gamma) + 2.19\cos(2\omega t + \gamma) \quad (41c)$$

These last equations are in the same form as that given by Doherty and Nickle in a previous paper.[3]

Inspection of figures 9, 10, 11 shows the expected reduction in second-harmonic current; a slight reduction

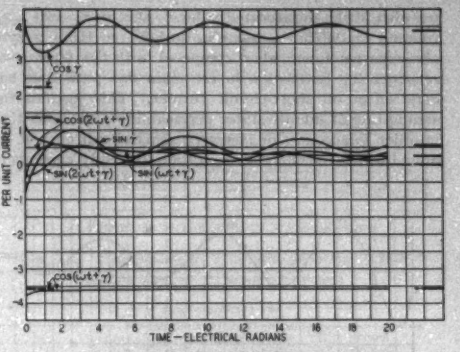

Fig. 9. Coefficients of trigonometric functions in expression for short-circuit current of solid-rotor turbine generator, case 1

Dashed lines are for machine with laminated rotor

for the unsaturated case ($\mu = 1{,}000$) and a great reduction for $\mu = 100$, which corresponds roughly to a small degree of saturation. It is interesting to note that the "fundamental" component of current is practically unaffected by the rotor eddy currents and is a function principally of the assumed values of field and armature-leakage reactance. The constant values approached by the coefficients are indicated on the figures and are very closely realized after a few cycles. We observe that although the expressions for current are somewhat complicated the general effect of the rotor eddy currents is simply to produce a more nearly sinusoidal wave shape of current and an effective phase shift. This phase shift is indicated by the presence of sine terms in the current equations 39 in addition to the cosine terms of the laminated rotor case (equations 41). Therefore according to equations 39 there is no switching angle which will completely eliminate the d-c component and result in a perfectly symmetric current.

The results further show that in the laminated-rotor machine the current is not affected appreciably by changes in rotor permeability in the range $\mu > 100$, while even for $\mu = 10$ the change is not great. For example, for $l_a = 0.18$,

$$\mu = \infty,\ i = 2.18\cos\gamma - 3.55\cos(\omega t + \gamma) + 1.37\cos(2\omega t + \gamma) \quad (42a)$$

$$\mu = 10,\ i = 2.46\cos\gamma - 3.64\cos(\omega t + \gamma) + 1.18\cos(2\omega t + \gamma) \quad (42b)$$

for $l_a = 0.09$,

$$\mu = \infty,\ i = 3.07\cos\gamma - 5.26\cos(\omega t + \gamma) + 2.19\cos(2\omega t + \gamma) \quad (43a)$$

$$\mu = 10,\ i = 3.42\cos\gamma - 5.40\cos(\omega t + \gamma) + 1.98\cos(2\omega t + \gamma) \quad (43b)$$

These currents indicate a 2.5 per cent decrease in transient reactance and a 38 per cent decrease (these changes are in

per cent of the unsaturated values; that is, x_d' (sat.)/x_d' (unsat.) = 0.975; x_d (sat.)/x_d (unsat.) = 0.62) in synchronous reactance when compared with the formula of reference 2. Saturation in the main flux path thus has little effect on short-circuit current. This justifies the assumption of infinite stator permeability and shows that in order to account for increased short-circuit current we must include the effect of saturation and eddy currents in the leakage paths. The magnitude of the short-circuit current shown by tests cannot be ascribed wholly to a "subtransient" reactance; it must be accounted for in part by a decrease in transient reactance (or field and armature leakage reactance) due to saturation.

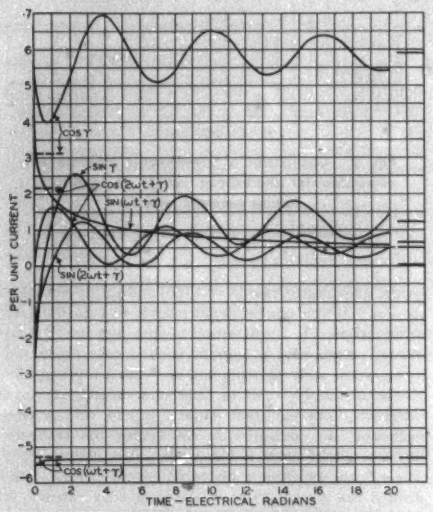

Fig. 10. Coefficients of trigonometric functions in expression for short-circuit current of solid-rotor turbine generator, case 2

Dashed lines are for machine with laminated rotor

The subtransient effect has been calculated from figures 9, 10, and 11 by comparing the magnitudes of the oscillatory component of current extrapolated to zero time with those after the iron transient has died out. The subtransient reactance computed on this basis is about 85 or 90 per cent of the transient reactance for $\mu = 100$ and about 97 per cent for $\mu = 1{,}000$. This indicates the importance of taking account of saturation and eddy currents in the leakage paths. In the present work field and armature leakage reactances have been assumed as constant quantities unaffected by the eddy currents, but the effect of eddy currents on the leakage reactances will be shown later.

Field Current Build-Up

As a second application of the general equations developed in this paper, the field current on sudden application of field voltage (with open-circuited armature) has been determined. The operational expression for field current is:

$$I_r = \frac{Qe_r}{QR + p\left(QL + \frac{KA_1^2}{a}\cosh ag\right)} \tag{44}$$

Taking $\mu = 100$ and solving equation 44, we obtain, for a solid rotor,

$$I_r = 1 + 0.0054\, e^{47.8t}\, erfc\,(21.8t^{\frac{1}{2}}) - 0.507\,[e^{(-0.214+j0.053)}\, erfc\,(0.452\, e^{j1.44t^{\frac{1}{2}}}) + e^{(-0.214-j0.053)}\, erfc\,(0.452\, e^{-j1.44t^{\frac{1}{2}}})] \tag{45a}$$

and for a laminated rotor,

$$I_r = 1 - e^{-t/4.34} \tag{45b}$$

Figure 12 shows the computed currents for both a laminated and solid rotor. The curve for the solid rotor case may be approximately represented by an equation of the form

$$I_r = 1 - 0.89e^{-t/4.35} - 0.11\, e^{-t/0.39} \tag{45c}$$

showing that a representation of the solid rotor by an equivalent short-circuited winding is in this case satis-

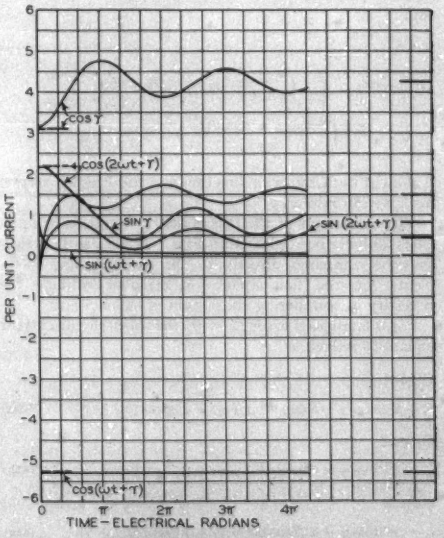

Fig. 11. Coefficients of trigonometric functions in expression for short-circuit current of solid-rotor turbine generator, case 3

Dashed lines are for machine with laminated rotor

factory. If the curve of figure 12 is regarded as a single exponential function, the time constant (determined as the time required to reach $(1 - e^{-1})$ of its final value) is 11 per cent less than that for a laminated rotor.

The transient problem of a stationary magnetic circuit linked with a single coil has been presented in a somewhat more simplified form by at least 2 previous writers.[3,4] Here we have taken account of the actual flux distribution in the iron and gap and of the distribution of the field winding, but since the whole effect of rotor eddy currents is seen from figure 12 to be rather small (at least for $\mu > 100$), the results in the case of field build-up show no great discrepancies from their work.

Flux Decay

A third application of the theory has been to the determination of the rate at which the flux changes following a sudden change in stator current. In the example given here we consider the field to be open-circuited and compute the flux decay following opening of the stator circuit. This will correspond to the decay of the quadrature axis component of flux.

From equation 49 it follows that for sudden changes in stator current there is the operational expression:

$$\psi \text{ is proportional to } \frac{\cosh ag + q \sinh ag}{q \cosh ag + \sinh ag} \qquad (46)$$

Here we are not concerned with the absolute magnitude but only with the shape of the flux-time curve. For a

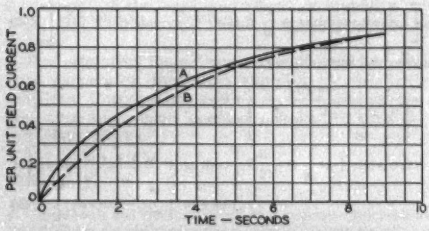

Fig. 12. Field current of a turbine generator with solid rotor, upon sudden application of field voltage

A—With solid rotor *B*—With laminated rotor

machine for which $2g/l = 0.051$ and $l_s = 0$, we obtain the equations of flux decay (per unit initial value): for $\mu = 1{,}000$,

$$\psi = 0.985\, e^{3.1\cdot 3t}\, erfc\,(4.67t^{\frac{1}{2}}) - 0.007\, erfc\,(0.032t^{\frac{1}{2}}) \qquad (47a)$$

for $\mu = 100$,

$$\psi = 1.048\, e^{3.13t}\, erfc\,(1.48t^{\frac{1}{2}}) - 0.071\, erfc\,(0.10t^{\frac{1}{2}}) \qquad (47b)$$

Note that the flux drops immediately to 98 per cent of its initial value, the drop representing that portion of the quadrature axis flux which did not link the rotor but was

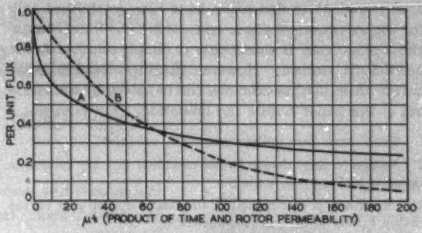

Fig. 13. Flux decay in a turbine generator, upon sudden removal of armature current

A—Quadrature-axis flux
B—Exponential through value $1/e$

only in the air gap. Although the expressions appear rather complicated it becomes evident by inspection that, with less than about 5 per cent error, a very simple relation exists between the flux at any time and the assumed permeability. That is, we may assume the flux to be a function of the product of permeability and time (see figure 13), so that the time constant is inversely proportional to the permeability.

Steady State Impedances

In order to show the relation between the design factors used in the present theory and the circuit constants of ideal synchronous machine theory,[5] we shall find the expression for synchronous impedance. From either equation 30*b* with $p = 0$ and $I_r = 0$, or equation 31*b* with $p = 0$ and $e_r = 0$,

$$\frac{C}{D} = r_s + j\omega\left[l_s + \frac{3KB_1^2}{2a}\left(\frac{\cosh ag + \mu^{-1}\sinh ag}{\mu^{-1}\cosh ag + \sinh ag}\right)\right]$$

Thus

$$\text{Synchronous Reactance} = \omega\left[l_s + \frac{3KB_1^2}{2a}\left(\frac{1 + \mu^{-1}\tanh ag}{\mu^{-1} + \tanh ag}\right)\right]$$

Similarly, from equations 53 the field self-inductance[6] may be recognized as

$$L + \frac{KA_1^2}{a}(\mu^{-1} + \tanh ag)^{-1}$$

Conclusions

In order to account completely for the observed phenomena of turbine-alternator transient performance and to compute correctly the behavior under specified terminal conditions it may be necessary to include the effects of the slots, of harmonics, of saturation, of hysteresis, of eddy currents, of the rotor surface curvature and of their influence not only on the main flux path but also on the leakage flux paths. For this reason the present paper should be regarded as presenting merely a first step in the complete solution of the general problem. Also, the

final equations of this paper have been established only for the symmetric 3-phase case. This was done because the 3-phase case is susceptible to simple solution by the operational method. However, many problems in addition to those used as examples can be solved by the methods of this paper despite this limitation. For example:

1. Short circuit from any symmetric load condition
2. Sudden (or any) change in field excitation with any symmetric armature load
3. Calculation of flux change, in addition to current and voltage change, for any of the other cases solved
4. Sudden change of load impedance (switching)
5. Prescribed change of terminal voltage.
6. Transient torque and forces for any of the conditions listed above
7. Negative-sequence reactance
8. Current for continuous load pulsation
9. Speed-torque relation for a solid rotor machine running as an induction motor
10. Eddy current losses

From the results of the calculations the following specific conclusions may be drawn:

1. Saturation in the main flux path does not affect appreciably the magnitude of the short-circuit current.
2. Eddy currents in the main body of the solid rotor may account for a 10 to 15 per cent reduction in subtransient reactance below transient reactance.
3. The larger difference between transient and subtransient reactance shown by tests must be due to (*a*) retaining ring saturation and eddy currents; (*b*) tooth tip saturation (and eddy currents in case of the rotor teeth).
4. Eddy currents in the solid rotor may account for about a 10 per cent decrease in the apparent field open circuit time constant.
5. The effective time constant of the quadrature axis flux varies inversely as the rotor permeability (at least in the range of permeability greater than 100).

Appendix I—Symbols and Nomenclature

H = magnetic intensity vector
i = current-density vector
E = electric-intensity (voltage-gradient) vector
B = magnetic flux-density vector
t = time
λ = specific conductivity
μ = permeability
$\beta^2 p = \beta^2 \dfrac{\partial}{\partial t} = 4\pi\lambda\mu 10^{-9} \dfrac{\partial}{\partial t}$
x, x_1, y, z are co-ordinate directions as shown in figure 1; x and x_1 tangential, y radial, and z axial; x, y, z are fixed in the rotor while x_1 is fixed in the stator
ψ = vector magnetic potential
ω' = angular velocity of rotor (see figure 1)
r = radius of rotor
I = coil currents; I_r rotor coil current; I_a, I_b, . . . stator coil currents; I_s resultant of all stator ampere-turns
l = length along rotor surface of 2π electrical radians or twice pole pitch
a = $2\pi/l$
A_n, B_n are coefficients of Fourier series for the ampere turn distributions
R = rotor-coil resistance
L = rotor coil leakage inductance
r_s = stator coil resistance
l_s = stator coil leakage inductance in the direct (or quadrature) axis
l_0 = zero phase sequence stator coil leakage inductance
e = applied voltage; e_a = voltage applied to coil a; e_r = voltage applied to rotor coil, etc.
k = number of pairs of poles
ω = electrical angular velocity = $k\omega'$
γ = angle by which the rotor "leads" the stator
C, C', c_0 = coefficients of complex components of stator terminal voltage
D, D', i_0 = coefficients of complex components of stator current
g = air-gap length
Z = machine axial length
$K = 2\pi 10^{-9} Z l k$
$q = \dfrac{\beta}{\mu a}\left[p + \left(\dfrac{a}{\beta}\right)^2\right]^{\frac{1}{2}}$
$Q = q \cosh ag + \sinh ag$
$u = l_s \cosh ag + \dfrac{3KB_1^2}{2a} \sinh ag$
$v = l_s \sinh ag + \dfrac{3KB_1^2}{2a} \cosh ag$
$2V$ = magnitude of open-circuit armature phase voltage

Appendix II

The solutions of the field equations 17 and 18, subject to the boundary conditions expressed by equations 19 and 20, and considering only the fundamental components, yield:
At the rotor surface, $y = 0$,

$$\psi = \frac{-4\pi 10^{-9} e^{pt}}{\left[\dfrac{\sqrt{\beta^2 p + a^2}}{\mu a} + \tanh ag\right] a \cosh ag} \times \left[I_r A_1 \cos ax \cosh ag + \frac{3}{2} B_1 (De^{j(ax-\gamma)} + D' e^{-j(ax-\gamma)})\right] \quad (48)$$

At the stator surface, $y = g$,

$$\psi = \frac{-4\pi 10^{-9} e^{pt}}{\left[\dfrac{\sqrt{\beta^2 p + a^2}}{\mu a} + \tanh ag\right] a \cosh ag} \times \left\{I_r A_1 \cos(ax_1 + \omega t + \gamma) + \frac{3}{2} B_1 \left[\cosh ag + \frac{\sqrt{\beta^2 p + a^2}}{\mu a} \sinh ag\right] \times \right.$$
$$\left. [De^{j(ax_1+\omega t)} + D' e^{-j(ax_1+\omega t)}]\right\} \quad (49)$$

From equation 48 the electric intensity at the rotor surface is simply

$$E_r(x) = \frac{\partial}{\partial t}\psi = p\psi \quad (50)$$

while, from equations 49 and 23, at the stator surface

$$E_s(x_1) = \frac{\partial}{\partial t}\psi(x_1) = \frac{-4\pi 10^{-9} e^{pt}}{\left[\dfrac{\sqrt{\beta^2 p + a^2}}{\mu a} + \tanh ag\right] a \cosh ag} \times$$
$$\left\{\frac{I_r A_1}{2} [(p + j\omega)e^{j(ax_1+\omega t+\gamma)} + (p - j\omega)e^{-j(ax_1+\omega t+\gamma)}] + \right.$$
$$\frac{3}{2} B_1 \left[\cosh ag + \frac{\sqrt{\beta^2 p + a^2}}{\mu a} \sinh ag\right] \times$$
$$\left.\left[D(p + j\omega)e^{j(ax_1+\omega t)} + D'(p - j\omega)e^{-j(ax_1+\omega t)}\right]\right\} \quad (51)$$

(*Concluded on page 179*)

Electrical Characteristics of Suspension-Insulator Units

By C. L. DAWES
FELLOW AIEE

REUBEN REITER
ASSOCIATE AIEE

Effects of humidity, corona, and mechanical stress on the electrical characteristics of porcelain and glass suspension-insulator units are shown in this paper. Moisture, alone and combined with corona, is found to produce surface deposits which cause hysteresis effects in the power, power factor, and capacitive characteristics, and mechanical stress is found to reduce the power, power factor, and capacitance. The effect of stress is reduced where soft metal is used in place of cement in assembling the unit.

ALTHOUGH for a number of years the flashover and puncture characteristics of suspension-insulator units have been investigated extensively, very little study has been made of their power-loss, power-factor, and capacitance characteristics. The only published work of any importance is that of Draeger.[1] The extent and value of his measurements were limited, however, by the bridge facilities available to him at the time (1925). Moreover, he did not take into consideration the effect of humidity on the characteristics, which has been found by the authors to be the factor which, with corona, has the greatest effect on the electrical characteristics of the insulators. Furthermore, the authors have been able to carry the investigation much further than Draeger and to relate "corona hysteresis" to the combined effects of humidity, corona, and a microscopic surface deposit produced by corona.

The insulators tested were 10-inch porcelain disk-type suspension insulators supplied by the Locke Insulator Corporation, and a Pyrex 776, 10-inch glass disk-type suspension insulator supplied by the Corning Glass Works.

Summary

1. The electric and dielectric circuits of a suspension-disk insulator consist of the porcelain and cement between cap and pin which is practically invariable, and the capacitance between the surfaces of the shell in series combinations with the surface resistance. This circuit is highly variable due to changes in surface resistance.

2. The surface resistance is a function of adsorbed moisture and decreases with increase in absolute humidity and increases with decrease in absolute humidity. The surface resistance also decreases with corona formation.

3. At any fixed voltage the electrical characteristics of the insulator vary with time. This is due to the change in surface resistance caused by Joule heating and to "island formation." The resistance may increase with time or it may decrease, depending on the part of the test cycle at which it is operating.

4. The electric and dielectric characteristics of the insulator are functions of the absolute humidity or of the absolute amount of moisture in the atmosphere.

5. Corona forms at lower voltage with increasing values of absolute humidity.

6. The power factor is practically a linear function of the absolute humidity.

7. Corona reacting with oxygen, nitrogen, and moisture of the atmosphere forms acidic compounds which deposit on the insulator surface, causing change in the surface resistance.

8. The combined action of the corona, acidic compounds, and the sputtering of the metal of the cap and pin form semipermanent conducting microscopic "island" deposits which cause a decrease in surface resistance. Such island deposits can be removed only by vigorous rubbing.

9. The moisture film on the insulator surface together with the island deposits causes a hysteresis effect in the electrical characteristics of the insulator.

10. The changes in surface resistance also vary the amount of shell capacitance connected between cap and pin. Hence the total insulator capacitance increases with decrease in surface resistance and *vice versa*.

11. The electric and dielectric characteristics of the insulator are not greatly affected directly by temperature, but are affected indirectly in that absolute humidity of air is a function of temperature.

12. Mechanical stress for the most part causes a decrease in the power factor and capacitance due to the compression of the cementing material. After such material has a permanent "set" further change is slight and with glass insulators the characteristics remain independent of further stress.

Method of Measurement

The electrical characteristics were measured by means of the mutual-inductance type of high-voltage bridge developed and used in the high-voltage laboratories at Harvard University. The simplified diagram of connections of the bridge and the test insulator is shown in figure 1.

In order to facilitate the connection of the high-voltage lead and the low-voltage shielding, the insulator was tested in an inverted position. No differences in effects between this position and the upright one were noted.

The details of the bridge connections have already been published.[2] The shielding S_3 surrounding the low-voltage lead ab to the specimen is balanced to the

A paper recommended for publication by the AIEE committee on power transmission and distribution. Manuscript submitted August 17, 1936; released for publication November 10, 1936.

1. For all numbered references see list at end of paper.

C. L. Dawes is associate professor of electrical engineering in the graduate school of engineering at Harvard University, Cambridge, Mass. Reuben Reiter is a graduate student at Harvard University.

The authors wish to express their thanks to K. A. Hawley, formerly of the Locke Insulator Corporation, Davidge H. Rowland, and C. W. Roberts, both of the Locke company, and Dr. J. T. Littleton of the Corning Glass Works for their co-operation in the conduct of this research. The authors also are indebted to Dean Harry E. Clifford of the graduate school of engineering, Harvard University, for his assistance and to Victor G. Mooradian and Dr. Carl Shapiro of the metallurgical department for their assistance in the microphotography.

same potential as the lead *ab* so that capacitive effects between them are eliminated. The bridge is provided with an amplifier to give it the necessary sensitivity, and filters to eliminate harmonics from the circuit.[3]

Equivalent Circuits of Disk Insulators

In figure 2*a* is shown the cross section of a typical insulator unit and the approximate electrical circuits. There is a capacitance C of approximately 30 micromicrofarads between the cap and the pin. The dielectric is the porcelain, and the cement used to fasten the cap and pin in place. Such dielectrics obviously involve dielectric loss so that in the equivalent circuits of figures 4*b* and 4*c*, the capacitance C is shown shunted by a resistance R to simulate this loss. The dielectric characteristics of the porcelain and the cement remain practically constant under all conditions, although a slight increase in power factor with increase in voltage may be attributed to the ionization of occluded gases. The values of C and R may be changed slightly by mechanical stress.

The glazed porcelain shell may be considered as consisting of a number of capacitances C' between the upper and lower surfaces. If the surface resistance were infinite, the capacitances C' would have very little effect on the total insulator characteristics. These capacitances are, however, connected in the insulator circuit by the surface resistance R' which is caused by moisture and other conducting deposits on the surface, as well as by corona which is also conducting. As will be shown later, the surface resistance R' depends on the humidity and the voltage, and it has a very large effect on the insulator characteristics. Hence the effects of the shell capacitance depend on the surface resistance and they will vary with changes in the surface resistance.

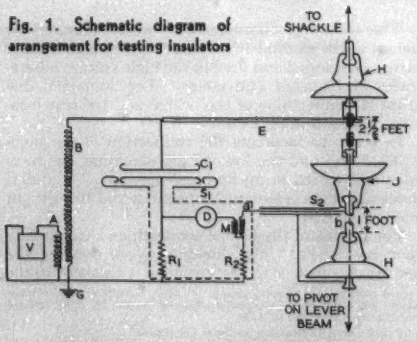

Fig. 1. Schematic diagram of arrangement for testing insulators

A—Voltmeter coil
B—Step-up transformer secondary
C_1—Air capacitor
D—Detector
E—High-voltage lead, one inch in diameter
G—Ground
H—Insulators, mechanical strength, 25,000 pounds
J—Test specimen, mechanical strength 18,000 pounds
M—Mutual inductance
R_1, R_2—Series resistors
S_1, S_2—Shielding
V—Voltmeter

The equivalent circuit of the insulator shown in figure 2*a* is shown directly in *b*. The cap and pin capacitance C is shunted by a resistance R to simulate the dielectric losses. The capacitances C' and the surface resistance R' combine to form equivalent

A—Insulator cap
B—Corona
C—Main capacitance, 30 micromicrofarads
R'—Surface resistance
D—Insulator pin
C_1, R_1—Equivalent parallel circuit of insulator shell

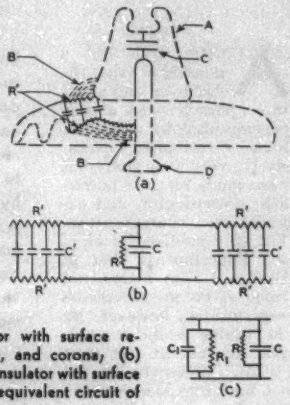

Fig. 2. (a) Insulator with surface resistance, capacitance, and corona; (b) equivalent circuit of insulator with surface resistance; (c) total equivalent circuit of insulator

T-circuits and this combination is connected in parallel with C and R to give the equivalent circuit of the entire insulator. The entire diagram of figure 2*b* may be simplified to that of *c* in which the over-all effect of the capacitances C' and the surface resistance R' for any one set of conditions are replaced by the capacitance C_1 and the resistance R_1. The variation of the surface resistance R' with humidity, corona, and elapsed time of test for the most part accounts for the changes in the characteristics of the insulator.

Time Lag

In making the measurements of power, power factor, and capacitance, it was found that very much higher values for these factors were obtained with decreasing values of voltage than with increasing values, thus giving a hysteresis effect. This effect is illustrated in figure 3 as well as in figures 4, 5, 6, and 7. It was also found that the hysteresis effect increased with absolute humidity, as is shown in figure 5.

Moreover, in making the measurements, it was found that the values of power, power factor, and capacitance for any definite voltage were not fixed, but varied with time. At low humidity and with increasing values of voltage, these factors increased with time. At high humidity and with increasing values of voltage, at low voltage, they decreased with time, but after corona formed they increased with time due to the surface deposits to be described later. These effects are illustrated in figures 3 and 4.

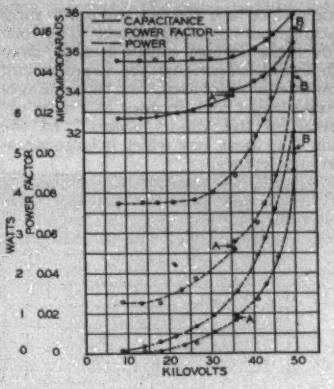

Fig. 3. Characteristics of porcelain insulator, showing time lag and hysteresis effects at 60 cycles and 20 degrees centigrade

A—Lapse of time of 10 minutes

B—Lapse of time of 2 hours

In figure 3 the increases in power, power factor, and capacitance for an interval of 10 minutes at 35 kv are shown. Also, the same effects are shown for a 2-hour interval at 50 kv, but the increases are much greater.

Careful study of this phenomenon showed that the values of power, power factor, and capacitance varied almost as does a direct current in an inductive circuit with resistance in series when a continuous voltage is suddenly switched across it, or when such a circuit is short-circuited. The change is at first rapid but the rate of change diminishes with time. It seemed that theoretically steady conditions would be reached only after infinite time. To reach the steady condition for each bridge balance would therefore require a prohibitively long time. Moreover, in order to interpret the phenomena, it is not necessary that the exact values corresponding to the ultimate steady state be obtained. Hence, in making the measurement it was decided to choose such values of time as would give from 85 to 90 per cent of the difference between the ultimate and initial readings.

The relationships among the characteristics obtained at the different values of time are shown in figure 4, *A* and *B* giving those for increasing values of voltage, and *C* and *D* giving those for decreasing values of voltage. In all the figures the characteristics aa' give the values of power factor which would be obtained if the measurement were made instantaneously. The characteristics bb' give the values of power factor which would be obtained if the measurement were made at infinite time. The characteristics cc' are those actually obtained and they lie at approximately 85 to 90 per cent of the distance from aa' to bb'. As will be shown later, these time-lag effects are due to the humidity of the atmosphere and to the accumulation of a deposit on the insulator surface.

It was found that the value of the time necessary to obtain curves cc' was not constant but varied with the voltage, the humidity, and the amount of corona formation. In a large measure, the time was determined by experience combined with watching the rate at which the bridge balance changed. The approximate values of time are as follows:

Kilovolts Across Insulator	Elapsed Time Before Taking Reading, Minutes
3	5 to 20
10	5 to 20
20	10 to 25
30	15 to 45
40	25 to 80
50	30 to 120

Electrical Characteristics and Absolute Humidity

Early in the research it was found that the electrical characteristics of the insulators were, in a large measure, functions of the humidity. First it was attempted to relate the characteristics to the relative humidity, but there seemed to be no remote relationship, even, between them. Further investigations showed that the characteristics were closely related to both specific humidity and to absolute humidity. (Specific humidity is the actual amount of moisture per unit weight of dry air.) In this paper absolute humidity in grains of moisture per cubic foot of air is used (7,000 grains of moisture equal one pound).

In the authors' experimental work there were little means for controlling the humidity so that usually it was necessary to await natural changes in the laboratory. As a rule, high values of humidity occurred in summer and low values on cold winter days.

In figure 5 are shown the power-factor characteristics for a porcelain insulator with increasing and decreasing values of voltage for 3 different values of absolute humidity, $s = 2.6$, $s = 4.48$, and $s = 7.56$.

The very low value (2.6) was obtained on a cold,

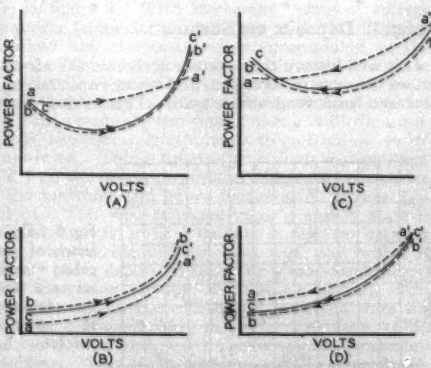

Fig. 4. Effect of time lag on insulator characteristics

A—High humidity, increasing voltage
B—Low humidity, increasing voltage
C—High humidity, decreasing voltage
D—Low humidity, decreasing voltage

dry winter day; the intermediate value (4.48) was obtained on a cool, autumn day, and the high value (7.56) was obtained during a hot, muggy day in July. Similarly, in figure 6 are shown the capacitance characteristics for the same insulator at these same 3 values of absolute humidity. In figure 7 is shown the power-factor characteristic of a glass insulator obtained at an absolute humidity of 4.7. It may be noted that with all the characteristics of figures 5, 6, and 7, the values for decreasing voltage are greater than for increasing voltage.

It will also be noted in figure 5 that with the low value of absolute humidity, $s = 2.6$, the power factor increases continuously with increase in voltage and decreases continuously with decrease in voltage. With the intermediate value of absolute humidity, $s = 4.48$, the power factor remains constant until 35 kv and then increases. This increase in power factor is caused by the corona which forms at approximately 35 kv. With the high value of absolute humidity, $s = 7.56$, the power factor first decreases rapidly with increase in voltage, reaches a minimum at approximately 25 kv, and then increases due to corona formation. The characteristic for descending values of voltage is similar, except that it lies above the first characteristic.

These characteristics are typical. With low values of absolute humidity, the power factor always increases with voltage, rising more rapidly after corona formation. With larger values of absolute humidity, the power factor at first decreases with increase in voltage until corona forms, when it increases. It is also found that with large values of absolute humidity the difference between the ascending and the descending characteristic increases (see figure 5). Corona forms at lower values of voltage with increasing values of absolute humidity. For example, in figure 5 corona formation begins at 34 kv when $s = 4.48$, and at 26 kv when $s = 7.56$ (also see figure 12).

"Island" Deposits on Surface

It is well known that corona activates the air and causes the oxygen, nitrogen, and water vapor to combine and form weak nitric acid. This acid deposits on the insulator surface near the cap and pin to form initially conducting spots or small islands. The voltage gradient over the surface causes arcs to snap from island to island, vaporizing the deposits and scattering them over a wider area. At high voltages these arcs become longer and brighter and more explosive scattering of the vapors occurs. In the authors' opinion it is these arcs which in large measure cause radio interference.

These acidic islands are more or less conducting and it is in part due to their formation that the power factors, etc., increase with time.

Several factors led to the belief that, in addition to the acidic spots, a more or less permanent deposit must form on the insulator surface, but it was some time before this fact could be substantiated. After the voltage had initially been increased to its maximum value and then lowered, the power, power factor, and capacitance were greater than with increasing values of voltage, as is shown by the descending voltage characteristics, figures 5, 6, and 7. In subsequent tests these quantities always remained above their initial values, and, in fact, they increased continuously with continued application of voltage, particularly if the absolute humidity were large. However, if the surface were cleaned, vigorous wiping

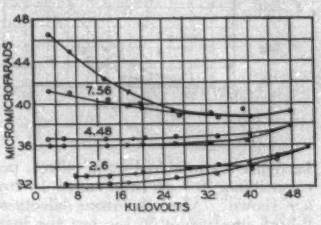

Fig. 6. Capacitive characteristics of porcelain insulator at 3 values of absolute humidity

Numbers on curves are humidities in grains of moisture per cubic foot of air

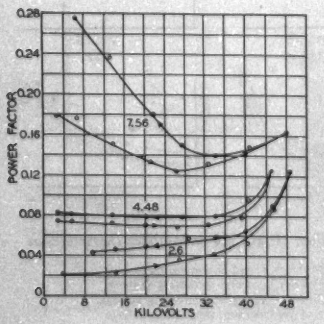

Fig. 5. Power factor of porcelain insulator as a function of voltage at different absolute humidities

Numbers on curves are absolute humidities in grains of moisture per cubic foot of air

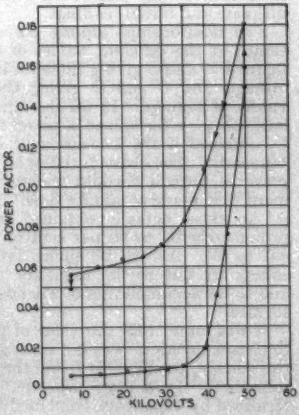

Fig. 7. Power-factor characteristics of glass insulator at 60 cycles, 21.5 degrees centigrade, and 4.7 absolute humidity

being necessary, the characteristics returned to the initial values.

Carefully polished surfaces of metals were then subjected to a corona discharge with moisture present and island formations could be readily seen under the microscope. (One of the authors has found that corona makes a very effective etching agent in micro-

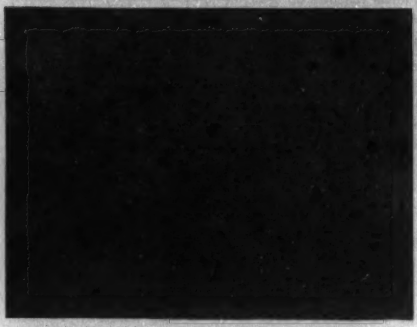

Fig. 8. Microphotograph of deposit near pin on porcelain insulator caused by corona and moisture

Magnification 120 diameters

photography.) Later, by means of a dark-field type of microscope, it became possible to detect the island deposits on porcelain, and a microphotograph taken near the pin is shown in figure 8. The examination of the surface is made difficult by the fact that microscopes are not adapted to bring to the objective the portions of the porcelain surface near the cap and pin, and thecurved surfaces make microphotography very difficult. Hence, it is necessary to break the porcelain without disturbing the deposits, and to select suitable pieces for examination. It is the island deposits such as are shown in figure 8 that cause the permanent changes in the insulator characteristics to which reference has already been made.

The authors have made several attempts to learn more about the nature of the deposit. It can be removed by wiping the surface vigorously and, as has already been stated, the characteristics of the insulator return to their initial values. The deposit is a very thin film consisting of microscopic islands, some of which are crystalline in form. The film is so thin and so difficult to remove that, so far, a chemical analysis has not been possible. The authors believe, however, that it consists of the nitric-acid deposit already discussed in combination with the metal of the cap or pin which has been deposited by the sputtering effect of the corona. This is substantiated by some experiments made on pieces of porcelain placed within a corona field, with moisture present. If a sheet of glass was interposed between the high-voltage electrode and the porcelain, no deposit occurred. If, however, moist air is interposed between the high-voltage metal electrode and the surface of the porcelain, a deposit almost identical with that shown in figure 8 results. A microphotograph of this deposit is shown in figure 9. This seems to show that the deposit involves the metal of the electrodes. Further study of these deposits, with chemical, X-ray, and microscopic aid, is now in progress.

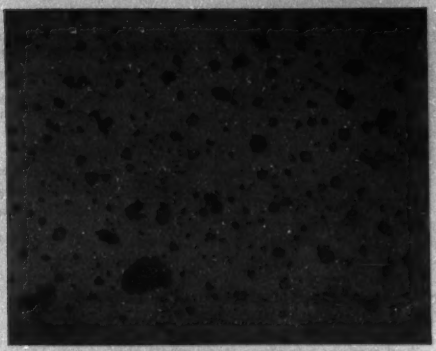

Fig. 9. Microphotograph of deposit on glazed porcelain formed artificially by simulating natural conditions in the presence of corona and moisture

Magnification 300 diameters

Hysteresis in Power Factor Curves

With the preceding discussions of humidity, corona, and the surface deposits on the insulator surface, it now becomes possible to analyze the corona hysteresis characteristics.

Consider, for example, the characteristic for $s = 7.56$ in figure 5. With increasing values of voltage the power factor decreases. Due to the humidity an adsorbed film of moisture has accumulated on the surface of the insulator, accounting for the resistance R' in figures 2*a* and 2*b*. At the lower values of voltage, if the voltage is brought to any particular value and held constant, the power factor will diminish, that is, the characteristic tends to go from aa' to bb' in figure 4*A*. This is due to the joulean heating effect (I^2R') on the insulator surface which vaporizes some of the moisture and hence increases R' (figure 2, *a* and *b*). This will continue until a steady state is reached, that is, until a balance is reached between the moisture removed by heat and that which is steadily being deposited from the humid atmosphere. With increasing voltage, the surface heating effect is increased, and more moisture is driven from the insulator surface. This increases the value of R' (figure 2*b*) and the power factor again diminishes with time. This effect continues until corona forms.

Corona itself is an energy loss and will accordingly of itself increase the power factor. Moreover, it is conducting in character and causes the surface resistance R' to decrease (figure 2, *a* and *b*). Up to a certain point a decrease in R' increases the power fac-

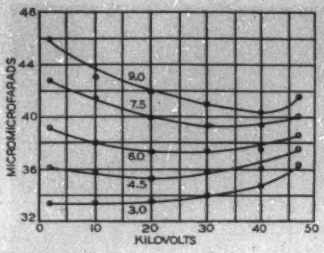

Fig. 10 (left). Capacitance of porcelain insulator as a function of voltage at different absolute humidities; interpolated data from increasing voltage

Numbers on curves are absolute humidities in grains of moisture per cubic foot

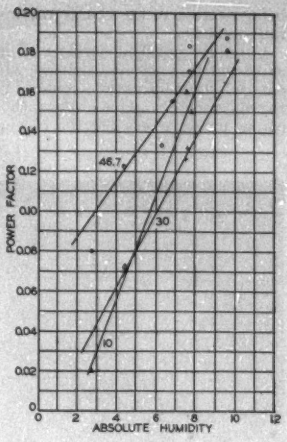

Fig. 11 (right). Power factor of porcelain insulator as a linear function of absolute humidity at constant voltage; data from increasing voltage

Numbers on curves are potentials in kilovolts

tor. Corona thus accounts for the increase in power factor which occurs at the higher values of voltage.

With low values of absolute humidity, the adsorbed surface moisture is so small that it has very little and at times negligible effect on the power and power factor. As the voltage is raised with very low absolute humidities, a slight increase in power factor occurs as is shown by the characteristic, $s = 2.6$, in figure 5. This undoubtedly is due to corona formation occurring in the pores of the porcelain and cement and in any small voids that may exist between cap and pin. With a higher value of absolute humidity, $s = 4.48$ (figure 5), the value of power factor remains substantially constant until corona forms. This undoubtedly occurs because the effects of humidity, which cause a decrease in power factor, are being balanced with the corona formation in the voids, which causes an increase in power factor.

With decreasing voltage the power-factor characteristics lie above those for increasing voltage as has already been stated. This is due primarily to the conducting surface deposits resulting from the combined action of corona and moisture. As the voltage decreases, the corona formation itself decreases and the resulting power factor decreases. A point will, however, be reached when corona ceases and the characteristic will reach a minimum (see characteristic $s = 7.56$, figure 5). With further decrease in voltage, and hence in surface heating, moisture will again deposit on the insulator surface and the power factor will now increase. As the voltage becomes less, less heat is evolved on the insulator surface, more moisture deposits, and the power factor continues to increase with diminishing values of voltage.

With low values of humidity the effect of surface loss is negligible so that the rise in power factor with diminishing voltage does not occur as is shown by the characteristics for $s = 4.48$ and $s = 2.6$ in figure 5.

Capacitance Characteristics

A study of a and b in figure 2 shows that the total capacitance of the insulator consists of the sum of the capacitance C of the head of the insulator and the capacitances C' between the conducting surfaces of the shell. The effectiveness of the capacitances C', however, depends on the value of the surface resistance R'. With R' infinite, the capacitances C' have negligible effect on the total capacitance of the insulator. The effect of C' increases as R' diminishes and the maximum effect of C' occurs when R' is zero. Hence the value of the total capacitance C of the insulator depends on the conductance of the film of surface moisture.

With low values of absolute humidity, the capacitance changes little with voltage. There is a steady rise in capacitance with voltage, as is shown by the 2 characteristics at $s = 2.6$ and $s = 4.48$ in figure 6. This rise is undoubtedly due to corona formation in the voids in the porcelain and cement between cap and pin. There is but slight rise in capacitance after corona formation at the edges of the cap and the pin. This is because the corona probably does not extend sufficiently far out from the cap and the pin to include much of the capacitance C' of the shell.

The effect of the adsorbed surface moisture is well illustrated by the characteristic for $s = 7.56$. At first the capacitance dimin-

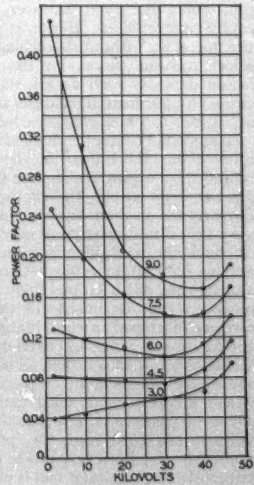

Fig. 12. Power factor of porcelain insulator as a function of voltage at different absolute humidities; interpolated data from increasing voltage

Numbers on curves are absolute humidities in grains of moisture per cubic foot of air

ishes with increasing voltage due to the increasing surface resistance R'. When corona forms the capacitance increases slightly due to reduction in surface resistance by corona and island deposits. With diminishing voltage the capacitance increases due to the combined effect of returning adsorbed surface moisture and the permanent island deposits. Hence the total capacitance of a disk insulator is a function of the deposit and the adsorbed moisture on the surface, and of the corona.

In figure 10 is shown a complete family of capacitance-kilovolt characteristics with increasing values of voltage for 5 different values of absolute humidity. These characteristics further illustrate the analysis of the relationship of capacitance to absolute humidity. That is, at low values of absolute humidity, the changes in capacitance are small; at large values, they are considerable.

Power Factor and Absolute Humidity

It is found that if the values of power factor for constant voltage be plotted as functions of absolute humidity, the best representative characteristics are

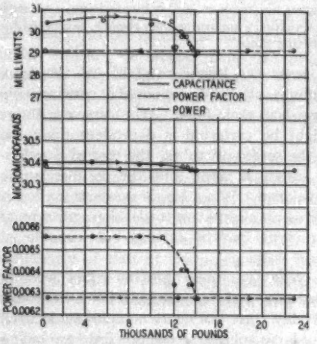

Fig. 13. Electrical characteristics of glass insulator as functions of mechanical stress at 60 cycles, 21.5 degrees centigrade, and 30 kv

linear. Three such characteristics for 10, 30, and 46.7 kv are shown in figure 11. For the sake of clearness, similar characteristics for other values of voltage are omitted.

If the data for the characteristics of power factor versus absolute humidity such as are given in figure 11 are replotted, with power factors as functions of kilovolts at constant values of absolute humidity, characteristics similar to those of figure 12 are obtained. These characteristics are similar to those of figures 3 and 5 except that they include more values of absolute humidity. A study of these curves shows that with increasing voltage the rise due to corona formation at the edges of cap and pin begins at lower values of voltage with increasing values of absolute humidity. With decreasing voltage the reverse is true.

In the foregoing relationships, the effect of temperature has not been mentioned. The authors' studies showed no explicit relationship of any of the characteristics to temperature over the annual range of atmospheric temperature variation. Over extreme ranges of temperature Draeger[1] shows a relationship. However, it must be remembered that absolute humidity is a function of the temperature. Hence indirectly, temperature does affect the electrical characteristics of suspension disks.

Electrical-Mechanical Characteristics[1]

In order to study the effects of mechanical stress on the electrical characteristics, the suspension disk was so mounted that mechanical stress could be applied and measured simultaneously with the high-voltage electrical measurements. It was anticipated that any dislocation of the cap or pin by mechanical stress would affect the electrical characteristics of the insulator. The stress was applied by means of a large automobile jack acting through a lever with a 5 to 1 ratio. With this arrangement, stresses as high as 40,000 pounds could be applied.

The stress was measured by means of an extensometer. A steel rod $1^1/_4$ inches in diameter for 10-inch length was connected in series with the insulator. It was necessary to choose a diameter which would give an elongation sufficiently great for measurement and yet permit the steel to retain perfect elasticity and not be stressed beyond the yield point.[8] The ends of the rod were reduced to $^3/_4$ inch diameter to adapt them to the special fittings. The elongation of only

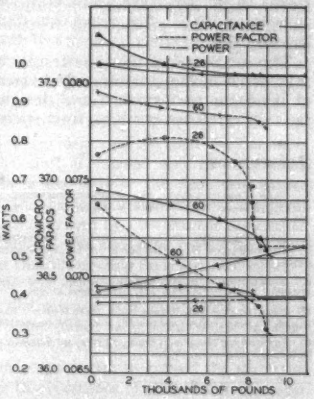

Fig. 14. Electrical characteristics of porcelain insulator as functions of mechanical stress at constant frequencies of 26 and 60 cycles, 19 degrees centigrade, 30 kv, and 4.3 absolute humidity

Numbers on curves are frequencies in cycles per second

3 inches of the rod at the center was measured. The extra length of 10 inches is necessary in order to insure stress equalization over the cross sections near the center. The elongation was measured by means of a combination of mirrors, knife edges, and telescopes. The elongation of the rod was magnified 10^6 times.

The effects of mechanical stress on power, power factor, and capacitance for the glass insulator are shown in figure 13. For an applied potential of 30 kv until a stress of 12,000 pounds is reached, little or

no effect on the characteristics occurs. Then all 3 quantities show a small decrease. (The quantities in figure 13 are plotted to a large scale.) The change in the power and the power factor is approximately 4 or 5 per cent and the change in the capacitance is extremely small. The stress is then carried to 23,000 pounds. All these quantities remain constant up to this value of stress. They also remain constant as the stress is carried back to zero.

Similarly, in figure 14 are shown the effects of stress on the porcelain insulator. The characteristics are obtained at 30 kv and at the 2 frequencies, 26 and 60 cycles. The stress at 60 cycles was not carried back to zero because of the insulator's failure. It may be noted that although the effects of stress are in general similar to those for glass, yet the characteristics are not so simple. They tend to have a steady drop before the critical stress of 8,500 pounds is reached, when they drop rapidly. Moreover, after the application of the critical stress, the quantities, except the power at 26 cycles, do not remain constant as with glass. This would be expected. With glass the pin is held by a soft metal. With application of stress the metal would be pressed more firmly against the glass and little change in conductive relationships of this metal to the glass would be expected. On the contrary, with the porcelain insulator the cement used to fasten the cap and pin is an imperfect dielectric probably containing moisture. Under mechanical stress its dielectric properties would be expected to change considerably. The effect of stress appears to diminish the power, power factor, and capacitance, undoubtedly because of changes in the geometrical relationships between cap and pin.

The authors feel that the results of this research may assist in the obtaining of a better understanding of insulator performance and design, as well as of radio interference resulting from surface discharge.

References

1. Über Verlustwinkel und Kapazetätmessung an Porzellan Isolatoren, Draeger. *Elektrotechnische Zeitschrift*, volume 46, May 1925, pages 683–8.

2. Some Problems in Dielectric-Loss Measurements, C. L. Dawes, P. L. Hoover, and H. H. Reichard. AIEE Transactions, volume 48, 1929, pages 1271–80.

3. Subharmonics in Non-Linear Systems, W. M. Goodhue. *Journal* of the Franklin Institute, volume 217, 1934, pages 87–101.

4. Discussion by C. L. Dawes and Reuben Reiter. Electrical Engineering (AIEE Transactions), volume 53, Nov. 1934, pages 1534–5.

5. Fatigue of Metals (a book), Moore and Kommers. McGraw-Hill Book Company, New York, 1927.

Sealed-Off Ignitrons for Welding Control

(*Continued from page 40*)

The welding of large pieces, particularly when done rapidly with automatic machinery, usually requires the use of water-cooled tubes. There are few resistance-welding machines in use today requiring currents higher than these tubes are able to control.

Advantages of Sealed-Off Ignitrons

The sealed-off ignitron tube provides the following attractive features for welding control. No other device offers all of these advantages:

1. Tubes have no moving parts and so require little or no attention throughout their normal life. They are designed for long life. As compared with mechanical devices for rapidly opening and closing high current circuits, maintenance expense is low.

2. Tubes provide flexibility, short timing, and accuracy of control otherwise unobtainable. This reduces surface heating, thus minimizing deformation and oxidation of work and lengthening electrode life. They permit welding of metals or alloys which were previously difficult if not impossible to weld.

3. Ignitron tubes, because of their ability to pass very high peak currents, are connected directly in the primary circuit of the welding transformer.

4. Ignitron tubes, particularly the metal models, are not fragile and so do not require extreme care in handling. They may be safely installed by unskilled workmen.

5. Sealed-off ignitrons are replaceable units. Tube failure results in only the few minutes shutdown necessary to accomplish replacement. When welding equipment is one link in a continuous production line, the avoidance of long forced shutdowns may result in sizeable savings.

6. Sealed-off ignitrons are small in size, comparatively, and, with the small amount of auxiliary apparatus they require, save valuable space in high production shops.

At higher currents the longer total life of the more completely demountable and repairable continuously pumped tanks weigh in their favor. The capacity above which tanks might be preferred is dependent upon the ultimate life of the sealed-off tubes, the cost of development of larger sealed-off sizes, and the manufacturing cost of those developed. When higher power is needed it may be desirable as an alternative to develop ignitrons of approximately present current ratings but capable of operating at higher voltages.

Two or three years ago these ignitron tubes were in the developmental stage and were used in a few commercial applications.[8] Today there are many equipments located in key positions of large volume production lines producing more consistent welds at higher speed than is practical with other types of control.

References

1. "Ignitron" Control, *Power Plant Engineering*, volume 37, May 1933, pages 218–19.

2. Ignitron—A New Controlled Rectifier, D. D. Knowles. *Electronics*, volume 6, June 1933, pages 164–6.

3. A New Method of Starting an Arc, J. Slepian and L. R. Ludwig. Electrical Engineering (AIEE Transactions) volume 52, September 1933, pages 605–08.

4. Applications of Electron Tubes in Industry, D. E. Chambers. Electrical Engineering (AIEE Transactions), volume 54, January 1935, pages 82–92.

5. The Theory of the Immersion Mercury-Arc Ignitor, J. M. Cage. *General Electric Review*, volume 38, October 1935, pages 464–5.

6. High-Speed Pictures of Mercury-Arc Spots, H. W. Lord. Presented before IRE national convention, Cleveland, Ohio, 1936; AIEE winter convention, New York, N. Y., 1936. Reported in *Electronics*, May 1936, page 11.

7. Glass-to-Metal Seals, Albert W. Hull and E. E. Burger. *Physics*, volume 5, December 1934, pages 384–405.

8. A New Timer for Resistance Welding, Ralph N. Stoddard. Electrical Engineering (AIEE Transactions), volume 53, October 1934, pages 1366–70.

Short-Time Spark-Over of Gaps

By J. H. HAGENGUTH
ASSOCIATE AIEE

In this paper data are presented on spark-over values of rod gaps, insulators, bushings, sphere gaps, and solid insulation for a range of spark-over times of approximately from 0.2 to 4 microseconds. The problems of accurate measurement that are involved are also discussed, and a shielded resistance voltage divider is described.

DURING the last few years considerable progress has been made in impulse testing technique.[1,2] The results obtained in different laboratories on the spark-over of sphere and rod gaps with the standard 1.5 x 40 wave where spark-over occurs after the crest of the wave agree well and have permitted standardization of such spark-over curves.

There has been little data published on spark-over values of gaps and insulation at very short time lags (less than 2 microseconds).[3,4] These data become important when insulation co-ordination is considered. A given gap might protect a piece of insulation when a 1.5x40 wave of low amplitude is applied to the combination, such that spark-over takes place after the crest of the wave, but the insulation might fail if a wave of much higher voltage or steeper front is applied. Therefore, to enable satisfactory co-ordination of various insulating structures it is important to know the behavior of gaps and insulation for the steepest waves expected on transmission lines.

The greatest rate of voltage rise of traveling waves due to lightning is not definitely known. However, from some oscillograms obtained in field investigations it is quite safe to assume that 1,000 kv per microseconds or more is a rate of voltage rise, which can occur quite frequently at least at the point where lightning strikes a line. If a rate of 1,000 kv per microseconds is assumed, this means, for instance, a spark-over at 300 kv at 0.3 microseconds.

The problems concerning the accuracy of the impulse measurements when high spark-over voltage and short spark-over time are involved are discussed in part I of the paper. Definitions of rate of voltage rise and of time to spark-over are discussed since they are important for comparison of results obtained in different laboratories. In part II of the paper, results of tests on rod gaps, insulators, bushings, sphere gaps, and solid insulation covering a range of spark-over time of approximately 0.2 to 4 microseconds, are presented.

I. Impulse Testing Technique

The Voltage Divider

The resistance type of divider has been found to be an ideal tool for the reduction of high impulse voltages to true images of low enough amplitudes, which permit recording with a cathode ray oscillograph, when tests are made to determine the minimum spark-over of gaps with the standard 1.5x40 wave. The resistance can be measured conveniently and the true ratio between oscillograms and actual spark-over voltage can be established with certainty.

For the standard wave the distributed constants of the divider such as its inductance, capacitances to ground, and capacitance between successive turns of the non-inductively wound cards, are of negligible importance. However, the presence of the distributed constants changes the apparent ratio of the divider when high potentials with spark-over occurring at short times are to be measured. For instance, a 10,000-ohm divider, which is used in the range between 200 kv and 1,000 kv slants a rectangular front to about a 0.4-microsecond front and a $^1/_2$-microsecond front to about $^2/_4$-microsecond front in certain positions of the divider with respect to a ground plane. Consequently the breakdown voltage of a sphere gap might be recorded much too low as shown on figure 1*a*, which was taken with a $6^1/_4$-centimeter gap illuminated both by a mercury quartz lamp and a spark from a gap. Although the gap did not spark every time (see full wave on same figure), the amplitude of the recorded spark-over voltage was only $^1/_2$ the amplitude of the full wave. When the waves of figure 1*b* are considered, however, it is evident that the spark-over actually occurred after the crest is reached and the disturbing result in figure 1*a* is due only to the distortion caused by the divider. In the appendix equations are given showing the distortion caused by the different distributed constants of the divider and also some curves pertaining to some particular case illustrating their separate effect.

When examining the effect of the various distributed constants on the distortion, it was found, that the main offender was the capacitance to ground which together with the resistance of the divider slants the wave front. Therefore for equal capacitance to ground the distortion will be greater as the resistance of the divider increases. In the above test, this capacitance had been equally distributed by placing the divider about 6 feet above and parallel with the ground plane. In usual practice such a divider will be moved around in the laboratory, to place it in the optimum position with respect to the test

A paper recommended for publication by the AIEE committee on instruments and measurements. Manuscript submitted October 31, 1936; released for publication December 1, 1936.

J. H. HAGENGUTH is electrical engineer with the General Electric Company, Pittsfield, Mass.

The author is indebted to the personnel of the high voltage engineering laboratory for procuring test results.

1. For all numbered references see list at end of paper.

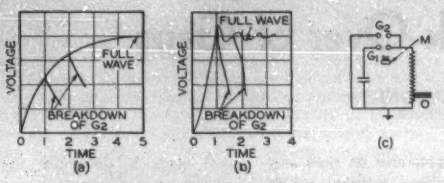

Fig. 1. Comparative tests with ordinary and shielded resistance divider

a—Measured wave front with ordinary divider
b—Measured wave front with shielded divider
c—Test circuit
G_1, G_2—6¼-centimeter spheres
M—Mercury-arc lamp
O—Oscillograph

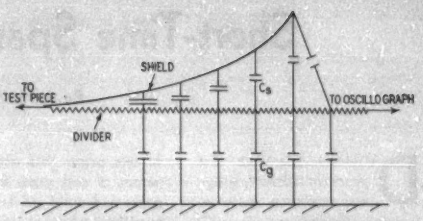

Fig. 2. Schematic diagram of shielded resistance divider

C_s—Capacitance from shield to divider
C_g—Capacitance from divider to ground

piece and the effect of the capacitance to ground will be greater or smaller depending on any particular case.

Another source of error obtained with any divider at rapid changes of voltage is the presence of the rapidly changing fields produced from the impulse generator proper, from the connecting lines, sphere gaps, etc., each changing at a somewhat different rate but all contributing a part to the distortion of the field around the divider.

Therefore, 3 conditions are imposed in eliminating the distortion:

1. The effect of the capacitance to ground must be compensated.
2. A change in position of the divider must not change the compensation.
3. The influence of external fields should be kept as small as possible.

To eliminate the effect of the capacitance to ground a method similar to that used in shielded winding transformers[5] has been employed. This method is shown diagrammatically in figure 2. The shield is shaped in such a manner, that by means of capacitance C_s it supplies just the right amount of current through capacitance C_g to ground, which is required to maintain the voltage e at an amplitude equal to the ratio of resistances at that point. Such a divider also will meet condition 2 by fixing the ground plane permanently to the divider. However, condition 3 cannot be met very readily without going to a very large grounded shield above the divider, which the available space in the laboratory usually would not permit.

To meet all 3 of the conditions a different type of divider was developed which is shown in figure 3. In this divider a center cylindrical electrode serves as the line shield. The tank serves as the ground plane as well as the shield against external fields. The resistor is placed in the field between the line and ground shield in such a way that equal parts of resistances are placed on equipotential lines of correct potential differences. The divider as shown can be used up to 700 kv for minimum breakdown voltage tests on a 1.5x40 wave and up to 2,000 kv on front of the wave tests. In addition to the shielding, the distortion effect has been minimized by keeping the divider resistance low—7,000 ohms. The tank is filled with oil to avoid forming of corona. The minimum ratio of the divider is 100 to 1, since the surge impedance of the delay cable of 100-ft. length, which is used to transmit the surges to the oscillograph plates, equals 70 ohms. This ratio can be increased to approximately 1,400 to 1 by placing a required low resistance parallel to the cable at the divider end of the cable.

Fig. 3. Shielded oil-immersed divider

The Impulse Circuit

For testing with high rates of voltage rise, it is very important, that the divider is connected as closely to the test piece as possible, to avoid reflections of connecting lines and also to avoid measuring the inductive drop on long connecting lines from the steep wave fronts. One factor which produces distortion on the front as well as on the tail of chopped waves is the position of the test piece in the generator discharge circuit, figure 4*a*. The inherent inductance of the circuit is divided into 3 parts; the inductance of the impulse generator proper L_v the inductance of the line to the test piece L_L, and the inductance of the ground return L_g. The effect of these inductances is twofold:

1. On the front of the waves, the rate of rise is influenced by the apparent addition of a superimposed oscillation. This is due to the fact, that at the initial moment, when the impulse generator discharges, the voltages in the circuit distribute according to the inductances. Depending then on the ratio of L_g to the total inductance in the circuit $L_i + L_L + L_g$ the amplitude of this initial inductive kick will be large or small. This inductive effect will have largely disappeared at the time the gap breaks down, provided

the breakdown occurs between 50 per cent and 100 per cent of the wave crest.

2. After spark-over of the test piece the load capacitance is short circuited by the low resistance of the arc and the discharge circuit changes practically into a L, R, C circuit with an oscillatory discharge with a time constant approximately proportional to LC. In the extreme case then the breakdown voltage would be of sinusoidal form of long time constant (8 to 10 microseconds) while the true time constant of the gap breakdown is of the order of a fraction of a microsecond.

To avoid the above discrepancies it is desirable to keep L_s as small as possible by connecting the grounded end of the test piece to the generator through short leads,

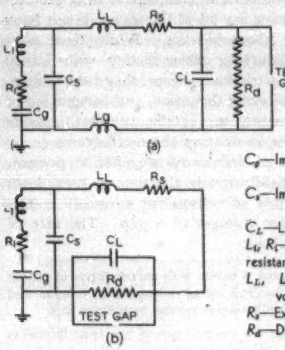

Fig. 4. Impulse-generator discharge circuit

a—Usual connection
b—Preferred connection

C_g—Impulse generator capacitance
C_s—Impulse generator stray capacitance
C_L—Load capacitance
L_i, R_i—Internal inductance and resistance of impulse generator
L_L, L_g—Inductance of high voltage and ground leads
R_s—External series resistance
R_d—Divider resistance

figure 4*b*. The actual position of true ground with respect to the generator is then not so important as long as discharge currents do not flow through the ground straps. It can be seen from figure 4*a*, that traveling waves of considerable amplitude would be set up in the divider cable sheath, if the cable sheath were connected to the grounded side of the test piece, while in case of figure 4*b*, the cable can be connected at that point without complications.

Effect of Circuit Constants on the Spark-Over on the Front of Waves

The control of wave fronts depends on the inductance and resistance in series with the discharge circuit, on the generator stray capacitance to ground and the capacitance of the test piece or any additional load capacitance. Usually the inductance inherent to the circuit is fixed and it is more convenient to control fronts by choosing the proper values of load capacitances and series resistances. For tests on minimum spark-over especially of air gaps, it is quite immaterial whether a relatively large resistance or a large load capacitance is chosen except that the resistance must be large enough to prevent superimposed oscillation. For breakdown on the front of waves, somewhat different results are obtained using the same time constant RC but using either high R or high C.

Figure 5 shows a typical wave front, with breakdown at t_1 and t_1'. Breakdown at t_1' would occur with large resistance, (for instance, 2,000 ohms) and at t_1 with the small resistance, (for instance 400 ohms). The difference between the 2 waves is due to the voltage drop caused across the resistance by the relatively large charging and especially streamer currents[4] through the gap shortly before breakdown. Naturally the larger the resistance the greater will be the drop and the more will the voltage wave depart from that natural to the circuit. It is evident that the spark-over voltages would be quite different in the 2 tests although the rate of voltage rise as determined by conventional methods, is practically the same for the 2 waves. Therefore if plotted on a curve showing rate of rise against breakdown voltage, a considerable spread of test points would be observed. The importance of this phenomenon with respect to evaluation of results will be discussed later.

With respect to the maximum rate of rise and maximum voltage, that can be obtained from an impulse generator, curves of figure 6 are prepared. The generator has a rating of 2,500 kv at a discharge capacitance of 0.011 microfarads and an inherent inductance of 120 microhenries including leads.

It was desired to determine whether the generator was of sufficient size to test transformers with steep fronts of

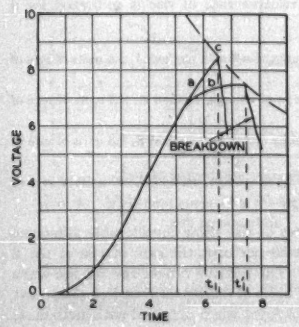

Fig. 5 (left). Change of wave shape due to change in circuit constants

a—RC = constant, R small, C large
b—RC = constant, R large, C small
c—Volt-time curve

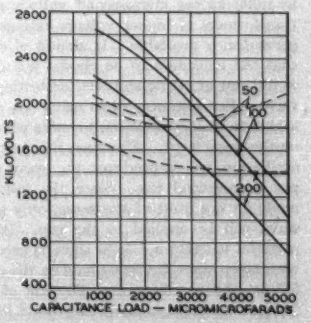

Fig. 6 (right). Rate of rise and maximum spark-over voltages obtainable with a 2,500-kv impulse generator as a function of series resistance and capacitance load

Solid lines—Kilovolts per microsecond
Dashed lines—Kilovolts crest
Numbers on curves are series resistances in ohms

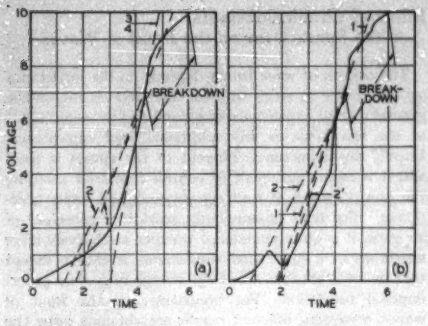

Rate of Rise

1. 10/3.8 = 2.6 units
2. 7/3.2 = 2.2 units
3. 10/1.9 = 5.3 units
4. 7/1.4 = 5.0 units

Rate of Rise

1. 10/3.7 = 2.7 units
2. 7/3.7 = 1.9 units
2'. 7/2.3 = 3 units

Fig. 7. Comparison of definitions of rate of voltage rise

the order of 1,000 kv per microsecond. A transformer can be represented by a capacitance equal to its impulse capacitance when chopped waves of short duration are applied. The impulse capacitance of transformers ranges from approximately 300 to 2,500 micromicrofarads.

Tests were made with the electrical transient analyzer.[7] The analyzer represents an ideal tool for such purposes and eliminates a large amount of routine labor in evaluating the equations. In the curves of figure 6 the rate of rise is calculated by using the crest voltage as measured with the analyzer and dividing it by the time interval from zero to crest. The maximum rate of rise obtainable is therefore greater than indicated on the curves of figure 6. It is seen from figure 6, that in the range of load capacitances of 300 to 2,000 micromicrofarads, rates of rise between 2,000 and 2,800 kv per microsecond can be obtained with maximum voltages of approximately 2,000 kv. These values are sufficiently high to permit spark-over of test gaps parallel to transformers with spacings up to 70 inches at 1,000 kv per microsecond voltage rise. For tests on transformers of higher voltage ratings, a larger impulse generator is available. It should of course, be realized, that the constants to be chosen for the wave front test would not at all be suitable for testing on the tail of the wave. For instance, when using $R_2 = 50$, $C_2 = 5{,}000$, a high-frequency oscillation results which is superimposed on the wave front. However, it is just this superimposed oscillation which produces the wave front of 1,200 kv per microsecond rise. Since the test is required to be made on the front of the wave, only the first rise of the wave will be applied to the gap. It is, therefore, immaterial whether a 1.5x40 wave is used for testing a gap with steep wave fronts as long as the rate of voltage rise follows the specification. The use of 1.5x40 waves for tests on the front of the wave would limit the spark-over tests to relatively small gap spacings or else would require an impulse generator of uneconomical proportions.

Definition of Breakdown Voltage, Time to Breakdown, and Rate of Voltage Rise

If impulse generators contained resistances and capacitances only, it would be an easy matter strictly to define terms determining the time to breakdown, and the rate of voltage rise on wave fronts. However, throughout the impulse discharge circuit, especially of the high-voltage impulse generators, inductance of sometimes considerable value is distributed. These inductances, together with the generator capacitance and capacitances to ground, such as stray capacitances and load capacitance, produce oscillations on the wave front and the waves do not have strictly exponential characteristics. While these phenomena are not disturbing when testing with 1.5x40 waves for minimum spark-over of gaps, they tend to magnify the difficulties of exact definition, and comparison of results of different investigators is difficult unless the same procedure is used for evaluating the oscillograms.

Two main groups of definitions are used at present, both of which practically ignore the time to breakdown but rather use the rate of voltage rise to record results of tests of spark-over voltages of a gap. The rate of voltage rise is defined as:

(*A*) A line drawn through 2 points with an amplitude of 10 per cent and 90 per cent of the crest voltage intersects the zero line and a line through the maximum voltage parallel to the zero axis.

(*B*) A tangent drawn to the steepest part of the front intersects the zero line and a line through the maximum voltage parallel to the zero axis.

In both cases division of the maximum voltage by the time interval between the 2 intersection points gives the rate of voltage rise.

Method *A* has the advantage of a clearer definition since in most cases, it is quite a simple problem to define the 10 per cent and 90 per cent point and the 2 intersection points, while it is generally extremely difficult to determine a tangent. Both methods however, have slight inconsistencies as follows:

Figure 7*a* shows a wave front without superimposed oscillations. The relative rate of rise is indicated for 4 conditions:

1. Spark-over at 10 units of voltage, method *A*, 2.6 units of rate of voltage rise.
2. Spark-over at 7 units of voltage, method *A*, 2.2 units of rate of voltage rise.
3. Spark-over at 10 units of voltage, method *B*, 5.3 units of rate of voltage rise.
4. Spark-over at 7 units of voltage, method *B*, 5.0 units of rate of voltage rise.

The resulting rates of rise show considerable difference although for about 50 per cent the rate of rise of the 2 waves is identical. The relative rate of rise for the wave breaking down at 7 units of voltage is even less than that for the 10 unit breakdown when obtained with method *A*.

The method of B would indicate a rate of rise twice as large as that of A. Further actual wave fronts are often of a form as shown on figure 7*b*, because optimum test conditions cannot be obtained. The method A would practically give the same rates of rise as that in figure 7*a*, while it would be very difficult to use method B. From the above discussion it appears that the use of the rate of voltage rise to determine spark-over voltages is at least confusing if used with any of the above definitions.

From comparative tests such as mentioned in connection with figure 5, it appears that the maximum rate of rise as defined above is relatively unimportant, while the crest voltage and the time to spark-over seem to be quite definitely related. For instance, spark-over voltages obtained with the same time constant RC but large and small series resistance R lie on a smooth curve when plotted against time to spark-over but when plotted against rate of voltage rise (by standard definition) a considerable spread is observed.

From these considerations, it was found to be an advantage to use the average rate of rise as the factor which determines the breakdown. Average rate of rise is obtained by dividing crest voltage by the time to spark-over. The wave zero under this definition would be defined as the point of intersection with the zero axis of a line drawn through the 10 per cent and 90 per cent points of crest voltage.

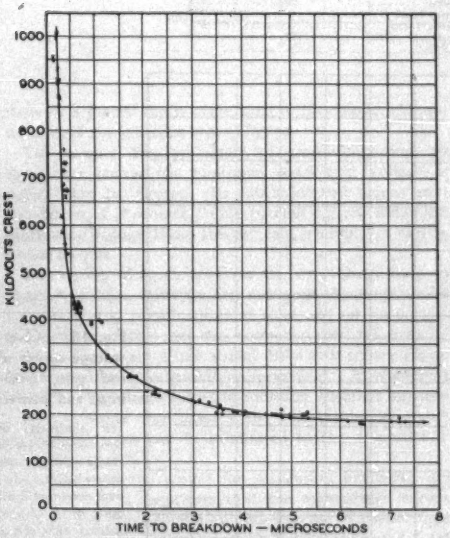

Fig. 8. Volt-time curve of a 10-inch rod gap: $^1/_8$-inch square rods

· 2,000 ohms series resistance
+ 1,500 ohms series resistance
× 0 ohms series resistance
1.5x40-microsecond wave for tests with 2,000 ohms series resistance, positive polarity

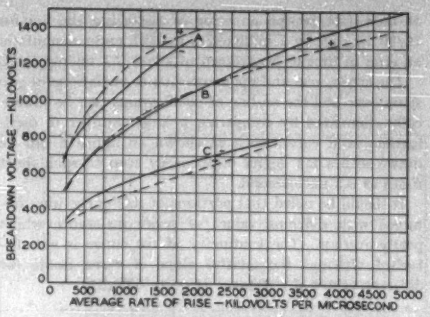

Fig. 9. Variation of spark-over voltage with steepness of applied wave corrected for standard conditions

Solid curves negative polarity; dashed curves positive polarity
A—30-inch rod gap *B*—20-inch rod gap
C—10-inch rod gap

Necessary discrimination has to be used when due to enforced testing conditions the front of a wave is not smooth but has for instance the shape of figure 7*b*. At the spark-over at 7 voltage units, the 10 per cent point should not be chosen at the first rise in voltage, but on the zero extension of the following voltage rise as shown by line 2′.

II. Results of Breakdown Tests

Accuracy of Test Results

Tests of breakdown on the front of waves are conducted in the following manner. Beginning at minimum spark-over of the gap for a 1.5x40 wave the charging voltage of the impulse generator is raised in 10 per cent steps. For each charging voltage usually 3 arc-overs are recorded by oscillograms. As the voltage is raised higher the losses in the series resistance due to streamer currents become greater than the increase in voltage. At this point the series resistance is lowered or removed completely which changes the wave front accordingly. The oscillograms are then analyzed for spark-over voltage and the time to spark-over. Figure 8 is included to show what accuracy can be expected from a single random calibration point. It is evident that down to 0.4 microsecond the spread of values is of the order of 10 per cent and usually less. This spread is partly due to variations in gap spark-over, partly to errors in scaling of oscillograms, partly to the error inherent to the divider and oscillograph. For breakdown times of less than 0.4 microsecond the error becomes greater. Here the greatest error is due to the scaling of the oscillograms. Usually the time to spark-over is the greater source of error, although for these fast times the sweep is chosen such that 1 microsecond represents 40 to 60 millimeters on the time axis of the oscillogram. Even

at these fast sweeps an error in displacing the line for 10/90 per cent by 2 millimeters at both ends amounts in an error in time to breakdown of about 0.1 microsecond.

The errors, real and apparent, due to variations in gap spark-over and the scaling of oscillograms can be practically eliminated by comparing a large number of oscillograms, and curves such as shown on figure 8 can be drawn with a fair degree of accuracy even to such short times as 0.2 microsecond.

It should be noted that portions of this curve were obtained with different values of series resistance which partly overlap. The continuity of the curve is not disturbed, although the relative slope of wave fronts for different values of resistance is quite different.

Spark-Over Curves of Gaps

The results of tests on 10, 20, and 30-inch rod gaps are shown on figure 9 for positive and negative polarity. These curves were drawn by using the average curves obtained as outlined above. The kilovolts per microsecond values were calculated by using crest voltage and time to breakdown as explained earlier in the paper. The curves level somewhat at the high rates of rise and appear to approach some straight line characteristic. The left-hand portion of figure 8 seems to substantiate this. Here the voltage rises almost abruptly while the time to breakdown hardly changes. A difference of about 10 per cent is indicated between positive and negative breakdown voltages.

To compare gaps of different size and different character it is an advantage to use some common basis for comparison. As a characteristic curve the overvoltage-time to spark-over curve is considered. Overvoltage is defined as the voltage required to spark over a gap in excess of the minimum impulse spark-over voltage, for instance due to a 1.5x40 wave, at a spark-over time less than the minimum impulse spark-over time. Such curves

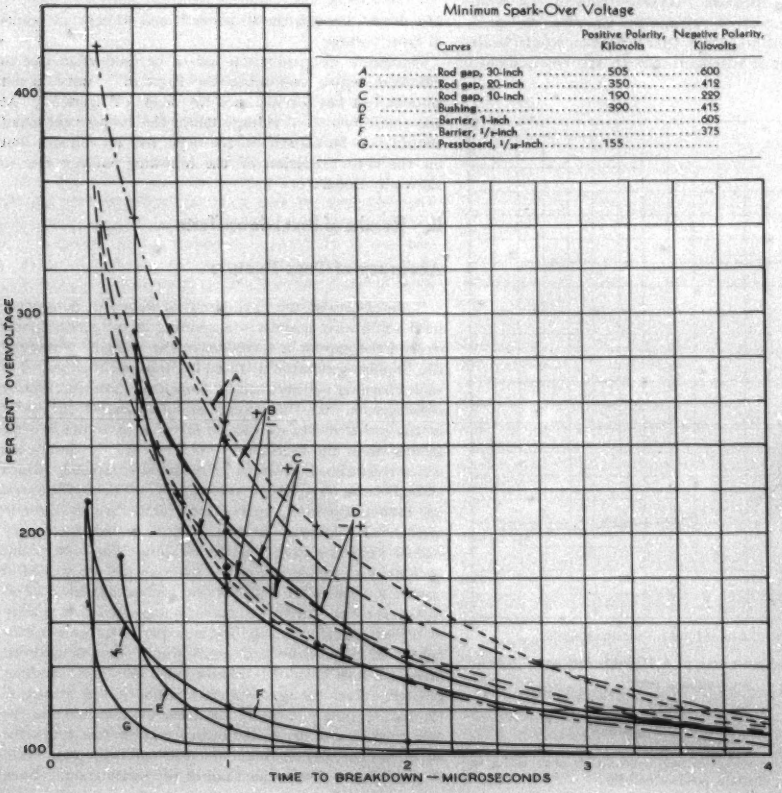

Fig. 10. Overvoltage curves of rod gaps, bushings, and barriers

Test electrodes of barriers are 4-inch round disks with square edges. Barriers consist of 3 oil ducts of 1/4 of total spacing each and 2 pressboard sheets 1/8 of total spacing each

Rod gap of 1/2-inch square rods

+ indicates positive polarity, − indicates negative polarity

Fig. 11. Overvoltage curves of suspension insulators

Spacing 5¾ inches; diameter 10 inches

+ indicates positive polarity; - indicates negative polarity

Minimum Spark-Over Voltage

Curve	Number of Units	Positive Polarity, Kilovolts	Negative Polarity, Kilovolts
Solid	1	150	155
Dashed	2	258	270
Dot-dash	3	355	358

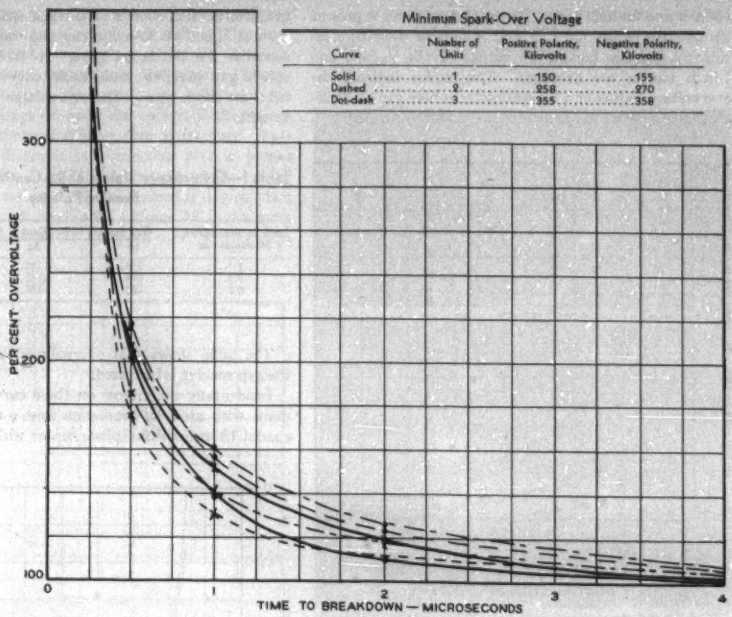

show at a glance the relative time to breakdown characteristics of the different types of gaps.

To increase the usefulness of overvoltage-time to spark-over curves the minimum spark-over voltage is noted below the figures. To obtain kilovolt values from the curves, it is necessary only to multiply the minimum spark-over voltage times the per cent overvoltage and to divide by 100.

The curves of figure 10 show the overvoltage-time to spark-over characteristics for rod gaps, bushings, solid insulation, and combinations of solid and oil insulation. It should be noted that the electrodes used for tests on solid insulation are 4-inch round disks with square edges, which produce a somewhat uniform field. It is evident that the overvoltage values of rods and bushings are considerably higher than those of the solid insulation. Part of this difference can be attributed to the difference in electrostatic field.

In figure 11 the curves for suspension insulators are shown. It is surprising that the overvoltage curves have such a small spread and an increase of overvoltage with increase in string length is hardly indicated. On the contrary the curves for pedestal insulators, figure 12, show larger differences in characteristic shape and a high increase in overvoltage as the number of insulators is increased, especially for positive polarity.

Figure 13 shows a summary of the previous curves. The curves for rod gaps correspond to the average of the

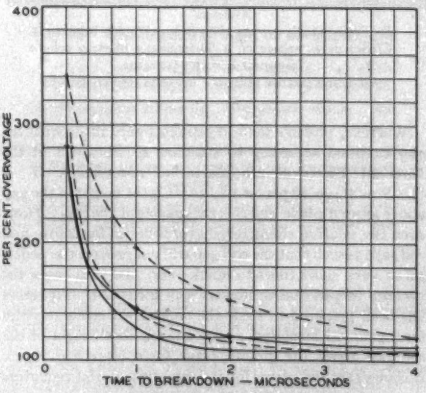

Fig. 12. Overvoltage curves of pedestal insulators

Spacing 14½ inches; diameter 17 inches

+ indicates positive polarity; - indicates negative polarity

Minimum Spark-Over Voltage

Curve	Number of Units	Positive Polarity, Kilovolts	Negative Polarity, Kilovolts
Solid	1	240	300
Dashed	2	400	600

10-inch and 20-inch gap. The insulator curves represent the average values for 1, 2, and 3 units of suspension insulators and the breakdown values for the $^1/_2$-inch and 1-inch barrier are averaged. The circles indicate the overvoltage values of a 50-centimeter sphere gap at 34.25-centimeter (68 per cent) spacing at negative polarity.

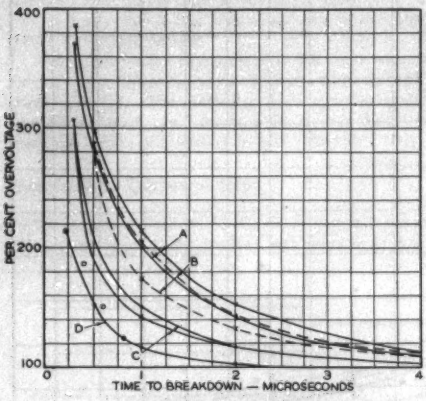

Fig. 13. Comparison of overvoltage characteristics of different types of gaps

A—Rod gap; average values of 10-inch and 20-inch gaps
B—Bushing
C—Insulator; average values of 1, 2, and 3 suspension insulators
D—Solid and oil; average of $^1/_2$-inch and 1-inch barriers
Circles show voltage of a 50-centimeter diameter sphere gap spaced 34.25 centimeters
+ indicates positive polarity; · indicates negative polarity

Wherever possible the rod gap tests were made with the gap mounted according to standard specifications of the National Electrical Manufacturers Association, $H = (1.3\,S + 4'') \pm 10$ per cent where H is the height of the gap above ground plane and S is the spacing of the gap. However, the relative characteristics of pedestal insulators and rod gaps is such that the rod gap will not protect the pedestal at very short times to spark-over. In such cases the number of pedestal insulators was increased. Figure 14 has been prepared to show the breakdown characteristics for 2 pedestal insulators giving the specified height of the rod gap above the ground plane for a 20-inch rod gap. It shows that the curves for rod gap and pedestal insulators cross at 1 microsecond for the positive wave and approach at $^1/_2$ microsecond for a negative wave, which indicates that either may arc. It appears desirable to modify the NEMA rules for the condition of tests on the front of waves.

The above gaps with exception of the solid and barrier type represent strictly non-uniform fields. Contrary to this a sphere gap is considered to have a fairly uniform field. Figure 15 is included to show the spark-over characteristics of such a gap, when spark-over occurs at a short time. A 25-centimeter gap was chosen as representative for the larger gaps. It is evident that the sphere gap requires considerable overvoltage to spark-over at short time. The overvoltage values are shown in table I.

Table I—Overvoltage Values of 25-Centimeter Sphere Gap, Positive Polarity

Time to Breakdown, Microseconds	Gap Spacing in Per Cent of Sphere Diameter		
	16	32	76
1	113	115	109
0.5	154	140	137
0.2	191	155	

The table shows that overvoltage values decrease as the gap spacing is increased.

Incidentally the crosses on these curves indicate tests made with artificial irradiation from a mercury arc light spaced 18 inches from sphere center with 60 watts input.

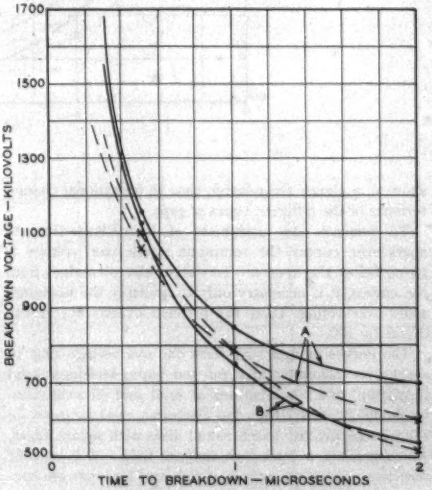

Fig. 14. Volt-time characteristics of 2 pedestal insulators (A) and a 20-inch rod gap (B). The pedestal represents the standard mounting for this size gap

+ indicates positive polarity; · indicates negative polarity

The effect of this ionization appears to be negligible for large gaps at relatively large spacings. From these curves it appears that for spark-over time of 1 microsecond or more the sphere gap indicates spark-over at the same voltage irrespective of voltage application.

For times shorter than 1 microsecond the established values of sphere gap spark-over do not apply. The over-voltage-time to spark-over characteristics for different spacings of the same gap are not the same. This requires a complete short time spark-over calibration for a number of spacings on each size sphere, if the sphere is to be used for measuring short time spark-over. Fortunately the oscillograph in connection with a proper divider has become a reliable instrument which can be used with confidence as a voltage measuring device when the sphere gap is not applicable. Figure 16 shows some representative oscillograms of spark-over of rod gaps

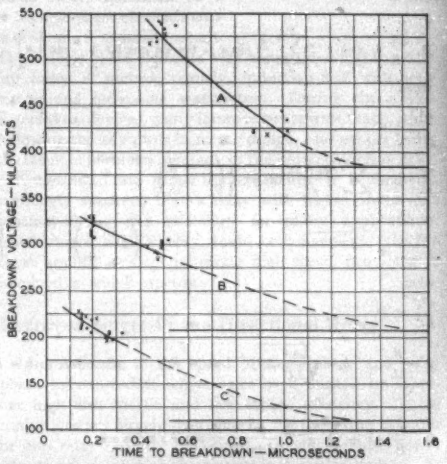

Fig. 15. Spark-over voltage of a 25-centimeter sphere, at positive polarity

Horizontal lines *M* are minimum breakdown voltages

A—19-centimeter spacing *B*—8-centimeter spacing
C—4-centimeter spacing

without and with transformer load and a sphere gap spark-over.

Summary

1. A shielded resistance divider is described which incorporates the desirable features of the ordinary resistance divider and by means of shielding eliminates distortion inherent to such dividers on application of fast wave fronts.

2. The over-all accuracy of measurements of waves at short times is approximately 10 per cent or better for spark-over times of 0.4 microsecond or more, 15 per cent to 20 per cent for shorter times. This applies for individual test points. For a more accurate determination a series of 3 to 5 breakdowns can be used under identical condition of test circuits with a probable accuracy of better than 10 per cent.

3. The curves presented show that the relative short time spark-over voltages are highest for gaps with non-uniform field such as rod gaps, bushings, pedestal, and suspension insulators in the order named, figure 13. The gaps with more nearly uniform field such as

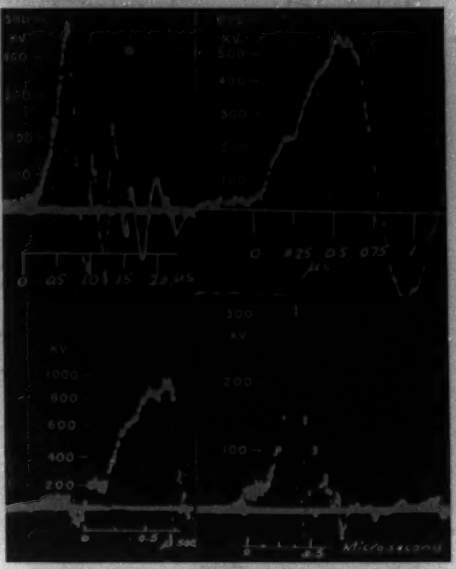

Fig. 16. Oscillograms of front of wave spark-over

A—1/8-inch square rod gap, 10-inch spacing. Rate of rise 850 kv per microsecond, crest 475 kv, negative polarity

B—25-centimeter sphere gap, 19-centimeter spacing. Rate of rise 950 kv per microsecond, crest 551 kv, positive polarity

C—1/8-inch square rod gap, 20-inch spacing. Rate of rise 1,300 kv per microsecond, crest 913 kv, transformer load, negative polarity

D—1/2-inch square rod gap, 3-inch spacing. Rate of rise 1,330 kv per microsecond, crest 300 kv, transformer load, negative polarity

sphere gaps and the 4-inch disks used in tests with solid insulation show relatively high overvoltages but they occur at considerably shorter times than those of gaps with non-uniform fields.

4. Although a large number of volt-time curves has been made, a considerable amount of additional tests are required to complete the experiments, on which co-ordination can be perfected for the fastest rates of rise of natural lightning waves. Experience in the latter field is very restricted. However, rates of rise of 1,000 kv per microsecond and higher can be expected at least at the point of lightning contact. Further data are needed to enable a better understanding of requirements.

5. Impulse breakdown tests on front of waves can be made with similar ease as those on the tail of waves. The limits of accuracy, however, should be more liberal to allow for the greater spread in breakdown voltages of gaps when subjected to high rates of voltage rise.

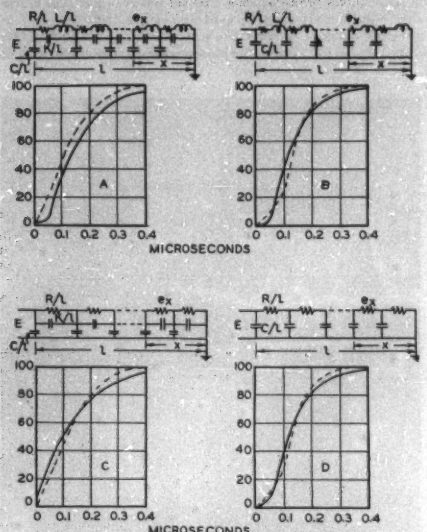

Fig. 17. Comparative wave shapes obtained with ordinary resistance divider and equivalent circuits

Solid curves from calculations; dashed curves from tests

For conditions *A* and *C*, *K'* has been added externally to the divider

Inherent constants—$R = 10{,}200$ ohms; $C = 81 \times 10^{-12}$F; $L = 34 \times 10^{-6}$h; $K = 3 \times 10^{-12}$F

Appendix

To study the behavior of a resistance divider, the divider was placed horizontally 6 feet above ground. Under this condition an extremely steep wave was applied to the divider and the response was measured at the grounded end. Since the effect of the series capacitance K is beneficial, such series capacitance was externally applied to the divider (condition *A* and *C*, figure 17). However, it was found that the amount of series capacitance which could reasonably be connected to the divider was not nearly sufficient to benefit the transmission of the wave.

The equations for the 4 possible combinations of divider constants were solved and the results plotted together with the test results. From a comparison of tested and calculated waves, it appears that the calculations ignoring the inductive component of the divider (conditions *C* and *D*, figure 17) show as good agreement between test and calculation as those with the inductance included. It appears therefore that for simplicity of calculations the circuit *D* of figure 17 can be considered as being representative of the resistance divider circuit.

The equations for the voltage e at a point x to ground of the divider for the 4 conditions are:

A. $$\frac{e_x}{E} = x + \epsilon^{-\alpha t}\sum_1^\infty \frac{2}{\pi s}\sin \pi s x \quad \cos \pi s \frac{\alpha^2}{\alpha^2 + \pi^2 s^2}\left(\cos b_s t + \frac{\alpha}{b_s}\sin b_s t\right)$$

when

$$\frac{\pi^2 s^2}{LK(\alpha^2+\pi^2 s^2)} > \alpha^2$$

$$\frac{e_x}{E} = x + \sum_1^\infty \frac{\sin \pi s x}{\pi s} \cos \pi s \frac{\alpha^2}{\alpha^2 + \pi^2 s^2}\left\{\left(1 + \frac{a}{\omega_s}\right)\epsilon^{-(a-\omega_s)t} + \left(1 - \frac{a}{\omega_s}\right)\epsilon^{-(a+\omega_s)t}\right\}$$

when

$$\frac{\pi^2 s^2}{LK(\alpha^2 + \pi^2 s^2)} < \alpha^2$$

$$a = \frac{R}{2L}; \quad b_s = \sqrt{\frac{\pi^2 s^2}{LK(\alpha^2 + h^2 s^2)} - a^2}; \quad \omega = jb_s; \quad \alpha^2 = \frac{c}{K}; \quad l = 1$$

B. $$\frac{e_x}{E} = x + \epsilon^{-at}\sum_1^\infty \frac{2}{\pi s}\sin \pi s x \cos \pi s\left[\cos b_s t + \frac{a}{b_s}\sin b_s t\right]$$

when

$$\frac{\pi^2 s^2}{LC} > \alpha^2$$

$$\frac{e_x}{E} = x + \sum_1^\infty \frac{\sin \pi s x}{\pi s}\cos \pi s \left\{\left(1 + \frac{a}{\omega_s}\right)\epsilon^{-(a-\omega_s)t} + \left(1 - \frac{a}{\omega_s}\right)\epsilon^{-(a+\omega_s)t}\right\}$$

when

$$\frac{\pi^2 s^2}{LC} < \alpha^2$$

$$a = \frac{R}{2L}; \quad b_s = \sqrt{\frac{\pi^2 s^2}{LC} - a^2}; \quad \omega_s = jb_s; \quad \alpha^2 = \omega; \quad l = 1$$

C. $$\frac{e_x}{E} = x + \sum_1^\infty \epsilon^{-\alpha t}\frac{\alpha^2}{\alpha^2 + \pi^2 s^2}\frac{2}{\pi s}\sin \pi s x \cos \pi s$$

$$a = \frac{\pi^2 s^2}{RK(\alpha^2 + \pi^2 s^2)}; \qquad \alpha^2 = \frac{K}{C}; \qquad l = 1$$

D. $$\frac{e_x}{E} = x + \sum_1^\infty \epsilon^{-\alpha t}\frac{2}{\pi s}\sin \pi s x \cos \pi s$$

$$a = \frac{\pi^2 s^2}{RC}; \qquad l = 1$$

References

1. Laboratory Measurement of Impulse Voltages, J. C. Dowell and C. M. Foust. AIEE Transactions, volume 52, 1933, page 537.

2. The Measurement of High Surge Voltages, P. L. Bellaschi. AIEE Transactions, volume 52, 1933, page 544.

3. Factors Influencing the Insulation Co-ordination of Transformers, P. L. Bellaschi and F. J. Vogel. AIEE Transactions, volume 53, 1934, page 871.

4. Sphere Gap Characteristics on Very Short Impulses, P. L. Bellaschi and W. L. Teague. *Electric Journal*, March 1935.

5. The Non-Resonating Transformer, W. A. McMorris and J. H. Hagenguth. *General Electric Review*, October 1930.

6. Ionization Currents and the Breakdown of Insulation, J. J. Torok and F. D. Fielder. AIEE Transactions, volume 49, 1930, page 382.

7. The Electrical Transient Analyzer, N. Robats. *General Electric Review*, March 1936.

A Single-Element Polyphase Directional Relay

By A. J. McCONNELL
ASSOCIATE AIEE

Increased speed because of reduced inertia and greater torque is obtained from the polyphase directional relay described in this paper. A single cup-like moving element is used in place of multiple disks as used heretofore, the polyphase function being obtained by the use of multiple poles.

THE IMPORTANCE of polyphase directional relays in relay protective arrangements is generally recognized today.

The first polyphase directional relays consisted of 2 or 3 single-phase elements connected to a common shaft. These single-phase elements were almost identical to existing forms of meters, namely, induction-disk watt-hour meters and indicating wattmeters. During the evolution of these devices, many improvements were made, some following the advances in meter design, and others being the result of problems met only in the protective relay field.

Notwithstanding these improvements, it became increasingly apparent that a relay with higher speed and greater torque was necessary for many applications. Furthermore, such a relay would be convenient even for those applications not requiring high speed, providing it involved no added expense.

Improved Single-Phase Directional Relay

Improvements in the speed of single-phase and polyphase induction-disk relays have been limited by inherent high disk inertia and low torque efficiency. These limitations are largely overcome in the induction cylinder or cup relay recently developed. A single-phase power directional element of this design is shown in figure 1.

It consists of a stator with 8 laminated salients projecting inward and arranged symmetrically around a central magnetic core. The salients are fitted with alternate current and potential coils. In the annular air gap between the stator and central core is the cylindrical part of the cup-like induction rotor. The central core is fixed to the stator frame. The cup alone turns. The combination of the smaller rotor inertia and the greater efficiency of this design greatly increases the speed.

For some time, polyphase directional relays of this type of construction have been built using 3 elements having 3 rotors mounted on a single shaft.

Single-Unit 3-Phase Directional Element

Engineers have long considered the economy of using one directional unit to perform the polyphase function. In fact, methods utilizing potential and current switching have been in use for some time, mainly in other countries. These, however, have the disadvantage of being complicated by auxiliary switching relays, in addition to the time lost in performing the switching function.

The multiple-pole induction-cylinder relay makes it possible, as will be shown, to combine the polyphase function of 3 elements in a single element without the use of auxiliary switching. This has resulted in a large reduction in size and weight, together with low inertia and high speed, as illustrated in table I.

The relay operating element is similar to the element shown in figure 1, but a magnetic return path is provided for each salient.

The production of torque is like that in the induction-disk directional relay and the unit may be considered to be a number of directional magnets acting upon the same rotor.

Referring to figure 2, each coil produces rotor currents which react with the flux of each other coil to produce torque. The torque of adjacent pairs of salients is large, relative to that of other pairs. For example, the torque produced by combination 1 and 3 is approximately 15 per cent of the torque produced by combination 1 and 2, while that produced by combination 1 and 4 is about 2 per cent, a negligible amount. The torques of alternate salients (*e. g.*, 1 and 3 or 2 and 4) being appreciable, the connections are so arranged that these torques balance out substantially to zero; an adjustment being provided in addition, for more accurate balance of the current torques.

Table I—Comparison of Types of 3-Phase Relays

	Two-Disk Relay (Per Cent)	Three-Cup Relay (Per Cent)	One-Cup Relay (Per Cent)
Size	100	100	50
Weight	100	100	50
Torque per watt input	100	190	156
Inertia of moving element	100	17	6.6
Speed (equal input)	100	330	480
Speed (rated input)	100	330	280

Thus, in analyzing the action of the relay, it is necessary to consider only the adjacent combinations.

Although the same performance characteristics of all the usual connections (quadrature, etc.) are possible, the connections shown in figure 2 appear to be the most suitable. Considering the interaction of adjacent combinations, I_a acts with E_B and with E_A. Since E_B and E_A are on opposite sides of I_a, combination 1–2 is of opposite sign to combination 2–3. Assuming the reaction of each

A paper recommended for publication by the AIEE committee on protective devices. Manuscript submitted October 31, 1936; released for publication November 27, 1936.

A. J. McCONNELL is design engineer, relay engineering department, General Electric Company, Philadelphia, Pa.

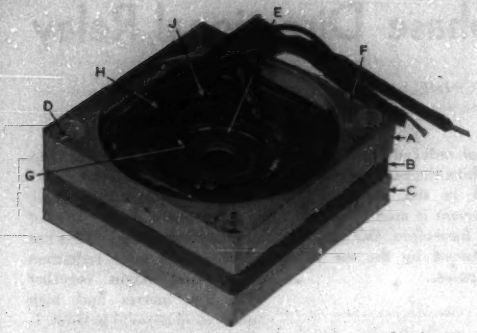

Fig. 1. Element of single-phase directional relay

A—Upper stator casting
B—Laminations
C—Lower stator casting
D—Rivets which fasten parts *A*, *B*, and *C* together
E—Central core (laminated iron) fixed to part *C*
F—Notch to facilitate disassembly
G—Air gap in which rotor cup turns
H—Position for current coils
J—Position for potential coils

current coil with the counterclockwise potential coil as positive, and with the clockwise potential coil as negative, the total input (watts and reactive volt-amperes) to the relay will be[1]

$$P_R + jQ_R = (E_B - E_A)I_a + (-E_A - E_B)I_b + (E_A - E_C)I_c + (E_A + E_C)I_b$$

With the above power quantities supplied to the relay, it will have average torque proportional to

$$(|E_1|)(|I_1|)\cos(\phi_1 - 60 + \theta) + (|E_2|)(|I_2|)\cos(\phi_2 + 60 + \theta) \quad \text{(appendix IA)}$$

The corresponding equation for the torque of the standard quadrature connection of the usual type of induction-disk relay is

$$(|E_1|)(|I_1|)\cos(\phi_1 - 90 + \theta) + (|E_2|)(|I_2|)\cos(\phi_2 + 90 + \theta) \quad \text{(appendix IIA)}$$

It may be seen that there is agreement between the 2 connections, except for 30 degrees in both the positive- and negative-phase-sequence terms.

With the connections of figure 2, there is a difference of 30 degrees in phase angle between a 3-phase fault and a dead phase-to-phase fault; maximum torque being at the more lagging angle in the phase-to-phase condition (appendix IB).

This characteristic is desirable because a 3-phase fault, from the relay point of view, is likely to be nearer unity power factor than is a phase-to-phase fault. This is because the phase angle at the relay during a 3-phase fault depends only on the impedance (line and arc) from the relay to the fault, whereas, during a phase-to-phase fault,

1. For numbered references see end of paper.

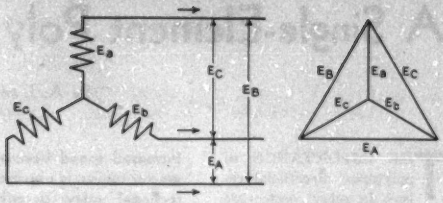

Fig. 2a (right). Diagram illustrating relay connection

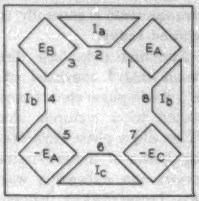

Fig. 2b (above). Diagrams of current and voltage relations

the phase angle depends on the impedance back to and including the generator as well as the impedance to the fault (appendix III). This inherent 30 degree shift is advantageous for another reason, namely, less resistance is required in the potential circuit than with the quadrature connection in order to obtain the same 3-phase phase-angle characteristics. The loss is therefore less.

Quadrature and Other Connections

It is possible to obtain the performance characteristics of the well-known quadrature connection in several ways; 2 ways are illustrated in figure 3. Figure 3*a* utilizes phase-to-neutral voltages, the neutral being either ground or an artificial neutral formed by a common connection of the potential coils. Figure 3*b* uses a delta voltage on each potential coil. Appendix IV shows how each of these connections is equivalent to the quadrature connection.

It is also possible to obtain the equivalent of the adjacent connections by changing the cyclic order of either the voltages or currents of figure 3.

Relays Using the 3-Phase Element in Combination With Other Elements

The element described in the preceding is, of course, a plain directional relay. On the same shaft have been added certain other elements of like construction in order to modify the characteristics. For example, it is often advantageous to prevent a directional relay from operating except during fault conditions. For this purpose, a voltage restraining element has been added. This type of relay is shown in figure 4.

Although a plain directional relay will often take care of ground faults as well as phase faults, it is necessary to add ground-fault protection when the torque caused by ground-fault voltage and current is less than that caused by load current, or when generation is present at one end only. To meet this requirement a strong ground-fault

element may be added to the 3-phase element, this combination being sufficient for almost any relay location.

The addition of a voltage-restraining element to the 3-phase directional and ground directional elements has resulted in an entirely new combination. A relay of this type is shown in figure 5.

The successful use of the induction-cup element for the applications described above gives encouragement for the development of other forms of polyphase high-speed relays having a higher torque-to-input ratio and lower inertia of the moving parts.

Nomenclature

P_R = total power applied to relay
Q_R = total reactive volt-amperes applied to relay
I = current vector as a complex quantity (of the form $a + jb$)
$\bar{I}$ = conjugate of $I(a - jb)$
$|I|$ = absolute value of the vector $I(\sqrt{a^2 + b^2})$
E = voltage vector as a complex quantity
a = operator which rotates a vector 120 degrees in the counter-clockwise direction
α_1 = angle by which the vector E_1 leads a reference line
β_1 = angle by which the vector I_1 leads a reference line
ϕ_1 = $\alpha_1 - \beta_1$ = angle by which I_1 lags E_1
α_2 = angle by which the vector E_2 leads a reference line
β_2 = angle by which the vector I_2 leads a reference line
ϕ_2 = $\alpha_2 - \beta_2$ = angle by which I_2 lags E_2
θ = angle of lead (current leading voltage) at which maximum torque of a pair of adjacent salients occurs
Z_1 = positive-phase-sequence impedance of the generator
Z_2 = negative-phase-sequence impedance of the generator
Z_L = positive- and negative-phase-sequence line impedance
R = phase-to-neutral arc resistance
K = relay torque constant per pair of adjacent salients

Subscripts a, b, c, A, B, C are defined by figure 2b.
Subscripts 1, 2, and 0 denote positive, negative, and zero phase sequence, respectively.

Appendix IA

Connections according to figure 2.
The total input to the relay is[1]

$$P_R + jQ_R = (E_B - E_A)\bar{I}_a + (\underline{-E_A} - E_B)\bar{I}_b + (-E_C + E_A)\bar{I}_c + (\underline{E_A} + E_C)\bar{I}_b$$

The underlined terms cancel, leaving

$$P_R + jQ_R = E_B\bar{I}_a - E_A\bar{I}_a + E_C\bar{I}_b - E_B\bar{I}_b + E_A\bar{I}_c - E_C\bar{I}$$

Fig. 3. Relay connections for quadrature equivalent

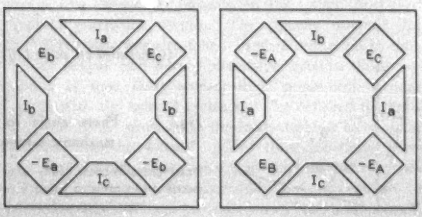

These power quantities can be expressed in terms of symmetrical components as follows:

$$E_BI_a = (E_a - E_c)\bar{I}_a = E_a + E_1 + E_2 - E_0 - aE_1 - a^2E_2$$
$$(\bar{I}_a + \bar{I}_1 + \bar{I}_2)$$
$$= (1-a)E_1\bar{I}_a + (1-a)E_2\bar{I}_1 + (1-a)E_1\bar{I}_2 + (1-a^2)E_2\bar{I}_2 + (1-a^2)E_2\bar{I}_1 + (1-a^2)E_2\bar{I}_2$$

The following table gives the coefficients of all of the sequence voltage-current products.

Relay Quantities	$E_1\bar{I}_1$	$E_1\bar{I}_2$	$E_1\bar{I}_0$	$E_2\bar{I}_1$	$E_2\bar{I}_2$	$E_2\bar{I}_0$	$E_0\bar{I}_1$	$E_0\bar{I}_2$	$E_0\bar{I}_0$
$E_B\bar{I}_a$	$1-a$	$1-a$	$1-a$	$1-a^2$	$1-a^2$	$1-a^2$	0	0	0
$-E_A\bar{I}_a$	a^2-a	a^2-a	$a-a^2$	$a-a^2$	$a-a^2$	$a-a^2$	0	0	0
$E_C\bar{I}_b$	$1-a$	$a-a^2$	a^2-1	a^2-a	$1-a^2$	$a-1$	0	0	0
$-E_B\bar{I}_b$	a^2-a	$1-a^2$	$a-1$	$1-a$	$a-a^2$	a^2-1	0	0	0
$E_A\bar{I}_c$	$1-a$	a^2-1	$a-a^2$	$a-1$	$1-a^2$	a^2-a	0	0	0
$-E_C\bar{I}_c$	a^2-a	$a-1$	$1-a^2$	a^2-1	$a-a^2$	$1-a$	0	0	0
Total	$3-6a+3a^2$	0	0	0	$6a^2-3a-3$	0	0	0	0
Total	$-9a$	0	0	0	$-9a^2$	0	0	0	0

$$P_R + jQ_R = -9aE_1\bar{I}_1 - 9a^2E_2\bar{I}_2$$
but $a = \epsilon^{j120}$ $\quad a^2 = \epsilon^{j240}$
$E_1 = |E_1|\epsilon^{j\alpha_1}$ $\quad E_2 = |E_2|\epsilon^{j\alpha_2}$
$I_1 = |I_1|\epsilon^{-j\beta_1}$ $\quad \bar{I}_2 = |I_2|\epsilon^{-j\beta_2}$

(Note: Angles are in degrees.)

Therefore:

$$P_R + jQ_R = -9(|E_1|)(|I_1|)\epsilon^{j(\alpha_1-\beta_1+120)} - 9(|E_2|)(|I_2|)\epsilon^{j(\alpha_2-\beta_2+240)}$$
$$= 9(|E_1|)(|I_1|)\epsilon^{j(\alpha_1-\beta_1-60)} + 9(|E_2|)(|I_2|)\epsilon^{j(\alpha_2-\beta_2+60)}$$
$$P_R + jQ_R = 9(|E_1|)(|I_1|)[\cos(\alpha_1-\beta_1-60) + j\sin(\alpha_1-\beta_1-60)] + 9(|E_2|)(|I_2|)[\cos(\alpha_2-\beta_2+60) + j\sin(\alpha_2-\beta_2+60)]$$
$$= (|E_1|)(|I_1|)[\cos(\phi_1-60) + j\sin(\phi_1-60)] + 9(|E_2|)(|I_2|)[\cos(\phi_2+60) + j\sin(\phi_2+60)]$$

This is the total input to the relay in terms of symmetrical components. It is seen that the input consists of a positive-phase-sequence term with a voltage E_1, a current I_1, and an angle between E_1 and I_1 equal to $(\phi_1 - 60)$ and a similar negative-phase-sequence term with an angle $(\phi_2 + 60)$.

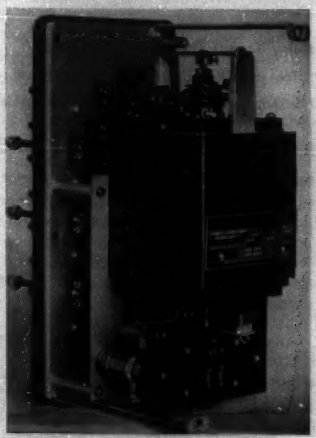

Fig. 4. Three-phase directional relay with voltage restraint

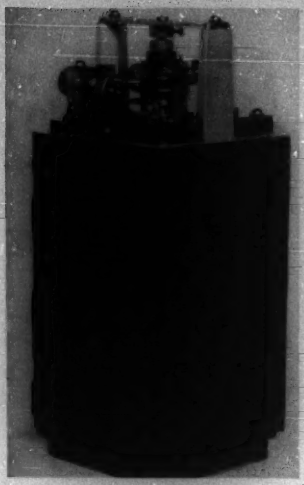

Fig. 5. Three-phase and ground directional relay with voltage restraint

On the basis of a pair of adjacent salients, the relay has average torque proportional to $(|E|)(|I|)\cos(\phi + \theta)$ where

ϕ = the angle by which the current lags the voltage
θ = the angle of lead (current leading voltage) at which maximum torque occurs

Thus, with the above input, the relay will have torque equal to

$$9K[(|E_1|)(|I_1|)\cos(\phi_1 - 60 + \theta) + (|E_2|)(|I_2|)\cos(\phi_2 + 60 + \theta)]$$

where K is the relay torque constant per pair of adjacent salients.

Appendix IB

Connections according to figure 2.

Relay Torque During 3-Phase Fault

$$\text{Torque} = 9K(|E_1|)(|I_1|)\cos(\phi_1 - 60 + \theta)$$

Maximum torque is when $\phi_1 + \theta - 60 = 0$, that is, when $\phi_1 + \theta = 60$ (see figure 6)

Relay Torque During Dead Phase-to-Phase Fault

Assuming $|E_1| = |E_2|$, $|I_1| = |I_2|$, and $\phi_2 = \phi_1 + 180$

$$\text{Torque} = 9K[(|E_1|)(|I_1|)\cos(\phi_1 - 60 + \theta) + (|E_1|)(|I_1|)\cos(\phi_1 + 180 + 60 + \theta)]$$

$$= 9K(|E_1|)(|I_1|)[\cos(\phi_1 - 60 + \theta) + \cos(\phi_1 + 240 + \theta)]$$

$$= 9\sqrt{3}K(|E_1|)(|I_1|)\cos(\phi_1 - 90 + \theta)$$

Maximum torque occurs when $\phi_1 - 90 + \theta = 0$ that is, when $\phi_1 + \theta = 90$ degrees (See figure 7)

Appendix IIA

Quadrature Connection

With the quadrature connection, E_A operates with $-I_a$, E_B with $-I_b$, and E_C with $-I_c$.

The total input to the relay is

$$P_R + jQ_R = -E_A I_a - E_B I_b - E_C I_c$$

Relay Quantities	$E_A I_1$	$E_1 I_1$	$E_a I_1$	$E_2 I_1$	$E_a I_2$	$E_2 I_2$	$E_1 I_2$	$E_a I_2$	$E_2 I_2$
$-E_A I_a$	$a^2 - a$	$a^2 - a$	$a^2 - a$	$a - a^2$	$a - a^2$	0	0	0	
$-E_B I_b$	$a^2 - a$	$1 - a^2$	$a - 1$	$1 - a$	$a - a^2$	$a^2 - 1$	0	0	
$-E_C I_c$	$a^2 - a$	$a - 1$	$1 - a^2$	$a^2 - 1$	$a - a^2$	$1 - a$	0	0	
Total	$3a^2 - 3a$	0	0	0	$3a - 3a^2$	0	0	0	

$$P_R + jQ_R = 3(a^2 - a)E_1 I_1 + 3(a - a^2)E_2 I_2$$
$$= -3\sqrt{3}\,j\,E_1 I_1 + 3\sqrt{3}\,j\,E_2 I_2$$
$$= 3\sqrt{3}(|E_1|)(|I_1|)\epsilon^{j(\alpha_1 - \beta_1 - 90)} + 3\sqrt{3}(|E_2|)(|I_2|)\epsilon^{j(\alpha_2 - \beta_2 + 90)}$$
$$= 3\sqrt{3}(|E_1|)(|I_1|)[\cos(\alpha_1 - \beta_1 - 90) + j\sin(\alpha_1 - \beta_1 - 90)] + 3\sqrt{3}(|E_2|)(|I_2|) \times [\cos(\alpha_2 - \beta_2 + 90) + j\sin(\alpha_2 - \beta_2 + 90)]$$

which is the total input to the relay in terms of symmetrical components and the relay torque is

$$3\sqrt{3}K[(|E_1|)(|I_1|)\cos(\phi_1 - 90 + \theta) + (|E_2|)(|I_2|)\cos(\phi_2 + 90 + \theta)]$$

Appendix IIB

Quadrature Connection

Relay Torque During 3-Phase Fault

$$\text{Torque} = 3\sqrt{3}K(|E_1|)(|I_1|)\cos(\phi_1 - 90 + \theta)$$

Maximum torque is when $\phi_1 - 90 + \theta = 0$ that is, when $\phi_1 + \theta = 90$ (See figure 7)

Relay Torque During Dead Phase-to-Phase Fault

Assuming $|E_1| = |E_2|$, $|I_1| = |I_2|$, and $\phi_2 = \phi_1 + 180$

$$\text{Torque} = 3\sqrt{3}K[(|E_1|)(|I_1|)\cos(\phi_1 - 90 + \theta) + (|E_1|)(|I_1|)\cos(\phi_1 + 180 + 90 + \theta)]$$
$$= 6\sqrt{3}K(|E_1|)(|I_1|)\cos(\phi_1 - 90 + \theta)$$

Maximum torque is when $\phi_1 - 90 + \theta = 0$ that is, when $\phi_1 + \theta = 90$ (See figure 7)

(*Concluded on page 113*)

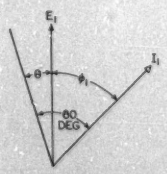

Fig. 6. Phase angle for maximum torque

Three-phase fault; connections according to figure 2

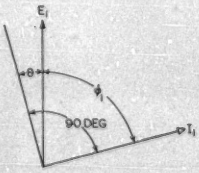

Fig. 7. Phase angle for maximum torque

Dead phase-to-phase fault; connections according to figure 2 or quadrature connections

Ultrahigh-Speed Reclosing of High-Voltage Transmission Lines

By PHILIP SPORN
FELLOW AIEE

D. C. PRINCE
FELLOW AIEE

Reclosure of circuit breakers following a fault on a high-voltage transmission line with a minimum of delay in order that synchronous load will not fall out of step is described in this paper. Apparatus that performs a complete operation in approximately 20 cycles on a 60-cycle system may be used to obtain a high degree of service continuity from a single-circuit transmission line.

HIGH-SPEED reclosing of high-voltage transmission lines has been practiced for a number of years and has been described previously.[1] This method of reclosing has sometimes been termed "instantaneous reclosing." The term "instantaneous" obviously admits of no latitude. It has always, however, been broadly interpreted. As applied to reclosing of high-voltage circuits, as heretofore practiced, it is obviously a misnomer because the time involved has always been appreciable, running into a considerable fraction of a second. In this paper the authors have given the name of ultrahigh-speed reclosing to a reclosing operation at the maximum speed physical phenomena, particularly arc deionization, will permit. So far as is known, this is the first time that high-voltage transmission circuits have been set up to reclose on that basis.

Background of the Problem

The experience back of high-speed reclosing and ultrahigh-speed reclosure is considerable. It has accumulated with the vast extension of transmission networks in the United States and with the experience in interruptions to service, particularly to industrial service, as a result of voltage surges or dips occurring on systems. The basic reason for these voltage dips was generally found to be the long time taken to clear faults occurring on the system. Going back 10 years, these times were frequently of the order of from 3 to 4 seconds. This long duration of reduced voltage, coupled with the fact that many of the industrial control systems were using extensively instantaneous undervoltage devices (instantaneous in this case involving times of from 5 to 10 cycles in the terms of a 60-cycle system) gave serious interruptions in section after section of the United States where transmission service was extensively substituted for rather short-feed localized generation service. The remedy adopted for these difficulties was two-fold. First, a reduction in time of relay action, and second, extensive work in the introduction of time delay undervoltage protection in connection with the control systems. The detailed methods for handling the problem in the latter fashion have again been described elsewhere.[2] All of these solutions, however, had definite limitations, first because many types of motor drives are fundamentally not susceptible to time-delay undervoltage protection as a cure and, second, there is always the problem of complete loss of service where a single line is utilized to take care of the supply into an area or station. One of these difficulties has lately been taken care of by extremely fast clearing of faults. Thus, in recent practice with the use of one-cycle carrier relaying it has been possible, even by using nothing more than a standard 8-cycle breaker, to get a maximum time clearing under all conditions of 0.15 second (9 cycles) and under these conditions the disturbance is not of sufficiently long duration to cause synchronous motor drives to drop out of step. However, there is still the problem of the single line which even with such rapid clearing of faults, of necessity, has to have a service interruption when the line is faulty. It is this particular problem that the authors and their associates had in mind and set themselves to solve in the development described herein.

In a measure this development is an outgrowth of the work done on high-speed breakers and high-speed relaying. Each of these particular developments has previously been described.[3,4,5,6] The problem posed was the attainment of a breaker reclosure so quickly that the net effect on load would be as if no interruption had taken place and no load would be lost. It is apparent that as regards lightning the same result could be obtained by the use of expulsion deionizing gaps. However, although considerable work in that direction has been carried out and some of it has been described,[7] it is a fact that the experience with gaps is still rather limited. Further, the gap has the disadvantage that it will not take care of anything but lightning difficulties and there are other difficulties besides lightning that may cause momentary flashovers which can be cleared and re-established by sufficiently fast reclosure. Besides, since there must be circuit breakers on the line in any event, if these circuit breakers by a special reclosing provision can approach the service standard of a line with both breakers and expulsion gaps, a considerable economic advantage is possible.

From all this it was apparent that a thorough exploration of the possibilities of ultrarapid reclosure by circuit breakers was in order. An examination of the problem

A paper recommended for publication by the AIEE committee on protective devices. Manuscript submitted October 31, 1936; released for publication November 21, 1936.

PHILIP SPORN is vice-president and chief engineer of the American Gas & Electric Company, New York, N. Y. D. C. PRINCE is chief engineer, Philadelphia (Pa.) works, General Electric Company.

1. For all numbered references see list at end of paper.

indicated that the following were essential parts of the solution to the problem:

1. Relaying must be provided which will locate the fault and communicate the trip impulse to all breakers involved in the shortest possible time and, if possible, in a time not exceeding one cycle.

2. Reclosing mechanisms must be provided which will open and reclose the breakers in a total time somewhere between 0.25 and 0.50 second, or a total time of somewhere between 15 and 30 cycles, with the chances very great of need in the direction of the smaller as against the larger of the 2 interyals.

3. The circuit breaker must extinguish the arc in the least possible time and in a period possibly not to exceed 5 or 6 cycles.

4. The actual arc causing the service interruption must not restrike when voltage is restored.

Some of these parts of the complete solution were already available or the facts with regard to the phenomena involved definitely known. Thus, it was definitely known that standard breakers could be obtained to operate in a period not to exceed 8 cycles, and special breakers in a period not over 3 cycles.[4] Again it was definitely known and experience had been previously obtained with a relay system functioning in a period not exceeding one cycle. However, the problem of getting a mechanism applicable to a standard breaker that would reclose in a period of from 7 to 8 cycles, or a total period from initiation of fault of 15 cycles, definitely had not been solved. Again, although the action of the arc upon re-establishment of potential had been previously explored[8] by others, insufficient and inconclusive data was available for complete guidance to a satisfactory solution of the problem presented. Nevertheless, it was decided that the period had arrived when it was necessary and desirable to attempt to bring to a solution this particular problem, taking advantage of what was available, and developing or exploring those parts that were unavailable from an equipment standpoint or unknown from a fundamental theoretical standpoint. This paper describes the developments thus made, the investigations both in the laboratory and in the field, and the performance of a system of rapid circuit interruption and ultrahigh-speed reclosing.

Carrier Current Relaying System

Choice of relay equipment was determined by the desirability of high-speed operation combined with nearly simultaneous energization of the trip circuits of the breakers at each terminal. Carrier-current relaying is the only practical system which provides high-speed operation for any fault at any location on the circuit being protected.[9] When it came to a decision as to the type of carrier to be employed, one was confronted with the fact that as a matter of plain arithmetic a one-cycle system was almost essential. Thus, if 6 cycles is allowed for arcing and 8 cycles is permitted for reclosure after the arc has been extinguished, the total time available for relaying, if the total time of 15 cycles is to be adhered to, is only one cycle. It was obvious that if a larger amount of time was satisfactory for reclosure, some leeway was available in the relaying time but the one-cycle system, if practically available, was ideally suited for this problem.

The one-cycle relaying system utilized here has been previously described[5,6] as can be seen by reference to such previous data. The trip circuit is normally held open by the receiver relays and it is closed only by the dropping out of these relays when no carrier signal is received. Since the relays controlling the trip circuits at both ends are simultaneously de-energized by the stoppage of the carrier signal, the actual closing of the trip circuits will occur at nearly the same instant.

Because of the importance that the relaying plays in the entire scheme, it may be pertinent to review the salient parts of the relay scheme, their function and performance. Figure 1 shows the fundamental scheme and involves in essence the following equipment:

1. *Receiver Relay.* This is a polarized relay having a field winding and an operating winding arranged to be energized either from the local battery circuit or from the received carrier signal. The relay

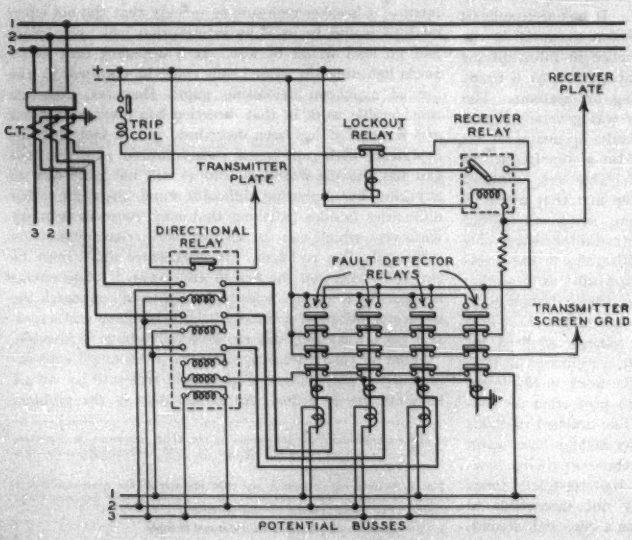

Fig. 1. High-speed carrier-current relay circuit

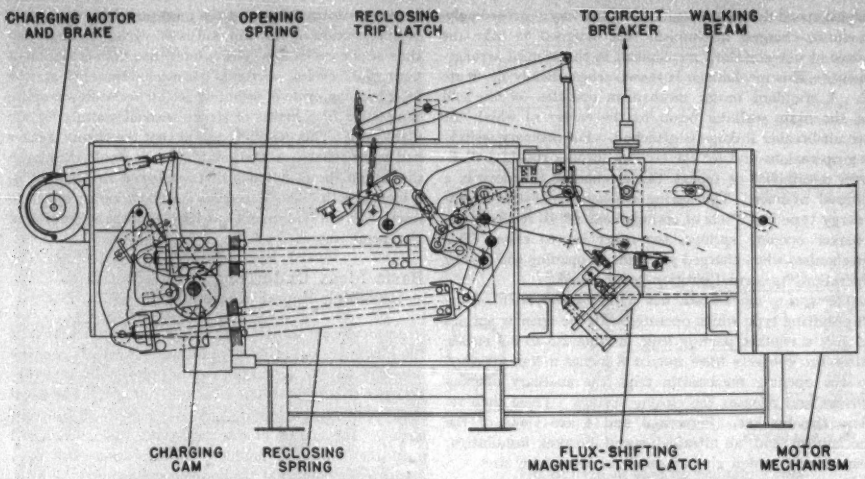

Fig. 2. Schematic diagram of ultrahigh-speed reclosing mechanism for oil circuit breakers

will close its tripping contacts when de-energized and hold the tripping contacts open normally when excited from the battery circuit and during fault conditions when excited from the received carrier signal. The relay will close its lockout contacts when energized and hold them closed normally when excited from the battery circuit and during fault conditions when excited from the received carrier signal.

2. *Fault Detecting Elements.* Three for phase faults, these being of the impedance type, that is, having a current operating winding and a voltage restraining winding, and one for ground faults having only a current winding. All of these fault detectors were equipped with 4 independent contacts for performing the following functions:

a. A circuit-opening contact for starting carrier by the removal of the grid bias.

b. A circuit-opening contact for disconnecting the receiver relay coil from the local battery supply.

c. A circuit-opening contact for removing voltage restraint from the directional relay.

d. A circuit-closing contact which is in series with the receiver relay contact and the tripping circuit.

3. *Directional Relay.* This is the polyphase type, having voltage restraint. This relay is of the new induction cup type, giving it greater speed than was obtainable with previous types of power directional relays.

4. *Lockout Relay.* This is a time-delay circuit-opening and circuit-closing auxiliary relay of the plunger bellows type which is adjusted to give a time delay of 5 cycles in opening or closing its contacts.

The sequence of operation is comparatively simple and may be described briefly as follows: Under normal conditions the directional-relay contacts are held closed by voltage restraint, applying plate voltage to the transmitter but the transmitter does not operate because of the normally closed contacts of the fault-detector relays which apply a negative bias to the screen grid of the transmitter. Further, the receiver-relay contacts are held open by the closed contacts of the fault-detector relays energizing the receiver-relay coil from the station battery. In case of an internal fault the directional relays will operate to stop the transmission of carrier at both ends of the line. When the carrier from both ends has been stopped then the receiver relays are de-energized and they both drop out, completing the trip circuits. The receiver relay operates in an average time of 0.35 cycle. The directional relay opens its contacts in an average time of 0.40 cycle so that the fundamental fastest time possible is approximately 0.75 cycle. Some variations on either side of that value are obviously possible. On an external fault one of the directional relays on the end where power is flowing from the line into the bus will permit the carrier signal to be maintained, thereby preventing tripping. The function of the lockout relay is to open the trip 5 cycles after the circuit-closing contacts of the fault detector have closed to prevent false tripping on a through fault as the result of sudden reversals of power flow and also to prevent tripping in case of system instability.

Tripping and Reclosing Mechanisms and Circuit-Breaker Operation

Most standard mechanisms require about 0.5 second to close the circuit breaker. Reclosing mechanisms have been made providing an over-all time of this order by connecting 2 mechanisms together through a walking beam. One of the 2 mechanisms is at all times at rest with its latch reset. When tripped the circuit breaker opens until the energized mechanism builds up enough force to overcome the opening springs and momentum. It was obviously necessary in this case to secure a much

higher speed than was obtainable in this way. Accordingly, a spring-charged mechanism was designed to take the place of one standard mechanism in the teamed arrangement. This mechanism is shown schematically in figure 2. A standard motor mechanism operates on one end of the main walking beam to the center of which the circuit-breaker linkage is attached. For ordinary switching operations and for the second opening should a flashover re-establish or repeat, this mechanism functions in a normal manner. The spring mechanism of the stored-energy type has 2 sets of springs; one set to reinforce the breaker opening springs, the other set to close. This mechanism when charged performs an opening and closing operation, its normal position being closed.

The spring mechanism has a high-speed latch of the flux-shifting type which operates with the opening springs to give a contact parting time of from 2.5 to 3.5 cycles. After the contacts have moved 8 inches a link attached to the opening mechanism trips the auxiliary opening springs and releases the closing springs. These then reclose the breaker. Figures 3 and 4 are views of the mechanism and an ultrahigh-speed breaker installation, respectively, which give an excellent idea of the size.

During the reclosing stroke the tripping circuit is transferred to the motor mechanism so that a permanent fault will be tripped off at once. As adjusted for test, one of these mechanisms gave an over-all time from initial trip impulse to contact make of 15 cycles. It proved rather difficult to hold this fine adjustment throughout so that the service record aimed at was much nearer 18 cycles. A typical calculated travel record is shown in figure 5. It may be noticed first that the total time from the instant of energization of the trip coil is 16 cycles: taking relay time at one cycle, this gives a total time from initiation of fault of 17 cycles. Second, the mechanism once started on a tripping cycle is definitely set for reclosure upon the completion of 8 inches of stroke without waiting for arc extinction. This definitely meant that the circuit breaker had to be reliable to the point where it would extinguish the arc on the completion of the allowed stroke, that is, 8 inches, with enough to spare for the tripping relays to reset. As will be brought out later, this was accomplished in general very successfully.

Basic Ideas Underlying Ultrahigh-Speed Reclosing

As previously pointed out, one of the essential parts of the solution of the problem of ultrarapid reclosing was the necessity for the actual arc causing the service interruption not to restrike when voltage is restored. The usual fault against which protection is sought is a lightning stroke. The circuit in this case cannot be re-energized until the ionization produced by the stroke has been dissipated enough that the restored voltage may be withstood. This time was investigated in both field and laboratory tests. Griscom and Torok[8] have made a series of such tests, varying the current from 800 to 1,500 amperes and the voltage from 66 kv to 130 kv with the spacing of electrodes from 12 inches to 93 inches. They concluded that:

1. The restriking of arcs is a random phenomenon.

Fig. 3. Ultrahigh-speed circuit-breaker reclosing mechanism

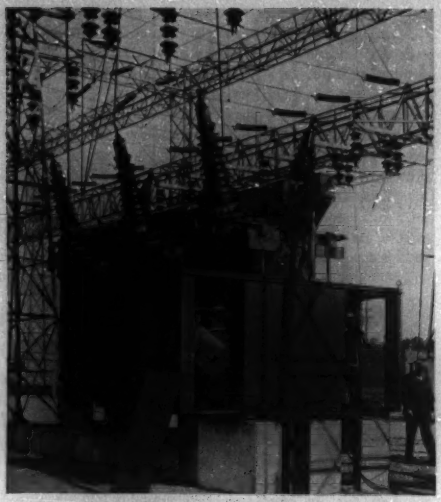

Fig. 4. A 132-kv installation of the ultrahigh-speed reclosing breaker

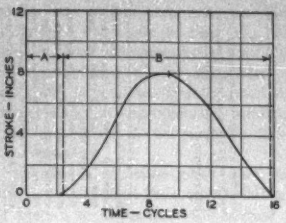

Fig. 5. Travel record of ultra-high-speed mechanism

A—Trip impulse of 2.4 cycles until contacts part

B—Contacts part to make 8-inch stroke during 13.4 cycles

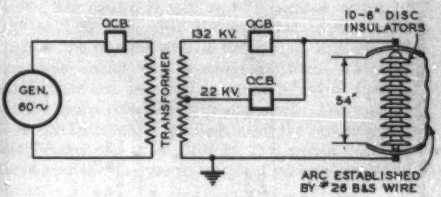

Fig. 6. Circuit used for laboratory tests

2. The probability of restrike increases with operating voltage for spacings ordinarily used.

3. The probability of restriking is only slightly affected by large variations in current.

4. For a given recovery voltage above a certain spacing, the probability of restriking is but slightly affected by the spacing of electrodes; below this value, spacing plays an important part.

The restriking times found by Griscom and Torok vary from about $1^1/_2$ cycles at 66 kv to a little over 3 cycles at 130 kv. The authors made some preliminary tests in 1935, under conditions similar to those used by Griscom and Torok but with currents of the order of 5,000 amperes, from which a probable restriking time of nearly 5 cycles resulted. These tests seemed to indicate that insufficient current range had been used in the earlier tests. Several other variables seemed to require attention, including velocity of wind, duration of arcing, and position of gap. In addition to these, the weatherman's part in the picture had to be determined. What would be the practical effect of multiple strokes of lightning? Would field experience show a larger or smaller proportion of successful reclosures than obtained in fair weather tests? It was decided to undertake additional tests along 3 lines:

1. Additional laboratory tests to further clarify the effects of voltage, current, distance between electrodes, wind, arc duration, etc.

2. Staged field tests to cross check against laboratory tests and determine the operation of high-speed reclosure under practical field conditions.

3. An extended field-operation test to determine from experience the service improvement possible with high-speed reclosure.

Laboratory Tests

The method employed in the laboratory tests is indicated in figure 6. A fine-wire fuse is suspended between the ends of an insulator string, arcing horns, or other electrodes. The arc is drawn by closing a 20-kv circuit through this fuse. The fuse is quickly vaporized. The 20-kv circuit is then opened and after a time another circuit of higher voltage is closed. Some 300 tests have been made from which some conclusions seem justified, while others are in doubt. Figure 7 is a chart and table I is a summary of all the tests made. On the chart, crosses indicate a restrike and circles an absence of restrike. A line is drawn from the cross representing the longest restriking time to the circle representing the shortest non-restriking time. The center of this line should represent 50 per cent probability of restriking.

Any conclusions drawn are subject to modification as more experimental evidence becomes available.

In the meantime, the data on the chart and table may be examined to determine different tendencies. As a matter of probabilities, one may conclude that:

1. Restriking times are longer with a high-current arc.

2. Restriking times are longer the longer the arc is sustained.

3. Restriking times are longer in still air.

4. Moderate changes in electrode form, spacing, and location of arc are not important although a wider range might disclose differences as in 1, 2, and 3.

5. Restriking times vary from $2^1/_2$ to 12 cycles.

The line of development which would give a minimum

Table I—Summary of Laboratory Tests on Effect of Various Changes on Restriking Time on String of Suspension Insulators

Conditions of Test								Restriking Time, Cycles										Conclusions
Voltage, Kilovolts	Current, Amperes	Rain	Number of 5½-in. Insulator Units	Arcing Rings	Wind Velocity, Miles per Hour	Faults to Lee or Wind of String	Initial Fault Duration, Cycles	800 Amperes Low	800 Amperes High	800 Amperes Mean	6,000 Amperes Low	6,000 Amperes High	6,000 Amperes Mean	Difference Low	Difference High	Difference Mean	Number of Tests Geometric Mean	Weighted Difference Low	Weighted Difference High	Weighted Difference Mean	
80		No	12	Yes	20–30	Lee	8	2.0	5.0	3.5	5.3	5.6	5.4	3.3	0.6	1.9	19	63	11	36	On the average approximately 2½ cycles or 50 per cent more dead time is required at 6,000 amperes than at 800 amperes
80		No	12	No	10–15	Lee	8	4.0	4.5	4.3	4.4	4.6	4.5	0.4	0.0	0.2	13	5	0	3	
80		No	12	Yes	0– 5	Lee	8	5.8	6.4	6.1	6.8	9.4	8.1	1.0	3.0	2.0	9.5	10	29	19	
80		No	12	No	0– 5	Lee	8	4.3			6.8	11.9	9.3	2.5			10	25			
80		No	9	Yes	0– 5	Lee	8	2.7	7.1	4.9	9.0	9.9	9.4	6.3	2.8	4.5	15.5	98	43	69	
80		No	12	Yes	0– 5	Lee	2	4.6	5.6	5.1	5.3	6.2	5.8	0.7	0.6	0.7	9.8	7	2	4	
80		Yes	12	No	0– 5	Lee	8	6.0	7.0	6.5	9.5	10.0	9.8	3.5	3.0	3.3	14.5	50	43	47	
																	91.3	81.3	81.3	258	130	178	
																	Weighted average difference				2.8	1.6	2.2	

							0–5 Miles per Hour Low	0–5 Miles per Hour High	0–5 Miles per Hour Mean	5–10 Miles per Hour Low	5–10 Miles per Hour High	5–10 Miles per Hour Mean	10–15 Miles per Hour Low	10–15 Miles per Hour High	10–15 Miles per Hour Mean	20–30 Miles per Hour Low	20–30 Miles per Hour High	20–30 Miles per Hour Mean	
80	6,000	No	12	Yes		Lee	8	6.8	9.4	8.1				8.6	9.2	8.7	5.3	5.6	5.4	Effect of wind velocity negligible below 10 miles per hour without arcing rings and 15 miles per hour with arcing rings Between 10 and 15 miles per hour, it allows a reduction in dead time of about 2.0 cycles without arcing rings Between 20 and 30 miles per hour, it allows a reduction in dead time of about 2.5 cycles even with arcing rings
80	6,000	No	12	No		Lee	8	6.8	11.9	9.3				4.4	4.6	4.5				
80	800	No	12	Yes		Lee	8	5.8	6.4	6.1							2.0	5.0	3.5	
80	800	No	12	No		Lee	8	4.3			4.0	4.2	4.1	4.0	4.6	4.3				
80	800	No	9	Yes		Lee	8	2.7	7.1	4.9				6.7	7.2	6.9				
80	800	No	12	No		Wind	8	4.7	6.1	5.4	7.5	7.7	7.6	2.9	5.5	4.2				

							2 Cycles Low	2 Cycles High	2 Cycles Mean	8 Cycles Low	8 Cycles High	8 Cycles Mean	30 Cycles Low	30 Cycles High	30 Cycles Mean	
80	6,000	No	12	Yes	0– 5	Lee	5.3	6.2	5.8	6.8	9.4	8.1	9.3	9.7	9.5	At 6,000 amperes, 2 cycles less dead time is required for 2-cycle initial fault duration than for 8 cycles Between 8 and 30 cycles, the loss is only one cycle At 800 amperes, the difference is reduced only one cycle between 2- and 8-cycle initial fault duration
80	800	No	12	Yes	0– 5	Lee	4.6	5.6	5.1	5.8	6.4	6.1				

							Arcing Rings Low	Arcing Rings High	Arcing Rings Mean	No Arcing Rings Low	No Arcing Rings High	No Arcing Rings Mean	Difference Low	Difference High	Difference Mean	Number of Tests Geometric Mean	Weighted Difference Low	Weighted Difference High	Weighted Difference Mean	
80	6,000	No	12		10–15	Lee	8.6	9.2	8.9	4.4	4.6	4.5	4.2	4.6	4.4	12	50	55	53	Wind velocity between 10 and 15 miles per hour showed a decrease in necessary dead time of 4½ cycles when arcing rings were removed. Wind velocity less than 5 miles per hour shows no appreciable effect of the presence or absence of arcing rings
80	6,000	No	12		0– 5	Lee	6.8	9.4	8.1	6.8	11.8	9.3	0.0	−2.4	−1.2	13	0	−31	−16	
80	800	No	12		0– 5	Lee	5.8	6.4	6.1	4.3			1.5			8	12			
80	800	No	12		0– 5	Lee	4.3									20.5	−14	+14	0	
80	800	No	9		0– 5	Lee	2.7	7.1	4.9	3.4	6.4	4.9	−0.7	+0.7	0	53.5	45.5	45.5	48	38	37	
																Weighted average difference			0.9	0.8	0.8	

							Lee Low	Lee High	Lee Mean	Windward Low	Windward High	Windward Mean	Difference Low	Difference High	Difference Mean	Number of Tests Geometric Mean	Weighted Difference Low	Weighted Difference High	Weighted Difference Mean	
80	800	No	12	No	10–15		4.0	4.6	4.3	2.9	5.5	4.2	−1.1	+0.9	−0.1	11.5	−13	+10	−1	Necessary dead time is about 1½ cycles less on the lee than on the windward side of the string
80	800	No	12	No	5–10		4.0	4.2	4.1	7.5	7.7	7.6	3.5	3.5	3.5	8.5	30	30	30	
80	800	No	12	No	0– 5		4.3			4.7	6.2	5.4	0.4			5.5	2			
																25.5	20	19	40	29	
																Weighted average difference			0.7	+2	+1	

							12 Units Low	12 Units High	12 Units Mean	9 Units Low	9 Units High	9 Units Mean	Difference Low	Difference High	Difference Mean	Number of Tests Geometric Mean	Weighted Difference Low	Weighted Difference High	Weighted Difference Mean	
80	6,000	No		Yes	0– 5	Lee	6.8	9.4	8.1	9.0	9.9	9.4	2.2	0.5	1.3	10.4	23	5	14	Within the limits investigated, the number of insulator units makes no difference in the necessary dead time
80	800	No		Yes	0– 5	Lee	5.8	6.4	6.1	3.7	7.1	4.9	−3.1	+0.7	−1.2	14	−43	10	−17	
80	800	No		No	0– 5	Lee	4.3			3.4	6.4	4.9				11				

							No Rain Low	No Rain High	No Rain Mean	Rain Low	Rain High	Rain Mean	Number of Tests Geometric Mean	Weighted Difference Low	Weighted Difference High	Weighted Difference Mean	
80	6,000		12	No	0– 5	Lee	6.8	11.9	8.3	9.5	10.0	9.7	16.5	31	23	28	Presence of rain appears to increase the necessary dead time about 1½ cycles
80	800		12	No	0– 5	Lee	4.3			6.0	7.0	6.5	11.5	39	17	28	
													28	70	40	56	
													Weighted average difference		2.5	1.4	2.0

outage time should combine high-speed tripping to give short fault duration with high-speed reclosing.

If reclosing is to be at a long enough interval to give little probability of a restrike, voltage must not be applied to the line for about 12 cycles after the arc has been interrupted. With an 8 cycle breaker this gives 20 cycles for the over-all reclosure time. At the other extreme, reclosure after $2^1/_2$ cycles will be successful sometimes. If a flashover is caused by multiple lightning strokes, some reclosures longer than 20 cycles over-all may still be followed by restriking. For that reason, the final limits will not have been determined until after a considerable period of experience under actual service conditions.

Field Tests

The actual installation of ultrahigh-speed reclosing breakers was made on the 59.2-mile 132-kv line between the Fort Wayne, Ind., station of the Indiana & Michigan Electric Company and the Deer Creek (Marion) station of the Indiana General Service Company. High-speed reclosing mechanisms of the type described herein were installed on the breakers at both stations. One-cycle carrier-current relaying was employed on the line for fast and simultaneous tripping of breakers at both ends of the line. Automatic high-speed oscillographs were installed at both stations to determine the performance of the breakers under actual operating conditions. As a preliminary to long-time test operation, a series of complete tests was made on May 17, 1936, and another on June 14, 1936, the object being not only to test thoroughly the performance of the assembled equipment but to ascertain, if possible, the likelihood of successful performance under actual operating conditions and the actual time to be used as the reclosure interval for such long time tests.

In all, 35 reclosure tests were made. A tabulated summation of 20 of these tests is indicated in table II.

Tests 1 to 4 illustrate the normal performance of the breakers and relays for an internal phase-to-ground fault. The carrier-current relays operated within from 0.70 to 1.00 cycle after the inception of the fault to energize the trip circuits of the circuit breakers. The line was completely de-energized from 5.3 to 7.2 cycles later and remained so for a period of from 10.7 to 12.0 cycles before being re-energized. The total time from the initiation of the fault until the reclosing of the last breaker was from 21.0 to 21.8 cycles. On all of these tests the line was re-energized without restriking of the arc.

Tests 5 to 7 show the performance for internal phase-to-phase faults not involving ground. Here it will be noted that in 2 of the tests the arc was restruck after the line was energized. The line was de-energized for periods of from 11.5 to 14.1 cycles, and the test where the line was de-energized for 14.1 cycles was the only case where the arc did not restrike after energization of the line.

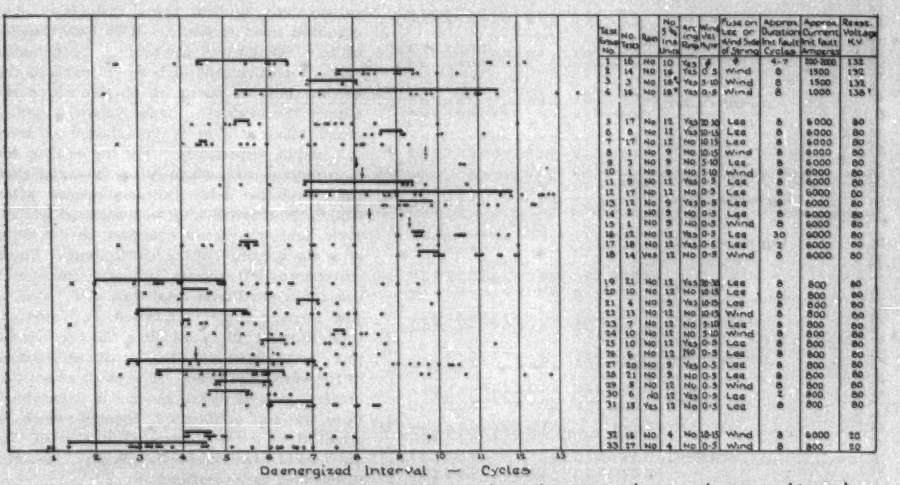

Test Group No.	No. Tests	Rain	No. § Wind Units	Arc re-est.	Wind Vel. m.p.h.	Fuse on Lee or Wind Side of String	Approx. Duration Arc Faults Cycles	Approx. Current Arc Faults Amperes	Recept. Voltage Kv
1	16	No	10	Yes	?	?	4-7	100-2000	132
2	14	No	18	Yes	0-5	Wind	8	1500	132
3	3	No	18	Yes	5-10	Wind	8	1500	132
4	16	No	18	Yes	0-5	Wind	8	1000	138 †
5	17	No	12	Yes	20-30	Lee	8	6000	80
6	8	No	12	Yes	10-15	Lee	8	6000	80
7	17	No	12	No	10-15	Lee	8	6000	80
8	1	No	9	No	10-15	Wind	8	6000	80
9	3	No	9	No	5-10	Lee	8	6000	80
10	1	No	9	No	5-10	Wind	8	6000	80
11	9	No	12	Yes	0-5	Lee	8	6000	80
12	17	No	12	No	0-5	Lee	8	6000	80
13	12	No	9	Yes	0-5	Lee	8	6000	80
14	2	No	9	No	0-5	Lee	8	6000	80
15	1	No	9	No	0-5	Wind	8	6000	80
16	12	No	12	Yes	0-5	Lee	30	6000	80
17	18	No	12	Yes	0-5	Lee	2	6000	80
18	14	Yes	12	No	0-5	Wind	8	6000	80
19	21	No	12	Yes	20-30	Lee	8	800	80
20	10	No	12	No	10-15	Lee	8	800	80
21	4	No	9	Yes	10-15	Lee	8	800	80
22	13	No	12	No	10-15	Wind	8	800	80
23	7	No	12	No	5-10	Lee	8	800	80
24	10	No	12	No	5-10	Wind	8	800	80
25	10	No	12	Yes	0-5	Lee	8	800	80
26	6	No	12	No	0-5	Lee	8	800	80
27	20	No	9	Yes	0-5	Lee	8	800	80
28	21	No	9	No	0-5	Lee	8	800	80
29	8	No	12	No	0-5	Wind	8	800	80
30	6	No	12	Yes	0-5	Lee	2	800	80
31	13	Yes	12	No	0-5	Lee	8	800	80
32	16	No	4	No	10-15	Wind	8	6000	20
33	27	No	4	No	0-5	Wind	8	800	20

Fig. 7. Chart of laboratory reclosing tests on insulator string for tendency to restrike versus de-energized interval

Crosses indicate arc re-establishment; circles indicate no arc re-establishment

* Insulator string suspended horizontally

† Supplied by 2 transformers at 120 degrees, each supplying 80 kv, common point grounded

§ Wind velocity not recorded; believed to be about 15 miles per hour

Position of fuse wire changed from test to test

Table II—Summary of Field Tests on 132-Kv Ultrahigh-Speed Reclosing Oil Circuit Breakers, Fort Wayne-Deer Creek Line, May 17 and June 14, 1936

Test Number	Date	Time*	Type of Fault	Line Dead Time, Cycles	Fault Arc Restruck	Primary Amperes	Relay Time	Fort Wayne: Time, Cycles: Breaker Clearing Time	Fort Wayne: Time, Cycles: Breaker Reclosing Time	Fort Wayne: Time, Cycles: Total Time	Fort Wayne: Travel, Inches: Breaker to Interrupt	Fort Wayne: Travel, Inches: Breaker to Reclose	Fort Wayne: Breaker Restripped	Deer Creek: Primary Amperes	Deer Creek: Relay Time	Deer Creek: Time, Cycles: Breaker Clearing Time	Deer Creek: Time, Cycles: Breaker Reclosing Time	Deer Creek: Time, Cycles: Total Time	Deer Creek: Travel, Inches: Breaker to Interrupt	Deer Creek: Travel, Inches: Breaker to Reclose	Deer Creek: Breaker Restripped	Remarks
1.	5/14/36	8:34	e1 to Grd.	11.8	No	275	1.00	7.2	19.0	20.0	6.25	9.25	No	690	0.90	5.4	20.9	21.8	5.75	11.5	No	
2.	5/14/36	8:54	e1 to Grd.	12.0	No	270	0.95	6.55	18.55	19.5	6.25	9.25	No	745	0.90	5.1	20.2	21.1	4.75	10.0	No	
3.	5/14/36	9:07	e1 to Grd.	12.0	No	270	0.95	6.55	18.55	19.5	6.25	9.25	No	745	0.70	5.2	20.8	21.5	4.75	10.0	No	
4.	5/17/36	9:40	e1 to Grd.	10.7	No	300	1.00	5.3	16.0	17.0	6.0	7.0	No	800	0.80	4.8	20.2	21.0	6.0	11.6	No	
5.	5/17/36	2:36	e1 to e3	14.1	No	740	0.90	6.8	20.9	21.8	6.0	8.0	No	510	0.80	5.0	21.3	22.1	6.0	13.0	No	
6.	6/14/36	12:10	e1 to e3	13.9	Yes	750	0.70	6.4	20.3	21.0	6.25	10.3	Yes	520	0.70	5.45	22.6	23.2	5.75	11.5	Yes	
7.	6/14/36	12:30	e1 to e3	11.5	Yes	750	0.70	5.4	18.5	19.5	6.25	10.0	Yes	520	0.70	5.45	23.6	24.2	5.75	11.6	Yes	
8.	6/14/36	2:10	e1 to e3 to Grd.	13.3	No	750	0.90	6.4	19.7	20.6	6.25	10.5	No	760	0.90	5.0	21.2	22.1	5.75	12.75	No	
9.	5/17/36	1:33	e1 to Grd.	7.4	No	290	0.70	5.3	15.9	16.6	4.5	7.0	No	860	0.75	3.75	24.6	24.6	6.0	13.0	No	Tripping delayed 3 cycles at Deer Creek
10.	5/17/36	6:30	e1 to Grd.	6.2	No	300	0.90	5.1	15.8	16.7	4.5	8.0	No	930	0.70	9.9	24.8	25.5	6.0	11.5	No	Tripping delayed 4 cycles at Deer Creek
11.	5/17/36	6:40	e1 to Grd.	5.5	No	290	0.85	6.15	16.00	16.9	6.0	7.0	No	860	0.70	10.3	25.8	26.5	6.0	11.6	No	Tripping delayed 5 cycles at Deer Creek
12.	5/17/36	7:09	e1 to Grd.	5.5	Yes	270	1.00	5.3	15.5	16.5	4.5	7.0	Yes	840	0.70	9.9	25.5	26.2	6.0	11.0	Yes	Tripping delayed 5 cycles at Deer Creek
13.	5/17/36	6:57	e1 to Grd.	3.6	Yes	290	0.90	5.8	14.9	15.8	4.5	7.0	Yes	840	0.70	11.0	27.2	27.9	6.75	11.6	No	Systems out of parallel; 9,000 kw over line
14.	6/14/36	10:31	e1 to Grd.	10.2	No	290	1.00	8.35	18.35	19.6	6.25	9.25	No	835	1.00	6.0	21.2	23.2	5.75	12.75	No	Systems out of parallel; 28,000 kw over line
15.	6/14/36	10:50	e1 to Grd.	11.6	No	290	1.00	6.9	18.5	19.6	6.25	9.25	No	750	1.00	6.8	21.3	23.3	5.75	12.75	No	Systems out of parallel; 28,000 kw over line
16.	6/14/36	12:24	e1 to Grd.	11.6	No	230	1.10	6.9	18.5	19.6	6.25	9.25	No	750	1.00	6.8	21.3	23.3	5.75	12.75	No	Systems out of parallel; 28,000 kw over line
17.	6/14/36	5:31	e1 to Grd.	11.7	No	210	0.70	7.2	18.9	19.6	7.0	9.25	No	850	1.00	6.7	20.6	21.6	7.25	11.6	Yes	Systems out of parallel; 40,000 kw over line
18.	6/14/36	4:10	e1 to Grd.	11.8	No	250	1.33	6.3	18.1	19.4	6.25	9.25	No	1,000	1.00	6.3	20.1	21.1	5.75	10.0	No	Systems out of parallel; 0 kw over line
19.	6/14/36	4:50	e1 to Grd.	11.4	No	250	0.70	6.9	18.3	19.0	6.25	9.25	No	1,110	1.00	5.8	20.0	21.0	5.75	11.5	No	Systems out of parallel; 9,000 kw over line
20.	6/14/36	5:08	e1 to Grd.	12.5	No	290	0.70	6.3	18.8	19.5	6.25	9.25	No	1,000	1.00	6.1	19.9	20.9	5.75	10.0	No	Systems out of parallel; 10,000 kw over line

* Light face indicates time a.m.; bold face indicates time p.m.

In test 8 an internal phase-to-phase-to-ground fault was applied. Here the line was de-energized for 13.3 cycles and the line was re-energized without the arc restriking.

Tests 9 to 13 were made to determine the minimum time that the line could be de-energized on an internal phase-to-ground fault without the arc restriking upon energization of the line. This was accomplished by intentionally delaying the tripping time of the breaker at Deer Creek station by inserting a time-delay auxiliary relay in the trip circuit. It may be noted that the minimum time the line had to be de-energized averaged approximately 6.0 cycles in order to prevent the arc restriking. In test 13, voltage was reapplied a second time when the breaker at Deer Creek station finally reclosed. The dead time in the second interval was only 2.0 cycles.

Tests 14 to 20 were made to determine the performance of the reclosing equipments on a single tie line between 2 systems (not otherwise connected in parallel) with varying amounts of load transfer over the tie line. The system arrangement used on these tests represented a single 132-kv tie line approximately 340 miles long between the 2 generating stations.

With load transfers up to 28,000 kw over the tie line, the breakers and relays performed satisfactorily to hold the 2 systems in synchronism upon reclosure. With load transfer up to 40,000 kw over the tie line, the breakers reclosed satisfactorily at both terminals of the tie line but the operation of the relays retripped the breakers. Figure 6 shows 3 oscillograms taken at Fort Wayne station for tests 4, 7, and 15, respectively. The top oscillogram is for test 4 from which it will be noted that the directional relay contacts opened after 0.50 cycle, that blocking was removed in 0.60 cycle, and trip circuit energized in 1.0 cycle after the inception of the short circuit. Fault current was 300 amperes, primary current, and was interrupted in a total time of 6.3 cycles. The breaker contacts reclosed in 17 cycles, total time, or 16 cycles after the trip circuit was energized, as indicated by the oscillations in the current element. The point where the breaker contacts reclose can also be determined from the top oscillograph element which is attached to a travel recorder and gives the mechanical position of the breaker contacts throughout the operation.

The middle oscillogram is for test 7, which was a phase-to-phase short circuit in which the arc restruck. The relay operating time was somewhat faster in this case, the directional-relay contacts opening in 0.4 cycle, blocking being removed in 0.5 cycle, and the

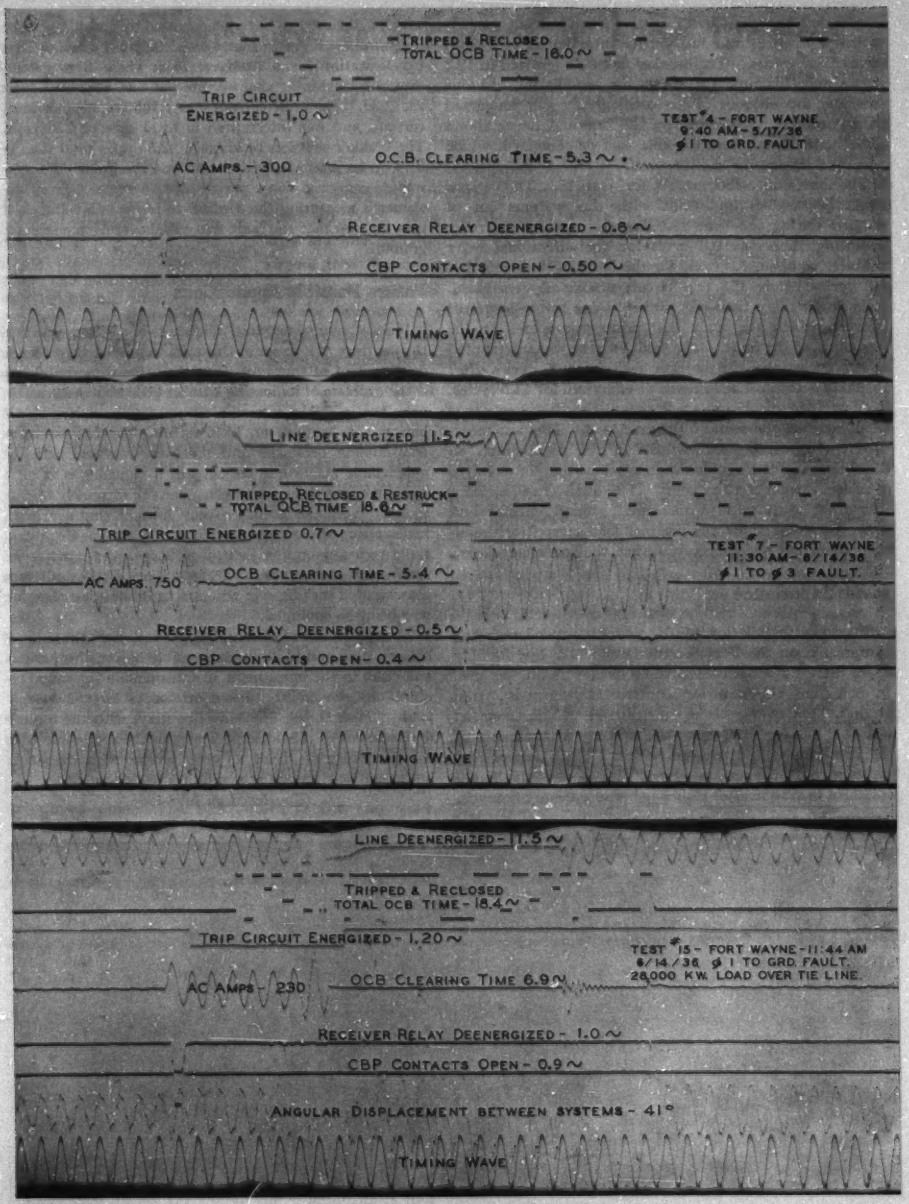
TRIPPED & RECLOSED
TOTAL OCB TIME - 16.0 ~
TRIP CIRCUIT
ENERGIZED - 1.0 ~
TEST 4 - FORT WAYNE
9:40 AM - 5/17/36
ϕ1 TO GRD. FAULT
AC AMPS. - 300
O.C.B. CLEARING TIME - 5.3 ~
RECEIVER RELAY DEENERGIZED - 0.6 ~
CBP CONTACTS OPEN - 0.50 ~
TIMING WAVE
LINE DEENERGIZED 11.5 ~
TRIPPED, RECLOSED & RESTRUCK
TOTAL OCB TIME 18.6 ~
TRIP CIRCUIT ENERGIZED 0.7 ~
TEST 7 - FORT WAYNE
11:30 AM - 6/14/36
ϕ1 TO ϕ3 FAULT.
AC AMPS. 750
OCB CLEARING TIME - 5.4 ~
RECEIVER RELAY DEENERGIZED - 0.5 ~
CBP CONTACTS OPEN - 0.4 ~
TIMING WAVE
LINE DEENERGIZED - 11.5 ~
TRIPPED & RECLOSED
TOTAL OCB TIME - 18.4 ~
TRIP CIRCUIT ENERGIZED - 1.20 ~
TEST 15 - FORT WAYNE - 11:44 AM
6/14/36 ϕ1 TO GRD. FAULT.
28,000 KW. LOAD OVER TIE LINE.
AC AMPS - 230
OCB CLEARING TIME 6.9 ~
RECEIVER RELAY DEENERGIZED - 1.0 ~
CBP CONTACTS OPEN - 0.9 ~
ANGULAR DISPLACEMENT BETWEEN SYSTEMS - 41°
TIMING WAVE

Fig. 8. Oscillograms of field tests

trip circuit energized in 0.7 cycle. Fault current was 750 primary amperes and was finally interrupted in a total time of 7.7 cycles. The breaker contacts reclosed in 19.3 cycles and this time the arc was re-established. In this case the top element of the oscillograph was connected to a potential transformer on the line and hence shows directly the total time the line was de-energized, which was 11.6 cycles.

The bottom oscillogram is for test 15. This was a single phase-to-ground fault with the systems out of parallel during the time the line was open. The relay operating time was 0.9 cycle for the directional relay contacts to open, 1.0 cycle for the blocking to cease, and 1.2 cycles before the trip circuit was finally energized. This slower relay time was probably due to the low fault current, which was only 230 primary amperes at the beginning of the fault. The fault current was interrupted in 8.1 cycles and the breaker reclosed 19.6 cycles after the fault began. The line was de-energized for 11.5 cycles. The angular displacement between the 2 systems was 41 degrees at the instant they reclosed. This was measured by connecting an element of the oscillograph so as to measure the vector difference between the voltages of phases one on the 2 systems. The oscillograph element measuring fault current measured ground current and hence does not show the original load current or the in-rush of current which occurred when the line was reclosed.

Field Experience

Since the installation of the ultrahigh-speed reclosing equipments on the Fort Wayne-Deer Creek line in May 1936, there have been 4 lightning flashovers on this line. In all 4 cases, the flashover occurred between phase 3 and ground. The average time that the line was de-energized was 13.0 cycles. In 3 cases the breakers at both ends of the line tripped and reclosed within a total time of 22.0 cycles without the arc restriking. In one case, the breakers failed to stay in after reclosing because the arc restruck, which is believed to have been caused by a multiple lightning stroke. Figure 9 shows an oscillogram taken at Deer Creek station for a flashover from phase 3 to ground caused by lightning that occurred at 8:59 a.m. on August 28, 1936. The fault current was 1,165 amperes, primary current, and was interrupted in total time of 6.0 cycles. The breaker contacts reclosed in 22.5 cycles total time or 21.5 cycles after the trip circuit was energized. The line was de-energized for a period of 12.5 cycles. From the elements measuring the 3 phase-to-phase bus voltages, it may be seen that the fault was a flashover from phase 3 to ground.

Future Possible Applications

It is, of course, extremely difficult, nor is it well within the province of a paper of this sort, to predict the course a development of this type will take. Even more difficult is the problem of indicating with so little experience available the possible immediate application. One thing, however, is certain, on lines forming part of extensive transmission networks and particularly where loads of appreciable magnitude are carried, if lightning is at all a factor it ought to be found economically extremely attractive to equip the 2 ends of any lines of that sort with mechanisms of the type described to make possible ultra-rapid reclosing on any lightning outage. As a matter of fact, on the power system with which one of the authors is associated, 2 such lines in addition to the one described are now being so equipped.

The application of ultrahigh-speed reclosing, the authors believe, may eventually make possible in some instances a reduction in the investment in transmission lines now required to give uninterrupted service to large industrial loads. That is, the duplicate line may, with the further development of this idea, give way to the single line with the possibility of giving as good service with the single line as can be given with the multiple feeds now used.

(*Concluded on page 100*)

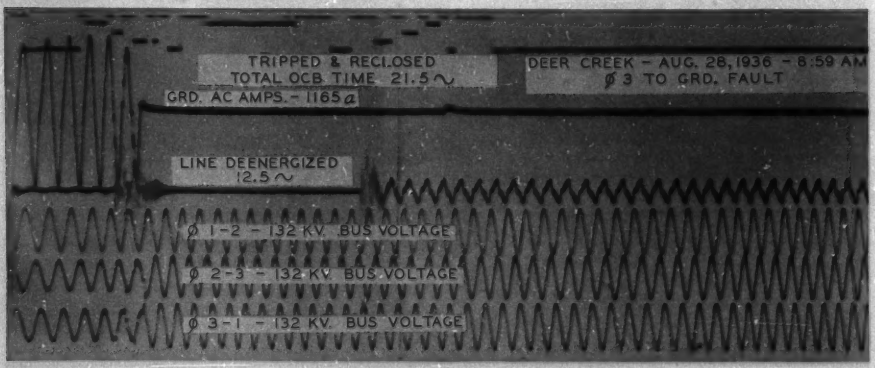
TRIPPED & RECLOSED
TOTAL OCB TIME 21.5 ~
GRD. AC AMPS. - 1165 a
DEER CREEK - AUG. 28, 1936 - 8:59 AM
Ø 3 TO GRD. FAULT
LINE DEENERGIZED
12.5 ~
Ø 1-2 - 132 KV. BUS VOLTAGE
Ø 2-3 - 132 KV. BUS VOLTAGE
Ø 3-1 - 132 KV. BUS VOLTAGE

Fig. 9. Oscillogram of operation resulting from lightning

Pole Flexibility as a Factor in Line Design

By HOWARD P. SEELYE
MEMBER AIEE

MYRON ZUCKER
[MEMBER AIEE

Poles are ordinarily considered as rigid struts in designing structures for supporting overhead lines, even in situations where they are not restrained by guys and it is known that movement takes place under variation in loading. This paper points out the importance of making allowance for this factor under certain conditions and gives the theory and practical methods for its solution.

ALTHOUGH it is customary, in designing a structure for supporting overhead lines, to consider a pole as a rigid strut, there are situations where this assumption leads to considerable error. The processes whereby the flexibility of the supports can be taken into account are by no means obvious.

In certain cases, which are not at all infrequent in practice however, the neglect of this inherent characteristic of the materials will lead to unnecessary strength in some parts and insufficient strength in others. It is the purpose of this paper to point out some of these cases, to discuss methods by which this effect may be determined, and to indicate how these may be applied to the development of working rules and charts which can be applied to field problems with sufficient accuracy for practical purposes.

Typical Cases in Which Flexibility Is of Importance

As a simple illustration of the effect of pole flexibility, consider a line dead-ended on a pole which, for some reason, cannot be guyed. A common practice in such a case would be to guy the next-to-last pole, either to an anchor or to the end pole itself, holding the greater part of the conductor tension on the guyed pole. The conductors in the end span are then slacked off to reduce the tension to an amount which will not exceed the allowable load on the unguyed pole under the heaviest condition of loading which is anticipated (see figure 1). If it is assumed that the total dead-end tension of the conductors must be held by the guy on pole A, that guy will be made unnecessarily strong, since part of this load is balanced by the tension of the conductors in the end span. If, on the contrary, the end pole B is considered rigid, and full allowance is made for the guying effect of the conductors in the slack span on this basis, the load assigned to the guy will be too small. This is evident when the actual effect of the flexing of the pole B is considered. As the load on the wires (wind and ice) increases, the tension in the end span would tend to increase. This increase in tension applied to pole B will cause it to deflect toward pole A. This, in turn, will increase the sag in the conductors, tending to reduce their tension. Equilibrium is reached when, under the assumed loading conditions, the sag in the conductors is just sufficient to produce a tension which will deflect the pole an amount necessary to produce that sag. The tension in these conductors will naturally be less than it would be if pole B were rigid, hence the load actually held by the guy must be more than would be indicated by a calculation based on the assumption of rigidity. However, the strength necessary in pole B will be appreciably less than would be required if no deflection occurred.

Figure 2 shows a dead-end pole guyed to an unguyed stub, with a guy on the pole ahead. Here the deflection of both pole A and the stub, acting together, affects the conductor tension in the end span and allowance must be made for it if the sizes of pole B, the stub, and the 2 guys are to be accurately determined. Such a situation is frequently encountered in alleys in Detroit, wherein the stub is a telephone pole subject to joint use. Consideration of flexibility allows an appreciably smaller class of pole to be used for the stub than would be required under the usual assumption of rigidity.

Figure 3 shows a short run between 2 dead-end poles. Considering flexibility, it may be feasible to leave both poles unguyed, if guying is difficult. Figure 4 shows an unguyed angle in the line with the adjacent poles guyed. Here the effect of deflection is somewhat different due to the angle, but it can sometimes be used to advantage in determining the size of the corner pole and the guys. Figure 5 shows a street lamp supported on a span wire. Allowance for the reduction in stress resulting from pole flexibility may make guying unnecessary.

There are other similar situations wherein the allowance for flexibility will serve to give a better and more economical design, but these are typical and will serve to illustrate the problem.

General Method of Solution

The general method of attacking the problem of making proper allowance for pole flexibility may be indicated by reference to the simple case shown in figure 1. The movement of the pole under a varying applied force, such as the tension in the wires, may be plotted in the form of line B in figure 6. The relation between the tension in the wires and the span length or the change in span length (that is, the pole

A paper recommended for publication by the AIEE committee on power transmission and distribution. Manuscript submitted October 16, 1936; released for publication November 19, 1936.

HOWARD P. SEELYE and MYRON ZUCKER are engineers of the Detroit (Mich.) Edison Company.

movement) may also be plotted in the form of curve A in figure 6. The point at which these curves intersect gives the solution at which equilibrium is reached, that is, the tension which is just sufficient to move the pole an amount which will sag the wire

Fig. 1. Dead end on unguyed pole

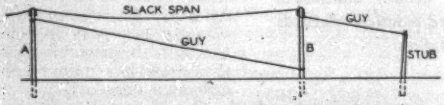

Fig. 2. Dead-end pole guyed to unguyed stub

sufficiently to produce that tension. This is the basis of the methods followed in this study.

Two methods will be described. The first is an elaboration of the general solution by the plotting of the 2 curves just discussed. This is accurate within the limits of accuracy of the methods used in determining tension-span relations but is somewhat cumbersome for general application to a variety of problems. The second method, which is more convenient to use, introduces several approximations, the errors involved being relatively insignificant, however.

Exact Solution

Pole Characteristic. The derivation of the curves shown on figure 6 requires some explanation. In order to plot curve B, the relation between the flexure in a pole and the applied force must be determined. The theory for calculating this characteristic for any given pole is shown in the appendix. A "deflection constant" is derived which gives the number of pounds of applied horizontal load per foot of deflection, the butt being held fixed. It is recognized that in some cases there may be a movement of the pole in the ground which will add to the effect of its flexure. Allowance can be made for this in choosing the deflection constant if its magnitude is known. Since this quantity is indeterminate, however, and the data which are available are meager, and also since it is practicable to support the pole by blocking or concreting against any considerable foundation movement under the loads considered, the effect of such movement has been ignored in this paper. This relationship is assumed to be reasonably constant throughout an ordinary range of loading, within the elastic limit, hence the stress-strain curve (and curve B of figure 6) is a straight line. The slope of the line is equal to the deflection constant p. For the condition illustrated, where the horizontal scale is in terms of movement from the position of initial loading, the intercept with the vertical axis (load for 0 movement) is T_1, which is the applied load or the tension in the wires under the assumed initial loading conditions. The intercept with the horizontal axis (pole position at zero load) is at a negative value equal to the deflection of the pole under initial conditions. The scale may be arranged to show total pole movement from the unloaded condition, if desired, in which

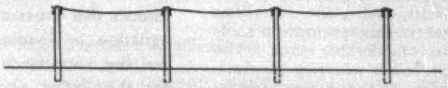

Fig. 3. Short line with neither end guyed

Fig. 4. Plan of angle with corner pole unguyed

case the intercept with the horizontal axis will be the zero point.

Wire Characteristic. The A curve may be derived by any of the well-known methods of determining sag-tension relations in a wire span. The Thomas chart has been found convenient for ordinary spans with copper wire. If composite conductors such as *ACSR* (aluminum-cable steel-reinforced) are used, or if greater accuracy is desired with copper, some of the more refined methods using stress-strain curves obtained by test may be necessary. The Thomas chart method will be described in the following.

It may be remembered that the Thomas chart uses a curve showing the relationship between tension and length of wire in the span. Specifically, the co-ordinates are a "stress factor" (T/wS) equal to

$$\frac{\text{tension}}{\text{load per foot span} \times \text{span}}$$

and length of wire per foot span, $(L/S) = l$, as shown in figure 7. For a given span S, an initial loading w_1 per foot, and an initial sag, the initial value of $T_1/(w_1S)$ is calculated and the value of l_1 found from the chart. From this, a quantity l_0, the "unstressed length," is derived by subtracting from l_1 the elongation resulting from the tension in the wire

$$l_0 = \frac{l_1}{1 + \frac{T_1}{AE}}$$

where A is the cross-sectional area of the wire and E the modulus of elasticity. The line l_0r_1 plotted on the chart, figure 7, is the stress-stretch line of the

wire for loading w_1. For a change in load to w_2, a new stress-stretch line similar to l_0r is plotted between l_0 and a point r' whose co-ordinates are $T_1/(w_1S)$ and $l_0 + (w_2/w_1)(l_1 - l_0)$. The intersection of l_0r' with the curve at r_2 gives the new value of $T_2/(w_2S)$ and hence of T_2.

For a change in temperature, the unstressed length l_0 changes to a new length $l_0' = l_0(1 + \alpha t)$, where α is the coefficient of expansion and t the change in temperature, using the proper sign for t. The new stress-stretch line for load w_1 at the new temperature (not shown on figure 7) is parallel to l_0r_1; the new stress-stretch line for w_2 is parallel to l_0r_2.

Determination of the effect of a change in span as the result of pole movement is quite similar to that for temperature change. The actual unstressed length of the wire remains the same, but, since the span changes, L_0/S (and hence l_0) will change. If the pole should move so that the span will be shortened

Fig. 5. Street-lamp suspension with customary guys shown

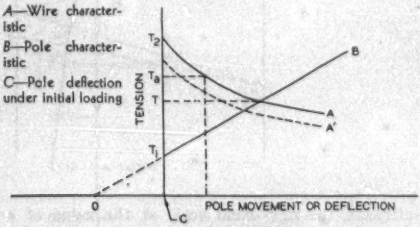

Fig. 6. Construction of graphic solution for flexible span

one per cent, $l_0 = L_0/S$ changes to $l_0'' = L_0/0.99S = l_0/0.99$. The stress-stretch line through this new point l_0'' for the new span will be parallel to the one through l_0 for the same loading, since the slope of this line is

$$\frac{T}{wS} + \frac{L - L_0}{S} = \frac{T}{w(L - L_0)}$$

which is independent of span length. On figure 7, $l_0''r_a$ is parallel to l_0r_2, for loading w_2, and its intersection with the curve at r_a gives the solution for $T_a/(w_2S_a)$ and hence T_a for the reduced span.

This is the basis for plotting curve A of figure 6. For example, if initial conditions w_1, S_1, and sag are given, T_1 and l_0 may be determined. The pole is initially deflected by T_1 an amount T_1/p. If the pole were held fixed at that point, T_2 for a new loading, w_2, would be found by figure 7. This T_2 will give the intercept of the curve A (figure 6) with the vertical axis, since it is the tension in the wire for zero movement. Assume a certain reduction in span such as one foot or one per cent, and find the corresponding T_a as herein described. Plot this as a second point on the A curve. Assume other possible pole movements and find the corresponding values of T_a, locating other points on the A curve until it is completely plotted. The intersection of this A curve with the B line is the solution for the loading w_2. For other loadings, such as w_3, another A curve such as A' in figure 6 can be similarly derived and the solution obtained. It should be remembered that the load applied to the pole is the total of all the wires carried, hence the A curve must represent the sum of all the wire tensions. Where different sizes are present, separate curves may be plotted and totaled into one combined A curve. The error is usually not great, however, if the combined curve is obtained by using the total cross-sectional area, loading, and tensions of all wires.

This method, although relatively accurate and not difficult for a specific problem, is somewhat cumbersome for general use, where various wire sizes, spans, and loadings are being considered. The second method to be described is sufficiently accurate for most purposes and is more easily handled for a variety of problems. This method and the resulting charts will also be found useful in solving spans with rigid supports as well as those with flexible supports.*

Approximate Method

For this solution the parabolic formulas for wire-span relationship are used instead of the catenary

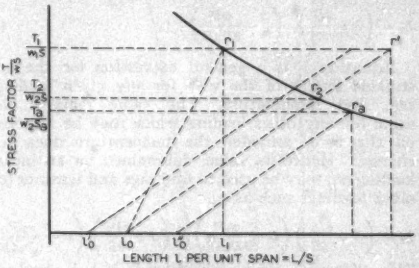

Fig. 7. Thomas chart

as being more convenient and not introducing serious error. For any wire hanging in a span, the following relationships exist:

$$\text{Length of wire} = L = S + \frac{8D^2}{3S} \qquad (1)$$

* Originality is not claimed for this method of solving spans with rigid supports since the principles are referred to in several previous publications, both in this country and abroad. See "Sag Problems Readily Solved by Aid of Alignment Chart," by D. C. Stewart, *Electrical World*, volume 96, September 20, 1930, page 518, and others. The detailed application here is somewhat different, however, and the development for flexible supports is believed to be new.

$$\text{Tension in wire} = T = \frac{wS^2}{8D} \tag{2}$$

Where

S = span in feet
D = sag or deflection in feet
w = load in pounds per foot

Rigid Supports. For the ordinary case of rigid supports, the span length is fixed, hence the relationship of equation 1 is between 2 variables, length of wire and deflection, the latter also being dependent upon loading and tension in accordance with equation 2. On account of its elastic characteristic, the length of wire varies with the tension; it also varies with the temperature. The unstressed length of the wire at a given temperature, that is, its length if removed from the span and laid on the ground is a fixed quantity, however, and can be used as a reference in determining the effect of various changes in conditions. The unstressed length can be obtained from equation 1 by subtracting from L the elongation caused by the tension obtained from equation 2.

$$L = L_0\left(1 + \frac{T}{AE}\right) \qquad L_0 = \frac{L}{1 + \frac{T}{AE}}$$

For the present purpose it is somewhat more convenient to change this to a form which is approximately as correct:

$$L_0 = L\left(1 - \frac{T}{AE}\right)$$

Substituting equations 1 and 2, respectively,

$$L_0 = \left(S + \frac{8D^2}{3S}\right)\left(1 - \frac{T}{AE}\right)$$

$$L_0 = \left(S + \frac{8D^2}{3S}\right)\left(1 - \frac{wS^2}{8DAE}\right) \tag{3}$$

Equation 3 is a general expression for the unstressed length of the wire for any given loading, sag, and temperature. The value remains the same for any other loading which may be imposed on the wire, provided the temperature does not change. Hence its value, determined for an initial loading w_1, may be used to find sags and tensions for other loadings such as w_2.

$$L_0 = \left(S + \frac{8D_1^2}{3S}\right)\left(1 - \frac{w_1S^2}{8D_1AE}\right) = \left(S + \frac{8D_2^2}{3S}\right)\left(1 - \frac{w_2S^2}{8D_2AE}\right)$$

This expression can be solved for D_2 if L_0 is obtained from w_1 and D_1.

If equation 3 is expanded, the expression becomes

$$L_0 = S + \frac{8D^2}{3S} - \frac{wS^2}{8DAE} - \frac{wSD}{3AE}$$

It will be found that the last term is of insignificant size compared with the others and may be dropped from the equation without appreciable error, leaving

$$L_0 = S + \frac{8D^2}{3S} - \frac{wS^2}{8DAE} \tag{4}$$

For convenience equation 4 may be operated upon mathematically by subtracting the span length S (a constant for any problem with rigid supports) from both members and also by dividing both members by S. The deflection per foot of span, $d = D/S$ is also introduced. This gives a quantity designated as e, which is the difference per unit span between unstressed length of wire and span length.

$$e = \frac{L_0 - S}{S} = \frac{8}{3}d^2 - \frac{1}{8d}\frac{wS}{AE} \tag{5}$$

It is possible to plot a nomograph from this equation using as variables e, d, and $(wS)/(AE)$ as illustrated by figure 8. If the value of $(w_1S)/(AE)$ is computed for an initial loading w_1, a straight line from that point on the left-hand scale through the value of initial deflection d_1 on the middle scale

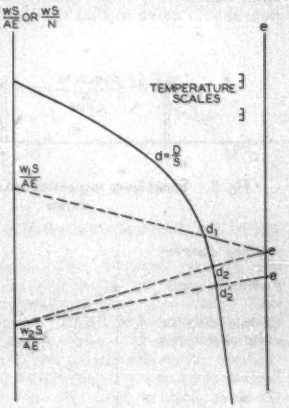

Fig. 8. Nomographic method of solution for rigid or flexible span

intersects the right-hand scale at the value of e. Since e is constant (for a given temperature) another straight line from e to the calculated value of $(w_2S)/(AE)$ for a new loading w_2 will give a new deflection d_2, from which the new tension can be computed from the formula

$$T = \frac{wS^2}{8D} = \frac{wS}{8d} \tag{6}$$

A change in temperature changes the unstressed length, L_0, to some new value $L_0(1 + \alpha t)$ where

α = temperature coefficient of expansion
t = change in temperature in degrees, positive for a rise, negative for a fall

If L_0 has been determined for given initial conditions including temperature t_1, L_0' for some other temperature t_2 will be

$$L_0' = L_0[1 + \alpha(t_2 - t_1)] = L_0 + L_0\alpha t$$

Since the length L_0 is not greatly different from the span length S, no appreciable error is introduced if the last term is written $S\alpha t$.

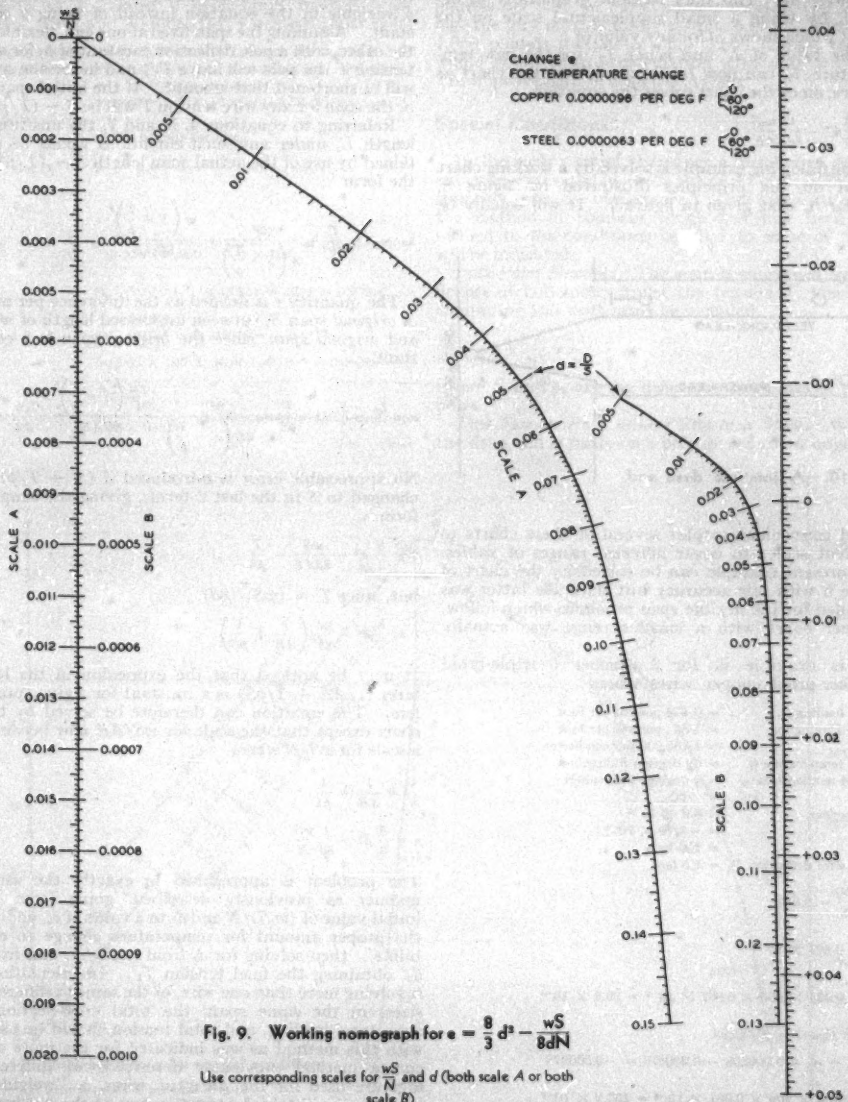

Fig. 9. Working nomograph for $e = \frac{8}{3}d^2 - \frac{wS}{8dN}$

Use corresponding scales for $\frac{wS}{N}$ and d (both scale *A* or both scale *B*)

Introducing this quantity into the equation for e,

$$e' = e + \alpha t \tag{7}$$

If e has been determined from the chart as described, e' can be found by adding or subtracting the quantity αt. This may be done graphically, if desired, by using a small supplemental scale on the chart which shows αt for any value of t.

The value of d_2' and hence T_2' for the new temperature, t_2, can now be obtained from the chart as before, since the chart solves the equation

$$e' = \frac{8}{3} d_2^3 - \frac{1}{8d_2} \frac{w_2 S}{AE}$$

The following example is solved by a working chart based on the principles illustrated by figure 8, similar to that given in figure 9. It will usually be

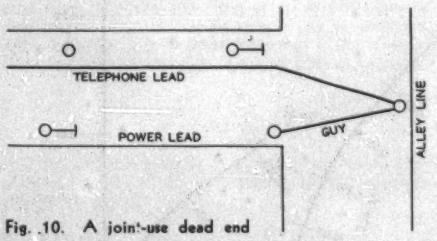

Fig. 10. A joint-use dead end

found convenient to plot several of these charts to different scales to cover different ranges of values. The present example can be solved by the chart of figure 9 with fair accuracy but since the latter was intended for the flexible span problems which follow, another chart with a smaller range was actually used.

This example is for 3 number 0 triple-braid weather-proof copper wires where

Initial loading w_1	= 0.424 pounds per foot
Heavy loading w_2	= 1.55 pounds per foot
AE	= 1,160,000 per conductor
Initial temperature t_1	= 60 degrees Fahrenheit
Loaded temperature t_2	= 0 degrees Fahrenheit
t	= −60
α for copper	= 9.6×10^{-6}
αt	= -5.76×10^{-4}
Span	= 100 feet
Initial wire deflection D_1	= 1.5 feet

$$d_1 = \frac{D_1}{S} = 0.015$$

$$\frac{1}{AE} = 0.861 \times 10^{-6}$$

$$\frac{w_1 S}{AE} = 0.424 \times 100 \times 0.861 \times 10^{-6} = 36.5 \times 10^{-6}$$

e_1 (from chart) = 0.000298

$$e' = e_1 + \alpha t = 0.000298 - 0.000576 = -0.000278$$

$$\frac{w_2 S}{AE} = 1.55 \times 100 \times 0.861 \times 10^{-6} = 133.2 \times 10^{-6}$$

d_2 (from chart) = 0.0166

$T_2 = (w_2 S)/(8d_2) = 155/(8 \times 0.0166) = 1{,}165$ pounds per wire or 3,495 pounds for 3 wires

Flexible Span. If the support is not fixed, but can move as the wire tension changes, the span becomes a variable in the equation instead of being a constant. Assuming the span fixed at one end, flexible at the other, with a pole deflection constant of p, for any tension T the pole will move T/p and hence the span will be shortened that amount. If the initial span is S, the span for any wire tension T will be $S - (T/p)$.

Referring to equations 4, 5, and 7, the unstressed length L_0 under any such conditions would be obtained by use of the actual span length $S - (T/p)$ in the form

$$L_0 = S - \frac{T}{p} + \frac{8D^2}{3\left(S - \frac{T}{p}\right)} - \frac{w\left(S - \frac{T}{p}\right)^3}{8DAE}$$

The quantity e is defined as the difference per unit of *original* span S, between unstressed length of wire and *original span*, since the original span is a constant.

$$e = \frac{L_0 - S}{S} = -\frac{T}{pS} + \frac{8D^2}{3S\left(S - \frac{T}{p}\right)} - \frac{w\left(S - \frac{T}{p}\right)^3}{8DAES}$$

No appreciable error is introduced if $(S - T/p)$ is changed to S in the last 2 terms, giving the simpler form

$$e = \frac{8}{3} d^2 - \frac{wS}{8dAE} - \frac{T}{pS}$$

but, since $T = (wS)/(8d)$,

$$e = \frac{8}{3} d^2 - \frac{wS}{8d}\left(\frac{1}{AE} + \frac{1}{pS}\right) \tag{8}$$

It may be noticed that the expression in the last term $(1/AE + 1/pS)$ is a constant for a given problem. The equation can therefore be solved by the chart except that the scale for wS/AE now becomes a scale for wS/N where

$$\frac{1}{N} = \frac{1}{AE} + \frac{1}{pS}$$

$$e = \frac{8}{3} d^2 - \frac{1}{8d} \frac{wS}{N} \tag{9}$$

The problem is approached in exactly the same manner as previously described, going from an initial value of $(w_1 S)/N$ and d_1 to a value of e; adding the proper amount for temperature change to obtain e'; then solving for d_2 from $(w_2 S)/N$, and from d_2' obtaining the final tension T_2'. In calculations involving more than one wire, of the same or different sizes, in the same span, the total cross-sectional area, total loading, and total tension should be used with this method as was indicated for the more accurate method previously described. If different sags are used for the different wires, a "weighted sag" can be obtained from the sum of the products

of sag and loading for each wire, divided by total loading.

The chart in figure 9 is a working chart for such problems. Taking as a typical example the same conditions used in the previous example, except for the rigidity of the pole, the solution is carried out as follows for 3 number 0 triple-braid weather-proof copper wires and 40-foot class 4 western-cedar pole:

Stringing load w_1 = $3 \times 0.424 = 1.272$ pounds per foot for 3 wires
Heavy loading w_2 = $3 \times 1.55 = 4.65$ pounds per foot for 3 wires
AE = 1,160,000 per conductor
αt = $-60 \times 9.6 \times 10^{-6} = -5.76 \times 10^{-4}$
Deflection constant p = 600 pounds per foot
Initial wire deflection D_1 = 1.5 feet

$$d_1 = \frac{1.5}{100} = 0.015$$

$$\frac{1}{N} = \frac{1}{AE} + \frac{1}{pS} = \frac{1}{3 \times 1{,}160{,}000} + \frac{1}{600 \times 100} = 16.954 \times 10^{-4}$$

$$\frac{w_1 S}{N} = 1.272 \times 100 \times 16.954 \times 10^{-4} = 0.00216$$

$$e = -0.0174$$

$$e' = e + \alpha t = -0.0174 - 0.000576 = -0.01798$$

$$\frac{w_2 S}{N} = 4.65 \times 100 \times 16.954 \times 10^{-4} = 0.00788$$

$$d_2 = 0.043$$

$$T_2 = \frac{w_2 S}{8 d_2} = \frac{465}{8 \times 0.043} = 1{,}350 \text{ pounds or } 450 \text{ pounds per wire}$$

It is apparent by comparing these results with those previously calculated for the rigid span that if the pole B had been assumed rigid, its load would have been calculated as 3,495 pounds instead of 1,350 pounds. If the tension in the normal span to the left of pole A (figure 1) were calculated at 2,000 pounds per wire, or 6,000 pounds total at full loading, the guy must actually assume 6,000 − 1,350 = 4,650 pounds instead of only 2,505 pounds which would result from a calculation with pole B rigid. The improvement in design is evident.

Special Conditions

In the early part of the paper a number of different cases were cited in which the effect of flexibility of supports was of importance. The application of the method of solution which has just been described to the conditions peculiar to some of these will be indicated.

Both Poles Flexible. The span is shortened by the flexure of both poles under the tension T, hence in computing $1/N$ both must be included

$$\frac{1}{N} = \frac{1}{AE} + \frac{1}{p_1 S} + \frac{1}{p_2 S}$$

where p_1 and p_2 are the deflection constants of the 2 poles.

Two Flexible Poles at One End of a Span. Where the dead end is made on a pole guyed to an unguyed

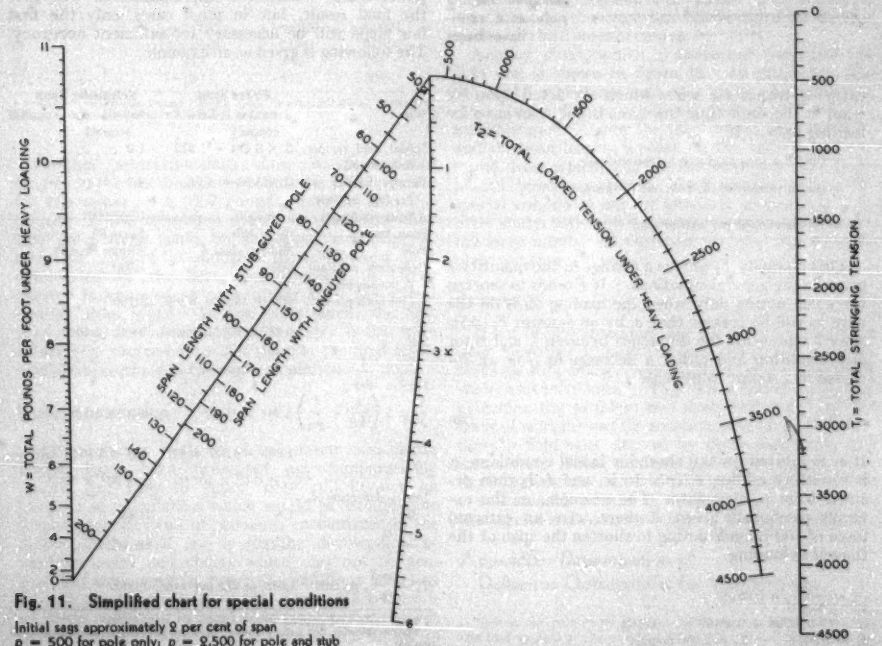
W = TOTAL POUNDS PER FOOT UNDER HEAVY LOADING
SPAN LENGTH WITH STUB-GUYED POLE
SPAN LENGTH WITH UNGUYED POLE
T2 = TOTAL LOADED TENSION UNDER HEAVY LOADING
T1 = TOTAL STRINGING TENSION

Fig. 11. Simplified chart for special conditions

Initial sags approximately 2 per cent of span
p = 500 for pole only; p = 2,500 for pole and stub

stub, both enter into the change in the span caused by flexure. In this case, if the guy is short and tight, the deflection constant of the 2 poles acting together is equal to the sum of their individual deflection constants.

$$\frac{1}{N} = \frac{1}{AE} + \frac{1}{(p_1 + p_2)S}$$

The load divides between pole and stub in proportion to their deflection constants.

External Force. Sometimes there will be forces other than the tension in the wires acting to bend the pole. An example of such a case would be a pole

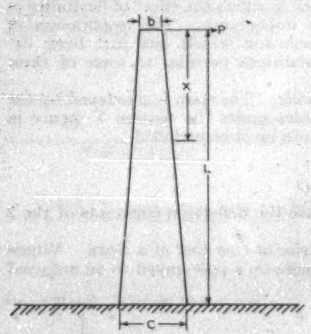

Fig. 12. Representation of a pole as a cantilever beam

carrying transverse wires which are acted upon by wind at the same time the wires in the span have ice loading only. If

F = the force thus produced on the end pole

$\frac{F}{p}$ = the movement of the pole due to this force

$\frac{F}{pS}$ = the movement per unit of span

This quantity $F/(pS)$ is a change in the quantity e given in the general equations. If F tends to shorten the span, acting only when the loading w_2 is on the wire, e_2 will be greater than e_1 by an amount $F/(pS)$, since e represents the difference between L and S for any condition and either a decrease in S or an increase in L tends to increase e.

$$e_2 = e_1 + \frac{F}{pS} \qquad (10)$$

If e_1 is located on the chart for initial conditions, e_2 is found by adding $F/(pS)$ to it, and d_2 is then derived from e_2 as before. For example, in the example previously given, if there were an external force of 100 pounds acting to shorten the span at the time of w_2 loading,

$$\frac{F}{pS} = \frac{100}{60{,}000} = 0.00167$$

$$e_2 = -0.01798 + 0.00167 = -0.0163$$

$$d_2 = 0.0451 \qquad T_2 = 1{,}290 \text{ pounds}$$

Joint Use. In certain cases the pole which acts as a guy stub for the end pole acts also as a dead-end pole for telephone cable carried on a parallel lead (see figure 10). The tension in the messenger supporting the telephone cable changes with the loading. If telephone and power spans are of approximately equal length, the problem may be solved just as if all wires were on the same poles. If span lengths are different, however, a solution may be reached by a series of convergent approximations as follows: Consider the loaded tension T_T in the telephone messenger first as a constant external force similar to that discussed in the preceding paragraph. It is assumed that the initial span for the power wires is that obtained after T_T is applied to the end pole. The equivalent deflection constant for the whole system is the same whether T_T and T_P are applied to the same pole or to different poles, being equal to $p_1 + p_2$ for the total tension. The power span is solved in the usual manner and a value for tension in the power wires found. Returning to the telephone span, a solution is made similarly except that in determining e_2, an amount $(T_2 - T_1)_P/(pS_T)$ is added to e_1 to allow for the *increase* in tension in the power wires $(T_2 - T_1)_P$, S_T being the telephone span. The resulting tension in the telephone messenger having thus been determined, the power span is recalculated, increasing e_1 now by the amount $(T_2 - T_1)_T/(pS_P)$ where $(T_2 - T_1)_T$ is the *increase* in messenger tension and S_P the power span. Successive approximations will give the final result, but in most cases only the first few steps will be necessary for sufficient accuracy. The following is given as an example:

	Power Span	Telephone Span
Wire	3 number 0 *TBWP* copper†	202–24 cable, on 6*M* strand‡
Initial load w_1 per foot, pounds	$3 \times 0.424 = 1.272$	1.9
Heavy loading w_2 per foot, pounds	$3 \times 1.55 = 4.65$	4.3
AE per conductor	1,160,000	1,757,000
Span, feet	$S_P = 100$	$S_T = 60$
Pole	40-foot, class 4	30-foot class 2
Deflection constant p, pounds per foot	600	1,500
p_{eq} for both poles	$600 + 1500 = 2{,}100$	2,100
$\frac{S}{AE}$	0.287×10^{-4} (3 wires)	0.341×10^{-4}
$\frac{S}{p_{eq}S} = \frac{1}{p_{eq}}$	4.76×10^{-4}	4.76×10^{-4}
$\frac{S}{N} = S\left(\frac{1}{AE} + \frac{1}{p_{eq}}\right)$	5.047×10^{-4}	5.10×10^{-4}
$\frac{w_1 S}{N}$	$1.272 \times 5.047 \times 10^{-4} = 6.42 \times 10^{-4}$	$1.9 \times 5.10 \times 10^{-4} = 9.697 \times 10^{-4}$
Initial deflection d_1, feet	1.5	0.85
$d_1 = \frac{D_1}{S}$	0.015	0.0142
$T_1 = \frac{w_1 S}{8d_1}$, pounds	1,060, or 353 per wire	1,000

† Triple-braid weather-proof.
‡ Number 24 wire, 202 pairs in cable; breaking strength of messenger 6,000 pounds.

	Power Span	Telephone Span
$e_1 = \frac{8}{3}d_1 - \frac{w_b S}{8d_1 N}$ (chart)	−0.0048	−0.0081
α (temperature coefficient)	9.6×10^{-6} (copper)	6.6×10^{-6} (steel)
αt for −60 degrees	-6×10^{-4}	-4×10^{-4}
$e' = e_1 + \alpha t$	−0.0048 − 0.0006 = −0.0055	−0.0081 − 0.0004 = −0.0084
$\frac{w_b S}{N}$	$4.65 \times 5.047 \times 10^{-4} = 23.5 \times 10^{-4}$	$4.3 \times 5.10 \times 10^{-4} = 21.95 \times 10^{-4}$
$\frac{1}{p_{eq} S}$	$\frac{1}{210{,}000} = 4.76 \times 10^{-6}$	$\frac{1}{126{,}000} = 7.94 \times 10^{-6}$

Successive Approximations*

	Power Span		
	1	2	3
$\frac{(T_2 - T_1)_T}{p_{eq} S_T}$	0	−0.0008	−0.0009
$e_T = e' + \frac{(T_2 - T_1)_T}{p_{eq} S_T}$	−0.0055	−0.0063	−0.0064
d_2 (from chart)	0.0340	0.0324	0.0320
$T_2 = \frac{w_b S}{8d_2}$	1,710 lbs	1,795	1,820
$(T_2 - T_1)_P$	650	735	760
	Telephone Span		
	1	2	3
$\frac{(T_2 - T_1)_P}{p_{eq} S_T}$	0.0052	0.0058	0.0060
e_2	−0.0032	−0.0026	−0.0024
d_2	0.0384	0.040	0.0405
T_2	840	805	795
$(T_2 - T_1)_T$	−160	−195	−205

* Proceed from column 1 under "Power Span" to column 1 under "Telephone Span," to column 2 under "Power Span," etc.

Further approximations show no appreciable change in the tensions so the solution is 1,820 pounds for the power span (607 pounds per wire) and 795 pounds in the telephone span. It is evident that this calculation could be shortened somewhat if, after the trend of the change in the telephone span is discovered in the first approximation, a larger change is assumed at once rather than the actual change thus found. In the table given, the first step shows a reduction of 160 pounds; if this were arbitrarily increased to 200 pounds the final result would be obtained in the next calculation.

Field Application

Although the methods of calculation and charts which have been presented are comparatively simple and easy to apply, they still involve an amount of calculation which would be troublesome in the everyday run of problems encountered in the field. Their chief use is for the development of working rules and charts which may not be general but may cover a range of conditions sufficient for the greater majority of the cases. Since there is so much variation in local conditions and standards of construction, such working rules should be set up for one's own system in accordance with the combinations of circumstances most often occurring on that system. Two examples of such specific instructions will be given as illustrations.

Study of many actual cases of unguyed end poles and pole-stub combinations in the Detroit territory, both with and without joint use with telephone lines, led to the working rule:

"The initial load on an unguyed end pole or pole-stub combination should not exceed one half the ultimate allowable load."

This does not give actual resulting load under storm conditions but it does assume that a severe overload will be avoided and also that too much stress and deflection will not be placed on the pole under ordinary loading conditions. For pole-stub combinations, the criterion will be the load on the weaker of the 2 poles of course.

Another chart, which is somewhat simplified for field use, is shown in figure 11. In preparing this the initial sags were fixed at a given percentage of span, and ordinary values for deflection constants were assumed. From the total heavy load per foot and the span length, a point on the turning scale is found, from which, and the initial tension, the total loaded tension is found. Still simpler charts for special conditions can be similarly prepared with a little study, although it must be recognized that with the large number of variables no very simple complete solution is possible.

Table I—Pole Deflection Constants and Ultimate Strengths

Individual Poles				Combinations			
Length, Feet	Class	p	Ultimate Strength, Pounds	Length, Feet	Class	p	Ultimate Strength, Pounds
25	1	3,000	4,500	25	1	4,200	6,300
25	2	2,800	3,700	35	2		
25	3	1,700	3,000				
30	1	2,000	4,500				
30	2	1,500	3,700	25	2	3,100	5,000
30	3	1,100	3,000	35	4		
35	2	1,200	3,700				
35	4	800	2,400	30	2	2,250	3,500
40	2	850	3,700	40	2		
40	4	600	2,400				
45	2	650	3,700	30	2	2,150	3,300
45	4	450	2,400	45	2		

Summary

It has been pointed out that the flexure of supports may constitute a major factor in the design of structures for supporting overhead lines, and examples of such cases have been given. The general method of attacking the problem was described and 2 specific ways of working out the solution were given in detail. Simpler field rules derived by these means are also mentioned. These methods have been used in practical applications and it is believed that they can be of considerable benefit to those who are interested in the careful and accurate design of their structures.

Appendix—Determination of Deflection Characteristics for Wood Poles

Assume the pole to be in effect a tapered cantilever beam, with the load applied at the end (see figure 12). The increment deflec-

tion at the load end of the beam resulting from the stress at any point at distance x from that end is

$$dQ = \frac{Mx}{EI}\,dx = \frac{Px^2}{EI}\,dx$$

The total deflection therefore is

$$Q = \int_0^L \frac{P}{EI}\,x^2 dx$$

$I = 0.0491\,d^4$ for circular cross section of diameter d

For a taper of a per foot,

$$d = ax + b \qquad a = \frac{c - b}{L} \qquad I = 0.0491(ax + b)^4$$

Therefore

$$\frac{0.0491\,E}{P}\,Q = \int_0^L \frac{x^2}{(ax + b)^4}\,dx$$

$$= \frac{1}{a^3}\left[-\frac{1}{ax + b} + \frac{2b}{2(ax + b)^2} - \frac{b^2}{3(ax + b)^3}\right]_0^L$$

Substituting for a,

$$\frac{0.0491\,E}{P}\,Q = \frac{L^3}{(c - b)^3}\,\frac{(c - b)^3}{3bc^3}$$

$$= \frac{L^3}{3bc^3}$$

"Deflection constant" $p = \dfrac{P}{Q} = \dfrac{0.0491E \times 3bc^3}{L^3}$

$$= 0.1473Eb(c/L)^3 \text{ pounds per inch deflection}$$

All quantities must be expressed in inches. The deflection constant in pounds per foot deflection will be 12 times that given by the equation.

Values of E given in the 1935 "Wood Handbook" of the U.S. Department of Agriculture are as follows:

Northern white cedar	800,000 pounds per square inch
Western red cedar	1,120,000 pounds per square inch
Southern yellow pine	1,800,000 pounds per square inch

Example

35-foot class 4 western-cedar pole

b = top diameter, average for class approximately 8.5 inches
c = ground line diameter, average for class approximately 11.7 inches
L = length from 2 feet below top to ground line = 35 − 8 = 27 feet = 324 inches

$$p = \frac{P}{Q} = 0.1473 \times 1{,}120{,}000 \times 8.5\left(\frac{11.7}{324}\right)^3$$

$$= 66 \text{ pounds per inch}$$

$66 \times 12 = 800$ pounds per foot

For a pole and stub acting together, connected by a guy, the deflection of both is the same, hence the deflection constant of the combination is equal to the sum of their individual deflection constants. The ultimate strength of the combination is limited by the strength of the one which has the lower ratio of strength to deflection constant, since that one reaches its ultimate strength before the other one does. For example,

	p	Ultimate Strength, Pounds
35-foot class 2 pole	1,200	3,700
25-foot class 1 stub	3,000	4,500
Combination	4,200	$4{,}200\,\dfrac{4{,}500}{3{,}000} = 6{,}300$

Table I gives deflection constants and rated ultimate strengths for a number of common sizes of western-cedar poles and stubs and some typical combinations.

Ultrahigh-Speed Reclosing of High-Voltage Transmission Lines

(*Continued from page 90*)

In a large measure the field of application of this development will be determined, as would be expected, by the additional cost of ultrahigh-speed mechanisms as against standard mechanisms but here the reverse is also true that the cost will in turn be influenced to a considerable extent by the development of applications for the mechanisms and by whether quantity production will be possible. In any event it would appear that a very definitely new and ingenious tool has been made available to the transmission-system designer and operator that gives promise of improved service and lower costs.

Conclusions

The authors believe that it is perhaps premature to draw final conclusions as to the nature, scope, and significance of the development described herein and such was not within the limited scope of this paper, but nevertheless it would appear that the following have been fairly well established:

1. On high-voltage lines, particularly on overhead lines, outages caused by lightning and possibly other outages can be materially reduced, perhaps to the extent of 75 per cent, by ultrarapid reclosing.

2. Apparently the occurrence in nature of intervals between multiple strokes is such as to give a fortuitously happy arrangement from the standpoint of possible reclosure. This, however, is a phase that needs not only further theoretical but a great deal of practical verification.

3. While a great deal of benefit can be obtained in the reducing of outage resulting from phase-to-ground troubles, phase-to-phase troubles are much more bothersome and a great deal of additional work needs to be done either in the way of bringing them within the range of treatment that can be so successfully applied to phase-to-ground faults or in the direction of reducing their frequency.

4. Finally, it appears that as is true in so many other cases of research and development, the by-product of the search for speed in circuit-breaker practice and speed on relay protection has given most fruitful results, perhaps equal to those obtained from the original line of research, and promises to yield a great deal more.

References

1. Automatic Reclosing of Oil Circuit Breakers, A. E. Anderson. Electrical Engineering (AIEE Transactions), volume 53, January 1934, pages 48–53.

2. Motors Need Not Stop When Voltage Dips, D. W. McLenegan. *Electrical World*, volume 96, September 6, 1930, pages 433–6.

3. Oil Circuit Breaker Tests—Philo 1930, Philip Sporn and H. P. St. Clair. AIEE Transactions, volume 50, 1931, pages 498–505.

4. Circuit Breakers for Boulder Dam Line, D. C. Prince. Electrical Engineering (AIEE Transactions), volume 54, April 1935, pages 366–72.

5. One-Cycle Carrier Relaying Accomplished, Philip Sporn and C. A. Muller. *Electrical World*, volume 105, October 12, 1935, pages 26–8.

6. A Faster Carrier Pilot Relay System, O. C. Traver and E. H. Bancker. Electrical Engineering (AIEE Transactions), volume 55, June 1936, pages 685–96.

7. Expulsion Protective Gaps on 132 Kv Lines, Philip Sporn and I. W. Gross. Electrical Engineering (AIEE Transactions), volume 54, January 1935, pages 66–73.

8. Keeping the Line in Service by Rapid Reclosing, S. B. Griscom and J. J. Torok. *Electric Journal*, volume 30, May 1933, pages 201–4.

9. Carrier-Current Relaying Proves Its Effectiveness, Philip Sporn and C. A. Muller. *Electrical World*, volume 100, September 10, 1932, pages 339–6.

Lightning Investigation on Transmission Lines—VI

By W. W. LEWIS
MEMBER AIEE

C. M. FOUST
MEMBER AIEE

Continuing a series of papers reporting a study of lightning on transmission lines, the authors present herewith data obtained during 1935 and part of 1936 on 66-, 110-, 132-, and 220-kv lines. Values of lightning current are presented, and the effectiveness of overhead ground wires and low footing resistance in preventing tripouts is shown.

IN PREVIOUS papers the authors have reported the results of an investigation of lightning effects on transmission lines, which began in the year 1926. The immediately preceding paper[1] gave the results for 1933 and 1934. The present paper will summarize the 1935 and part of the 1936 results. The participating power companies in this investigation are the Pennsylvania Power and Light Company, Appalachian Electric Power Company, Philadelphia Electric Company, Pennsylvania Water and Power Company, Public Service Company of New Jersey, Consumers Power Company, American Gas and Electric Company, and the Electric Bond and Share Company.

In the years 1935 and 1936 data were gathered by means of the surge crest ammeter[2] on lightning currents in tower legs and crossarms, overhead ground wires, counterpoise wires and lightning rods erected at the tops of towers. These data, together with supplementary data from lightning stroke recorders, surge indicators, and automatic oscillographs have permitted a rather complete picture to be drawn of the effects of individual strokes. Additional mass statistics permit further confirmation of the theories in regard to the behavior of overhead ground wires and counterpoise wires.

Summary

Line performance data and current and voltage measurements now at hand give a reasonably clear qualitative and quantitative idea of the essential elements in the line protection problem.

First, it is apparent from line performance data that overhead ground wires reduce tripouts in the order of 20 to 1. Current measurements on the ground wire have demonstrated that it is serving as a lightning stroke terminal for many strokes which otherwise might reach the conductor and cause flashover. Measurement experience seems to bear out that the overhead ground wires also act to assist in reducing tower potentials for strokes to a tower.

The second important element has been shown by measurement to be the tower footing resistance. With marked consistency it has been shown that when a stroke terminates on a tower, flashover and tripout will quite likely result if footing resistance is high. The product of current and footing resistance must be below insulator flashover for the wave shape applied if flashover is to be prevented.

Both the parallel and radial type counterpoise wires have been shown to be effective in reducing the voltage drop at the tower footing. The tower-to-tower buried ground wire has been shown in one case to have entirely eliminated flashover of insulation at a point previously very susceptible to flashover. The radial counterpoise has been shown in one case to be effective for most lightning currents when some 150 feet long.

Simultaneous measurements of lightning currents have been made in counterpoise wires, in tower legs, in tower arms, in ground wires and lightning rods. Such readings have permitted the location of the general point of contact of the stroke to be known, the direction of flow of current from positive ground to negative cloud to be definitely determined, and have provided quantitative values of lightning current.

Flashover on Lines With and Without Overhead Ground Wires

In table VII of paper IV of this series[3] data were given as to the insulation and conductor and ground wire arrangement for 9 systems in eastern United States, ranging from 66 kv to 220 kv, also data as to the number of tripouts on these lines for a period of years up to and including 1933. In table I of the present paper the same systems are listed, with the tripout data brought up to and including 1935. In addition, data for the section of the Wallenpaupack-Siegfried line without overhead ground wires are given.

Two of the lines have an almost perfect record of 0.4 tripouts per 100 miles per year. The other lines with overhead ground wires range up to 2.8 tripouts per 100 miles per year, while the one line without overhead ground wires had 47 tripouts per 100 miles per year, that is, 17 or more times as many tripouts as on the lines with overhead ground wires.

In table II are given the location of the flashovers which caused tripout on the Wallenpaupack-Siegfried line,[4] segregated with respect to the overhead ground wire construction and method of grounding, for the 10 years from 1926 to 1935 inclusive. Of the 112 faults whose locations are known, 108 occurred on the section of line

A paper recommended for publication by the AIEE committee on power transmission and distribution. Manuscript submitted October 30, 1936; released for publication December 1, 1936.

W. W. Lewis and C. M. Foust are electrical engineers with the General Electric Company, Schenectady, N. Y.

1. For all numbered references see list at end of paper.

Table I—Tripouts on Transmission Lines, Data Up to and Including 1935

	Line Name	Kilovolts	Miles	Average Length of Span, Feet	Footing Resistance, Ohms	Tripouts	Years	Tripouts per 100 Miles per Year
1a	Wallenpaupack-Siegfried (Without overhead ground wires)	220	38.9	1,100	5–325	138†	8	47
1b	Wallenpaupack-Siegfried (With overhead ground wires)	220	27.8	1,100	1–1.5* 5–75**	6†	8	2.8
2	Bushkill-Roseland	220	47	1,150	5–300	4†	4	2.1
3	Siegfried-Plymouth	220	49	1,270	5–60	6	8	1.5
4	Conowingo-Plymouth (No. 1)	220	57	1,170	5–100	8	8	1.8
	Conowingo-Plymouth (No. 2)	220	57	1,170	5–100	8	8	1.8
5	Roseland-Plymouth	220	72	1,050	5–100	9	5	2.5
6	Safe Harbor-Westport	220	70	1,050	2–85	1	4	0.4
7	Philadelphia-Chester	66	14	480	Below 5	1	18	0.4
8	Greenbush-Pleasant Valley	110	64	735	1–175‡	7	4	2.74
9	Pleasant Valley-Millwood	132	40.5	620	5–800‡	4	4	2.47

* Section with continuous counterpoise.
** Section with radial counterpoise.
† The location of faults causing 53 tripouts on lines 1a, 1b, and 2 were not known definitely, but these have been assigned to section with or without ground wires in accordance with correlated information.
‡ Before counterpoise and ground rods installed.

without overhead ground wire and 4 on the overhead ground wire section. In 7 years the section with tower-to-tower counterpoise had no flashovers. It is interesting to know that in the same section in the years 1926, 1927, and 1928, before the counterpoise was installed, there was a total of 29 flashovers.

Relation Between Tower Voltage and Flashover

In table III are given the data for 15 records of tower current exceeding 30,000 amperes, secured on the Wallenpaupack-Siegfried line during the years 1933 to 1935 inclusive.

It will be noted that 5 cases of flashover occurred on the section without overhead ground wire, and that the product of current and resistance in all but one case exceeded 1,500 kv. The assigned flashover voltage[5] for this line with standard test waves is as follows:

Units	Positive Wave	Kilovolts
14	1.5x40	1,265
14	1x5	1,565
16	1.5x40	1,425
16	1x5	1,775

An analysis of items 11 to 15, inclusive, indicates strokes to the towers in all cases. This analysis follows:

Item 11—The stroke was confined to a single tower. All 3 phases flashed over.

Item 12—The stroke was confined to a single tower. All 3 phases flashed over.

Item 13—A current reading of 4,000 amperes was obtained in the legs of adjacent tower *WT* 28–1. This tower had a footing resistance of 45 ohms. It is believed that the stroke hit tower *WT* 27–6 and flashed over to *Y*-phase conductor. This conductor was in turn raised in potential and flashover took place from this conductor to the tower at *WT* 28–1.

Item 14—Only one tower was involved in this stroke, and the flashover took place to 2 conductors. Current measurements were made on only one leg and the actual tower current may have been somewhat larger than estimated from the one leg reading. On the other hand, a long wave with low flashover value is possible.

Item 15—Five towers were involved in this stroke and the data pertaining to these towers follow:

Tower	Footing Resistance	Tower Amperes	Product I × R, Kv	Flashed Phases
SR 9–2	15	10,000	150	*W*
SR 9–3	28	29,000	810	*W* and *Y*
SR 9–4	28	54,000	1,510	*W* and *X*
SR 9–5	34	7,000	240	*W* and *Y*
SR 10–1	15	8,000	120	*Y*
		108,000		

It would appear from this record that the stroke hit tower *SR* 9–4, causing flashover from this tower to conductors *W* and *X*. The surge then traveled to the 2 adjacent towers in both directions, flashing over from conductor to tower. There is some incousistency in the phases affected at the different towers in that the surge started on *W* and *X* phases and wound up on *W* and *Y*

Table II—Locations of Flashovers Causing Tripouts on Wallenpaupack-Siegfried 220-Kv Line Tabulated With Respect to Overhead Ground Wire Construction and Method of Grounding

Year	Location Unknown	Overhead Ground Wires: No Overhead Ground Wires	Overhead Ground Wires: Standard Grounding*	Overhead Ground Wires: Tower-to-Tower Counterpoise	Overhead Ground Wires: Radial Counterpoise	Total
1926		15				15
1927	3	4	0			7
1928	11	2	1			14
1929	27	10	1	0		38
1930	9	14	1	0	0	24
1931	0	20		0	0	20
1932	1	8		0	1	10
1933	2	13		0	0	15
1934	1	11		0	0	12
1935	2	11		0	0	13
Total	56**	108	3	0	1	168
Miles†		36.9		2.6	25.2‡	64.7

* After the latter part of 1930 this section was equipped with radial counterpoise wires.
** This necessarily includes unknown locations on the Bushkill-Roseland line, the probable number of which is 2.
† Present mileage of each item. This mileage has changed from time to time as construction has been changed.
‡ Includes diverter cable section.

Table III—Relation Between Tower Voltage and Flashover, Wallenpaupack-Siegfried 220-Kv Line

Item	Tower Number	Overhead Ground Wire	Footing Resistance, Ohms	Amperes in Tower Legs	Product I × R, Kilovolts	Flash-over	Year
1.	*WT* 12–3	Yes	14	36,700	54	No	1934
2.	*WT* 8–5	Yes	7	40,000	280	No	1933
3.	*WT* 8–4	Yes	8	35,000	280	No	1933
4.	*SR* 2–4	Yes	10	36,000	360	No	1933
5.	*SR* 2–1	Yes	15	38,000	570	No	1933
6.	*SR* 2–2	Yes	15	30,000	450	No	1934
7.	*SR* 4–4	Yes	19	35,000	665	No	1933
8.	*SR* 21–2	No	20	42,000	840	No	1933
9.	*SR* 8–4	No	20	49,000	980	No	1934
10.	*SR* 33–2	No	18	30,800	555	No	1933
11.	*SR* 31–3	No	34	51,000	1,730	Yes	1933
12.	*SR* 19–3	No	45	40,000	1,800	Yes	1933
13.	*WT* 27–6	No	58	36,000	2,100	Yes	1933
14.	*SR* 18–1	No	28	30,000	840	Yes	1934
15.	*SR* 9–4	No	28	54,000	1,510	Yes	1935

phases. It is barely possible that tower 9–3 was raised sufficiently high in potential by the flashover of phase *W* to involve phase *Y* in the trouble. It is also possible that flashover took place on *Y*-phase at *SR* 9–4 but left no marks that could be detected.

The Glenlyn-Roanoke line[8] of the Appalachian Electric Power Company is a double circuit line, approximately 65 miles long, with one overhead ground wire at the peak of the towers. It is not possible from the measuring equipment on this line to associate the point of flashover with a particular tripout as definitely as on the Wallenpaupack-Siegfried line.

The Glenlyn-Roanoke line is insulated with 10 units, spaced 4¾ inches apart, with flashover voltage approximately as follows:

1½x40 positive wave—820 kv
1x5 positive wave—970 kv

In 1934 there were 51 lightning strokes to this line. Tower potentials, that is, the product of tower current and tower footing resistance, for the towers which appeared to be the center of disturbance in each of the 51 strokes, ranged as shown in the following tabulation:

Kilovolts Range	Number
40– 200	13
201– 800	23
801–1,000	5
1,001–4,200	10
Total	51

In 15 of the 51 cases listed the tower potential was of sufficient magnitude to be in the flashover range. In 13 of the 15 cases a possible correlating tripout was reported. There were 3 other tripouts which may have correlated with tower potentials lower than the assigned flashover voltage.

In 1935 there were 32 strokes to the Glenlyn-Roanoke line. Potentials of the towers which were the apparent center of disturbance may be grouped as follows (excluding 3 cases in which the tower current was classified as a "trace").

Kilovolts Range	Number
20– 200	6
201– 800	17
801–1,000	0
1,001–2,610	6
Total	29

Of the 32 cases there were 6 cases in which the tower potential was of the order of the insulator flashover and 6 tripouts due to lightning occurred on this line during the period of measurements.

Table IV—Range of Tower and Probable Stroke Currents in 4 Transmission Lines, 1933, 1934, and 1935

Range of Current, Amperes	Tower Current										Probable Stroke Current									
	W-S*			G-R**			SH-W-T†		P-D‡	Total	W-S*			G-R**			SH-W-T†		P-D‡	Total
	1933	1934	1935	1933	1934	1935	1934	1935	1935		1933	1934	1935	1933	1934	1935	1934	1935	1935	
1,000–5,000	4	4	9	0	2	0	0	14	0	33	4	4	8	0	2	0	0	14	0	32
5,001–10,000	3	5	8	8	3	7	11	28	2	75	3	1	3	7	3	7	9	20	1	54
10,001–20,000	7	2	6	9	7	4	7	30	2	74	6	4	7	10	2	2	8	22	3	64
20,001–30,000	0	0	2	4	11	3	17	22	5	64	1	2	4	2	10	4	7	23	1	54
30,001–40,000	8	3	1	0	15	8	16	16	6	71	3	2	2	1	11	2	11	12	6	50
40,001–50,000	2	0	0	0	4	2	8	4	0	20	4	0	1	1	7	4	8	9	1	35
50,001–60,000	1	0	1	1	2	1	1	1	0	8	1	0	0	0	1	1	3	7	1	14
60,001–70,000				1	3	0	1	0	1	6	0	0	1	1	0	2	7	4	2	17
70,001–80,000				0	1		1	0	0	2	1	0	0	0	3	0	1	1	0	6
80,001–90,000				0					0	0	0	0	0	0	2	1	2	1	0	6
90,001–100,000				2					0	2	0	0	0	1	0	2	0	1	0	4
100,001–110,000									0	0	1	1	0	1	0	0	1	0	0	4
110,001–120,000									1	1			1	1	1	0	0	0	0	3
120,001–130,000									1	1				1	2	2	0	0	0	5
130,001–140,000									1	1				2		1	1	1	1	5
140,001–150,000														0			0	0	0	0
150,001–160,000														0			1	2	0	3
160,001–170,000														0						0
170,001–180,000														0						0
180,001–190,000														0						0
190,001–200,000														1						1
200,001–210,000														0						0
210,001–220,000														1						1
Total	23	14	27	23	49	26	61	116	19	358	23	14	27	23	49	26	61	116	19	358

* Wallenpaupack-Siegfried 220-kv line.
** Glenlyn-Roanoke 132-kv line.
† Safe Harbor-Westport-Takoma 220-kv line.
‡ Philadelphia-Delaware 66-kv line.

Current in Towers and Strokes

Table IV gives the range of current and the number of times these currents were recorded by surge crest ammeter for 4 systems during the years 1933 to 1935 inclusive.

Records of 358 strokes were obtained in these years. The table gives data for the tower with the highest current where several towers are involved in a stroke, and for the probable total stroke current, obtained by adding the currents in all the towers affected by a stroke.

Figure 1 summarizes in cumulative curves, the tower current and probable stroke current of the 4 transmission lines based on the data of table IV. It will be noted from figure 1 that although the tower currents go to approximately 130,000 amperes, only about one per cent exceed 100,000 amperes and about 6 per cent exceed 50,000 amperes, also that the probable stroke currents go to 220,000 amperes but only about 6 per cent exceed 100,000 amperes. Of the 358 strokes recorded approximately 95 per cent were of negative polarity, that is, top of tower negative with respect to bottom of tower and ground.

The use of surge measuring instruments of several types, and in many cases a great number of each type, permits analysis of results on a statistical basis as well as for single strokes. The statistical method establishes the range of stroke current, voltage, and frequency of occurrence, but the exact electrical mechanism of the stroke in the transmission structure can be established only through correlation of a great number of records for a single stroke. For instance, the single stroke surge voltage recorder data, obtained at a number of stations along the conductor resulted in the practical attenuation formula previously given.[7] Also each cathode-ray oscillogram of conductor voltage when examined with accompanying surge voltage recorder and surge indicator data for the same stroke provides a more complete record of the surge mechanism. The surge crest ammeter is peculiarly adapted to the securing of a great number of current records at all parts of the line structure for each stroke.

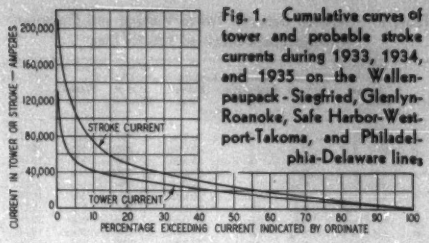

Fig. 1. Cumulative curves of tower and probable stroke currents during 1933, 1934, and 1935 on the Wallenpaupack - Siegfried, Glenlyn-Roanoke, Safe Harbor-Westport-Takoma, and Philadelphia-Delaware lines

In figure 2 is shown a sample of current measurements in the counterpoise, tower legs, tower arms, and overhead ground wire. Polarity directions are indicated by the arrows pointing in the conventional plus to minus direction. The 2 counterpoise wires fed into the base of tower 10 from the adjacent earth some 15,800 amperes. The longer, or 150-foot, counterpoise gathered some 120 amperes per foot and this was about the same for each foot of its length. The shorter, or 40-foot, counterpoise gathered about 80 amperes per foot. Assuming that the long and short counterpoise wires on which no measurements were taken also carried 15,800 amperes, a total counterpoise current of 31,600 is obtained. This agrees with the upward current of the 4 legs which measured some 28,600 amperes. This current flowed into the tower arms and into the ground wire at the tower tip, being joined here by about 12,000 amperes coming from the left. These currents together gave a crest of 33,000 amperes in the overhead ground wire just a few feet to the right of the tower tip. As the measurement station on the ground wire at the left of tower 9 showed 12,500 amperes flowing

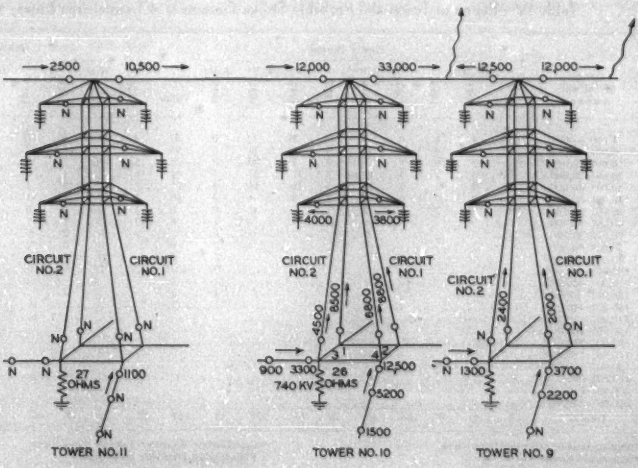

Fig. 2. Current measurements obtained during stroke occurring on Glenlyn-Roanoke line, June 1936

Circles indicate measurement stations

N—Current less than measuring range of station

in the opposite direction, the assumption of the stroke to the ground wire between these 2 stations appears justifiable. The current of the stroke is some 45,500 amperes. It will be noted that the individual currents do not add to exactly equal the measured sum. Two factors are important in this connection. First, the magnetic links are adjusted to read crest current to 10 per cent accuracy. Second, the measurement station at the right of tower 9 on the ground wire showed 12,000 amperes flowing to the right. Another stroke along the line in this direction is indicated, but this stroke occurred further to the right than tower 8, as this tower did not show any leg current within the measurable range.

To the left of tower 10 the measurement station in the ground wire on the right side of tower 11 gave a reading of 10,500 amperes. This 10,500 amperes is made up of 2,500 amperes coming in over the ground wire from tower 12 and some tower leg current in tower 11, which was below the measurement range of the magnetic link setting. The middle phase insulator assemblies of circuit number 1, towers 8 and 10, flashed over. The tower footing resistance at tower 10 of 26 ohms with 28,600 amperes flowing gives a tower potential of 740 kv. At tower 8 the high resistance of 147 ohms requires only 5,000 amperes to give insulator flashover voltage, and this value divided among the 4 legs evenly gives but 1,250 amperes per leg, a value below the measuring level of the magnetic links as installed.

Reviewing briefly this one set of records locates the point of contact of the stroke and gives the magnitude and direction of the component surge currents in the structure. The overhead ground wire shields the line conductors and the counterpoise wires operate to reduce footing resistance, but the high ground resistance gives a high tower potential which causes insulator flashover. Many similar records have been obtained of strokes to the ground wire and occasional records indicate strokes to the conductor and to the tower.

Table V—Current in Long (150-Foot) Counterpoise Wire at Different Distances From Tower, Glenlyn-Roanoke 132-Kv Line, 1935

Reference Number	Tower Number	Amperes at Indicated Distance From Tower		
		3 Feet	80 Feet	147 Feet
1–3	22 G.	750	Trace*	0
1–3	24 G.	1,600	750	Trace*
1–3	25 G.	8,500	5,600	0
1–3	26 G.	2,900	2,400	0
1–3	27 G.	2,800	0	0
2–1	7 R.	3,500	2,000	Trace*
2–1	8 R.	8,900	3,800	Trace*
2–1	9 R.	2,300	1,400	Trace*
3–1	13 G.	1,800	1,400	0
3–2	16 G.	−3,000+**	−4,200**	N. I.
3–3	18 G.	3,300	1,400	0
3–3	19 G.	2,600	1,300	0
3–3	20 G.	9,400	5,900	1,300
3–3	21 G.	10,700	5,400	Trace*
3–3	22 G.	17,500	13,000	2,300
3–3	23 G.	11,600	7,700	2,700
3–3	24 G.	2,500	800	0
3–3	25 G.	0	0	1,000
3–3	27 G.	0	900	0
4–1	18 R.	1,000	0	0
1–2	9 G.	15,000	4,700	2,600
1–2	10 G.	5,700	2,800	800
1–2	11 G.	1,600	1,000	0
6–1	12 G.	9,300	8,100	1,000
6–1	14 G.	800	Trace	0
6–1	15 G.	700	Trace	0
Summation		124,750	68,850	14,200

* For the purpose of this tabulation a trace is assumed to be 500 amperes.

** In this case the polarity indicates current flowing from tower to free end of counterpoise. In all other cases current flows from free end of counterpoise toward tower. Values for this reading have been omitted from the summation.

N. I. = not installed.

The Counterpoise

On the Glenlyn-Roanoke line the counterpoises are made of $^1/_{16}$ by 1.5 inch galvanized iron strap. Two lengths each 150 feet long extend out from diagonally opposite tower legs and run parallel with the conductors; 2 lengths each 40 feet long extend at right angles to the line from the other 2 tower legs. The counterpoise conductors are buried approximately 18 inches under the surface of the ground. The counterpoise wires on 20 towers near each end of the line were equipped with current measurement means as follows:

In 1934 one 150-foot wire and one 40-foot wire, each had one magnet bracket installed at approximately 3 feet from the tower leg. In 1935 the equipment on the short cable was unchanged, but on the long cable 2 additional brackets were mounted at approximately 80 and 147 feet from the tower leg.

In 1935 readings were obtained in 26 cases of current at all 3 points on the 150-foot counterpoise. These readings are given in table V. In all cases but one, the polarity indicates current flowing from the free end of the counterpoise toward the tower.

In figure 3 are plotted a summation of counterpoise currents for each of the 3 stations located along the wire. This summation was made by arranging the data in order of increasing current magnitudes for the station nearest the tower, and beginning at the lowest current adding each time the next higher current value.

Table VI—Relation Between Current in Long (150-Foot) and Short (40-Foot) Counterpoise Wires, Glenlyn-Roanoke 132-Kv Line, 1935

Reference Number	Tower Number	Amperes		Ratio Long to Short
		Long Counterpoise	Short Counterpoise	
1–3	25 G.	8,500	1,900	4.48
2–1	7 R.	3,500	1,200	2.92
2–1	8 R.	8,900	1,300	6.85
3–3	18 G.	3,300	1,100	3.0
3–3	19 G.	2,600	700	3.72
3–3	20 G.	9,400	1,600	5.87
3–3	21 G.	10,700	2,400	4.46
3–3	22 G.	17,500	6,800	2.58
3–3	23 G.	11,600	2,900	4.0
3–3	24 G.	2,500	750	3.34
1–2	9 G.	15,000	2,600	5.77
1–2	10 G.	5,700	900	6.33
6–1	12 G.	9,300	1,100	8.46
Summation		108,500	25,350	4.3

Ratio of counterpoise lengths 3.75. Total counterpoise current approximately double above values. In all cases the polarity indicates current traveling from free end of counterpoise toward tower.

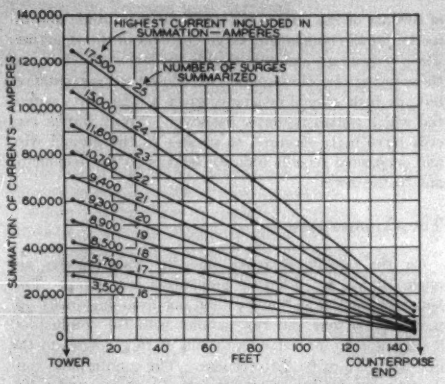

Fig. 3. Summation of currents in 150-foot counterpoise wire at different distances from tower

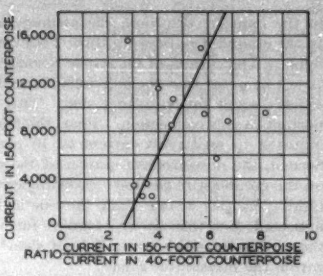

Fig. 4. Relation between current in 150-foot and 40-foot counterpoise wires

The figure shows that for all current levels the collection of current from the ground by the counterpoise is about the same for each foot of its length. There seems to be an indication, however, that at lower currents the portion nearer the tower collects a greater proportion per unit length than that away from the tower while for the higher currents the remote sections gather in the greater proportion of currents. Although not brought out clearly by the figure, a consideration of all the data indicates that the 150-foot counterpoise takes care of about 10,000 amperes with uniform collection of current throughout its entire length. This gives about 70 amperes earth current collected per foot of wire. Such an even ground current must be accompanied by good uniformity in distribution of earth potentials and an elimination of points of high earth current density and great earth potential differences, which result in high tower potentials. An effective utilization of the entire length of the counterpoise wire is therefore indicated at approximately 10,000 amperes. If the current ranged above this value more length would appear to be desirable, while for lower currents the remote end of the 150-foot wire would be of questionable value. On this basis 4 radial 150-foot wires would take care of a 40,000-ampere tower current, which is considerably above the average in magnitude.

In 13 cases simultaneous readings were obtained on the long and short counterpoise wires. In Table VI are given the readings in the short counterpoise and in the long counterpoise at the 3-foot station. Comparing the summation of all the readings on the long and short counterpoise wires, we find the ratio of current in long counterpoise to current in short counterpoise to be about 4.3. The ratio of lengths is 3.75, indicating that the current taken by a radial counterpoise of this sort, all conditions being equal, is practically in proportion to its length.

In figure 4 are plotted the ratio of current in the 150-foot counterpoise to the current in the 40-foot wire as abscissas against the current in the 150-foot counterpoise as ordinates from the data of table VI.

With these data a tendency for the higher counterpoise currents to give higher ratios can be noted. This again shows the remote section of a buried ground wire to be gathering in a proportionally greater amount of current at higher stroke currents. At some 5 to 6 thousand amperes the 2 wires are carrying currents in the same proportion as their lengths. Below this value on an average the short counterpoise carries a greater proportional part and above it the longer wire carries the greater proportion. Now, it seems to be a reasonable rule that that wire will carry the most current which performs most effectively in reducing earth potentials. This reduction in earth potentials is also the mechanism whereby the counterpoise serves to hold down the tower potential and prevent insulator flashover. Accordingly, a reasonable conclusion from the ratio data appears to be that for currents below 5 to 6 thousand amperes the 150-foot wire is more than necessary and for higher currents the 40-foot wire too short. These considerations, of course, pertain to relative length and it is important to observe that the ratio-current magnitude trend is not clearly demonstrated by the available data. The variations in soil conductivity quite likely partially obscure this trend.

Table VII shows the relation between the total current

(*Concluded on page 189*)

Table VII—Relation Between Current in Tower Legs and Counterpoise Wires, Glenlyn-Roanoke 132-Kv Line, 1935

Reference Number	Tower Number	Total Tower Current, Amperes	Total Counterpoise Current, Amperes	Ratio Tower Current to Counterpoise Current
1–3	25 *G*	30,300	20,800	1.46
2–1	7 *R*	7,000	9,400	0.75
2–1	8 *R*	10,800	20,400	0.53
3–3	20 *G*	16,700	22,000	0.76
3–3	21 *G*	22,000	26,200	0.84
3–3	22 *G*	52,100	48,600	1.07
3–3	23 *G*	21,500	29,000	0.74
3–3	24 *G*	9,000	6,500	1.39
1–2	9 *G*	34,200	35,200	0.98
1–2	10 *G*	17,000	13,200	1.29
6–1	12 *G*	20,000	20,800	0.96
Summation		240,800	252,100	0.95

In all cases the polarity indicates current traveling from free end of counterpoise to tower and from bottom of tower to top.

Arc Characteristics Applying to Flashing on Commutators

By R. E. HELLMUND
FELLOW AIEE

This paper gives the results of experimental investigations relating to arc characteristics as they apply in commutator flashing. A knowledge of these characteristics is necessary for the application of the theory outlined in a previous paper[1] on flashing of commutators by the same author, as well as for the investigation of flashing due to other causes.

IN A previous paper,[1] a method of analyzing flashing on commutators caused by jumping of the brushes was given. This method assumes that an arc (*S*) is formed between segment (*a*) and brush (*b*) when the brush leaves the commutator, as indicated in figure 1*A*. This arc is likely to persist as shown in figure 1*C* after the commutator has moved a certain distance and the brush has returned to the commutator. The method consists essentially in comparing during successive periods the voltage necessary for sustaining the arc with the voltage induced in the armature coils and existing between the arc terminals. For a practical application of this method, a knowledge of the arc characteristics applying to the commutators is therefore a prerequisite, and it is the purpose of the present paper to give the results of experimental investigations of this nature.

The data given will also be of value in investigations of flashing brought about by other causes. In railway motors, for instance, flashing is caused at times by certain transient conditions applying when the voltage of the motor is suddenly re-established while the motor is running and after an interruption of power supply caused by section breaks in the line, trolley bouncing, etc. Flashing is further caused by transient conditions applying in generators when a short occurs in the line, or in large motors when there is a short-circuit in the system and the motors temporarily act as generators feeding current into the short. Under these various operating conditions, flashing is caused by an appreciable voltage being induced in the short-circuited armature coil (*g*) during these temporary or transient conditions. When, as shown in figure 1*B*, this short-circuit current is opened because of segment (*a*) leaving the brush (*b*), an arc (*S*) is formed. As in the case of brush jumping, the sustaining of this arc depends upon the relative values of the voltage necessary for sustaining it and the voltages existing between the terminals of the arc for various successive positions of the commutator segment (*a*). Therefore, we are again interested in a knowledge of the arc characteristics around the commutator. This case may be somewhat complicated by the fact that a new arc is formed on each segment leaving the brush, resulting possibly in the formation of a number of different arcs on the several commutator segments, as indicated in figure 2 by *S*, S_1, S_2, and S_3. However, a knowledge of the arc characteristics of the individual arcs formed should prove a desirable first step toward a complete analysis of the various transient conditions.

In order to study the arc characteristics around the commutator, a simple arrangement as shown in figure 3 was used in our experimental work. A number of connected segments (*a*) of a commutator (*C*) were connected to a slip ring (*D*). A d-c voltage source was connected through an adjustable resistance (*r*) to the brushes (*b* and b_1). Whenever the segments (*a*) are in contact with the brush (*b*), current flows and is interrupted by means of an arc (*S*) when the last segment (*a*) leaves the brush (*b*). With this operating condition, oscillograms were obtained giving the current as well as the voltage across the arc terminals. An example of these oscillograms is shown in figure 4. Tests were carried out with different initial current values and also for different speeds of the commutator. From an analysis and careful scaling of these oscillograms, curves such as shown in figures 5 and 6 were derived for a number of different speeds of the commutator.

The results for only 2, but widely different, speeds are given in these 2 figures. The full-line curves show the relation between arc current and arc voltage as scaled directly from the oscillograms. The test points thus obtained and entered in the figures gave in most cases rather smooth curves, which is to be expected because of the fact that the oscillograms gave rather smooth curves, as indicated in figure 4, and were void of erratic irregularities frequently encountered in connection with arc phenomena. Whatever discrepancies do exist are due essentially to difficulties in scaling the oscillograms, some of which were not taken on as large a scale as that of figure 4. It was furthermore observed that in spite of the widely diverging speeds at which these tests were made, the solid-line curves of figures 5 and 6, when compared for an equal initial current, did not vary appreciably from each other for different speeds. In considering all the curves drawn, it is difficult to find any marked tendency of variation with speed in one direction or another in the solid-line curves. Further analysis revealed, however,

A paper recommended for publication by the AIEE committee on electrical machinery. Manuscript submitted October 29, 1936; released for publication December 1, 1936.

R. E. HELLMUND is chief engineer of the Westinghouse Electric & Manufacturing Company, East Pittsburgh, Pa.

The author acknowledges the assistance of W. B. Batten, R. P. Hanna, and J. N. Jones, of the Westinghouse Electric & Manufacturing Company, in the preparation of this paper.

1. For all numbered references see list at end of paper.

that with a given current, a certain arc voltage corresponds to different arc lengths with different operating speeds. By means of the timing curves taken with the oscillograms, it was possible to calculate the arc length corresponding to any test points. This was done

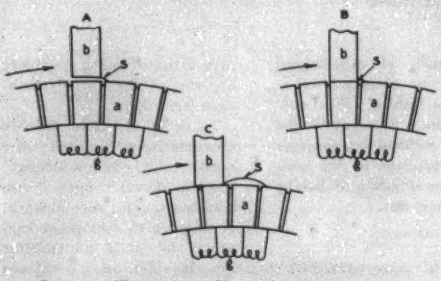

Fig. 1. Illustration of arc formation prior to flashing on commutators

and the points entered in figures 5 and 6 corresponding to a certain arc length were marked by like designations; thus the dotted-line curves each corresponding to a given arc length, as indicated, were obtained.

The agreement of the test points with the dotted-line curves is not quite so good as with the solid-line curves, nevertheless the consistency of the results is quite remarkable, taking into consideration the usual difficulty in obtaining consistent results with arc phenomena. The reason for this seems to be that in these tests the condition of the air currents near the arc was more or less definitely established by the nature of the air film carried around near the surface of a rotating cylinder for any given speed. Usually arc phenomena tested in open air are subject to varying air currents caused by convection and other causes, and they frequently are further influenced by electromagnetic effects, all of which lead to irregularities. Furthermore, the electrode spots are often moved about by these irregularities, which further increases

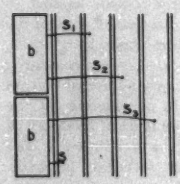

Fig. 2. Illustration of multiple arcs forming on commutators under certain conditions of flashing

the difficulty of obtaining consistent results. (This is noticeable on some of the oscillograms given toward the end of the paper which show very irregular curves during periods when the location of the electrode spots is changing. See figure 12.)

In considering the phenomena further, it must be appreciated that while the dotted-line curves somewhat simulate the usual arc characteristic curves, they do not represent a static relation between current and voltage because the points to which the curves are drawn are in all cases the points from a transient arc condition obtained by starting with a certain value and lengthening the arc while the current decreases and the voltage increases. By means of the full-line curves, it is possible to determine the starting currents corresponding to the current values at the points of intersection between the

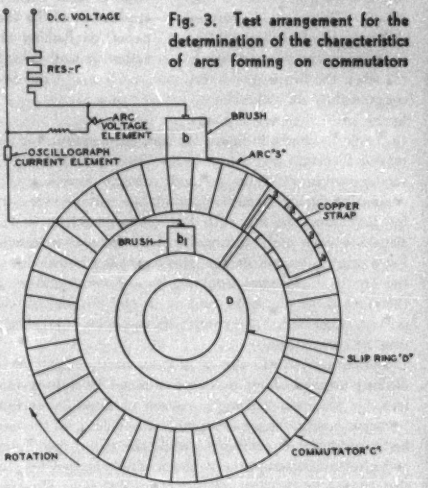

Fig. 3. Test arrangement for the determination of the characteristics of arcs forming on commutators

solid-line and the dotted-line curves. Normally, that is with constant length of arc and without high air velocity around the arc, it is to be expected that with a diminishing arc current the voltage will be the lower the shorter the time interval allowed for the decrease in current. The reason for this is that during a shorter time interval, less deionization will take place. Comparison of definite points between the low- and the high-speed curves in figures 5 and 6, respectively, shows that the opposite condition applies here. If we consider, for instance, the 20-ampere point for the $2^1/_2$-inch arc length in figure 5, which corresponds to a starting current of about 28 amperes, we find a voltage of 167 volts for the slow speed. If we then consider the 20-ampere point for the $2^1/_2$-inch arc length in figure 6, we find a higher voltage of 215 volts in spite of the fact that the time of drawing this arc was only $^1/_3$ that of figure 5 and that the starting current was over 30 amperes. Likewise, if we consider the 14-ampere point of the 1-inch arc length, with a starting current of about 18 amperes the voltage indicated is 115 volts for the low speed, while with approximately the

same starting current, a voltage of 155 is obtained for the high speed. The conclusion drawn from this is that the speed at which the commutator is rotating has a marked influence upon the deionization, resulting in higher voltages for a given current with the higher speed. This is more clearly shown in figure 7, which gives the arc voltages for certain arc lengths at different speeds for instantaneous arc currents of 10 and 60 amperes. As should be expected, the speed is of relatively minor influence with the shorter arcs but is, in general, of greater influence with the longer arcs. It will be further noted that with the heavier currents the influence of the speed is not very marked, while with the small currents it is appreciable. Since the voltages for the transient currents for which the curves of figure 7 are plotted may be influenced by the initial currents

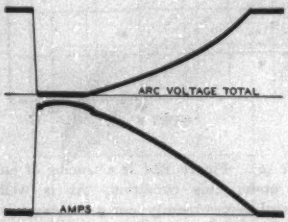

Fig. 4. Tracing of oscillogram giving arc current and arc voltage

and the corresponding ionization, the values of the initial currents are of interest. The values of these initial currents happen to be practically constant for each of the curves and therefore the difference in voltages evidently is caused by the difference in speed; these values are shown at the right of the curves in figure 7.

Although, as already pointed out, the curves in figures 5 and 6 cannot be considered as representing static arc characteristics, figure 8 has been prepared showing a comparison of some of the curves of figures 5 and 6 with the static-arc characteristics as calculated from a formula given by Rüdenberg.[2]

In commutator flashing we do not at any time deal with constant arc currents, but the conditions are much the same as the test conditions of figure 3. What we are really interested in, especially in the light of the theory advanced in my previous paper,[1] is the arc voltage for different lengths of arc for any given initial arc current and for various commutator speeds. The curves in figures 9*A* and 9*B* show this. These curves can be directly applied as the arc voltage curves designated *A*-*B* in the previous paper and compared with the curves of the voltages induced in the armature between the arc terminals. Figure 10 gives a number of these voltages as compared with the curves applying to given initial currents indicated for a speed of 2,200 feet per minute. The distance to the points at which the arc-characteristic curves and the induced-voltage curves cross each other should, therefore, be a direct indication of the comparative likelihood of motor flashing at 2,200 feet per minute for the different initial currents and for the 3 different curves of induced voltage corresponding to different main-pole shapes.

In order to check any influence which different brush locations might have upon the arc characteristics, a number of tests were made with the brush mounted at the bottom of the commutator. The results thus obtained did not differ materially from those obtained with the brush mounted at the top. Visual inspection indicated that the arc formed close to the surface of the commutator with the brush in either position, and, in general, the phenomena seemed to be the same.

With the testing arrangement in figure 3, it is evident

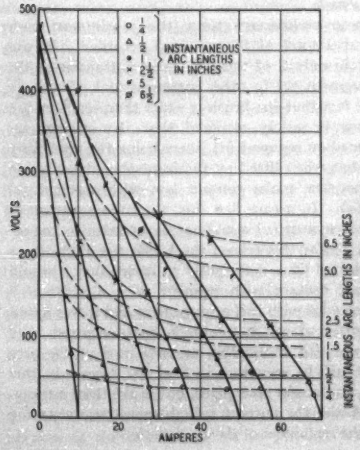

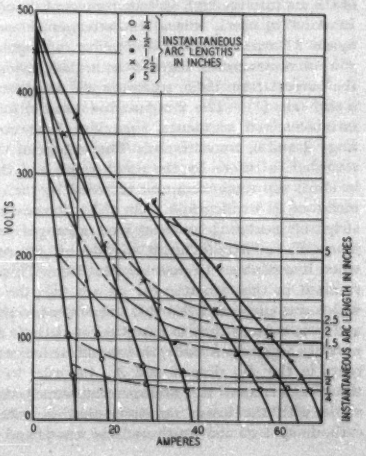

Figs. 5 (left) and 6 (right). Curves showing relation of voltage to current as obtained from oscillograms such as shown in figure 4 (full lines), and curves showing relation of voltage to current for various lengths of arc (dotted lines)

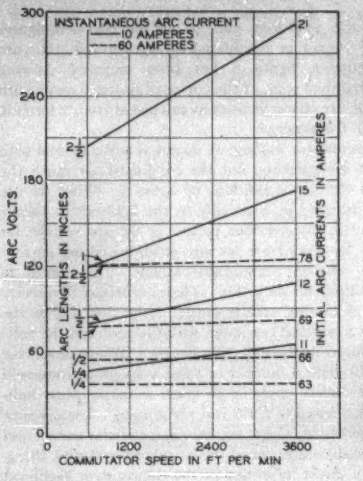

Fig. 7 (left). Curves showing arc voltage as influenced by speed for various currents and arc lengths

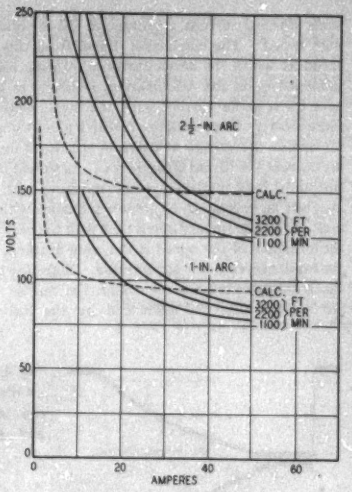

Fig. 8 (right). Comparison of calculated static arc characteristics with transient characteristics tested on commutators

that the hot-cathode spot would very likely remain on the last segment (*a*) for the entire duration of the arc, unless there were appreciable air currents or magnetic effects to disturb conditions. However, in checking some tests made on motors with artificially produced brush jumping, it seemed that at times flashing did not occur when according to the basic theory given in my previous paper[1] it should have occurred. This theory assumes that the hot-cathode spot remains on the segment on which it originally forms. The only possible explanation therefore seemed to be that in reality the hot-cathode spot moved from the original segment in a backward direction to other segments, thus preventing the drawing of the arc into the high-voltage regions of the commutator. In order to check this a test arrangement as shown in figure 11 was devised. A number of segments (*a*, *z*, *y*, *x*) were connected together as in the previous tests and the current from these segments was conducted through a slip ring (1). The 2 segments (*b* and *c*) following the interconnected segments were also connected to slip rings 2 and 3, respectively. The voltage of the arc was recorded as before by the oscillograph and the currents in the 3 slip rings were also recorded by the current elements of an oscillograph. On the commutator surface 2 strips of insulating material were arranged as shown in figure 11 to lift the brush slightly off the commutator when it was about to pass segment (*a*). This, of course, resulted in the formation of an arc (*S*), the current of which was measured through the current of slip ring (1) and it is evident that in case the hot-cathode spot would move to segments *b* and *c*, this would be indicated by currents in the slip rings 2 and 3. In order to determine the effectiveness of this arrangement, some tests were first made with the brush negative—that is, with the hot-cathode spot on the brush and the anode end of the arc forming on segment (*a*). Figure 12*A* is a tracing of an oscillogram taken under this condition. As is well known, the anode spot moves readily and it will be seen that the arc formed on segment (*a*) at the left end of the oscillogram, persisted for a short period, and then transferred to segment (*b*). Subsequently the current was divided for a time between segments (*b*) and (*c*) and finally transferred entirely to segment (*c*). In the case of the second arc on the same oscillogram, the current again is on segment (*a*) for a certain period, then is transferred for a short time to (*b*); and then instead of dividing as in the first case, is entirely transferred to segment (*c*). The latter condition is obtained in the majority of cases with a negative brush.

After these preliminary tests, the brush was made positive and a total of 22 arcs was recorded. It was found that in only 2 of these 22 cases a transfer of the arc from segment (*a*) to other segments took place. In view of the fact that the brush is wider than segment (*a*), it could not be safely assumed that the original arc always formed on segment (*a*), there being the possibility that the brush when lifted by the insulating strips would tilt and therefore make contact last with segment (*z*) preceding (*a*). In a case like this, the subsequent move of the arc to segment (*a*) would not be recorded by the oscillograph. For this reason the brush was beveled, as shown by dotted lines, sufficiently to insure that it would make its last contact with segment (*a*). A total of 7 arcs were recorded with this arrangement and it was found that a transfer of the hot-cathode spot occurred in 2 cases. Figure 12*B* shows the currents in 3 of the arcs formed. It will be seen that in 2 of the 3 cases in this oscillogram no transfer took place, but in the third a transfer occurred and the current split between segments (*b*) and (*c*) for the remainder of the arc duration.

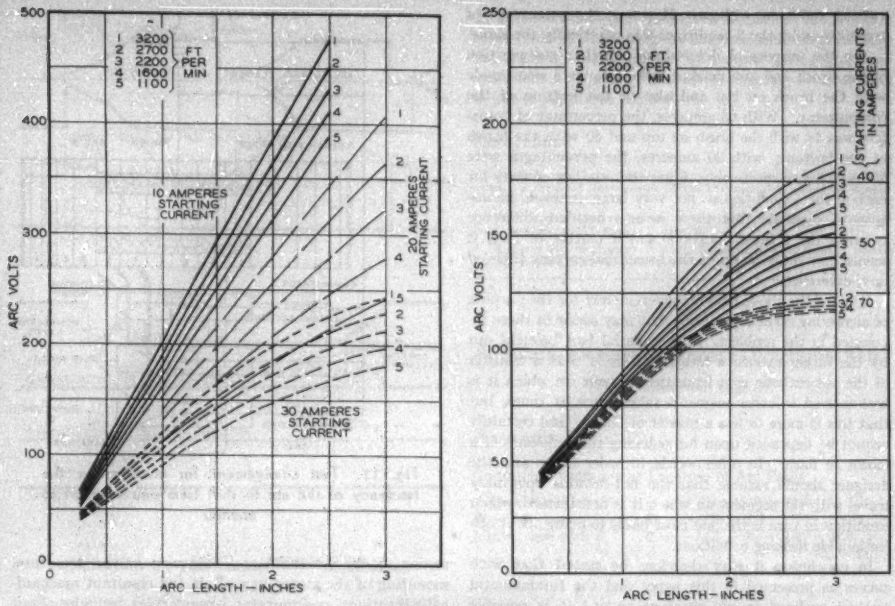

Fig. 9A (left) and 9B (right). Curves showing relation of arc voltages to arc lengths for various values of speeds and initial currents

In order to provide for the possibility of the arcs transferring to segments following segment (*c*), the arrangement was changed so that segment (*c*) was connected to a number of succeeding segments (*f*, *g*, and *h*), as indicated by the dotted connection in figure 11. A typical oscillogram taken under this condition is shown in figure 12*C*. It will be seen that with the first 2 arcs no transfer took place; with the third a transfer of current to segment (*b*) occurred, and subsequently to the sector including segment (*c*). The sudden breaks in the current of slip ring (3) seems to indicate a further shift of the hot-cathode spot from one of the connected segments to another. The formation of the fourth arc seems to be similar to that of the third, except that the arc transferred from the leading to the lagging sector without touching the intermediate bar.

In another oscillogram shown in figure 12*D*, it will be noted that a transfer from the leading to the lagging segment took place in 2 instances, while no transfer occurred in the third. It will also be noted that the time at which the transfer took place in the first 2 cases differs. The oscillogram shows no definite evidence of an intermediate time during which segment (*b*) carried the current.

Summarizing: It is found that of 125 arc formations recorded, no transfer took place in 84, or 67 per cent of the total. Eliminating the tests with unbeveled brushes because of the uncertainty as to whether transfer took place between segments (*g*) or (*a*), it is found that of the remaining 103 arc formations there was no transfer of any kind in 64, or about 62 per cent of the cases. Current values of 30 and 65 amperes were used in the tests. With the 30-ampere current, transfer took place in 21 out of 55 cases, or 38 per cent; with the 65-ampere current, in 20 out of 71, or 28 per cent. Considering only the tests with beveled brushes, with the 30-ampere current a transfer took place in 44 per cent of the cases; with the 65-ampere current, in 33 per cent. There is, therefore, a general indication that with a lower current the tendency to transfer is greater, though it may be inadvisable to draw such a definite conclusion without carrying on a greater number of tests. At speeds of about 1,600, 2,200, and 3,200 feet per minute, the percentages of cases in which transfers took place were 43 per cent, 19 per cent, and 44 per cent, respectively, when all tests are considered; at speeds of 1,600, 2,200, 3,200, 4,300, 4,900, and 5,400 feet per minute, the percentages are 53 per cent, 18 per cent, 47 per cent, 11 per cent, 22 per cent, and 45 per cent, respectively, when only the tests with the beveled brushes are taken into account. These figures do not indicate any very definite tendency to transfer with increasing speed.

It was thought that the tendency of the arc to transfer might be influenced somewhat by the undercutting of the commutator and some tests were therefore run with under-

cutting and some without. However, the percentage of transfers under the 2 conditions was practically the same.

For the purpose of determining whether the position of the brush had any marked influence, tests were made with the brush on top and also at the bottom of the commutator. With 65 amperes, the percentage of transfers was 44 with the brush on top and 40 with the brush at the bottom; with 30 amperes, the percentages were 40 and 62.5, respectively. Since the number of tests for each of the 4 conditions is not very large, it would be unwise to conclude that there is any decided difference between the 2 brush locations; as a matter of fact, it seems that the location of the brush makes very little, if any, difference.

Some of the above data are given merely for the purpose of answering certain questions that may occur to those interested in the problem. The essential fact brought out by the rather extensive series of tests is that a transfer of the hot-cathode spot from the segment on which it is first formed to other segments takes place at times, but that this is more or less a matter of chance and certainly cannot be depended upon for reducing the tendency of a motor to flash. In other words, in order to be safe the designer should assume that the hot-cathode spot may travel with the segment on which it is first formed, which condition in turn is the one most likely to bring about objectionable flashing conditions.

In conclusion it may therefore be stated that with curves as presented in this paper and the fundamental method outlined in my previous paper,[1] it is possible to analyze the inherent electrical tendency of motors to flash when the brushes jump. It is appreciated that this phenomenon is also greatly influenced by the length of time the brush is off the commutator, which in turn is influenced by a great many mechanical factors, such as workmanship in the building of the commutators, seasoning of the commutators, balancing of the armature, mounting of the motor as a whole and resultant mechanical vibrations, commutator irregularities brought about by commutation characteristics and the type of brush used, brush tension applied to the brushes, weight and elasticity of the brushes, etc. It is obvious that the great variety of influencing factors makes it practically impossible to determine theoretically the time the brush is likely to leave the commutator at different commutator speeds and that a complete and exact theoretical analysis of this flashing problem therefore seems impossible. However, the method and data given are useful and of practical value in a comparative quantitative analysis of different motor designs and, in particular, of their field distributions. Moreover, some of the variables enumerated, such as the commutation characteristics, the choice of brushes, etc., can be handled by the designer in such a way as to eliminate them as factors of practical importance. On the other hand, the variations caused by manufacturing and maintenance operations can, with reasonably controlled shop processes, be reduced to chance phenomena of a limited amplitude of variation. Consequently, the comparative analysis outlined furnishes a means by which the adequacy of new designs can be predicted with a considerable degree of assurance. As already indicated at the beginning of the paper, the experimental results given here will also be useful in other types of flashing. A more complete analysis of these will require experimental investigations regarding the initial current that may exist at the brush when a short-circuited coil passes from under the brush under different conditions of load and commutation. Furthermore, it would be necessary to make a quantitative analysis of the transient current, field, and

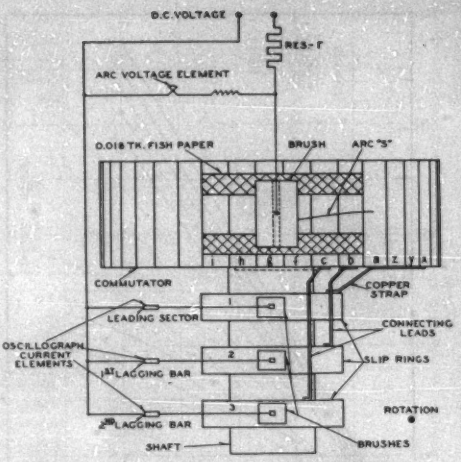

Fig. 11. Test arrangement for investigating the tendency of the arc to shift from one segment to another

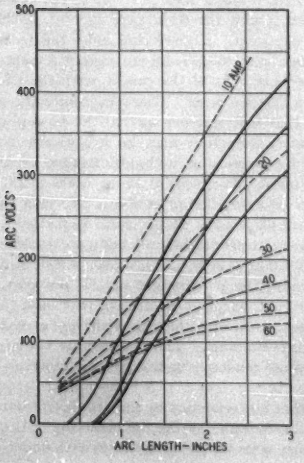

Fig. 10. Curves comparing arc voltages with voltages as induced in armature with various field forms

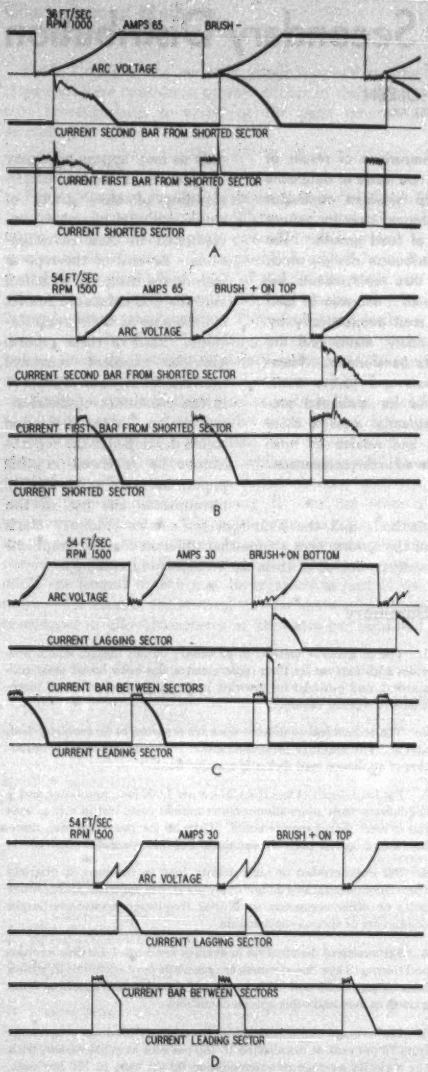

Fig. 12. Oscillograms showing tendency of arc to shift from one segment to another

voltage conditions existing in the machine at the time when flashing is likely to occur. However, through the judicious use of a qualitative analysis of these factors given by the author in an earlier article,[2] together with the considerations and data given in this and the previous paper,[1] considerable progress has been made in predicting the flashing characteristics of motors during transient conditions such as may exist after temporary interruptions of power supply to the motors.

References

1. Flashing of Railway Motors Caused by Brush Jumping, R. E. Hellmund. Electrical Engineering (AIEE Transactions), volume 54, November 1935, page 1178.

2. Elektrische Schaltvorgänge (a book), R. Rüdenberg. Published by Julius Springer, Berlin, chapter V, page 190.

3. Railway Motor Commutation and Flashing, R. E. Hellmund. *Electric Railway Journal*, January 1915, page 105.

A Single-Element Polyphase Directional Relay

(*Continued from page 80*)

Appendix III

Conductor Voltages at Location of Arc Fault

Three-Phase Fault	Phase-to-Phase Fault
$E_1 = I_1 R$	$E_1 = -I_1(Z_1 + Z_L)$
I_1 is in phase with E_1	$E_1 = -I_1(Z_1 + Z_L + 2R) = I_1(Z_1 + Z_L + 2R)$
	$-I_1$ and I_1 lag E_1 and E_1, respectively

Appendix IV

A. Connections Figure 3a

The total input to the relay is

$$P_R + jQ_R = E_c I_b + \underline{E_b I_b} - E_b I_c + E_a I_c - E_a I_b - \underline{E_b I_b} + E_b I_a - E_c I_a$$

The underlined terms cancel and

$$-E_a I_b + E_c I_b = (E_c - E_a) I_b = -E_B I_b$$
$$-E_b I_c + E_a I_c = (E_a - E_b) I = -E_C I_c$$
$$-E_c I_a + E_b I_a = (E_b - E_c) I_a = -E_A I_a$$

Therefore

$$P_R + jQ_R = -E_A I_a - E_B I_b - E_C I_c$$

B. Connections Figure 3b

The total power to the relay is

$$P_R + jQ_R = -E_C I_a - E_A I_a + E_A I_c + E_B I_c - E_B I_a - E_A I_a + E_A I_b + E_C I_b$$

since $E_A + E_B + E_C = 0$

$$E_A I_b + E_C I_b = (E_A + E_C) I_b = -E_B I_b$$
$$E_A I_c + E_B I_c = (E_A + E_B) I_c = -E_C I_c$$
$$-E_C I_a - E_A I_a - E_B I_a - E_A I_a = -(E_C + E_A + E_B + E_A) I_a = -E_A I_a$$

therefore

$$P_R + jQ_R = -E_A I_a - E_B I_b - E_C I_c$$

Reference

1. Symmetrical Components (a book), C. F. Wagner and R. D. Evans. Chapters II and XV.

A Review of Overhead Secondary Distribution

By W. P. HOLBEN
MEMBER AIEE

This paper provides a comparison of results of 5 economic studies* that were made to determine the economic relationship between conductor sizes and distribution transformer sizes for various load densities and rates of load growth. The progressive method of distribution design, which provides additions rather than replacements, has been found most economical. Increase in load density can be handled most economically by the subdivision of secondary mains and the installation of intermediate transformers. Numbers 4, 3, or 2 conductors and 15-kva transformers should be favored for overhead secondary distribution in residential areas in cities and towns. Rural lines and service to rural communities are not considered in this comparison.

SPECIAL interest in the economics of secondary distribution design has developed during recent years among the various electric utility companies. Extensive studies covering technical and practical features of secondary design have been made and reports completed to show the results of these studies in a most interesting and enlightening manner. Through the courtesy and co-operation of 5 operating companies, and the authors of the respective reports, it is now possible to present the combined results of these studies in a comparative form.

The comparisons of the conclusions reached in the various investigations are especially interesting, since they represent a variety of operating conditions, locations, and engineering and operating opinions. There is sufficient similarity in the conclusions reached to indicate that all these reports are based on sound engineering principles and that, in general, the economic and technical solutions of such problems are not restricted by local conditions or individual opinions. On the other hand, certain qualified conclusions indicate the effects of good engineering judgment to meet special local problems, and provide ample reason for separate and independent studies based on conditions and practices in the various operating territories.

While no technical analysis will be undertaken in this paper, it is proposed to present the essential data and results in a concise manner, adding explanatory discussion only as may appear necessary to provide a better understanding of the variety of conditions and variables encountered in these investigations. Several of the reports include the complete technical analysis and tabulated results of each step of their computations. Each of these reports provides excellent reference material for any one interested in the economics of distribution design. Many of the fine points developed in the reports cannot be reviewed in this paper, but the writer highly recommends the use of the methods and the technique for similar studies. Each of the reports uses a somewhat different form of graphical analysis but all of them are extremely interesting.

A paper recommended for publication by the AIEE committee on power transmission and distribution. Manuscript submitted October 29, 1936; released for publication November 30, 1936.

W. P. HOLBEN is engineer in the engineering and construction department of the Duquesne Light Company, Pittsburgh, Pa.

* This paper represents a composite review of the findings resulting from 5 separate studies on the subject of "Economics of Overhead Distribution Design." The author is therefore indebted to the company managements and the authors of the respective company reports, without whose contributions a paper of this type would be impossible at this time. The author is especially grateful for the constructive suggestions made as a result of the review of the paper in preliminary form. The following contributed to the studies on which this paper is based:

Boston Edison Company; report by A. H. Sweetman and St. George T. Arnold, dated December 29, 1934.

Detroit Edison Company; report by H. P. Seelye and R. L. Leinbach, dated September 1, 1935.

Duquesne Light Company; report by C. T. Sinclair and W. P. Holben, dated January 16, 1934.

Philadelphia Electric Company; report by A. H. Kidder, dated November 5, 1934.

West Penn Power Company; report by Merrill DeMarit and R. C. McKee, dated June 1928.

Summary

1. The progressive method of secondary circuit design, which provides additions rather than replacements, has been found most economical, and provides for growing loads on the basis of small increments of system capacity.

2. The economical conductor sizes are reported to be numbers 4, 3, and 2. The majority recommendation is number 2 where the reduction of appliance load flicker is a major need.

3. For load densities less than 20 kw per 1,000 feet, numbers 6 and 4 conductors show some advantage in annual costs but in some cases fail to meet flicker requirements. Over 20 kw per 1,000 feet, numbers 3 and 2 meet both the economy and flicker conditions.

4. For concentrated or high density load in commercial districts these recommendations do not apply, as lack of sufficient transformer poles or other congested conditions frequently necessitate larger conductors or special construction.

5. For overhead distribution in average residential districts in cities and towns, 15 kva transformers are generally most economical, with a later change to 25 and 37½ kva for higher densities resulting from growth in load and other special conditions.

6. For average residential loads, transformer loadings may range from 75 per cent at installation to 165 per cent at replacement, with the majority average recommendation 90 per cent to 150 per cent. (The overloading becomes permissible because of the usual low ambient temperature at the time of the winter peak load on transformers on overhead lines.)

7. Growing loads in overhead distribution areas can be handled most economically when the secondary system is designed on a progressive basis to allow for subdivision of secondary mains and the installation of intermediate transformers as required, including possibly some transformer relocations.

Comparison of Methods, Assumptions, and System Conditions

Table I outlines the methods, conditions, and assumptions that were considered by the authors in their respective investigations, to arrive at the most economical secondary design.

Type of System

The comparison in item 1 shows that each of the 5 companies has studied the problems and economics relating to a 3-wire single-phase overhead radial system of secondary distribution. Companies *A* and *B* have selected the "straight line" plan of distribution with continuous secondaries on streets with long blocks, using the 2-way feed from transformers. Three- and 4-way feeds are rare because of difficulty in locating transformers on corner poles Cross ties between secondary mains and "H" construction are generally considered unnecessary and uneconomical as a result of these studies, except where closed radial loops or banked secondaries are in use. Company *D* reports the use of some radial loop construction, although not used extensively, while company *E* uses banked secondaries as well as radial circuits, with the former predominating. Company *C* does not state a preference. Where short branches from secondary mains are in use, the load on such branches may generally be considered located at the point of connection to the main, while the longest branch may be regarded as part of the main. For most of the studies, the load density has been considered in kilovolt-amperes or kilowatts per thousand feet, distributed uniformly along the main at the respective pole locations.

Method of Comparison

Item 2 indicates that companies *A*, *B*, and *D* have based their investigations on a study of annual costs and companies *C* and *E* on a study of investment costs. Company *E* also includes capitalized losses in the total costs. It is interesting to note that company *B* has included also the annual lost revenue due to secondary drop.

Annual costs include the following items:

(*a*). Fixed annual charges (included by all companies)
1. Interest
2. Dividends
3. Taxes
4. Insurance
5. Depreciation

(*b*). Energy losses (included by all companies)
1. Transformer iron losses
2. Transformer copper losses
3. Secondary copper losses

(*c*) Operation and maintenance for (included by company *A*)
1. Transformers
2. Secondaries

(*d*). Lost revenue due to secondary drop (included by company *B*)

Depreciation as expressed in item (*a*)-5 is dependent on the life of transformers and secondaries resulting from failure, inadequacy, and obsolescence, but must also provide for retirement to meet new conditions resulting from growth in load. Replacement before the end of a normally useful life requires a larger retirement re-

Table I—Comparative Statement of Methods, Assumptions, and System Conditions

		Company				
		A	B	C	D	E
1.	Type of system	3-wire 1-phase overhead radial straight-line	3-wire 1-phase overhead radial straight-line	3-wire 1-phase overhead radial	3-wire 1-phase overhead radial straight-line, 2-way and 4-way	3-wire 1-phase overhead radial and banked
2.	Method of comparison	Annual costs	Annual costs incl. lost revenue due to secondary drop	Investment costs	Annual costs per peak kilowatt	Investment costs incl. capitalized losses
3.	Cost of losses					
	Secondary copper	0.0164			0.00436 and 0.01	0.005
	Transformer iron	0.0073	0.0035 and 0.007		0.003 and 0.01	0.005
	Transformer copper	0.0155	0.0070 and 0.014		0.00456 and 0.01	0.005
4.	Losses capitalized @					15 per cent
5.	Equivalent hours of full load use per year	1,500	1,095 and 2,190		1,200	1,095
6.	Voltage regulation					
	Secondary drop, per cent	2–3	3			2½
	Total regulation			121 volts (first customer) 109 volts (last customer)	4–7 per cent (113–121)	
7.	Allowable flicker				5 per cent of 115 volts 20 amp @ 50% power factor	2–4 per cent of 115 volts 20 amp @ 50% power power factor
	Noticeable flicker	2 per cent of 115 volts 15 amp @ 50% power factor				
8.	Wire cost, triple-braided weatherproof, cents	12	20			5, 10, 20, and 30 copper
9.	Standard wire sizes	Nos. 6, 3, 1/0, and 4/0	Nos. 6, 4, 2, 1/0, 2/0, and 4/0	Nos. 6, 4, 2, and 2/0	Nos. 6, 4, 2 2 No. 1/0 and 1 No. 2 2 No. 4/0 and 1 No. 2/0	Nos. 6, 4, 2 1/0, and 4/0
10.	Type of load	Residential and light commercial	Residential	Residential including ranges	Residential	Residential
11.	Load growth rates, per cent	7½	5, 10, and 15	5	5 linear 5 and 10 compound	"a," "b," and "c"
12.	Load density, kilowatts per 1,000 feet	10 to 110	10 and 20, initial load		7½, 15, 22½, and 30	10 to 100

serve, and most of the companies have therefore extended their investigations to include accumulated annual charges over a considerable period of years, ranging from 15 to 25 years.

Cost of Losses

There is a wide variation in cost of energy losses used by the various companies in calculating this portion of the annual cost. This is apparently due at least in part to one being twice as great as the other, with cost curves resulting that are similar in form and an average variation in total costs of 7 per cent.

Rate of Capitalizing Losses

Company *E* based their study on the total cost of transformers and secondaries in place on the system and included losses capitalized at 15 per cent. Company *C* refers to their comparison of investment costs but does

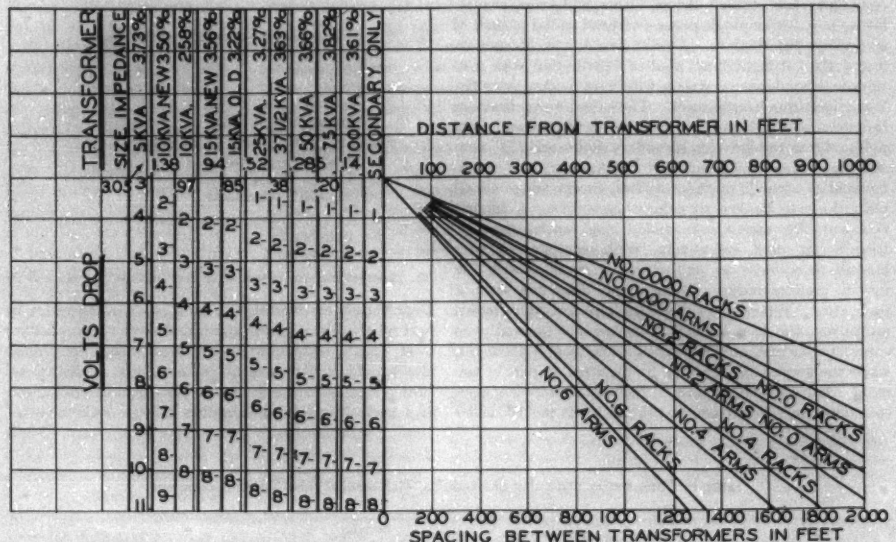

Fig. 1. Flicker chart showing voltage drop with 20 amperes at 115 volts and 50 per cent power factor (company E)

Use scale at left corresponding to transformer used for radial secondaries. This chart may be used for banked transformers by dividing scale readings at voltage drop by 2 if motor is midway between transformers

a difference in opinion regarding the demand charge factor as well as the load factor for such energy losses. Generally speaking, there should be very little difference in generating costs on these representative systems, but there will be a substantial variation when different points on the system to which the energy is to be delivered are taken into consideration. For example, since the secondaries are the remote part of the system, the unit cost for energy at that point will be a great deal more than at the generating station

It is unnecessary, however, to be greatly concerned about this point since losses represent less than 20 per cent of the total annual costs and regardless of the values used, the form of the annual cost curves are similar and therefore do not materially affect the choice of conductor or transformer sizes. This fact was substantiated by company *B* which included as part of their study the effect of using 2 values, not state the percentage for capitalizing losses. It is suggested however that a good practice to follow on this point provides a percentage for capitalizing losses equal to the annual fixed charges.

Load Factor

The load factor based on the equivalent hours of full load use per year for the calculation of losses is reasonably uniform, as shown in table I, with one company somewhat more optimistic about their load curve for distribution transformers.

Voltage Regulation

The allowable voltage drop in the secondaries represents a fairly uniform practice among all the companies. The total voltage regulation at the customer's service is the important consideration, and must include the voltage

drop in primary conductors beyond the regulating point on the main, the transformer drop, and the drop in the secondaries to the point of service. When transformers are located near the regulating point or when not fully loaded, it is possible to allow a greater drop in the sec-

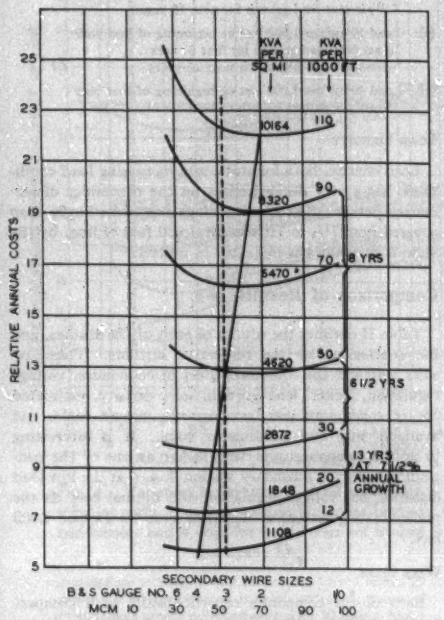

Fig. 2. Annual costs of transformers and secondaries for various conductor sizes, pole spacing 100 feet, 2 per cent secondary regulation, and transformers 100 per cent loaded (company A)

ondaries and still maintain satisfactory voltage at the customer's service, within the limits specified by company practice, or public service commission requirements.

A great deal of discussion has resulted from the claim that the feeder regulators may be used to correct transformer regulation. It should be noted that 2 conditions react against complete success in the use of regulators for this purpose:

1. The daily load cycle is not the same for all the transformers on a primary distribution circuit. Large present-day distribution circuits include transformers to supply residential, commercial, and industrial load.

2. The per cent loading of distribution transformers on any primary circuit is not the same, partly due to the difference in rate of growth and also because of the need to handle a large variety of load conditions and densities, therefore resulting in the use of a variety of transformer sizes.

Allowable Flicker

The allowable flicker has been investigated by companies *B*, *D*, and *E*. The results in each case indicate that sudden voltage variations in excess of 2 per cent are noticeable and if they occur frequently will become the cause of complaints. Refrigerator motors and similar appliances are subject to starting currents of 15 to 20 amperes at 115 volts and 50 per cent power factor. As the density of these appliances increases, the question of flicker becomes a problem of major importance, and directly affects the choice of wire sizes and transformers as well as transformer spacing. Figure 1 has been prepared by company *E* to show voltage flicker due to appliance motors.

Wire Costs

The effect of considerable variation in wire costs has been thoroughly investigated by company *E*. While an increase in wire price shows the effect of favoring smaller wire sizes, it is not a controlling factor in the choice of wire sizes. There is, of course, a natural reason for favoring larger conductors when copper prices are low but it cannot be adopted as a standard practice over an extended period of time. The use of an average price, such

Iron losses 0.007 per kilowatt-hour for 8,760 hours annually

Copper losses 0.014 per kilowatt-hour for 1,095 hours annually

Sizes of wire for main sections designated on each curve. Number 4 wire used in all cases for short sections on side streets

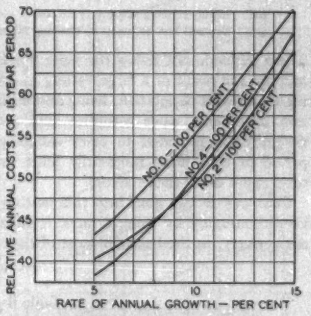

Fig. 3. Total annual charges with varying yearly growth of load for straight line secondary distribution (company B)

Initial loading on transformers 100 per cent, maximum loading approximately 150 per cent, and maximum secondary voltage drop of 3 per cent or less; initial load density of 20 kva per 1,000 feet. Total life of each layout 15 years with assumption for transformer life 30 years and wire 15 years

as 15 cents per pound for comparative studies, appears to be logical as a result of the facts developed in this investigation.

Standard Wire Sizes

It will be noted that 4 of the companies use the even numbered wire sizes, while company *A* stocks and uses numbers 6, 3, 1/0, and 4/0. This naturally has some ef-

fect on the selection of the economical wire size as will be noted later, especially in the lower load densities.

Type of Load

All of the studies apply to loads and economical designs in residential districts, but at the higher densities may apply equally well to light commercial districts, unless pole congestion and street conditions enter into the picture. Electric range load was studied by one company and is an important factor in some parts of the country. As ranges increase in number, the diversity and demand factors are expected to show a substantial improvement, and will be less of a problem than in the early stages of scattered and isolated installations.

Load Growth Rates

Estimated load growth must necessarily include an element of speculation, although over a limited period of years, experience records show some fairly definite trends. Depressions have a serious effect not only on load growth records and charts but also result in greater caution in the selection of per cent load growth.

It should be noted that in residential districts growth in load may result from:

1. Increased usage
2. Additional customers
   - (*a*). Along existing secondary mains.
   - (*b*). Beyond but adjacent to existing mains.

These items do not follow the same trends in all districts and are the result of a large variety of conditions including changes in population, living and business conditions, new inventions, sales activities, and rates. Secondary design when intended to meet conditions over a long period of time must necessarily meet the composite or total result of all these factors.

Company *B* has gone into this matter of load growth very thoroughly by using 3 rates, 5, 10, and 15 per cent, respectively, as the basis for most of their charts. All of the companies have selected rates of load growth in connection with their computations of accumulated annual charges as indicated in table I.

Company *E* defines the rates of load growth *a*, *b*, and *c* as follows:

(*a*). Load 10 kw per 1,000 feet at beginning of first year
20 per cent load growth for first 5 years
7.5 per cent load growth for next 15 years

(*b*). Load 10 kw per 1,000 feet at beginning of first year
10 per cent load growth for first 5 years
5 per cent load growth for next 15 years

(*c*). Load 30 kw per 1,000 feet at beginning of first year
10 per cent annual growth to load density, 75 kw

Load Density

Load density, both for static and increasing load conditions, has a very decided effect on the economics of secondary design. The density range has accordingly been covered from 7½ to 110 kw per 1,000 feet of line, by the various companies as indicated in table I.

Comparison of Results

Table II outlines the results of each of the studies, and the conclusions by the respective authors. These results represent the combined effect of economics, voltage regulation, flicker, load growth, load density, estimated life of conductors and transformers, copper costs, and available wire and transformer sizes. It is interesting to note 3 companies reporting flicker as one of the controlling factors in secondary system design at the low load densities, but voltage regulation and annual cost as the predominating factors at densities over 20 kw per 1,000 feet.

Wire Sizes

Each of the companies reports results of a comprehensive study of costs to determine economical conductor sizes and 4 reports demonstrate in graphical form the

Table II—Comparative Results of Economic Studies

	Company A	B	C	D	E
1. Wire size numbers					
20 kva per 1,000 feet and under	3	4	4 minimum	2	2
Over 20 kva per 1,000 feet	3	2	2,000 to 5,000 circular mils per kilovolt-ampere	2	2
2. Transformer sizes, kilovolt-amperes	15 for 12–60 kw/M feet 25 for 60–100 kw/M feet 37½ for 100–110 kw/M feet		2/0 maximum 25 maximum generally	15 and 25 37½ maximum	10 to 37½
3. Transformer loading					
At installation, per cent	90	100	100 for 3, 5, 7½ kva 125 for 10 kva 140 for 15 kva and over	75–100	50 minimum
At replacement, per cent	140	150	165	150	Over 125
4. Transformer spacing, feet	1,200 for 5–19 kva/M feet 800 for 20–29 kva/M feet 600 for 30–49 kva/M feet 400 for 50 kva and over			800 to 400	800 to 600 (3,000 to 600 studied)
5. Load growth handled by*	Subdivision and replacement	Replacement and subdivision	Subdivision and replacement	Replacement and subdivision	Replacement and subdivision

* Preferred method is shown first.

procedure followed in reaching their conclusions.

Both companies showing number 4 as the economical conductor size at low load densities, recognize the flicker limitations, but until complaints become numerous they seem to be willing to recommend the use of that size. This disadvantage may be offset to some extent by closer spacing of transformers. The other 3 companies report number 6 or number 4 conductors economical under 20 kw per 1,000 feet, but do not recommend them in order to avoid an early change to a larger size. Company *E* states the additional cost of number 2 is small and avoids flicker as well as the expensive operation of replacing secondary conductors. The choice of number 3 by company *A* is, of course, influenced considerably by the fact that numbers 4 and 2 are not stock sizes for them. This item of the respective reports shows unusual similarity of results. While conditions are recognized that may necessitate larger conductors for special applications, the consensus of engineering opinion favors these wire sizes over a large range of load densities.

Figures 2, 3, 4, 5, and 6 are typical graphs that were developed to demonstrate the relative economy of various conductor sizes. Company *C* did not include the charts used in reaching the conclusions stated in their report. Companies *B*, *D*, and *E* include an extensive series of charts for various conditions, but only typical charts are shown here.

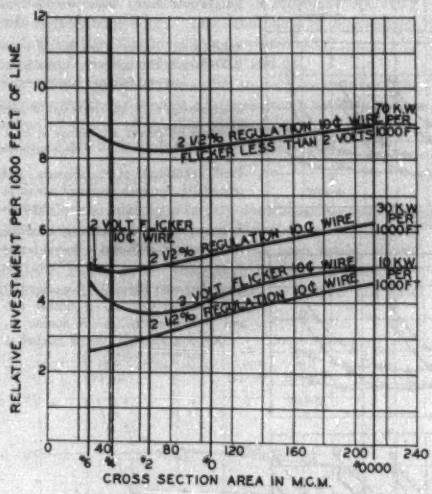
RELATIVE INVESTMENT PER 1000 FEET OF LINE
2 V2% REGULATION 10¢ WIRE
FLICKER LESS THAN 2 VOLTS
70 KW PER 1000 FT
2 VOLT FLICKER 10¢ WIRE
2 V2% REGULATION 10¢ WIRE
30 KW PER 1000 FT
2 VOLT FLICKER 10¢ WIRE
2 V2% REGULATION 10¢ WIRE
10 KW PER 1000 FT
CROSS SECTION AREA IN M.C.M.

Fig. 4. Variation in investment in secondary distribution with 2 volts allowable flicker for banked transformers and 4 volts for transformers not banked (company E)

Assumptions include starting current of 115 volt motor, 20 amperes at 50 per cent power factor, voltage dip computed to customer's service pole, and wire price 10 cents. Motor location assumed to be midway between transformers

Transformer Sizes

On the question of transformer sizes the reports are not specific in their conclusions, except in the case of company *A*. This report illustrates by means of figure 7 the economy of 15-kva transformers up to 60 kw per 1,000 feet, 25-kva for 60 to 100, and 37½-kva above 100 kw per 1,000 feet for 2-way feed. Company *B* does not state any recommended size of transformer, but apparently uses the voltage drop and loading limitations to determine transformer sizes. Company *C* is very specific in stating the maximum size they consider most desirable, but do not indicate the extent of economical use for smaller sizes. Company *D* finds 15- and 25-kva transformers most economical and are explicit in recommending 37½-kva as the

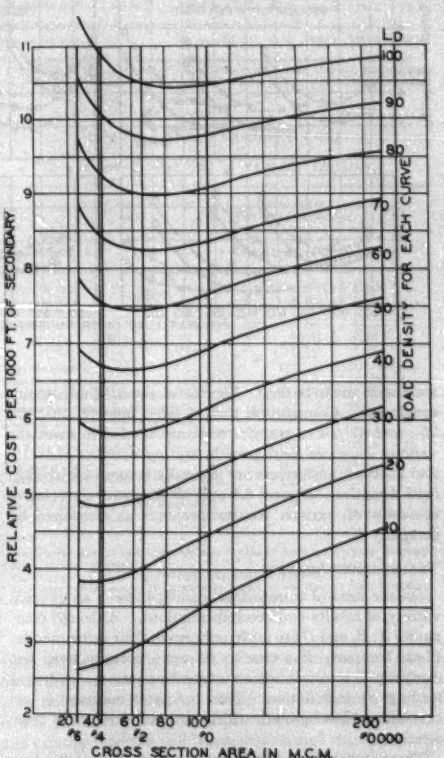

Fig. 5. Relative total cost per 1,000 feet of secondaries and transformers, with wire at 10 cents per pound and capitalized losses included (company E)

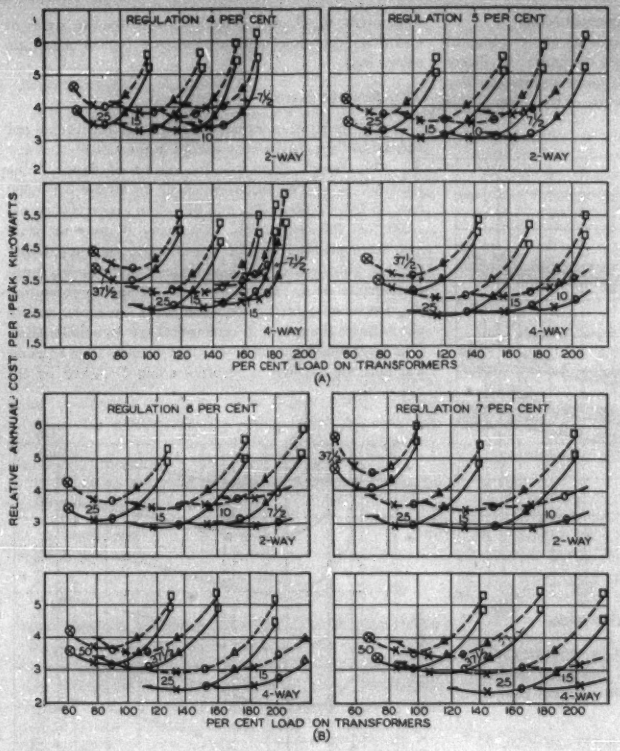

Fig. 6. Annual cost of transformers and secondaries at various per cent loads on different transformer sizes for 2 assumed values of energy costs (company D)

Broken line curves—Copper loss at 0.01 per kilowatt-hour; transformer loss at 0.01 per kilowatt-hour

Solid line curves—Copper loss at 0.00456 per kilowatt-hour; transformer loss at 0.003 per kilowatt-hour

Load density—15 kw per 1,000 feet

Numbers on curves are ratings in kilovolt-amperes

Total regulation of transformers and secondaries for each group of curves as shown

Two-way and 4-way distribution from transformers as indicated. Power factor 97 per cent

Secondary wire sizes: □—2 number 4/0 and 1 number 2/0; △—2 number 1/0 and 1 number 2; ⊙—3 number 2; ×—3 number 4; ⊗—3 number 6

maximum size to be used. Figures 6*A* and 6*B* illustrate this conclusion. Company *E* finds 4 sizes, namely, 10-, 15-, 25-, and 37½-kva transformers, are needed to meet the various stages of load growth, stating however that 15- and 25-kva transformers are generally favored for average load densities. Figures 8*A* and 8*B* illustrate the relative economy of various transformer sizes as developed by company *E*.

Transformer Loading

On the item of transformer loading there is an unusual variety of results and recommendations. Although companies *A*, *B*, and *D* are fairly uniform in their recommendations, company *E* seems to be extra conservative, but company *C* recommends an unusual percentage for initial loading at installation. This company assumes 5 per cent annual load growth which probably influences their conclusion.

These conclusions are based principally on the fact that peak loads on distribution transformers are expected during the winter season when ambient temperatures are low, whereas transformer ratings are based on temperature rise with 40-degree ambient. The increasing use of appliances may gradually change this condition and should therefore be checked from time to time. It should be noted also that this recommendation applies only to overhead transformer installations, and not to transformers in building or underground vaults, where the low ambient temperatures may not be available.

Generally, voltage regulation, rather than per cent overload, dictates the need for transformer replacement or respacing of transformers to reduce length of secondary mains. Increased transformer regulation is usually accompanied by a relatively high secondary drop hence both of these items will require attention, unless primary regulation is extremely favorable. The total voltage variation should be studied in each case, as well as the component voltage drops, to determine the best solution. It is evident therefore that the thermal capacity of distribution transformers is only part of the loading problem.

For small transformers, the annual transformation cost is materially reduced by overloading even up to 200 per cent. The exact effect on the life of the transformer under such conditions is not fully known, although

claimed by some to be satisfactory. There is no consensus of opinion on this point. Fortunately, on the 15-kva transformer and larger, the most economical loading ranges less than 150 per cent of name plate rating, hence there is less reason for risking failure on these larger units. In any event, the higher loadings may be expected to be troublesome and therefore result in increased operating and maintenance costs. The economics of transformer loading has been developed in a very interesting manner by company *D*, as shown in figures 6*A* and 6*B*.

It will be especially interesting to note the results of the various practices followed on transformer loading over a period of years. A further comparison of operating experiences will be desirable at a later date.

Transformer Spacing

Transformer spacing is largely determined by load density and secondary voltage drop, especially after the selection of the economical wire size has been made. Companies *B* and *C* do not state their findings on this point. While companies *A*, *D*, and *E* have developed this item very thoroughly, the spacings listed represent preferred distances between transformers under ideal pole conditions and uniform load density. Experience indicates that it is well to favor these spacings, but actual field conditions and existing facilities will frequently change the secondary design including the transformer spacing. Company *E* illustrates by means of figures 8*A* and 8*B* the economics of transformer spacing. The limits for $2^1/_2$ per cent voltage drop and 4 per cent flicker for radial secondaries are shown.

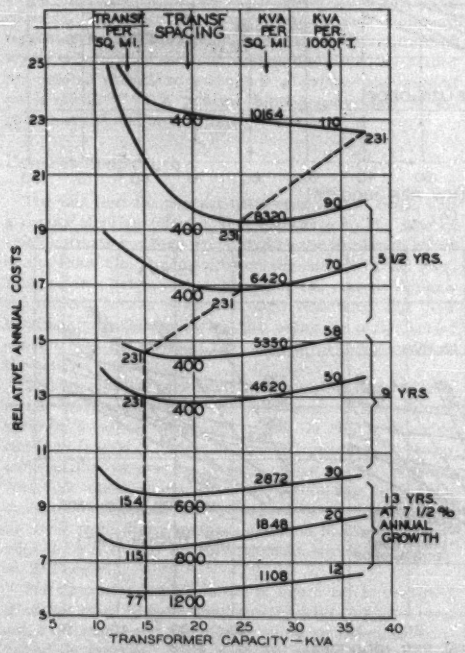

Fig. 7. Relative annual cost of transformers and secondaries for various transformer sizes, number 3 secondary conductors, pole spacing 100 feet, and transformer and secondary regulation approximately 4.5 per cent (company A)

Table III—Transformer Costs in Relative Units

Per Cent Loading	Transformer Rating in Kilovolt-amperes					
	$7^1/_2$	10	15	25	$37^1/_2$	50
Annual Transformer Cost*						
40	23.9	27.0	31.9	45.9	56.7	70.0
60	24.6	27.9	33.1	47.8	59.3	73.4
80	25.6	29.2	34.8	50.4	63.0	78.2
100	26.8	30.8	37.0	53.7	67.8	84.4
120	28.4	32.8	39.7	57.7	73.7	91.9
140	30.2	35.1	42.9	62.5	80.5	100.8
160	32.3	37.8	46.5	68.0	88.5	113.4
180	34.9	40.9	50.7	74.2	97.6	122.6
Transformer Retirement Costs						
Location maintained—transformer re-used on job						
A—Cost installed	140.0	159.0	183.5	270.0	328.0	409.0
B—Reclaim value	134.6	141.5	164.6	242.4	296.1	372.6
C—L. and D. to remove	5.0	5.0	5.0	8.0	8.0	8.0
D—Net reclaim (*B* — *C*)	119.6	136.5	159.6	234.4	288.1	364.6
E—Retirement cost (*A* — *D*)	20.4	22.5	23.9	35.6	39.8	44.3
Location maintained—transformer returned to storeroom						
Retirement cost	35.0	39.0	43.0	64.8	78.8	92.8
Location abandoned—transformer re-used on job						
Retirement cost	39.8	41.9	42.3	60.0	74.3	78.9
Location abandoned—transformer returned to storeroom						
Retirement cost	54.4	58.5	61.4	99.3	111.3	127.4

* Comprised of $12^1/_2$ per cent of installation cost as fixed charges, transformer iron losses, transformer copper losses, and transformer operation and maintenance cost.

Table IV—Annual Transformer Costs

Load Growth $7^1/_2$ Per Cent Per Year, 20-Year Period

Year	Kva Load	Transformer Per Cent Load $7^1/_2$–15 Kva	10–15 Kva	15 Kva	Annual Cost Per Cent Comparison $7^1/_2$–15 Kva	10–15 Kva	15 Kva
1	5.0	67	50	33	4.51*	4.97*	5.68*
4	6.2	83	62	41	4.69	5.14	5.82
8	8.3	111	83	55	4.95	5.47	6.00
12	11.0	73†	110	73	6.16†	5.76	6.18
15	13.7	91	91†	91	6.29	6.29†	6.29
20	19.7	131	131	131	7.54	7.54	7.54
Total annual cost (20 years)					113	117	124 (*A*)
Retirement cost					6	7	(*B*)
Total annual cost plus retirement cost					119	124	124 (*A* + *B*)
Depreciation reserve (compounded)					9	12	24 (*C*)
Total net cost after applying credit for depreciation reserve‡ (compounded at 6 per cent less retirement cost)					104	105	100 (*A* — *C*)
Total annual cost					113	117	124 (*A*)
Depreciation reserve (not compounded)					5	5	13 (*D*)
Total net cost after applying credit for depreciation reserve (not compounded) less retirement cost					108	112	111 (*A*-*D*)

* Transformer annual cost expressed in per cent of total net cost for 20 years using a 15-kva (column 3).
† The change to a 15-kva transformer was made at this time.
‡ The depreciation reserve is included as a part of the annual cost, therefore, any part not used for retirement costs may be applied as a credit to determine total net cost.

Various methods of handling load growth have been carefully studied to obtain the lowest total cost over a long period of years. This has been done by studying the accumulated annual costs for a number of possible methods. The method that involves the least retirements is usually most economical.

The subdivision method including the installation of additional or intermediate transformers is used by all the reporting companies but is especially favored by com-

(*Concluded on page 189*)

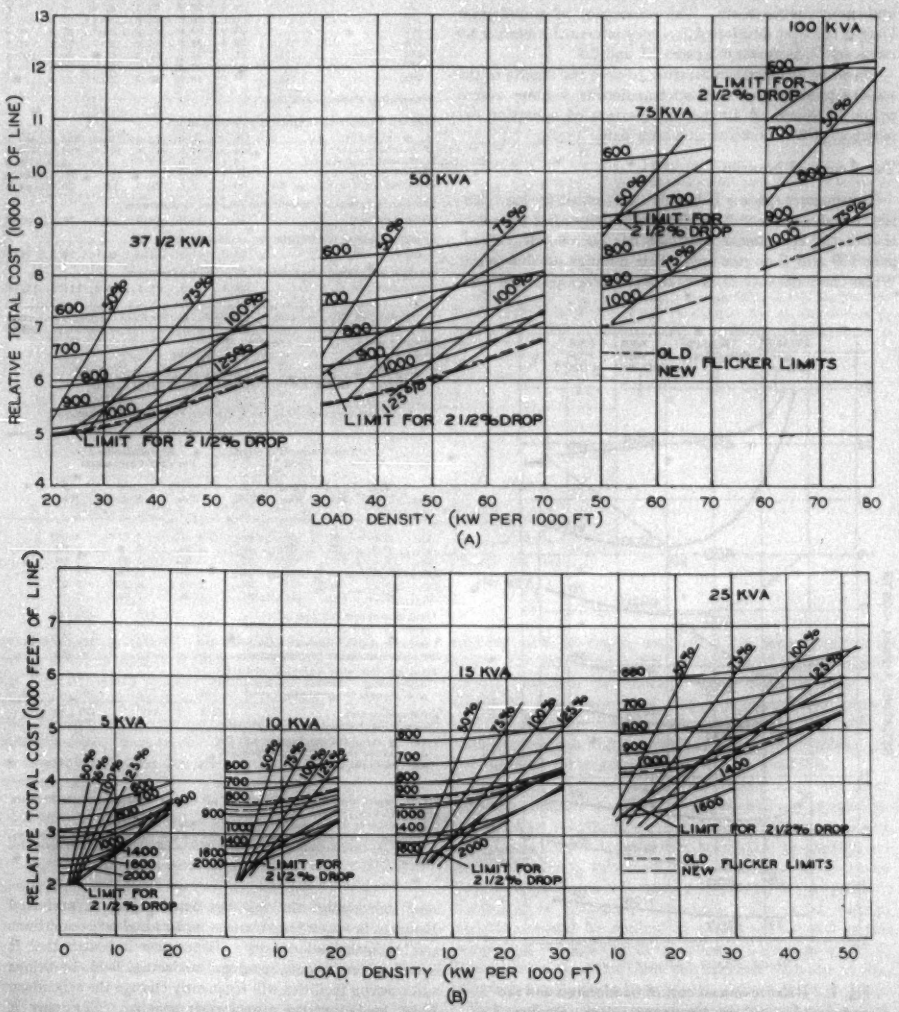

Figs. 8A and 8B. Total equivalent investment per 1,000 feet of line for different transformer spacing using various transformer sizes and number 2 wire at $2^1/_2$ per cent maximum voltage drop (company E)

Number 2 copper wire at 10 cents per pound

Contact Drop and Wear of Sliding Contacts

By R. M. BAKER
ASSOCIATE AIEE

G. W. HEWITT
Membership Application Pending

The results of a series of experiments, in which the processes of contact voltage drop and ring wear in sliding contacts are demonstrated by means of a direct method, are presented in this paper. The results show that the wear of metal-graphite brushes and the rings upon which they operate can be reduced if they be operated in an oxygen-free gas instead of air.

THE relatively small amount of accurate knowledge gained through the enormous amount of effort expended in the study of sliding contacts is evidence enough of the complicity of the processes involved. This paper is intended to be only another step forward toward the ultimate goal of a perfect understanding. Each such step makes it just that much easier for the design and operating engineer to analyze and solve those practical problems with which he is continually confronted. It is felt that the experiments described represent a real advance in our understanding of contact drop and wear of sliding contacts. In order to conserve space and eliminate repetition, certain concepts developed in earlier published works will be used without explanation, and the reader not familiar with these concepts is referred to the original publications.[1,2,3,4] A general bibliography also is included at the end of this paper.

Contact Resistance

The fact that the contact between a carbon brush and a copper slip-ring offers a high resistance to the flow of small currents has been attributed to the insulating effect of the oxide film which forms on the surface of the ring. Further, it is believed that increasing the current through the contact breaks down this high resistance film over certain areas, thus allowing the brush to make better contact with the metal of the ring and in this way lower the contact resistance.

This concept has been fairly well established[2] by experiments which show that the resistance of the contact between a carbon brush and a ring on which no oxide can form (a gold or carbon ring) is independent of current and remains low even for currents as low as 0.001 ampere. Although these experiments are convincing it seemed desirable to illustrate the correctness of the assumptions by some more direct method, and this has been accomplished by a special test arrangement which will be described below.

The apparatus used is shown in figure 1. It consisted of copper rings 13 inches in diameter driven by 2 motors; one a d-c motor and the other a synchronous motor connected in tandem. With such an arrangement it was possible to drive the rings at synchronous speed (1,800 rpm) or at any other speed differing slightly from synchronous speed. Each ring carried only one brush ($^3/_8$ inch thick and $^3/_4$ inch wide) of a soft electrographitic grade. Since the rings were electrically connected, the current flow at any instant was from one brush into its ring and from the other ring out into its brush. All tests were made with a resistance in series with the contacts and since the supply voltage was 40 volts, 60 cycle alternating, the current through the contacts was essentially sinusoidal and in phase with the applied voltage. The effective value of brush current was 12 amperes (42.8 amperes per square inch). The brush current was supplied from the same circuit which supplied the synchronous driving motor, thus insuring synchronism between the rotation of the rings and the current supplied to the brushes. A stroboscopic lamp was used to bring the rings into synchronism always with a definite phase relation to the brush current. This lamp was also used when it was desired to let the rings slip one or more revolutions before being thrown back into synchronism again. When it was desired to operate the rings nonsynchronously, the synchronous motor was disconnected from the line and the rings were driven by the d-c motor. It now will be shown how this apparatus was used to illustrate the part played by oxide films in determining contact resistance.

With the rings running synchronously (1,800 rpm) it is obvious that the 60-cycle current through the brushes became zero 4 times each revolution of the rings. As the positions of current zero occurred at the same points on the ring surface each revolution, there were 4 sections of the ring surface which were never called upon to carry current. (This is not strictly true because of the finite brush width but the discrepancy is of small consequence.) Other points of the ring surface were called upon once each revolution to carry some value of current between zero and the maximum current through the brushes (17 amperes or 60.5 amperes per square inch), and it is especially important to observe that the same section of the ring surface was subjected to exactly the same value of current each time it passed under a brush. The condition can be pictured best perhaps by thinking of a standing wave of current around the ring. One quarter of the ring surface carried all values of positive current, the next quarter all values of negative current, and so on around the ring.

If the oxide film on the ring is responsible for the commonly observed large variation of contact resistance with

A paper recommended for publication by the AIEE committee on electrical machinery. Manuscript submitted November 11, 1936; released for publication November 20, 1936.

R. M. BAKER and G. W. HEWITT are both research engineers for the Westinghouse Electric & Manufacturing Company, East Pittsburgh, Pa.

1. For all numbered references, see list at end of paper.

current, it would be expected that the film on the ring surface near each of the 4 points of zero current might have a very high resistance, for it is never called upon to carry heavy current and therefore does not become broken down. Thus, it would be expected that with a sinusoidal current passing through the brushes, the variation of contact drop would be represented by a flat topped wave. That is, one would expect a relation between current and voltage similar to that obtained in the static characteristic. To what extent this prediction is fulfilled by experiment is shown by the oscillograms of figure 2, all of which were taken with the rings running synchronously.

Figure 2*a* shows the current through the contacts and the voltage drop in each contact just after the ring surfaces had been cleaned with very fine alundum cloth. It will be seen that the contact drop was low and almost sinusoidal. The oxide film was still so thin that it was not appreciably affecting the contact resistance anywhere around the ring.

The oscillogram shown in the figure 2*b* was taken about $1^1/_2$ hours later and it can be seen that the curves of contact drop were beginning to flatten somewhat. The oxide film was forming on the ring surface and was increasing the contact resistance more in the regions of low current than in the regions of high current.

The oscillogram of figure 2*c* was taken after the rings had operated synchronously for several days. The oxide film was fully formed and the curves of contact drop had become quite flat, especially over those sections of the ring where the current flowed from the ring to the brush. The resistance of the contact near current zero is very high but drops off rapidly at first and then more gradually until it reaches a minimum at the point of maximum current.

One might ask at this point what happens if the rings are not running in exact synchronism. In this case, every section of the ring surface is called upon to carry all possible values of current from zero to the maximum brush current. Thus, all sections of the film on the ring surface are broken down to the same extent and all offer the same resistance to the flow of current. If a sinusoidal wave of current is forced through the contacts, it would be expected that the curves of contact drop also would be essentially sinusoidal. An oscillogram taken after the rings had run for some time out of synchronism is shown in figure 3*a*.

It is especially interesting and instructive to compare the contact drop curves of figure 3*a* with those of figure 2*c*. In both cases the brushes carried the same value of alternating current, so it is fair to assume that the condition of the brush face was the same in both cases. It follows, therefore, that the large variation of contact resistance with current during synchronous operation is due to a condition on the ring surface rather than to some property of the brush face. This is an especially important conclusion for it follows that the same must be true in general for all sliding contacts which show a large change in contact resistance with current.

To demonstrate this fact in another way, a separate experiment was made. After the rings had been running synchronously for several days with alternating current in the brushes, the brush current supply was switched off and replaced by a dry cell in series with a 6-ohm resistor and an oscillograph element as shown by the diagram of figure 4. The oscillogram, figure 4*a*, was taken as soon as possible after the change was made. The peaked current record shows that each time the brushes passed over a part of the ring surfaces which previously carried low current, the current through the oscillograph element decreased. This can be interpreted to mean only that the condition of the ring surface over these parts was such as to produce a high contact resistance. Thus one sees that it was possible to set up a standing wave of resistance around the ring, during synchronous operation, perma-

Fig. 1. Test equipment used for studying brush performance during synchronous and asynchronous operation

nent enough to be recorded or measured in a separate circuit some minutes after the a-c current supply had been disconnected from the brushes.

The record of figure 4*b* was taken after 10 minutes of operation with the dry cell connected in the brush circuit. In this time the oxide film on the ring surface had repaired considerably to produce an average increase in contact resistance. The high-resistance regions were gradually destroyed by the 1.5 volts applied across the contacts.

Figure 3*b* shows the current and contact drop curves with the rings stationary. The contact drop curves under this condition are practically sinusoidal, indicating constant resistance in the contact. The peculiar breakdown phenomena observed on the one ring (upper record) probably occurred because the ring happened to come to rest in such a position that the contact between the brush and the ring was especially poor. Such a record is seldom obtained and is included only as an oddity.

If one were to plot a curve between current and contact drop from the curves of figure 2*c*, the result would look very much like the static volt-ampere characteristic commonly taken by the tedious step-by-step method. In fact this might be a satisfactory and easy method of obtaining a static volt-ampere characteristic on a brush grade. It is in effect a method of operating a number of rings simultaneously with different currents and observing in rapid succession the contact drop in equilibrium with each value of current. The brushes are actually carrying alternating current but the individual sections of the ring surface have no way of detecting this unless the nature of the brush face is influenced by the current it carries. There is undoubtedly a difference in the polish of the brush face with different currents flowing but experiments indicate that this effect is small in comparison to that produced by the conditions on the ring surface.

A brush which is hard, or one which contains enough abrasive to prevent the formation of a uniform oxide film on the ring surface, will not build up such a high contact resistance at the very low current densities as will a soft nonabrasive brush such as used in the investigation described above. Neither will a hard abrasive brush produce contact drop curves with such sharp corners as those of figure 2*c*.

Previous experiments[3] have indicated that the breakdown of the oxide film and the resulting decrease in contact resistance occurs almost instantaneously when a high current is forced through the contact. It was expected therefore that allowing the rings to slip one revolution following synchronous operation before pulling them back into synchronism again would subject all sections of the ring surface to high current and make the surface uniformly conducting all around the ring. However, contrary to expectations, a record of contact drop taken immediately after the rings had slipped one revolution and were running synchronously again, showed curves

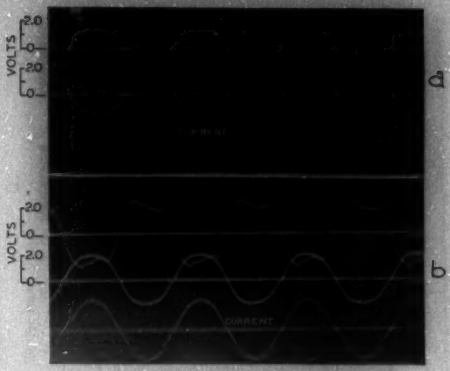

Fig. 3. Current and contact voltage drop oscillograms taken during asynchronous operation

(*a*)—Near synchronous speed
(*b*)—Rings stationary

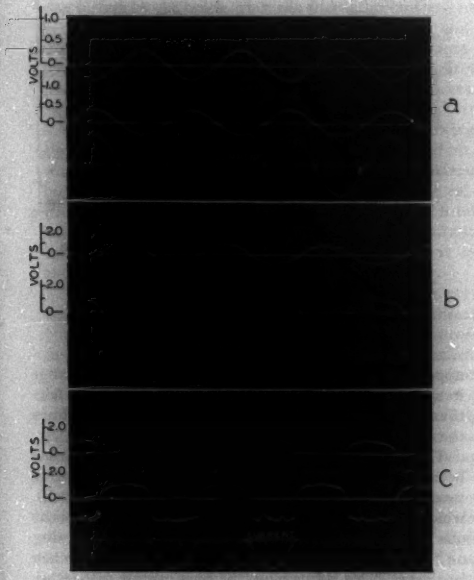

Fig. 2. Oscillograms of current and contact voltage drop taken during synchronous operation

A downward deflection of the contact voltage drop curve corresponds to a current flow from ring to brush

(*a*)—Ring surface free of oxide film
(*b*)—Taken after operation of 1¼ hours
(*c*)—Taken after operation of several days

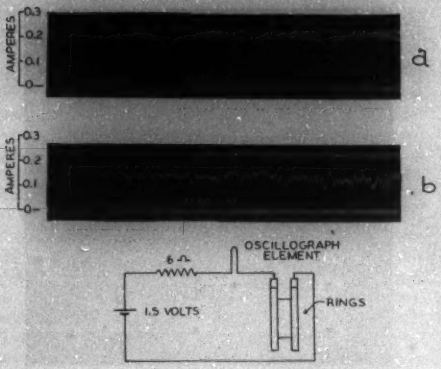

Fig. 4. Distribution of film resistance around periphery of ring

of contact drop almost identical with those of figure 2*c*. Only by allowing the rings to slip 10 revolutions (50 seconds nonsynchronous operation), could rounded contact drop curves similar to those of figure 3*a* be obtained. No attempt will be made at present to explain the unexpected results. It was necessary to operate the rings synchronously for half an hour or more to repair the damage done to the film during the 50 seconds of nonsynchronous operation and to obtain again contact drop curves similar to those of figure 2*c*.

Ring Wear

The track produced on the surface of a copper ring by a carbon or graphite brush is definitely characteristic of the direction of current flow through the contact. If the current flows from the ring to the brush, the track has a light color and may even be bright and show signs of threading. If the current flows from the brush to the ring, the track is dull and in some cases seems to be covered with a thin film of carbon. These effects are generally observed on rings operated with direct current but it was discovered in the present investigation that they may be observed also with alternating current in the brushes. It will be recalled from the early part of this paper that during synchronous operation of the rings, certain parts of the ring surface always experienced current flow from the ring to the brush. These parts showed the typical brush track for this direction of current flow. Other parts of the ring surface always experienced current flow in the opposite direction and showed the characteristic track for that direction of current flow. The contrast was so sharp that one could determine by visual observation of the ring surface, the exact point at which the direction of current flow reversed.

This observation is of considerable importance for it establishes the fact that the nature of the track produced at one polarity or the other is effected by the direction of current flow across the contact (an instantaneous process) rather than by some condition of the brush face, such as fine copper picking or the loosening of carbon particles as is sometimes supposed.

Another interesting observation connected with the difference in ring surface over different parts of the ring after synchronous operation, was the occasional appearance of burned spots or brush photographs on the ring surface. These generally occurred only with a hard brush grade which did not ride well on the ring surface. This is such a common phenomenon that it would not be worth mentioning except for the fact that these spots always occurred at points of zero current on the slip-ring surface. This is not so surprising when it is remembered that just at the point of zero current there is an abrupt change in the

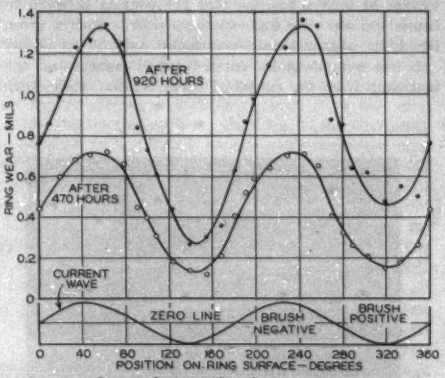

Fig. 5. Curves showing that the wear of rings is in synchronism with the brush current

"Brush negative" indicates current flow from ring to brush
"Brush positive" indicates current flow from brush to ring

appearance of the ring surface. This abrupt change in appearance is probably associated with a change in friction which causes the brush to dance just a little and burn the ring at this point.

The appearance of brush tracks, which already has been discussed at some length, is closely related to ring wear. The negative ring (current flow from ring to brush), which usually exhibits a bright clean-looking track, is the one which always shows rapid wear. The positive ring on the contrary usually shows a dull track and very much less wear. This is true when the rings operate with either graphite or metal-graphite brushes, although the wear is usually much more rapid with metal-graphite brushes than with graphite brushes.

The synchronous ring arrangement used throughout this set of experiments seemed likely to show some interesting facts regarding ring wear if enough wear could be produced to be measurable at all points around the ring. Since all values of current and both polarities would

be represented on the one ring surface, a single set of wear measurements should give a fairly complete story.

A test was made using metal-graphite brushes containing about 80 per cent of copper by weight. The brushes carried 35 amperes of 60-cycle alternating current. The rings ran synchronously at 1,800 rpm throughout the test.

The rings were measured at the beginning of the test, at the end of 470 hours, and again at the end of 920 hours. A special device was used to measure the ring wear with an accuracy of plus or minus 0.00002 inch.

The results of the test are shown in figure 5. The current wave shows the distribution of current around the ring surface, or more exactly, the current carried by each section of the ring surface as this section passed under the brush. The wear curves indicate the ring wear, measured at various angular positions around the ring. These curves show at once that the total wear of the ring surface is made up of 2 components, the one constant around the ring and the other alternating and almost exactly in phase with the distribution of current around the ring. Apparently the constant component of ring wear is caused by mechanical abrasion of the ring surface by the brush, while the alternating component is caused by the transportation of material across the contact by the current. The fact that the material transferred is roughly proportional to the current, indicates that the transfer might occur by an electrolytic process. Whether or not this is true is not definitely known. It is interesting however, to calculate what current, flowing electrolytically in parallel with the main brush current, would be required to transfer the amount of material indicated by the wear curves of figure 5. A simple calculation shows that if only 0.004 per cent of the total brush current flowed across the contact by electrolytic conduction, the material transfer would be sufficient to explain the wear curves obtained.

The results of this experiment show that a large percentage of the ring wear commonly observed with direct current in the brushes is due to an instantaneous process associated with the transfer of current across the contact. The curves of figure 5 show greater ring wear at the points of zero current than at the points of maximum current where the direction of flow is from the brush to the ring. Apparently metal is in some way picked up from one part of the ring surface and put down at another to bring about this result.

The maximum ring wear occurs on those sections of the ring where the current flows from the ring to the brush; the minimum wear occurs on those sections where the current flows from the brush to the ring. These observations agree with the fact that in direct current operation, the wear of the negative ring is much greater than that of the positive ring. As shown by figure 5, the ratio of maximum wear to minimum wear on the synchronous rings was 5.4 after 470 hours operation and 5.7 after 920 hours operation. This leads one to believe that if the rings had been operated with direct current in the brushes, the wear of the negative ring would have been about 5.5 times as rapid as that of the positive ring.

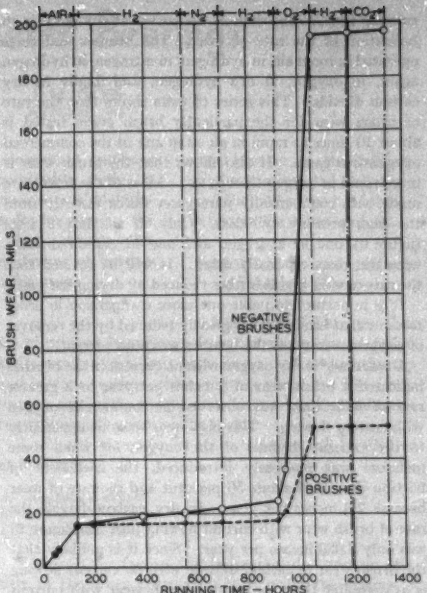

Fig. 6. Curves showing wear of metal-graphite brushes in various gases

However other factors which cannot be discussed here would probably make this ratio considerably greater if the test operated 1,000 hours or more.

Brush Wear in Various Gases

Previous experiments[4] have shown that carbon brushes wear very slowly when operating in an atmosphere of hydrogen. This observation led to the belief that oxygen in the atmosphere around the brushes was responsible for the brush wear commonly observed in service and that this wear could be greatly reduced if the brushes were surrounded by some oxygen-free atmosphere. The greater demand for a longer life of metal-graphite brushes led to the choosing of this type of brush for a special test which will be described below.

Copper slip rings and a driving motor were inclosed in a gastight housing which could be filled with any gas desired. The rings were 9.5 inches in diameter and operated at a speed of 1,750 rpm. Each ring carried 2 metal-graphite brushes, $\frac{1}{2}$ inch wide by $1\frac{3}{4}$ inches thick. The brushes operated on direct current, 160 amperes per ring (80 amperes per brush). The current flowed into one ring and out the other. The temperature of the gas inside the housing was about 55 degrees centigrade.

The results of a series of tests are shown in figure 6. These curves show brush wear plotted as a function of

running time, so the slope of the curves at any point is an indication of the rate of wear. The brushes and rings operated in room air, in hydrogen, in nitrogen, in hydrogen again, in oxygen, in dry hydrogen, and finally in dry carbon dioxide. This series of tests shows that the rate of brush wear for the particular brush grade tested is about 10 times as rapid in air as in any of the commercial oxygen-free gases. It also shows that the brush wear is more rapid in oxygen than in air. Most of the tests were made with commercially pure gases taken directly from the high pressure cylinders. Only in the last 2 tests (figure 6), one in hydrogen and one in carbon dioxide, were the gases especially dried. It will be noticed that the rate of wear is still further reduced by drying the gases.

It is important to make one more comparison in order to show that brush wear is greatly reduced by the removal of oxygen even when the brushes carry no current.

A test made in dry oxygen with no current in the brushes indicated a brush wear of 8 inches per year or a greater rate of wear than was observed in commercial oxygen with current flowing. This high wear was due apparently to the extreme dryness of the oxygen for when some moisture was purposely introduced, the coefficient of friction decreased about 50 per cent and the rate of wear became 2.8 inches per year. In dry carbon dioxide the rate of brush wear with current flowing (last test, figure 6) was only 0.028 inches per year. Since it is unlikely that the brush wear in carbon dioxide with no current flowing is any greater than the rate of brush wear with current flowing, it appears that the brush wear with no current in the brushes is about 100 times greater in oxygen, under the most favorable conditions, than it is in dry carbon dioxide.

The noticeable effect of moisture in reducing wear of the brushes during operation in oxygen is just opposite to the effect observed during operation in the oxygen-free gases. The evidence is that moisture is beneficial during oxygen operation and perhaps also during air operation, for it results in a decreased friction and a lower rate of brush wear. This is in line with field experience, where short brush life is often associated with low air humidity.

Although no actual measurements of ring wear were made, visual observation indicated that the ring wear during tests in oxygen-free gases was extremely low and that this wear was rapid (especially on the negative ring) when air or oxygen was introduced. This was also observed on another test in which graphite brushes operated on copper-alloy rings.

The brushes used to study brush wear in various gases contained 70 per cent copper and 30 per cent graphite by weight and were bonded with pitch. This specification is given because another grade bonded with bakelite showed less improvement with the introduction of an oxygen-free gas.

The results of the experiments described in this paper have been interpreted in so far as it was consistent with the limitations of space and our present knowledge. For the most part the results agree well with the ideas and experimental evidence presented in previous works to which the reader was referred in the introduction.

Bibliography

1. Electrical Sliding Contacts, R. M. Baker. *Electric Journal*, volume 31, 1934, page 359.

2. Voltage Drop in Sliding Contacts, R. M. Baker. *Electric Journal*, volume 31, 1934, pages 448–50.

3. Sliding Contacts—Electrical Characteristics, R. M. Baker. AIEE Transactions, volume 55, 1936, page 94.

4. Brush Wear in Hydrogen and in Air, R. M. Baker and G. W. Hewitt. *Electric Journal*, volume 33, 1936, page 287.

5. On the Theory of Stationary Metallic Contacts With and Without Surface Films, R. Holm. Wiss. Veroeff. a.d., Siemens-Konzern, volume 10, 1931, page 1.

6. Material Transfer in Contactor Contacts, R. Holm, F. Gueldenpfennig, R. Stoermer. Wiss. Veroef. a.d. Siemens-Konzern, volume 14, section 1, 1935, page 30.

7. Material Transfer in Opening Contactor Contacts, R. Holm, F. Gueldenpfennig. Wiss. Veroef. a.d., Siemens-Konzern, volume 14, section 3, 1935, page 53.

8. Electrical Contacts, Hermann Rohmann. *Phys. Zeit.*, volume 21, 1920, page 417.

9. On the Phenomena at the Brushes of Slip-Rings and Commutators, Ludwig Binder. Wiss. Veroef. a.d., Siemens-Konzern, volume 2, 1923, page 158.

10. On the Physics of Sliding Contacts, F. Schroeter. *Archiv. fur Electrotechnik*, volume 18, 1927, page 111.

11. Phenomena Connected With the Collection of Current From Commutators and Slip-Rings, H. G. Taylor. British I.E.E., volume 68, 1930, page 1356.

12. Humidity Control Prevents A. C. Brush Disintegration, E. F. Bracken. *Electrical World*, volume 102, 1933, page 410.

13. Investigation of Carbon Brushes, A. Schliephacke. *E. T. Z.*, volume 55, 1934, page 814.

14. Electrical Brush Wear, V. P. Hessler. AIEE Transactions, volume 54, 1935, page 1050.

A New Electrostatic Precipitator

(*Continued from page 163*)

V_d = velocity of drift of a charged particle through the gas under the influence of the electrostatic force

V_g = velocity of the gas parallel to the electrode face

A = spacing between parallel electrodes

L = length of parallel dust-collecting electrodes

t_A = time required for a charged particle to drift through the gas a distance A

t_g = time required for the gas to travel the length of the parallel dust collecting electrodes

r = radius of the dust particle assuming that an actual irregular particle can be represented by a sphere of equivalent radius

K = dielectric constant of the dust particle

References

1. Untersuchungen uber die physikalischen Vorgange bei der sogenannten elektrischen Gasreinigung, Von Rudolf Ladenburg. *Annalen der Physik*, volume 4, 1930, page 863.

2. The Impinger Dust Sampling Apparatus, Leonard Greenburg and J. J. Bloomfield. Reprint No. 1528 from the Public Health Reports, volume 47, No. 12, March 18, 1932.

3. Air Cleaning as an Aid in the Treatment of Hay Fever and Bronchial Asthma, Leo H. Criep and M. A. Green. *Journal of Allergy*, volume 7, number 2, page 120, January 1936.

4. An Electrostatic Dust Count Sampler, E. C. Barnes and G. W. Penney. *Journal of Industrial Hygiene and Toxicology*, volume 18, number 3, March 1936.

5. *Lehrbuch der Elektrizitat* (ninth edition) I, page 132.

6. *Annalen d. Physik*, 1922, page 335.

7. P. Arendt and H. Kallman, *Zeitschrift fur Physik*, 1926, volume 35, page 421.

8. H. Schweitzer, *Annalen der Physik*, 1930, volume 4, page 33.

Watt-Hour Meter Bearings

By I. F. KINNARD
MEMBER AIEE

J. H. GOSS
ASSOCIATE AIEE

Bearings for the moving element in watt-hour meters have received considerable study in recent years in order that maintenance might be reduced. The requirements for the bearing, the materials available and their characteristics, lubricants, and the various designs of bearings are discussed in this paper.

A GREAT DEAL of interest has always been exhibited in watt-hour meter design by the users as well as the manufacturers, because the watt-hour meter is so vital a factor in the sale of electrical energy. The emphasis has gradually shifted from one part of the meter to another as each has been perfected in turn to a high degree, until within the last few years much attention has been focused on the subject of bearings. Interest in meter bearings has been accentuated due to the tendency to increase the length of periodic test intervals and the necessity of eliminating as much servicing and as many replacements as possible. There are so many factors involved and it is so difficult to obtain conclusive data, that it is not surprising that there has existed a divergence of opinion on the part of many who have studied the problem.

The purpose of this article is to analyze the many factors that bear upon the design and operation of watt-hour meter bearings and to attempt to consolidate and clarify fundamental information on this subject. In searching for a complete explanation and evaluation of the various factors and their relative importance, a large amount of work has been done. The results of much of this work will be covered in this article, and it is the hope of the authors that it will assist in making a more complete understanding of the subject possible.

Historical Review

The groundwork of bearing design for electrical instruments and meters was, no doubt, laid by the designers of chronometers. For centuries prior to the birth of the electrical industry, builders of clocks and watches were faced with the problem of building rugged low-friction bearings to carry the weight of moving parts and to have long life. Much work had been done on the geometry of bearings as well as on the component parts to select the best combination of materials available.

With the advent of the electrical industry in the latter part of the 19th century, it was only natural that the builders of electrical instruments and meters turned to the watch industry as a guide in selecting materials and designs of bearings to carry the moving systems. A wide variety of bearings has been proposed and used in various instruments, meters, and measuring devices. Figure 1 shows a number that are, in general, applicable to watt-hour meters, but are also applicable to some forms of instruments. All of these arrangements can be resolved into either the pivot or the ball type, and for a theoretical consideration of the friction of the bearings the ball type and the pivot type lend themselves to the same analysis.

Important Considerations in Bearing Design

There are 2 bearings that are of primary importance from the standpoint of design and operation of a watt-hour meter. These are the top and bottom bearings of the moving element. The lower bearing carries the weight and the top bearing maintains the vertical alignment of the shaft.

For clarity of treatment this discussion will be divided as follows:

A. Mechanical design
B. Materials
C. Lubrication

Each of these factors will be examined in turn in relation to the lower bearing, as it is really the essence of successful long time operation of a watt-hour meter. A brief discussion of the top bearing will follow since it also performs an important function.

Mechanical Design

Friction Torque

The primary consideration in the design of a watt-hour meter lower bearing is the reduction of friction to a minimum value that can be maintained. If the weight of the moving system is designated by W and the coefficient of friction by μ, then from the definition of the coefficient of friction the frictional force of the bearing will be proportional to $W\mu$. It has been shown that the friction torque T_f is proportional to $WR\mu$, where R is the lever arm at which the force acts.[28] If it were possible to reduce R to zero which could be done if a true point contact could be provided, then the friction torque would be zero and there would be no friction effect. Unfortunately, this would require the bearing material to carry or sustain an infinite stress which is impossible. All materials deform under load until the area in contact is sufficient to carry the load. The contact area then has an equivalent R that determines the friction torque (T_f) of the bearing. As R cannot be reduced to zero, the next best

A paper recommended for publication by the AIEE committee on instruments and measurements. Manuscript submitted October 30, 1936; released for publication November 28, 1936.

I. F. KINNARD is executive engineer in charge of engineering department, and J. H. Goss is head of laboratory, General Electric Company, West Lynn works, Lynn, Mass.

28. For all numbered references see list at end of paper.

thing is to make it as small as possible which can be done by carrying the load of the moving element on a pivot point of small radius or ball of small radius in contact with a flat plate or a cupped jewel of a larger radius of curvature than the ball or pivot. As pointed out in a previous article[1] due to wear the initial condition cannot be maintained throughout the useful life of a watt-hour meter bearing. The friction torque is made low so that an increase of several times the initial value will not materially affect the meter calibration. Figure 2 shows the initial error due to friction that must be compensated for, as a function of the radius of the pivot point. The values shown in figure 2 have been confirmed experimentally both by V. Stott[2] and by the authors.

Rate of Wear and Shock Resistance

There are 2 important considerations aside from the fact that the geometrical requirement is that the contact area should be as small as possible for minimum initial friction. One of these is that the rate of increase of this area should be reduced to a minimum, and the other is that the bearing should have sufficient strength to withstand installation abuse and service abuse.

Figure 3 shows the manner in which the friction torque varies as a function of pivot radius for a given decrease in pivot length resulting from wear. The friction increases rapidly with an increase in the radius. This curve was drawn assuming the pivot in contact with a flat plate. V. Stott[2] has shown that little error is introduced by this assumption if the area in contact is small. The method of computing the friction torque as a percentage of the watt-hour meter load torque is given in a previous article.[1]

Figure 4 shows the relative shock resistance as a function of the radius of curvature for glass-hard steel pivots running in sapphire jewels. It is evident from a study of this curve that the shock resistance of a pivot falls off rapidly below 0.0175-inch radius and that in order to reduce impact failures under severe conditions to a minimum, a pivot should not have a radius below this value. The method of test will be discussed later in relation to the required shock resistance of bearing material.

A further treatment of the mechanical design of the types of bearings shown in figure 1 will be deferred until after materials and the subject of lubrication have been considered.

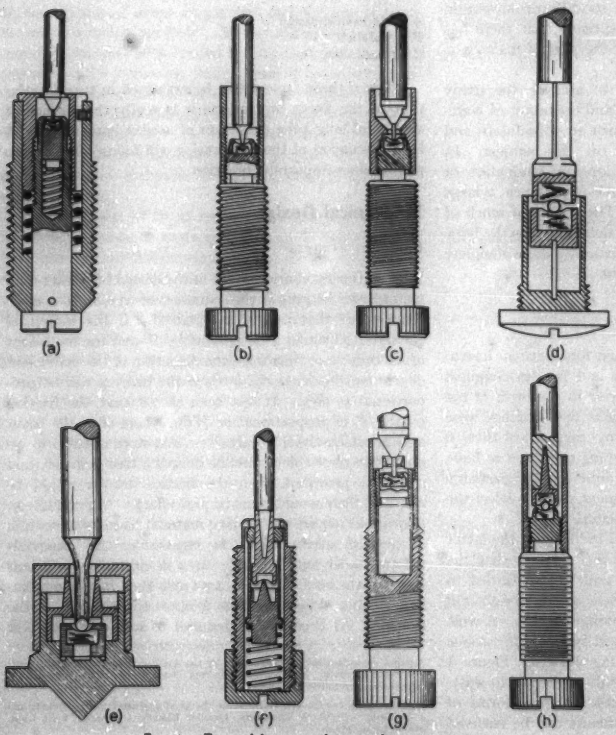

Fig. 1. Typical bearings for watt-hour meters

Materials

The material for any of the bearing designs shown in figure 1 must meet practically the same requirements and as the geometry of a watt-hour meter pivot is limited to a ball or spherical point, improved materials offer the best possibilities in developing bearings with increased life.

Jewel Material

The material for the jewel cup should have the following characteristics:

1. Hardness—That gives high resistance to wear.
2. Toughness—That will protect the surface against shattering under shock.
3. Low coefficient of friction—Should have a low friction coefficient in contact with the pivot or ball.
4. Workability—Should be such that the jewel cup can be produced at a cost which will not be prohibitive.

It is extremely difficult to give quantitative data of the above requirements for a given material, due to the lack of an accurate method of measuring perform-

ance. In the past hardness has been measured in accordance with the Moh scale which is based on the ability of one material to scratch another. This scale makes no allowance for the toughness of the material which is also a factor in wear resistance just as hardness is a factor in protecting the surface against shattering.

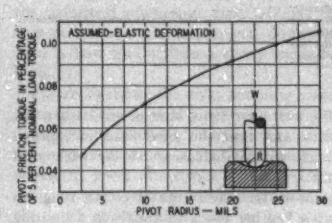

Fig. 2. Calculated friction torque as a function of pivot radius

Recently work has been done[3] and results published that have given an illuminating picture of the Moh scale when applied to bearing material. Instead of the scratch hardness, the ability of a given material to resist abrasion was taken as a measure of its hardness. This is precisely the thing of interest in a bearing material. The Moh scale and the new wear hardness scale are plotted in figure 5.

It is evident from this curve that the Moh scale of hardness gives erroneous results when used as a basis for

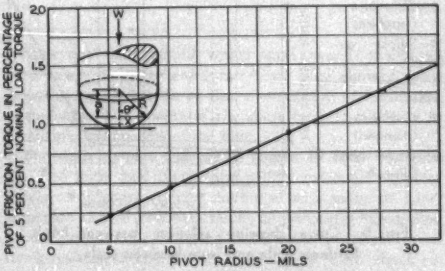

Fig. 3. Friction torque as a function of radius for a given decrease in length of the pivot due to wear

Decrease in length is $(R - a)$

judging the relative wear resistance of materials. The new scale based on abrasion resistance gives a much better indication of the relative performances of the materials as is borne out by the results obtained in service with diamond jewels for severe applications as compared with sapphire jewels. The Moh scale if assumed to be linear would indicate a small difference between sapphire and diamond (sapphire 9, diamond 10), while on the scale of wear hardness the diamond is superior in the ratio of over 4 to 1.

Fig. 4. Curve showing the variation of pivot shock resistance as a function of pivot radius

Data obtained from short-circuit test using high carbon steel pivots and natural sapphire jewels

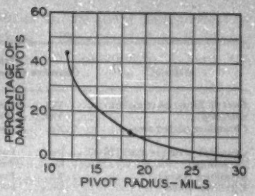

Diamond, according to figure 5, should be the most desirable material to satisfy specification 1, and if it is assumed that wear hardness is also a measure of toughness diamond is the most desirable from specification 2. Both diamond and sapphire take a good polish and satisfy specification 3. It is, however, difficult to grind a cup into diamond, and the cost of the raw material plus the high cost of working it into cups makes the cost prohibitive except for meters yielding a large revenue.

Silicon carbide and boron carbide are seen to be between diamond and sapphire on the wear hardness scale. Jewel cups made from these materials are not commercially available although much work has been done to investigate their properties. Present practice, the outgrowth of long experience, shows that sapphire approaches nearer to the perfect material as defined by the specifications than any other material and is the best available.

Pivot or Ball Material

Glass-hard steel approximately 1.25 per cent carbon, running in a polished sapphire jewel cup, has from the beginning of meter and instrument manufacture been the most widely used combination of materials. A large amount of operating data has been obtained on meters operating with bearings of these materials both with and without lubrication. Based on these data certain specifications have been drawn up as desirable for a pivot material.

1. Non-corrosive—Material should not corrode under operating conditions.

2. Non-abrasive—Products of wear should be non-abrasive. (Most important when pivot operates on a sapphire without lubrication.)

3. Wear-resistive—Should have a low rate of normal wear. (To be considered with and without lubrication.)

4. Shock-resistive—Should be capable of resisting high impact loads caused by rough handling of the watt-hour meter during transportation and installation and impact loads imposed by short circuits while in service.

5. Low coefficient of friction—Initial friction should be low in combination with sapphire.

6. Workable—Should be capable of being produced in the form of pivots and balls at a reasonable price.

Table I shows some of the more promising pivot materials rated in accordance with the above specifications.

To check materials to this set of specifications, one test was to run the bearings in meters at an accelerated speed without lubrication to see how well they stood up

Table I—Properties of Pivot Materials

Material	Corrosive	Non-abrasive	Wear-Resistive	Shock-Resistive	Workable	Low Coefficient of Friction	
Steel (1.25 per cent carbon)	Yes	Poor	Good	Good	Satisfactory	Satisfactory	
Nitralloy	Yes	Poor	Good	Good	Satisfactory	Satisfactory	
Chromium plated steel	No	Poor	Good	Good	Probably satisfactory	Satisfactory	Initially wears well with or without lubrication but plate wears off
Cyanided stainless steel (18–8)	No	Poor	Good	Fair	Probably satisfactory	Satisfactory	
Tantalum	No	Fair	Fair	Poor	Probably satisfactory	Satisfactory	Hard outer shell breaks down under impact
Beryllium copper	No	Poor	Fair	Poor	Satisfactory	Satisfactory	
Beryllium nickel	No	Fair	Fair	Fair	Satisfactory	Satisfactory	
Cobalt-tungsten	No	Good	Good	Good	Satisfactory	Satisfactory	

in comparison with high-carbon steel. The high-carbon steel and even alloys with a small percentage of iron were found to form appreciable quantities of iron oxide which, due to its highly abrasive character, rapidly wore away the pivot point. It is interesting to note that a bearing that is adequately lubricated with the proper lubricant does not form this oxide. The formation of the iron oxide has been investigated by Shotter[4] and has been shown to be dependent upon the presence of a certain amount of water vapor which may in a measure serve to explain why a bearing that is properly lubricated does not form the abrasive oxide.

In table I the material approaching nearest to the requirements is an alloy of cobalt and tungsten (75 per cent cobalt and 25 per cent tungsten). This alloy is the development of Sykes[4,5] who has applied it for wire-drawing dies to resist the high temperatures necessary for the drawing of tungsten wire for lamp filaments. The material belongs to the group of precipitation-hardening alloys. Figure 6 shows a typical hardening curve for actual pivot samples.

Accelerated Tests of Cobalt-Tungsten

It is very valuable to be able to check a material against the specifications in terms of values obtained by actual measurements. This can be done under stated conditions as there are several methods of obtaining data on watt-hour meter bearings.[1] In the preparation of the results for table I and figure 7, an accelerated test was used.

Figure 7 shows the results of the test run to compare the wear rate of the cobalt-tungsten material with that of high-carbon steel and to check the abrasion characteristics of the wear products in accordance with specification 2. The worn area on the end of the pivot is approximately circular in shape and its diameter can be measured readily by means of a microscope with a calibrated eye-piece. From time to time as the test progressed the pivots were removed and the diameter of the worn area was measured. These measurements as a function of revolutions of the watt-hour meters are shown in figure 7.

Without lubrication the cobalt-tungsten pivots averaged 34×10^6 revolutions for a worn area diameter of 0.003 inch as compared to 12×10^6 for high carbon steel. This shows a ratio of 2.8 to 1 for cobalt-tungsten over steel. The mean diameter of the worn area of the jewels run with the steel pivots and the jewels run with the cobalt-tungsten pivots were as shown in table II.

These results show definitely that the cobalt-tungsten material has a life well over twice that of steel when run without lubrication and that the jewel wear is approximately $^1/_3$ as much with cobalt-tungsten as with steel based on this test.

Figure 7 also shows the worn area of cobalt-tungsten in a well lubricated bearing tends to approach a limiting value and become stable. While it is difficult to measure the small amount of wear of the jewels with the 2 materials running in well lubricated bearings, the cobalt-tungsten definitely showed less wear on the jewels than did the steel pivots. Further tests made on a large number of watt-hour meters in actual service have confirmed the conclusions drawn from the accelerated test. For example, a field test in which 175 steel pivots and 153 cobalt-tungsten pivots operated with lubricated bearings for a one year

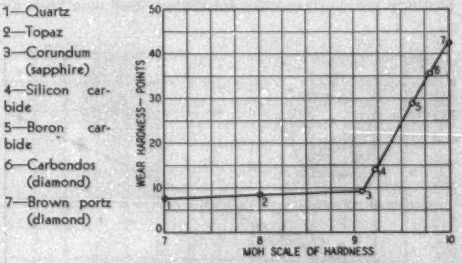

Fig. 5. Curve showing relation between Moh hardness scale and wear hardness scale

period showed an average jewel wear area diameter of 0.004 inch for cobalt-tungsten as compared to 0.0084 inch for steel.

Shock Resistance of Pivot Materials

In order to check the shock resistance of different materials, 2 watt-hour meters rated at 5 amperes, 115 volts were connected in series with a 30-ampere fuse and the load side was short-circuited with a heavy knife switch. An oscillogram was taken to determine the point on the wave at which the switch was closed and the magnitude of the short-circuit current. It was found that a peak value of 1,500 amperes was obtained. Further tests showed that currents under 1,000 amperes were not suffi-

cient to crack jewels or damage the steel pivots used. The 1,500 ampere value was selected as a reasonable one to use as it represents a value that is likely to be obtained in service.

The disk is thrown upward when the short circuit is applied and springs between the damping magnets and the driving element so that energy is stored elastically in the deformed aluminum disk. When the short circuit is removed, the pivot is driven downward like an arrow from a bow and strikes a sharp impact blow upon the jewel.

Figure 8*a* shows the disk, damping magnet, and driving element in the normal position, and figure 8*b* shows the deformed disk under short-circuit conditions. An attempt was made to study the energy of the blow with which the jewel was struck by the pivot by replacing the sapphire jewel with a polished brass plug and observing the depth of the indentation made by the pivot.

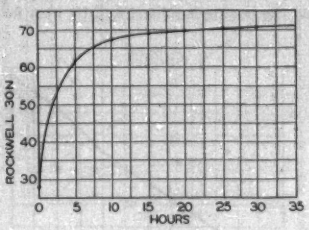

Fig. 6. Age hardening of cobalt - tungsten pivot material at 650 degrees centigrade

After one short circuit which was opened within 1/4 cycle after its occurrence, the brass plug showed *seven* indentations. This shows that a condition of oscillation existed after the release of the short circuit, resulting in a multiple hammering of the plug.

The data to plot the curve, shown in figure 4, were obtained with steel pivots and solidly mounted sapphire jewels using short circuits having a peak value of 1,500 amperes. These tests were made, as previously mentioned for the purpose of evaluating the effect of pivot radius on shock-resistance and show conclusively that shock-resistance increases very rapidly with increase in radius.

In making the tests to obtain the data for figure 4, 13 per cent of the jewels were damaged by steel pivots of 0.0185-inch radius. The tests were repeated using 0.0185-inch radius cobalt-tungsten pivots and no jewels were damaged. The cobalt-tungsten pivots are softer than steel pivots and in this test tended to flatten slightly, thereby reducing the stress on the jewel and preventing damage to the jewel surface. The extent of the flattening was not sufficient, however, to measurably increase the friction of the bearing.

Table II—Wear in Pivot Material

Material	Number of Meters	Number of Revolutions	Mean Diameter of Worn Area, Inches
Steel (1.25 per cent carbon)	4	62.9×10^6	0.031
Cobalt-tungsten	4	63.8×10^6	0.0113

Lubrication

It was shown by Abbott and Goss[1] that the most successful operation of a pivot type bearing is obtained when the bearing is properly lubricated, but the provision of a good lubricant is not a simple matter. The requirements for a lubricant are exacting due to the fact that a small quantity put into the bearing at the time of installation is expected to last for periods up to 10 years. Based on experience and tests on watt-hour meter bearing lubricants over a period of years, the following empirical set of specifications has been developed to serve as a criterion for judging a lubricant for this application:

1. Low evaporation—The evaporation loss shall not exceed 20 per cent in a dry atmosphere at 75 degrees centigrade after 50 days. Free circulation of air shall be provided. The evaporation shall be tested in glass dishes approximately 2 inches in diameter and the depth of oil shall not exceed 1/8 inch or an equivalent ratio of area to volume shall be maintained.

2. Stable viscosity—The viscosity during the evaporation test shall not change more than 10 per cent and no gummy deposits or precipitates shall be formed.

3. Wide temperature range—The viscosity of the oil shall not affect the calibration of a standard watt-hour meter more than 0.10 per cent between +25 and −40 degrees centigrade. The test shall be made with 5 per cent nominal load on the watt-hour meter.

4. High chemical stability—The oxidation or acid forming properties of the oil shall be checked by the following method: 500 cubic-centimeters of oil shall be placed in a 1,000-cubic-centimeter glass beaker which also contains 40 inches of number 18 iron wire and 40 inches of number 18 copper wire. The beaker shall be placed in

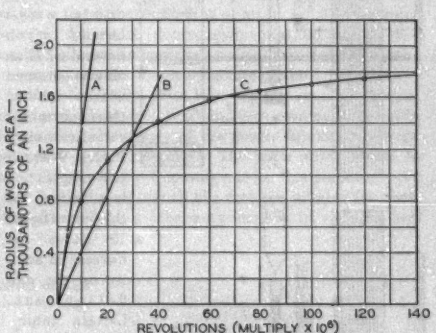

Fig. 7. Accelerated life test wear curves

A—Standard steel pivot without lubrication; 12×10^6 revolutions for a worn area radius of 0.0015 inch

B—Cobalt-tungsten pivot without lubrication; 34×10^6 revolutions for a worn area radius of 0.0015 inch

C—Cobalt-tungsten pivot with ideal lubrication

Pivot radius 0.0185 inch

a water bath at 75 degrees centigrade and an excess of free oxygen bubbled through the oil. The initial acidity shall not be over 0.50 per cent and at the end of 500 hours on this test it shall not exceed 1.0 per cent.

5. Low creepage—The oil should have low creepage tendencies.

6. Corrosion protection—The oil should not corrode steel or the other bearing materials used and should also afford good corrosion protection to the pivots.

Over 60 different oils were checked to these specifications during a recent investigation and table III gives the results of a few typical oils.

The literature contains an abundance of material on the properties of different mineral oils, fish oils, animal, and vegetable oils. This information is not, however, of particular value in selecting an oil or the components of an oil to meet the above set of specifications because of the fact that the evaporation requirement is particularly exacting when combined with the low temperature requirement. This subject has been treated by Holtz[7] for the mineral oils. The mineral oils in general are too volatile at the upper temperature (75 degrees centigrade) if they will meet the low temperature viscosity requirements, and too viscous at low temperatures if they will meet the evaporation requirement. There are exceptions, however, as shown by mineral oil *E* in table III.

The fish oil *F* has the unusual property of combining low evaporation with good low temperature performance and meets the specifications very well. The acidity is high, however, and as seen from the table when blended with mineral oil *E* an oil was obtained which fulfilled the requirements satisfactorily. Figure 9 shows the evaporation loss curve for this oil and figure 10 shows the increase in acidity on the oxidation test. Certain inhibitors can be added to oils as shown by Dornte[8] that will materially retard the rate of oxygen absorption in an oil. The chemistry of the reaction of oxygen with oil is complex, but by adding the proper inhibitor, as was done in the case of the blend *A*, the rate of acid formation can be reduced to a very low value.

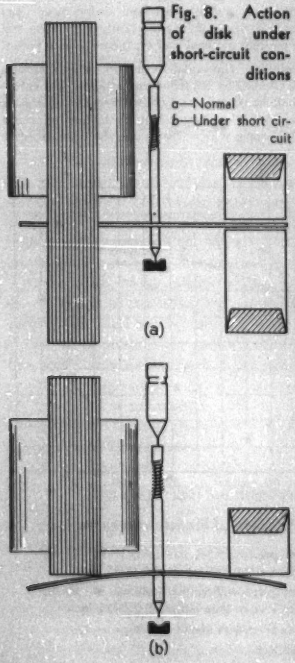

Fig. 8. Action of disk under short-circuit conditions

a—Normal
b—Under short circuit

Table III shows that oil *A* meets all of the specifications by a liberal margin. It represents a good balance between evaporation rate and temperature range so that it can be safely used for the wide temperature range to which outdoor metering subjects the bearing. Ordinary lubricants and many special blends of expensive ingredients will not meet these specifications which are so important to long bearing life. This oil meets the need for a lubricant that can be used in modern watt-hour meter bearings to give the full advantages of reduced wear and long life that good lubrication can produce.

Top Bearing

Figure 11 shows a typical top bearing for a watt-hour meter. As previously stated, the load this bearing must carry is small and the bearing is subject to little wear for this reason. At the present time a brass washer and steel pivot lubricated with petroleum jelly are the most widely used combination of materials.

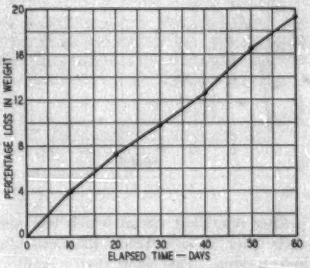

Fig. 9. Evaporation loss of jewel oil A at 75 degrees centigrade

Induction-type watt-hour meters require that the clearance between the pivot and washer be kept small in order to provide accurate alignment of the moving element, and to minimize the bearing noise set up by vibration. The addition of the lubricant also serves to reduce this noise as well as to provide the necessary lubrication to the bearing.

This discussion of the top bearing may be summed up by saying that while some improvements may be made in the top bearing by the use of new materials and by improved design, little trouble is experienced at the present time with millions of meters in service.

Discussion of Typical Bearing Designs

It is evident from the discussion of friction and impact considerations that the radius of curvature for a pivot or ball must be a compromise between initial friction, rate of increase of friction, and impact strength. Figure 12

shows the range within which the radius of curvature for pivots and balls shown in figure 1 falls. These limits have been selected by the different manufacturers of watt-hour meters, based on years of experience, as being a suitable compromise among the various factors for their particular watt-hour meter design.

Too much emphasis should not be placed on the initial or elastic conditions of pivot or ball deformation because it is almost impossible to maintain them due to wear. This was shown by Abbott and Goss[1] for the pivot-type bearing with lubrication and is shown in figure 7 for the pivot-type bearing without lubrication.

Up to this point the design requirements have been considered without reference to any of the particular bearing arrangements shown in figure 1. It will be of value to consider some of the design details together with the advantages and disadvantages of the 3 principal designs.

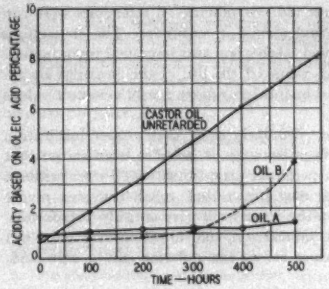

Fig. 10. Oxidation of oils in stability test

Pivot Type Bearing

A typical example of a pivot-type bearing is shown in figure 1*c*. The radius of curvature of the pivot point is 0.0185 inch and the radius of the jewel is 0.035 inch.

The metal guide bearing shown in the figure is to limit the side motion of the pivot and shaft as the load on the meter is increased above a given value. This side motion is due to the combined action of the driving force and the damping force of the meter acting to move the disk out of the meter air gap. Were the side thrust bearing not provided, the meter element shaft would eventually come in contact with the sleeve and the resulting friction would be much greater due to the greatly increased lever arm at which the friction would act. The necessity for such a bearing comes from the wide range over which modern watt-hour meters hold their calibration accuracy and over which they may be used without exceeding their thermal rating. It is possible for a modern watt-hour meter to operate for long periods at 400 per cent to 500 per cent of rated nominal load with good accuracy and no damage to the meter.

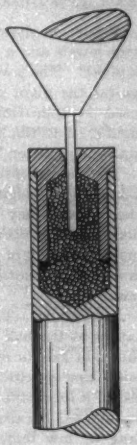

Fig. 11. Cross section of top bearing

Interchangeability. In order to insure interchangeability of the pivot and jewel without appreciably affecting the watt-hour meter calibration, it is necessary that the position of the disk in the air gap shall not be materially altered when the bearing is changed. The distribution of the fluxes in the gap is such that both the driving torque and the damping torque vary with the vertical position of the disk in the gap. The speed of the watt-hour meter on a given load will therefore vary with the vertical position of the disk. Figure 13 shows an actual curve taken on a standard make of watt-hour meter rated 5 amperes, 115 volts. It will be noted that as the disk moves down from the top of the air gap, the meter speeds up For an extreme case this change may be well over 1 per cent.

The control of the position of the disk in the gap necessitates the manufacture of the jewel screw and pivot to within a few one-thousandths of an inch. The sapphire jewel is subject to dimensional variations due to the method of manufacture that makes it necessary to take it into account in the manufacture of the brass screw.

Lubrication. The pivot type bearing requires lubrication for the best operation[1] and provision must be made for an adequate supply of the proper lubricant and the retention of this lubricant. The jewel screw shown in figure 1*g* provides a deep reservoir for this purpose.

At low temperatures all oils that are suitable for watt-hour meter bearing lubricants increase in viscosity and

Table III—Properties of Oils

Oil	Composition	(1)* Evaporation Loss, Per Cent	(2)* Viscosity After Evaporation at 75 Deg C	(3)* Viscosity at −40 Deg C	(4)* Percentage Acidity Final	(4)* Per Cent of Initial	(5)* Creepage Property	(6)* Corrosion Protection
A	Mineral and fish oil	16.4	Unchanged	Satisfactory	0.09	167.0	Medium	Satisfactory
B	Castor oil**	1.0	Solid	Solid	0.75	3,850.0	Low	Fair
C	Castor oil** and fish oil	16.0	Solid	Solid (−18 deg C)	0.33	185.0	Medium	Satisfactory
D	Mineral oil**	26.0	Tacky and gummy	Solid	0.10	100.0	High	Fair
E	Mineral oil	13.4	Unchanged	Satisfactory	0.25	183.0	Medium	Satisfactory
F	Fish oil**	14.0	Substantially unchanged	Satisfactory	0.38	240.0	Medium	Satisfactory

* See specifications for details of test method. ** Retarded.

tend to retard the rotation of the moving element. By the proper choice of a lubricant and by minimizing the area of the moving parts (such as the pivot) in contact with the oil, the viscous drag can be reduced to the point where the operation of the watt-hour meter is not affected over a wide range of temperature.

Ball Type Bearing

Figure 1*d* shows a good example of a bearing using 2 cup jewels and a small ball instead of one cup jewel and a pivot. The jewel radius is the same for this construction as for the pivot construction but the radius of the balls used is approximately 0.030 inch which as shown by figure 12 is the upper limit of radius of curvature for watt-hour meter bearings.

The side thrust for this bearing must of necessity be taken by the shaft and sleeve. It is necessary to make the parts so they will not come in contact until the watt-hour meter is operating under a load sufficiently great to make the effect of the side thrust bearing friction negligible and at the same time not allow the ball to ride out of the jewel cup.

Lubrication. This bearing is operated without lubrication as the ball is free to move with the sudden application of load or mechanical vibration and constantly presents new points of contact to the jewel surface. The use of a lubricant in this type of construction is not recommended because it introduces an appreciable viscous drag at low temperatures which slows down the watt-hour meter and is, therefore, objectionable for installations where low temperatures are encountered.

Cup and Cone Type Bearing

Figure 1*h* shows a modification of the pivot type and the ball type which combines some of the advantages of each. The cone is either metal, or sapphire set into a metal plug. The friction between the ball and cone is greater than between the ball and the lower jewel but still is not great enough to prevent the shifting of the position of the ball with changes in load and with vibration. Added rigidity of the system is obtained by the use of the cone and the construction also makes it possible to take the overload side thrust on a thrust bearing of small radius.

Lubrication. This bearing should not be lubricated because of the viscous drag introduced by the oil at low temperatures just as with the ball type with 2 cup jewels. Dependence must be placed on the movement of the ball to distribute the wear over the surface of the ball rather than to rely upon lubrication to reduce the wear to a low value. An alloy ball that will meet the specifications that have been set up for a pivot or ball material should materially increase the life of the bearing over that obtained with a steel ball.

Field Tests

Based on the material covered under the headings of the component parts of watt-hour meter top and lower bearings, the question naturally arises as to the improvement in bearing life that is to be obtained by carrying out the improvements in construction, materials, and design.

Figure 7 shows the results of accelerated tests on one bearing combination consisting of the jewel screw shown in figure 1*g*, the lubricant oil *A*, and cobalt-tungsten pivots. Figure 7 also shows results for the same combination except without the oil run in comparison with high-carbon-steel pivots. Many accelerated tests of this nature have been run. It is realized, of course, that tests of this nature are not the final method of evaluating any bearing combination and that actual field tests under service conditions offer the final basis for judgment of the true value of a bearing. Hundreds of bearings have been studied that were placed in meters in actual service and the results obtained verify the statements made in this paper. While tests have been for but one and 2 year periods, high-carbon-steel pivots and old designs of jewel screws that did not provide oil reservoirs were run in comparison and served as controls. The indications are that improved lubrication and improved pivot materials have added years to the life of the bearings by reducing wear and maintaining more nearly constant values of friction.

While all tests definitely show that proper lubrication increases the life of bearings, it has also been shown that cobalt-tungsten performs exceptionally well even without oil. Experience may prove that cobalt-tungsten pivots running on sapphire jewels will give entirely satisfactory service without lubrication, but much service data will have to be obtained before this question can be answered.

Summary

1. It has been shown that the meter bearing problem can be rationalized and simplified by careful analysis and that specific requirements or specifications can be formulated for each component part.

2. Definite limitations on the mechanical design result from the requirements of low initial and sustained friction of the bearing

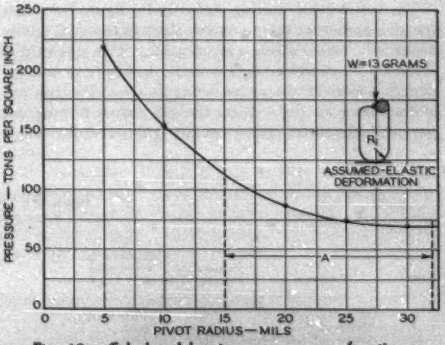

Fig. 12. Calculated bearing pressure as a function of pivot radius

A—Present range of watt-hour meter bearings

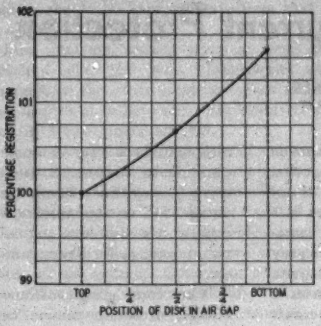

Fig. 13. Variation of meter calibration as a function of vertical position of the disk in the air gap

and the shock resistance requirements. Improved materials, therefore, offer the best possibilities for increased bearing life.

3. Although the hardness of sapphire is considerably lower than that of diamond on the new scale of hardness, the high cost and the difficulty of working the latter leave sapphire the best material available for jewel cups.

4. Various alloys offer possibilities of improved bearing life but an alloy of cobalt and tungsten very definitely shows all around superiority to all other materials tested.

5. Research and development work on watt-hour meter bearing oils has resulted in improvements which have made possible a wide temperature-range oil with a low evaporation rate for outdoor meter installations.

6. For pivot bearings, tests indicate that best results are obtained with a jewel screw that maintains a liberal supply of oil in the jewel cup. This is not true for the ball type for which lubrication is not recommended.

7. Improved materials and design may make possible some improvements in watt-hour meter top bearings, but little trouble is experienced with them at the present time.

8. The maximum service for the pivot type bearing is obtained by adopting the 3 improvements mentioned in paragraphs 3 to 5 inclusive of this summary, namely:

(*A*) A jewel screw designed to provide a liberal oil reservoir.

(*B*) Improved oil suitable for a wide temperature range.

(*C*) Cobalt-tungsten pivots which reduce jewel breakage under impact, decrease jewel wear, and reduce abrasion in the event of the loss of the lubricant.

References

1. Lubrication Increases Life of Meter Bearings, T. A. Abbott and J. H. Goss. Electrical Engineering (AIEE Transactions), volume 54, April 1935, pages 425–31. Discussion, September 1935, pages 992–3.

2. Investigation of Problems Relating to Use of Pivots and Jewels in Instruments and Meters, V. Stott. National Physical Laboratory, volume 24 (1931).

3. How Hard Is the Diamond? J. K. Smith & Sons, Inc. *Diamonds in Industry*, volume 2, number 2, May 1936.

4. Material presented at the fourteenth annual convention of the American Society for Steel Treating, Buffalo, New York, 1932, by W. P. Sykes.

5. Cobalt-Tungsten Alloys, W. P. Sykes. U. S. Patent 2,050,865, 1936.

6. Experience With, and Problems Relating to, Bottom Bearings of Electricity Meters, O. F. Shotter. IEE *Journal*, volume 75, December 1934, pages 755–84.

7. A Study of Meter Lubrication, F. C. Holtz. *Electric Journal*, June 1933.

8. Modern Loads Require Improved Methods of Jewel Inspection, P. E. Alger. *Electrical West*, volume 77, July 1936, pages 15–18.

9. Friction Check for Meter Jewels, J. Lang. *Electrical World*, volume 106, December 7, 1935, page 2920.

10. How Nearly Perfect Should Meter Jewels Be? H. H. Brown. *Electrical World*, volume 103, May 26, 1934, page 771.

11. Standardization Would Aid Meter Jewel Maintenance, H. H. Brown. *Electrical World*, volume 105, May 12, 1934, page 587.

12. Tests of Instrument Bearings, P. Maurer. *Revue Générale de l'Electricité*, volume 36, Dec. 1, 1934, pages 783–7. French instruments and methods of testing meter bearings.

13. Carbon Tetrachloride Good for Jewel Cleaning, F. N. Steel. *Electrical World*, volume 103, January 13, 1934, page 89.

14. Oiled Jewels Winning in Meter Bearing Test. *Electrical World*, volume 103, April 14, 1934, page 554.

15. Pivots and Jewels in Your Meter. *Electric Journal*, volume 31, July 1934, page 293.

16. Bearings for Watt-Hour Meters, F. G. Giles. *Journal* of the Institution of Engineers of Australia, volume 5, Sept. 1933, pages 314–18.

17. Microscopic Inspection Aids Study of Meter Jewels, L. H. Kistler. *Electrical World*, volume 102, October 21, 1933, page 527.

18. Bearings for Electric Meters, and a Bearing Testing Device, P. May. *E. T. Z.*, volume 54, April 13, 1933, pages 349–50.

19. Synthetic Corundum for Jewel Bearings, E. G. Sandmeier. IEE *Journal*, volume 72, June 1933, pages 505–14. *Arch. fur Tech. Messen*, volume 3, number 28, October 1933, page T149.

20. Jewel Bearings Protected During Meter Handling, F. Holtz, Jr. *Electrical World*, volume 99, April 2, 1932, page 624.

21. Research on the Operation of the Pivoting Elements in Electricity Meters, G. Grunberg. *Revue Générale de l'Electricité*, volume 29, May 30, 1931, pages 869–74. Compares sapphire pivots with steel.

22. Bearings for Electric Meters, G. Grunberg. *Revue Générale de l'Electricité*, volume 28, Aug. 23, 1930, pages 273–82. Method for the rapid testing of meter bearings.

23. Rotor Bearings of Electricity Meters, E. G. Sandmeier. IEE *Journal*, volume 68, November 1930, pages 1319–22.

24. Rotor Bearings of Electricity Meters, W. Lawson. IEE *Journal*, volume 67, September 1929, pages 1147–56. Discussion, volume 67, pages 1156–66.

25. Small Machine Tools Applied to Instrument Manufacture: Bronzes and Jewel Bearings for Watt-Hour Meters, F. J. Oliver, Jr. *American Machinist*, volume 71, August 29, October 3, 1929, pages 343–5, 581–3.

26. Electricity Meter Jewels. *Electrical Review*, London, volume 105, October 11, 1929, pages 593–6.

27. Electrical Measuring Instruments, C. V. Drysdale and A. C. Jolley 2 volumes, 1924, Benn Lond. Pivoting and pivots, jewels and jewel bearings, volume 1, page 29. Ball bearings for supply meters, volume 2, page 68. (Brit. discussion.)

28. Mechanical Factor of Merit With Respect to Electrical Instruments, J. H. Goss. *General Electric Review*, volume 36, April 1933, pages 188–91.

29. Synthetic Jewels, Their Manufacture and Technical Application, A. Werner. *Zeitschrift fuer Inst. Kunde*, Dec. 1925.

30. The Chemical Mechanism of Lubrication, W. F. Parish and Leon Cammen. Presented at annual meeting of The American Society of Mechanical Engineers (1932).

Dielectric Strength of Transformer Insulation

(*Continued from page 171*)

5. Breakdown Curve for Insulation, V. M. Montsinger. Electrical Engineering (AIEE Transactions), volume 54, December 1935, page 1300.

6. Discussion of reference 5 by P. L. Bellaschi and W. L. Teague. Electrical Engineering, volume 55, April 1936, pages 399–401.

7. Characteristics of Surge Generators for Transformer Testing, P. L. Bellaschi. AIEE Transactions, volume 51, December 1932, page 936.

8. The Measurement of High Surge Voltages, P. L. Bellaschi. AIEE Transactions, volume 52, June 1933, page 544.

9. Impulse Calibration of Sphere Gaps, P. L. Bellaschi and P. H. McAuley. *Electric Journal*, volume 31, June 1934, page 228.

10. Sphere Gap Characteristics on Very Short Impulses, P. L. Bellaschi and W. L. Teague. *Electric Journal*, volume 32, March 1935, page 120.

11. Impulse Voltages Chopped on Front, P. L. Bellaschi. Electrical Engineering, volume 55, September 1936, pages 985–90.

12. Progress Report on Impulse Testing of Commercial Transformers, F. J. Vogel and V. M. Montsinger. AIEE Transactions, volume 52, June 1933, page 409.

13. Recommended Transformer Standards, H. V. Putman and J. R. Clem. Electrical Engineering (AIEE Transactions), volume 55, December 1936, page 1504.

Trends in Distribution Overcurrent Protection

By G. F. LINCKS NONMEMBER AIEE P. E. BENNER ASSOCIATE AIEE

The provision of suitable overcurrent protection for distribution systems at low cost is an important problem, for upon the satisfactory solution of that problem depends the continuity of service of a great many consumers of electric energy; consequently, the relations of a public utility company with its customers also depend upon adequate overcurrent protection. This paper presents a discussion of the various trends in overcurrent protection, with the aim of providing for the distribution engineer some basis for selecting the particular protective system best suited to his particular requirements.

LOW-COST overcurrent protection on distribution systems has commanded the attention of the utility industry. New devices and applications have opened new avenues of thought on this phase of distribution problems. It is proposed to make an impartial presentation of the facts pertaining to the problem of overcurrent protection, from the plug or cartridge fuse on the meter board on the consumer's premises to the co-ordination of the main feeder breaker relays with those on the transmission system. This presentation, by correlating the various trends of thought as they are related to the whole overcurrent protection program, should assist utility engineers in choosing the one best suited to their present and future requirements.

Continuity and quality of service, protection of equipment, and low initial and maintenance costs are often divergent factors governing the application of overcurrent protective apparatus on distribution systems. Where the stressing of one necessitates sacrificing another, it is important to know all the facts so the most efficient balance can be secured. The facts governing such a balance will differ somewhat on urban, suburban, and rural systems. Of first importance is a knowledge of the causes of outages evaluated for different parts of the distribution system in terms of some unit for measuring the service being rendered the consumer.

Review of the Causes and Evaluation of Outages

Protection of consumer service is of fundamental importance. There is little duplication of equipment on the distribution system for reducing consumer outage, and so the equipment must be used with the greatest possible efficiency. Thus, the protection problem involves the handling of fault conditions more with the idea of minimizing consumer outage rather than from the standpoint of protecting the equipment. In analyzing the effect of troubles with the idea of using an overcurrent protective device to improve the continuity of service, it is necessary to know the duration of the fault, how often it is likely to occur, and the number of consumers affected.

Consumer minutes of outage, which is conventionally used as a measure of continuity is determined from the number of consumers affected by any particular outage and the length of time for which the service is interrupted. The importance of including time is, of course, obvious, although there may be some question as to whether it is correct to say that a 60-minute outage for one consumer is equally undesirable as a one-minute outage for 60 consumers.

When considering consumer outage, attention cannot be confined to the outage of any one particular consumer or group of consumers, but must be given to all the outages of all the consumers. For instance, it might be possible to reduce the outages of a small group of consumers at the expense of increasing the outages for a larger group of consumers. This, of course, would be generally undesirable but nevertheless it can easily happen if one does not have a thorough knowledge of all the factors involved or if one places emphasis on just one part of the system without correlating it with the whole system.

A major factor in the efficient application of protective equipment is the relative percentage of temporary versus permanent outages which occur on that particular part of the system. Temporary outages usually refer to fault conditions which will clear themselves with the interruption of power and before the first or second reclosing of the breaker or fuse cutout, whereas permanent outages are those which require the attention of a line crew. Temporary outages would ordinarily be of less than one minute duration, whereas a study of the records of a number of operating companies shows that faults which require the attention of a line crew last anywhere from several minutes up to several hours and average something like 45 minutes.

Outage Records

Outage information is an indication of the type of service being rendered. However, to be usable in system design, the outage data should be segregated into those parts of the distribution circuit which might be sectionalized, such as main feeder, branch feeder, distribution transformer, and secondary. Another important segregation should correspond to the nature of the area and the load served. For instance, line outage data on rural

A paper recommended for publication by the AIEE committee on power transmission and distribution. Manuscript submitted October 9, 1936; released for publication November 27, 1936.

G. F. LINCKS is an engineer in the lightning arrester, cutout, and capacitor engineering department of the General Electric Company, Schenectady, N. Y.; P. E. BENNER is an engineer in the central station engineering department of the same company.

1. For all numbered references, see list at end of paper.

feeders should be kept separate from that on suburban or urban feeders.

Line data are usually given in terms of outages per hundred miles per year. Transformer and secondary outages, on the other hand, are given as the per cent of the number of transformer installations or as the number per 100 transformers per year.

An analysis of the outage data of a number of operating companies, some of which is given in table I, shows that the number of outages on primary lines varies from only a few to as high as 70 or 80 per hundred miles per year. The per cent of these faults which are temporary also varies over a wide range. Trees are a very important cause of line outage. Conditions between various localities differ greatly in the possibility to trim or avoid trees, which accounts for the smaller number of outages per hundred miles on many rural lines as compared with urban or suburban feeders on the same system.

Lightning is still of major importance as a cause of distribution-transformer outage due to the large number of older transformers still in service, to the omission of lightning arresters, etc. Fuse blowing and transformer burnouts due to lightning have been greatly reduced by

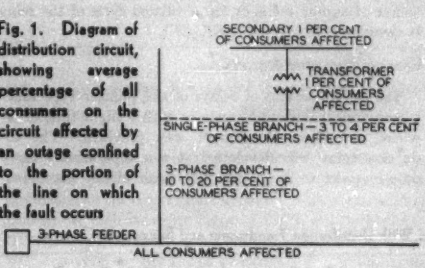
SECONDARY 1 PER CENT OF CONSUMERS AFFECTED
TRANSFORMER 1 PER CENT OF CONSUMERS AFFECTED
SINGLE-PHASE BRANCH — 3 TO 4 PER CENT OF CONSUMERS AFFECTED
3-PHASE BRANCH — 10 TO 20 PER CENT OF CONSUMERS AFFECTED
3-PHASE FEEDER
ALL CONSUMERS AFFECTED

Fig. 1. Diagram of distribution circuit, showing average percentage of all consumers on the circuit affected by an outage confined to the portion of the line on which the fault occurs

the interconnection of the lightning arrester grounds with the secondary neutral. This, and the present trend toward connecting the lightning arrester so the discharge currents do not pass through the fuse link, has tended to improve the undesirable situation in which the prevalence of lightning dictated the use of fuse-link ratings larger than might otherwise have been selected.

In analyzing the distribution transformer and secondary outage data from which table I was obtained, it is found that the number of outages accompanied by transformer burnouts is relatively small. For instance, of the distribution transformer and secondary outages tabulated, the transformer burnouts occurred with only 12.5 per cent of the total outages due to lightning (0.256 per 100 transformers average), 6.4 per cent of the total outages due to secondary faults and miscellaneous (0.255 per 100 transformers average), and 30 per cent of the total outages due to overload (0.091 per 100 transformers average). These figures demonstrate the overcurrent protection afforded the distribution transformer by the primary fuse.

As is to be expected, there is a wide variation in the frequency and nature of outages for the various companies which emphasizes the necessity of each company maintaining outage records for its own particular use. If a company attempts to make use of an average value as indicated from a study of the records of other companies, a type of design might result which would not be at all suitable for the particular condition under which the system operates.

Consumers Affected

The number of consumers affected by a fault accompanied by the functioning of some overcurrent protective device varies from one to all those on a feeder or perhaps even more if the feeder breaker relay is not properly coordinated with devices between it and the source of supply. With the usual type of construction, trouble occurring anywhere from the consumer service fuses to the transformer primary fuses involves all the consumers on the particular transformer. This varies from one consumer in the case of rural areas to over a hundred, and averages from 25 to 40 for the usual type of urban residential construction. The number of transformers on any particular primary branch varies from one or more, in the case of single-phase branches, up to 100 in the case of 3-phase branches. Trouble on branch circuits may, therefore, involve from one up to 1,000 or more consumers. In the case of feeders and branches having a higher percentage of residental consumers, fairly accurate estimates of the actual number of consumers can be obtained by multiplying the peak load in kilowatts by 4. This applies when the kilowatt consumption of the consumers in the area considered averages 600 kw or 700 kw per year.

In studying a distribution system with the idea of reducing the consumer minutes of outage, it is usually important to know the relative importance of troubles on the primary lines, in the distribution transformer, and on the secondary lines; with respect to which causes most of

Table I—Outage Data for 2,400/4,160 Y Volt Distribution Circuits

Company	1	2	3	4	5	6	7	8	9	Average
Total outages due to line troubles (urban) per 100 miles of line	29.1	13.5	41.6	53.7	20.9	13.4	40.1	29.3	2.5	27.04
Total outages due to distribution transformer and secondary troubles (per 100 distribution transformers)	7.9	4.1	8.7	8.6	9.1	0.9	7.8	3.0	11.8	6.3
Total outages due to lightning (per 100 transformers)	2.03	0.86	2.53	1.84	4.05	0.998	1.07	0.09	5.87	2.05
Total outages due to secondary faults and miscellaneous (per 100 transformers)	4.54	3.08	6.0	3.84	3.43	0.612	6.11	2.70	5.68	3.98
Total outages due to overloads (per 100 transformers)	0.065	0.16	0.17	0.62	0.57	0.0	0.09	0.31	0.35	0.304

the consumer minutes of outage. Figure 1 shows graphically the probable range in percentage of consumers affected by faults on the various parts of the system for the more generally used types of radial feeders.

Table II, lines 1 and 2 show a study of the ratios of permanent line outages to distribution transformer and secondary outages for the various companies whose outage data are given in table I. The number of transformers per mile is also given in line 3 of table II, so that a direct comparison may be made between them on the same basis as in lines 4 and 5. These point conclusively to the importance of primary line trouble as a cause of consumer minutes of outage. This is confirmed by figure 2 which gives the actual records in percentage of consumer minutes outage for the different parts of two utility companies' systems. The comparisons of lines 4 and 6 show that a reduction of one-half the length of line decreases the effect of permanent line faults in transformer outages to $^1/_4$, whereas lines 5 and 7 show it only decreases the effect of transformer and secondary faults on transformer outages to $^1/_2$.

Therefore branch-line fusing or other sectionalizing of the line to confine the effect of faults to smaller areas, not only attacks the problem at one of the most important causes of consumer minutes outage, but also produces a greater reduction per protective unit installed. The growing interest in the co-ordination of line protection is a natural outcome of an understanding of these facts.

Time-Current Characteristics

The co-ordination of overcurrent protective apparatus to reduce to a minimum the number of consumer-minutes outage on distribution circuits, is based on the correlation of their time-current characteristics. These are usually plotted as curves so as to show the variations in the shape for different types and ratings of apparatus. This is important as the comparison of one or 2 points may not insure proper co-ordination over the complete range of fault currents that can occur in the section protected. The fault currents will vary with the total impedance of the line, the connected apparatus and the fault.

The total time to clear the circuit is comprised of 2 parts for most protective apparatus: For circuit breakers these parts are (1) the time to complete the electrical cycle of the relay and (2) the time for the breaker to open mechanically and extinguish the arc (see figure 3 $E'' - E^2''$); for fuse links (more especially those used on the primary lines) they are (1) the time to melt the fuse link and (2) the time to extinguish the arc (see figure 3 $B'' - B'''$). Both are essential for the proper co-ordination of protective apparatus. The device farthest out on the line must clear the circuit (total clearing time figure 3 B''', C''', D''') before the fuse link between it and the source of supply melts or the electrical cycle of the relay is completed (figure 3 E', E^2', E^1'):

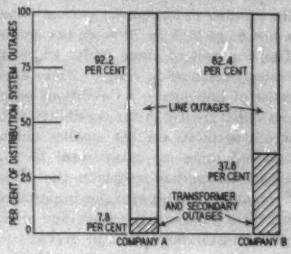

Fig. 2. Diagrammatic representation of the outage record of 2 companies

Circuit-Breaker Relays

The earlier designs of relays of the plunger type functioned almost instantaneously or with a slight time delay where a bellows attachment was provided. The induction relay was developed at a comparatively early date in order to meet operating requirements, necessitating greater time delay to permit a wider range for co-ordination with the current-carrying and current-interrupting characteristics of other apparatus further out on the line. These have been adopted quite universally. The induction relay curves have the inverse time-current characteristic of figure 3 E' or the very inverse time-current characteristic of figure 3 E^2'. The latter provides a sharper knee which is especially valuable at the low time lever settings, where the less inverse curves tend to approach the fuse link curves at the low currents.

Attachments are available for induction relays to permit instantaneous completion of the electrical cycle at any desired current. The use of this attachment allows

Table II—Comparison of Permanent Primary Line Outages With Distribution Transformer and Secondary Outages

	Company	1	2	3	4	5	6	7	8	9
1	Permanent line outages (per 100 miles of lines)	18.65	8.3	2.54	35.0	14.	1.0	.84	1.7	4.0
2	Distribution transformer and secondary outages (per 100 distribution transformers)	7.2	4.1	8.7	5.6	8.1	0.9	7.8	3.	11.6
3	Transformers per mile	11.9	9.5	13.5		10.7		7.9		8.9
4	Transformer outages for one mile of line due to permanent line faults	1.22	0.79	3.43		1.5		3.58		0.36
5	Transformer outages for a one-mile line due to transformer and secondary faults	0.86	0.39	1.73		0.87		0.63		1.03
6	Transformer outages for a $^1/_2$-mile line due to permanent line faults	0.305	0.20	0.83		0.38		0.89		0.09
7	Transformer outages for a $^1/_2$-mile line due to transformer and secondary faults	0.43	0.20	0.86		0.44		0.31		0.52

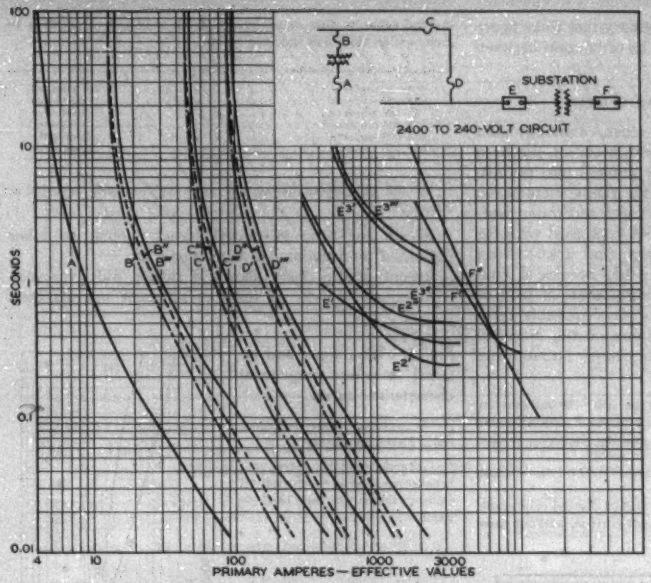

A—Household plug or cartridge fuse rated at 30 amperes
B—Fuses rated at 10 amperes in primary leads of a distribution transformer
B′—Time-current characteristic curve for 75 per cent of melting time to factor operating and manufacturing variables
B″—Melting time-current characteristic curve
B‴—Total clearing time-current characteristic curve
C—Branch line sectionalizing fuse rated at 30 amperes
C′, C″, C‴—Same as B′, B″, and B‴, respectively
D—Branch line sectionalizing fuse rated at 50 amperes
D′, D″, D‴—Same as B″, B‴ and B‴, respectively
E—Feeder oil circuit breaker and relay (minimum pick-up, 200 amperes)
E′—Inverse relay (number 1 time lever setting)
E²′—Very inverse relay (number 1 time lever setting)
E³″—Opening of oil circuit breaker
E²′—Very inverse relay (number 10 time lever setting)
E³‴—Instantaneous attachment on relay function
E³⁽⁴⁾—Opening of oil circuit breaker
F—Protective device on incoming transmission lines
F′—Very inverse relay (number 1 time lever setting)
F″—Fuse

Fig. 3. Co-ordinated time-current characteristics of protective devices on a typical distribution circuit

higher time lever settings (figure 3 $E^{3\prime}$), which makes possible a greater time-current range for other protective apparatus on the distribution system. The instantaneous pick-up at high currents (figure 3 $E^{3\prime\prime}$), will prevent distribution system faults from blowing the fuses of figure 3F'' or operating the relays of figure 3 F' on the transmission side of the substation.

Primary Fuse Cutouts and Fuse Links

As one phase of the marked improvement that has been incorporated in primary fuse cutouts and fuse links[1,2], the time-current characteristic curves for fuse links were made more inverse so as to permit closer co-ordination with the induction relay. Of more recent date, a further improvement figure 4 has resulted from an engineering study that took into consideration the 100 per cent continuous current carrying ability of the fuse links and cutouts, the motor starting demand currents figure 4A, the plunger type and the induction relay characteristics figure 4E and D, and the current-interrupting ability of the fuse cutouts.

Secondary Fuse Cutouts and Fuse Links

The use of secondary fuse cutouts while not new, has only very recently come into prominence because of the improvement made in the designs available. A large part of this improvement has resulted from making the time-current characteristics of the fuse links identical

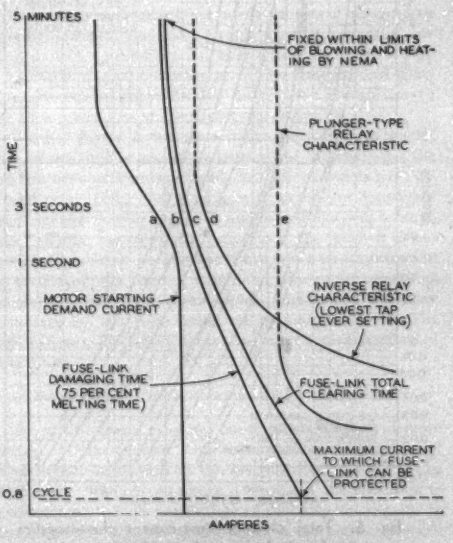

Fig. 4. Curves showing scientific development of universal cable-type fuse links

to those for the latest designs of primary fuse links figure 4. This similarity enables a closer co-ordination between the secondary and primary.

Plug and Cartridge Fuse Characteristics

The household plug and cartridge fuse, commonly used at the meter boards on the consumer's premises, has been a merchandised product that rarely entered into the distribution engineer's problems. The rapid increase in residential loads, especially due to ranges and water heaters, has so raised the ratings of these fuses used with the relatively low kva transformer ratings, that a knowledge of their time-current characteristics has become a vital factor. To date, the different manufacturers of plug or cartridge fuses, of the renewable or nonrenewable type, have complied with the specifications of the National Electric Code and the Fire Underwriters' Laboratories which state:

"*Rating.* Fuses shall be so constructed that with the surrounding atmosphere at a temperature of 24 degrees centigrade they will carry indefinitely 110 per cent current without causing the tubes to char or externally visible soldered connections to melt.

"Temperature and 110 per cent current tests shall be made simultaneously.

"With a room temperature between 18 and 32 degrees centigrade, fuses starting cold shall blow on 150 per cent current, without causing the tubes to char or externally visible soldered connections to melt, within the times specified below.

0– 30 amperes	1 minute
31– 60 amperes	2 minutes
61–100 amperes	4 minutes
101–200 amperes	6 minutes
201–400 amperes	12 minutes
401–600 amperes	15 minutes

"In the 150 per cent rating test, only one fuse shall be tested at a time."

Except for these specifications, as quoted, no other published information has been available.

Recent studies have shown a rather wide variation between the curves of fuses of different manufacture.

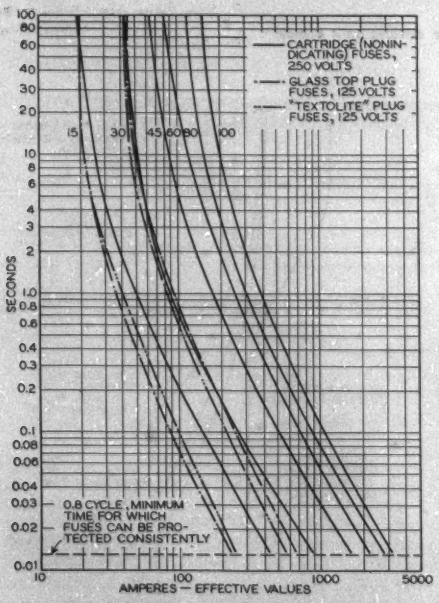

Fig. 5. Total clearing time-current characteristics of typical plug and cartridge fuses

Curves are based on tests at normal rated voltage

Fig. 6. Transformer and internal breaker time-current characteristic curves

A—Recommended time-load curve for a 10-kva transformer

B—Secondary breaker curve, with breaker mounted in transformer oil (setting similar to that used in practice)

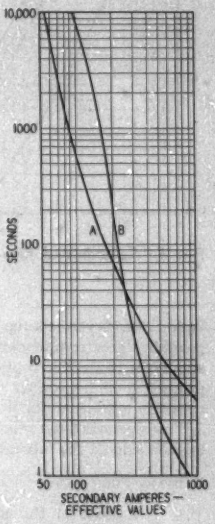

However, generally these all have an inverse-time-current characteristic, figure 5, quite similar to that of the fuse links and induction relays used on the primary and secondary lines.

Transformer Time-Load Characteristics

Heretofore transformer protection has been a problem of overvoltage rather than overcurrent. The interconnection of the lightning arrester ground and secondary neutral has so greatly reduced the failures caused by overvoltage, that those caused by overcurrent appear more important. This is accentuated in some places by the desire to increase the average loading of the transformers.

A recommended time-load curve for distribution transformers has been prepared by the AIEE and ASA as a guide (see figure 6*A* plotted for a 10-kva transformer).

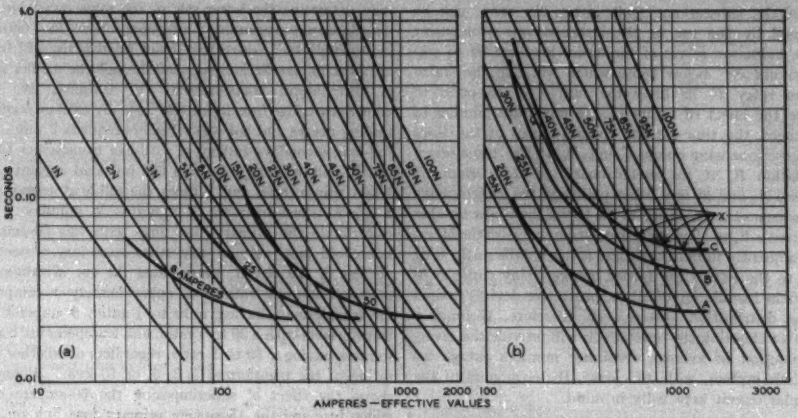

Fig. 7. Time-current characteristics of recloser and fast-blowing universal cable-type fuse links for enclosed, open, and drop-out cut-outs rated at from 50 to 100 amperes and from 5 to 15 kv

(a)—First opening of recloser and total clearing time for fuse links (fuse link curve must be to left of recloser curve for proper co-ordination)

(b)—Curves for 50-ampere recloser and melting time of fuse links

A—First opening of a typical recloser

B—Equivalent heating of fuse link by current during all operations to lock-out of the recloser, and taking into account the cooling for that part of the cycle during which no current flows

C—Equivalent heating, but including a factor for operating variables

This curve has the backing of a large group of utility and manufacturing engineers. In this analysis we are more interested in the shape rather than the exact positioning of this curve with respect to current and time.

The recommended transformer time-load curve (figure 6*A*) has an inverse time-current characteristic. The curve has much less slope, especially at the low-current long-time end, than is provided by the induction relay, the primary and secondary fuse links, or the household plug and cartridge fuses.

The Low Voltage Breaker

The time-current characteristic curve for the low-voltage breaker recently developed for household application is slightly less inverse than the induction relay and the fuses whose characteristics have to be co-ordinated with it. The breaker characteristics were made to co-ordinate with the fusing of the wire used in buildings so as to afford the maximum fire protection.

Secondary Breakers in Distribution Transformers

A breaker has been developed for use inside the tank of distribution transformers. It is mounted so as to obtain some of the heating characteristics of the transformer and has a time-current characteristic curve figure 6*B* that approaches the transformer time-load curve at the low-current, long-time end and is more inverse (much faster) at the high-current short-time end. The average slope is less than for induction relays and the fuses.

Characteristics of Circuit Reclosers

The circuit recloser is a recent development designed to provide low-cost reclosing circuit breaker operation for rural or troublesome branch lines where there are a high percentage of temporary faults. The time-current characteristic curves figure 7*A* for the recloser are similar to the characteristics of plunger-type relays.

Another factor is introduced by the recloser, namely, that of the time to reclose. During the interval after the arc has been extinguished and until the contacts have reclosed, relays connected in series will partially or completely reset to the normal position and fuse links will tend to cool. Thus the resultant effect of the periods when current flows and no current flows must be considered in co-ordinating the recloser with other protective apparatus so as to permit the recloser to lock out before the relay functions or the fuse links are partially melted. The curves figure 7*B* and 7*C* factor the cumulative heating of fuse links.

The Problem of Co-ordinating the Characteristics

In most cases, existing conditions impose a definite range of time-current characteristics within which all overcurrent protection on the distribution system must be obtained. The curves figure 3 represent the condition in existence on a high percentage of distribution systems in the country. The maximum limit is the highest possible setting of the feeder breaker relay *E* that will permit co-ordination with the relay *F'* or fuse *F''* on the transmission

side of the substation. Quite often the range can be increased by the use of the instantaneous attachment on the induction relays of the feeder breakers set to trip at currents $E^{3\prime\prime}$ below those which will trip the transmission relay F' or blow the fuse F''. In order to confine the effect of faults to the minimum number of consumers, the time-current characteristics of the fuses at the sectionalizing points C and D, at the transformer installation B, at the meter board on the consumer's premises A, and at any other points on the system, have to be squeezed in the range to the left of the feeder breaker relay curve E, so that each is co-ordinated with the other. It is frequently found that there is not a sufficiently wide range to the left of the feeder breaker relay curve E to permit the installation of all the protective devices desired on the distribution system. It, therefore, becomes a matter of choosing the ones which will provide the greatest reduction in average consumer minutes outage for the whole system, with, of course, the economics of the particular circuit kept fully in mind.

The Household Fuse and Breaker

The plug and cartridge fuses located on the meter board of the consumer's premises are becoming a factor to be considered. Their time-current characteristics may determine the lower side of the range available for distribution overcurrent protection. This has become increasingly true where the higher rated household fuses are used for installations supplied through the smaller sizes of distribution transformers. For instance, the 60-ampere cartridge fuse, figure $8A''$, usually used on services feeding ranges and hot-water heaters requires 2 times the full-load secondary current of a 10-kva transformer (220- to 250-volt winding), 4 times the full load current of a 5-kva transformer, and 7 times the full-load current of a 3-kva transformer to blow within 2 minutes. To co-ordinate the primary fuse links with this 60-ampere household fuse, without any other secondary protective devices in the circuit, necessitates the use of minimum primary fuse-link ratings of approximately 15 amperes for transformers having a 10 to 1 ratio, 5 amperes for transformers with a 20 to 1 ratio, and 3 amperes for transformers having a 30 to 1 ratio, regardless of whether the rating of the transformer is 3, 5, or 10 kva. Figure 8 shows the effect of superimposing the 60-ampere cartridge fuse and the 15-ampere primary fuse link on the curves of figure 7 shaded. As a high percentage of urban distribution circuits use 2,400 to 120 and 240-volt distribution transformers for serving residential loads, this may present an overcurrent protection problem for a great many systems. A factor in this problem is the

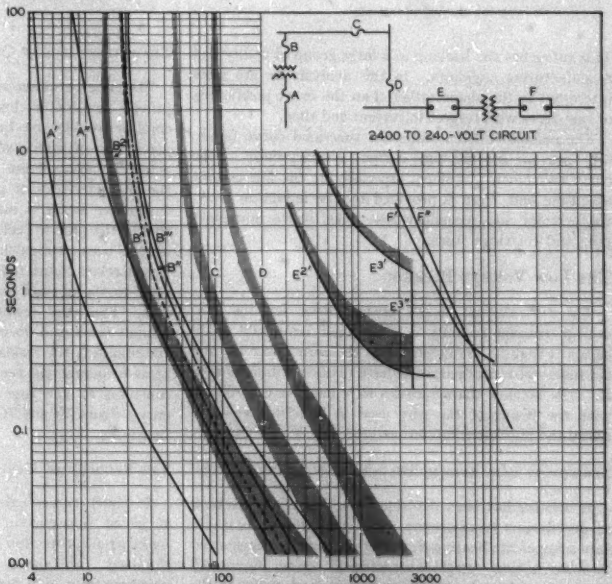

A—Household plug and cartridge fuses
A'—30-ampere rating
A''—60-ampere rating
B—Fuses in primary leads of distribution transformer
B^N—10*N* ampere rating
B'—Time-current characteristic curve for 75 per cent of melting time to factor operating and manufacturing variables
B''—Melting time-current characteristic curve
B'''—Total clearing time-current characteristic curve
C—Branch line sectionalizing fuse rated at 30 amperes
D—Branch line sectionalizing fuse rated at 50 amperes
E—Feeder oil circuit breaker and relay
$E^{2\prime}$—Very inverse relay (number 1 time lever setting)
$E^{3\prime}$—Very inverse relay (number 10 time lever setting)
$E^{3\prime\prime}$—Instantaneous attachment on relay functions
F—Protective device on incoming transmission lines
F'—Very inverse relay (number 1 time lever setting)
F''—Fuse

Fig. 8. Time-current curves for 60-ampere household cartridge fuse and 15-ampere primary fuse link superimposed on curves of the conventionally co-ordinated system of figure 3

A—Household plug and cartridge fuses
A'—30-ampere rating
A''—60-ampere rating
B—Fuses rated at 15 amperes, in primary leads of distribution transformer
C—Branch line sectionalizing fuse rated at 30 amperes
D—Branch line sectionalizing fuse rated at 50 amperes
E—Feeder oil circuit breaker and relay
E'—Very inverse relay (number 1 time lever setting)
E''—Very inverse relay (number 10 time lever setting)
E'''—Instantaneous attachment on relay functions
F—Protective device on incoming transmission lines
F'—Very inverse relay (number 1 time lever setting)
F''—Fuse
G—Recommended transformer time-load curve
H—Internal secondary breaker
H'—Overload indicator lights
H''—Breaker opens
I—Internal "weak link" or fuse in primary leads
I' and I''—Available designs

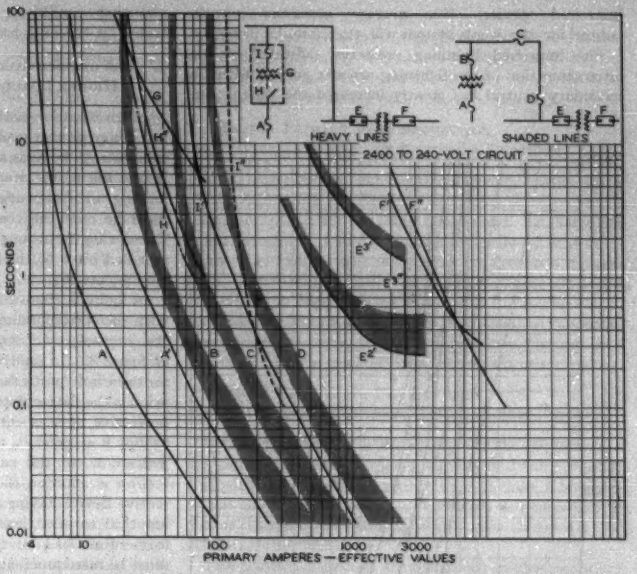

Fig. 9. Time-current curves for unit-type distribution transformer superimposed on curves of the conventionally co-ordinated system of figure 1, showing comparative use of range available for distribution protection

probable frequency of faults, occurring, now and later, on the short comparatively new wiring or in the range or water heater fed directly through the 60-ampere fuse. A large majority of the faults should occur on the other house wiring, and should be isolated by lower rated branch fuses, provided these fuses are not short-circuited malicious or otherwise. On the higher-voltage systems, the 60-ampere cartridge fuse or equivalent breaker is not such a limiting factor, except in cases where other secondary protection is introduced into the problem.

Protection on Secondary Circuits

The protection on secondary circuits from overcurrent faults involves a number of different factors including not only the continuity of service, but the quality and the protection of equipment. Overcurrent protective devices, such as fuses, are installed at the points where the individual service entrances are connected to the main secondary circuit, so as to:

1. Isolate old and faulty installations.
2. Protect against outages from services through buried cable.
3. Isolate services where pennies are inserted behind plug fuses.

The insertion of an overcurrent protective device at the individual service entrance may or may not necessitate using more than a justifiable share of the range available for protection on the whole system. This depends upon several factors. A low rated household plug or cartridge fuse and/or a high transformation ratio makes available a greater range for protection at the service entrances. It will be readily apparent that a protective device such as a fuse, having a time-current characteristic similar in shape to the household fuse and the fuse link on the primary of the transformer permits the closest co-ordination and thus requires the least range for its insertion. If the introduction of a protective device in the service entrance lead necessitates increasing the fusing on the primary of the transformer, an analysis may show the advantages secured for a few consumers have increased the average consumer minutes outage for the whole system.

For example, if the insertion of a secondary fuse cutout in the service leads to confine outages to individual consumers necessitates substituting a $20N$ ampere primary fuse link for the $15N$ ampere rating, figure 8*B*, it cannot be co-ordinated with the $30N$ ampere sectionalizing fuse link, figure 8*C*. Substituting any higher rating for the $30N$ ampere link, in turn, requires the replacing of the $50N$ ampere rating, figure 8*D*, with a larger fuse link which then cannot be co-ordinated with the relay, figure 8*E*. If the relay setting cannot be changed, either the $30N$ or the $50N$ ampere sectionalizing fuse links must be omitted. Then each fault on that portion of the primary line will cause an outage to a larger number of consumers, totaling a great many times those securing

improved service. The average consumer minutes outage for the whole system will, therefore, be increased.

The improved lightning protection afforded by the interconnection of the lightning arrester ground with the secondary neutral has greatly increased the relative importance of overcurrent protection for distribution transformers. Augmenting this relative importance is the desire in some places for higher loading of distribution transformers. New applications of overcurrent protective devices are involved in attempts to meet these changing conditions and requirements. Three major trends in thinking have developed as a result:

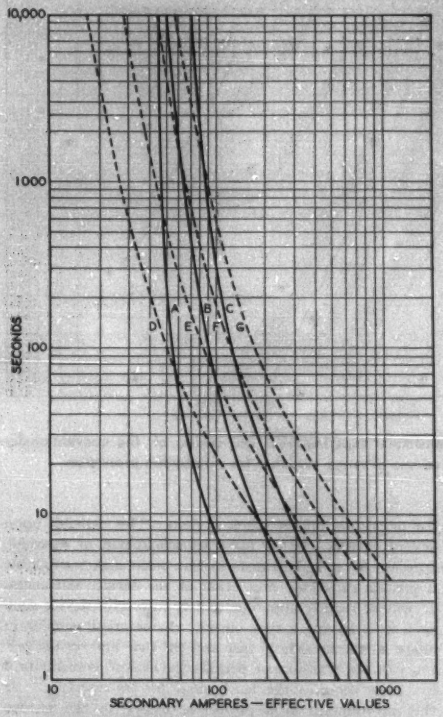

Fig. 10. Co-ordination of time-current curves for 30-, 45-, and 60-ampere household fuses with those for the time load of 3-, 5-, 7.5-, and 10-kva distribution transformers

A—30-ampere plug or cartridge household fuse
B—45-ampere plug or cartridge household fuse
C—60-ampere plug or cartridge household fuse
D—3-kva transformer time load
E—5-kva transformer time load
F—7.5-kva transformer time load
G—10-kva transformer time load

1. Use of Secondary Protection for Higher Loading

Much attention has been and is being given to the use of a secondary protective device supplemented by an overload indicator, to serve as a stop gap against excessive decrease in the life of the transformer so as to permit increased loading at distribution transformers. Such protection must be over the complete range of excessive currents. These vary from long-time, overload currents which are repeated often to the less frequent short-time high short-circuit currents.

In figure 9, the transformer time-load curve *G* is drawn with the corresponding internal secondary breaker *H* and the internal fuse *I* superimposed on the (shaded) curves of figure 8. In studying the effect of time-load curve *G* on the whole protection problem, the important consideration is the flatter slope of the curve, which may make the protective devices curves *H* and *I* co-ordinated with it, occupy too great a portion of the available range for protection on the entire distribution system. If protection is afforded the transformer by a secondary protective device having a time-current characteristic curve identical to or at least closely approximating the transformer time-load curve *G*, the internal primary fuse *I'* or *I''* must be rated much higher than the normal fusing practice *B* so the breaker *H''* will open first and without damage to the fuse *I'* or *I''*. The attendant decrease in the available range may prevent any sectionalizing of the primary lines as indicated in figure 9. The economics of this situation depend wholly upon the degree of protection which can be afforded transformers and the actual number of transformer burnouts saved thereby. Against this must be balanced the increase—or the inability to effect future decreases—in the consumer minutes outage resulting from the utilization of a major portion of the available range for protection on the whole distribution system for protecting the transformer.

For example, consider the degree of protection which can be afforded transformers using as a basis the recommended transformer time-load characteristic curves, figure 10*D*, *E*, *F*, and *G* (for the 3, 5, 7½, and 10-kva ratings, respectively). As shown in figure 10, these curves cross the curves for the household fuses *A*, *B*, and *C* (30-, 45-, and 60-ampere ratings, respectively) due to the dissimilarity in the slopes. Thus any attempt to secure complete protection involves having the secondary protective device interrupt service for all the consumers fed by the transformer for any fault on individual consumer's premises of such magnitude and duration that when plotted on figure 10 the point lies to the left of the fuse curves *A*, *B*, or *C* and to the right of the transformer curves *D*, *E*, *F*, or G.

Complete protection involves a further increase in consumer minutes outage. Any lesser degree of protection means some decrease in the life of the transformer. Therefore, using the recommended transformer time-load curves figure 10 as a basis, it is necessary to strike

a balance between the permissible increase in outages and the degree of protection deemed necessary for the transformer, just as has been done for years in choosing the primary fusing practice.

There is another factor entering the problem; namely, the equipment available and its ability to afford protection to the transformer. Breakers are mounted internally in transformers below the oil level to obtain a portion of the heating characteristic of the transformer. However, curve C'', figure 11*a* approaches but does not quite equal the flatter transformer time-load curve B, figure 11*a*, at the low current long-time end. The breakers are usually set to trip so the curve C'' is well to the right of the transformer time-load curve B at the low current long-time end. Even the overload indicator trips on curve C', to the right of the time-load curve B.

The primary and secondary fuse links have more inverse time-current characteristics D, E, F, figure 11*b*, than the transformer curve B, figures 11*b* and *c*, and the breaker curve C'', figures 11*a* and *c*. Thus in general the primary or secondary fuse link affords a slightly lesser degree of protection to the transformer than the breaker at the low current long-time end as shown by the shaded portion X of figure 11*c*. An exception to this is shown by the shaded portion Y, figure 11*c*, indicating a range where the fuse link affords better protection. Comparing the curves D and F, figure 11*b* with the curve E shows that the primary and secondary fuse links, respectively, will afford an equal degree of protection to the transformer assuming both halves of the secondary are equally loaded. The secondary fuse link or protective device can be used to afford a greater degree of protection without decreasing service continuity only where it can be co-ordinated with the household fuse and the primary fuse link without increasing the fusing practice on the primary.

2. Better Primary Fuse Protection With Increased Transformer Capacity

Some distribution engineers are giving consideration to the economics of affording complete, or very nearly complete, protection to the transformer by installing larger transformers and fusing on the primary at a minimum value which will not cause unnecessary outages from overcurrent surges. They are thinking in terms of having the improved regulation and the saving due to decreased transformer burnouts and the omission of extra protective devices pay the interest on the increased investment for the greater installed transformer capacity.

3. Use of Protective Devices and Secondary Banking for Higher Loading

Increasing attention is being given to the protection of the transformer with normal low primary fusing practice and with the banking of transformers to take advantage of the diversity of loads on individual transformers to reduce extremes of loading which also improves the instantaneous regulation.

The protective devices are connected in the secondary lines at sectionalizing points between adjacent transformers, which are tied solidly to these lines. Outages

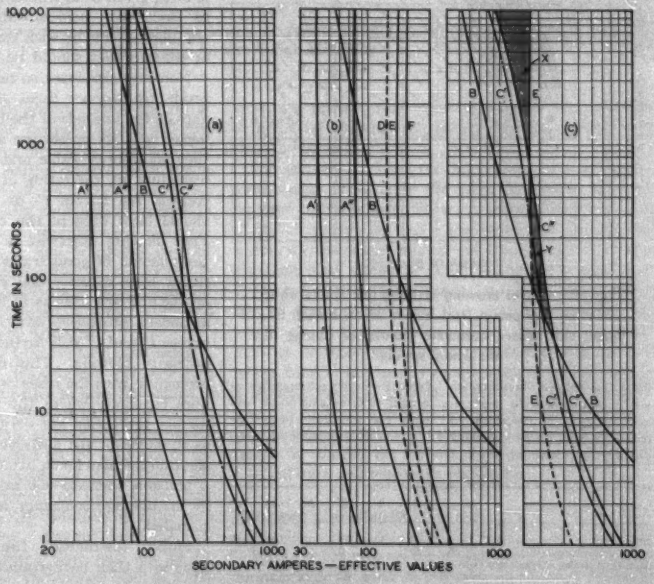

Fig. 11. Curves showing relative degree of protection afforded distribution transformer by secondary breaker, secondary fuse, or primary fuse on a 2,400 to 240-volt circuit

A—Household plug or cartridge fuse
A'—30-ampere rating
A''—60-ampere rating
B—Recommended transformer characteristic curve
C—Secondary breaker and overload indicator
C'—Overload indicator lights
C''—Breaker opens
D—Primary fuse rated at 15 amperes, with no secondary protective device
E—Secondary fuse rated at 85 amperes
X—Shaded portion showing degree of improved protection afforded by secondary breaker
Y—Shaded portion showing degree of improved protection afforded by secondary fuse

from transformer or secondary faults are isolated to the consumers fed by the one transformer. It is not fundamentally important to burn off secondary faults in order to obtain successful operation. The resulting permissible low rating of the secondary and primary protective devices affords generally normal overload protection to the transformer and no decrease in the range available for protection on the primary lines. The co-ordination of the household and secondary fuses can be close since only a maximum of approximately 50 per cent of the current through the household fuse passes through the secondary fuse link.

In some cases the protective devices are placed in the transformer secondary leads and the secondaries of adjacent transformers are tied solidly together to isolate faulty transformers without interrupting service. Faults on the secondary lines or service leads then affect all the consumers on the particular secondary circuit by causing low voltage or the complete loss of service, due to the opening of the secondary protective devices on several or all of the transformers banked on the circuit, known as cascading. The successful operation of banking through protective devices in the transformer leads requires that the majority of the secondary faults clear themselves.

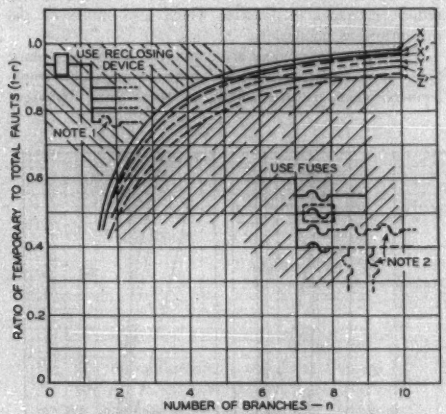

Fig. 12. Curves showing dividing line above which reclosing equipment, and below which branch line fuses, will reduce consumer minutes of outage for the whole system

Note 1—Isolating branches on which permanent faults predominate may raise the percentage of temporary faults for the remainder of the system, above the curves

Note 2—Fusing sub-branches or several sectionalizing points will raise the temporary percentage values of the curves

	X	Y	Z	X'	Y'	Z'
Minutes to go to location (a)	30	30	30	60	60	60
Minutes per branch to locate fault (b)	10	5	0	10	5	0
Minutes duration of temporary fault (c)	1					

Burning a fault clear, demands that secondary and primary protective devices allow the full use of the transformer thermal capacity which involves all of the problems just discussed as attendant upon the use of secondary protection for the higher loading of individual transformer. A similar compromise must be made between overload protection and service continuity. The higher rating of the protective devices reduces the available range for the protection on the primary lines.

The foregoing consideration of the trends in thinking on solutions for the overcurrent protection of distribution transformers has shown that it evolves into a decision on the relative value of protection to the transformer versus present and future improvements in service continuity for the system as a whole. The success of an operating practice intended to reduce the number of consumers affected by each fault and decrease the length of each outage, centers about the ratings of the fuses required on the primary of the distribution transformers. Schemes for reducing outages due to secondary faults, decreasing transformer burn-outs with increased loading, and improving regulation, should be used with caution if they require increasing the primary fusing practice. Where higher rated fuse links are necessitated in the primary leads of the transformer, the available range is decreased for existing or future protection on the primary lines against the major causes of consumer minutes outage.

Fusing Transformer Primaries

Among the various trends in thinking, consideration is being given as to whether transformer primaries should be fused with nonrenewable fuses mounted inside the transformer case or with external renewable fuse cut-outs, or whether they should be fused at all.

Nonrenewable fuses, so called "weak links," are mounted inside transformer cases to permit connecting internal gaps on the line side of the fuses and/or to make the transformer and its protective apparatus one unit. Because they are nonrenewable and in blowing will carbonize the insulating oil, the rating of the fuses must be greatly increased, see curves I' or I'', figure 9. Internal fuses should blow only in the case of a transformer failure. Fuse blowing otherwise would damage and necessitate the removal of good transformers. The higher primary fusing may decrease the range available for protection on the primary lines as in figure 9, I', I''. The lack of a secondary protective device requires the moving of the curves I' and I'' still further to the right to prevent unnecessary blowing. This may even prevent proper co-ordination with the fuses or breaker relay on the primary lines, especially where the fuse ratings or relay settings for line protection are very low on long rural circuits so as to interrupt the flashover of external gaps installed on the transformers for lightning protection. In either case, a probable increase—or prevention of future decrease—in the average consumer minutes outage should be anticipated.

Modern distribution fuse cutouts and renewable fuse links with their background of over 14 years of intensive

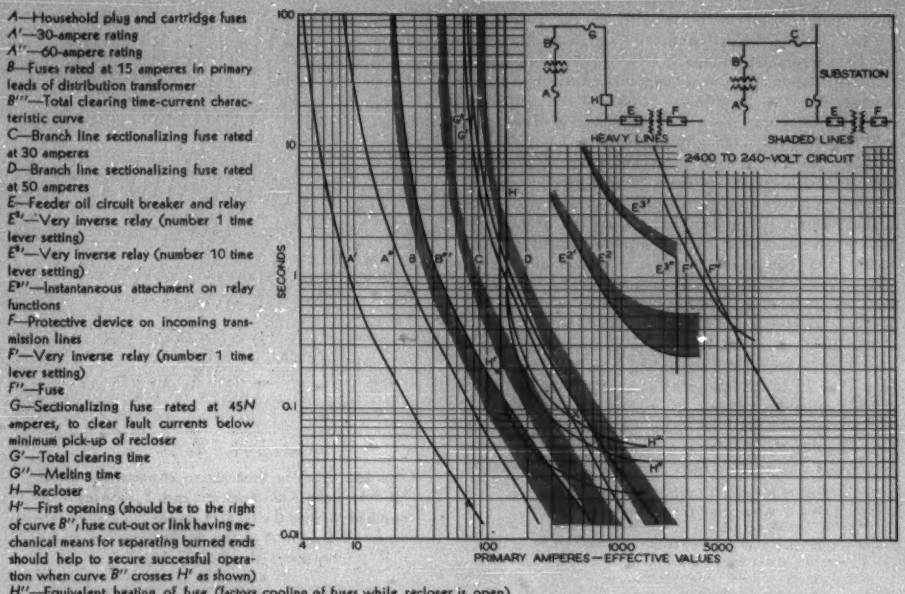
A—Household plug and cartridge fuses
A'—30-ampere rating
A''—60-ampere rating
B—Fuses rated at 15 amperes in primary leads of distribution transformer
B'''—Total clearing time-current characteristic curve
C—Branch line sectionalizing fuse rated at 30 amperes
D—Branch line sectionalizing fuse rated at 50 amperes
E—Feeder oil circuit breaker and relay
E³'—Very inverse relay (number 1 time lever setting)
E²'—Very inverse relay (number 10 time lever setting)
E''—Instantaneous attachment on relay functions
F—Protective device on incoming transmission lines
F'—Very inverse relay (number 1 time lever setting)
F''—Fuse
G—Sectionalizing fuse rated at 45N amperes, to clear fault currents below minimum pick-up of recloser
G'—Total clearing time
G''—Melting time
H—Recloser
H'—First opening (should be to the right of curve B''', fuse cut-out or link having mechanical means for separating burned ends should help to secure successful operation when curve B''' crosses H' as shown)
H''—Equivalent heating of fuse (factors cooling of fuses while recloser is open)
H'''—Equivalent heating of fuse, with 25 per cent factor added to permit direct comparison with melting-time curves for fuse G
X—Maximum current up to which recloser will lock out before fuse link melts
100
10
1
0.1
0.01
SECONDS
4
10
100
1000
5000
PRIMARY AMPERES—EFFECTIVE VALUES
HEAVY LINES
SHADED LINES
SUBSTATION
2400 TO 240-VOLT CIRCUIT

Fig. 13. Time-current curves for a recloser protecting part of a long line and a fuse cut-out protecting the rest, superimposed on the curves for a conventionally co-ordinated system as shown in figure 3, showing the comparative use of the rangeavail able for distribution protection

research and engineering development permit the utility engineer to choose the lowest primary fusing practice with assurance of a successful operating record. This cannot be said of some of the earlier designs upon which much of the present-day service data are based. The primary fuse link rating is usually chosen so as to provide a balance between unnecessary fuse blowing and protection afforded the apparatus, and/or proper co-ordination with protective devices on the secondary of the transformer. A fuse cutout provides an easy means for manually disconnecting transformers and for easily and quickly locating those which are damaged.

The prevalence of lightning in some localities makes it desirable to limit the size of transformer primary fuse links to a certain minimum in order to take advantage of the ability of the larger links to more successfully withstand lightning impulses. This is especially true where the lightning arrester is connected on the load side of the fuse cutout. A minimum rating of 10 amperes will generally eliminate the majority of unnecessary fuse blowing and will not ordinarily interfere greatly with proper primary co-ordination. Saving one fuse replacement trip will usually more than pay for the installation of secondary fuses on the smaller sizes of transformers to provide the same overload protection as would be given by the smaller primary fuse link that would normally be used.

The omission of fuses on the primary of distribution transformers is virtually the same as adding miles of exposure to the primary lines. A service interruption to all the consumers on such a line may result from a line fault or a transformer flashover or burnout; or a secondary line fault if no secondary protective device is employed. The cause of each outage must be sought among every one of these possibilities, thus greatly increasing the length of each interruption. The use of secondary fuses or breakers while affording a degree of protection to the transformer, merely removes the secondary line as a possible cause of trouble. Therefore, where primary fuses are omitted, a marked increase in consumer minutes outage can be anticipated over that occurring where protection is afforded the individual transformer by modern fuse cut-outs and renewable fuse links.

Primary Line Faults

With the fuse link on the primary of distribution transformers kept as small as possible, the effect of faults on

the primary lines can be reduced by the introduction of the properly located protective devices. The choice between fuses and automatic reclosing devices is largely dependent upon the ratio of temporary faults to permanent faults on the whole and each portion of the distribution system. Of course, there is also the question of economics and the importance of loads. Superior service continuity can be secured by the use of fuses at a number of sectionalizing points on the primary lines especially where a fairly high percentage of the faults are permanent. Automatic reclosing equipment will reduce the average consumer minutes outage where temporary faults predominate. This equipment may be a breaker or a recloser which reset themselves after interrupting temporary fault currents, or a reclosing fuse cutout which requires periodic inspection and renewal of blown fuse links.

The dividing line between the percentage of temporary versus permanent faults above which reclosing equipment located either in the station or at branch lines, and below which sectionalizing fuses, will reduce the consumer minutes outage is shown in figure 12. These values were derived using the following formula, with the indicated assumptions as to the times required to restore service.

r = ratio of permanent to total number of faults
$1 - r$ = ratio of temporary to total number of faults
P = faults per branch
$a + nb$ = duration of permanent fault
a = minutes to go to location
b = minutes to locate fault per branch
n = number of branches
e = duration of temporary fault
N = number of consumers per branch

Total consumer minutes outage per year with reclosing device = $nPr\,(a + nb)\,(nN) + Pn\,(1 - r)\,(e)\,(nN)$
Total consumer minutes outage per year with sectionalizing fuses at each branch or sub-branch = $nP\,(a + b)\,N$

$$\text{ratio} = \frac{\text{minutes outage with reclosing device}}{\text{minutes outage with sectionalizing fuse}}$$

$$= \frac{n^2 PN\,[r\,(a + nb) + e\,(1 - r)]}{nPN\,(a + b)}$$

$$= \frac{n\,(ra + rnb + e - er)}{a + b}$$

The lower cost, nonreclosing fuse cutout can perform a real service for reducing consumer minutes outage both as to the effect and the length of outages. The curves figure 12 show the advantage of connecting fuse cutouts and fuse links in several branch lines. The use of additional fuses at sub-branches or in series at various sectionalizing points, will raise the curves figure 12. For example, with 3 fused branches each having one fused sub-branch, curve x figure 12 will be raised from 79.1 per cent to 84.7 per cent and with 2 sub-branches each to 89.2 per cent. Connecting one and 2 fuses in series with each branch line fuse will raise curve x figure 12 from 79.1 per cent to 84.7 per cent, respectively. In addition to those greater benefits due to the confinement of the effect of faults to fewer consumers, the time to locate the faults will be reduced and the curves figure 12 raised, for example, the 89.2 per cent and 84.7 per cent values given above will be raised to 91.2 per cent and 86.9 per cent, respectively, with a proportionate reduction in time to the length of line affected.

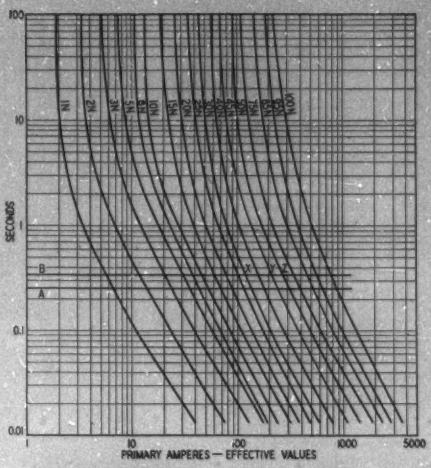

Fig. 14. Melting time-current characteristic curves for fuse links with lines A and B showing time required to open the feeder breaker, the limiting factor for co-ordinating so that the first opening of the breaker is ahead of the fuse link

A—Time required for instantaneous ground relay and breaker to open
B—Factor of 25 per cent added to curve A to permit direct comparison with melting-time curves of fuse links
X—Maximum current up to which breaker will clear ahead of 30*N* ampere fuse link
Y—Maximum current with 45*N* ampere fuse link
Z—Maximum current with 50*N* ampere fuse link

The effectiveness of reclosing fuse cutouts depends on the periodic inspection and replacement of blown fuse links before an outage occurs. If they are not refused until both or all 3 fuse links have blown, their use should tend to raise the curves figure 12 up to which they will improve service continuity. If periodically inspected and a majority of the blown fuse links are replaced before an outage occurs, their performance approximates the reclosing devices indicated on the curves, figure 12.

Both conventional reclosing oil circuit breakers and the lower cost mechanical breakers known as circuit reclosers, are available for use at sectionalizing points. The relay actuating the conventional oil circuit breaker functions with the induction relay characteristics which are similar to those for the modern distribution fuse links, figure 8*B*, *C*, and *D*. Thus the introduction of this equipment permits reasonably close co-ordination with the fuse links at transformer installations and at any desirable sectionalizing point.

The instantaneous plunger type relay characteristics of the circuit recloser figure 13*H'* definitely limit the rating of fuse links which will blow before the first opening

of the recloser, to low values (the fuse link curves which are to the left of the respective recloser curves figure 7*a*). The ratings of practically all internal fuses, or "weak links," are too high to blow soon enough to prevent lockout of the recloser. If the fuses further out on the system are too large to blow before the recloser locks out, a fuse cutout can be connected across the recloser to permit manually by-passing it through a fuse after the recloser locks out. The fuse link in the cutout should be large enough to allow the internal fuses or sectionalizing fuses beyond the recloser to blow first, so as to indicate the location of the fault.

On long lines the recloser can be used for that portion where the fault currents will be greater than the minimum current required to pick up the contact so that it actuates the lockout mechanism. A fuse cutout, installed within this portion, can be fused, figure 13*G*, so as to permit the recloser to lock out on fault currents above the minimum pick-up. The location of the cutout should be such that the maximum fault current available at the point of installation does not exceed the value at which the melting time current curve 13*G'* crosses the recloser curve, figure 13*H'''*, at *X*. Then the fuse cutouts will afford protection for all fault currents below the minimum pick-up of the recloser; in most cases reaching out to the end of a long line. The fuse link can also be co-ordinated with the relay on the main feeder breaker, figure 13*F'* and *F''*.

Automatic reclosing oil circuit breakers are more generally installed at the substation to improve continuity of service to the more important consumers on the main feeder and larger branches. By fusing branches of the circuit where permanent faults predominate, the percentage of temporary faults on the important parts may be raised so the reclosing breakers will reduce the consumer minutes outage for the whole system, note 1, figure 12, as well as for the important loads.

Several large utility companies report an improvement in service continuity resulting from the combination of branch line fusing and automatic reclosing breakers at the substation. Their scheme is applicable on grounded neutral systems where the instantaneous relay, connected to operate on ground and/or neutral currents, can be set to pick up at very low currents for the initial opening of the breaker. A grounding bank can be used to provide the neutral on delta systems. After the first opening, the instantaneous relay locks out and the induction relays, connected in the phase wires are automatically switched on for the subsequent operations to the lockout of the breaker. However, in the case of a permanent fault on a branch line the fuse links and induction relays are co-ordinated so a time delay is provided and the fuse links clear ahead of the second relay operation. The ground relay is automatically reconnected in the case of a temporary fault or after the fuse disconnects the branch. A practical set-up for the fusing of branch lines in this way automatically differentiates between temporary and permanent faults to neutral and ground.

The successful functioning of such an arrangement depends on the time required for the breaker to open and interrupt the fault current, after the instantaneous ground relay has closed the trip circuit. For example, a relay and breaker requiring a total time of 15 cycles (0.25 second) to clear the circuit, will successfully clear temporary faults up to 125 amperes without damaging a 33*N* ampere branch line sectionalizing fuse link of the design for which the curves figure 14 are plotted. This is indicated by the point *X*, figure 14, where the melting time curve for the fuse link crosses the curve *B* plotted so as to allow a 25 per cent factor for operating and manufacturing variables above line *A* drawn at 0.25 second. Under similar conditions, a 45*N* ampere fuse link will not be damaged up to 205 amperes, and a 50*N* ampere fuse link up to 270 amperes (points *Y* and *Z*, figure 14, respectively). If the short-circuit current available at the point of installation for the sectionalizing fuse cutout exceeds these values, the fuse link may be partially melted. If it is not replaced subsequent melting on load currents may cause arcing which will not clear and will burn the fuse tube of cutouts that provide no mechanical means for separating the burned ends of the fuse link.

One utility company reports that it has been their experience based on observations of actual operating conditions, as well as field tests, that those circuits which are fused with the 30*N* ampere fuse links usually have shorts which range between 100 and 150 amperes, while the circuits on which the 50*N* (60) ampere fuse links are used, run between 200 and 300 amperes. In the cases where it is definitely known a heavy phase short circuit has taken place, it is the operating practice to replace both fuses. From this it would appear practical to secure the combined advantages of automatic reclosing for temporary line-to-ground or line-to-neutral faults and fused sectionalizing for isolating permanent line-to-ground and line-to-neutral and line-to-line faults to small areas. Such a practice should afford a marked decrease in the consumer minutes of outage.

Summary

In the foregoing an attempt has been made to make an impartial study of the various trends in thinking with respect to the overcurrent protection on distribution systems. This has been done from the standpoint of the effect of each on the service continuity, the protection to apparatus, and the system economy. Major emphasis has been given to service continuity as present-day consumer requirements have increased the utility companies' interest in reducing outages to a minimum. A number of pertinent factors have been brought out which are generally applicable to any such studies that might be made on specific systems. A tabulation of these without doubt, will be of value.

1. Actual operating records on the system in question are essential.
2. The data in such records will be enhanced in value if selected to show the differences,
   - *a*. On urban, suburban, and rural sections,
   - *b*. On main feeders, branch feeders, distribution transformers, and secondary lines,
   - *c*. Between causes of faults such as lightning, short circuits, overloads, etc.,

d. Between types of faults, temporary vs. permanent,

e. Between modern and old equipment.

3. Such records will show that one permanent fault on the primary lines will cause upward to 100 times as many consumer minutes outage as one fault in a transformer or on the secondary lines, and that generally a greater percentage of faults occur on the primary lines.

4. Secondary protection to continuity and/or apparatus which can be secured without increasing the normal fusing practice on the primary of the distribution transformer (generally 2 or 3 times the full load current of the transformer) will improve service continuity.

5. Conversely, any increasing of the normal primary fusing practice to secure other advantages very likely will increase—or prevent future decreases in—the average consumer minutes outage for the whole system.

6. The use of the external fuse cutout with renewable fuse links enables the use of the lowest possible fusing practice, spoken of as normal. Modern equipment insures an improved service record.

7. The normal fusing practice while termed short-circuit protection, affords a fairly high degree of protection to the transformer as indicated by operating records; such as those where higher internal fusing has been employed with no secondary protection.

8. The use of nonrenewable internal fuses necessitates increasing the primary fusing practice, and without a secondary fuse or breaker affords no protection to the transformer.

9. The omission of fuses on the primary virtually adds miles of exposure to cause and on which to locate, trouble on the primary lines.

10. The ratio of temporary to permanent faults on the whole and various parts of the system governs the benefits in improved continuity of service rendered by fuse cutouts at sectionalizing points and by automatic reclosing equipment.

a. Fusing sectionalizing points on the primary lines to confine the effect of outages to small areas will reduce the average consumer minutes outage even with high ratios of temporary to permanent faults (see figure 12).

b. Automatic reclosing equipment or reclosers at the substation or in branch lines will reduce the consumer minutes outage where the percentage of temporary faults is high. This percentage in some instances can be improved by fusing branches where permanent faults predominate.

c. A practical arrangement for automatically combining sectionalizing fuse and automatic reclosing protection so as to differentiate between temporary and permanent faults will produce the best results.

References

1. Co-ordinating Fuses and Relays for Distribution Reliability, G. F. Lincks. *Electrical World*, July 29, 1933.

2. Fuse Link Improvement Gives Co-ordinated Protection, G. F. Lincks, *Electrical World*, November 4, 1933.

Expansion Theorems for Ladder Networks

(*Continued from page 158*)

7. Spulen und Wanderwellen, W. Rogowski. *Archiv fuer Elektrotechnik* volume 6, 1918, pages 285–300, 377–88, and volume 7, 1919, pages 33–40, 161–75, 330–36.

8. Überspannungen und Eigenfrequenzen einer Spule, W. Rogowski, *Archiv fuer Elektrotechnik*, volume 7, 1919, pages 240–62.

9. Building up of Sinusoidal Currents in Long Periodically Loaded Lines, J. R. Carson. *Bell System Technical Journal*, volume 3, number 4, 1924.

10. Electric Circuit Theory and Operational Calculus (a book), J. R. Carson. McGraw-Hill Book Co., N. Y., chapter 8.

11. Transient Oscillations in Electric Wave-Filters, J. R. Carson and O. J. Zobel. *Bell System Technical Journal*, volume 2, July 1923, pages 1–32.

12. Theory and Design of Uniform and Composite Electric Wave Filters, O. J. Zobel. *Bell System Technical Journal*, volume 2, January 1923.

13. Transmission Characteristics of Electric Wave Filters, O. J. Zobel. *Bell System Technical Journal*, volume 3, October 1924.

14. A Note on the Theory of Artificial Telephone and Transmission Lines, A. C. Bartlett. *Philosophical Magazine*, volume 48, 1924, page 859.

15. Properties of the Generalized Artificial Line, A. C. Bartlett. *Philosophical Magazine*, volume 49, 1924, page 859.

16. Transient Analysis of Artificial Lines, Y. H. Ku, T. C. Tsao, and Y. Chu. University of Chekiang Publications in Electrical Engineering, number 7, September 1930.

17. Die Eigenschaften symmetrischer 4n-Pole und höherer symmetrischer Schaltungen und Anwendungen derselben, H. G. Baerwald. *Sits. Preuss. Akad. der Wiss. (Phys. Math. Kl.)* 1931, pages 784–729.

18. Note on a Method of Solution of a Certain Type of Homogeneous Linear Difference Equation, A. F. Stevenson. *Transactions* of the Royal Society of Canada, volume 3, September 25, 1931, pages 49–55.

19. On the Operational Solution of Linear Finite Difference Equations, Milne-Thomson. *Proceedings* of the Cambridge Philosophical Society, volume 27, 1931, pages 36–38.

20. Sequenzen von Zahlen, die sich aus einer linearen homogenen Rekursionsformel berechnen, B. I. Baldaff. *Sol. Mat.*, volume 4, 1931, pages 137–40 and volume 5, 1932, pages 17–18.

21. Die Siebschaltungen der Fernmeldetechnik, W. Cauer. *Zeitschrift fuer Angewandte Mathematik und Mechanik*, volume 10, 1930, pages 425–33.

22. Siebschaltungen (a book), W. Cauer. Published by D. I. Verlag G. m. b. H., Berlin, 1931.

23. New Theory and Design of Wave Filters, W. Cauer. *Physics*, volume 2, number 4, 1932, page 242.

24. Erweiterung der Siebkettentheorie, M. J. O. Strutt. *Archiv fuer Elektrotechnik*, volume 26, 1932, pages 273–78.

25. A Method for Calculating Transmission Properties of Electrical Networks Consisting of a Number of Sections, A. Alford. *Proceedings* of the Institute of Radio Engineers, volume 21, number 8, 1933, pages 1210–30.

26. On the Operational Solution of Linear Mixed Difference Differential Equations, J. Neufeld. *Proceedings* of the Cambridge Philosophical Society, volume 30, 1934, pages 380–91.

27. A General Theory of Electric Wave Filters, H. W. Bode. *Bell System Technical Journal*, volume 14, 1935, pages 211–14.

28. A Generalized Infinite Integral Theorem, M. G. Malti. Electrical Engineering (AIEE Transactions), volume 54, November 1935, pages 1222–27.

29. Die gewöhnlichen und partiellen Differenzengleichungen der Baustatik (a book), F. Bleich and E. Melan. Julius Springer, Berlin.

30. Vorlesungen über Fouriersche Integrale (a book), S. Bochner. Published by Akad. Verlagsgesellschaft m. b. H. Leipzig, 1932, chapter 5.

31. Differenzenrechnung (a book), N. E. Nörlund. Julius Springer, Berlin.

32. An Introduction to Linear Difference Equations (a book), F. M. Batchelder. Harvard University Press, Cambridge, Mass.

A New Service Restorer

(*Continued from page 182*)

Film *B* shows the record of 2 interruptions with 12,000 volts across the terminals, the current being 960 and 880 amperes, respectively. Film *C* shows 4 interruptions (3 reclosures and a final lockout) of 400 amperes at 12,000 volts. Reclosure is immediate after each opening, the average reclosing time from the instant the fault occurs until the device recloses being 31 cycles.

The service restorer was developed primarily for low-capacity low-revenue lines and it is hoped that it will be a real contribution toward the improvement of electric power service by providing an economical and efficient automatic reclosing device for such applications. It should be ideally suited for sectionalizing lines and protecting feeders in rural and suburban districts as well as for use at small isolated industrial and mining properties where a continuous power supply is important.

Expansion Theorems for Ladder Networks

By MICHEL G. MALTI
MEMBER AIEE

S. E. WARSCHAWSKI
NONMEMBER

The well-known expansion theorem of Heaviside applies to circuits whose current-electromotive force relations may be expressed through differential equations, whereas in some networks such as filters and artificial lines, in which the network consists of a repeated pattern or mesh, the relations give what are known as difference equations. These are equations involving the mesh number of the network. The solutions of such networks are given in this paper in the form of expansion theorems similar to Heaviside's expansion theorem and its extensions.

THE current-electromotive force relations of filter circuits, artificial lines, and other ladder networks lead to difference equations whose solutions have been given by Pupin,[1] Rüdenberg,[3] Wagner,[4-6] Rogowski,[7,8] Carson,[9-11] Zobel,[11-13] Cauer,[21-23] Alford,[25] and others.[2,14-20,24,26,27] Mathematical work on difference equations has been going on since the days of Newton, Laplace, and Gauss (18th century). Treatises on difference equations have been written by Nörlund,[31] Batchelder,[32] and F. Bleich[29] and E. Melan.[29]

Although Laplace transformations have been used in the treatment of linear difference equations with constant coefficients, particularly by Bochner,[30] the authors do not know of any results which parallel Heaviside's expansion theorem and its extensions for differential equations.[28] The object of this paper is to develop such expressions by the use of Laplace transformations.

1. Solution of a Difference Equation

Consider the following linear difference equation of the nth order with constant coefficients a_k:

$$a_0 f(x) + a_1 f(x+1) + \ldots + a_n f(x+n) = \phi(x) \tag{1}$$

In equation 1, $a_0 \neq 0$, $a_n \neq 0$. This does not detract from the generality of equation 1 because if $a_0 = 0$, then substituting x for $x + 1$ reduces equation 1 to a difference equation of lower order. On the other hand if $a_n = 0$ then again the order of equation 1 is reduced.

Again $\phi(x)$ is a given function which satisfies the following conditions:

1. $\phi(x)$ is of bounded variation in any finite interval
2. $\phi(x) \equiv 0$ for $x < 0$
3. $\phi(x) = [\phi(x+0) + \phi(x-0)]/2$ for every x
4. $\int_0^\infty |\phi(x)\epsilon^{-ux}|\,dx$ converges if the real part of u is sufficiently large.

It may be here observed that all functions encountered in engineering practice do satisfy these conditions.

In addition to equation 1 certain boundary conditions must be given. As boundary conditions we shall assume that $f(x)$ is known over the interval $0 \leq x < n$ and that in this interval $f(x)$ is of bounded variation and $f(x) = [f(x+0) + f(x-0)]/2$. The solution of equation 1 consists in determining $f(x)$ which

1. Satisfies equation 1 for all $x \geq 0$;
2. Is equal to the given boundary function for $0 \leq x < n$

Multiply both sides of equation 1 by $\epsilon^{-ux}dx$ and integrate between zero and infinity thus:

$$\sum_{k=0}^{n} \int_0^\infty a_k f(x+k)\epsilon^{-ux}dx = \int_0^\infty \phi(x)\epsilon^{-ux}dx \tag{2}$$

where u is any complex number whose real part is positive and sufficiently large.

Consider a typical term of the sum in equation 2. Let $x + k = y$ then $dx = dy$, $x = y - k$. When $x = 0$, $y = k$ and when $x = \infty$, $y = \infty$. Substitute these relations in the left side of equation 2 and obtain:

$$\sum_{k=0}^{n} a_k \epsilon^{ku} \int_k^\infty f(y)\epsilon^{-uy}dy = \int_0^\infty \phi(x)\epsilon^{-ux}dx \tag{3a}$$

or

$$\sum_{k=0}^{n} a_k \epsilon^{ku} \left[\int_0^\infty f(x)\epsilon^{-ux}dx - \int_0^k f(x)\epsilon^{-ux}dx\right] = \int_0^\infty \phi(x)\epsilon^{-ux}dx \tag{3b}$$

Since $f(x)$ is known for $0 \leq x < n$ and since $k \leq n$, therefore the second integral in each term of the sum to the left of equation 3b is known. Again since $\phi(x)$ is known the integral to the right of equation 3b is also known. Let:

$$\Psi(u) = \sum_{k=0}^{n} a_k \epsilon^{ku} \int_0^k f(x)\epsilon^{-ux}dx \tag{4a}$$

$$\Phi(u) = \int_0^\infty \phi(x)\epsilon^{-ux}dx \tag{4b}$$

Substitute equation 4 in 3b and obtain:

$$\sum_{k=0}^{n} a_k \epsilon^{ku} \int_0^\infty f(x)\epsilon^{-ux}dx = \Phi(u) + \Psi(u) \tag{5a}$$

or

$$\int_0^\infty f(x)\epsilon^{-ux}dx = F(u) \tag{5b}$$

where

$$F(u) = [\Phi(u) + \Psi(u)] \Big/ \sum_{k=0}^{n} a_k \epsilon^{ku} \tag{5c}$$

A paper recommended for publication by the AIEE committee on electrophysics. Manuscript submitted November 6, 1936; released for publication December 1, 1936.

MICHEL G. MALTI is assistant professor of electrical engineering, and S. E. WARSCHAWSKI is a research assistant at Cornell University, Ithaca, N. Y.

1. For all numbered references see list at end of paper.

Equation 5*b* is a well-known integral equation whose solution is:

$$f(x) = \frac{1}{2\pi j}\int_{b-j\infty}^{b+j\infty} F(u)\epsilon^{ux}du \tag{6}$$

where b is a sufficiently large positive number.

Equation 6 is the solution of equation 1. It is given in the form of a complex integral which may be readily evaluated (see section 3).

2. Solution of a System of Difference Equations

Consider the following system of linear difference equations of the nth order with constant coefficients a_{lrk}:

$$\sum_{r=1}^{m}\sum_{k=0}^{m_r} a_{1rk}f_r(x+k) = \phi_1(x) \tag{7a}$$

$$\sum_{r=1}^{m}\sum_{k=0}^{m_r} a_{2rk}f_r(x+k) = \phi_2(x) \tag{7b}$$

$$\cdots\cdots\cdots\cdots\cdots\cdots$$

$$\sum_{r=1}^{m}\sum_{k=0}^{m_r} a_{mrk}f_r(x+k) = \phi_m(x) \tag{7m}$$

where $\phi_l(x)$ are given functions which satisfy the conditions imposed on $\phi(x)$ in section 1; $f_r(x)$ are unknown functions. As to the boundary conditions we shall assume that $f(x)$ is known over the interval $0 \leqq x < m$, and that in this interval $f_r(x)$ is of bounded variation and $f_r(x) = [f_r(x+0) + f_r(x-0)]/2$. The problem is to determine $f_r(x)$ which satisfy the system of difference equations 7 for all $x \geqq 0$ and the boundary conditions for $0 \leqq x < m_r$.

Multiply both sides of each of equations 7 by $\epsilon^{-ux}dx$ and integrate between zero and infinity. Then a typical equation becomes:

$$\sum_{r=1}^{m}\sum_{k=0}^{m_r}\int_0^\infty a_{lrk}f_r(x+k)\epsilon^{-ux}dx = \int_0^\infty \phi_l(x)\epsilon^{-ux}dx \tag{8}$$

where $l = 1, 2, 3, \ldots m$.

Substitute $x + k = y$ in equation 8 and obtain as in equation 3*b*:

$$\sum_{r=1}^{m}\sum_{k=0}^{m_r} a_{lrk}\epsilon^{uk}\left[\int_0^\infty f_r(x)\epsilon^{-ux}dx - \int_0^k f_r(x)\epsilon^{-ux}dx\right] = \int_0^\infty \phi_l(x)\epsilon^{-ux}dx \tag{9}$$

Since $f_r(x)$ is known for $0 \leqq x < m_r$ and since in each inner sum $k \leqq m_r$, therefore the second integral to the left in equation 9 is known. Again, since each $\phi_l(x)$ is known, the integral to the right of equation 9 is also known. Let:

$$\Psi_l(u) = \sum_{r=1}^{m}\sum_{k=0}^{m_r} a_{lrk}\epsilon^{uk}\int_0^k f_r(x)\epsilon^{-ux}dx \tag{10a}$$

$$\Phi_l(u) = \int_0^\infty \phi_l(x)\epsilon^{-ux}dx \tag{10b}$$

Substitute equations 10 in 9 and obtain:

$$\sum_{r=1}^{m}\sum_{k=0}^{m_r} a_{lrk}\epsilon^{uk}\int_0^\infty f_r(x)\epsilon^{-ux}dx = \Phi_l(u) + \Psi_l(u) = M_l(u) \tag{11}$$

Let:

$$\sum_{k=0}^{m_r} a_{lrk}\epsilon^{uk} = A_{lr}(\epsilon^u) \tag{12a}$$

$$\int_0^\infty f_r(x)\epsilon^{-ux}dx = F_r(u) \tag{12b}$$

Substituting equations 12 in equation 11 and remembering that we have m such equations because l assumes all integer valves between 1 and m, we have:

$$\sum_{r=1}^{m} A_{1r}(\epsilon^u)F_r(u) = M_1(u) \tag{13a}$$

$$\sum_{r=1}^{m} A_{2r}(\epsilon^u)F_r(u) = M_2(u) \tag{13b}$$

$$\cdots\cdots\cdots\cdots\cdots\cdots$$

$$\sum_{r=1}^{m} A_{mr}(\epsilon^u)F_r(u) = M_m(u) \tag{13m}$$

Expanding equations 13 we obtain

$$A_{11}(\epsilon^u)F_1(u) + A_{12}(\epsilon^u)F_2(u) + \ldots + A_{1m}(\epsilon^u)F_m(u) = M_1(u) \tag{14a}$$

$$A_{21}(\epsilon^u)F_1(u) + A_{22}(\epsilon^u)F_2(u) + \ldots + A_{2m}(\epsilon^u)F_m(u) = M_2(u) \tag{14b}$$

$$\cdots\cdots\cdots\cdots\cdots\cdots\cdots\cdots\cdots\cdots$$

$$A_{m1}(\epsilon^u)F_1(u) + A_{m2}(\epsilon^u)F_2(u) + \ldots + A_{mm}(\epsilon^u)F_m(u) = M_m(u) \tag{14m}$$

Solving equations 14 simultaneously for $F_r(u)$ we have:

$$F_r(u) = [\Delta_{1r}(\epsilon^u)M_1(u) + \Delta_{2r}(\epsilon^u)M_2(u) + \ldots + \Delta_{mr}(\epsilon^u)M_m(u)]/\Delta(\epsilon^u) \tag{15}$$

where

$$\Delta(\epsilon^u) = \begin{vmatrix} A_{11}(\epsilon^u) & A_{12}(\epsilon^u) \ldots A_{1m}(\epsilon^u) \\ A_{21}(\epsilon^u) & A_{22}(\epsilon^u) \ldots A_{2m}(\epsilon^u) \\ \cdots\cdots\cdots\cdots\cdots\cdots \\ A_{m1}(\epsilon^u) & A_{m2}(\epsilon^u) \ldots A_{mm}(\epsilon^u) \end{vmatrix} \tag{16}$$

and $\Delta_{pq}(\epsilon^u)$ is the minor of Δ obtained by omitting the pth row and qth column and multiplying the determinant so obtained by $(-1)^{(p+q)}$.

Substituting equation 15 in 12*b* we have

$$\int_0^\infty f_r(x)\epsilon^{-ux}dx = F_r(u) = \sum_{l=1}^{m}\Delta_{lr}(\epsilon^u)M_l(u)/\Delta(\epsilon^u) \tag{17}$$

Equation 17 is of the same form as 5*b*. Hence its solution is:

$$f_r(x) = \frac{1}{2\pi j}\int_{b-j\infty}^{b+j\infty} F_r(u)\epsilon^{ux}du \tag{18}$$

3. Evaluation of the Integrals of Equations 6 and 18

The complex integrals given in equations 6 and 18 are not usable in their present form. They must be evaluated before the functions $f(x)$ and $f_r(x)$ can be computed in any engineering problem. These integrals have, accord-

ingly been evaluated by us. The actual evaluation is of mathematical interest only. We therefore give here the results.

Referring to the difference equation 1 let:

$$P(\epsilon^u) = \sum_{k=0}^{n} a_k \epsilon^{ku} \tag{19a}$$

$$Q_s(\epsilon^u) = \sum_{k=0}^{n-s} a_{(k+s)} \epsilon^{ku} \tag{19b}$$

If the polynomial $P(\epsilon^u)$ has distinct (unequal) roots α_k then by decomposition into partial fractions we obtain:

$$1/P(\epsilon^u) = \sum_{k=1}^{n} B_k/(\epsilon^u - \alpha_k) \tag{20a}$$

$$Q_s(\epsilon^u)/P(\epsilon^u) = \sum_{k=1}^{n} B_{ks}/(\epsilon^u - \alpha_k) \tag{20b}$$

where

$$B_k = 1/P'(\alpha_k); \qquad B_{ks} = Q_s(\alpha_k)/P'(\alpha_k) \tag{21}$$

On the other hand if the polynomial $P(\epsilon^u)$ has λ roots α_k, each repeated n_k times, then decomposition into partial fractions gives:

$$1/P(\epsilon^u) = \sum_{k=1}^{\lambda} \sum_{r=1}^{n_k} B_{kr}/(\epsilon^u - \alpha_k)^r \tag{22a}$$

$$Q_s(\epsilon^u)/P(\epsilon^u) = \sum_{k=1}^{\lambda} \sum_{r=1}^{n_k} B_{krs}/(\epsilon^u - \alpha_k)^r \tag{22b}$$

where

$$B_{kr} = [\psi_k^{(n_k-r)}(\alpha_k)]/(n_k - r)! \tag{23a}$$

$$B_{krs} = [\psi_{ks}^{(n_k-r)}(\alpha_k)]/(n_k - r)! \tag{23b}$$

$$\psi_k(\epsilon^u) = [\epsilon^u - \alpha_k]^{n_k}/P(\epsilon^u) \tag{23c}$$

$$\psi_{ks}(\epsilon^u) = Q_s(\epsilon^u)[\epsilon^u - \alpha_k]^{n_k}/P(\epsilon^u) \tag{23d}$$

With these notations the integral equation 6 becomes, for distinct and repeated roots respectively of $P(\epsilon^u)$:

$$f(x) = \sum_{k=1}^{n} B_k \sum_{c=0}^{[x]-1} \alpha_k^c \phi(x - c - 1) + \sum_{s=1}^{n} \sum_{k=1}^{n} B_{ks} \alpha_k^{[x]} f(x - [x] + s - 1) \tag{24a}$$

$$f(x) = \sum_{k=1}^{n} \sum_{r=1}^{n_k} B_{kr} \sum_{c=0}^{[x]-r} \binom{r+c-1}{c} \alpha_k^c \phi(x - r - c) + \sum_{s=1}^{\lambda} \sum_{k=1}^{\lambda} \sum_{r=1}^{n_k} B_{krs} \binom{[x]}{[x]-r+1} \alpha_k^{([x]-r+1)} f(x - [x] + s - 1) \tag{24b}$$

In equations 24:

1. $\binom{a}{b} = 0$ if $b < 0$
2. x is a positive non-integer
3. If x is a positive integer then $f(x) = [f(x + 0) + f(x - 0)]/2$ and $f(0) = f(0 + 0)/2$

Equation 24*a* may be termed Heaviside's expansion theorem for difference equations; while equation 24*b* is the extension of that theorem to the case of repeated roots[28] of $P(\epsilon^u)$.

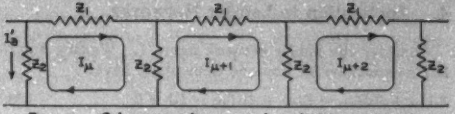

Fig. 1. Schematic diagram of a ladder network

Next referring to the system of difference equations 7 let:

$$\Delta(\epsilon^u) = \sum_{k=0}^{n} b_k \epsilon^{ku}, \quad \Delta_{lr}(\epsilon^u) = \sum_{r=0}^{q_{lr}} b_{lrr} \epsilon^{ru} \tag{25a}$$

$$Q_{lrps}(\epsilon^u) = \sum_{k=s}^{m_p} a_{lpk} \epsilon^{ku} \Delta_{lr}(\epsilon^u) = \sum_{r=0}^{m_p+q_{lr}} \beta_{lrpsr} \epsilon^{ru} \tag{25b}$$

Then the expansion of $1/\Delta(\epsilon^u)$ in partial fractions is given by equations 20*a* and 22*a* respectively where $\Delta(\epsilon^u)$ replaces $P(\epsilon^u)$. With these notations the integral in equation 18 becomes:

$$f_r(x) = \sum_{l=1}^{m} [f_{lra}(x) + f_{lrb}(x)] \tag{26}$$

where

(*a*) *For distinct roots of* $\Delta(\epsilon^u)$

$$f_{lra}(x) = \sum_{r=0}^{q_{lr}} b_{lrr} \sum_{k=1}^{n} B_k \sum_{c=0}^{r+[x]-1} \alpha_k^c \phi_l(r + x - c - 1) \tag{27a}$$

$$f_{lrb}(x) = \sum_{p=1}^{m} \sum_{s=1}^{m_p} \sum_{r=0}^{m_p+q_{lr}} \beta_{lrpsr} \sum_{k=1}^{n} B_k \alpha_k^{[x]} f_p(x - [x] + s - 1) \tag{27b}$$

(*b*) *For repeated roots of* $\Delta(\epsilon^u)$

$$f_{lra}(x) = \sum_{r=0}^{q_{lr}} b_{lrr} \sum_{k=1}^{\lambda} \sum_{r=1}^{n_k} B_{kr} \sum_{c=0}^{r+[x]-r} \binom{r+c-1}{c} \times \alpha_k^c \phi_l(r + x - r - c) \tag{28a}$$

$$f_{lrb}(x) = \sum_{p=1}^{m} \sum_{s=1}^{m_p} \sum_{r=0}^{m_p+q_{lr}} \beta_{lrpsr} \sum_{k=1}^{\lambda} \sum_{r=1}^{n_k} B_{kr} \times \binom{[x]}{[x]-r+1} \alpha_k^{([x]-r+1)} f_p(x - [x] + s - 1) \tag{28b}$$

In equations 27 and 28:

1. $\binom{a}{b} = 0$ if $b < 0$
2. x is a positive non-integer
3. $\Delta(\epsilon^u)$ has no zero roots

If $\Delta(\epsilon^u)$ has a zero root of the n_0th order then x in equations 27 and 28 should be replaced by $x - n_0$ and $\Delta(\epsilon^u)$ in 25, 20*a*, and 22*a* should be replaced by $\Delta_1(\epsilon^u)$ where

$$\Delta(\epsilon^u) = \epsilon^{n_0 u} \Delta_1(\epsilon^u) \tag{29}$$

Equations 26, 27, and 28 correspond to the extensions of Heaviside's expansion theorem[28] to systems of differential equations.

4. Application to Ladder Networks

Consider the ladder network figure 1. Writing Kirchhoff's equations for any one element we have:

$$Z_3 I_{\mu+1} + Z_3(I_{\mu+1} - I_{\mu+1}) + Z_3(I_{\mu+1} - I_\mu) = 0 \tag{30a}$$

or

$$Z_3 I_\mu - (Z_1 + 2Z_3) I_{\mu+1} + Z_3 I_{\mu+1} = 0 \tag{30b}$$

Equation 30*b* is a difference equation of the second order similar to equation 1 where:

$$f(x) = I_\mu \text{ for } \mu - 1 < x < \mu \tag{31a}$$

$$a_0 = Z_3, \qquad a_1 = -(Z_1 + 2Z_3), \qquad a_2 = Z_3 = a_0 \tag{31b}$$

$$\phi(x) \equiv 0, \qquad n = 2 \tag{31c}$$

From equations 19 we have

$$P(\epsilon^w) = \sum_{k=0}^{2} a_k \epsilon^{kw} = a_0 + a_1 \epsilon^w + a_2 \epsilon^{2w} \tag{32a}$$

$$Q_1(\epsilon^w) = \sum_{k=0}^{2-1} a_{(k+1)} \epsilon^{kw} = a_1 + a_2 \epsilon^w \tag{32b}$$

$$Q_2(\epsilon^w) = \sum_{k=0}^{0} a_{(k+2)} \epsilon^{kw} = a_2 \tag{32c}$$

The roots of $P(\epsilon^w)$ are:

$$\begin{matrix} \alpha_1 \\ \alpha_2 \end{matrix} = \left[\begin{matrix} -a_1 + \sqrt{a_1^2 - 4a_0a_2} \\ -a_1 - \sqrt{a_1^2 - 4a_0a_2} \end{matrix} \right] \Big/ 2a_2; \tag{33}$$

We shall assume that $\alpha_1 \neq \alpha_2$. It must be also noted that:

$$\alpha_1\alpha_2 = 1 \tag{34}$$

Equations 21 reduce, in this case, to:

$$B_1 = 1/(a_1 + 2a_2\alpha_1) \qquad B_2 = 1/(a_1 + 2a_2\alpha_2) \tag{35a}$$

$$B_{11} = (a_1 + a_2\alpha_1)/(a_1 + 2a_2\alpha_1) \qquad B_{12} = a_2/(a_1 + 2a_2\alpha_1) \tag{35b}$$

$$B_{21} = (a_1 + a_2\alpha_2)/(a_1 + 2a_2\alpha_2) \qquad B_{22} = a_2/(a_1 + 2a_2\alpha_2) \tag{35c}$$

Substituting equations 31 to 35 in 24*a* and remembering that $\phi(x) \equiv 0$ and that (see equation 31*a*) $f(x - [x] + s - 1) = I_s$ and $[x] = \mu - 1$ we have:

$$I_\mu = \sum_{s=1}^{2} \sum_{k=1}^{2} B_{ks} \alpha_s^{(\mu-1)} I_s \tag{36a}$$

$$= (B_{11}I_1 + B_{12}I_2)\alpha_1^{(\mu-1)} + (B_{21}I_1 + B_{22}I_2)\alpha_2^{(\mu-1)} \tag{36b}$$

$$= K_1 \epsilon^{\mu \ln \alpha_1} + K_2 \epsilon^{\mu \ln \alpha_2} \tag{36c}$$

Equation 36*c* is the form generally encountered in engineering literature.

One more fact might be brought out before leaving this illustrative problem. Quite often the boundary conditions relate not to 2 successive elements but to the 2 ends of a line (say I_1 and I_N are given). Such cases could be readily worked out by the use of equation 36*b* or equation 36*c*. Thus in equation 36*b*, substitute $\mu = N$ and solve for I_2 thus reducing the problem to the given boundary conditions. On the other hand, if we assume both

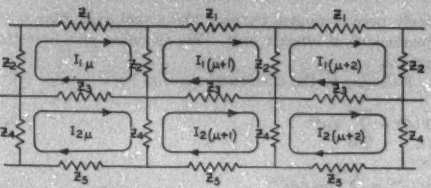

Fig. 2. Schematic diagram of a ladder network

K_1 and K_2 in equation 36*c* to be unknown, then by substituting $\mu = 1$ and $\mu = N$ in equation 36*c* we obtain 2 equations with 2 unknowns. The latter is the classical mode of procedure.

In order to illustrate the use of the solution for systems of difference equations consider the ladder network figure 2. Writing Kirchhoff's equations we have:

$$Z_1 I_{1\,(\mu+1)} + Z_3(I_{1\,(\mu+1)} - I_{1\,(\mu+2)}) + Z_3(I_{1\,(\mu+1)} - I_{2\,(\mu+1)}) + Z_3(I_{1\,(\mu+1)} - I_{1\mu}) = 0 \tag{37a}$$

$$Z_2 I_{2\,(\mu+1)} + Z_4(I_{2\,(\mu+1)} - I_{2\,(\mu+2)}) + Z_3(I_{2\,(\mu+1)} - I_{1\,(\mu+1)}) + Z_4(I_{2\,(\mu+1)} - I_{2\mu}) = 0 \tag{37b}$$

whence:

$$Z_3 I_{1\mu} - (Z_1 + 2Z_3 + Z_3) I_{1\,(\mu+1)} + Z_3 I_{1\,(\mu+2)} + Z_3 I_{2\,(\mu+1)} = 0 \tag{38a}$$

$$Z_4 I_{2\mu} - (Z_2 + 2Z_4 + Z_3) I_{2\,(\mu+1)} + Z_3 I_{2\,(\mu+2)} + Z_3 I_{1\,(\mu+1)} = 0 \tag{38b}$$

Equations 38 are a system of difference equations of the second order similar to equation 7 where

$$I_{1\mu} = f_1(x) \text{ for } \mu - 1 < x < \mu \tag{39a}$$

$$I_{2\mu} = f_2(x) \text{ for } \mu - 1 < x < \mu \tag{39b}$$

$$\phi_2(x) \equiv 0, \qquad m_1 = m_2 = m = 2 \tag{39c}$$

In order to obtain a clearer insight into the correspondence of equations 38 and the system of difference equations 7 we shall write 7 more explicitly for the case at hand. Thus:

$$a_{110}f_1(x) + a_{111}f_1(x+1) + a_{112}f_1(x+2) + a_{120}f_2(x) + a_{121}f_2(x+1) + a_{122}f_2(x+2) = 0 \tag{40a}$$

$$a_{210}f_1(x) + a_{211}f_1(x+1) + a_{212}f_1(x+2) + a_{220}f_2(x) + a_{221}f_2(x+1) + a_{222}f_2(x+2) = 0 \tag{40b}$$

Comparing equations 40 with equations 38 we have:

$$a_{110} = Z_3 \tag{41a} \qquad a_{112} = a_{113} = 0 \tag{41a'}$$

$$a_{111} = -(Z_1 + 2Z_3 + Z_3) \tag{41b} \qquad a_{111} = Z_3 \tag{41b'}$$

$$a_{113} = Z_3 \tag{41c} \qquad a_{220} = Z_4 \tag{41c'}$$

$$a_{120} = a_{121} = 0 \tag{41d} \qquad a_{221} = -(Z_2 + 2Z_4 + Z_3) \tag{41d'}$$

$$a_{131} = Z_3 \tag{41e} \qquad a_{223} = Z_4 \tag{41e'}$$

Referring to equations 12 we have

$$A_{11}(\epsilon^w) = \sum_{k=0}^{2} a_{11k} \epsilon^{kw} = a_{110} + a_{111}\epsilon^w + a_{112}\epsilon^{2w} \tag{42a}$$

$$A_{12}(\epsilon^w) = \sum_{k=0}^{2} a_{12k} \epsilon^{kw} = 0 + a_{121}\epsilon^w + 0 \tag{42b}$$

$$A_{21}(\epsilon^{\mu}) = \sum_{k=0}^{2} a_{21k}\epsilon^{k\mu} = 0 + a_{211}\epsilon^{\mu} + 0 \tag{42c}$$

$$A_{31}(\epsilon^{\mu}) = \sum_{k=0}^{2} a_{31k}\epsilon^{k\mu} = a_{310} + a_{311}\epsilon^{\mu} + a_{312}\epsilon^{2\mu} \tag{42d}$$

The determinant $\Delta(\epsilon^{\mu})$ equation 16 is:

$$\Delta(\epsilon^{\mu}) = (a_{110} + a_{111}\epsilon^{\mu} + a_{112}\epsilon^{2\mu})(a_{220} + a_{221}\epsilon^{\mu} + a_{222}\epsilon^{2\mu}) - a_{210}a_{120}\epsilon^{3\mu} \tag{43a}$$

$$= b_0 + b_1\epsilon^{\mu} + b_2\epsilon^{2\mu} + b_3\epsilon^{3\mu} + b_4\epsilon^{4\mu} \tag{43b}$$

where:

$$b_0 = a_{110}a_{220} \qquad b_1 = a_{110}a_{221} + a_{220}a_{111} \tag{44a}$$

$$b_2 = a_{110}a_{222} + a_{111}a_{221} + a_{112}a_{220} - a_{210}a_{120} \tag{44b}$$

$$b_3 = a_{111}a_{222} + a_{112}a_{221} \qquad b_4 = a_{112}a_{222} \tag{44c}$$

Moreover:

$$\Delta_{11} = A_{22}, \quad \Delta_{12} = -A_{21}, \quad \Delta_{21} = -A_{12}, \quad \Delta_{22} = A_{11} \tag{45}$$

Finally the values of $\beta_{lr\,p_{2r}}$ in equation 25*b* are given in table I.

Table I—Values of $\beta_{lrp_{2r}}$

lrp_{2r}	$r=0$	$r=1$	$r=2$	$r=3$	$r=4$
1111	$a_{220}a_{111}$	$a_{220}a_{112}+a_{221}a_{111}$	$a_{221}a_{112}+a_{222}a_{111}$	$a_{222}a_{112}$	
1112	0	$a_{220}a_{112}$	$a_{221}a_{112}$	$a_{222}a_{112}$	
1121	$a_{220}a_{121}$	$a_{221}a_{121}$	$a_{222}a_{121}$	0	
1122	0	0	0	0	
1211	0	$-a_{111}a_{121}$	$-a_{112}a_{121}$	0	
1212	0	0	$-a_{112}a_{121}$	0	
1221	0	$-a_{121}a_{111}$	0	0	
1222	0	0	0	0	
2111	0	$-a_{121}a_{111}$	0	0	
2112	0	0	0	0	
2121	0	$-a_{121}a_{122}$	$-a_{122}a_{121}$	0	
2122	0	0	$-a_{122}a_{122}$	0	
2211	$a_{120}a_{111}$	$a_{111}a_{111}$	$a_{112}a_{111}$	0	
2212	0	0	0	0	
2221	$a_{120}a_{112}$	$a_{111}a_{112}+a_{111}a_{112}$	$a_{111}a_{112}+a_{112}a_{112}$	$a_{112}a_{112}$	
2222	0	$a_{120}a_{122}$	$a_{111}a_{122}$	$a_{112}a_{122}$	

Assuming that the roots of $\Delta(\epsilon^{\mu})$ are distinct and equal to α_1, α_2, α_3, α_4, and using equation 20*a* where $P(\epsilon^{\mu})$ is replaced by $\Delta(\epsilon^{\mu})$ we have:

$$1/\Delta(\epsilon^{\mu}) = \sum_{k=1}^{4} B_k/(\epsilon^{\mu} - \alpha_k) \tag{46}$$

where

$$B_k = 1/[b_1 + 2b_2\alpha_k + 3b_3\alpha_k^2 + 4b_4\alpha_k^3], \qquad k = 1, 2, 3, 4 \tag{47}$$

Substituting equations 39 to 47 in 27 and the result in 26 and remembering that $\phi_l(x) \equiv 0$ and that (see equation 39) $f_p(x - [x] + s - 1) = I_{ps}$ and that $[x] = \mu - 1$ we have:

$$I_{\mu r} = \sum_{l=1}^{2}\sum_{p=1}^{2}\sum_{s=1}^{3}\sum_{v=0}^{4}\beta_{lr\,p_{2r}}\sum_{k=1}^{4}B_k\alpha_k^{\mu-1}I_{ps}, \text{ where } r = 1, 2 \tag{48}$$

This problem could, of course, have been solved by reducing, through elimination, the system of difference equations to 2 difference equations, each of the fourth order, and each involving only one unknown function. The choice between the 2 modes of solution is determined by the nature of the problem. The above example simply illustrates the applicability of our results and could have been solved through elimination.

5. Extension to Other Boundary Conditions

Quite often, in physical problems, the boundary conditions are not what we assumed in sections 1 and 2 of this paper. In fact, the boundary conditions are often specified at the beginning and end of a network. It needs but a slight addition to this theory, as indicated in the first illustrative problem, to obtain the solution for any boundary conditions whatever.

Consider equations 24 which are solutions of the difference equation 1. Let, for distinct and repeated roots, respectively:

$$A(x) = \sum_{k=1}^{n} B_k \sum_{c=0}^{[x]-1} \alpha_k^{\,c}\phi(x - c - 1) \tag{49a}$$

$$A(x) = \sum_{k=1}^{\lambda}\sum_{r=1}^{n_k} B_{kr} \sum_{c=0}^{[x]-r} \binom{r+c-1}{c} \alpha_k^{\,c}\phi(x - r - c) \tag{49b}$$

Let, for distinct and repeated roots, respectively:

$$H_s(x) = \sum_{k=1}^{n} B_{ks}\alpha_k^{[x]} \tag{50a}$$

$$H_s(x) = \sum_{k=1}^{\lambda}\sum_{r=1}^{n_k} B_{krs}\binom{[x]}{[x]-r+1}\alpha_k^{([x]-r+1)} \tag{50b}$$

Then equations 24 may be written in both cases as follows:

$$f(x) = A(x) + \sum_{s=1}^{n} H_s(x) f(x - [x] + s - 1) \tag{51}$$

In equation 51, $A(x)$ and $H_s(x)$ are both known functions. $f(x - [x] + s - 1)$ is the value of $f(x)$ in the interval $s - 1 < x < s$. In our solution $f(x - [x] + s - 1)$ is given for $s = 1, 2, \ldots n$.

It is our object to show that equation 51 gives an explicit solution even when the boundary values are not given for the first n intervals but for any n arbitrary intervals $k_1 - 1 < x < k_1$; $k_2 - 1 < x < k_2$, $\ldots$ $k_n - 1 < x < k_n$.

In the first place it must be observed that $f(x - [x] + s - 1)$ is periodic in one, or:

$$f((x + k) - [x + k] + s - 1) = f(x - [x] + s - 1) \tag{52}$$

Moreover:

$$x = x - [x] + k_r - 1 \text{ if } k_r - 1 < x < k_r \tag{53}$$

Substituting for x its value from equation 53 in 51 for the various intervals where $f(x)$ is known and using the relation 52 we have:

$$f(x - [x] + k_1 - 1) - A(x - [x] + k_1 - 1) = \sum_{s=1}^{n} H_s(x - [x] + k_1 - 1) f(x - [x] + s - 1) \tag{54a}$$

$$f(x-[x]+k_2-1)-A(x-[x]+k_2-1)=\sum_{s=1}^{n}H_s(x-[x]+k_2-1)f(x-[x]+s-1) \quad (54b)$$

. . . . . .

$$f(x-[x]+k_n-1)-A(x-[x]+k_n-1)=\sum_{s=1}^{n}H_s(x-[x]+k_n-1)f(x-[x]+s-1) \quad (54n)$$

Equations 54 are n equations with n unknowns, the unknowns being the values of $f(x)$ for the first n intervals, *viz.*:

$$f(x-[x]), \quad f(x-[x]+1), \quad \ldots \quad f(x-[x]+n-1)$$

The solutions of equations 54 give these values of $f(x)$ which can now be substituted back in 24. The process is the same for each $f_r(x)$ in a system of n difference equations.

It should be here remarked that if, as is generally the case, some of the boundary values are given for the first β-intervals then the number of unknowns and therefore of equations in 54 is reduced to $(n-\beta)$.

Summary

We have developed 2 expansion theorems applicable to difference equations and to systems of difference equations such as occur in ladder networks. These theorems are given by equations 24, 26, 27, and 28, respectively. The equations presuppose that the boundary conditions are given for the values of $f(x)$ in the first n successive intervals. As, in physical problems, the boundary conditions vary widely, the theorems are adapted to any boundary conditions in section 5 of the paper. Finally 2 problems are worked out in section 4 to illustrate the use of these theorems.

Notations

a_k = constant coefficient in the difference equation 1
a_{lrk} = constant coefficient in the system of difference equations 7
A_{lr} = see equation 12*a*
$A(x)$ = a function defined by equations 49
b_k = coefficient of the kth term of the polynomial $\Delta(\epsilon^w)$
b_{lrs} = coefficient of the sth term in the polynomial $\Delta_{lr}(\epsilon^w)$ see equation 25*a*
B_k = see equation 21
B_{k2} = see equation 21
B_{kr} = see equation 23*a*
B_{krs} = see equation 23*b*
$\binom{a}{b}$ = $\begin{cases} a(a-1)(a-2)(\ldots)(a-b+1)/b! \text{ if } b \geqq 0,\ a \geqq 0 \\ 0 \text{ if } b<0,\ a \geqq 0 \end{cases}$
c = any non-negative integer
$f(x)$ = The unknown function in the difference equation 1 See also equations 6 and 24
$f_r(x)$ = The unknown functions in the system of difference equation 7 See also equations 18, 26, 27 and 28
$f(x+0)$ = $\lim_{\delta \to 0} f(x+\delta),\ \delta>0$
$f(x-0)$ = $\lim_{\delta \to 0} f(x-\delta),\ \delta>0$
$f_{lr\beta}(x)$ = see equations 27*a* and 28*a*
$f_{lr\beta}(x)$ = see equations 27*b* and 28*b*
$F(u)$ = see equations 5
$F_r(u)$ = see equations 12*b* and 15
$H_s(x)$ = a function defined by equations 50
I_μ = mesh current in the μth mesh of the ladder network figure 1
$I_{1\mu}$ = mesh current in the first row of the μth mesh of the ladder network figure 2
$I_{2\mu}$ = mesh current in the second row of the μth mesh of the ladder network figure 2
k = any positive integer
K_1, K_2 = constants defined by equation 36*c*
l = any non-negative integer
m = number of difference equations in the system 7
m_r = order of the difference equation involving $f_r(x)$ in the system of equations 7
$M_1(u)$ = see equation 11
n = order of the difference equation 1
n_k = multiplicity of the root α_k of $P(\epsilon^w)$ (see equation 22*b*) and of $\Delta(\epsilon^w)$
p = any non-negative integer
$P(\epsilon^w)$ = see equation 19*a*
q = any non-negative integer
q_{lr} = the degree of the polynomial $\Delta_{lr}(\epsilon^w)$
$Q_s(\epsilon^w)$ = see equation 19*b*
$Q_{lr\rho s}(\epsilon^w)$ = a polynomial defined by equation 25*b*
r = any non-negative integer
s = any non-negative integer
t = a variable of integration
u = any complex number whose real part is positive
x = independent variable in a difference equation or a system of difference equations
$[x]$ = greatest integer which is equal to or less than x
y = a variable of integration
Z_k = an impedance in the ladder networks figures 1 and 2
α_k = roots of the polynomial $P(\epsilon^w)$ or of the polynomial $\Delta(\epsilon^w)$
$\beta_{lr\rho s}$ = coefficient of the sth term in the polynomial $Q_{lr\rho s}(\epsilon^w)$
$\Delta(\epsilon^w)$ = see equation 16
$\Delta_{lr}(\epsilon^w)$ = the minor of $\Delta(\epsilon^w)$ obtained by omitting row l and column r
$\Delta_1(\epsilon^w)$ = a polynomial having no zero roots (see equation 29)
ϵ = base of napierian logarithms
λ = any positive integer
μ = any non-negative integer
ν = any non-negative integer
$\phi(x)$ = given function in the difference equation 11
$\phi_r(x)$ = given function in the system of difference equations 7
$\phi(x+0)$ = $\lim_{\delta \to 0} \phi(x+\delta),\ \delta>0$
$\phi(x-0)$ = $\lim_{\delta \to 0} \phi(x-\delta),\ \delta>0$
$\Phi(u)$ = see equation 4*b*
$\Phi_1(u)$ = see equation 10*b*
$\psi_k(\epsilon^w)$ = see equation 23*c*
$\psi_{k2}(\epsilon^w)$ = see equation 23*d*
$\Psi(u)$ = see equation 4*a*
$\Psi_1(u)$ = see equation 10*a*

References

1. Wave Transmission Over Non-Uniform Cables and Long-Distance Air Lines, M. I. Pupin. AIEE Transactions, volume 17, 1900, pages 445–512.

2. Dämpfung von Pupinleitungen in Beziehung zur Wellenfrequenz. F. Breisig. *Elektrotechnische Zeitschrift*, volume 30, 1909, pages 683–88.

3. Die Spannungsverteilung an Kettenisolatoren, R. Rüdenberg. *Elektrotechnische Zeitschrift*, volume 35, 1914, pages 413–14.

4. Die Theorie des Kettenleiters nebst Anwendungen, K. W. Wagner. *Archiv fuer Elektrotechnik*, volume 3, 1915, pages 315–32.

5. Spulen und Koordinatorleitungen, K. W. Wagner. *Archiv fuer Elektrotechnik*, volume 8, 1920, page 61.

6. Wanderwellen-Schwingungen in Transformatorwicklungen, K. W. Wagner. *Archiv fuer Elektrotechnik*, volume 6, 1918, pages 301–26 and volume 7, 1919, page 32.

(Concluded on page 152)

A New Electrostatic Precipitator

By G. W. PENNEY
ASSOCIATE AIEE

The cleaning action upon gases of a corona discharge has been known since 1824, however, the technique of electrostatic precipitation has been improved slowly because of the inherent difficulties of the process and the somewhat limited field of its application. With accurately controlled industrial processes and delicate laboratory measurements came the necessary incentive for improving electrostatic precipitation equipment, and recently it has been applied in the field of medicine for the treatment of such maladies as hay fever. The theory of electrostatic precipitation is reviewed briefly in this paper, and a new precipitator is described.

ELECTROSTATIC precipitation has long been recognized as the outstanding method of removing very fine particles from gases, especially at elevated temperatures.

The cleaning of gases by a corona discharge was observed by Hohlfield in 1824. His experiments were extended by Sir Oliver Lodge who made a working installation in a lead smelter in 1884. In 1906 Dr. Cottrell developed a practical form which has been very successful in handling difficult cleaning problems which could not be accomplished by other cleaning methods. The application of electrostatic precipitation has, however, been limited. The most serious factors limiting the use of electrostatic precipitation are as follows:

1. D-c voltages of from 30,000 to 100,000 and appreciable current are required.
2. The space required is large both for the precipitator proper as well as the high-voltage transformer and rectifier.
3. The corona discharge of the conventional precipitator generates so much ozone that the cleaned air, although free of dust, is too irritating to the nose and throat to be used for ventilation.
4. First cost and maintenance are both high as compared to other types of cleaning equipment.

In considering the field of gas purification, the larger particles (above 10 microns) are readily removed by various means, such as centrifugal devices, simple filters, washers, or by viscous coated devices which depend on impinging the particle onto the coated surface. Somewhat finer particles can be removed by the better grade of filters. However, in many cases the dust particles are only a fraction of a micron in diameter. Such particles approach the resolving power of the ordinary microscope. The diameter of these particles is comparable with the mean free path of air molecules. Such particles defy almost all air cleaning devices except precipitation, although in most cases this could not previously be used for the reasons given.

An analysis of the process of precipitation has pointed the way to the development of a new type of precipitator which reduces the size, voltage, power required, and ozone and compounds of nitrogen generated so that this new device can be applied in fields in which electrostatic precipitation was not previously practical.

A paper recommended for publication by the AIEE committee on electrochemistry and electrometallurgy. Manuscript submitted November 6, 1936; released for publication December 2, 1936.

G. W. PENNEY is manager of the electrophysics division of the research laboratories of the Westinghouse Electric & Manufacturing Company, East Pittsburgh, Pa.

1. For all numbered references, see list at end of paper.

Generation of Ozone

In air, the generation of ozone by a given discharge current depends somewhat upon the geometry of the electrodes. By selecting a favorable design of electrode the generation of ozone per unit of current can be limited to a minimum value. The problem then becomes one of designing the precipitator to clean the air with the minimum discharge current. The analysis given in this paper has resulted in a precipitator which gives a generation of ozone which is small as compared with that found in outdoor air in bright sunlight and at the same time the space, voltage, and power required are small as compared to previous practice.

Analysis of Electrostatic Precipitation

The Corona Discharge

The conventional process of electrostatic precipitation uses a wire or system of points at high potential so that there is a corona discharge which carries the dust to the opposite electrode. The forces acting on the particles have been analyzed by R. Ladenburg.[1] The primary effect is an accumulation of charge on each dust particle. The particle is then acted upon by the electrostatic field which carries it toward the electrode of opposite polarity. There is another effect which Ladenburg refers to as the electrostatic wind. This electrostatic wind consists of a movement of air away from discharge points and carries dust toward the collecting electrode. However, the movement of air toward the electrode must also displace air

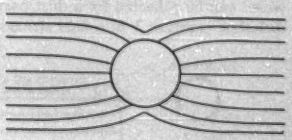

Fig. 1. Sketch showing how an electrostatic field is distorted by a dust particle

away from the collecting electrode. The net result increases the precipitation of dust but it appears to be a very inefficient method. In this paper the electrostatic wind is ignored and an attempt made to develop the most efficient device for charging the particles and attracting them out of the air. The resulting device accomplishes results not considered possible in devices where the electrostatic wind is utilized.

Effect of the Electrostatic Field

The particles are charged in the region of a corona discharge. Here a high local electrostatic field is produced by impressing a high voltage on points or a fine wire. This local voltage gradient is sufficiently high to produce ionization by collision and a self-maintaining discharge. If the point or wire is negative, the positive ions generated in the discharge are attracted to the negative electrode but the electrons are repelled and drift toward the large positive electrode. Probably most of the electrons quickly become attached to air molecules forming negative ions. This space charge forms a high opposing voltage which limits the current and produces a stable discharge.

The electrons or ions drifting through the gas tend to follow the electrostatic lines of flux. Dust particles usually have a dielectric constant greater than one and distort the field tending to concentrate the flux through the particle (figure 1). This drives the drifting charges toward the particle. Any charge on the particle exerts a force tending to repel ions from the particle. The maximum charge which the particle can attain is that at which this repulsive force cancels the effect of the main electrostatic field. Ladenburg's equation expressing the balance of forces acting on an electron just outside the dust particle at this limiting charge is

$$e\left(1+2\frac{k-1}{k+1}\right)E_0-\frac{ne^2}{r^2}=0 \qquad (1)$$

Solving for n,

$$n=E_0\left(1+2\frac{k-1}{k+1}\right)\frac{r^2}{e} \qquad (2)$$

This equation gives the maximum number of electrons which can be collected by a dust particle of radius r and dielectric constant k in a field strength E_0. Experiments

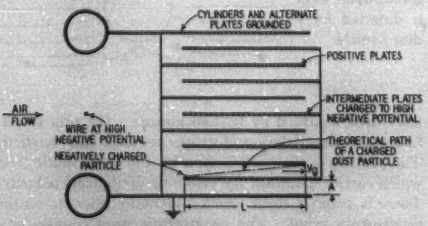

Fig. 2. Cross section of the ionizing unit and parallel dust-collecting plates of an electrostatic precipitator, showing the path of a dust particle

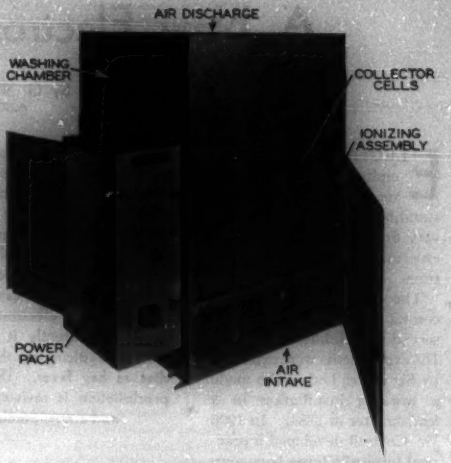

Fig. 3. An electrostatic precipitator developed for use with a spray booth in a pottery plant

indicate that this charge is approached in a small fraction of a second as compared to the 2 to 10 seconds ordinarily required for precipitation in conventional practice.

Effect of Molecular Motion of Electrons or Ions

In addition to the driving force of the electrostatic field the heat or molecular motion of the electrons or ions tends to charge the dust particles. The effect of this heat motion becomes increasingly important as the particle size decreases. Ladenburg considers this effect to be the controlling factor for particles less than $^1/_4$ micron in diameter. When the dust particle is uncharged, the ion will not be repelled but as a charge accumulates on the particle, this charge tends to repel ions so that there will be relatively few ions having sufficient velocity to overcome the repulsive force. This gives a rapid rate of charging the particle as long as the ion velocity required is below the most probable velocity but when the charge on the particle reaches such a value that only a few ions have sufficient energy to reach the dust particle, the charging proceeds very slowly. The mathematical theory is rather long[5,6,7,8] to review here but a few values are given in table I which compares the values of n obtained by this theory with that given by equation 2. The particle will, of course, tend to take the maximum number of charges.

Separation of Particles From the Gas

In the conventional precipitator the charging of the particles and their separation from the gas was accomplished in one chamber with a discharge taking place throughout the length of travel of the gas. Both experiment and theory indicate that the charging of the particles

Fig. 4. The ionizing unit of the precipitator

Fig. 5. Parallel-plate dust-collecting assembly

takes place very rapidly as compared to their separation from the gas. Furthermore, the charging process inherently requires a nonuniform field while for most efficient separation the field should be uniformly high. It has been found possible to make the process much more efficient by first ionizing the particles and then separating them from the gas in the electrostatic field between parallel charged plates.

Figure 2 is a schematic drawing showing a cross section of a precipitator using an ionizing unit and a separate dust collector consisting of parallel plates, alternate plates being grounded and the remaining plates being connected to a source of high d-c potential.

If we assume any given charge ne on a dust particle, in an electrostatic field, there will be a force neE_0 acting to pull the particle toward the opposite electrode. The drift of the particle through the gas is opposed by the viscous resistance of the gas and can be calculated by Stokes' Law.

$$neE = V_d 6\pi\mu r \tag{3}$$

$$V_d = \frac{neE_0}{6\pi\mu r} \tag{4}$$

The velocity of a given charged particle will then be proportioned to the field strength. The time required to travel the distance A perpendicular to the air is given by

$$t_d = \frac{A}{V_d} = A\frac{6\pi\mu r}{neE_0} \tag{5}$$

If we assume such a negatively charged particle moving between 2 parallel electrodes (figure 2) and starting near the negative electrode, the maximum allowable air velocity is that at which the charged particle will just reach the positive electrode before passing out of the region between the plates. The time required to travel the distance L is given by

$$t_v = \frac{L}{V_v} \tag{6}$$

Equating

$$t_d = t_v = \frac{A}{V_d} = \frac{A}{V_v} \tag{7}$$

$$V_v = \frac{LV_d}{A} \tag{8}$$

To secure the maximum capacity, V_v should be as large as possible. It is evident that V_v is inversely proportional to the plate spacing A for a given electrostatic field strength. Over a considerable range of plate spacing the electrostatic field strength can be greater as the plate spacing is decreased, so that the capacity of a given precipitator increases faster than inversely proportional to the plate spacing. The lower limit of plate spacing is usually determined by manufacturing limitations and by space required for the collection of dust.

The arrangement of separate ionization and parallel dust collecting plates has been proposed years ago. But the use of this construction to obtain a more compact and efficient unit for removing low concentrations of dust with a very low generation of ozone and oxides of nitrogen does not appear to have been appreciated.

This discussion has been based on the assumption of streamline flow between parallel electrodes. Actually some turbulence frequently exists but tests have demonstrated that these relations approximate most of the actual conditions and constitute a very valuable guide in the general discussion of precipitation.

Effect of Particle Size

From equation 2 it is evident that the charge collected by a particle due to the effect of the electrostatic field is proportional to the square of the diameter. While from equation 3 the resistance offered by the air is proportional to the first power of the diameter, the allowable velocity is according to this theory proportional to the diameter of the particle to be removed. As the particle size decreases, the heat motion of the ion gives an additional charge

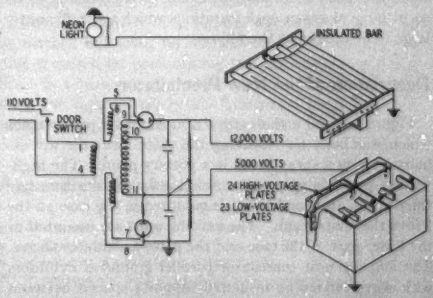

Fig. 6. Wiring diagram of the precipitator

above that due to the electrostatic field so that actually the allowable velocity does not decrease directly with the particle size, although the fine particles are more difficult to remove than large particles.

Retention of Particles on Collecting Electrodes

The electrostatic force exerted by the field on the charged particle acts to carry the particle through the air toward the oppositely charged electrode.

But when the particle touches that electrode if the dust is conducting the charge leaves the particle and a surface charge of opposite sign appears representing the condenser charge of the electrodes. This tends to repel the particle from the electrode. On the other hand, if the particle could be a perfect insulator, at least on the second layer of particles, the charge would remain on the particle and the attraction be maintained. The actual case will be somewhere between these extremes. But in any case we cannot rely on the electrostatic force to hold the particle on the electrode. It must be held by adhesion. Most fine particles normally adhere. In special cases the plates may be coated with oil or other material which will cause particles to adhere, although in this case they adhere so well that cleaning of the plates is very difficult. With some types of dust, it may collect normally but a jar may loosen agglomerations of dust.

Table I—Theoretical Maximum Charge on a Dust Particle

Radius of Particle, Centimeter	Diameter Microns	Dielectric Constant	Maximum Charge Due to Field Equation 2, $E_0 = 5$	Maximum Charge Due to Heat Motion
1×10^{-4}	20	1	1.05×10^4	
1×10^{-4}	20	4	2.1×10^4	2,100
1×10^{-4}	20	∞	3.15×10^4	
1×10^{-4}	2	1	105	
1×10^{-4}	2	4	210	207
1×10^{-4}	2	∞	315	
1×10^{-4}	0.2	1	1	
1×10^{-4}	0.2	4	2	19
1×10^{-4}	0.2	∞	3	

Many cases of this type can be solved by using a simple mechanical filter past the precipitator. Such a filter would not remove the dust in its original, finely divided state but when the dust breaks loose from the plates it tends to do so in large pieces or agglomerations which are sufficiently large to be caught by the filter.

Description of the New Precipitator

Figure 3 shows a photograph of a complete precipitator which was built for removing the glaze from the air exhausted from a spray booth in a pottery plant. The high-voltage power supply unit consisting of transformer, rectifier tubes, and condensers, is mounted in the case at the left of the photograph. The ionizing units are mounted at the lower part of the case and the plate assemblies above. The ionizing unit consists of parallel grounded cylinders with wires carried on insulated supports spaced between the cylinders. The wires are connected to the high-potential power source giving 12 to 14 kilovolts d-c. Figure 4 shows a photograph of an ionizing unit removed from the case.

Some dust collects on the grounded cylinders of the ionizing unit. However, most of the dust is deposited in the dust collection plate assemblies. Figure 5 shows one of these units removed from the case. Alternate plates are grounded, being supported from the case. The remaining or intermediate plates are supported by insulated bars and are charged to a lower voltage than the ionizing units. Figure 6 shows a wiring diagram.

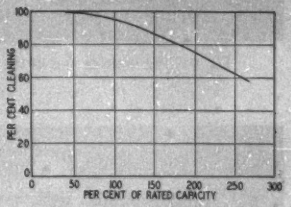

Fig. 7. Efficiency-volume curve of the precipitator

Efficiency of Precipitation

The equations derived on the basis of maximum charge obtainable would indicate 100 per cent efficiency up to a given critical velocity (equation 8) and a rapid reduction in efficiency above this velocity. In practice, this abrupt transition is not obtained for several reasons. Particles vary greatly in size. All particles of a given size do not obtain the same charge because the dielectric constant varies, the field is not uniform over the ionizing region, the shape of the particles vary, and the equations governing the charging of small particles depend on the probable movement of ions and in the smaller particles the numbers involved are too small to give a uniform result. Figure 7 shows a typical curve obtained by test. This shows that we can increase the efficiency of a given unit to almost any desired value by merely reducing the volume of gas cleaned.

The initial development on this precipitator was for the purpose of removing the dust, mainly black smoke particles, from air particularly in cities where soft coal is burned. In this application we are interested primarily in the tendency of the air to blacken wall paper, draperies, merchandise, etc. This characteristic can be measured by drawing the air to be tested at a measured rate, through a piece of white cloth. Figure 8 is a photograph of 3 such samples taken simultaneously. One shows unfiltered air. The second sample shows air which had passed through a common commercial oil-coated filter. On coarse dusts, tests can be made which will give a weight efficiency of over 99 per cent for this same coated filter, but when tested using these fine smoke particles, the cleaning effect of the coated filter was almost negligible. The third sample shows air which had been passed through an electrostatic precipitator.

Another method of determining efficiency is to count the number of particles suspended in the air before and after passing through the cleaning device, using the Greenburg Impinger[3] recommended by the Bureau of Public Health. A test made using a dust of ground silica rock and counting the particles by this method gave the following results:

1. Unfiltered air—430 × 10^7 particles per cubic foot.
2. Air filtered through the viscous coated filter—350 × 10^5 particles per cubic foot or 19 per cent efficiency of cleaning.
3. Air passed through the electrostatic cleaner—2.3 × 10^5 particles per cubic foot or 99.5 per cent efficiency.

Another method of making such particle counts is the electrostatic dust sampler.[4]

The efficiency of a given unit will vary over wide limits based on the method of test. Usually a weight test gives a high efficiency, since the larger particles are efficiently removed and constitute a large portion of the weight. It is possible on filters for instance, to make tests where the weight efficiency will be above 95 per cent and yet the particle count using the impinger may show an efficiency below 20 per cent. The tests used to obtain the curve of figure 7 were made using a smoke and air mixture and measuring the time required to produce a given blackness of a piece of cloth. A condition giving 95 per cent based on this test would give well over 99 per cent using a weight test.

Fields of Application

This type of precipitator is particularly adapted to removing light concentrations of fine dust. Some of the principle fields of application are:

1. Removal of industrial dusts which constitute a hazard to health of employees.
2. Air cleaning to protect delicate apparatus or processes.
3. Air cleaning in homes and offices in soft-coal burning cities to reduce cleaning of walls, draperies, etc.
4. Air cleaning for the relief of hay fever and asthma.
5. Air cleaning in stores to reduce damage to merchandise.

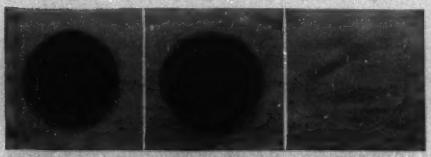

A B C

Fig. 8. Results of passing through cloth filters a volume of 10,000 cubic feet of air cleaned by 3 different methods

A—Uncleaned air
B—Mechanically cleaned air
C—Electrostatically cleaned air

Fig. 9. A type of electrostatic air cleaner used for the relief of hay fever and asthma

In the operation of delicate relays such as automatic telephone switching equipment, considerable trouble may be caused by atmospheric dust which is so fine that it is not removed by ordinary means. Precipitators are giving satisfactory results in such service.

Experimental electrostatic air cleaners have been operated in connection with hot air furnaces and have shown a remarkable reduction in household cleaning required in locations where atmospheric pollution is serious.

Hay fever has been recognized as a disease caused by pollen carried by the air. Some types of asthma are also caused by air-borne dust, some of this dust being very fine. Early in the experimental work on the precipitator, 2 hospital rooms were equipped with electrostatic air cleaners. Very satisfactory results were obtained on hay fever and certain asthma cases. This work has been reported by Criep and Green.[3] Since the publication of this paper even more startling results have been obtained in relieving certain asthma cases. Figure 9 shows a picture of a precipitator designed for this service. This unit consists of a fan, ionizing unit, dust collection chamber, and high-voltage power supply consisting of transformer, 2 rectifier tubes and condensers. It is equipped with a small neon light which glows when the unit is operating. The dust collecting element is easily removed for cleaning and is constructed entirely of metal and porcelain so that it can be washed out using an ordinary hose and nozzle. The time required for precipitating the dust (including ionization) is a measure of the size of the unit. In the unit shown in figure 9 the precipitation time is $^1/_4$ second as compared to 2 to 10 in older conventional precipitators.

Appendix I—Symbols

μ = viscosity of the gas
e = charge on the electron
n = number of electrons on a dust particle
E = electrostatic field strength in volts per centimeter

(*Concluded on page 128*)

Dielectric Strength of Transformer Insulation

By P. L. BELLASCHI
MEMBER AIEE

W. L. TEAGUE
ASSOCIATE AIEE

This paper presents a summary of the results of over 2,000 tests on the dielectric strength of transformer oil and insulating material for impulse, switching, and 60-cycle voltages. From these tests the voltage-time characteristics of the 2 insulations tested may be established over the entire range from a fraction of a microsecond to more than one minute.

THE voltage-time characteristic of insulation is of great importance in engineering and theoretical dielectric problems. A practical case is the early recognition that the time of application of voltage be reduced when testing transformers at industrial frequencies higher than the normal.[1,2] Later when the protection of electrical apparatus against lightning received close attention, naturally insulation was studied in considerable detail in the impulse region which extends from about 100 microseconds to a fraction of a microsecond.[3,4] Recently some data[5,6] have been reported to the AIEE to establish the voltage-time characteristic of insulation over its range up to the order of one minute, but these data are limited in scope. More data are therefore required to establish adequately the voltage-time characteristics of insulation.

The purpose of this paper is to fulfill this need more fully. It presents the data and results of a comprehensive investigation on solid and liquid insulations (0.056- and 0.125-inch fullerboard; 0.25-, 0.50-, and 1.00-inch transformer oil). Some 2,000 tests were made and approximately 750 cathode-ray and magnetic oscillograms recorded. These data permit establishing the voltage-time characteristics of the insulation tested over the entire range from a fraction of a microsecond to beyond one minute. Tests were also made on insulation structures similar to those in large high-voltage electrical apparatus, thus enhancing the usefulness of the investigation. In the paper the technique and test methods developed, always an important factor in fundamental work, are given in detail. These methods can be applied in similar investigations on other insulation materials. Besides the data reported in curve form, other pertinent observations and findings (such as corona, character of breakdown, etc.) are reported, which should be of guidance in the correct interpretation of the mechanism of insulation breakdown.

Test Methods

The voltages which appear on electrical systems may conveniently be classified according to their duration as impulse, switching, and normal-frequency voltages. Means were therefore provided to produce corresponding testing voltages and to measure the voltage and its duration.

Impulse Tests

These tests were made with the standard impulse generator set up to produce a nominal $1^1/_2 \times 40$ microsecond wave. Voltage and time were measured with a cathode-ray oscillograph connected across the test piece through a capacitance divider which was calibrated against a resistance divider. The equipment and general procedure conform to the established practice in impulse testing[7–10]. Typical oscillograms of impulse voltages applied to the test piece are shown in figure 8*A*, *B*, and *C*.

Switching Surge Tests

The circuit in figure 1 was devised for these tests. The surge generator is arranged for a high capacitance (C_s = 0.1 microfarad) and supplies a voltage of 350 kv or less. The generator discharges into a load capacitance of 0.08 microfarad through an inductance of 1.2 henries. The test piece is across the load capacitance. The duration and wave form of the surge across the test piece is fixed by the constants of the circuit and the magnitude can be controlled by the charging voltage applied to the surge generator. A typical oscillogram of the surge voltage employed in these tests is given in figure 8*D*.

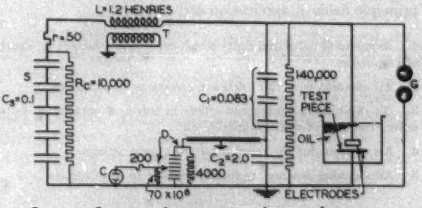

Fig. 1. Circuit and arrangement for switching-surge tests

Resistances in ohms; capacitances in microfarads

C—Cathode-ray oscillograph
D—Voltage divider
G—25-centimeter sphere gap
S—Surge-voltage generator
T—1,000-kva 132-kv transformer

The method of measuring the voltage was by means of the cathode-ray oscillograph connected through the

A paper recommended for publication by the AIEE committees on electrophysics and electrical machinery. Manuscript submitted October 31, 1936; released for publication December 2, 1936.

P. L. Bellaschi is development and research engineer, and W. L. Teague is engineer, for the Westinghouse Electric & Manufacturing Company, Sharon, Pa.

1. For all numbered references see list at end of paper.

Fig. 2. Circuit and arrangement for short-time 60-cycle tests

Resistances in ohms
A—Switch
B—600-kva single-phase 60-cycle generator
C—Circuit-breaker tripout coil
G—25-centimeter sphere gap
M—Release magnet for switch *A*
R—500-kva step induction regulator
R_1—Initiating relay operated by magnetic oscillograph
R_2—Time relay
T—300-kv 150-kva testing transformer
T_1—Current transformer, 5 to 50 amperes
V—Voltmeter coil

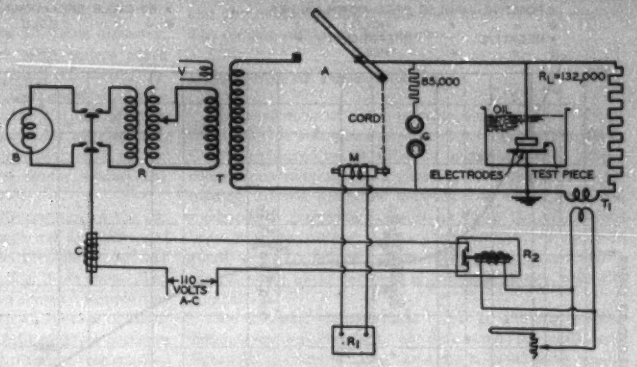

capacitance divider as indicated in figure 1. The capacitance divider was calibrated against a resistance divider connected across the load. The resistance divider calibration established that the wave form of the surge applied to the test object was faithfully recorded at the cathode-ray oscillograph with the capacitance divider. The testing set was also calibrated against a 25-centimeter sphere gap and the relation between the output voltage at the load and the charging voltage of the surge generator was established. The 2 methods of voltage measurement checked within 3 per cent.

Short-Time 60-Cycle Tests

The circuit diagram and test arrangement for the short-time 60-cycle tests are shown in figure 2. The arrangement is such that a voltage of a desired magnitude can be applied for only a short time in the range of 5 to 90 cycles. The voltage was supplied from a 300-kv 150-

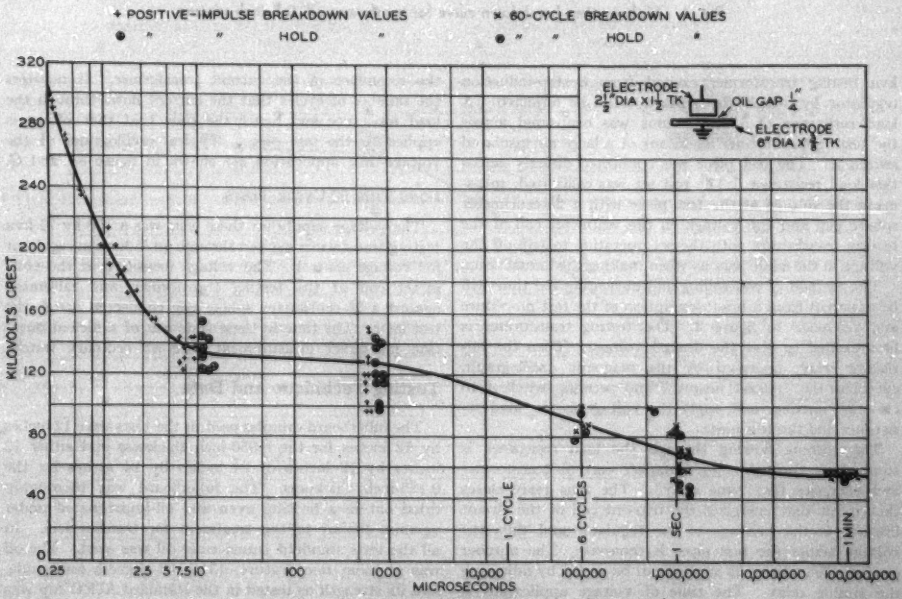

Fig. 3. Voltage-time breakdown curve for transformer oil, 0.25-inch spacing

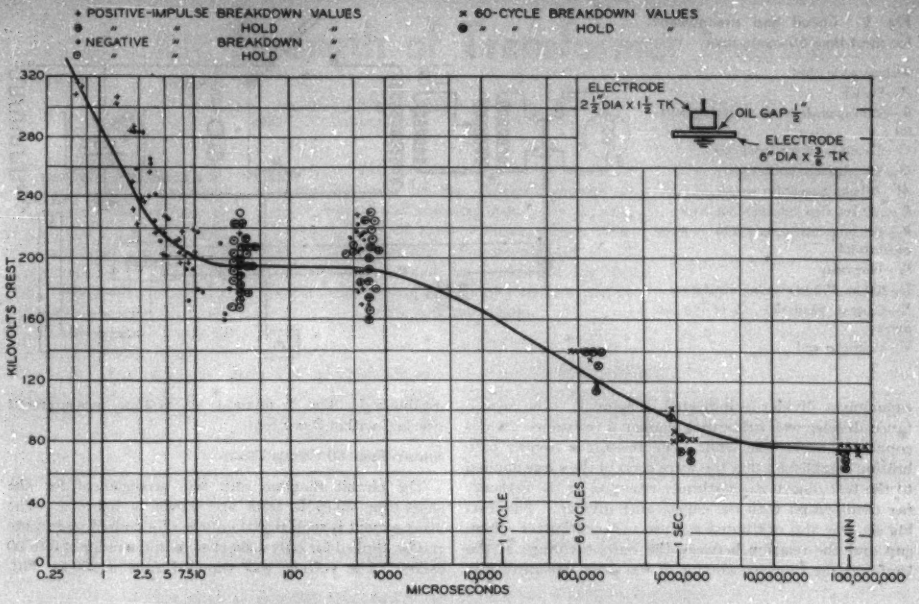

Fig. 4. Voltage-time breakdown curve for transformer oil, 0.5-inch spacing

kva testing transformer excited from a step-induction regulator by which the voltage could be adjusted. A load resistance of 132,000 ohms was connected across the testing transformer by means of a large air insulated switch *A*. The test piece was connected directly across this load resistance. The test set was calibrated, measuring the voltage at the test piece with a 25-centimeter sphere gap and the voltage on the voltmeter coil of the testing transformer with the set operating to trip off the voltage in the same way as when making the actual tests.

The method of controlling and measuring the time will be apparent from a brief description of the test procedure and reference to figure 2. The testing transformer is first excited to give the desired voltage. Then the initiating relay, operated by the magnetic oscillograph, energizes the "release magnet" and permits switch *A* to close by gravity, and apply the voltage to the load resistance and the test piece.

The current flowing through the load resistance is stepped up through a 5/50-ampere current transformer and energizes the "time relay". The time relay closes the circuit that energizes the trip-out coil of the circuit breaker in the primary of the regulator and thus the voltage across the test piece is removed. The number of cycles the voltage is applied can be varied by adjusting the timing relay. The time of voltage application is measured by the magnetic oscillograph connected across the secondary of the current transformer. It registers the number of cycles that the current flows through the load resistance and hence the time that the voltage is applied to the test piece. Typical oscillograms of the voltage-time application are shown in figure 8*F* and *G*.

Long-Time 60-Cycle Tests

The voltage supply for these tests was a 150-kv 75-kva testing transformer excited through an induction regulator for voltage control. The voltage measured at the voltmeter coil of the testing transformer was calibrated against a 25-centimeter sphere gap connected across the test load. The time in these tests was of sufficient duration for direct measurement with an ordinary watch.

Testing Technique and Data

The fullerboard samples used in the tests were 12 inches by 12 inches for the 0.056-inch thickness and either 12 inches by 12 inches or 24 inches by 24 inches for the 0.125-inch thickness. The fullerboard was thoroughly dried out in a heating oven and oil-impregnated under vacuum similar to the treatment for transformers. In all the tests standard transformer oil was used. The oil was at room temperature, 13 to 22 degrees centigrade, and its strength as tested in the standard AIEE cup was between the limits of 28 to 36 kv (root mean square)

which is well above the accepted value for good oil.

In all tests the line electrode was a 2 1/2 inch diameter, 1 1/2-inch thick polished brass disk with square edges and the grounded electrode was a 6-inch diameter, 1/2-inch thick smooth brass plate. The electrodes were arranged coaxially and supported by a rigid Micarta framework. In the oil tests the electrodes were set and rigidly clamped at the desired separation and in the fullerboard tests they were pressed firmly against the test sample.

All tests were started at 60 to 70 per cent of the expected breakdown value. The voltage was first increased in steps of about 10 per cent and as breakdown was approached the steps were reduced to 2 to 3 per cent. The total number of voltage applications on each sample was from a few up to as many as 25 with an average of about 10. In the impulse tests where the breakdown occurred on the front of the wave (figure 8*A*), the first test resulted in failure. A rest period of 2 minutes or more was allowed between repeated voltage applications on a sample.

The minimum corona voltage was determined starting at a low voltage and increasing it in small increments until corona could just be detected. In the impulse, switching, and short-time 60-cycle tests corona was first detected visually, whereas in the long-time 60-cycle tests it was first detected audibly.

From these tests the voltage-time characteristic curves for transformer oil and oil-impregnated fullerboard are plotted in figures 3, 4, 5, 6, and 7. Both the breakdown and the maximum hold values are given on the curves. The corona values are also shown.

Discussion of Tests and Data

The breakdown of oil on impulse, switching, and short-time 60-cycle voltages was somewhat erratic. The variation was reduced to an apparent minimum when proper precautions were taken in cleaning the electrodes, in replacing burned oil from between the electrodes with fresh oil, in removing trapped air from the oil, and in beginning the tests at low voltage and increasing it in small steps to failure. Even with these precautions a spread of 20 to 30 per cent is found as shown in figures 3, 4, and 5.

One inherent characteristic of oil is the long time-to-breakdown on impulses, as illustrated in oscillogram figure 8*C*. In some cases the time-to-breakdown was as great as 25 microseconds, as can be seen in figure 4.

No corona could be observed previous to breakdown in any of the tests on oil except there appeared to be a slight amount just preceding breakdown of the 1-inch spacing in the short-time 60-cycle tests. Most of the failures occurred from the edge of the line electrode, though for the 1-inch spacing a considerable proportion was from the face of the line electrode.

Tests with positive and negative impulse and switching voltages were made on the 1/2-inch oil gap. There is no marked difference in breakdown voltage for the 2 polar-

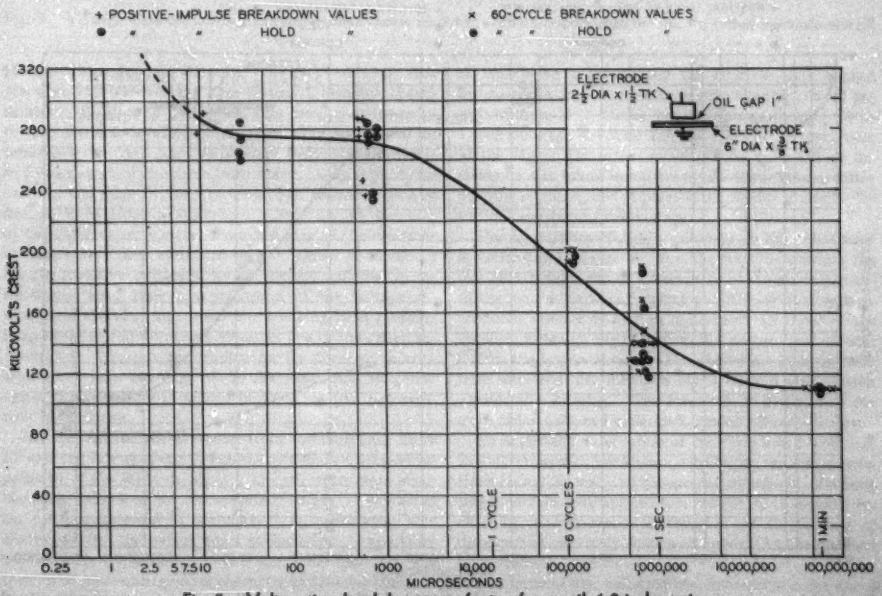

Fig. 5. Voltage-time breakdown curve for transformer oil, 1.0-inch spacing

ities, though the negative breakdown values are on the average somewhat greater than the positive. In the short-time 60-cycle tests the polarity of the 60-cycle voltage at failure could be determined from the magnetic oscillograms. Of 22 tests, 15 failed on positive polarity.

The voltage-time characteristic curves for the $^1/_4$-inch, $^1/_2$-inch, and 1-inch oil gaps (figures 3, 4, and 5) are essentially of the same form. They are flat in the region between 10 to 1,000 microseconds, rise rapidly for impulse voltages shorter than 10 microseconds and fall gradually from 1,000 microseconds to one minute. The close similarity of the 3 curves can be seen by comparing the ratios of voltage at any time value to the one-minute voltage (impulse ratio). For example, the impulse ratios for the $^1/_4$-inch, $^1/_2$-inch, and 1-inch oil gaps are respectively 2.4, 2.6, and 2.5 at 40 microseconds. The relation between voltage breakdown (V) and oil gap spacings (d) for these curves is closely expressed by $\log V = 0.5 \log d$.

The voltage-time characteristic curves of oil-impregnated fullerboard tested in transformer oil are given in figures 6 and 7 for 0.056-inch and 0.125-inch thicknesses respectively. In these tests breakdown was definitely preceded by corona. In the impulse tests the corona voltage for the 2 thicknesses appeared at approximately 45 per cent of breakdown voltage. On increasing the impulse voltage above the corona value visible streamers in increasing length extended from the edge of the line electrode along the surface of the fullerboard reaching a length at breakdown of about $2^1/_8$ inches for the 0.056-inch fullerboard and $3^1/_8$ inches for the 0.125-inch fullerboard. These observations of corona were confirmed by the inspection of the marking on the fullerboard after test. The maximum time-to-breakdown in the impulse tests on fullerboard occurred near the crest, figures 6 and 7 and oscillogram figure 8B, as compared to the long time breakdown in oil. It is of interest to note that the corona voltages of the 2 thicknesses of fullerboard (60 kv and 95 kv) correspond closely to the estimated breakdown voltage for the same spacing of oil gaps.

An important observation is the nature of breakdown. For the positive polarity impulse tests somewhat more than 80 per cent of failures for the 2 thicknesses of fullerboard were from the face of the line electrode and less than 20 per cent were from the edge. Whereas for the negative polarity tests, which were made on the 0.125-inch fullerboard alone, only 35 per cent of the failures were from the face of the electrode and 65 per cent occurred at the edge. The location of these failures indicates the grading effect of the positive streamers on the edge of the line electrode and also suggests a considerable voltage drop along the length of the streamer from the base to the tip. Apparently negative impulse streamers are of a different character than the positive and do not produce the same grading effect on the edge.

The length of the corona streamers for the switching surges (oscillograms, figures 8D and E) were considerably

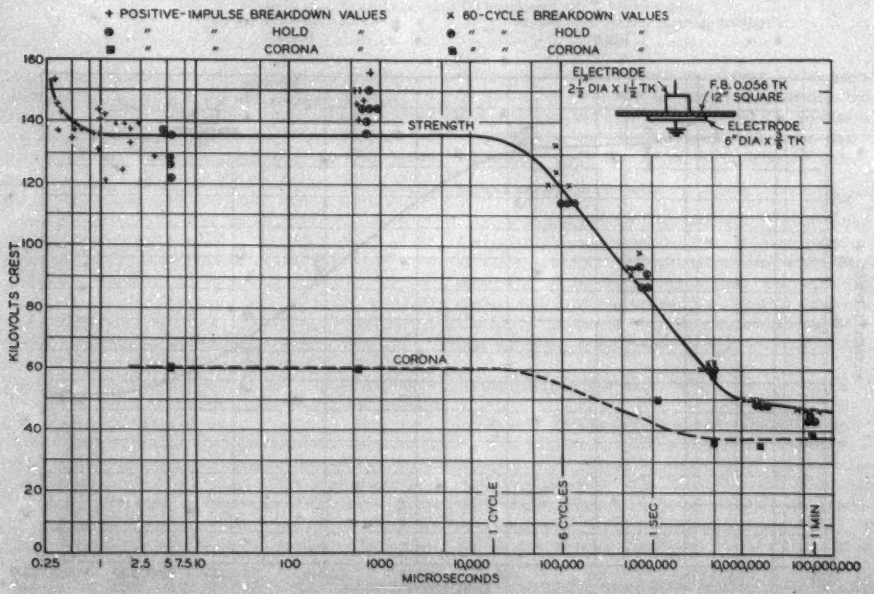

Fig. 6. Voltage-time breakdown and corona-time curves for 0.056-inch oil-impregnated fullerboard tested in transformer oil

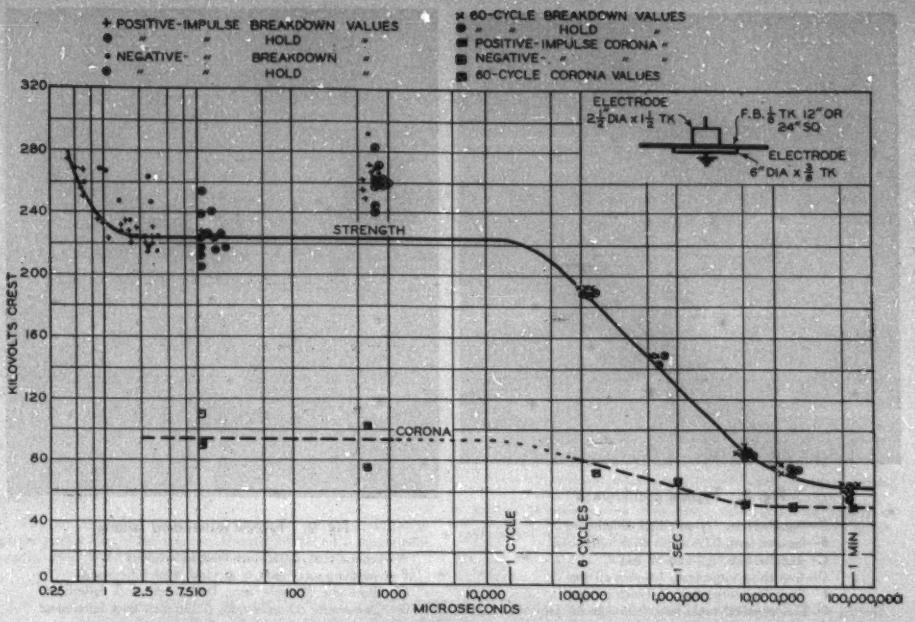

Fig. 7. Voltage-time breakdown and corona-time curves for 0.125-inch oil-impregnated fullerboard tested in transformer oil

greater than for the impulse. In fact creepage took place at 160 kv over the edge of the 12-inch by 12-inch samples, 0.125-inch thickness, this making it essential to use 24-inch by 24-inch samples. The location of the breakdown for the positive polarity switching surges was in 55 per cent of the tests from about $^1/_2$ to $1^1/_2$ inches outside the edge of the line electrode. These points of failure were from a streamer. The other 45 per cent of the failures were either from the edge of the electrode or from the face near the edge. These observations for the positive switching surges suggest that due to the relatively long time of application of the voltage the streamers develop into a more conducting path resulting frequently in failure from a streamer rather than from the electrode. The points of failure for the negative polarity were at or near the edge of the electrode, thus indicating again the difference in nature between positive and negative breakdown.

In the short-time 60-cycle tests (oscillograms figure 8*F* and *G*), 12 out of the 13 failures occurred on the positive polarity of the 60-cycle wave. The streamers were about the same length as for the switching surges. One-half of the failures occurred on streamers $^1/_4$ to 1 inch away from the electrode, the others were at the edge. Apparently the nature of breakdown for the short-time 60-cycle tests is of the same general character as that for the positive switching surges. Further evidence on the nature of breakdown is given from the 60-cycle tests applied for durations from 5 seconds to one minute. In 80 per cent of these tests, failure occurred on a streamer $^1/_4$ to 1 inch from the electrode and the other 20 per cent were at the edge. The extent of the visible corona from the electrode was much less pronounced than for short-time 60-cycle switching and impulse voltages, due undoubtedly to the lower breakdown voltage.

The appearance of the breakdown in the fullerboard is illustrated in figure 9. For the impulse voltages the failures are distinctly of a disruptive character with practically no indication of burning. The switching tests produced failures similar in appearance to those of the impulse, although the extent of the rupture was greater due to the larger current. The short-time 60-cycle tests were somewhat disruptive in character and also showed considerable burning. The 5 seconds to one minute 60-cycle failures showed a decided burned effect.

An important observation of the fullerboard tests was in connection with the surface marking on the test sample. Even though as many as 25 repeated impulse or switching surge voltages were applied to a sample up to breakdown, entailing profuse corona discharges, yet the amount of damage was extremely small and appeared to be confined to the surface layer.

The form of the voltage-time characteristic for the 2 thicknesses of fullerboard (figures 6 and 7) is of the same

Fig. 8. Typical oscillograms

A—Impulse tests, 1/8-inch thick fullerboard
B—Impulse tests, 0.056-inch thick fullerboard
C—Impulse tests, 1.0-inch oil gap
D—Switching surge tests, 1.0-inch oil gap
E—Switching surge tests, 1.0-inch oil gap
F—Short-time 60-cycle tests, 0.25-inch oil gap
G—Short-time 60-cycle tests, 1.0-inch oil gap

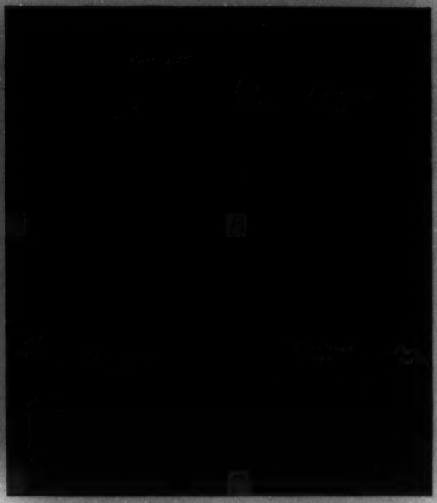

Fig. 9. Typical fullerboard failures

A—Impulse tests, 0.056-inch thick fullerboard
B—Switching surge tests, 0.056-inch thick fullerboard
C—Short-time 60-cycle tests, 0.056-inch thick fullerboard
D—One-minute 60-cycle tests, 0.056-inch thick fullerboard

type. As compared to the characteristic of oil however, the fullerboard characteristic is flat for a greater range of time in the impulse and switching surge regions. The fullerboard curves are flat from 2 to 10,000 microseconds, rise for shorter times than 2 microseconds, and fall quite rapidly from 10,000 microseconds to one minute. The corona curves are of similar shape. The data points are quite consistent from 6 cycles to one minute. In the switching surge region the spread in the points is about 20 per cent, which is the same as in the impulse region, but the values are higher than for the long impulses, apparently due to a better grading effect.

The impulse ratio for the 2 thicknesses of fullerboard is of the same order for the entire range of time and at 2 microseconds the average is 3.1.

The relation between voltage strength (V) and thickness over the greater range of the 2 curves for fullerboard is expressed by $\log V = 0.6$ to $0.7 \log d$.

Combined Solid and Liquid Insulation

To further extend the investigation, tests were made on a barrier structure of 2 0.056-inch thick, 36-inch by 36-inch fullerboard sheets and 3 1/8-inch oil ducts arranged alternately. A 4-inch disk and a plate were used for the line and the ground electrodes, respectively. Impulse tests were made by applying 100 repeated applications at each voltage setting up to failure. The one-minute 60-cycle breakdown strength was also established. The average test values were 300, 300, 280, and 130 kv for 0.35 microsecond, 2.5 microseconds, full 40 microseconds, and one-minute 60-cycle test (crest), respectively. These results show an average impulse ratio of 2.2. These tests for a large number of repeated impulses confirm the constant strength over the impulse region even down to the very short times, as previously established.[4] For the longer times these values indicate the same form of voltage-time characteristic as shown for the fullerboard and oil alone.

Though this barrier and the fullerboard and oil alone are elements of electrical apparatus insulation, they do not conform to the best design structure used in practice. Therefore 2 power transformers, a 132 kv core-type and a 132 kv shell-type were tested, as shown in figure 10. The impulse tests from 1 microsecond and less were made with a 24-inch rod gap chopping the wave on the front.[11] From about 2.5-microsecond duration to the 40-microsecond full wave the tests were made in the same manner as in the recommended practice[12,13] using a test rod gap. Switching surges limited by a 38 1/4-inch co-ordinating rod gap were made on the core-type transformer and in a few of the tests the gap actually flashed over. Furthermore this transformer had previously been used in the switching surge tests in the set-up of figure 1 and had been subjected to more than 500 of these tests from 350 kv and less.

The standard one-minute 60-cycle test had also been made.

The dotted line at 860 kv (391 × 2.2) shows the maximum permissible impulse test level corresponding to the standard AIEE 60-cycle test.[3,4] It will be seen that the tests above this line in region *E* encroach on the margin of the insulation impulse strength. The tests in region *D* verify the adequate impulse strength levels of the transformers. The tests in region *C* represent AIEE recommended impulse tests.[12,13] The highest switching tests are indicated at *B*. These tests on the transformer are amply indicative that the voltage-time characteristic of this and other apparatus of the kind is similar in shape to that for the oil and fullerboard. These large numbers of tests over the entire time range, from a fraction of a microsecond to a minute, indicate that impulse and 60-cycle tests are sufficient to establish the adequacy of a transformer design for practically all conditions of service.

Conclusions

1. In the oil tests corona and breakdown apparently occurred simultaneously.

2. The impulse ratio at the full impulse wave for the oil tested is approximately 2.5. The average strength of the oil is practically constant from 15 to 1,000 microseconds.

3. In the fullerboard tests even though profuse corona preceded breakdown, no appreciable damage could be observed on the insulation.

4. The strength of fullerboard is practically constant from 2 to 16,000 microseconds. Over this range the impulse ratio is close to 3.1.

5. In the fullerboard tests a distinct difference was found in the nature of breakdown between the positive and the negative polarity as indicated by the corona streamers, the failures and the 60-cycle tests.

6. The character of the breakdown for the impulse, switching, short-time 60-cycle, and long-time 60-cycle voltages was progressively from a distinct disruptive character to a burning effect.

7. The strength of fullerboard and oil is essentially the same for switching surges as for impulse voltages at the full 40-microsecond wave. This characteristic and the tests on the transformers indicate that 60-cycle and impulse tests are proof of the adequacy of design for practical service conditions.

References

1. Insulation Tests of Transformers as Influenced by Time and Frequency, F. J. Vogel. AIEE Transactions, volume 43, 1924, page 348.

2. Effects of Time and Frequency on Insulation Test of Transformers, V. M. Montsinger. AIEE Transactions, volume 43, 1924, page 337.

3. Factors Influencing the Insulation Co-ordination of Transformers, F. J. Vogel. AIEE Transactions, volume 52, 1933, page 411.

4. Factors Influencing the Insulation Co-ordination of Transformers—II, P. L. Bellaschi and F. J. Vogel. Electrical Engineering (AIEE Transactions), volume 53, June 1934, page 870.

(*Concluded on page 137*)

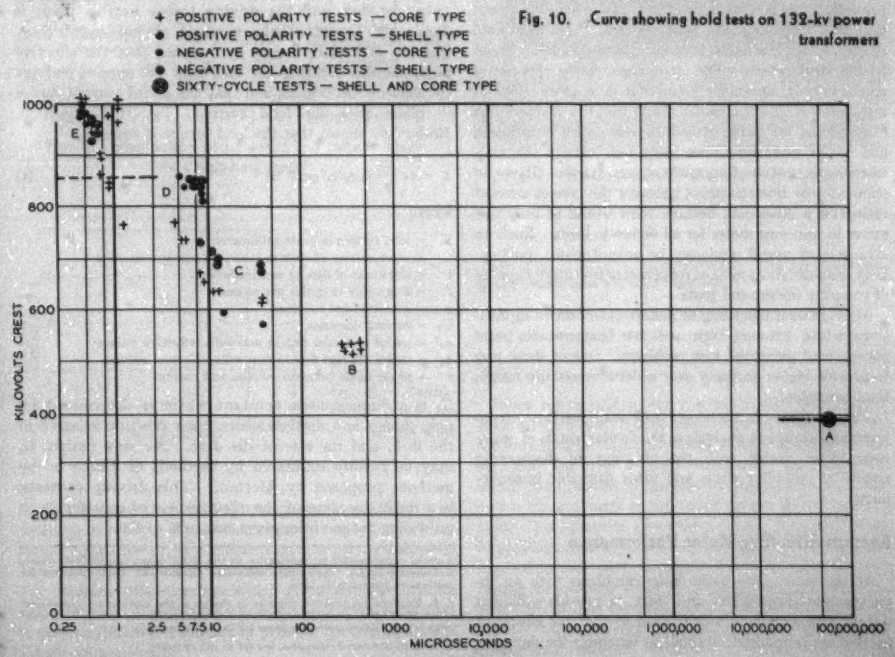

Fig. 10. Curve showing hold tests on 132-kv power transformers

Development of a Modern Watt-Hour Meter

By I. F. KINNARD
MEMBER AIEE

H. E. TREKELL
ASSOCIATE AIEE

A comprehensive discussion of the factors affecting the performance of a watt-hour meter is presented in this paper, and the general discussion is applied to a description of the development of a new type of domestic watt-hour meter. Design and performance data on the new meter also are presented.

THE a-c watt-hour meter has undergone many stages of development and improvement since the first ac-dc meter designed by Thomson in 1889 and the first induction watt-hour meter by Shallenberger in 1894. Meters have grown smaller, they have become much more accurate under varying load conditions, and their cost has been reduced. There has been a definite tendency to increase the current range over which a meter will operate successfully. Another important improvement has been the minimizing of errors due to variations in ambient temperature. Both of these features are of particular significance when considered from the standpoint of modern metering conditions.

Watt-hour meters as they exist today have built up a deserved reputation for accuracy and reliability and at first thought it might appear that further attempts to improve performance might be unwarranted, if not impossible. When carefully analyzed, however, it is evident that the "long range accuracy" that has been built into recent meters has really been an attempt to reach closer to the ideal, which would be a single meter capable of measuring all currents encountered in a given class of installations. Such a meter would simplify the problem of providing for future growth of load on an installation and at the same time adequately take care of the very small loads that are frequently of importance. It would eliminate the uncertainty of choosing the correct current rating for a given job, because there would be only one meter to use—one meter for all domestic loads. Such an arrangement would obviously be advantageous, particularly from the standpoint of reduction in inventory expense of complete meters and parts.

More general mounting of meters out-of-doors in locations where extreme high and low temperatures were encountered presented new problems. One of these was to provide higher accuracy over wider temperature ranges than heretofore.

There appeared, therefore, sufficient justification to warrant a complete analysis of the fundamentals of watt-hour meter design with the objective of discovering means of providing these and other desirable improvements.

Factors Affecting Meter Performance

At the outset, the basic design problems with an induction watt-hour meter are: first, to provide sufficient torque with a minimum of friction so that the effects of friction are minimized; second, to minimize the damping effects of the a-c fluxes in order that the performance will be good at abnormal voltages and at heavy loads; third, to decrease the inherent lagging angle and the potential circuit watts loss in order that wave form, frequency, low power factor, and class II temperature errors will be minimized. The induction meter is inherently accurate but it is these details that are the main causes of any inaccuracy. A good design must incorporate a consideration of all these factors.

Analysis of Element Driving and Damping Torques

To analyze the inherent effects of the a-c fluxes in the driving element of a watt-hour meter, it is well to consider how these fluxes determine the element driving and damping torques. At normal conditions of load—that is, rated frequency and voltage, unity power factor, and nominal-load current, there will be established definite values of flux, and the driving torque at this point is commonly known as the nominal or full-load torque. For this condition, it may be assumed that the effective potential flux crossing the disk lags the applied voltage by 90 electrical degrees and that the useful current flux is in phase with the load current. For this condition, Jimbo[1] has shown that the load torque is equal to

$$T = 4\pi \frac{stf}{g} G_d \phi_v' \phi_i' \cos\theta \, 10^{-8} \qquad (1)$$

where

T = load torque in gram-millimeters
s = conductivity of disk in mhos per centimeter cube
t = thickness of disk in centimeters
f = frequency in cycles per second
g = gravitational constant
G_d = driving constant
ϕ_v' = useful potential flux in maxwells, effective values
ϕ_i' = useful current flux in maxwells, effective values
θ = phase angle between voltage and current

G_d is a dimensionless constant which is determined by pole shapes and displacements, their position relative to the disk, and the size of the disk. For any design, G_d may be readily estimated by methods of Jimbo or by methods proposed by Morton.[2] This driving constant is a direct measure of the effectiveness of any design in producing torque from given amounts of flux.

A paper recommended for publication by the AIEE committee on instruments and measurements. Manuscript submitted October 30, 1936; released for publication December 3, 1936.

I. F. KINNARD is executive engineer in charge of the engineering department of the West Lynn works, General Electric Company, Lynn, Mass. H. E. TREKELL is meter development engineer for the same company.

1. For all numbered references, see list at end of paper.

The current and potential fluxes not only produce a driving torque but each also provides a damping torque which in the case of the current flux is the major cause of heavy-load droop, and in the case of the potential flux is the major cause of meter voltage errors. These damping torques are expressed as follows:

$$T_i = \frac{s\omega}{g} G_i (\phi_i')^2 10^{-8} \quad (2)$$

$$T_e = \frac{s\omega}{g} G_e (\phi_e')^2 10^{-8} \quad (3)$$

where

T_i = current flux damping torque in gram-millimeters
T_e = potential flux damping torque in gram-millimeters
ω = speed of disk in radians per second
G_i = current damping constant
G_e = potential damping constant

These damping constants are also dimensionless and depend upon the inherent meter design. The designer's problem is to provide the useful potential and current fluxes from appropriate windings, so designing the magnetic structure that the driving constant G_d is as large as possible and the damping constants G_i and G_e are as small as possible. By knowing these constants, the inherent qualities of any element are largely established although there are other features that must be considered. For instance, the structure which gives desirable driving and damping constants may not be at all practical in that it may be difficult to efficiently provide the required magnitude of a-c fluxes.

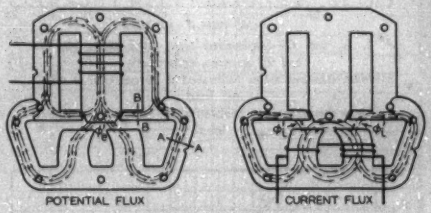

Fig. 1. Distribution of potential and current fluxes in a watt-hour meter

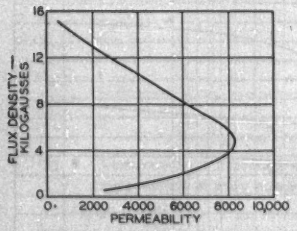

Fig. 2. Permeability curve for silicon steel

Equations 1, 2, and 3 have further value for they show that:

1. The a-c damping torques in a meter are proportional to the meter speed so it is desirable to make the nominal speed as small as possible. This is accomplished by the use of a high-strength control magnet.

2. For small current damping, the ratio ϕ_e'/ϕ_e' should be small and for small potential damping the inverse is true. The final choice depends upon the errors and the relative ease of correcting for them in the design.

3. For given amounts of flux, the driving torque is proportional to frequency so that for the higher frequency ratings the damping effects of the a-c fluxes are relatively smaller. The damping torques do not depend upon the rated frequency.

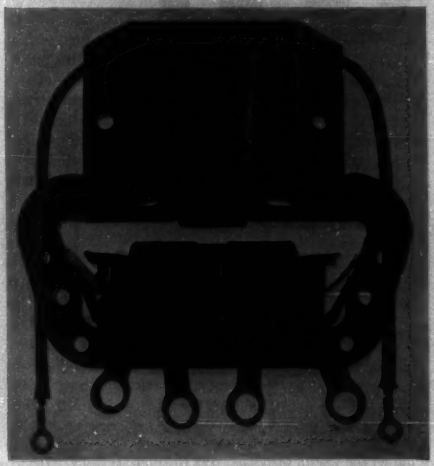

Fig. 3. Element assembly of a new 3-wire domestic watt-hour meter

High-conductivity aluminum is used for the disk because of the superior torque to weight ratio that results.

The Voltage Curve

Since commercial power systems usually hold voltage within 10 per cent, it is necessary that a meter be correct for only a rather limited voltage range. Because of this and since the error is easily corrected in the design, the useful potential flux in modern watt-hour meters is usually 4 or 5 times as large as the useful current flux at nominal load. This practice gives less current damping torque, improving the heavy load registration curve. A common method in use today to correct for the voltage damping torque or voltage error is to proportion the magnetic structure so that the useful potential flux increases more rapidly than the applied voltage. This has been accomplished[3] without resorting to saturation. In this

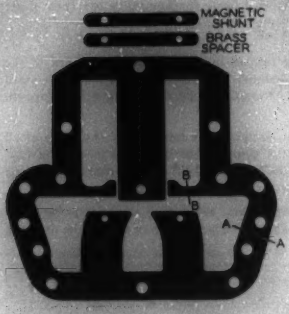

Fig. 4. The type of lamination used for all sizes of watt-hour meters

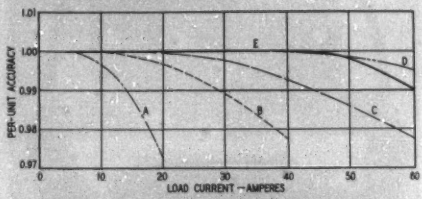

Fig. 5. Heavy-load curves of the new domestic watt-hour meter and the superseded type of meters at unity power factor

A, *B*, *C*, and *D*—Superseded type, rated at 5, 10, 15, and 25 amperes, respectively
E—New domestic meter

scheme, the useful potential flux through sections *A*—*A*, figure 1, works below the point of maximum permeability in the iron and is operated in parallel with the shunt path at section *B*—*B* which works above the point of maximum permeability.

The Load Curve

The factors which determine the shape of the speed-load or meter-accuracy curve, some of which have been previously published,[4] may be divided into 2 classes: (1) those that are significant in affecting the light load performance and (2) those that have the most influence on heavy load performance. These factors include:

1. Ratio of friction to load torque.
2. Variation of iron permeability.
3. Variation of torque due to anticreep holes.

These factors affect light-load performance.

4. Damping effect of current flux.
5. Torque due to load current alone.

These factors affect heavy-load performance.

These 5 factors are the inherent factors in any meter that determine the load curve. A sixth factor which is a powerful tool to correct for error is load compensation which will be considered later in this paper.

Friction. Friction largely determines the reliability of sustained performance and its presence is the principal reason for a high driving torque which minimizes the effect of the friction torque. Friction is essentially constant in value at light loads where it is significant and provides a constant retarding torque which, unless compensated, will cause a drooping characteristic in the registration curve as light load is approached from nominal load. In a meter, this retarding torque is balanced by the light-load adjustment torque. At normal voltage, the 2 torques cancel and the shape of the load curve is not affected. It is very desirable to keep the total friction

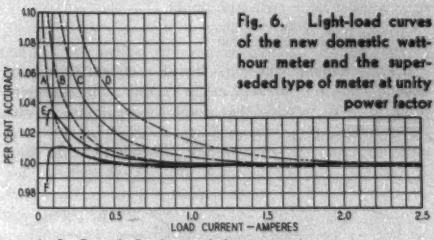

Fig. 6. Light-load curves of the new domestic watt-hour meter and the superseded type of meter at unity power factor

A, *B*, *C*, and *D*—Superseded type, rated at 5, 10, 15, and 25 amperes, respectively
E—New domestic meter calibrated at 10 per cent of nominal load
F—New domestic meter calibrated at 5 per cent of nominal load

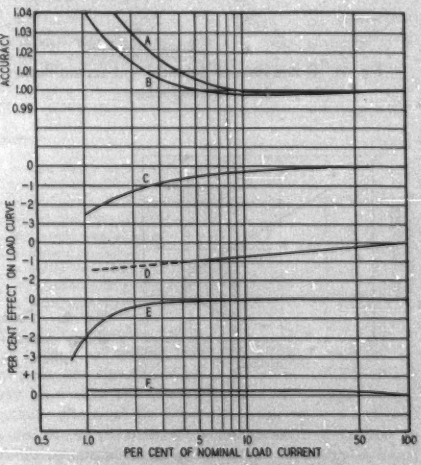

Fig. 7. Components of light-load curve without load compensation at unity power factor

A—Load curve, calibrated at 10 per cent of nominal load
B—Load curve, calibrated at 5 per cent of nominal load
C—Friction
D—Iron
E—Anticreep holes
F—Current damping

torque low in order to decrease variations and to reduce the compensation required. With latest improvements in bearing design which have been described recently,[8] the total bearing and register friction as measured[4] is approximately 0.013 gram-millimeter. With a nominal load torque of 52 gram-millimeters, the friction represents only 0.25 per cent of the torque at 10 per cent nominal load. In the earlier days of the metering art, friction was a greater limitation, and the introduction of high-torque meters was a significant advance. Further refinements in bearings which give long life and low friction have reduced the effect of friction until other factors at light load are equally or more important.

Iron Permeability. With iron in the element magnetic circuit, the current flux is usually more than proportional to the load current. This is due to the fact that in most designs the current flux magnetic circuit operates below the point of maximum permeability. The effect on the load curve is often confused with friction since the effect of the permeability change is also a drooping characteristic as light load is approached, unless it is corrected by means

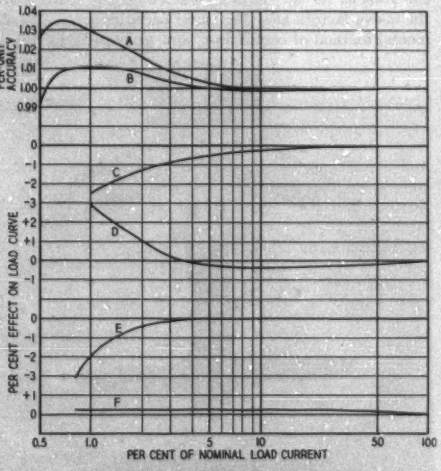

Fig. 8. Components of light-load curve with load compensation at unity power factor

A—Load curve, calibrated at 10 per cent of nominal load
B—Load curve, calibrated at 5 per cent of nominal load
C—Friction
D—Iron
E—Anticreep holes
F—Current damping

of the light-load compensation. Usually the compensation required at 10 per cent nominal load, the usual calibration point, is more than that required at smaller loads so the net result is a rising load curve below 10 per cent nominal load. The effect of the iron can be minimized by the proper choice of magnetic sections, the use of high-

Fig. 9. Heavy-load curves, with and without load compensation, at unity power factor

A—Compensated
B—Uncompensated

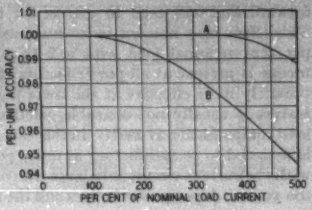

permeability iron, and by using a large main air gap with a large number of ampere-turns in the current coils.

Anticreep Holes. The anticreep holes in the disk reacting with the potential flux cause a small locking torque which must be overcome by load torque due to both current and potential flux before the meter will start. It is in this manner that the anticreep holes keep the disk from rotating when there is no load current flowing even though the light-load compensation torque has an average positive value. At loads just above starting, the meter speed varies due to the anticreep holes and the variation causes the average meter speed to be lower than it would be without the holes. This influence is present to a significant extent only at loads below 5 per cent of nominal rating. It may be considered beneficial because it he ps to correct for the effect of iron permeability variation.

Current Flux Damping Torque. The presence of the current flux damping torque has been explained with the analysis of the element driving and damping torques. The current flux damping torque is the largest cause of heavy load errors. For any design, this error is approximately proportional to the square of the load current since the current damping torque increases as $(\phi_i'^2)$ and ω whereas the load torque is proportional to ϕ_i'. Meter speed ω is proportional to ϕ_i' neglecting the meter error. There has been much progress in design to decrease this inherent error. In early meters, the error at 400 per cent nominal load amounted to as much as 12 per cent, thus limiting the load range for acceptable accuracy within 150 per cent of nominal rating. This error at 400 per cent nominal load had been reduced to less than 2.7 per cent by the year 1927.[9] This was accomplished by designing a meter element to make the best known possible use of the a-c fluxes as regards driving and damping torques, by using a high useful potential flux and a low useful current flux, and by using a strong permanent magnet and a low meter speed. This design gave very good performance without the use of heavy load compensation, giving satisfactory operation up to 300 per cent nominal load and still retaining good operation at light loads.

Current Torque. It is well known by designers and has been experimentally determined that when there is an unbalance in the current flux magnetic circuit caused by having more turns on one current pole than on the other, there will be a driving torque generated in the disk due to the current flux alone. By making the proper pole have the greater number of turns, this torque will be

forward and will tend to correct for heavy load droop. This effect may amount to as much as 1 per cent at 400 per cent nominal load with a 2 to 1 unbalance. This torque is present at all power factors so that it is proportionately more effective at the lower power factors. This feature is usually not desirable, particularly when heavy load compensation is used. In this case, the compensation is designed to be satisfactory at unity power factor so that with the current circuit unbalance the compensation will be too great at lower power factors and the meter will run fast.

Potential and Current Flux Circuits

The design of the current flux circuit is determined largely by the ampere-turns desired, the ratings in which a line of meters must be manufactured, and the space limitations. Provision must be made to include sufficient section so that temperature rise will be small, and the coils must be insulated for abnormal voltages. These features, with a consideration of the driving and damping constants, establish the current pole shapes and the current coil designs.

The potential coil and core must provide useful flux at a phase angle not far from quadrature with the applied voltage. The design problem is to provide sufficient sections so that the watts loss is low. Furthermore, the ratio of resistance to reactance must be as small as possible. This is helped by using a coil of small mean length of turn and a good space factor. The number of potential coil turns should be low, calling for potential air gaps of small reluctance. This takes loss from the copper and places it in the iron where it is not so effective in determining the inherent lagging angle.

Temperature Errors

The causes of temperature errors have been considered by Kinnard and Faus.[7] These errors are divided into 2 classes, depending upon their influence on the meter. These 2 classes are:

Class I. Those errors which affect all loads alike and which are equivalent to a change in magnet strength.

Class II. Those errors caused by a change in phase angle between the useful potential and current fluxes. These errors appear only at lower power factors.

The common method of class I temperature compensation is that described in the paper referred to, in which a material having a negative permeability-temperature characteristic is used to shunt some of the permanent magnet flux. With increases in temperature, the shunt is less effective and the magnet damping strength is held within desired limits. Much research has been undertaken since 1925 to extend the range of compensation to wider temperature differences.

Class II errors should first be minimized by designing with a small inherent lagging angle. The error can be reduced by using lag plates and lag coils of low resistivity-temperature coefficient materials. A common method of compensation, described by Brooks,[8] is to overlag the useful potential flux with a low-coefficient material and then correspondingly lag the useful current flux with a high-coefficient material. With the proper balance, the phase angle will remain unchanged with change in temperature. This method has its disadvantages because it introduces additional watts loss and in some cases makes the low power factor operation poor. A more successful method of class II compensation is described later in this paper.

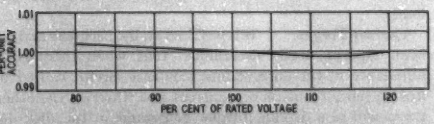

Fig. 10. Voltage calibration curve for the new domestic watt-hour meter

Consideration of a Specific Design

Inherent Accuracy

The real criterion of any meter is its performance, but the reasons for all characteristic curves are related with the above factors affecting meter performance. A fundamental method of comparison and analysis is to prepare a table listing the major design constants for any design. The choice of any design is then very straightforward, for the various factors can be weighed in their true sense. In developing the meter described below, many samples were tested and analyzed. All designs were compared by listing the characteristic constants as

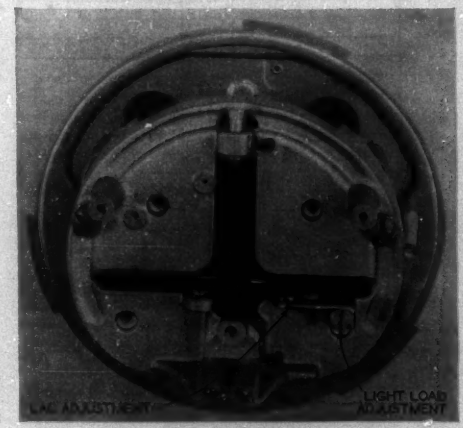

Fig. 11. Interior view of the new domestic watt-hour meter, showing the light-load and lag adjustments mounted on the frame

shown in table I, which in this instance includes only the data for the design finally chosen.

Table I shows the inherent errors of the latest design to be small without compensation. It was found that better and more consistent operation was obtained by thus reducing inherent errors and applying a minimum amount of compensation.

Sufficient amounts of flux and a large driving constant result in a high torque-to-weight ratio. It was necessary to keep the watts loss down to a reasonable value in deciding on flux values.

The slow meter speed and the small damping constants G_1 and G_2 result in small inherent errors for abnormal voltages and heavy loads. Improved compensations then result in negligible resultant errors due to voltage and temperature variations and permit a much longer load range than before possible.

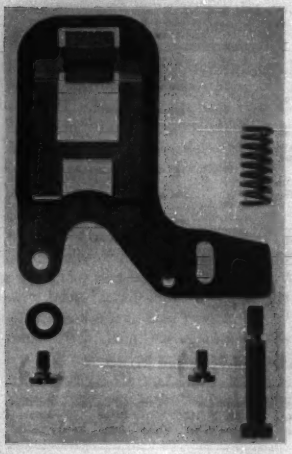

Fig. 12. Lag plate and support, showing class II temperature-compensating device

The choice of current circuit ampere-turns is limited on the low side by the required flux and necessary air gap; it is limited on the high side by the same factors, also heating and volt-ampere burden. The number within this range found to be most suitable for all ratings was 100. This number makes it possible to use an equal number of turns on each current pole on one iron structure for all ratings, 2-wire and 3-wire. This insures most consistent performance and simplifies manufacture and stocking due to having only one iron structure, magnet strength, and adjustment mechanism with which to deal.

Ratings

Figure 3 shows the complete assembled element. Form-wound current coils are used and are readily placed on the current poles. Figure 4 shows the laminations and the load shunt and spacer which are securely attached to the current laminations and also serve to hold the current coils in place. Using this iron structure, 3 self-contained sizes are suggested: a long-range domestic meter, a long-range commercial meter, and a low-capacity meter.

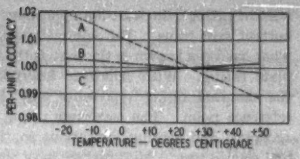

Fig. 13. Temperature calibration curve for the new domestic watt-hour meter

A—Without temperature compensation at 0.5 lagging power factor

B—With temperature compensation at 0.5 lagging power factor

C—With temperature compensation at unity power factor

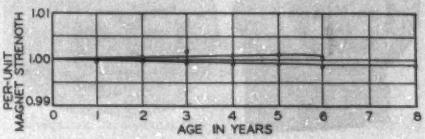

Fig. 14. Typical aging curves for the magnet used in the new watt-hour meter

The domestic meter is proposed for modern home loads, including the latest advances in lighting, appliances, cooking, refrigeration, and air conditioning. At the same time, this meter should measure small loads such as clocks and night lights. A 2-wire 115-volt meter of this type will start at 4 watts and will measure accurately loads up to 6,000 watts.

The commercial meter is intended to handle heavier loads. This meter will start at 16 watts and will measure loads accurately up to 150 amperes.

The low-capacity meter is proposed for use where small loads are of primary importance and provision for higher loads is not required.

It will be interesting to compare the performance of the domestic meter just described with existing meters rated 5, 10, 15, and 25 amperes, respectively. This is shown in figures 5 and 6 where meter accuracy is plotted as a function of load current. At heavy currents up to 60 amperes, the accuracy of the domestic meter is superior to that of any of the 3 lower ratings of the existing meter and about equal to that of the 25-ampere rating. At light loads, its accuracy is definitely superior to the 10-, 15-, and 25-ampere ratings. When the domestic meter is calibrated at 5 per cent nominal load, its performance is superior to the existing 5-ampere meter except from the standpoint of starting watts. Even when calibrated at 10 per cent nominal load, the performance is comparable.

Because of this long load range, the number of essential self-contained ratings required is reduced from 5 to 2. These 2 ratings, together with the proposed low-capacity meter, are shown in table II with the nominal and maximum

current ratings, the watt-hour constant, and the balanced current coil turns. The nominal rating corresponds to what has been known in the past as the full-load or nameplate rating. With improved heavy-load performance, the nominal rating represents only a calibration and reference point. The maximum rating is determined by accuracy and heating limitations so that it does have real significance. All 3 ratings have the same speed and

A B

Fig. 15. Types of the new watt-hour meter

A—Type *A* bottom-connected meter
B—Type *S* socket meter

torque obtained by the use of 100 ampere-turns in the current circuit at nominal load.

The domestic meter has a watt-hour constant of 1.5. This provides a good compromise between the 2 basic meter speed systems in general use today. Assuming all meters concerned to be 100 per cent accurate, a given even number of revolutions of this domestic meter corresponds to integral numbers of revolutions of all watt-hour meter standards now in production. Other possible constants do not have this desirable feature.

The Load Curve

The load shunt not only compensates for heavy load droop but also improves the performance at light loads. Figure 7 shows the light-load curve and the relative values of all the factors comprising it when no compensation is used. These curves are plotted on a semilogarithmic scale in order to expand the extremely light load portions. As described previously the curve rises at light loads due to the effect of the iron.

When the load shunt is applied, figure 8, the droop due to the iron is reduced because the shunt was designed so that its permeability decreases with decrease in load from the nominal rating. This reduces the light-load compensation necessary for correct calibration and the resulting load curve is accurate to lower values.

At heavy loads, compensation for the droop is accomplished as a result of the load shunt approaching saturation so that the current flux is more than proportional to load current. Figure 9 shows the compensated and uncompensated heavy-load curves at unity power factor. The use of balanced ampere-turns on the current poles and

Table I—Analysis Chart of a Watt-Hour Meter

Quantity*	Symbol	Unit	Value
Rated voltage	V	volts	115
Nominal current	I	amperes	12.5
Frequency	f	cycles per second	60
Watt-hour per revolution	K		1.5
Speed at nominal load	ω	radians per second	1.672
Disk diameter	D	inches	3.5
Disk thickness	t	inches	0.027
Disk thickness	t	centimeters	0.0688
Disk weight	W_d	grams	13.3
Torque at nominal load	T	gram-millimeters	83.5
Torque-to-weight ratio	T/W		3.95
Friction constant†	$\frac{T}{W^{4/3}}$		1.67
Potential coil turns	N_1	turns	2,400
Exciting current	I_0	amperes	0.098
Potential coil resistance	R_0	ohms	58
Out-of-phase voltage	I_0R_0	volts	5.5
Potential watts loss	W_iL	watts	1.25
Potential ampere-turns	N_0I_0		238
Total potential flux	ϕ_t	maxwells	13,700
Useful potential flux	ϕ_t'	maxwells	2,490
Current ampere-turns	$A \cdot T$		100
Useful current flux	ϕ_i'	maxwells	495
Current damping torque at nominal load	T_i	gram-millimeters	0.130
Potential damping torque at nominal load	T_e	gram-millimeters	1.17
Driving constant	G_d		0.237
Current damping constant	G_i		1.28
Potential damping constant	G_e		0.455
Inherent droop at 400 per cent nominal load**	R	per cent	3.85
Inherent voltage error at 120 per cent rated voltage‡	S	per cent	0.98
	G_i/G_d		5.63
	G_e/G_d		2.00

* Unless otherwise indicated values are given for nominal load.
† $\cos\phi$ has shown friction to vary as $(W)^{4/3}$.

** $R = 100\,\frac{15\,T_i/T}{1 + 15\,T_i/T}$

‡ $S = 100\left(\frac{(1.2)^2 T_e}{1.2T} - \frac{T_e}{T}\right) = 44.4\,\frac{T_e}{T}$

Table II—Self-Contained Ratings

Meter	Nominal Rating, Amperes	Maximum Rating, K (115 Amperes Volts)		Turns on Current Poles			Nominal Ampere-Turns
				Right	Left	Total	
Commercial	50	150	6.0	1	1	2	100
Domestic	12.5	60	1.5	4	4	8	100
Low capacity	5	20	0.6	10	10	20	100

the particular design of load shunt result in equivalent performance at low power factors.

The Voltage Curve

The inherent voltage error at 120 per cent of rated voltage is shown in table I to be 0.98 per cent. As previously described, this error can be compensated for effectively by the use of the proper sections at *B*—*B* and *A*—*A* in the magnetic circuit (figure 4). The resulting voltage curve obtained is shown in figure 10. It was found possible to reduce the actual error to less than 0.2 per cent for 40 per cent voltage range.

Light-Load and Lag Adjustment

The most straightforward and effective method of providing light-load and lag adjustment in this design was found to be modification of a mechanism already in general use, as shown in figures 11 and 12. The lag

plate is supported in the proper position by a bracket made of high-resistivity alloy. For light-load adjustment, this support is rotated by the light-load adjusting screw. A spring mounted on this screw between the lag plate support and the frame prevents backlash. The lag adjustment is accomplished by moving the lag plate radially with respect to the disk.

Temperature Compensation

Class II temperature compensation is accomplished by a novel method proposed by Faus.[10] The lag plate is made with a small core linking it, composed of a material having a negative permeability-temperature characteristic similar to that used for magnet compensation. This core imposes an impedance in the lag circuit which becomes less effective with increases in temperature so that the lag plate becomes more effective. In this manner, the necessary increase in lagging is obtained to compensate for the shift in flux angles. Figure 13 shows the resulting temperature curves with both class I and class II compensation. Improvements in characteristics of the temperature-sensitive material has made possible more effective compensation of class I errors.

Control Magnet

The control or damping magnet is of standard construction that has been used for many years. It is designed to give a high braking torque, making possible the slow meter speed which is so desirable for improved accuracy and a long load range. Magnets of this form are unusually stable. Figure 14 shows typical aging curves on 2 groups of magnets over periods of 6 and 8 years, respectively. At no time does the strength vary more than 0.2 per cent from the initial value.

Summary

1. It is shown that fundamental analysis of meter theory can be used effectively in meter design and provides a basis of accurate comparison of inherent characteristics.
2. Emphasis is laid on the importance of minimizing the inherent errors, thereby reducing the magnitude of the required compensations. This results in improved accuracy and more consistent performance.
3. Slow meter speeds are desirable from the standpoint of higher accuracies and greater suitability for operation over a long load range.
4. The meter described with long range performance reduces the number of ratings required. It also provides for growth of load without sacrificing light load accuracy.
5. An improved temperature compensation is described which insures accurate registration under conditions of extreme temperature variations.
6. With improved performance, "full load" has lost its significance and should be replaced by a "nominal" and "maximum" rating. Nominal rating aids in comparisons and in calibration, but a maximum rating, corresponding to both accuracy and thermal limits, is the real criterion of a meter's capacity.

References

1. The Characteristics of Induction Watt-Hour Meters, S. Jimbo. Researches of the Electrotechnical Laboratory, Tokyo, Japan, Nos. 255 and 330.
2. Torque in a Bipolar Induction Meter, R. M. Morton. Electrical Engineering, volume 55, April 1936.
3. United States Patent No. 1,771, 929, I. F. Kinnard.
4. Electric Power Metering (a book), A. E. Knowlton. McGraw-Hill Book Company, New York, 1934, chapter VIII.
5. Lubrication Increases Life of Meter Bearings, T. A. Abbott and J. H. Goss. Electrical Engineering, volume 54, April 1935.
6. General Electric type *I*-16 meter.
7. Temperature Errors in Induction Watt-Hour Meters, I. F. Kinnard and H. T. Faus. AIEE Transactions, volume 44, 1925, page 275.
8. Discussion by H. B. Brooks on reference 7.
9. Mechanical Factor of Merit With Respect to Electrical Instruments, J. H. Goss. *General Electric Review*, April 1933.
10. United States Patent No. 2,050,881, H. T. Faus.

Synchronous Machines With Solid Cylindrical Rotor

(*Continued from page 58*)

By equation 22, assuming that e_r also varies as e^{pt}, we obtain the rotor-coil equation:

$$RI_r = e_r + Zk\int_0^c A_1 \cos \alpha x\, E_s(x)dx = e_r - \frac{Kp\left[I_r A_1^2 \cosh \alpha g + \frac{3}{2} A_1 B_1 (De^{-jr} + D'e^{jr})\right]}{\alpha(q \cosh \alpha g + \sinh \alpha g)} \quad (52)$$

where

$$q = \frac{\beta}{\mu\alpha}\left[p + \left(\frac{\alpha}{\beta}\right)^2\right]^{\frac{1}{2}}, K = 2\pi 10^{-9} Zlk$$

Similarly by equation 24, the voltage equation of stator coil a is

$$r_s I_a = e_a + Zk\int_0^c B_1 \cos \alpha x_1 E_s(x_1)dx_1 = Ce^{j\omega t} + C'e^{-j\omega t} + e_a - \frac{K}{\alpha(q \cosh \alpha g + \sinh \alpha g)}\left\{\frac{1}{2} I_r A_1 B_1 [(p + j\omega)e^{j(\omega t + \gamma)} + (p - j\omega)e^{-j(\omega t + \gamma)}] + \frac{3}{2} B_1^2 [D(p + j\omega)e^{j\omega t} + D'(p - j\omega)e^{-j\omega t}][\cosh \alpha g + q \sinh \alpha g]\right\} = r_s(De^{j\omega t} + D'e^{-j\omega t} + i_a) \quad (53)$$

Equation 53 is seen to be composed of 3 components, constant terms, terms containing $e^{j\omega t}$ as a factor, and terms containing $e^{-j\omega t}$ as a factor. By combining this equation with 2 similar equations for coils b and c it may be separated into its 3 component equations. Thus from equations 49 and 53 are formed the 4 final equations 30 given in the body of the paper.

References

1. Fourier Integrals for Practical Applications, G. A. Campbell and R. M. Foster. Bell System Technical Publication B-584, page 58, No. 545-7.
2. Three-Phase Short Circuit Synchronous Machines—V, R. E. Doherty and C. A. Nickle. AIEE Transactions, volume 49, 1930, page 706, equation 15.
3. Transients in Magnetic Systems, C. F. Wagner. AIEE Transactions, volume 53, 1934, page 418.
4. Field Transients in Magnetic Systems, E. Weber. AIEE Transactions, volume 50, 1931, page 1234.
5. Two Reaction Theory of Synchronous Machines—I, R. H. Park. AIEE Transactions, volume 48, July 1929, page 716.
6. Operational Impedances of a Synchronous Machine, M. L. Waring and S. B. Crary. *General Electric Review*, volume 35, November 1932, page 578.
7. Funktionenatlas, E. Jahnke and F. Emde. B. G. Teubner, Leipzig.

A New Service Restorer

By E. F. SIXTUS
ASSOCIATE

W. R. NODDER
NONMEMBER

Equipment capable of restoring service automatically after temporary interruptions on transmission and distribution systems has been developed to a high degree of effectiveness; however, most of such equipment is suitable only for systems of high capacity, and comparatively little attention has been given to systems of low and intermediate capacities. An automatic service restorer, designed primarily for use on systems of low capacity, is described in this paper, and some data on its operating characteristics are presented.

IN RECENT years there has been an increasing demand on the part of operating companies for equipment capable of automatically restoring service after interruptions due to momentary or self-clearing faults on transmission and distribution systems. Where protective equipment of high interrupting capacity is involved, this demand has been met by the use of the conventional oil circuit breaker in conjunction with protective relays and an adjustable timing relay to control the reclosing cycle. This equipment has been developed to such an extent that immediate reclosing breakers, capable of reclosing so quickly that in most cases service will be restored before synchronous motors can fall out of step, are now available for use on systems as high as 115,000 volts.

Up to the present time little has been done to extend the line of automatic reclosing breakers to the lower capacities, due mainly to the fact that the cost of such equipment could not be justified in the low-revenue field where it would be applied. The 7,500-volt breaker with an interrupting capacity of 50,000 kva has so far set the lower limit at which the conventional reclosing equipment has been economically feasible for outdoor service.

A study of outages on rural distribution systems has shown that from 75 to 90 per cent of the faults are momentary and self-clearing, but will blow a fuse and thereby cause a long power outage. It is evident, therefore, that a low-capacity automatic-reclosing breaker, if used in place of fuses, would result in a great improvement in service. Reclosing fuses have, of course, been available but they cannot be expected to give service equivalent to an enclosed high-speed reclosing breaker.

To be completely successful a breaker to fill this low-capacity requirement must have certain very definite characteristics:

1. It must be low in cost—considerably lower than the conventional reclosing breakers now on the market. It must be simple to install, to keep the labor and cost of installation at a minimum.

2. It must be simple to operate, so that it can be opened, closed or reset by an inexperienced person and thus save trained power company employees from making long trips to isolated installations.

3. It must be suitable for outdoor service and for pole mounting.

4. It must provide dependable overload and short circuit protection under all weather conditions with very little maintenance.

5. It should provide at least 3 automatic reclosures with the first reclosure immediate if so desired.

6. It should be multipole with all poles opening simultaneously to prevent single phase operation of three phase equipment.

7. It should trip on extremely low currents, about 10 amperes minimum, to provide dependable overload protection for lightly loaded lines.

After giving careful consideration to the above requirements it was decided that conventional designs must be discarded and it was on this basis that the type *AP*-1 automatic service restorer illustrated in figure 1 was developed.

One of the first problems to be solved in the design of the device was that of securing power to provide 3 automatic reclosures. Two types of control were considered; one where the operating power is derived from a relatively inexhaustible source such as an auxiliary battery and charger unit, or the line voltage or current itself; and the other where the actuating power is derived from an exhaustible source such as a spring.

If an inexhaustible power supply were used it would be necessary for an attendant to visit the switch every time it locked open for the purpose of resetting the lockout mechanism. Assuming that 75 per cent of the shorts are self clearing, the device would lock out and require the service of an attendant after every 4 short circuits.

With an exhaustible power supply, such as a spring that could be wound to provide sufficient energy for 4 openings and 3 reclosures, the attendant would be required to reset the lockout mechanism after every lockout as above and in addition would be required to restore the energy in the spring after every 4 shorts which were cleared, because the spring would be completely unwound. This would result, let us assume, in the attendant making twice as many trips to a device with a spring type of power supply as to one with an inexhaustible power supply. It is possible, of course, that a carrier current control could be used in lieu of an attendant to reset the lockout mechanism, although such an arrangement does not seem economically advisable at present.

The inexhaustible power supply could be provided by:

1. The use of a potential transformer placed in the tank of the device and connected to a small motor arranged to rewind an operating spring and keep it wound at all times.

2. The use of some sort of capacitance device in place of the potential transformer to supply energy to the rewinding motor. The out-

A paper recommended for publication by the AIEE committee on protective devices. Manuscript submitted October 29, 1936; released for publication November 20, 1936.

E. F. SIXTUS is vice-president in charge of sales, Pacific Electric Mfg. Corporation, San Francisco, Calif. W. R. NODDER is an engineer for the same company.

put of such a device would necessarily be small but rewinding could be accomplished over a relatively long period of time, as the spring could be designed to provide enough energy for 4 openings without rewinding.

3. The use of a falling weight heavy enough to provide energy for a large number of operations, possibly 20 or 30.

4. Using the short-circuit current, which causes the device to trip, to store sufficient energy for the next closing and opening operation.

In the design of the type *AP*-1 the first 2 methods listed above were discarded because they added materially to the cost of the device, and it was felt that the increased expense would not be justified in the majority of installations. The third alternative, that of using the falling weight was considered impractical and was not used because of the probable unfavorable reception such construction would receive from prospective users of the device. The fourth idea, that of using the short-circuit current to provide energy for closing and reopening the circuit, was not considered favorable because of the high current required to trip a device of this kind; a low tripping current being one of the requisites of the design.

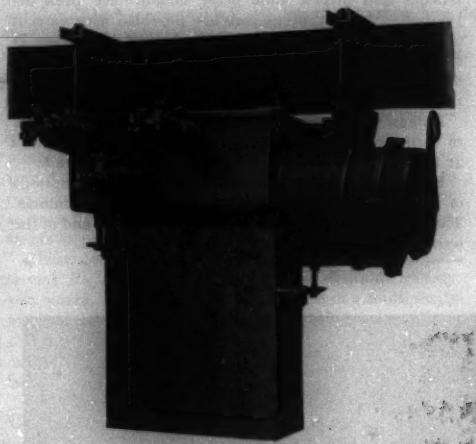

Fig. 1. Type AP-1 automatic service restorer, 7,500/12,500 Y volts

In view of the disadvantages of the inexhaustible power supply as applied to this particular device, the *AP*-1 was designed to use, as an operating mechanism, a manually wound spring which when fully wound, would store enough energy to give 3 closing and 4 opening operations. A helical twist spring was selected because its unidirectional motion was most easily adapted to the reciprocating motion of the switch blades. In actual construction one end of the spring is connected to a rewinding lever and the other, through a 4-to-1 reduction gear, to a crankshaft to which the blades are connected. See figure 2. The 4-to-1 reduction gear is used so that a $\frac{1}{4}$ turn on the rewinding lever will rewind the spring sufficiently for one reclosing cycle and a dial has been added to indicate to what extent the spring is wound. A stop is provided to hold the contacts in the open position upon completion of the last opening stroke.

The crankshaft is fitted with a latch plate engaging a latch to hold the breaker closed with the spring wound. This latch, which is actuated by a series trip coil in each pole, is released on overload permitting the contacts to open at high speed under the action of the helical spring. There being no latch to hold the switch open, it recloses and remains closed until the latch is again released by one of the trip coils, except in the case of the last opening when it locks in the open position.

In order to provide a timing mechanism to control the reclosing interval a special dashpot was developed. Upon attempting to determine the reclosing interval to use it was found that prospective users required different reclosing cycles. Some required an immediate first reclosure and others 3 reclosures at equal time intervals. In order to give the device as wide an application as possible the dashpot was designed so that it could be set to provide either 3 reclosures at an adjustable time interval, or one immediate reclosure with 2 additional reclosures at an adjustable time interval. In each case the reclosing interval is adjustable from 1 to 10 seconds.

The design of the arc-rupturing chamber for such a low interrupting capacity

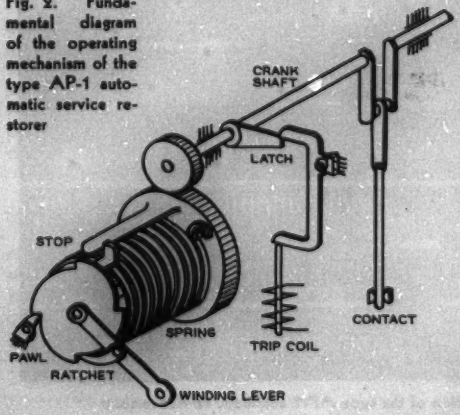

Fig. 2. Fundamental diagram of the operating mechanism of the type AP-1 automatic service restorer

Fig. 3. Cross-sectional view of expulsion contact chamber of the automatic service restorer

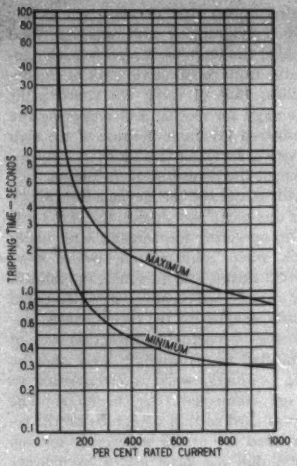

Fig. 4. Time-current curves of delayed trip attachment

device presented no problem, as previous papers have demonstrated the ability of the expulsion chamber contact to easily interrupt currents both greater and smaller than those required in this instance. The contact design used is shown in cross section in figure 3. It consists essentially of a moving blade engaging with high-pressure full-floating stationary contacts and separating at high speed in an enclosed chamber provided with baffles and vents to secure the most efficient arc extinguishing action.

The continuous current rating of the service restorer was set at 100 amperes in order to include the full current range normally covered by fuses. It was felt inadvisable to provide for larger currents because of the desire to keep the dimensions as small as possible and because investigation indicated that a 100-ampere capacity would be ample for most applications.

Consideration was, of course, given in the design to the need for co-ordinating the series trip coils with the blowing characteristics of fuses and the time current characteristics of oil circuit breaker relays. Trip coils for instantaneous and inverse time delay action have been developed. Instantaneous coils are provided with current adjustments so that they can be adjusted to operate at either 100, 150, or 200 per cent of the coil rating. Time-delay coils are provided with current and time adjustments, the characteristics of which are shown in figure 4.

Extensive tests were performed on the service restorer to verify its assigned interrupting rating of 1,200 amperes at 12,500 volts. Typical results are shown in figure 5.

Film *A* shows the performance during 2 interruptions of 1,780 amperes with 2,600 volts across the terminals. The total fault time in the first case is 7.0 cycles and in the second 7.4 cycles.

(*Concluded on page 152*)

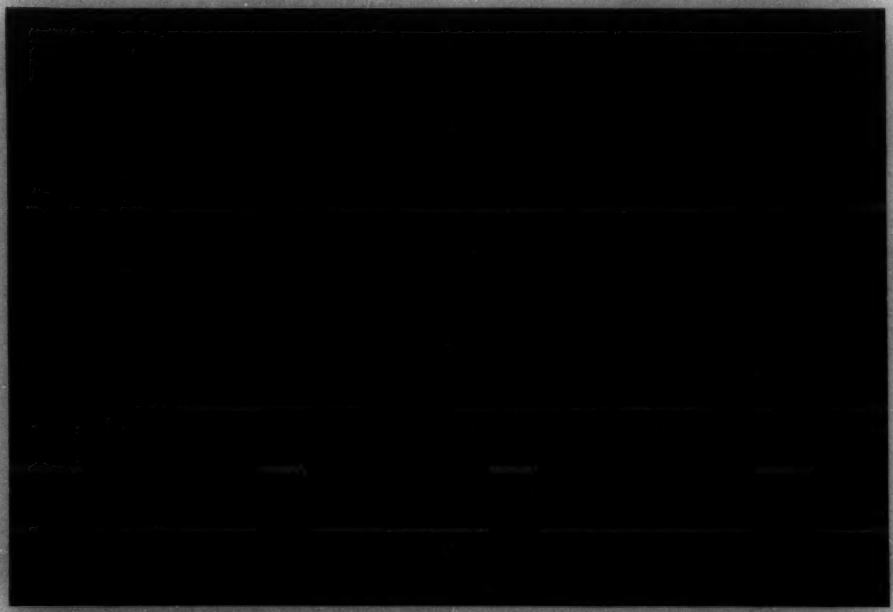

Fig. 5. Typical oscillographic records of the operation of the type AP-1 automatic service restorer

Impulse-Generator Voltage Charts for Selecting Circuit Constants

By J. L. THOMASON
ASSOCIATE AIEE

It is suggested in this paper that impulse generator voltage waves for commercial testing may be compared not only on the basis of wave shape but also on the basis of relations between circuit constants. The charts and graphs included are intended to show how desirable this is, and they may be used to facilitate both front-of-wave and full-wave testing.

PREVIOUSLY published articles[1–6] have indicated the need of an accurate method of comparing impulse voltage waves, and although it has already been recommended[1] that impulse voltage waves be designated by the "2 point" method, that is, 1.5x40, a considerable range for wave shape variation is possible even if it is specified that the wave is smooth. It seems desirable therefore in those cases where more accurate determination of wave shape is required to specify the generator circuit constants and to compare the wave shapes on some definite basis such as on a basis of ratios between the different circuit constants as presented here.

There are numerous impulse-generator circuits, each having its merits, which will produce desirable voltage test waves. However, to escape the use of a multiplicity of circuits it seems desirable to use one or 2 circuits. Then the small differences and oddities in waves produced by the different circuits can be eliminated, theoretically at least, in comparing test results.

Circuits Analyzed

In this paper only 2 impulse-generator circuits are considered, figures 1 and 2. Such circuits of the impulse generator are well enough known and are in such common use that they need only a brief explanation. Referring[7] to figure 2, C_1 is the generator capacitance, L_1 is the total series inductance, R_1 is the total series resistance, R_2 is the shunt resistance, and C_2 is the total load capacitance. These constants are basic in the impulse generator circuit, and although in an actual generator they may be distributed and have mutual effects on each other, for the purpose of this paper they alone are considered. This circuit of figure 2 is recommended as basic by the International Electrochemical Commission.[8]

In the first circuit, figure 1, the inductance is considered negligible.

In the second circuit, figure 2, the inductance is considered and in the calculations is made of such value that neglecting R_2 as in figure 3 the series resistance R_1 will just damp out oscillations. That is, the critical resistance is $R_1^2 = 4L_1/C$, or transposing, $L_1 = R_1^2C/4$, where $C = (C_1C_2)/(C_1 + C_2)$. By using this relation the oscillations are negligible (less than one per cent) at the crest. Thus using this relation between various circuit constants, the impulse generator applies to the test piece a voltage wave which has 3 desirable characteristics, considering that each is dependent upon the others:

1. A practically smooth wave
2. A minimum wave front
3. A maximum crest voltage

Relationship Between Circuit Constants

In analyzing the circuits, the relationship of the constants is considered also from the point of practical importance. The available capacitance of the generator is frequently a limiting factor both theoretically and economically, and when oscillograms are taken the shunt resistance may frequently be the divider resistance only, so both C_1 and R_2 are limiting factors. In making the tests the relation of the load to the generator capacitance, C_2/C_1, as well as the relation of the series resistance to the shunt resistance, R_1/R_2, must be considered if the proper voltage and wave shape are to be applied to the test piece.

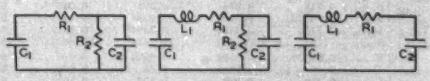

Figs. 1–3. Schematic diagrams of impulse generator circuits

Calculated Charts

With these relationships in mind the characteristics of the voltage test waves applied to a capacitance load were calculated for a wide range of circuit constants in the 2 circuits and the characteristics were so expressed in the calculated charts, charts I and II. In chart I the impulse generator circuit of figure 1 is considered in which the inductance is made equal to zero. At the top of the chart K_2 shows the ratio between the load and generator ca-

A paper recommended for publication by the AIEE committee on instruments and measurements. Manuscript submitted October 26, 1936; released for publication December 4, 1936.

J. L. THOMASON is electrical engineer and gas plant supervisor, General Electric Company, Pittsfield, Mass.

1. For all numbered references see list at end of paper.

Chart I

$K_1 = \frac{R_1}{R_2}$		$K_2 = C_2/C_1$										
		0.00	0.01	0.02	0.04	0.10	0.20	0.40	1.00	2.00	4.00	10.00
0.00	*F*	0.00000	0.000000	0.00000	0.00000	0.00000	0.0000	0.0000	0.0000	0.0000	0.0000	0.0000
	D	0.693	0.700	0.707	0.721	0.762	0.833	0.970	1.39	2.08	3.46	7.62
	C	1.000	0.990	0.980	0.961	0.909	0.833	0.714	0.500	0.333	0.200	0.0909
	R	0.00000	0.00000	0.00000	0.00000	0.00000	0.0000	0.0000	0.0000	0.0000	0.0000	0.0000
	a	1.0000	0.9901	0.9804	0.9615	0.9091	0.8333	0.7143	0.5000	0.3333	0.2000	0.0909
	b	OC	OC	OC	OC	OC	OC	OC	OC	OC	OC	OC
0.01	*F*	0.00000	0.000908	0.00167	0.00302	0.00641	0.0109	0.0177	0.0299	0.0408	0.0516	0.0648
	D	0.700	0.708	0.715	0.731	0.776	0.850	0.995	1.40	2.13	3.53	7.70
	C	0.990	0.979	0.969	0.951	0.896	0.820	0.702	0.496	0.328	0.198	0.0903
	R	0.00000	0.00128	0.00233	0.00413	0.00826	0.0128	0.0178	0.0213	0.0192	0.0146	0.00840
	a	0.9901	0.9805	0.9711	0.9538	0.9017	0.8275	0.7106	0.4987	0.3330	0.1999	0.0909
	b	OC	10199.02	5149.03	2624.05	1109.10	604.17	351.79	200.50	150.17	125.05	110.01
0.02	*F*	0.00000	0.00167	0.00304	0.00547	0.0115	0.0195	0.0313	0.0531	0.0724	0.0921	0.117
	D	0.707	0.715	0.724	0.741	0.790	0.866	1.02	1.46	2.17	3.58	7.77
	C	0.980	0.969	0.960	0.939	0.885	0.809	0.692	0.484	0.325	0.196	0.0899
	R	0.00000	0.00233	0.00420	0.00738	0.0146	0.0228	0.0308	0.0364	0.0334	0.0258	0.0150
	a	0.9804	0.9711	0.9619	0.9441	0.8943	0.8219	0.7070	0.4975	0.3326	0.1998	0.0909
	b	OC	5149.03	2599.04	1324.05	559.106	304.18	176.08	100.50	75.167	62.550	55.009
0.04	*F*	0.00000	0.00302	0.00547	0.00979	0.0204	0.0342	0.0547	0.0925	0.126	0.162	0.208
	D	0.721	0.731	0.741	0.759	0.814	0.896	1.06	1.51	2.24	3.68	7.88
	C	0.961	0.951	0.939	0.919	0.864	0.789	0.672	0.473	0.318	0.193	0.0891
	R	0.00000	0.00413	0.00738	0.0129	0.0251	0.0381	0.0518	0.0612	0.0564	0.0445	0.0264
	a	0.9615	0.9528	0.9441	0.9272	0.8799	0.8107	0.6999	0.4950	0.3318	0.1998	0.0909
	b	OC	2624.05	1324.05	674.073	284.120	154.19	89.300	50.505	37.968	31.300	27.509
0.10	*F*	0.00000	0.00641	0.0115	0.0204	0.0419	0.0695	0.113	0.187	0.255	0.335	0.439
	D	0.762	0.776	0.790	0.814	0.878	0.974	1.16	1.65	2.43	3.89	8.18
	C	0.909	0.896	0.885	0.864	0.810	0.739	0.630	0.445	0.303	0.187	0.0873
	R	0.00000	0.00826	0.01481	0.0251	0.0477	0.0714	0.0974	0.113	0.106	0.0861	0.0537
	a	0.9091	0.9017	0.8943	0.8799	0.8390	0.7786	0.6790	0.4875	0.3296	0.1992	0.0908
	b	OC	1109.10	559.106	284.120	119.161	64.221	36.831	20.512	15.170	12.551	11.009
0.20	*F*	0.00000	0.0109	0.0195	0.0342	0.0695	0.115	0.183	0.308	0.430	0.566	0.758
	D	0.832	0.850	0.866	0.896	0.974	1.09	1.30	1.87	2.69	4.21	8.59
	C	0.833	0.820	0.809	0.789	0.739	0.671	0.574	0.410	0.284	0.178	0.0846
	R	0.00000	0.0128	0.0235	0.0381	0.0714	0.105	0.140	0.165	0.160	0.134	0.0882
	a	0.8333	0.8275	0.8219	0.8107	0.7786	0.7296	0.6459	0.4750	0.3255	0.1984	0.0908
	b	OC	604.1725	304.178	154.189	64.2214	34.270	19.354	10.535	7.8742	6.3016	5.5092
0.40	*F*	0.00000	0.0177	0.0313	0.0547	0.113	0.182	0.295	0.492	0.695	0.933	1.28
	D	0.970	0.995	1.02	1.06	1.16	1.30	1.71	2.23	3.15	4.79	9.39
	C	0.714	0.702	0.692	0.672	0.630	0.574	0.499	0.361	0.254	0.163	0.0807
	R	0.00000	0.0178	0.0308	0.0518	0.0974	0.140	0.172	0.222	0.221	0.195	0.138
	a	0.7143	0.7106	0.7070	0.6999	0.6790	0.6459	0.5244	0.4505	0.3179	0.1968	0.0908
	b	OC	351.7894	176.079	89.3001	36.8210	19.354	10.735	5.5495	3.9321	3.1783	2.7594
1.00	*F*	0.00000	0.0299	0.0531	0.0925	0.187	0.308	0.492	0.860	1.25	1.72	2.48
	D	1.39	1.40	1.46	1.51	1.65	1.87	2.22	3.06	4.25	6.18	11.1
	C	0.500	0.496	0.484	0.473	0.445	0.410	0.361	0.275	0.204	0.127	0.0731
	R	0.00000	0.0213	0.0364	0.0612	0.113	0.165	0.222	0.281	0.294	0.279	0.232
	a	0.5000	0.4987	0.4975	0.4950	0.4875	0.4750	0.4505	0.3820	0.2929	0.1910	0.0901
	b	OC	200.5012	100.502	50.5050	20.5125	10.525	5.5495	2.8180	1.7071	1.3090	1.1099
2.00	*F*	0.00000	0.0408	0.0724	0.126	0.255	0.430	0.695	1.25	1.85	2.62	3.80
	D	2.08	2.13	2.17	2.24	2.43	2.69	3.18	4.25	5.71	8.06	13.6
	C	0.333	0.328	0.325	0.318	0.306	0.284	0.254	0.204	0.158	0.113	0.0639
	R	0.00000	0.0192	0.0334	0.0564	0.106	0.160	0.221	0.294	0.323	0.325	0.286
	a	0.3333	0.3330	0.3326	0.3315	0.3290	0.3258	0.3179	0.2929	0.2500	0.1798	0.0901
	b	OC	150.1670	75.1674	37.6882	15.1704	7.8742	3.9321	1.7071	1.0000	0.8052	0.5808
4.00	*F*	0.00000	0.0516	0.0921	0.162	0.335	0.5666	0.933	1.72	2.62	3.84	5.93
	D	3.46	3.53	3.58	3.66	3.89	4.21	4.79	6.16	8.06	11.0	17.7
	C	0.200	0.198	0.196	0.193	0.187	0.178	0.163	0.137	0.112	0.0849	0.0517
	R	0.00000	0.0148	0.0258	0.445	0.0861	0.134	0.195	0.279	0.325	0.349	0.336
	a	0.2000	0.1999	0.1998	0.1998	0.1992	0.1984	0.1968	0.1910	0.1798	0.1524	0.0867
	b	OC	125.0501	62.5502	31.3002	12.5508	6.3016	3.1783	1.3090	0.8052	0.4101	0.2883
10.00	*F*	0.00000	0.0646	0.117	0.208	0.439	0.758	1.28	2.48	3.89	5.95	9.83
	D	7.62	7.70	7.77	7.88	8.18	8.59	9.29	11.1	13.6	17.7	27.0
	C	0.0909	0.0903	0.0899	0.0891	0.0872	0.0846	0.0807	0.0721	0.0629	0.0517	0.0357
	R	0.00000	0.00840	0.0150	0.0264	0.0537	0.0852	0.138	0.222	0.286	0.336	0.384
	a	0.09091	0.09090	0.09089	0.09087	0.09085	0.0908	0.0906	0.0901	0.0891	0.0867	0.0730
	b	OC	110.0091	55.0091	27.5091	11.0091	5.5092	2.7594	1.1099	0.5808	0.2883	0.1370

OC indicates an infinite value.

pacitances. At the left of the chart K_1 shows the ratio between the series and shunt resistances.

For any particular values, for instance, $K_1 = 0.04$ and $K_2 = 0.20$, line *F* gives the wave front divided by C_1R_2. Thus *F*, or here 0.0342, times C_1R_2 equals the wave front. Likewise *D*, or here 0.896, times C_1R_2 gives the duration of the wave. As before explained[1] the wave front is the time from zero to crest and the wave duration is the time from zero to half crest on the tail of the wave.

Line *C* expresses as a ratio the crest magnitude of the test wave in terms of the initial voltage charge on the generator. For the example given, $C = 0.789$ which means that the voltage on the test piece will be 78.9 per cent of the initial voltage on the impulse generator.

Line *R* is the ratio between the wave front and duration. For the example, $R = 0.0381$. For a 1.5x40 wave $R = 0.0375$.

Lines *a* and *b* give the values of the 2 exponents of the

equation expressing the test wave. See appendix I. The values are expressed in terms of C_1R_2, that is, $a = m \times C_1R_2$ and $b = n \times C_1R_2$.

In chart II the inductance is considered and has the value previously determined, $L_1 = R_1^2C/4$. The symbols have meanings similar to those in chart I and there is added the term w which equals $\omega \times C_1R_2$, as shown in appendix II. In chart II there are 3 values of w, indicated by asterisks, which denote that the roots are real numbers and that these waves are perfectly smooth.

Curves and Illustrative Example

From these 2 charts a set of curves is plotted in figure 4. In figures 4*a*, 4*b*, and 4*c*, $L_1 = 0$ and in figures 4*A*, 4*B*, and 4*C*, $L_1 = R_1^2C/4$ where $C = (C_1C_2)/(C_1 + C_2)$.

These curves show (1) that with widely different values of circuit constants the same wave front, wave shape, and crest can be obtained, and (2) that wave shape is to a considerable extent a function of ratios between circuit constants.

Figure 5 shows the relation between L_1, R_1, and C and is an aid in making tests and calculations.

For purposes of mathematical interest numerous curves could be drawn to show the relation between a, b, and w and the wave characteristics but these curves will be omitted here for the sake of brevity. However, the data are presented in the charts for such use.

As an example of how to use these charts and curves suppose a 1.5x40 wave is desired where $C_1 = 0.005$ microfarad and $C_2 = 0.001$ microfarad. In circuit I neglect the inductance and in circuit II consider that the inductance has a value determined from figure 5. Then constant by constant,

Constant	Circuit I	Circuit II	Remarks
K_2	0.2	0.2	$K_2 = C_2/C_1$
K_1	0.04	0.08	Figures 4*b* and 4*B*
F	0.035	0.034	Figures 4*c* and 4*A*
R_2	8,600	8,800	Front = FC_1R_2
R_1	340	530	$K_1 = R_1/R_2$
L_1	0	58	Figure 5

The procedure is to first determine from figures 4*b* and 4*B* the values of K_1. Then determine from figures 4*a* and 4*A* the values of F. The values of R_2 and R_1 can then be quickly calculated and the value of L_1 can be obtained from figure 5. In case the stipulated values of inductance cannot be obtained, the values of the circuit constants will have to be estimated on a straight line basis.[7] Thus in circuit II hereinbefore if $L_1 = 40$ microhenries, make $R_2 = 8{,}700$ and $R_1 = 460$.

Front-of-Wave Testing and Example

Charts I and II and figure 4 show how easy it is even with widely varying circuit constants to make front-of-wave tests approximating the same rate of voltage rise. The main stipulation is to have the waves for the different circuits reach the same crest voltage at the same time.

For the smooth wave characteristics shown in figure 4, the first thing to do is to choose circuit constants giving the same wave fronts (same C_1R_2 values in figures 4*a* and 4*A*) and the second thing to do is to choose the proper charging voltages on the generators to give the same crest voltages on the test pieces. The refining stipulation would be to have in all circuits, if possible, equal values of L_1, K_1, and K_2.

As an example, suppose figure 2 with series inductance was used to get a long wave for test purposes and that $C_1 = 0.02$ microfarad, $C_2 = 0.001$ microfarad, $R_1 = 4{,}000$, $R_2 = 10{,}000$, and the crest voltage = 1,500 kv. Therefore $K_1 = 0.4$, $K_2 = 0.05$, and from figure 4*A*, $F = 0.053$. Suppose that only series resistance as in figure 1 was available for securing the same rate of voltage rise, given $C_1 = 0.008$ microfarad, and as before $C_2 = 0.001$ microfarad. Since the wave fronts must be equal $(FC_1R_2)_1 = (FC_1R_2)_2 = 10.6$ microseconds, and $R_{s1} = (0.053 \times 0.02 \times 10{,}000)/(0.053 \times 0.008) = 25{,}000$. As $K_2 = 0.001/0.008 = 0.125$ and $F = 0.053$, K_1 must equal 0.12 from figure 4*a* and $R_1 = 3{,}000$. The charged voltage on the second generator must be from figure 4*c*, 1,500/0.77 = 1,950 kv.

In constructing an impulse generator for wave-front testing, adjunct load capacitances as well as series resistances and inductances could be used for increasing the wave front.

By using the data presented here the slope of the wave-

Chart II

$K_1 = R_1/R_2$		$K_2 = C_2/C_1$ 0.00	0.01	0.10	1.00	10.00
0.00	F	0.000000	0.000000	0.00000	0.00000	0.00000
	D	0.603	0.700	0.762	1.39	7.62
	C	1.000	0.990	0.909	0.500	0.0909
	R	0.000	0.000	0.000	0.000	0.000
	a	1.000	0.990	0.909	0.500	0.0909
	b	OC	OC	OC	OC	OC
	w					
0.01	F	0.000258	0.000589	0.00444	0.0213	0.0462
	D	0.700	0.707	0.774	1.42	7.67
	C	0.990	0.981	0.898	0.493	0.0905
	R	0.000389	0.000832	0.00574	0.0150	0.00802
	a	0.990	0.989	0.902	0.499	0.0909
	b	40.399	20.249	2.304	400.2	220.0
	w		1.407	141	14.16	*1.414
0.10	F	0.0130	0.00441	0.0318	0.157	0.334
	D	0.777	0.774	0.881	1.83	8.01
	C	0.899	0.898	0.820	0.456	0.0885
	R	0.0167	0.00571	0.0369	0.0969	0.0404
	a	0.911	0.902	0.840	0.457	0.0908
	b	439	2070	235	40.2	21.5
	w		445	44.6	4.50	4.70
1.00	F	0.385	0.0213	0.170	0.883	2.21
	D	1.81	1.41	1.60	2.91	10.5
	C	0.437	0.495	0.461	0.296	0.0765
	R	0.213	0.0151	0.106	0.303	0.211
	a	0.536	0.499	0.490	0.337	0.0903
	b	7.46	252	26.7	4.31	2.20
	w		133	13.5	1.48	0.0988
10.00	F	4.80	0.143	0.965	4.26	11.9
	D	26.2	7.75	8.60	12.4	26.6
	C	0.0691	0.0900	0.0856	0.0723	0.0394
	R	0.183	0.0184	0.112	0.344	0.447
	a	0.128	0.0911	0.0926	0.1016	0.0781
	b	0.312	70.1	7.15	0.849	0.331
	w		*22.5	*1.91	0.257	0.0547

* The asterisks indicate that the roots are real.
OC indicates an infinite value.

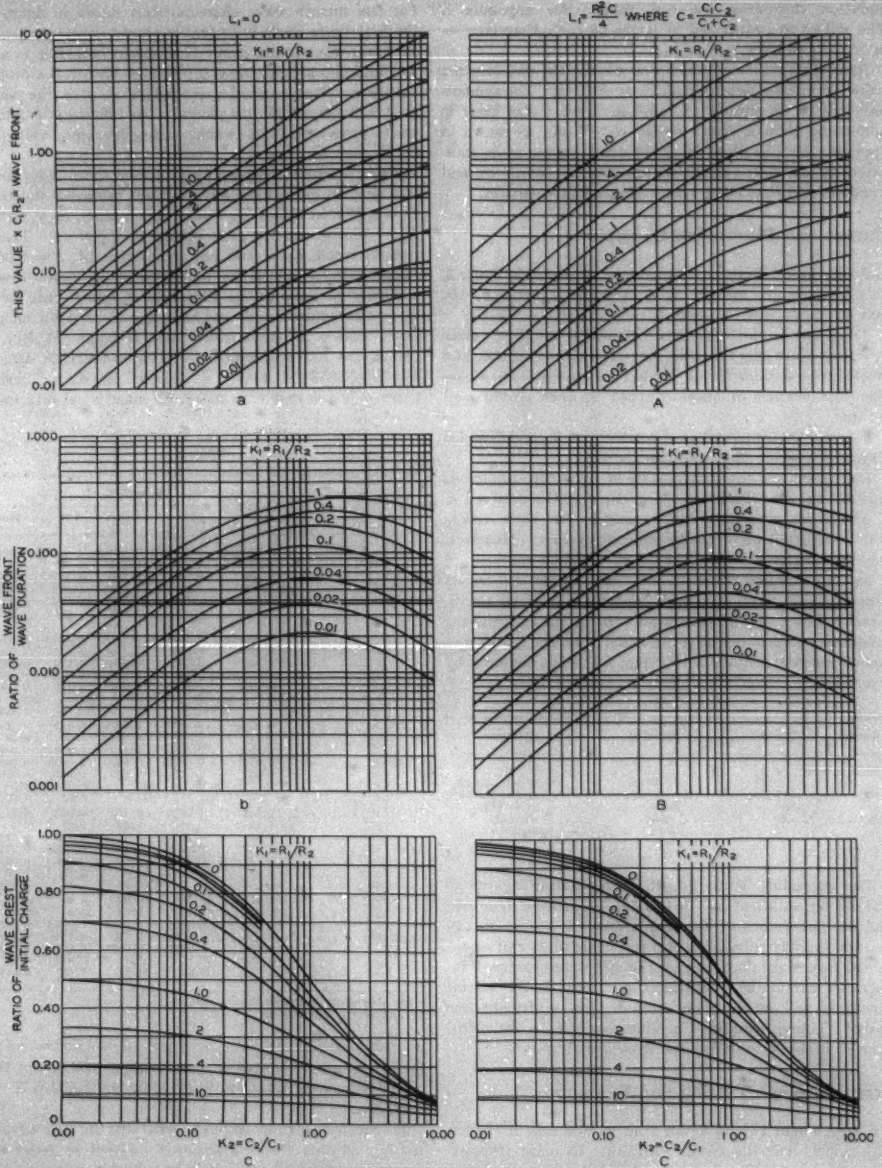

Fig. 4. Curves for wave shape as related to circuit constants

front could be calculated between points other than the zero and the crest points of the wave. Some laboratories may wish to use the slope equal to the tangent at the mid-point (50 per cent crest) of the front, others may wish to use the slope determined by 2 points on the front such as the points at 10 and at 90 per cent of crest, and so on. After the method of determining the slope had been agreed upon, the slopes could be determined from a set of calculated fronts, then tabulated similarly to charts I and II and plotted similarly to figure 4 so that any desired time rate of voltage rise could be easily applied to a test piece.

Accuracy of Charts and Curves

The charts were calculated on the calculating machine and on the slide rule with the intent that the third significant figure of the F, D, and C values would be approximately correct. On the curves of figure 4 the second significant figure should be approximately correct.

Oscillograms Verifying Tables and Curves

Up to this point the paper has been devoted to presenting the desirability of comparing and securing impulse voltage test waves on the basis of ratios between circuit constants. In practice, isolated, lumped circuit constants cannot be dealt with and the distribution of the generator capacitors, the effect of stray capacitance, and the idiosyncrasies of the divider and oscillograph must be considered. In general most of these factors are pretty well under control as proved by the fact that cathode-ray oscillograms closely duplicate calculations.

To show this verification, 2 oscillograms are shown in figures 6 and 7 and compared with the calculated charts and curves. In figure 6 a 1.9x40 wave is shown. C_1 = 0.00926 microfarad, C_2 = 525 micromicrofarads, L_1 = 110 microhenrys, R_1 = 1,250 ohms, R_2 = 4,250 ohms, the charged voltage on the generator = 1,300 kv, and the test-piece voltage = 932 kv. Therefore the similarity between the test results and the charts results can be compared as follows:

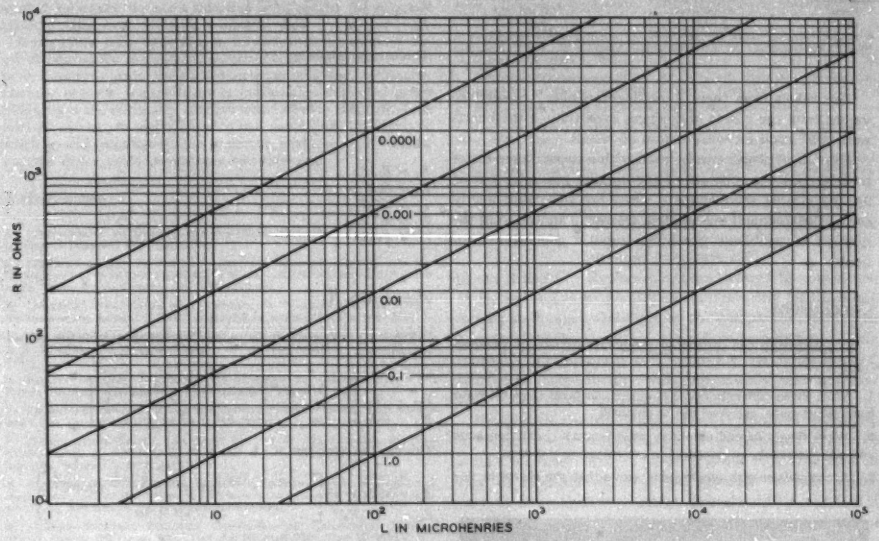

Fig. 5. Relations between inductance, resistance, and capacitance

Numbers on curves are capacitances in microfarads $L = R^2C/4$

Constant	By Test	By Chart
K_1	0.30	0.30
K_2	0.057	0.057
Front	1.9 microseconds	1.9 microseconds
Duration	40 microseconds	39 microseconds
Crest	72 per cent	71 per cent
R	0.047	0.048
L	110 microhenrys	110 microhenrys

In figure 7 a 1.4x44 wave is shown. C_1 = 0.00476 microfarad, C_2 = 0.00035 microfarad, L_1 = 160 microhenry, R_1 = 1,375 ohms, R_2 = 10,700 ohms, the charged voltage

on the generator = 550 kv, and the test-piece voltage = 446 kv. Then

Constant	By Test	By Chart
K_1	0.128	0.128
K_2	0.073	0.073
Front	1.4 microseconds	1.5 microseconds
Duration	44 mferoseconds	44 microseconds
Crest	81 per cent	80 per cent
R	0.032	0.034
L	160 microhenrys	154 microhenrys

The values from these 2 oscillograms check closely the values from the charts and curves even though the charts were calculated for wide ranges of values.

Thus these charts can be used with a capacitance meter to determine the constant of the impulse generator circuit for any desired wave shape. These are also conveniently used to supplement the electric transient analyzer[8] in the solution of problems involving impulse generator transients.

Conclusions

In conclusion the following observations can be pointed out:

1. With widely different values of circuit constants the same wave front, wave shape, and crest can be obtained.
2. Wave shapes depend upon the ratios between circuit constants and may frequently be compared to advantage on this basis.
3. A comparison with oscillograms shows that the charts in this paper are accurate enough for practical work and the examples show how easily the charts can be used for selecting circuit constants.

Fig. 6. Oscillogram for 1.9x40 microsecond wave

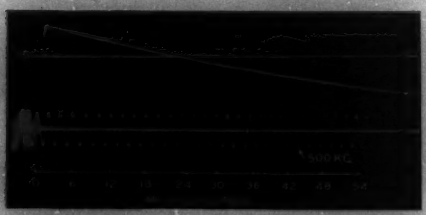

Fig. 7. Oscillogram for 1.4x44 microsecond wave

Appendix I

Referring to figure 1, the equation[7] for voltage across the capacitance load is

$$\frac{E_{c2}}{E_{c1}} = \frac{1}{a-m}\left[\frac{\epsilon^{-mt}-\epsilon^{-at}}{C_2R_1}\right]$$

This may be rewritten

$$\frac{E_{c2}}{E_{c1}} = \frac{1}{b-a}\left[\frac{\epsilon^{-T}-\epsilon^{-bT}}{K_1K_2}\right]$$

where

$K_1 = R_1/R_2$
$K_2 = C_2/C_1$
$a = mC_1L$
$b = nC_1R_2$
$t = TC_1R_2$

Appendix II

Referring to figure 2, the equation[7] for voltage across the capacitance load is

$$\frac{E_{c2}}{E_{c1}} = \frac{1}{C_2L_1}\left[\frac{\epsilon^{-\alpha t}-\epsilon^{-\beta t}\left\{\cos\omega t+\dfrac{\beta-\alpha}{\omega}\sin\omega t\right\}}{(\alpha-\beta)^2+\omega^2}\right]$$

This may be rewritten

$$\frac{E_{c2}}{E_{c1}} = \frac{4(K_2+1)}{(K_1K_2)^2}\left[\frac{\epsilon^{-aT}-\epsilon^{-bT}\left\{\cos wT+\dfrac{b-a}{w}\sin wT\right\}}{(a-b)^2+w^2}\right]$$

where

$L_1 = R_1^2C/4$
$C = (C_1C_2)/(C_1+C_2)$
$K_1 = R_1/R_2$
$K_2 = C_2/C_1$
$a = \alpha C_1R_2$
$b = \beta C_1R_2$
$w = \omega C_1R_2$
$t = TC_1R_2$

References

1. Recommendations for Impulse Voltage Testing, AIEE subcommittee report, AIEE Transactions, volume 52, June 1933, pages 486–71.
2. Impulse Testing of Commercial Transformers, F. J. Vogel and V. M. Montsinger. AIEE Transactions, volume 52, June 1933, pages 409–10.
3. Better Standards Needed for Surge Testing, F. D. Fielder. *Electrical World*, volume 102, September 30, 1933, pages 433–5.
4. The Production of Impulse Test Voltages, C. S. Sprague. Electrical Engineering (AIEE Transactions), volume 54, October 1935, pages 1100–04.
5. Characteristics of Surge Generators for Transformer Testing, P. L. Bellaschi. AIEE Transactions, volume 51, December 1932, pages 936–45.
6. International Electrochemical Commission, Advisory Committee No. 8 on Standard Voltages and Currents and High-Voltage Insulators. Unconfirmed minutes of the meeting held in Brussels on 24th, 25th, and 26th June 1935.
7. Impulse Generator Circuit Formulas, J. L. Thomason. Electrical Engineering (AIEE Transactions), volume 53, January 1934, pages 169–76.
8. The Oscillograph Electric Transient Analyzer, N. Rohats. *General Electric Review*, volume 39, March 1936, pages 146–9.

Inductive Co-ordination

(*Continued from page 26*)

phone pairs, and the importance, therefore, of suitable telephone-circuit transpositions.

Figure 5 shows exposure conditions such as may be encountered in a small community serving a nearby rural area and table IX shows the noise conditions at several locations during heavy power loads.

The extent to which various measures of co-ordination could be applied to reduce the noise induction or to restrict the extent of special arrangements is shown in table X.

It is evident from table X that, for the conditions assumed, the use of reasonably co-ordinated telephone-circuit transpositions will be necessary to care for the stations served by open wire. Ordinarily the use of such transpositions in combination with such other measures as are reasonably effective would serve to take care of the stations served by telephone cable and would limit the extent to which special telephone-station apparatus might be needed for the stations served by the longer open-wire extensions.

References

1. Improvement in Distribution Methods, S. B. Hood. AIEE Transactions, volume 44, 1925, page 1038.

2. Interconnection of Primary Lightning Arrester Ground and the Grounded Neutral of the Secondary Main, C. F. Harding and C. S. Sprague. AIEE Transactions, volume 51, 1932, page 234.

3. Lightning Protection for Distribution Transformers, K. B. McRachron and L. Saxon. AIEE Transactions, volume 51, 1932, page 239.

4. Lightning Protection for Distribution Transformers, A. M. Opsahl, A. S. Brookes, and R. N. Southgate. AIEE Transactions, volume 51, page 245.

5. Studies of Lightning Protection on 4,000-Volt Circuits—III, D. W. Roper. AIEE Transactions, volume 51, 1932, page 253.

6. Lightning Protection for Distribution Transformers, T. H. Haines and C. A. Corney. AIEE Transactions, volume 51, 1932, page 259.

7. Distribution System Lightning Studies by Philadelphia Electric Company, H. A. Dambly, H. N. Ekvall and H. S. Phelps. AIEE Transactions, volume 51, 1932, page 265.

8. Engineering Reports 8, 9, 13, and 15, Volumes I and II of Engineering Reports of Joint Subcommittee on Development and Research of National Electric Light Association and Bell Telephone System.

9. Common-Neutral Practice Confirmed in California. *Electrical World*, June 4, 1932, page 980. (See also *Electrical West*, May 15, 1932.)

10. Provisional Report No. 18 of Joint Subcommittee on Development and Research of Edison Electric Institute and Bell Telephone System.

11. Measurement of Telephone Noise and Power Wave Shape, J. M. Barstow, P. W. Blye and H. E. Kent. AIEE Transactions, volume 54, 1935, page 1307.

12. Reports of Joint General Committee of National Electric Light Association and Bell Telephone System on Physical Relations Between Electrical Supply and Signal Systems, edition of December 9, 1932.

Lightning Investigation on Transmission Lines

(*Continued from page 106*)

in the tower legs and counterpoise wires on the Glenlyn-Roanoke line for 11 cases in which a comparison could be obtained. It was assumed that the total counterpoise current was twice the current measured in one long and one short wire. This comparison shows the summation of the tower currents to be 0.95 of the summation of the counterpoise currents.

It is quite important in considering the comparison between leg currents and counterpoise currents to bear in mind that some leg current may pass directly to earth through the tower footings without passing through the counterpoise wires. Also the counterpoise wires may occasionally carry some current which passes through cross members of the tower structure and is not included in the leg measurements. In all cases polarity indicated the current to be traveling from the free end of the counterpoise to the tower and from the bottom of the tower to the top.

References

1. Lightning Investigation on Transmission Lines—V, W. W. Lewis and C. M. Foust. Electrical Engineering (AIEE Transactions), volume 54, September 1935, pages 934–42.

2. Direct Measurement of Surge Currents, C. M. Foust and J. T. Henderson. Electrical Engineering (AIEE Transactions), volume 54, April 1935, pages 373–8.

3. Lightning Investigation on Transmission Lines—IV, W. W. Lewis and C. M. Foust. Electrical Engineering (AIEE Transactions), volume 53, August 1934, pages 1180–6.

4. Lightning Investigation on 220-Kv Lines—II, Edgar Bell. Electrical Engineering, volume 55, December 1936, pages 1306–13.

5. Edison Electric Institute *Bulletin*, August 1936, pages 351–2.

6. Lightning Performance on 132-Kv Lines, P. Sporn and I. W. Gross Electrical Engineering, volume 53, August 1934, pages 1195–1200.

7. Lightning Investigation on Transmission Lines, W. W. Lewis and C. M. Foust. Electrical Engineering, volume 49, July 1930, pages 917–28.

A Review of Overhead Secondary Distribution

(*Continued from page 122*)

panies *A* and *C*. Replacements are favored by companies *B*, *D*, and *E* but frequently involve re-using transformers in new locations. Only one of the companies anticipates a general replacement of secondary conductors. This company has assumed a 15-year life for triple-braided weatherproof conductors, which apparently has influenced their choice of the replacement method.

Experience records indicate that conductors remaining in service in the same location have been used to a large extent for more than 15 years. While it is true that in case of replacement, it would generally become necessary to scrap such conductors, this should be avoided, if possible, as wires would continue to be serviceable for a good many more years if left in place in the same location. Some real savings are possible therefore by selecting the most economical wire size for the first installation and adding or respacing transformers.

Replacement costs of transformers should also be studied carefully whenever additional capacity is required. Since overloaded operation is considered permissible this should be given first consideration where voltage regulation permits. Additional transformers and subdividing secondaries with possibly some relocations should come next, and finally replacements. A table of annual costs for various per cent loadings of transformers and the net cost of replacements will prove very helpful in selecting the most economical method. Table III contains such typical information. While this information will vary somewhat for various companies, due possibly to a difference in operating or accounting practices, the table is shown here as a typical means of finding the best solutions.

Table IV shows a comparison of accumulated annual costs and indicates the economy of using transformers as long as possible in the same location. In order to benefit fully through long use of transformers, it is necessary to provide new poles, or poles in good condition, for new transformer installations.

News

Of Institute and Related Activities

AIEE Winter Convention Program Provides Attractive Features

TECHNICAL developments in many specialties and attractive social functions comprise the program for the Institute's 1937 winter convention, which will be held in New York, N. Y., January 25–29. Headquarters will be in the Engineering Societies Building, 33 West 39th Street, and registration will begin at 10:00 a.m. on Monday. Thereafter technical sessions, conferences, and committee meetings, together with the social functions, the smoker, Edison medal presentation, dinner-dance, and inspection trips in the city and vicinity provide ample opportunity for a busy and profitable week. In addition, for those who would enjoy a few days vacation in a mild climate during midwinter a Bermuda cruise has been arranged as a post-convention trip. The women's entertainment committee, under the chairmanship of Mrs. George Sutherland, also is arranging a most attractive program for the visiting women. A summarized schedule of events is given in an accompanying tabulation.

Edison Medal Presentation

The AIEE 1936 Edison Medal will be presented to Doctor Alex Dow at a special session of the convention to be held in the engineering auditorium Wednesday evening, January 27, at 8:15 p.m. Doctor Dow was awarded the medal "for outstanding leadership in the development of the central station industry and its service to the public." A biographical sketch of Doctor Dow is given on page 197 of this issue.

Technical Program

The technical program is comprised of 13 technical sessions at which a wide variety of timely technical papers will be presented and discussed. The tentative technical program announced in ELECTRICAL ENGINEERING for December 1936, pages 1388–9, is complete with the changes which have been made in the following sessions. These sessions, as revised, are repeated for convenience.

Selected Subjects

Electronic Transient Visualizers, H. J. Reich, University of Illinois.
December issue, pages 1314–18

Studies of Stability of Cable Insulation, Herman Halperin and C. E. Betzer, Commonwealth Edison Company. October issue, pages 1074–82

Proposed Transformer Standards, J. E. Clem, General Electric Company.
January issue, pages 32–6

A New Electrostatic Precipitator, G. W. Penney, Westinghouse Electric & Manufacturing Company. January issue, pages 159–63

Induction Machinery

Induction Motor Resistance Ring Width, P. H. Trickey, Diehl Manufacturing Company.
February 1936 issue, pages 144–50

Induction Motors Under Unbalanced Conditions, E. O. Lunn, Peterson and Cowan Elevator Company, Ltd. April 1936 issue, pages 387–93

Induction Motors on Unbalanced Voltages, H. R. Reed and R. J. W. Koopman, Michigan College of Mining and Technology.
November issue, pages 1206–13

Capacitor Motors with Windings Not in Quadrature, A. F. Puchstein and T. C. Lloyd, Robbins & Myers, Inc.
November issue, pages 1235–9

An Analysis of the Shaded Pole Motor, P. H. Trickey, Diehl Manufacturing Company.
September issue, pages 1007–14

Synchronous Machinery

Negative-Sequence Reactance of Synchronous Machines, W. A. Thomas, Antioch College.
December issue, pages 1378–84

Contributions to Synchronous-Machine Theory, A. S. Langsdorf, Washington University.
January issue, pages 41–8

Operational Solution of A-C Machines, A. R. Miller and W. S. Weil, Lehigh University.
November issue, pages 1191–1200

Two-Reaction Theory of Synchronous Machines, S. B. Crary, General Electric Company.
January issue, pages 27–31

Synchronous Machine With Solid Cylindrical Rotor, C. Concordia and H. Poritsky, General Electric Company. January issue, pages 49–58

Electrical Machinery

Self-Regulated Compound Rectifiers, W. M. Goodhue and R. B. Power, Harvard University.
November issue, pages 1200–06

Abrasion—A Factor in Electrical Brush Wear, V. P. Hessler, Iowa State College.
January issue, pages 8–12

Arc Characteristics Applying to Flashing on Commutators, R. E. Hellmund, Westinghouse Electric & Manufacturing Company.
January issue, pages 107–13

Table I—Issues of "Electrical Engineering" Containing 1937 Winter Convention Papers

February	1936	1 paper
April	1936	1 paper
August	1936	4 papers
September	1936	5 papers
October	1936	3 papers
November	1936	6 papers
December	1936	10 papers
January	1937	25 papers
February	1837	1 paper

Contact Drop and Wear of Sliding Contacts, R. M. Baker and G. W. Hewitt, Westinghouse Electric & Manufacturing Company.
January issue, pages 123–8

In addition to the technical conferences which were announced, an informal technical conference on the subject of noise will be held on Wednesday afternoon.

Smoker

Winter convention smokers for the last few years have been increasing so in popularity that it has become a difficult problem for the committee to meet satisfactorily the ticket demand. This year they believe

Summarized Schedule of Principal Events

Monday, January 25

10:00 a.m.	Registration
2:00 p.m.	Opening of convention
2:30 p.m.	Parallel technical sessions: —Communication —Selected subjects

Tuesday, January 26

10:00 a.m.	Parallel technical sessions: —Power transmission —Tensor analysis
2:00 p.m.	Address
2:45 p.m.	Parallel technical sessions: —Power distribution —Tensor analysis (continued)
6:30 p.m.	Smoker at the Commodore Hotel

Wednesday, January 27

10:00 a.m.	Parallel technical sessions: —Induction machinery —Protective devices
2:00 p.m.	Parallel technical sessions: —Synchronous machinery —Electronics
8:15 p.m.	Edison Medal presentation

Thursday, January 28

10:00 a.m.	Parallel technical sessions: —Electrical machinery —Electrophysics
2:00 p.m.	Parallel technical sessions: —Instruments and measurements —Electric welding demonstrations
7:00 p.m.	Annual dinner-dance

Friday, January 29

All day	Inspection trips

Saturday, January 30

3:00 p.m.	"Monarch of Bermuda" sails on post-convention cruise to Bermuda

that problem is solved, as the Grand Ballroom and West Ballroom at the Hotel Commodore have been engaged. The seating will be at tables of 10 with ample space to move around; an excellent supper served by the experienced Commodore staff and a satisfactory view for all of a full-sized stage will insure everyone's having a pleasant evening. The entire West Ballroom will be available as a lounge with service bar. Those planning to attend are urged to send in their reservations to the AIEE Smoker Committee, 33 West 39th Street, New York, N. Y., at an early date. All tables will be reserved. Tickets will be $3.50 per person.

Dinner-Dance

Continuing a social activity that has proved very popular in the past, a dinner-dance has been scheduled for Thursday evening, January 28, at the Hotel Astor, Broadway between 44th and 45th Streets. A combination dinner, dance, and buffet supper again will be featured. The flexibility of this arrangement will provide a very pleasant evening, which may be enjoyed by all according to their tastes, in one of New York's most popular hotels.

The Astor has been entirely redecorated and refurnished, making the surroundings more luxurious than ever. The Grand Ballroom and adjacent facilities will be reserved for the Institute's members and guests. Music will be furnished by George Ellner's Orchestra.

The program of the evening will be:

7:00 p.m.	Dinner
9:00 p.m. to 2:00 a.m.	Dancing
Midnight to 2:00 a.m.	Buffet supper

The rates for tickets will be the same as last year:

Dinner and dance	$5.00 per person
Dance and buffet supper	3.00 per person
Dinner, dance, and buffet supper	6.50 per person

The dinner-dance committee requests early purchase of tickets. Dinner reservation requests should indicate names of guests and the desired seating arrangement. Tables will be set up for 8 or 10 places, and every effort will be made to comply with the requests of members. Reservation requests should be sent to the AIEE Dinner-Dance Committee, 33 West 39th Street, New York City, N. Y., and checks should be made payable to H. H. Henline, national secretary.

Post-Convention Cruise to Bermuda Offered

A post-convention cruise to Bermuda will be offered to Institute members and their friends attending the AIEE 1937 winter convention. The party will sail on the "Monarch of Bermuda," which is shown above in the Hamilton Harbor, Bermuda, a thoroughly modern vessel in every respect. Those taking this cruise will have an opportunity to visit the engine room and the bridge of this quadruple-electric-turbine vessel, and to see the electrical equipment in action at sea.

Inspection Trips

A variety of interesting places has been included in the inspection trips arranged for the convention this year. An attempt has been made to arrange some trips during the week as complementary to the technical sessions. As in previous years, Friday has been set aside exclusively for inspection trips. The tentative schedule of inspection trips, which is subject to change, follows:

Monday, January 25

Sponsored broadcast, RCA Studios
Edison Wonder House

Tuesday, January 26

Public Service Electric and Gas Company—mercury turbine
S. H. Kress and Company—lighting and air conditioning
RCA Radiotron Company
The M. W. Kellogg Company—welding

Wednesday, January 27

Weston Electrical Instrument Corporation—cable testing equipment
Columbia Presbyterian Medical Center—Sloan X-ray generator

Thursday, January 28

Associated Press
Third Avenue Railway Company—grid-controlled rectifier
Board of Transportation, New York City—power-control board

Friday, January 29

Brooklyn Navy Yard
New York Stock Exchange
"Monarch of Bermuda"
Hastings-on-Hudson Mill, Anaconda Wire and Cable Company
Warner Brothers moving picture studio
National Broadcasting Company studios

Arrangements have been made to secure a very limited number of tickets to the General Electric Company "Hour of Charm" radio broadcast featuring Phil Spitalny and his all-girl orchestra. This program is given in the National Broadcasting Company studios on Monday afternoon. It is hoped that interested out-of-town members will indicate their desire for tickets when they register.

The Columbia Presbyterian Medical Center will exhibit the 1,000,000 volt high-frequency X-ray generator placed in operation this year. This generator was seen under construction by many members during the convention last year.

Interesting trips to plants of manufacturers of thermionic tubes, electrical instruments, welding equipment, and wire and cable have been arranged. A sightseeing tour of New York will be arranged for interested members if weather conditions are favorable.

Table II—A Few of the Hotels Available

Hotel	Location	Rooms With Private Bath	
		Single	Double
Astor	Broadway and 44th St.	$3.00– 6.00	$4.50– 7.50
Biltmore*	Madison Ave. and 43d St.	5.00–10.00	7.00–12.00
Bristol*	129 W. 48th St.	2.50– 4.00	3.00– 6.00
Commodore	Lexington Ave. and 42d St.	3.00– 5.00	4.50– 8.00
Edison	228–248 W. 47th St.	2.50– 5.00	4.00– 8.00
Governor Clinton	31st St. and 7th Ave.	3.00– 5.00	4.00– 7.00
McAlpin	Broadway and 34th St.	2.50– 7.00	4.00– 9.00
Montclair*	Lexington Ave. and 49th St.	3.00	4.00– 4.50
Murray Hill	Park Ave. and 40th St.	2.50– 5.00	3.50– 6.00
New Yorker	8th Ave. and 34th St.	3.50– 8.00	5.00–10.00
Pennsylvania	7th Ave. and 32d St.	3.50– 6.00	5.00– 9.00
Plaza	Fifth Ave. and 59th St.	6.00	8.00
Roosevelt	Madison Ave. and 45th St.	4.00– 8.00	6.00–12.00
Vanderbilt	Park Ave. and 34th St.	3.50– 5.00	6.00– 8.00
Waldorf-Astoria	Park Ave. and 50th St.	6.00– 8.00	9.00–11.00

* See advertising section for further details.

In addition to scheduled inspection trips, the committee will be pleased to arrange special trips for individuals and small groups. A list of possible items of interest will be available at the committee desk during the convention.

Bermuda Cruise Offered

For the first time, a post-convention cruise, to Bermuda, will be offered to Institute members and their friends. The party will leave New York on January 30, by the "Monarch of Bermuda"—a magnificent hotel on water with the appointments of an exclusive club. The cruise will include 3 days at the Hotel Bermudiana, Hamilton, which will give an opportunity to visit the near-by caves and submarine coral gardens, and to drive, rest, or golf on some of Bermuda's fine courses. Returning, the party will reach New York on the morning of February 5. The inclusive prices for the entire trip begin at $86.25. This includes all necessary expenses of the trip except the Bermuda tax of 12 shillings, 6 pence (about $3.25) which is payable in Bermuda. Reduced rates for rooms on shipboard are offered, as well as special rates at the Hotel Bermudiana, and stopover privileges for as long as desired. Members wishing to take this cruise are urged to make their reservations at once to avoid possible disappointment. Reservations may be cancelled later, if necessary. Detailed information may be obtained from Leon V. Arnold, 36 Washington Square, West, New York, N. Y.

Women's Entertainment

The women attending the convention this year are assured of plenty to occupy their time. The women's entertainment committee, under the chairmanship of Mrs. George Sutherland, is rapidly completing the details of a most attractive program. Monday, January 25, 1937, the first day of the Convention, will be devoted to registration at the women's headquarters on the 10th floor. On Tuesday several novel and interesting tours are scheduled with attendance at a radiobroadcast for the evening. On Wednesday there will be luncheon and bridge at the Engineering Woman's Club, and the Edison Medal presentation and lecture in the evening. Thursday will be devoted to a visit to the Edison Wonder House with the Dinner-Dance at the Hotel Astor for the evening. On Friday a visit is arranged to the Morgan Library. This necessarily will be for a limited group. If demand warrants, a visit to the Hayden Planetarium also will be provided.

Hotel Rates

Reservations for hotel accommodations should be made by writing directly to the hotel of your preference. In table II is included a brief list of some of the leading hotels in the vicinity.

Register in Advance

Members in near-by Districts should fill in and post promptly the mail registration card which was included with the mailed announcement of the winter convention sent them. This will permit the committee to have badges ready and prevent congestion at the registration desk upon arrival. There will be a registration fee of $2 for non-members with the exception of Enrolled Students of the Institute, and the immediate families of members.

The personnel of the 1937 winter convention committee is as follows: C. R. Beardsley, *chairman;* H. E. Farrer, *secretary;* T. F. Barton, O. B. Blackwell, E. E. Dorting, A. G. Oehler, C. S. Purnell, S. A. Smith, Jr., George Sutherland, and F. P. West. The chairmen of the subcommittees completing the arrangements are: C. M. Gilt, *dinner-dance;* E. S. Banghart, *smoker;* E. R. Thomas, *inspection trips;* and Mrs. George Sutherland, *women's entertainment.*

Student Conference Held by Middle Eastern District

The annual conference of Branch counselors and chairmen of the Institute's Middle Eastern District (2) was held at Ohio State University, Columbus, Friday and Saturday, November 13–14, 1936. The official attendance at the conference consisted of the 34 delegates listed in table I. The meeting was attended also by National Secretary H. H. Henline and W. H. Harrison, vice-president of the Institute representing the Middle Eastern District. The student attendance at the evening meeting Friday night was 75, and at the final joint meeting on Saturday, 64.

Following registration, which was held from 5 to 7 p.m. Friday, the evening meeting opened with a dinner. After dinner, Professor F. C. Caldwell gave the address of welcome, following which there were several talks. Professors H. W. Bibber and W. L. Everett, of Ohio State, outlined in detail the course in electrical engineering as it is taught at that institution. Professor E. O. Lange spoke on Branch activities, and recommended that all Branches consider seriously the installation of new officers at a much earlier date in the spring. National Secretary Henline presented a historical outline of student Branches and the national AIEE organization. Vice-President Harrison, who spoke on District activities, convinced all present that engineering societies offer some exceptional opportunities to engineers at the present time and that all student engineers should associate themselves actively with the engineering society of their choice. Professor E. E. Kimberly, chairman of the Institute's Columbus Section, and V. Frederiksen, secretary of that Section, outlined the constructive work being done between the Section and the Ohio State University Branch.

On Saturday morning, November 14, the group was taken on an inspection trip of the laboratories at Ohio State. This was followed by separate meetings of the Branch chairmen and counselors. The student group with R. P. Stokely, chairman of the Ohio State Branch presiding, carried out informal discussion of: (1) participation by students in meetings; (2) credit for attendance; (3) competition for prizes; (4) encouragement of attendance of upperclassmen, sophomores, and freshmen; (5) inspection trips; and (6) social activities.

At the counselors session, there was some discussion concerning the student convention of the Branches in the east section of the District to be held at Johns Hopkins University, Baltimore, Md., next spring. It was decided that the Branches at George Washington University, the University of Maryland, and the Catholic University of America be invited to participate in this convention, since they are situated near Baltimore. It was the consensus of opinion that Branches situated in a central area should work as a unit in holding student Branch conventions.

It was decided that the next District

Membership—

Mr. Institute Member:

Your response to our request for names of prospective members has been very helpful so far this year. We need your continued aid to reach the goal of 2,000 applications by May. Whether you have already suggested some one or not, send in the name of a good prospect now.

The busy season of the Institute year is now well under way. Take your fellow engineer who is not a member to your Section meetings, to the convention technical sessions, to the dinner-dance and the smoker, and show him what we do. When he is interested, send his name to your Section membership committee chairman. If you start the job he will finish it.

J. Elliot Du Comb

Vice-Chairman, District No. 3
National Membership Committee

Table I

Branch	Counselor	Delegate
Univ. of Akron	J. T. Walther	
Bucknell Univ.		Ripple Schumaker
Carnegie Inst. of Tech.	M. S. Schonvisner	J. C. Lynch
Case School of Applied Science	A. C. Seletzky	J. A. Harshaw
Catholic Univ. of America		
Univ. of Cincinnati	L. R. Culver	B. Baumsweiger
Drexel Inst. of Tech.	E. O. Lange	H. W. Graybill
George Washington Univ.	A. G. Ennis	E. W. Thomas
Johns Hopkins Univ.	J. H. Lampe	H. B. Peck
Lafayette College	F. W. Smith	R. S. Baum
Lehigh Univ.	J. L. Beaver	T. R. Brown
Univ. of Maryland	L. J. Hodgins	W. G. Calder
Ohio Northern Univ.	B. F. Wyandt	Glen Griffith
Ohio State Univ.	F. C. Caldwell	R. P. Stokely
Ohio Univ.	A. A. Atkinson	G. M. Kanable
Pennsylvania State College	L. A. Doggett	H. B. Stockham
Univ. of Pennsylvania		R. S. Graham
Univ. of Pittsburgh	H. E. Dyche	E. B. McKinney
Princeton Univ.		
Swarthmore College		
Villanova College	H. S. Baeche	
West Virginia Univ.	A. H. Forman	M. W. Henderson

conference of Branch counselors and chairmen should be held at Akron in October 1937, in conjunction with the District meeting to be held there at that time. Professor A. G. Ennis of George Washington University, was elected chairman of the conference for the year beginning August 1, 1937. Professor E. O. Lange was elected as a delegate to the Institute's 1937 summer convention to be held June 21–25, 1937, at Milwaukee, Wis.

At the conclusion of these sessions, the counselors and students reconvened for a final joint session during which the proceedings at the separate sessions were summarized.

Eta Kappa Nu Announces Awards

Frank M. Starr (A'30), central station engineering staff, General Electric Company Schenectady, N. Y., has been named by Eta Kappa Nu, honorary electrical engineering society, as America's outstanding young electrical engineer for 1936. Mr. Starr was selected from 47 nominees, and he becomes the first to be so recognized by this society in its plan to recognize outstanding young electrical engineers. (See announcement in March 1936 issue of ELECTRICAL ENGINEERING, pages 306–07.) Four other candidates were selected as recipients of honorable mention certificates; these men are: P. L. Bellaschi (A'28, M'34) development and research engineer, Westinghouse Electric & Manufacturing Company, Sharon, Pa.; E. W. Boehne (A'29) engineer, large oil circuit breaker engineering department, General Electric Company, Philadelphia, Pa.; A. C. Seletzky (A'29, M'35) assistant professor of electrical engineering, Case School of Applied Science, Cleveland, Ohio; and C. G. Veinott (A'28, M'34) electrical engineer, Westinghouse Electric & Manufacturing Company, Springfield, Mass. Biographical sketches of the recipients may be found in the "personal" columns of this issue.

The awards were made by a committee composed of: E. B. Meyer (A'05, F'27, past-president) chief engineer, electric engineering department, Public Service Electric and Gas Company, Newark, N. J.; L. W. Morrow (A'13, F'25) general manager, fiber products division, Corning Glass Works, Corning, N. Y.; the late General R. I. Rees; C. A. Butcher (M'22) eastern engineering manager, Westinghouse Electric & Manufacturing Company, New York, N. Y.; Everett S. Lee (A'20, F'30) engineer, general engineering laboratory, General Electric Company, Schenectady, N. Y.; and R. I. Wilkinson (A'35) engineer, Bell Telephone Laboratories, New York, N. Y.; the last 2 men are past-presidents of Eta Kappa Nu.

The recognition plan sponsored by Eta Kappa Nu is designed: (1) to assure due and appropriate honors to young electrical engineers for "meritorious service in the interest of their fellowmen"; (2) to give the engineering profession concrete examples of what young men under 35 years of age and not more than 10 years out of college can be expected to achieve; and (3) to inspire by these young men's careers, and furnish guides for, undergraduates and new engineering graduates to take up their own professional development as soon as possible. A very broad range of accomplishments from scientific research to civic and political activity and artistic creation is recognized, the aim being to encourage engineers to obtain a truly liberal and humanistic perspective at an early point in their careers.

Nominations of candidates for the 1936 recognition were received from heads of electrical engineering departments of colleges and universities throughout the country, from Sections of the AIEE, and from individual members of the Eta Kappa Nu Association. Mr. Starr will have the honor of being the first to have his name placed on a large bronze bowl created by Eta Kappa Nu, which will be kept on display at the headquarters of the AIEE in the Engineering Societies Building in New York. Mr. Starr will also be presented with a smaller reproduction of the bowl, engraved with a brief résumé of his accomplishments, at the citation ceremonies to be held in New York on the evening of January 25, 1937, during the AIEE winter convention.

Future AIEE Meetings

Winter Convention
New York, N. Y., Jan. 25–29, 1937

North Eastern District Meeting
Buffalo, N. Y., May 5–7, 1937

Summer Convention
Milwaukee, Wis., June 21–25, 1937

Pacific Coast Convention
Spokane, Wash., Date to be determined

Middle Eastern District Meeting
Akron, Ohio, Fall 1937

District and National Prizes for 1936 Technical Papers

All who have presented technical papers before the Institute during the calendar year 1936 are eligible under the AIEE paper prize regulations for competitive consideration for one or more of the established prizes. Papers are eligible for submission to the prize committees regardless of whether presented before a Branch meeting, a Section meeting, a District meeting, or a national convention, the several classes providing for equitable competition. Both District and national prizes are awarded each spring for papers presented during the preceding calendar year. Rules governing the awards were outlined in the December 1935 issue of ELECTRICAL ENGINEERING, pages 1414–15.

Although all 1936 papers are *eligible* for consideration, every paper for which prize consideration is desired must be *submitted* specifically for that purpose (except as noted below) not later than February 15, 1937, through the District secretary for consideration for the District prizes, or through the national secretary's office for consideration for the national prizes. There is no provision for automatic consideration of papers, with the exception that those approved by the technical program committee and presented at national conventions or District meetings, will be considered by the national prize committee for the national "best paper" and "initial paper" prizes without being formally offered for competition.

Executive Committee Meets at Institute Headquarters

A meeting of the executive committee of the American Institute of Electrical Engineers was held at Institute headquarters, New York, N. Y., December 10, 1936, in place of the regular meeting of the board of directors.

Present: A. M. MacCutcheon (chairman), O. B. Blackwell, Everett S. Lee, E. B. Meyer, L. W. W. Morrow, W. I. Slichter; National Secretary H. H. Henline.

Reports were presented and approved of meetings of the board of examiners held October 28 and December 2, 1936. Upon

the recommendation of the board of examiners, the following actions were taken: 3 applicants were transferred to the grade of Fellow; 17 applicants were transferred and 14 were elected to the grade of Member; 76 applicants were elected to the grade of Associate; 560 Students were enrolled.

Disbursements in November amounting to $20,511.61 were reported by the finance committee and approved.

Report was made and approved of the appointment, upon the nomination of the standards committee, of H. W. Samson as AIEE representative on the sectional committee on standardization of graphical symbols and abbreviations (Z32) of the American Standards Association.

Further consideration was given to the subject of broadening Institute activities to cover discussions of social and economic subjects. At its October 1936 meeting, the board of directors passed a motion concurring in the suggestion that such topics are of general interest to electrical engineers, calling attention to the fact that the Institute offers opportunity for discussion of such questions, and suggesting that papers on these subjects be submitted to the proper committees of the Institute for consideration for national presentation and publication. After a discussion of the procedure to be followed in this matter, it was voted that a special committee on broadening of Institute activities be appointed, consisting of the chairman of the technical program committee as chairman, and the chairmen of the committees on code of principles of professional conduct, co-ordination of Institute activities, economic status of the engineer, Institute policy, legislation affecting the engineering profession, publication, and Sections.

Other matters were discussed, reference to which may be found in this or future issues of ELECTRICAL ENGINEERING.

Weston Library Willed to Newark Engineering College

By the terms of the will of the late Doctor Edward Weston (A'84, M'84, HM'33, past-president) the Newark (N. J.) College of Engineering is to receive his general and technical library with a sum sufficient to provide for housing and maintaining it. The library is reported to contain complete sets of the proceedings of scientific societies not only in America, but from many foreign countries. In addition to his library, Doctor Weston willed the college the drawings and designs for his many patents and discoveries and much data accompanying them of great general interest and historical value. The college is planning to gather together this material and arrange it in such manner as to form a proper record of Doctor Weston's contribution to science and technology.

Doctor Weston was a member of the original board of trustees of the Newark Technical School, predecessor of the Newark College of Engineering, in which capacity he served for many years. Although forced to retire from the board because of increasing business obligations, he maintained an active interest in the college until his death, which occurred on August 20, 1936. A biographical sketch of his career appeared in the September 1936 issue of ELECTRICAL ENGINEERING, page 1049.

New automobile showroom in Chrysler Building, New York, N. Y., has distinctive lighting

AIEE Officers to Be Nominated Soon

In accordance with the Institute's by-laws, the national nominating committee of the AIEE will meet during the winter convention, New York, N. Y., January 25–29, 1937, for the purpose of nominating national officers to be voted upon by the membership in the spring of 1937. Members of the national nominating committee, named in accordance with the Institute's by-laws, are as follows:

Representing the Board of Directors

O. B. Blackwell — A. C. Stevens
N. E. Funk — J. B. Whitehead

(One additional member to be appointed)

Representing the 10 Geographical Districts

1—T. H. Morgan, Worcester Polytechnic Institute, Mass.
2—W. R. Wickenden, Case School of Applied Science, Cleveland, Ohio.
3—E. B. Meyer, Public Service Electric and Gas Company, Newark, N. J.
4—E. E. George, Tennessee Electric Power Co., Chattanooga, Tenn.
5—K. L. Hansen, Harnischfeger Sales Corporation, Milwaukee, Wis.
6—A. L. Turner, Northwestern Bell Telephone Company, Omaha, Neb.
7—J. W. Ramsay, University of Texas, Austin.
8—H. S. Lane, Pacific Gas and Electric Company, San Francisco, Calif.
9—R. E. Kistler, Pacific Telephone and Telegraph Company, Seattle, Wash.
10—C. V. Christie, McGill University, Montreal, Quebec, Can.

The provisions of the AIEE constitution and by-laws relating to nomination of officers were given in ELECTRICAL ENGINEERING for November 1936, page 1278, wherein members were invited to submit suggestions for nominations not later than December 15, 1936. The methods whereby nominations also may be made independent of the nominating committee were given in that item. Briefly, independent nominations may be made by a petition of 25 or more members sent to the national secretary at Institute headquarters, not later than March 25, to be placed before the nominating committee for inclusion in the ballot of such candidates as are eligible. Petitions for the nomination of vice-president may be signed only by members within the District concerned.

New York Gathering Honors Memory of Rudolph Diesel

In commemoration of the 40th anniversary of the introduction of Diesel power into the United States, some 250 or more leaders in American business, industry, engineering, research, and education gathered at the Waldorf-Astoria Hotel in New York City, December 2, for a special luncheon which coincided with "Diesel Day" at the then current annual power show in New York.

Diesel, Paris-born Bavarian refrigerating engineer, had specialized in the study of thermodynamics and was much impressed with the Carnot theory of a perfect engine, the continued study of which subject led him toward his ultimate development. In 1892 he obtained his first German patent covering claims for both simple and compound Diesel engines, the suggested fuel being coal dust. Later patents included the use of petroleum oils and the employment of high-pressure air to inject the oil charge into the cylinder. Early development, however, was slow, and it was Fate's decree that never during the inventor's lifetime did his engine become generally recognized as an important source of power. Doctor Diesel disappeared from a ship while en route from Germany to England, during September 1913, on the eve of his engine's career.

In 1896, Adolphus Busch of Anheuser-Busch fame acquired the American Diesel license, and built in St. Louis, Mo., a 60-horsepower 2-cylinder unit, which, placed in service in 1898, is said to be the first Diesel engine in the world to be put actually into industrial service. In the interim, re-

search and industrial progress, with their by-products of improved knowledge of thermodynamics and vastly improved materials of construction have permitted the development and improvement of the Diesel engine to a point where the new horsepower placed in service during 1936 is estimated at 2,100,000.

Chairman of the committee of arrangements was Gordon Rentschler, president of The National City Bank of New York; master of ceremonies was Radio-Commentator John B. Kennedy. Feature speakers, each of whom spoke briefly from the point of view of his own business activities, included: Edward B. Pollister, president, Busch-Sulzer Brothers Diesel Engine Company; Capt. Edward V. Rickenbacker, vice-president, Eastern Air Lines; Col. Robert H. Morse, president, Fairbanks-Morse & Company; Thomas H. Beck, president, Crowell Publishing Company; C. L. Cummins, president, Cummins Engine Company; Edward G. Budd, Edward G. Budd Manufacturing Company (streamlined trains); R. U. Blasingame, president, American Society of Agricultural Engineers; David S. Sarnoff (via radio from Chicago) president, Radio Corporation of America; B. C. Heacock, president, Caterpillar Tractor Company; and Charles F. Kettering (via radio from Detroit) vice-president in charge of research, General Motors Corporation, who emphasized the extent of the internal combustion engine market in America, by pointing out that during 1936 some 200,000,000 horsepower in new motors cars had been manufactured.

Insulation Stability Research to Be Extended

Engineering Foundation, with the sponsorship of the AIEE, has appropriated $5,000 for an experimental research on the stability of impregnated paper insulation. The work is to be done in the school of engineering of The Johns Hopkins University, Baltimore, Md., under the direction of Doctor J. B. Whitehead (A'00, F'12, past-president) professor of electrical engineering.

This work will be an extension of that completed several years ago by Doctor Whitehead and associates on the stability of impregnated paper as related to the physical properties of the impregnating oil. The new work will include a similar series of accelerated life tests as related to variations in the physical and chemical properties of the paper.

The present appropriation and plans are for a period of a year, but it is expected that both will be continued a second year.

Noble Prize Awarded to Institute Member

The Alfred Noble Prize for 1936 has been awarded to Abe Tilles (A'30, M'36) instructor in electrical engineering at the University of California, Berkeley, for his paper "Spark Lag of the Sphere Gap." This paper, which received the Institute's 1935 Pacific District prize for best paper, was published in ELECTRICAL ENGINEERING for August 1935, pages 868–76, and was presented at the AIEE Pacific Coast convention, Seattle, Wash., August 27–30, 1935. An item regarding Doctor Tilles is given in the personal columns of this issue. Presentation of the award will be made at the AIEE 1937 winter convention.

The Alfred Noble Prize was instituted in 1929 in honor of Alfred Noble, past-president of the American Society of Civil Engineers and the Western Society of Engineers, and consists of a $500 cash award and an engraved certificate. The award is made to a member of any grade of either the American Society of Civil Engineers, the American Institute of Mining and Metallurgical En-

Ambrose Swasey Receives Hoover and VDI Medals

Ambrose Swasey (center), "Knight of the Kindly Heart," Honorary Member of the Institute, founder and patron of The Engineering Foundation, as he appeared at the Astor Hotel in New York City, December 2, 1936, celebrating his ninetieth birthday by receiving simultaneously the Hoover Gold Medal, highest American engineering award, and the Gold Medal of the Verein Deutscher Ingenieure, outstanding German award. At Mr. Swasey's right is Herbert Hoover (HM'29), for whom the medal was named and to whom in 1930 its first award was made "for distinguished public service." Mr. Swasey is the second to receive the award. At Mr. Swasey's left is Dr. Gano Dunn, past-president of the Institute, and chairman of the Hoover Medal board of award. Other details pertaining to the award and its recipient were given in the November 1936 issue of ELECTRICAL ENGINEERING, pages 1278–9 and 1288.

In connection with the presentation ceremonies, Doctor Dunn outlined medallist Swasey's long and colorful career. Mr. Hoover amplified this in his "tribute to Mr. Swasey as an engineer for his 70 years of active service to engineers and to humanity," stating that the "sum of Mr. Swasey's contributions has brought more comfort and more security to more human beings than have come from any one other individual." Incidentally, Mr. Hoover flung an engineer's challenge to engineers by stating emphatically that "the engineer no longer can hold himself to design and administration, but must range out into broader fields if humanity's problems of today are to be solved satisfactorily."

gineers, The American Society of Mechanical Engineers, the American Institute of Electrical Engineers, or the Western Society of Engineers, for a technical paper of particular merit accepted by the publication committee of any of the foregoing societies for publication, in whole or in abstract in any of their respective technical publications, provided the author, at the time the paper is accepted in practically its final form, is not over 30 years of age. The recipient of the prize is selected by a committee of 5 members, consisting of one representative of each society, the award being based upon papers published by the societies within the 12 months preceding July 15 of each year.

The first award of the Alfred Noble Prize was made in 1931, and the second award, in 1932, was made to F. M. Starr (A'30).

Letters to the Editor

CONTRIBUTIONS to these columns are invited from Institute members and subscribers. They should be concise and may deal with technical papers, articles published in previous issues, or other subjects of some general interest and professional importance. ELECTRICAL ENGINEERING will endeavor to publish as many letters as possible, but of necessity reserves the right to publish them in whole or in part, or reject them entirely.

ALL letters submitted for consideration should be the original typewritten copy, double spaced. Any illustrations submitted should be in duplicate, one copy to be an inked drawing but without lettering, and other to be lettered. Captions should be furnished for all illustrations.

STATEMENTS in these letters are expressly understood to be made by the writers; publication here in no wise constitutes endorsement or recognition by the American Institute of Electrical Engineers.

Engineering Education—Opinions and Influencing Factors

To the Editor:

In their closing discussion on their paper "Engineering Education—Opinions and Influencing Factors" (see ELECTRICAL ENGINEERING, October 1936, page 1147), Professors King and Eshbach raise certain questions that should be answered. One of these points was discussed in my paper "A New General Engineering Curriculum" as presented before the electrical engineering conference of the Society for the Promotion of Engineering Education in Madison, Wis., in June 1936 (see *Journal of Engineering Education*, volume 26, number 10, June 1936, page 826).

The members of the committee that worked out the details of this new general engineering curriculum, debated at length concerning the choice of a proper descriptive name for this new curriculum. They felt that "basic" engineering most nearly described the content, but recognized the fact that this term had no generally accepted meaning in either the engineering world or in industry. At the same time, the committee realized that "general" engineering, in its ordinary usage, connoted considerable emphasis upon managerial studies, and usually a wide range of electives in liberal amounts. Finally, it was decided that perhaps it was best at first to label it, in the college catalog, as "general engineering" with the subtitle description of "composite course including the basic essentials of civil, electrical, industrial, and mechanical engineering."

It was recognized immediately that professional society activities would be a necessary concomitant of the academic program of study. A local General Engineering Society was formed and started functioning immediately after the curriculum was opened. Meetings are held just as frequently as those of the student branches of the various national engineering societies. Also, the General Engineering Society participates jointly with the other student engineering societies in the activities of the local engineering society, which includes in its membership students from all engineering departments. Senior students in general engineering are encouraged to attend in rotation the meetings of the student branches of the 4 national societies sponsored by the 4 co-operating departments, in addition to the meetings of their own General Engineering Society. In this way they get well acquainted with national professional engineering societies and should have every incentive for associating with one of the national engineering societies as soon as they become placed in industry.

Respectfully yours,

ALBRECHT NAETER (A'23, M'30)
Professor and Head of Electrical Engineering Department, Oklahoma Agricultural and Mechanical College, Stillwater

The Measure of an Engineer

To the Editor:

In his response, in receipt of the Lamme medal, Doctor Vannevar Bush stated that engineers were responsible and honest people, but too often inclined to mind their own business. ("The Measure of an Engineer," ELECTRICAL ENGINEERING, August 1936, page 854.)

Such modesty and a minding of his own business are very practical guides to the engineer's conduct in his social community. Viewing socio-economic matters of the past and present he is not so much inarticulate as incoherent, as would be a medical person should he presume to speak on such matters. Let the engineer stick out his neck too far, he will receive, as descriptive of society's understanding of his stimuli, such trivia as:

"... but think of his power. Think of the temptation of playing with his switchboard just for the fun of it. In his place and at his age I do not think I could have resisted it."

This appeared in an article "Notes on the Conventions," by R. deR. deSales, published in *Atlantic Monthly*, September 1936 issue.

There is a wide gulf between the ideas of Doctor Bush and those of M. deSales. Remember, however, the latter is a journalist. He writes for the general public. He thus reflects their viewpoint. What he asks us to "think" the public in general thinks. Note that there is no reference to responsibilities on the part of the technician he refers to, but merely to the hilarious effect that might capriciously be brought about by a wholesale confusion.

To get some further notion of the public mind and its relation to any sort of science, let us assume M. deSale's attitude and apply the words to one or 2 other classes of persons. First, let us think of medical doctors: "... but think of his power. Think of the temptation of playing with his patient just for the fun of it. In his place ... etc." "An unthinkable and monstrous ideal"—thus we could expect to hear from common men filled with a thumping indignation.

But let us continue with possible other changes in the original quotation. Though the thought intrigues, we pass charitably over the substitution of "plaintiff," or "defendant" or "witness" for "switchboard." Rather put "printing-press" in its place, meantime thinking "journalist" instead of "engineer." M. deSales himself would doubtless be among the most notable in rightly professing that inherent responsibility which the true journalist feels.

Yet it cannot be too clearly stated that his original words represent a popular conception of the mischievous possibilities inherent in a position of control and assigned as admissible to engineers' mentalities. It represents the popular mind's notion of the mental set of scientists. These are the persons whom the public suspects of being that vast impersonal THEY in vexatious control of present-day developments and operations

So, in all sincerity, I beg those who are capable to give us further encouragement along the line of Dr. Bush's "central function" thesis. The engineer needs encouragement to apply the principles of scientific action to human affairs rather than feeling pressure to rush himself uncritically at the "success" demands of a business-based social order. He needs his backbone stiffened so that he may courageously focus back the ills of society on itself by applications of science, not to try to use it to produce any sort of palliatives. In war, physicians attend the wounded, even though in their hate of war they know that larger mass death would sooner terminate hostilities. Such behavior is an aspect of scientific method applied to human behaviors. The public considers such action worthy.

The proper rôle of an engineer at a political convention is likewise a scientific one. If the proceedings are consequential, well and good. Should they be so much twaddle, it is his true office to let that fact appear. But in the cheerful disorder of his mind Johnny Q. Public is a long way from any such realization.

Yours very truly,

J. ANDREW DOUGLAS (A'18, M'29)
Physics and General Science Teacher, Murphy High School, Mobile, Alabama

Personal Items

ALEX DOW (A'93, F'13, member for life) president, Detroit (Mich.) Edison Company, has been awarded the AIEE Edison Medal for 1936 "for outstanding leadership in the development of the central station industry and its service to the public." The medal, which was founded by friends and associates of the late Thomas A. Edison (A'84, M'84, HM'28), and is awarded annually for "meritorious achievement in electrical science, electrical engineering, or the electrical arts," will be presented to Doctor Dow during the Institute's winter convention at New York, N. Y., January 25–29, 1937. Doctor Dow was born in Glasgow, Scotland, in 1862, and although he is not a graduate of a technical school, he has received the honorary degrees of master of engineering (1911) and doctor of engineering (1924) from the University of Michigan and doctor of science (1935) from the University of Detroit. During the period 1874–82, he was employed as junior clerk and stenographer in a railroad office and in the offices of a steamship company in Liverpool, England. In 1882 he came to the United States, and was employed in various departments of the Baltimore and Ohio Railroad Company. Later he was transferred to the Baltimore and Ohio Telegraph Company to take charge of local line and instrument maintenance, with some construction and experimental work on telephones. In 1888 he was employed by the Brush Electric Company, Cleveland, Ohio, as installation electrician in the Chicago (Ill.) office, becoming district engineer in that office in 1889. In 1893, he accepted the opportunity to design and supervise the construction of the original public lighting plant of the city of Detroit, and in 1896 he became vice-president and general manager of the Edison Illuminating Company of Detroit. This company was succeeded by the Detroit Edison Company in 1903, and Doctor Dow was retained as vice-president until 1913, when he was made president. He became a naturalized citizen in 1895. Doctor Dow has been a leading pioneer in the United States in the engineering, rate making, and general operation of the electric light and power utility, and is given credit for both the engineering and financial success of his enterprises. He has supervised the design and construction of several generating stations of the Detroit Edison system, and he is called the father of the so-called "big" steam boiler in the United States, having installed 2,350-horsepower boilers at a time when 600- to 750-horsepower units were commonly considered large. He was the first to adopt the underfeed stoker for large installations, and much of the earlier development of this type of equipment was made in his power plants. In addition to his electric utility activities, Doctor Dow served the city of Detroit as the engineer member of the Board of Water Commissioners from 1916 to 1921, and again from 1925 to 1927. He is a member of The American Society of Mechanical Engineers (president 1928), American Society of Civil Engineers, the Institution of Electrical Engineers (Great Britain), and the Detroit Engineering Society (charter member and past-president). He has recently been elected an honorary member of both the ASME and the ASCE. For his paper "On the Schooling of Engineers" (published in the December 1934 issue of ELECTRICAL ENGINEERING, pages 1589–91), he was awarded the AIEE 1935 national prize for best paper in public relations.

O. E. BUCKLEY (M'19, F'29) director of research for the Bell Telephone Laboratories, Inc., New York, N. Y., has been elected executive vice-president. Doctor Buckley was born at Sloan, Iowa, August 8, 1887, and received the degrees of bachelor of science from Grinnell College (1909) and doctor of philosophy from Cornell University (1914). In 1936 the honorary degree of doctor of science was conferred upon him by Grinnell College. Doctor Buckley was an instructor in physics at Grinnell College during 1909–10, an assistant in physics at Cornell University 1910–12, and instructor 1912–14. He was then employed in the engineering department of the Western Electric Company until he was given charge of the signal corps laboratory of the U. S. Army in Paris, France, during 1917–18. After he returned to the company (from which Bell Telephone Laboratories, Inc., later was derived) he engaged in work on continuously loaded cables. In 1927 Doctor Buckley was made assistant director of research, and 6 years later became director of research, a position in which he had charge of fundamental studies in a great variety of fields. Since 1926 Doctor Buckley has been a member of the Institute's committee on electrophysics, and from 1929–31 he was its chairman. During the period 1929–31 he was a member of the meetings and papers committee (now technical program) and since 1934 he has been a member of the committee on research. He is a member of the Franklin Institute, American Physical Society, and American Association for the Advancement of Science.

O. B. BLACKWELL (A'08, F'17, vice-president) formerly manager of staff departments, Bell Telephone Laboratories, Inc., New York, N. Y., has been elected vice-president of the laboratories with responsibility for the development of communication apparatus and telephone systems. Mr. Blackwell was born at Bourne, Mass., August 21, 1884. Receiving the degree of bachelor of science from Massachusetts Institute of Technology in 1906, he immediately entered the engineering department of the American Telephone and Telegraph Company. In 1914 he became transmission and protection engineer, and with the formation of the department of development and research in 1919 he became transmission development engineer. When that department was consolidated with Bell Telephone Laboratories in 1934, Mr. Blackwell was appointed director of transmission development. In 1935 he was made manager of staff departments. In his new position as vice-president he will have charge of the apparatus development, systems development, and protection development departments. His individual contributions to the communication art have been to the practical theory of transmission and cross-talk and to many problems which have arisen in transmission development. Mr. Blackwell has served on the Institute's committee on communication 1918–26 (chairman 1922–25) and from 1935 to the present time; in 1936 he was elected a vice-president representing the New York City District and was appointed a member of the standards committee. He is a member of the plant co-ordination committee and the joint sub-committee on development and research of the Edison Electric Institute and Bell System, and a member of the standards council of the American Standards Association.

E. W. BOEHNE (A'29) engineer in the large oil circuit breaker engineering department of the General Electric Company, Philadelphia, Pa., has received honorable mention in connection with the selection by Eta Kappa Nu, honorary electrical engineering society, of America's outstanding young electrical engineer for 1936 (see page 193). Mr Boehne was born at Laramie, Wyo., June 2, 1905. Following graduation in 1926 from the Agricultural and Mechanical College of Texas, Mr. Boehne entered the General Electric Company at Lynn, Mass., for a year and then undertook graduate work at Massachusetts Institute of Technology, receiving the degree of master of science in 1928. He was one of 2 men from that institution selected to take the advanced course

ALEX DOW

O. E. BUCKLEY

O. B. BLACKWELL

M. J. KELLY

J. H. HERRON

F. M. STARR

ABE TILLES

in engineering of the General Electric Company at Schenectady, N. Y. Since 1933 he has been in the switchgear plant of that company at Philadelphia. He has specialized in the protection of electrical equipment from surges due to lightning and switching, his early work on the calculation of arrester performance in connection with choke coils being notable. He was closely associated with the design of 287-kv circuit breakers for the Boulder Dam-Los Angeles transmission line, and is the author of several Institute papers. Mr. Boehne is a member of the Franklin Institute, and is interested in the activities of the Roerich Society, whose aim is "world peace through the arts."

M. J. KELLY (M'26, F'31) vacuum tubes and transmission instruments director, Bell Telephone Laboratories, Inc., New York, N. Y., has been appointed director of research. He was born at Princeton, Mo., February 14, 1894, and received the degrees of bachelor of science (1914) and master of science (1915) from the University of Missouri. In 1919 he received the degree of doctor of philosophy from the University of Chicago and in May 1936 he received an honorary degree of doctor of engineering from the University of Missouri in recognition of his contributions to communication engineering. Doctor Kelly joined the engineering department of the Western Electric Company, now Bell Telephone Laboratories, in 1919 and since then has been continuously engaged in researches in electronics and in the development of thermionic devices of all types. In 1922 he was placed in charge of the vacuum-tube development of the laboratories. In 1935 in addition to that work he was placed in charge of the development of transmitters and receivers for telephone instruments. Now, as director of research, he is in charge of all of the research activities of the laboratories. Doctor Kelly has served on the Institute's committees on communication and standards since 1934.

J. H. HERRON (M'35) president, The James H. Herron Company, Cleveland, Ohio, has been elected president of The American Society of Mechanical Engineers for the year 1936–37. Mr. Herron was born at Girard, Pa., January 4, 1875, and received the degree of bachelor of science in electrical engineering at the University of Michigan in 1909. From 1889 to 1897 he was employed in Erie, Pa., and subsequently was assistant engineer in charge of power for the Cambria Steel Company, Johnstown, Pa.; vice-president and chief engineer of the Bury Compressor Company, Erie; manager of the Motch & Merryweather Machinery Company, Detroit, Mich.; and chief engineer and works manager of the Detroit Steel Products Company. Since 1909 he has been president of The James H. Herron Company, engineers and chemists. He is also president of the Paragon Laboratories, director of the Baldwin Farms Land Company, and secretary of the National Engineering Inspection Association. He is the author of articles on metallurgical subjects published in technical periodicals, and is the inventor of the air-compressor inlet-valve unloader and of numerous devices for use with air compressors and metallurgical furnaces. Mr. Herron has served The American Society of Mechanical Engineers as manager (1922–25) and as vice-president (1934–36), and was president of the Cleveland Engineering Society during the year 1917–18. His other society affiliations include the American Society of Civil Engineers, American Institute of Mining and Metallurgical Engineers, American Chemical Society, American Society for Testing Materials, British Iron and Steel Institute, Society of Automotive Engineers, American Concrete Institute, and American Association for the Advancement of Science.

F. M. STARR (A'30) central station engineer, General Electric Company, Schenectady, N. Y., has been named by Eta Kappa Nu, honorary electrical engineering society, as America's outstanding young electrical engineer for 1936. Details of the award are given elsewhere in this issue. Mr Starr was born at Fowler, Colo., February 26, 1905, and was graduated with special honors from the University of Colorado in 1928 with the degree of bachelor of science in electrical engineering. He then joined the General Electric Company, entering on the test course at Schenectady, N. Y. The following year he entered the engineering general department and for the past 5 years has been a member of the central station engineering department. Mr. Starr's contributions to the electrical art have been chiefly in the field of central station design and power distribution. His researches and inventions in the devising of equivalent circuits for simulating complex networks resulted in the widespread adoption of new and more exact methods for calculating system performance under both normal and emergency conditions. His later work in establishing methods for detecting faults on ungrounded lines, and his study on the design, operation, and economics of various types of distribution systems, particularly networks, have also attracted wide attention. Mr. Starr has presented several papers before the Institute and received the Alfred Noble prize for his paper on equivalent circuits presented in 1932. The degree of electrical engineer was conferred upon him in 1933 by the University of Colorado in recognition of his work.

L. H. HILL (A'22, M'29) who has been assistant engineer in charge of transformer design for the Allis-Chalmers Manufacturing Company at Milwaukee, Wis., has been appointed engineer-in-charge of the transformer division. Mr. Hill was born at Toms River, N. J., March 8, 1899, and received the degree of electrical engineer from Cornell University in 1922. During the period 1920–22 he served as an instructor at the university, and following graduation accepted the position of design engineer in the transformer engineering department of the Westinghouse Electric & Manufacturing Company. In 1928 he became manager of the transformer division of the American Brown Boveri Electric Corporation at Camden, N. J., having charge of engineering and sales for the division. This company was absorbed by Allis-Chalmers Manufacturing Company in 1931, at which time Mr. Hill was made assistant engineer in charge of transformer design. Recently Mr. Hill was appointed vice-chairman of the national convention committee preparing for the 1937 summer convention of the Institute at Milwaukee.

ABE TILLES (A'30, M'36) instructor in electrical engineering at the University of California, Berkeley, has been awarded the Alfred Noble Prize for 1936, as reported elsewhere in this issue. The award was made for his paper "Spark Lag of the Sphere Gap," which was presented at the AIEE Pacific Coast convention, August 27–30, 1935. Doctor Tilles was born at New York, N. Y., March 10, 1907. In 1928 he received the degree of bachelor of science in mechanical engineering and electrical engineering with highest honors

from the University of California. In 1932 he received the degree of master of science in electrical engineering, and in 1934 that of doctor of philosophy in electrical engineering. During the period 1928–30 he was employed in the testing laboratories of the Bureau of Power and Light, Los Angeles, Calif., and in 1930 was for a time engaged in work for the testing and research laboratories of the California State Division of Highways at Sacramento before joining the faculty of the University of California as an associate. He was appointed instructor in 1933, specializing in electric power transmission and telephone transmission lines and transmission networks. Doctor Tilles received the annual best paper prize of the Pacific District at the 1936 AIEE summer convention for the same paper for which he now receives the Noble prize. He is counselor of the University of California Branch, and a member of Eta Kappa Nu and Sigma Xi.

ROSCOE SCHAEFFER (A'32, M'36) formerly resident electrical engineer for the Byllesby Engineering and Management Corporation, Oklahoma City, Okla., has been transferred to the Oklahoma Gas and Electric Company, Oklahoma City, as superintendent of engineering of that company. Mr. Schaeffer was born at Ludlow, Ill., in 1892, and was graduated from Iowa State College in 1915, with the degree of bachelor of science in electrical engineering. Upon graduation he served briefly as assistant superintendent of a small municipal power plant before entering the employ of the General Electric Company, Schenectady, N. Y., in 1916, serving first as a test engineer and subsequently as an assistant foreman and an assistant to the electrical superintendent of the Schenectady works of that company. In 1919 Mr. Schaeffer accepted a position as assistant engineer on standards with the Remy Electric Company, Anderson, Ind., where he remained for one year before affiliating himself with the William A. Baehr Company, Chicago, Ill., as resident engineer in charge of transmission-line construction at Ada, Okla. In 1923 he became assistant to the construction superintendent of the Oklahoma Gas and Electric Company, and later was made assistant to the general superintendent of operation of that company before being transferred to the Byllesby Engineering and Management Corporation in 1926.

C. G. VEINOTT (A'28, M'34) electrical engineer, Westinghouse Electric & Manufacturing Company, Springfield, Mass., has received honorable mention in connection with the selection by Eta Kappa Nu, honorary electrical engineering society, of America's outstanding young electrical engineer for 1936 (see page 193). Mr. Veinott was born at Somerville, Mass., February 15, 1905, and received the degree of bachelor of science in electrical engineering from the University of Vermont in 1926. He then entered the student course of the Westinghouse company at East Pittsburgh, Pa., and since then has been engaged chiefly with the problems of rotating machinery, making notable contributions. He was transferred to the small-motor engineering department at Springfield in 1929, and has been associated with the development of new methods of analysis of losses in single-phase motors, noise prevention studies, and new means of calculating single phase and polyphase induction motors. Mr. Veinott holds patents for disk-type thermostatic protection of motors, and has actively participated in the design and development of fractional-horsepower motors. Recently he was appointed to have charge of sales and engineering on all fractional-horsepower motors for fans and blowers. Mr. Veinott is the author of a number of papers, some of which have been presented to the Institute. He has been a member of the Institute's electrical machinery committee since 1934, and has been active in the work of the Springfield Section, of which he is now chairman.

J. M. TODD (M'32) consulting electrical engineer, New Orleans, La., has been elected a vice-president of The American Society of Mechanical Engineers for the year 1936–37. He was born at Franklin, La., May 25, 1896, and received the degrees of bachelor of engineering (1918) and mechanical engineer (1930) from Tulane University. He served (1918–19) as a lieutenant in the U.S. Army, seeing service in England and France, and in 1919 became chief engineer of the Marrero, La., plant of Penick and Ford, Inc. From 1921 to 1928 he was associated as assistant engineer with A. M. Lockert & Company, mechanical engineering contractors in New Orleans. He has since been retained as consultant in mechanical and electrical problems by the Orleans Parish School Board, the Board of State Engineers, the city of New Orleans, and Tulane University. Mr. Todd has been a member of the Institute's membership committee since 1935, and is a past-president of the Louisiana Engineering Society.

A. C. SELETZKY (A'29, M'35) assistant professor of electrical engineering, Case School of Applied Science, Cleveland, Ohio, has received honorable mention in connection with the selection by Eta Kappa Nu, honorary electrical engineering society, of America's outstanding young electrical engineer for 1936 (see page 193). Doctor Seletzky was born at Novostavtzy, Volynia, Russia, May 29, 1905. In 1927 he received the degree of bachelor of engineering and in 1930 that of doctor of engineering from The Johns Hopkins University, and in the latter year became an instructor in electrical engineering at Case School of Applied Science. He was made assistant professor in 1933. Doctor Seletzky is noted for his research work, which ranges from new analyses of various types of electric circuits and bridges to methods of magnetic analysis, thermionics, power transmission circuits, and a-c circuit theory. Doctor Seletzky is a second lieutenant in the Ordnance Reserve of the U.S. Army and has worked at Watertown Arsenal. He is the author of a number of AIEE papers and of papers published by the Franklin Institute. Since 1933 he has been a member of the AIEE committee on instruments and measurements, and is now serving as counselor of the Branch at Case School of Applied Science and as chairman of the membership committee of the Cleveland Section.

E. W. BURBANK (A'25, M'30) district manager, Allis-Chalmers Manufacturing Company, Dallas, Texas, has been elected a manager of The American Society of Mechanical Engineers for the year 1936–37. He was born at Sunbury, Ohio, February 15, 1889, and received the degree of bachelor of engineering from Tulane University in 1911. He then entered the employ of the Allis-Chalmers company as a student apprentice. Between 1913 and 1916 he was engaged in the experimental design and development of hydraulic machinery and in conducting extensive tests on this type of equipment. In 1916 he was transferred to the sales department and was sent to New Orleans, La., as sales engineer becoming district manager at Dallas 5 years later. He is a member of the American Petroleum Institute and the Dallas Technical Club.

P. L. BELLASCHI (A'29, M'34) section engineer in charge of transformer engineering, Westinghouse Electric & Manufacturing Company, Sharon, Pa., has received honorable mention in connection with the selection by Eta Kappa Nu, honorary electrical engineering society, of America's outstanding young electrical engineer for 1936 (see page 193). Mr. Bellaschi was born at Piedmont, Italy, February, 13, 1903, and came to the United States with his parents in 1913. In 1926 he received the degree of bachelor of science in electrical engineering from Massachusetts Institute of Technology and, following a year in the Westinghouse student course, received the degree of master of science in electrical engineering in 1928. Since that time he has been with the Westinghouse company in various capacities. Mr. Bellaschi is well known for his work in the field of lightning investigation, and has made many important contributions and discoveries. Many papers based on his researches have been published, both in the United States and in Europe. In 1936 he received a Westinghouse award of merit in recognition of his work in high-voltage research. Mr. Bellaschi has been active on the committees of the Sharon Section of the Institute. He is a member of the Associazione Elettrotecnica Italiana.

G. H. DUNSTAN (A'28) formerly assistant professor of general engineering at the University of Southern California, Los Angeles, now is enrolled as a graduate student at the University of Iowa, Iowa City. Mr. Dunstan is specializing in hydraulic engineering.

VINCENT HACKETT (A'36) student engineer, General Electric Company, Schenectady, N. Y., has been transferred to the Philadelphia, Pa., works of that company.

H. J. MASSHARDT (A'24) formerly with the International Paper Company, New York, N. Y., now is employed by the Scott Paper Company, Chester, Pa.

Obituary

CHARLES LEGEYT FORTESCUE (A'03 F'21) consulting transmission engineer, Westinghouse Electric & Manufacturing Company, East Pittsburgh, Pa., died December 4, 1936. Doctor Fortescue was born at York Factory, Manitoba, Canada, November 7, 1876, and received his earlier education at a private school in England. In 1898 he received the degree of bachelor of science from Queen's University, Kingston, Ont., and in that year joined the Westinghouse Electric & Manufacturing Company as an apprentice. The university conferred upon him a doctor's degree in 1931. From 1901 to 1918 he was in the transformer engineering department, and from 1918 to 1926 he was manager of the porcelain, insulator, and transmission engineering department. Since 1926 Doctor Fortescue had been consulting transmission engineer. Perhaps the best known of the many contributions to the engineering art that are credited to Doctor Fortescue is the development of the mathematical system known as "symmetrical coordinates" or "symmetrical components" and application of it to the solution of problems involving polyphase systems. For this work he was awarded the gold medal of the Franklin Institute in 1931. Other fields of his work were studies of stability and lightning protection. Doctor Fortescue also is credited with many improvements in transformer design, advancement of the art of measurement of high voltage by the sphere spark gap, development of basic principles for the form and proportions of insulating surfaces, and contributions to the design of transmission systems, receiving nearly 200 patents. He is said to have developed the first commercial 100,000-volt transformer, and advanced the theory that direct strokes were the cause of trouble on transmission lines. Many papers on various subjects were presented by him before the Institute, and others were published elsewhere. Doctor Fortescue had been a member of the Institute's committee on power transmission and distribution since 1932, serving previously from 1925 to 1929. He also had been a member of the committees on telegraphy and telephony (now communication) 1914–17, and electrophysics 1916–17 and 1920–31.

CLINTON JESSE AXTELL (A'09, M'30) assistant engineer of the control division, transportation engineering department of the General Electric Company, Erie, Pa., died October 16, 1936. He was born at Axtell, Kans., April 4, 1883, and was graduated from Kansas State College in 1904. For a short time he was employed by the Jackson (Mich.) Light and Power Company, then entered the testing department of the General Electric Company at Lynn, Mass. In 1907 he was transferred to Schenectady, N. Y., remaining until 1910. Between 1910 and 1913 he was employed by the Commonwealth Power Company of Michigan, the International Railway Company, Buffalo, N. Y., and the Cleveland (Ohio) Railway Company. He then returned to the General Electric Company in the railway department division, becoming assistant engineer of the division in 1930. He made many important contributions to the development of railway equipment and was an authority on electric control for all types of transportation vehicles including ships and naval equipment.

A. W. RUSSELL (A'31) chief engineer of the Hollywood mill, Buckeye Cotton Oil Company, Memphis, Tenn., died recently according to word just received at Institute headquarters. Mr. Russell was born December 22, 1876, at Little Rock, Ark. During the period 1910–19 he was chief engineer of the Little Rock (Ark.) Railway and Electric Company. In 1923 he was appointed chief engineer of the National Cotton Seed Products Corporation, where he remained until he entered the employ of the Buckeye Cotton Oil Company in 1929, as supervisor of power in the Memphis mills of that company. He was appointed chief engineer of the Hollywood mill in 1933.

Membership

Recommended for Transfer

The board of examiners, at its meeting on December 2, 1936, recommended the following members for transfer to the grade of membership indicated. Any objection to these transfers should be filed at once with the national secretary.

To Grade of Fellow

Bennett, C. E., electrical engineer, Federal Power Commission, Washington, D. C.

Bossard, G. L., president and director of engineering research, General Kontrolar Company Inc., Dayton, Ohio.

Lane, F. H., manager, engineering and construction, Byllesby Engineering and Management Corporation, Chicago, Ill.

MacNaughton, A. K., supervising engineer, The Commonwealth and Southern Corporation of New York, Birmingham, Ala.

Watson, A. E., associate professor of electrical engineering emeritus, Brown University, Providence, R. I.

5 to Grade of Fellow

To Grade of Member

Beck, Lester E., assistant professor of electrical engineering, Purdue University, West Lafayette, Ind.

Bodicky, A., underground engineer, Union Electric Light and Power Company, St. Louis, Mo.

Brady, G. B., assistant division superintendent, Oklahoma Gas and Electric Company, Enid, Okla.

Dueland, R., electrical engineer, Parsons, Klapp, Brinckerhoff and Douglas, New York, N. Y.

Dutton, T. D., district plant engineer, American Telephone and Telegraph Company, Washington, D. C.

Gerell, O. W., relay engineer, Union Electric Light and Power Company, St. Louis, Mo.

Hoyle, E. R., electrical engineer, Sinclair Oil and Refining Company, Houston, Texas.

Musgrove, A. M., Jr., assistant engineer, Public Service Electric and Gas Company, Englewood, N. J.

Nuttall, A., electrical engineer, Trinidad Leaseholds Ltd., Pointe-a-Pierre, B. W. I.

Stone, E. W., assistant superintendent, electric testing department, Central Illinois Light Company, Peoria, Ill.

Talley, T. J., 3rd, technical employee, American Telephone and Telegraph Company, Philadelphia, Pa.

Watts, F. W., vice-president, United Electric Controls Corporation, Hoboken, N. J.

Weiser, R. G., assistant engineer, Brooklyn Edison Company, Brooklyn, N. Y.

13 to Grade of Member

Applications for Election

Applications have been received at headquarters from the following candidates for election to membership in the Institute. If the applicant has applied for direct admission to a grade higher than Associate, the grade follows immediately after the name. Any member objecting to the election of any of these candidates should so inform the national secretary before Jan. 31, 1937, or March 31, 1937, if the applicant resides outside of the United States or Canada.

Allen, R. T., Jr., Consumers Power Company, Jackson, Mich.

Andrews, N. R. (Member), National Sugar Refining Company of New Jersey, Long Island City, N. Y.

Armstrong, D. K., Union Oil Company, Olean, Calif.

Armstrong, H. R., Detroit (Mich.) Edison Company.

Barrow, L. O. (Member), Brooklyn (N. Y.) Edison Company, Inc.

Behar, M. F. deM., (Member), Instruments Publishing Co. Pittsburg, Pa.

Bose, C. C. (Member), Indiana Bell Telephone Company, Indianapolis.

Bowen, R. E., Jr., City Light & Water Division, Memphis, Tenn.

Brandt, T. F., (Member), Ohio Brass Co. Barberton

Campbell, S. M., Cleveland Electric Illuminating Company, Ohio.

Capel, C. C., Indiana Bell Telephone Company, Indianapolis.

Dausman, O. D., Indiana Bell Telephone Company, Indianapolis.

Denison, H. C., Oklahoma Gas and Electric Company, Oklahoma City.

Dixon, A. R. American Tel. & Tel. Co., New York, N. Y.

Dotterweich, W. A. (Member), Consumers Power Company, Jackson, Mich.

Dunnewold, L. J., Indiana Bell Telephone Company, Indianapolis.

Dublin, M., Department of Docks, North River, New York, N. Y.

Falk, K. K. (Member), Bendix Products Corporation, South Bend, Ind.

Ferguson, B. (Member) 319 Homebuilders Bldg. Phoenix, Ariz.

Foster, C. D., Portland (Ore.) General Electric Company.

Green, I. V., Indiana Bell Telephone Company, Indianapolis.

Griffith, H. D., Westinghouse Electric & Manufacturing Company, Springfield, Mass.

Gruenberg, A. T., Gruenberg Elec. Co. Inc., New York, N. Y.

Heathman, E. J., Southwestern Bell Telephone Company, Bristow, Okla.

Henson, C. A., Pacific Gas and Electric Company, Sacramento, Calif.

Hyland, G. A., Westinghouse Electric and Manufacturing Company, Wilkes Barre, Pa.

Jack, C. E., 716 S. W. King Ave., Portland, Ore.

Johnson, J. E., Philadelphia (Pa.) Electric Company.

Johnson, W. C., Allis Chalmers Manufacturing Company, Chattanooga, Tenn.

Jones, D. J. (Member), Vapor Car Heating Company, Chicago, Ill.

Kanouse, E. L., Los Angeles (Calif.) Bureau of Power & Light.

Killoran, J. M., The Cleveland (Ohio) Electric Illuminating Company.

Langhauser, G. E. (Member), New York and Queens Electric Light and Power Company, Flushing, N. Y.

Larlee, D. H., Brooklyn (N. Y.) Union Gas Company.

Langhus, L., Central Electric and Telephone Company, Sioux City, Ia.

Lehman, J. J., Freeport Sulphur Company, Freeport, Texas.

Lincks, G. F., General Electric Company, Pittsfield, Mass.

Linders, J. R., Cleveland Electric Illuminating Company, Ohio.

Linke, H. M., Spruce Falls Power and Paper Company Ltd., Kapuskasing, Can.

Low, A. A. (Member), Brooklyn (N. Y.) Edison Co. Inc.

Mancib, A. S. (Member), Weston Electric Institute Corporation, West Somerville, Mass.

Markus, H. F., Arsenal Technical Schools, Indianapolis, Ind.

Mascaro, W. O., Atlantic Refining Company, Philadelphia, Pa.

McDowell, J. A., Sherwin Williams Company, Dallas, Tex.
Meyer, J. E., General Laminated Products Inc., New York, N. Y.
Meyer, J. M., Meyer Instrument Company, San Francisco, Calif.
Moody, W. S., General Electric Company, Schenectady, N. Y.
Muehlig, R. E., Westinghouse Electric & Manufacturing Company, Boston, Mass.
O'Brien, R. W. (Member), Southern Power Journal, Atlanta, Ga.
Packer, W., 1826 E. 82nd St., Cleveland, Ohio.
Pefferly, W. J., Phelps Dodge Copper Products Corporation, Detroit, Mich.
Personeus, L. H., Puget Sound Power and Light Company, Seattle, Wash.
Pierson, W. H., Croft Place, R. F. D. 3, Huntington, L. I., N. Y.
Powers, C. P., C. P. Powers Company, Cleveland, Ohio.
Risseeuw, B. J., Allis-Chalmers Manufacturing Company, Milwaukee, Wis.
Rivero, A. (Member), New York (N. Y.) Edison Company.
Robinson, W. F., Pacific Telephone and Telegraph Company, Portland, Ore.
Rockwell, F. H., United Light and Power Engineering and Construction Company, Kansas City, Mo.
Royal, A. B., Louis-Allis Company, Milwaukee, Wis.
Schoenfeld, S. S., Department of Parks, Bronx, N. Y.
Sessions, A. P. (Member), Southern California Edison Company, Ltd., Los Angeles, Calif.
Shepherd, R. H., R. H. Shepherd Company, Vancouver, Can.
Snowden, W. H., *Electrical West*, San Francisco, Calif.
Stahl, C. D., Oklahoma Gas and Electric Company, Ardmore.
Stanley, L. L., Klein & Saks, New York, N. Y.
Steinback, E. T., Homestake Mining Company, Lead, S. D.
Stinchcomb, L. M. (Member), H. B. Sherman Manufacturing Company, Battle Creek, Mich.
Stokien, A., Brooklyn (N. Y.) Edison Company, Inc.
Swenson, C. R., Indiana Bell Telephone Company, Indianapolis.
Taylor, A. Y., Rural Electrification Administration, Washington, D. C.
Thompson, J. K., France Manufacturing Company, Cleveland, Ohio.
Uphouse, W. F. (Member), Southwestern Bell Telephone Co. St. Louis, Mo.
Waag, H. B., North Eastern Construction Co. New York, N. Y.
Wald, S., 2715 Webb Avenue, New York, N. Y.
Williams, H. F., Bussmann Manufacturing Company, St. Louis, Mo.
Williams, N. W., CCC-SCS Iowa No. 18, Clariton, Iowa.
Wood, A. H., Virginia Electric and Power Company, Richmond, Va.

77 Domestic

Foreign

Lucas, F. N., Bardez Elec. Supply Co. Ltd., Mapuca, Bardez Goa, Portuguese India.
Robinson, J. E. L. (Member), Ferranti Ltd., Hollinwood, Lancashire, England.
Simmonds, J. C., University College, Nottingham, Eng.
Sreenivasaiengar, M., International General Electric Company (India) Ltd., Bombay, India.

4 Foreign

Engineering Literature

New Books in the Societies Library

Among the new books received at the Engineering Societies Library, New York, recently, are the following which have been selected because of their possible interest to the electrical engineer. Unless otherwise specified, books listed have been presented gratis by the publishers. The Institute assumes no responsibility for statements made in the following outlines; information for which is taken from the preface of the book in question.

SCIENTIFIC BASIS OF ILLUMINATING ENGINEERING. (Electrical Engineering Texts). By P. Moon, N. Y. and Lond., McGraw-Hill Book Company, 1936. 608 p., illustrated 10x8 in., cloth, $5.00. A textbook on the engineering of lighting. Presents the details of current practice and a thorough treatment of the scientific fundamentals. The text is based on courses at the Massachusetts Institute of Technology.

Die SCHLAUCHELEKTRODE zur LICHTBOGENSCHWEISSUNG von KUPFER. By W. Lessel. Berlin, VDI-Verlag, 1936. 57 p., illustrated, 8x6 in., paper, 3.80 rm. Describes a new process for arc welding copper for which several important advantages are claimed.

RADIO AMATEUR'S HANDBOOK. 14th ed. American Radio Relay League, West Hartford, Conn., 1936. 536 p., illustrated, 10x7 in., paper, $1.00 in U.S.A.; cloth, $2.50 in all countries. A reference book for amateurs, intended to provide accurate information on the practical design and construction of sending and receiving apparatus and the operation of amateur radio stations.

PRINCIPLES of ELECTRICAL ENGINEERING, Theory and Practice. By O. C. Blalock. 2 ed. N. Y. and Lond., McGraw-Hill Book Company, 1936. 584 p., illustrated, 9x6 in., cloth, $4.00. Provides a course in electrical theory and practice adapted to the needs of students who are preparing for work as civil, mechanical, or chemical engineers, but it may also be used by students of electrical engineering as an introduction.

Great Britain. Mines Dept. REPORT OF H. M. ELECTRICAL INSPECTOR of MINES for the Year 1935. London, His Majesty's Stationery Office, 1936. 78 p., illustrated, 10x8 in., paper (obtainable in British Library of Information, New York, $0.45). Presents statistics upon the use of electrical mining machinery and upon the accidents resulting from the use of electricity in mines.

ELEMENTS of PROBABILITY. By H. Levy and L. Roth. Oxford, England, Clarendon Press; N. Y., Oxford University Press, 1936. 200 p., illustrated, 9x6 in., cloth, $5.00. Presents an elementary treatment of the subject and provides a detailed criticism of the various self-contained theories of probability.

Das ELEKTRISCHE EISENBAHNWESEN der GEGENWART. (Elektrische Bahnen Ergänzungsheft, Jahrgang 1936.) p. Ed. by W. Wechmann. Berlin, Verlag für Sozialpolitik, Wirtschaft und Statistik, 1936. 212 p., illustrated, 12x8 in., paper, 6 rm. Contains 9 lectures by various authorities on the electrical railway.

EINFÜHRUNG in die KLASSISCHE ELEKTRODYNAMIK. By J. Fischer. Berlin, Julius Springer, 1936. 199 p., illustrated, 10x7 in., cloth, 13.80 rm. Presents the classic theory of electrodynamics, intended for advanced students.

BEITRAG zur BERECHNUNG von MASTFUNDAMENTEN. By H. Fröhlich. 3 ed. Berlin, Wilhelm Ernst and Sohn, 1936. 81 p., illustrated, 10x7 in., paper, 7.50 rm. (3.65 rm. in U.S.A.). Provides a study of the design of foundations for the masts and towers of transmission lines.

INDUSTRIAL DUST. By P. Drinker and T. Hatch. N. Y. and Lond., McGraw-Hill Book Co., 1936. 316 p., illus., 9x6 in., cloth, $4.00. Discusses the problem of dust control in its relation to the health of workmen, and presents methods for designing and operating dust-control equipment.

ENGINEERING ALLOYS, Names, Properties, Uses. By N. E. Woldman and A. J. Dornbiatt. Cleveland, Ohio, American Society for Metals, 1936. 623 p., tables, 10x6 in., lea., $10.00. Contains the trade names, manufacturers, composition, properties, and uses of 3,200 engineering alloys.

ELEMENTS of MECHANICS. By H. A. Erikson. 3 ed. N. Y. and Lond., McGraw-Hill Book Co., 1936. 269 p., illus., 8x6 in., cloth, $2.25. A text based on a course at the University of Minnesota.

DESCRIPTIVE GEOMETRY PROBLEM BOOK. By F. W. Bubb. N. Y., Macmillan Co., 1936. Diagrs., 8x11 in., paper, $1.75. Contains 300 problems on detachable sheets of white paper.

PUBLIC UTILITY INDUSTRIES. By G. L. Wilson, J. M. Herring, and R. B. Butler. N. Y. and Lond, McGraw-Hill Book Co., 1936. 412 p., illus., 9x6 in., cloth, $3.50. Affords a survey of the economic, legal, and social characteristics of public utility enterprises.

TEXTBOOK of ILLUMINATION. By W. Kuneth. 2 ed. N. Y., J. Wiley and Sons, 1936. 276 p., illus., 10x8 in., lea., $3.00. A short course in illumination, intended for undergraduates.

TELEVISION with CATHODE RAYS. By A. H. Halloran. San Francisco, Pacific Radio Publishing Co., 1936. Illus., 7x5 in., lea., $2.75. The operating principles of the cathode-ray tube and its application to television are explained in terms that can be understood by the amateur radio operator and radio service man.

PHYSIK und TECHNIK der ULTRAKURZEN WELLEN, v. 2. By H. E. Hollmann. Berlin, Julius Springer, 1936. 306 p., illus., 9x6 in., cloth, 33 rm. Describes the practical applications of ultra-short waves, and discusses reception, detection, and transmission.

INDUCTIVE CO-ORDINATION of ELECTRIC POWER and COMMUNICATION CIRCUITS. By L. J. Corbett. San Francisco, J. H. Neblett Pressroom Ltd., 500 Sansome St., 1936. 151 p., illus., 9x6 in., cloth, $3.00. Discusses the factors involved and suggests methods by which detrimental effects can be remedied. Written from the point of view of the power engineer, but considers the problems of the communication engineer also.

HEAVISIDE'S OPERATIONAL CALCULUS, as applied to Engineering and Physics. (Electrical Engineering Texts.) By B. J. Berg. 2 ed. N. Y. and Lond., McGraw-Hill Book Co., 1936. 258 p., illus., 8x6 in., cloth, $3.00. Contains appendices in which various numerical problems are solved. Additional information on the theory of the use of the "unit function" is given.

Der ERDSCHLUSS in HOCHSPANNUNGSNETZEN. By H. Weber. Munich and Berlin, R. Oldenbourg, 1936. 107 p., illus., 10x7 in., paper, 5.80 rm. Discusses the phenomena accompanying grounds in 3-phase distribution systems and the methods of preventing them. Intended for operating engineers and students.

ELEKTROTECHNIK und WITTERUNG. By U. Retzow. Berlin, Julius Springer, 1936. 121 p., 9x6 in., paper, 6.80 rm. Discusses the effects of weather in electrical engineering, including the influence of meteorological elements on overhead lines, the use of wind for generating electricity, influence of altitude on power stations, and disturbances of radio transmission.

Die ELEKTRISCHE KRAFTÜBERTRAGUNG, v. 3, pt. 1. Bau und Betrieb des Netzwerkes. By H. Kyser. Berlin, Julius Springer, 1936. 573 p., illus., 10x6 in., cloth, 48 rm. Devoted to the mechanical equipment of electric power plants from a practical point of view for the designer and operator.

ELECTRONICS and ELECTRON TUBES. By R. D. MacArthur. N. Y., John Wiley and Sons, 1936. 173 p., illus., 9x8 in., $2.50. Describes the fundamental principles governing the action of all electron tubes; mathematics is used sparingly. A chapter is devoted to electron tube construction. Much of the book has appeared serially in the *General Electric Review*.

ELECTRICAL LABORATORY EXPERIMENTS, Theory and Practice. By V. Karapetoff and B. C. Dennison. N. Y., John Wiley and Sons, 1936. 487 p., illus., 9x6 in., lea., $4.00. An abridgment of Karapetoff's "Experimental Electrical Engineering," prepared to meet the demand for a less comprehensive book with the same general method of treatment but better adapted to the average undergraduate course.

Engineering Societies Library

29 West 39th Street, New York, N. Y.

MAINTAINED as a public reference library of engineering and the allied sciences, this library is a cooperative activity of the national societies of civil, electrical, mechanical, and mining engineers.

Resources of the library are available also to those unable to visit it in person. Lists of references, copies or translation of articles, and similar assistance may be obtained upon written application, subject only to charges sufficient to cover the cost of the work required.

A collection of modern technical books is available to any member residing in North America at a rental rate of five cents per day per volume, plus transportation charges.

Many other services are obtainable and an inquiry to the director of the library will bring information concerning them.

Industrial Notes

Corning Glass Expands.—To meet the increased production demands, plant facilities of the fibre products division of the Corning Glass Works are being enlarged, and work is well under way in the erection of 3 new buildings having a total area of 46,000 sq. ft. L. W. W. Morrow, formerly editor of the "Electrical World," was recently appointed general manager of this division. Principal applications of the new glass fibre include building insulation, refrigerator linings and air conditioning filters. Potential markets include wire and cable covering and innumerable textile applications to which an inorganic thread or cloth made of glass can be applied. The new glass cloth is heat resistant, waterproof, and non-corroding.

Copperweld Appointment.—Roy C. Raasch has recently been appointed field representative for the Copperweld Steel Co., with headquarters at Chicago, Ill. For the past few years he has been in the engineering department of a large utility company.

Tower Order to Blaw-Knox.—According to a recent announcement, the Blaw-Knox Co., Pittsburgh, Pa., has received an order for approximately 2000 tons of transmission towers (which will number about 250) for a 220,000 volt line of the Pennsylvania Water & Power Co. of Baltimore.

New Connector.—Burndy Engineering Co., Inc., New York City, has announced an addition to their line of grounding connectors "Groundem," type GH. This low-cost connector is for use in joining a ground lead to a driven rod or pipe. Its construction permits it to be slipped over the top of the rod as a one-piece assembly, or, in the event that the rod or pipe has been splayed from driving, it may be readily disassembled and slipped around the conductors. The Groundem is constructed entirely of non-corrosive copper alloys, making it resistant to underground conditions. It is installed with an ordinary wrench and is made in three sizes, each of which will take a range of rod and wire diameters.

Pacific Electric Now Home Owned.—According to a recent announcement, the interest of the General Electric Co. in the Pacific Electric Manufacturing Corp., has been purchased by Joseph S. Thompson, president of the latter company. Some eight years ago General Electric secured a virtual half interest in the west coast company, but with the sale of the stock the latter is now an entirely independent organization. It operates a factory occupying two city blocks in San Francisco and a small branch maintenance and storage plant at Gary, Ind. Incorporated in 1906, it is engaged in the manufacture of high voltage air break switches, oil circuit breakers, high voltage fuses and kindred apparatus.

Calculating Board Kept Busy.—With increasing loads racing toward the capacity of equipment, many power companies find it necessary to solve quickly new generation and distribution problems. Five companies wishing to determine accurately the added power needed and the load limits and stability of their systems have recently engaged the Westinghouse a-c calculating board to analyze their problems. During the past year eighteen major system studies, involving plants up to 500,000 kva capacity, have been completed on this uniquely efficient board. These systems included eight utilities, six government projects, two industrial plants and two foreign power systems. This is the largest a-c calculating board built to date, and with its 300 circuits it can readily duplicate, by miniature replica, any power system in this country. With its aid, system stability, power factor correction, load-voltage regulation studies and the best location for new generating, transformer and line equipment are readily determined.

Trade Literature

Distribution Capacitors.—Bulletin 3381, 16 pp. Describes the use of "Permittors" (capacitors) for power factor correction in distribution circuits. Products Protection Corp., New Haven, Conn.

Meters.—Catalog Sec. 42–210, 16 pp. Describes various types of polyphase detachable meters, applications, construction, operation, adjustment, outline dimensions and wiring diagrams. Westinghouse Electric & Mfg. Co., E. Pittsburgh, Pa.

Stopwatches.—Folder. Describes and illustrates 40 different types of stopwatches for industrial and laboratory use. Circular describes stopwatch repair service. A. R. & J. E. Meylan, 268 W. 40th St., New York.

Motor Repair Supplies.—Catalog 49, 48 pp. Describes insulation, wire, tools and supplies for the motor repair shop. Prices are included. Reading Electric Co., 227 W. Van Buren St., Chicago, Ill.

Circuit Breakers.—Bulletin GEA-2450, 4 pp. Describes type AE-1 air circuit breakers for industrial and central station auxiliary service; 250 volts d-c; 600 volts a-c; 15–600 amperes, 20,000 amperes interrupting rating. General Electric Co., Schenectady, N. Y.

Measuring Instruments.—Catalog-type broadside "Power Plant Measuring Instruments, Telemeters, and Automatic Controls." Specific applications are illustrated in electrical generation and transmission, steam generation and distribution, hydro- and diesel power generation, in which the equipment is used. Leeds & Northrup Co., 4962 Stenton Ave., Philadelphia, Pa.

Oilostatic Transmission System.—Bulletin, 16 pp. Describes the Bennett Oilostatic transmission system, in which the insulated power cables are installed in buried metal pipe filled with oil maintained under a constant high pressure. Includes details of construction, cable design, cable splices, terminals, pressure maintaining equipment, etc., as well as a detailed outline of all information required to make a study of an Oilostatic application. The Okonite-Callender Cable Co., Paterson, N. J.

Monel Metal.—Bulletin, 48 pp. The publication has been prepared primarily as a guide book to Monel and other non-ferrous nickel alloys in the fields of engineering applications. It also covers the corrosion resistance and other properties of these metals. Twenty sub-divisions are included, each devoted to specific problems in fields from hydroelectric and steam power plants to highway maintenance, refrigeration and automobiles. The booklet also describes some of the newer forms of the alloy, including "K" and "S" Monel, etc. International Nickel Co., 67 Wall St., New York City.

Synchronous Motors.—Bulletin 1154A, 28 pp. Describes the construction and applications of modern, coupled and engine-type synchronous motors that may now be obtained with torque characteristics suitable for practically any drive, fifty horse power or over, where the squirrel cage induction motor could be used. It deals with the increasing usage of this type of motor due to its uniform high efficiency, at fractional as well as at full loads, and at all speeds, together with its all important function of power factor correction. Allis-Chalmers Mfg. Co., Milwaukee, Wis.

Industrial Wiring Survey.—Bulletin, 40 pp. This publication has been designed to facilitate investigation of the condition of the electrical equipment and wiring in industrial plants from the standpoint of ability to carry load, surplus or spare capacity, system defects, safety, deterioration and obsolescence. It gives the logical procedure for making such a survey, provides convenient space for recording findings, and includes recommendations for plans or plot sketches of the existing layout. It is stated that such a study will disclose the weaknesses, if any, in the electrical system, and become a permanent record for determining what parts of the system may be extended under pressing conditions. Anaconda Wire & Cable Co., 25 Broadway, New York City.

New Clip-On Ammeters.—Bulletin, 4 pp. Describes a complete new line of dual range clip-on ammeters now available. Originally introduced some 6 years ago, this instrument was at first available only in the standard 0–100/500 ampere combination. Recently additional low and high range combinations have been added to the line so that it is now stocked in 4 standard low range combinations and 3 high range combinations. With these instruments it is possible to measure currents from 1/5 ampere up to 1,000 amperes without opening the circuit or shutting down the equipment under test, or removing insulation from the conductors. The instruments are supplied with fully insulated clips as well as Bakelite handles and may be used with equal safety on insulated or bare conductors. Many minor improvements have been incorporated in the new line. Ferranti Electric, Inc., 30 Rockefeller Plaza, New York City.